

# MOLECULAR COMPONENTS OF STORE-OPERATED CALCIUM ENTRY IN HEALTH AND DISEASE

EDITED BY: Joanna Gruszczynska-Biegala, Francisco Javier Martin-Romero,  
Agnese Secondo and Tarik Smani

PUBLISHED IN: Frontiers in Cell and Developmental Biology,  
Frontiers in Cellular Neuroscience and  
Frontiers in Molecular Neuroscience



# frontiers

## Frontiers eBook Copyright Statement

The copyright in the text of individual articles in this eBook is the property of their respective authors or their respective institutions or funders. The copyright in graphics and images within each article may be subject to copyright of other parties. In both cases this is subject to a license granted to Frontiers.

The compilation of articles constituting this eBook is the property of Frontiers.

Each article within this eBook, and the eBook itself, are published under the most recent version of the Creative Commons CC-BY licence.

The version current at the date of publication of this eBook is CC-BY 4.0. If the CC-BY licence is updated, the licence granted by Frontiers is automatically updated to the new version.

When exercising any right under the CC-BY licence, Frontiers must be attributed as the original publisher of the article or eBook, as applicable.

Authors have the responsibility of ensuring that any graphics or other materials which are the property of others may be included in the CC-BY licence, but this should be checked before relying on the CC-BY licence to reproduce those materials. Any copyright notices relating to those materials must be complied with.

Copyright and source acknowledgement notices may not be removed and must be displayed in any copy, derivative work or partial copy which includes the elements in question.

All copyright, and all rights therein, are protected by national and international copyright laws. The above represents a summary only. For further information please read Frontiers' Conditions for Website Use and Copyright Statement, and the applicable CC-BY licence.

ISSN 1664-8714

ISBN 978-2-88971-756-9

DOI 10.3389/978-2-88971-756-9

## About Frontiers

Frontiers is more than just an open-access publisher of scholarly articles: it is a pioneering approach to the world of academia, radically improving the way scholarly research is managed. The grand vision of Frontiers is a world where all people have an equal opportunity to seek, share and generate knowledge. Frontiers provides immediate and permanent online open access to all its publications, but this alone is not enough to realize our grand goals.

## Frontiers Journal Series

The Frontiers Journal Series is a multi-tier and interdisciplinary set of open-access, online journals, promising a paradigm shift from the current review, selection and dissemination processes in academic publishing. All Frontiers journals are driven by researchers for researchers; therefore, they constitute a service to the scholarly community. At the same time, the Frontiers Journal Series operates on a revolutionary invention, the tiered publishing system, initially addressing specific communities of scholars, and gradually climbing up to broader public understanding, thus serving the interests of the lay society, too.

## Dedication to Quality

Each Frontiers article is a landmark of the highest quality, thanks to genuinely collaborative interactions between authors and review editors, who include some of the world's best academicians. Research must be certified by peers before entering a stream of knowledge that may eventually reach the public - and shape society; therefore, Frontiers only applies the most rigorous and unbiased reviews. Frontiers revolutionizes research publishing by freely delivering the most outstanding research, evaluated with no bias from both the academic and social point of view. By applying the most advanced information technologies, Frontiers is catapulting scholarly publishing into a new generation.

## What are Frontiers Research Topics?

Frontiers Research Topics are very popular trademarks of the Frontiers Journals Series: they are collections of at least ten articles, all centered on a particular subject. With their unique mix of varied contributions from Original Research to Review Articles, Frontiers Research Topics unify the most influential researchers, the latest key findings and historical advances in a hot research area! Find out more on how to host your own Frontiers Research Topic or contribute to one as an author by contacting the Frontiers Editorial Office: [frontiersin.org/about/contact](https://frontiersin.org/about/contact)

# MOLECULAR COMPONENTS OF STORE-OPERATED CALCIUM ENTRY IN HEALTH AND DISEASE

Topic Editors:

**Joanna Gruszczynska-Biegala**, Mossakowski Medical Research Institute PAS,  
Poland

**Francisco Javier Martin-Romero**, University of Extremadura, Spain

**Agnese Secondo**, University of Naples Federico II, Italy

**Tarik Smani**, Sevilla University, Spain

**Citation:** Gruszczynska-Biegala, J., Martin-Romero, F. J., Secondo, A., Smani, T., eds. (2021). Molecular Components of Store-Operated Calcium Entry in Health and Disease. Lausanne: Frontiers Media SA. doi: 10.3389/978-2-88971-756-9

# Table of Contents

- 05 Editorial: Molecular Components of Store-Operated Calcium Entry in Health and Disease**  
Joanna Gruszczynska-Biegala, Francisco Javier Martin-Romero, Tarik Smani and Agnese Secondo
- 08 Targeting Orai1-Mediated Store-Operated Ca<sup>2+</sup> Entry in Heart Failure**  
Rui Luo, Ana-Maria Gomez, Jean-Pierre Benitah and Jessica Sabourin
- 18 Calcium Channels in Adult Brain Neural Stem Cells and in Glioblastoma Stem Cells**  
Valérie Coronas, Elodie Terrié, Nadine Déliot, Patricia Arnault and Bruno Constantin
- 40 Store-Operated Calcium Channels in Physiological and Pathological States of the Nervous System**  
Isis Zhang and Huijuan Hu
- 53 Target Molecules of STIM Proteins in the Central Nervous System**  
Karolina Serwach and Joanna Gruszczynska-Biegala
- 76 Dysregulation of Neuronal Calcium Signaling via Store-Operated Channels in Huntington's Disease**  
Magdalena Czeredys
- 97 STIM2 Mediates Excessive Store-Operated Calcium Entry in Patient-Specific iPSC-Derived Neurons Modeling a Juvenile Form of Huntington's Disease**  
Vladimir A. Vigont, Dmitriy A. Grekhnev, Olga S. Lebedeva, Konstantin O. Gusev, Egor A. Volovikov, Anton Yu. Skopin, Alexandra N. Bogomazova, Lilia D. Shuvalova, Olga A. Zubkova, Ekaterina A. Khomyakova, Lyubov N. Glushankova, Sergey A. Klyushnikov, Sergey N. Illarioshkin, Maria A. Lagarkova and Elena V. Kaznacheyeva
- 110 Transmembrane Domain 3 (TM3) Governs Orai1 and Orai3 Pore Opening in an Isoform-Specific Manner**  
Adéla Tiffner, Lena Maltan, Marc Fahrner, Matthias Sallinger, Sarah Weiß, Herwig Grabmayr, Carmen Höglinger and Isabella Derler
- 126 Gain-of-Function STIM1 L96V Mutation Causes Myogenesis Alteration in Muscle Cells From a Patient Affected by Tubular Aggregate Myopathy**  
Elena Conte, Alessandra Pannunzio, Paola Imbrici, Giulia Maria Camerino, Lorenzo Maggi, Marina Mora, Sara Gibertini, Ornella Cappellari, Annamaria De Luca, Mauro Coluccia and Antonella Liantonio
- 141 SARAF and Orai1 Contribute to Endothelial Cell Activation and Angiogenesis**  
Isabel Galeano-Otero, Raquel Del Toro, Abdel-Majid Khatib, Juan Antonio Rosado, Antonio Ordóñez-Fernández and Tarik Smani
- 154 Corrigendum: SARAF and Orai1 Contribute to Endothelial Cell Activation and Angiogenesis**  
Isabel Galeano-Otero, Raquel del-Toro, Abdel-Majid Khatib, Juan Antonio Rosado, Antonio Ordóñez-Fernández and Tarik Smani

**155   *Molecular Components of Store-Operated Calcium Channels in the Regulation of Neural Stem Cell Physiology, Neurogenesis, and the Pathology of Huntington's Disease***

Ewelina Latoszek and Magdalena Czeredys

**175   *ORAI1  $\text{Ca}^{2+}$  Channel as a Therapeutic Target in Pathological Vascular Remodelling***

Heba Shower, Katherine Norman, Chew W. Cheng, Richard Foster, David J. Beech and Marc A. Bailey



# Editorial: Molecular Components of Store-Operated Calcium Entry in Health and Disease

Joanna Gruszczynska-Biegala<sup>1\*†</sup>, Francisco Javier Martin-Romero<sup>2†</sup>, Tarik Smani<sup>3,4†</sup> and Agnese Secondo<sup>5†</sup>

<sup>1</sup> Laboratory of Molecular Biology, Mossakowski Medical Research Institute, Polish Academy of Sciences, Warsaw, Poland, <sup>2</sup> Institute of Molecular Pathology Biomarkers, University of Extremadura, Badajoz, Spain, <sup>3</sup> Group of Cardiovascular Pathophysiology, Institute of Biomedicine of Seville, University Hospital of Virgen del Rocío, University of Seville, CSIC, Seville, Spain, <sup>4</sup> Department of Medical Physiology and Biophysics, University of Seville, Seville, Spain, <sup>5</sup> Department of Neuroscience, "Federico II" University of Naples, Naples, Italy

**Keywords:** SOCE, STIM1, STIM2, TRP channels, ORAI

## Editorial on the Research Topic

### Molecular Components of Store-Operated Calcium Entry in Health and Disease

## OPEN ACCESS

### Approved by:

Dirk M. Hermann,  
University of

Duisburg-Essen, Germany

### \*Correspondence:

Joanna Gruszczynska-Biegala  
jgruszczynska@imdmk.pan.pl

<sup>†</sup>These authors have contributed  
equally to this work

### Specialty section:

This article was submitted to  
Cellular Neuropathology,  
a section of the journal  
Frontiers in Cellular Neuroscience

**Received:** 05 September 2021

**Accepted:** 15 September 2021

**Published:** 05 October 2021

### Citation:

Gruszczynska-Biegala J,  
Martin-Romero FJ, Smani T and  
Secondo A (2021) Editorial: Molecular  
Components of Store-Operated  
Calcium Entry in Health and Disease.  
Front. Cell. Neurosci. 15:771138.  
doi: 10.3389/fncel.2021.771138

Store-Operated Calcium Entry (SOCE) is a ubiquitous  $\text{Ca}^{2+}$  influx mechanism first described in 1986 (Putney, 1986). This conserved mechanism results from the interaction between the tetraspanning ORAI1 channel located in plasma membrane and the unique endoplasmic reticulum (ER)  $\text{Ca}^{2+}$  sensor, stromal interaction molecule 1 (STIM1), via their respective intracellular domains (Roos et al., 2005; Csutora et al., 2008). Moreover, there are two homologs of ORAI1, namely ORAI2 and ORAI3, all generating SOCE with the same mechanism.

Molecularly, upon ER  $\text{Ca}^{2+}$  depletion, STIM1 senses the filling state of ER with its N-terminus characterized by a low affinity for  $\text{Ca}^{2+}$  ion (200 nM-600 microM). After dimerization, STIM1 diffuses to the plasma membrane regions where it interacts with ORAI1 inducing SOCE through Calcium Release-Activated Calcium (CRAC) channel opening. This event may mediate a localized increase in the intracellular  $\text{Ca}^{2+}$  concentration useful to recharge ER of  $\text{Ca}^{2+}$  content by sarco/endoplasmic reticulum  $\text{Ca}^{2+}$ -ATPase (SERCA) intervention. Besides STIM1, also STIM2 may induce activation of ORAI1 (Brandman et al., 2007) but with a weak  $\text{Ca}^{2+}$  entry that is nevertheless able to trigger NFAT1 activation (Son et al., 2020).

Accumulated evidence suggests that SOCE dysfunction may produce  $\text{Ca}^{2+}$  dyshomeostasis in both excitable and non-excitable cells, thus participating to the pathogenesis of a large spectrum of diseases most of which are due to the modification of ORAI1/STIM1 interaction in consequence of changes in their expression or following a disruption of SOCE machinery. However, genetic modification of the two major players could also occur. For instance, loss of function mutations of ORAI1 and STIM1/STIM2 abolishes SOCE, thus causing autoimmunity and severe combined immunodeficiency (SCID)-like diseases. In contrast, autosomal dominant gain-of-function mutations in ORAI1 and STIM1 determine a sustained increase in CRAC and SOCE causing a large spectrum of diseases like Stormorken syndrome and nonsyndromic tubular aggregate myopathy (TAM) (Lacruz and Feske, 2015). In this respect the study by Conte et al. shows some of the adaptive or compensatory mechanisms able to counteract the genetic-encoded  $\text{Ca}^{2+}$  dyshomeostasis and describes the alteration in the differentiation process of muscle cells deriving from TAM-patients carrying STIM1 L96V mutation.

Mechanistically, mutations in the transmembrane domains of the pore region of ORAI channels may produce SOCE alterations. Of note, the elucidation of the isoform-specific mutations may

provide useful targets for selective drug development. In this context, the study by Tiffner et al. shows the molecular consequences of the enhanced hydrophobicity along TM3 of ORAI1 or ORAI3 structure on the gain-of-function of SOCE and CRAC currents.

In this Research Topic, two manuscripts review the role of ORAI1 in cardiovascular remodeling and heart failure. The first article by Luo et al. provides an overview of the new role of ORAI1-mediated SOCE in the maladaptive cardiac hypertrophy and heart failure. The review discusses the current knowledge regarding the involvement of ORAI1 in hypertrophic development induced by neurohormonal stimulation *in vitro* or *in vivo*, using transgenic mice subjected to different procedures that induce cardiac hypertrophy and consequently heart failure.

The other review article by Shawer et al. provides a broad perspective of the role ORAI1-mediated vascular smooth muscle cell (VSMC) switching from contractile to synthetic phenotypes, a critical step for their proliferation and migration. Authors focus on the involvement of ORAI1 in the pathological vascular remodeling related to atherosclerosis, neointimal hyperplasia and restenosis. They also discuss the potential mode of action of a large list of SOCE inhibitors examined in different cell lines.

Both reviews consider that new pharmacological selective inhibitors are valuable tools to study the role of SOCE in health and disease, which might pave the way for the development of therapeutic ORAI1 inhibitors to mitigate pathologic cardiac and vascular remodeling.

Galeano-Otero et al. in an original article related to the circulatory system highlight for the first time the role of SARAF, SOCE-associated regulatory factor, in the activation of endothelial cells and angiogenesis. The study nicely demonstrates that SOCE participates in several steps of angiogenesis, such as endothelial cell proliferation and migration, tube formation, and sprouting, and shows that SARAF co-localizes and interacts with ORAI1, which might sustain an enhanced  $\text{Ca}^{2+}$  entry in these highly proliferative cells during angiogenesis.

Since the discovery of the molecular components of SOCE, including the STIM, ORAI and TRP proteins, a growing number of publications describe their functions in the healthy and diseased central nervous system (CNS) (Serwach and Gruszczynska-Biegala, 2019). In this regard, Zhang and Hu summarize the current literature reporting on the variable expression of STIM, ORAI and TRPC in neurons and glial cells from different parts of the CNS. The authors also provide a systematic overview describing the current understanding of the physiological and pathological role of SOCE and its molecular components in each of these brain regions. The impact of existing therapies on SOCE is also reviewed.

Two additional review articles describe the relationship between Huntington's disease (HD) and SOCE (Latoszek and Czeredys). As an inherited neurodegenerative disorder, HD is characterized by the loss of  $\gamma$ -aminobutyric acid (GABA)-ergic medium spiny neurons (MSNs) in the striatum (Vonsattel and DiFiglia, 1998), and SOCE has been shown to be elevated in several HD models. Czeredys's review provides a comprehensive update on the implications of SOCE,

STIM2, ORAIs and TRPCs in HD pathology using various HD models, including YAC128 mice (HD transgenic model), HD cellular models, and induced pluripotent stem cell-based GABAergic MSNs that are obtained from fibroblasts of adult HD patients. The author further discusses potential drug candidates that may restore normal SOCE and consequently prevent dendritic spine loss in HD. Latoszek and Czeredys review recent data indicating that HD is also a neurodevelopmental disease, as neuronal cells differentiated from juvenile HD patient-derived iPSCs show deficits in development and adult neurogenesis. Finally, the authors also review different protocols to obtain MSNs and brain organoids as powerful tools to study HD.

Also related to HD, Vigont et al. in an original article, demonstrate the role of STIM2 in the elevated  $\text{Ca}^{2+}$  entry in HD cellular models. More specifically, these authors generated MSNs modeling a juvenile form of HD and show high levels of SOCE using patch-clamp. Upregulation of STIM2 protein expression was also observed, and the shRNA-mediated suppression of STIM2 expression attenuated SOCE. For this reason, Vigont et al. used the anti-HD drug EVP4593 to demonstrate that this drug decreased huntingtin expression and also the expression of STIM2, postulating that STIM2 could be a novel therapeutic target for HD.

In addition to the main components of SOCE, being the STIM and ORAI proteins, an increasing number of proteins have been also reported to play an important role in the STIM-ORAI dependent regulation of SOCE. Serwach and Gruszczynska-Biegala thoroughly review and summarize the current knowledge about STIM protein target molecules, including positive (mGluR, septins, synaptopodin, POST, EB and Golli proteins) and negative (Homer, SARAF, presenilin1, and NEUROD2) regulators and effectors [L-type voltage-operated  $\text{Ca}^{2+}$  channels (VOCCs) and receptors such as AMPAR and NMDAR] in the CNS. This review also highlights the importance of the interaction of STIM proteins with their target proteins in pathology, such as hypoxic/ischemic neuronal injury, epilepsy, Alzheimer's, Huntington's and Parkinson's diseases, and in physiological conditions of the CNS.

Finally, in this issue Coronas et al. review the role of  $\text{Ca}^{2+}$  channels in neural stem cells (NSCs) and glioblastoma stem cells (GSCs), derived from oncogenic mutations in adult NSCs and responsible for the emergence of malignant brain tumors. The review focuses on the  $\text{Ca}^{2+}$  toolkit and its physiological role in GSCs, in NSCs and their progenies to show that stemness is controlled by VOCCs, store-operated  $\text{Ca}^{2+}$  channels (SOCs),  $\text{IP}_3$ Rs in NSCs, and by VOCCs, nicotinic receptors and TRPVs in GSCs.

In summary, this special issue of Frontiers in Cellular Neuroscience provides a comprehensive overview of the most recent data on the role of SOCE and related proteins: STIMs, ORAIs and others that regulate them, in the physiology and pathology of a variety of cells. It highlights the importance of SOCE and its regulatory proteins as potential drug targets for future therapies against neurodegenerative, cardiovascular or muscular diseases and brain tumors.

## AUTHOR CONTRIBUTIONS

All authors listed have made a substantial, direct and intellectual contribution to the work, and approved it for publication.

## FUNDING

JG-B was supported by the National Science Centre grant (research project no. 2017/26/E/NZ3/01144), FJM-R was supported by the Spanish Ministry of Science and Innovation (research project BFU2017-82716-P), TS was supported by the Spanish Ministry of Science and Innovation (research project

no. PID2019-104084GB-C22/ AEI/10.13039/501100011033), AS was supported by PRIN2015–Prot. 2015KRY5JN (Italian Ministry of Education and Research), Progetto Speciale di Ateneo CA.04\_CDA\_n\_103 27.03.2019 and Progetto di Ateneo Linea A CdA\_54\_2020\_FRA.

## ACKNOWLEDGMENTS

Editors thank deeply all the authors for their scientific contributions and the reviewers for their support and constructive criticism in refining the manuscripts in this Research Topic.

## REFERENCES

- Brandman, O., Liou, J., Park, W. S., and Meyer, T. (2007). STIM2 is a feedback regulator that stabilizes basal cytosolic and endoplasmic reticulum  $\text{Ca}^{2+}$  levels. *Cell* 131, 1327–1339. doi: 10.1016/j.cell.2007.11.039
- Csutora, P., Peter, K., Kilic, H., Park, K. M., Zarayskiy, V., Gwozdz, T., et al. (2008). Novel role for STIM1 as a trigger for calcium influx factor production. *J. Biol. Chem.* 283, 14524–14531. doi: 10.1074/jbc.M709575200
- Lacruz, R. S., and Feske, S. (2015). Diseases caused by mutations in ORAI1 and STIM1. *Ann. N. Y. Acad. Sci.* 1356, 45–79. doi: 10.1111/nyas.12938
- Putney, J. W. Jr. (1986). A model for receptor-regulated calcium entry. *Cell Calcium* 7, 1–12. doi: 10.1016/0143-4160(86)90026-6
- Roos, J., DiGregorio, P. J., Yeromin, A. V., Ohlsen, K., Lioudyno, M., Zhang, S., et al. (2005). STIM1, an essential and conserved component of store-operated  $\text{Ca}^{2+}$  channel function. *J. Cell Biol.* 169, 435–445. doi: 10.1083/jcb.200502019
- Serwach, K., and Gruszczynska-Biegala, J. (2019). STIM proteins and glutamate receptors in neurons: role in neuronal physiology and neurodegenerative diseases. *Int. J. Mol. Sci.* 20:2289. doi: 10.3390/ijms20092289
- Son, G. Y., Subedi, K. P., Ong, H. L., Noyer, L., Saadi, H., Zheng, C., et al. (2020). STIM2 targets Orail/STIM1 to the AKAP79 signaling complex and confers coupling of  $\text{Ca}^{2+}$  entry with NFAT1 activation. *Proc. Natl. Acad. Sci. U.S.A.* 117, 16638–16648. doi: 10.1073/pnas.1915386117

Vonsattel, J. P., and DiFiglia, M. (1998). Huntington disease. *J. Neuropathol. Exp. Neurol.* 57, 369–384. doi: 10.1097/00005072-199805000-00001

**Conflict of Interest:** The authors declare that the research was conducted in the absence of any commercial or financial relationships that could be construed as a potential conflict of interest.

**Publisher's Note:** All claims expressed in this article are solely those of the authors and do not necessarily represent those of their affiliated organizations, or those of the publisher, the editors and the reviewers. Any product that may be evaluated in this article, or claim that may be made by its manufacturer, is not guaranteed or endorsed by the publisher.

Copyright © 2021 Gruszczynska-Biegala, Martin-Romero, Smani and Secondo. This is an open-access article distributed under the terms of the Creative Commons Attribution License (CC BY). The use, distribution or reproduction in other forums is permitted, provided the original author(s) and the copyright owner(s) are credited and that the original publication in this journal is cited, in accordance with accepted academic practice. No use, distribution or reproduction is permitted which does not comply with these terms.



# Targeting Orai1-Mediated Store-Operated $\text{Ca}^{2+}$ Entry in Heart Failure

Rui Luo, Ana-Maria Gomez, Jean-Pierre Benitah\* and Jessica Sabourin\*

Inserm, UMR-S 1180, Signalisation et Physiopathologie Cardiovasculaire, Université Paris-Saclay, Châtenay-Malabry, France

## OPEN ACCESS

### Edited by:

Tarik Smani,  
Seville University, Spain

### Reviewed by:

Rajender Motiani,  
Regional Centre for Biotechnology  
(RCB), India  
Marc Freichel,  
Heidelberg University, Germany

### \*Correspondence:

Jean-Pierre Benitah  
jean-pierre.benitah@inserm.fr  
Jessica Sabourin  
jessica.sabourin@universite-paris-saclay.fr

### Specialty section:

This article was submitted to  
Signaling,  
a section of the journal  
Frontiers in Cell and Developmental  
Biology

**Received:** 01 August 2020

**Accepted:** 07 September 2020

**Published:** 08 October 2020

### Citation:

Luo R, Gomez A-M, Benitah J-P  
and Sabourin J (2020) Targeting  
Orai1-Mediated Store-Operated  
 $\text{Ca}^{2+}$  Entry in Heart Failure.  
Front. Cell Dev. Biol. 8:586109.  
doi: 10.3389/fcell.2020.586109

The archetypal store-operated  $\text{Ca}^{2+}$  channels (SOCs), Orai1, which are stimulated by the endo/sarcoplasmic reticulum (ER/SR)  $\text{Ca}^{2+}$  sensor stromal interaction molecule 1 (STIM1) upon  $\text{Ca}^{2+}$  store depletion is traditionally viewed as instrumental for the function of non-excitable cells. In the recent years, expression and function of Orai1 have gained recognition in excitable cardiomyocytes, albeit controversial. Even if its cardiac physiological role in adult is still elusive and needs to be clarified, Orai1 contribution in cardiac diseases such as cardiac hypertrophy and heart failure (HF) is increasingly recognized. The present review surveys our current arising knowledge on the new role of Orai1 channels in the heart and debates on its participation to cardiac hypertrophy and HF.

**Keywords:** orai1, store-operated  $\text{Ca}^{2+}$  entry, cardiomyocytes, heart, hypertrophy, heart failure

## INTRODUCTION

Spatiotemporal modulation of intracellular  $\text{Ca}^{2+}$  levels provides a signal transduction mechanism in virtually all cell types. This is used to determine which both short- and long-term cellular functions are activated and when. This fine control of  $\text{Ca}^{2+}$  handling is notably setup by various ion channels at the plasma membrane, including the store-operated  $\text{Ca}^{2+}$  channels (SOCs) and their corresponding store-operated  $\text{Ca}^{2+}$  entry (SOCE).

The notion of SOCE was first proposed in salivary gland cells as a “capacitative  $\text{Ca}^{2+}$  entry” (Putney, 1986, 1990), which couples the extracellular  $\text{Ca}^{2+}$  influx to the depletion of endoplasmic reticulum (ER)  $\text{Ca}^{2+}$  stores.  $\text{Ca}^{2+}$  influx into the cell *via* SOCs can be pumped back into the ER to replenish depleted stores and restore ER  $\text{Ca}^{2+}$  homeostasis.

After its initial study, direct evidence for the concept of a  $\text{Ca}^{2+}$  release-activated  $\text{Ca}^{2+}$  current ( $I_{\text{CRAC}}$ ) activated by  $\text{Ca}^{2+}$  store depletion in mast cells was provided by patch-clamp experiments (Hoth and Penner, 1992).  $I_{\text{CRAC}}$  was described as a sustained non-voltage-activated  $\text{Ca}^{2+}$  inward current with an inward rectification positive to reversal potential. It is highly selective for  $\text{Ca}^{2+}$  ions over  $\text{Ba}^{2+}$ ,  $\text{Sr}^{2+}$ , and  $\text{Mn}^{2+}$  (Hoth and Penner, 1992). The modern molecular period identifies two essentials molecular candidates responsible for the SOCE and the  $I_{\text{CRAC}}$ : one is the STIM1 protein, serving as an ER  $\text{Ca}^{2+}$  sensor *via* its N-terminal EF-hand domain; the second is Orai1 (also called CRACM1) forming the classical SOCs, which is highly selective for  $\text{Ca}^{2+}$ . The participation of the transient receptor potential canonical (TRPCs), which are non- $\text{Ca}^{2+}$  selective channels, as SOCs remains a highly contentious issue. The mechanism for SOCE activation was then elucidated by a series of elegant studies conducted primarily in non-excitable cells. Upon ER  $\text{Ca}^{2+}$  depletion,

$\text{Ca}^{2+}$  dissociates from the STIM1 EF-hand domain resulting in dimerization or oligomerization of STIM1 proteins and their translocation to the ER-plasma membrane (PM) junctions where they interact and activate Orai1 channels (Ma et al., 2015).

Orai1 is a ~33-kDa protein composed of 301 amino acids, although the predicted molecular weight might be significantly modified by post-translational modifications, with four putative transmembrane-spanning domains (M1–M4) and cytosolic NH<sub>2</sub>- and COOH-tails (Rosado et al., 2015). M1 lines the ion conduction pathway of Orai1 and contains several amino acid residues that define the biophysical properties of the channel (Lacruz and Feske, 2015). A crystal structure of the *Drosophila melanogaster* Orai channel, which shares 73% sequence identity with human Orai1 within its transmembrane region, has been determined (Hou et al., 2012). This study revealed a hexameric assembly of Orai1 proteins around a central ion pore, which crosses the membrane and extends into the cytosol, with extracellular glutamate residues forming a selectivity filter. The hexameric quaternary assembly is in contrast with several previous studies suggesting that Orai1 assembles as a functional tetramer (Penna et al., 2008; Maruyama et al., 2009).

Orai1 exhibits a wide functional distribution across mammalian cells and tissue types and is essential for SOCE (Feske et al., 2006; Vig et al., 2006). Indeed, Orai1 as the pore-forming SOC unit was discovered throughout a genetic analysis of patients with autosomal recessive loss-of-function (LOF) or gain-of-function (GOF) mutations in *ORAI1*, which are associated with severe combined immunodeficiency (SCID)-like disease, tubular aggregate myopathy (TAM), and Stormorken syndrome (Feske, 2019). The revealed missense *ORAI1* mutation is associated with defective SOCE and  $I_{\text{CRAC}}$ , resulting in loss of fine control of  $\text{Ca}^{2+}$ -mediated processes characterized by a severe immunodeficiency with myopathy. Nowadays, there is emerging evidence that Orai1 channels are important to almost every cell type. In cardiomyocytes, their potential physiological and pathological roles during cardiac hypertrophy and HF processes have been intensively investigated in the past few years.

The present review will survey our current knowledge on the expression and function of Orai1 in the heart and on its participation to cardiac hypertrophy and HF.

## PHYSIOLOGICAL ROLE OF ORAI1 IN THE HEART

### Expression and Cellular Location

The presence of SOCE was first described in embryonic and neonatal rat ventricular cardiomyocytes (NRVMs) (Hunton et al., 2002; Uehara et al., 2002) and then in adult rat ventricular cardiomyocytes (Hunton et al., 2004). This was further confirmed by the expression of the molecular SOC actors, such as Orai1 channels in the cardiomyocytes (Table 1).

Expression of Orai1 protein was first detected in 1-day-old neonate mice heart (Vig et al., 2008). Later on, many other studies described its expression in the NRVMs (Voelkers et al., 2010; Volkers et al., 2012; Zhu-Mauldin et al., 2012; Wang et al., 2015; Sabourin et al., 2016; Ji et al., 2017; Zheng et al., 2017; Dominguez-Rodriguez et al., 2018; Dai et al., 2018; Malette

et al., 2019). Orai1 expression decreased after birth in mice (Volkers et al., 2012). In the adult heart, ventricular tissues, and isolated ventricular cardiomyocytes from rats, mice, cats, chickens, zebrafish, or even hibernator animal squirrels, Orai1 was also detected with a low or even moderate level of expression in rodents (Gross et al., 2007; Takahashi et al., 2007; Volkters et al., 2012; Wang et al., 2012; Zhu-Mauldin et al., 2012; Collins et al., 2014; Guzman et al., 2014; Horton et al., 2014; Correll et al., 2015; Dominguez-Rodriguez et al., 2015; Liu et al., 2015; Saliba et al., 2015; Li et al., 2017; Lu et al., 2017; Maus et al., 2017; Nakipova et al., 2017; Troupes et al., 2017; Zheng et al., 2017; Dai et al., 2018; Dominguez-Rodriguez et al., 2018; Lee et al., 2018; Sabourin et al., 2018; Bartoli et al., 2019; Bonilla et al., 2019; Segin et al., 2020). Orai1 is also expressed in HL-1 atrial muscle cell line (Touchberry et al., 2011; Shiou et al., 2019), in left atrial rat and mice myocytes (Wolkowicz et al., 2011; Liu et al., 2015), in human embryonic stem cell-derived cardiomyocytes (Che et al., 2015; Wang et al., 2015), and in the sarcolemma of mouse sinoatrial node cells (SANs) and tissue (Zhang et al., 2013; Liu et al., 2015).

Of note, one research group could not detect the Orai1 expression in isolated adult rat cardiomyocytes (Zhang et al., 2015). This might be related not only to its weak expression but also to the antibody used.

Orai1 expression is more abundant in human myocardial tissue (Guzman et al., 2014), in human left ventricular tissue (Cendula et al., 2019), and in human atrial myocytes (Zhang et al., 2013) than in rodents.

Limited numbers of studies have investigated the cellular distribution of Orai1. The Orai1 location seems somewhat inconsistent depending on the cell types studied, in particular between neonatal and adult cardiomyocytes. This is probably due to the different techniques for cell fixation and permeabilization and/or the antibody specificities.

In NRVMs, a surprising perinuclear and cytosolic pattern for Orai1 has been reported (Voelkers et al., 2010). In NRVMs overexpressing Orai1, upon a passive  $\text{Ca}^{2+}$  SR depletion, Orai1 was redistributed as puncta in the SR-PM junctions, with STIM1 promoting their interaction (Zhu-Mauldin et al., 2012). Orai1 and STIM1 were also found in the form of aggregates at the peripheral membrane of cardiomyocytes derived from human pluripotent stem cells (hESC-CMs) in the absence of SR  $\text{Ca}^{2+}$  depletion (Wang et al., 2015).

In isolated adult ventricular cardiomyocytes from rats and mice, Orai1 has been located at the surface sarcolemma, with higher concentration at the intercalated disks (IDs) (Volkters et al., 2012; Bonilla et al., 2019; Bartoli et al., 2020). Furthermore, it has been shown that the STIM1/Orai1 complexes were enriched at N-cadherin-rich IDs sites over Cx43-rich sites in adult mice cardiomyocytes (Bonilla et al., 2019). We also noted occasional nuclear Orai1 labeling in isolated mice cardiomyocytes (Bartoli et al., 2020). Indeed, the location of Orai1/STIM1 complex in the nucleoplasm has been reported by other authors as well (Lee et al., 2018), suggesting Orai1 involvement in nucleoplasmic  $\text{Ca}^{2+}$  regulation. In isolated pacemaker cells, Orai1 was colocalized with the hyperpolarization-activated cyclic nucleotide-gated (HCN)4 channels at the surface membrane (Liu et al., 2015; Zhang et al., 2015).

**TABLE 1 |** Orai1 expression in the heart.

Interfering methods	Techniques	Expression level	Antibody	Species	Cell type/tissue	Proposed location	References
MO-Orai1/siRNA	qRT-PCR	mRNA/Protein	Santa Cruz Biotech. (KD validated)	Zebrafish	One-cell embryos	PM	Volkers et al., 2012
	WB			Rat	Neonatal cardiomyocytes		
				Mouse	Embryonic hearts		
	IHC				Adult hearts		
siRNA	PLA	mRNA/Protein	N/A (KD validated)		Isolated adult cardiomyocytes	Perinuclear and cytosolic	Voelkers et al., 2010
	qRT-PCR/WB/IC			Rat	Neonatal cardiomyocytes		
RNAi	RT-PCR/WB	mRNA/Protein	Millipore	Mouse	HL-1 cell line		Touchberry et al., 2011
Cardiomyocyte-specific expression dn-Orai1 <sup>R91W</sup>	qRT-PCR/WB/IC/IHC	mRNA/Protein	Sigma-Aldrich (08264) (KI and KO validated)	Mouse	Adult Hearts/Isolated adult cardiomyocytes	PM/IDs/nuclei	Bartoli et al., 2020
	qRT-PCR/WB	mRNA/Protein	Sigma-Aldrich (08264)	Rat	Isolated adult cardiomyocytes		Bartoli et al., 2019
siRNA/dn-Orai1 <sup>G98A</sup>	qRT-PCR/WB/IC/IP	mRNA/Protein	Alomone (ACC-062) (KD validated)	Human	hESC-CMs/Neonatal cardiomyocytes	Puncta along the PM/nuclei	Wang et al., 2015
Myc-tagged Orai1/Myc-tagged Orai1 <sup>S34A</sup>				Rat			
BTP2	qRT-PCR/WB/IC	mRNA/Protein	Sigma-Aldrich (08264)/ProSci (PM-5207)	Mouse	SAN tissue and cells/Atria/Ventricles tissue	PM	Liu et al., 2015
2-APB (as activator)	WB/IHC	Protein	ProSci (4281)/ProSci (4217)	Rat	Left atria tissue/Papillary muscle	Puncta	Wolkowicz et al., 2011
2-APB (as activator)	WB/IHC	Protein	ProSci (4281)/ProSci (4217)	Rat	Left ventricles tissue	Diffuse/Puncta	Wang et al., 2012
siRNA	qRT-PCR/WB/Co-IP	mRNA/Protein	Santa Cruz Biotech. (sc-68895)(KD validated)	Rat	Isolated adult cardiomyocytes		Saliba et al., 2015
siRNA	RT-PCR/WB/IC/Co-IP	mRNA/Protein	N/A (KD validated)	Human	Cardiac c-kit <sup>+</sup> progenitor cells	PM	Che et al., 2015
dnOrai1 <sup>E106A</sup> /S66/BTP2	qRT-PCR/WB/IC/Co-IP	mRNA/Protein	Sigma-Aldrich (08264)	Rat	Neonatal cardiomyocytes		Sabourin et al., 2016
Orai1 <sup>+/−</sup>	WB	Protein		Mouse	Adult heart tissue		Horton et al., 2014
	WB	Protein		Rat	Isolated adult cardiomyocytes		Dominguez-Rodriguez et al., 2015
dn-Orai1 <sup>R93W</sup>	qRT-PCR	mRNA		Mouse	Heart tissue		Maus et al., 2017
	qRT-PCR	mRNA		Chicken	Heart tissue		Li et al., 2017
BTP2/dn-Orai1 <sup>E106Q</sup>	qRT-PCR/IC	mRNA/Protein		Cat	Isolated adult cardiomyocytes	PM	Troupes et al., 2017
GSK7579A/S66	WB/IC	Protein	Alomone (ALM-25)	Mouse	Heart tissue/Isolated adult cardiomyocytes	IDs	Bonilla et al., 2019
	WB	Protein	Millipore	Mouse	Ventricle tissue		Correll et al., 2015
	IC	Protein		Mouse	Isolated adult cardiomyocytes	Nucleoplasm	Lee et al., 2018
	WB/IC	Protein	Cell signaling (#1280)	Rat	Heart tissue/Neonatal cardiomyocytes	Membrane fraction	Zhu-Mauldin et al., 2012
					Heart tissue	Puncta along the PM	Lu et al., 2017
CRACM1 <sup>+/+</sup> -LacZ	WB/Co-IP		Santa Cruz Biotech.		Heart tissue		Collins et al., 2014
	WB	Protein	ProSci (4281)	Mouse	Isolated adult cardiomyocytes		Malette et al., 2019
	WB/Co-IP	Protein	Abcam (sc-377281)	Rat	Neonatal cardiomyocytes		Vig et al., 2008
	LacZ staining	Protein		Mouse	Neonatal heart		Zheng et al., 2017
	WB	Protein	Sigma-Aldrich (08264) (KD validated)	Mouse	Heart tissue		
siRNA				Rat	Neonatal cardiomyocytes		
	qRT-PCR/WB/IHC	mRNA/Protein	Abcam	Mouse	Heart tissue/Neonatal cardiomyocytes		Dai et al., 2018

(Continued)

TABLE 1 | Continued

Interfering methods	Techniques	Expression level	Antibody	Species	Cell type/tissue	Proposed location	References
Orai1 <sup>Flx/Flx</sup> /α-MHC/Cre	qRT-PCR/IC	mRNA/Protein	N.A. (#1003) (KO validated)	Mouse	Isolated embryonic cardiomyocytes		Segin et al., 2020
	qRT-PCR	mRNA		Human	Isolated adult cardiomyocytes		Cendula et al., 2019
	IHC/IC	Protein	Alomone	Mouse	Left ventricle tissue	PM	Zhang et al., 2015
	WB	Protein	Santa Cruz Biotech (sc-68895)	Mouse	SAN/SANCs		Shiou et al., 2019
	RT-PCR/WB/Co-IP	mRNA/Protein		Human	HL-1 cell line		Zhang et al., 2013
siRNA	qRT-PCR	mRNA		Ground squirrels	Atria tissue		Nakipova et al., 2017
	Northern-blot	RNA		Mouse	Papillary muscles		Gross et al., 2007
	WB	Protein	Abcam	Rat	Heart tissue		Ji et al., 2017
	RT-PCR	mRNA		Mouse	Neonatal cardiomyocytes		Takahashi et al., 2007
	PCR-based micro-array/WB/PLA	Protein	Novus Biologicals (KD validated)	Rat	Heart tissue		Dominguez-Rodriguez et al., 2018
	IHC	Protein	mAb266.1/ProSci (4281)	Rat	Neonatal cardiomyocytes/Heart tissue		Guzman et al., 2014
	WB	Protein	Sigma-Aldrich (08264)	Human	Heart tissue		Sabourin et al., 2018
				Rat	Left and right ventricles tissues		

WB, Western-blot; IC, immunocytochemistry; IHC, immunohistochemistry; PLA, proximity ligation assay; IP, immunoprecipitation; Dn, dominant negative; hESC-CMs, human embryonic stem cell-derived cardiomyocytes; PM, plasma membrane; IDs, intercalated disks.

Orai1 Function

Overall, most of the reports have detected Orai1 expression in cardiomyocytes. However, the physiological role of the Orai1-mediated Ca<sup>2+</sup> entry into the heart remains somewhat unclear and enigmatic. As for other excitable cells, it has long been considered that SOCE contribution to cardiac Ca<sup>2+</sup> homeostasis is rather limited or non-existent, taking into account that Ca<sup>2+</sup> influx during each beat through voltage-dependent Ca<sup>2+</sup> channels is large enough to maintain cardiac excitation-contraction coupling (ECC). However, even a modest change in Ca<sup>2+</sup> signaling can progressively alter heart function if sustained. For a prolonged period, a source of Ca<sup>2+</sup> through SOCs can therefore potentially affect the heart.

The Orai1 knockdown (KD) in NRVMs did not affect the diastolic Ca<sup>2+</sup> level or the SR Ca<sup>2+</sup> load (Voelkers et al., 2010). However, the spontaneous Ca<sup>2+</sup> transients frequency was reduced, as well as the NRVMs size. This was associated with the reduced activity of Ca<sup>2+</sup>-sensing proteins, such as calcineurin (CaN), calmodulin-dependant kinase II (CaMKII), or extracellular signal-regulated kinases (ERK1/2), signaling pathways involved in cardiac hypertrophy, and HF. Conversely, the reduction of SOCE in the HL-1 cell line with Orai1 KD decreased the diastolic Ca<sup>2+</sup> level and SR Ca<sup>2+</sup> content, suggesting a role of Orai1 in the SR Ca<sup>2+</sup> load maintenance (Touchberry et al., 2011). More recently, we have demonstrated that the mineralocorticoid receptor pathway promotes an Orai1-dependent SOCE, which regulated the diastolic Ca<sup>2+</sup> level *via* the serum and glucocorticoid-regulated kinase 1 (SGK1) in NRVMs (Sabourin et al., 2016). In hESC-CMs, the functional inhibition of Orai1 using overexpression of a dominant negative Orai1<sup>G98A</sup> mutant or the KD with shRNA against Orai1 decreased the cell size and altered the sarcomere organization (Wang et al., 2015). In human cardiac c-kit<sup>+</sup> progenitor cells, Orai1-mediated SOCE regulated cell cycling and migration *via* cell cycle kinase cyclin D1 and cyclin E and/or phosphorylation of Akt (Che et al., 2015).

The role of Orai1 in maintaining cytosolic and intrareticular Ca<sup>2+</sup> levels during development therefore raises the question of its potential involvement in the adult heart.

A recent study, in adult mouse cardiomyocytes, has identified highly localized SOCE events preferentially at the IDs, where STIM1-Orai1 complex formation occurred in close proximity to intracellular mechanical junctions (Bonilla et al., 2019). This microdomain segregation might participate in arrhythmogenesis without interfering in the ECC process. This echoed that, in adult feline cardiomyocytes, the BTP2, a classic Orai1 inhibitor, did not modify the action potential duration (APD), neither Ca<sup>2+</sup> transients nor cell contraction (Troupes et al., 2017).

*In vivo*, antisense oligonucleotide strategy to knockdown Orai1 in zebrafish leads to spontaneous ventricular systolic dysfunction and bradycardia, reduced blood circulation, blood congestion without affecting cardiogenesis and cardiomyocyte differentiation (Volkers et al., 2012). This was associated with ultrastructure alterations of sarcomeres, leading to reduced expression and impaired z-disc localization of calsarcin involved in the activation of calcineurin/nuclear factor of activated T cell (CaN/NFAT) hypertrophic pathway. In addition, inducible RNAi

to specifically suppress Orai1 expression in the *Drosophila* heart resulted in significant delays in post-embryonic development, premature death in adults, and impaired cardiac function due to myofibril disorganization consistent with dilated cardiomyopathy (Petersen et al., 2020).

In contrast, heterozygous global Orai1-deficient mice did not present alteration of heart structure and function (Horton et al., 2014). Likewise, we have reported that cardiomyocyte-specific dn-Orai1<sup>R91W</sup> transgenic mice displayed normal cardiac electromechanical function and ECC despite reduced Orai1-dependent SOCE (Bartoli et al., 2020), as recently confirmed in cardiomyocyte-specific and temporally inducible Orai1 knockout (KO) mouse line (Segin et al., 2020). Although in the later study, this was associated with reduced body weight and a downregulation of Orai3, STIM2, and store-operated Ca<sup>2+</sup> entry-associated regulatory factor (SARAF) transcript expression, those results suggested that Orai1 is not instrumental for the ECC and cardiac function at rest. In addition, it has been shown that dn-Orai1<sup>R93W</sup> mice display abnormal amounts of lipid droplets in the heart, providing a potential role in lipid metabolism (Maus et al., 2017).

In pacemaker cells from mouse, SOCE inhibition by BTP2 reduced the frequency and the amplitude of spontaneous Ca<sup>2+</sup> transients and the SR Ca<sup>2+</sup> content (Liu et al., 2015). It has been speculated that STIM1/Orai1-dependent SOCE were activated by the rhythmic release of Ca<sup>2+</sup> from the SR, which activates Orai1 to refill the SR stores. In this way, STIM1 and Orai1 ensured the fidelity of SAN Ca<sup>2+</sup> dynamics and the integrity of the cardiac pacemaker (Zhang et al., 2015).

Two studies have linked the non-selective Orai1 activator, 2-aminoethoxydiphenyl borate (2-APB at 20  $\mu$ M) to the initiation of atrial and ventricular arrhythmias (Wolkowicz et al., 2011; Wang et al., 2012). Indeed, 2-APB induced sporadic or tachycardial ectopic activities, as well as automatic activity in the superfused left rat atrium and left rat ventricular papillary muscles. The common non-specific SOC inhibitor, the SKF-96365, suppressed those arrhythmic behaviors (Wolkowicz et al., 2011). In addition, on a model of isolated rat hearts perfused by the Langendorff method, 2-APB also promoted ventricular fibrillations, which were prevented by SKF-96365. These studies suggest that Orai1 may be an important regulator of the electrical stability in rat hearts (Wang et al., 2012).

Taken together, it is generally accepted that SOCE carried by Orai1 channels regulates the SR Ca<sup>2+</sup> content, the diastolic Ca<sup>2+</sup>, as well as cell growth during cardiac development. However, in adulthood, additional studies are clearly necessary to clarify the controversy over the role of SOCE machinery in the heart.

## PATHOPHYSIOLOGICAL ROLE OF ORAI1 IN CARDIAC HYPERTROPHY AND HEART FAILURE

Whether Orai1 role in heart physiology is still elusive, its involvement in pathophysiological situation has been more documented.

As terminally differentiated cells, adult cardiomyocytes are largely incapable of cell proliferation. Hypertrophic growth from different pathologic stimuli, including hypertension, coronary insufficiency, or valvular defects, is the primary adaptive mechanism by which the heart is able to preserve pump function and maintain adequate cardiovascular support. On the other hand, sustained hypertrophy can lead to altering myocardial architecture and to cardiac dysfunction, dilated cardiomyopathy, HF, and sudden death. The dysregulation of cardiac Ca<sup>2+</sup> homeostasis is an important and proximal player underlying the pathogenesis of heart diseases. As the main regulator of the cardiac ECC, mishandling of Ca<sup>2+</sup> is directly related to the mechanical dysfunction and certain arrhythmias associated with hypertrophy and HF. Moreover, the Ca<sup>2+</sup>-dependent intracellular signaling pathways activation, notably CaN/NFAT, CaMKII, and ERK promotes pro-hypertrophic gene expression, leading to pathological growth, cardiac remodeling, and dysfunction (Wilkins et al., 2004; Mattiazzi et al., 2015; Gallo et al., 2019). However, the sources of Ca<sup>2+</sup> responsible for the activation of these Ca<sup>2+</sup>-dependent signaling circuits are still elusive. Nonetheless, in the last 20 years, convincing evidences have proposed a key role for Orai1-mediated SOCE in such processes.

## Orai1 Expression During Hypertrophic Process

Several studies have found that the expression of Orai1 was enhanced in angiotensin II (AngII) or phenylephrine (PE)-induced hypertrophy of NRVMs or hESC-CMs (Wang et al., 2015; Ji et al., 2017; Zheng et al., 2017; Dai et al., 2018). Increased Orai1 expression was also observed after ischemia/reperfusion in NRVMs (Dominguez-Rodriguez et al., 2018). Several *in vivo* studies also found Orai1 mRNA and protein expression upregulation in mouse cardiac hypertrophic model induced by pressure and volume overload, such as transverse aortic constriction, abdominal aortic banding, chronic AngII infusion, or myocardial infarction (Volkers et al., 2012; Dai et al., 2018; Bartoli et al., 2020; Segin et al., 2020). In right ventricular hypertrophy and dysfunction secondary to pulmonary hypertension, we also observed an increased Orai1 expression (Sabourin et al., 2018). Surprisingly, Orai1 expression was decreased by 30% in the end-stage human failing left myocardium (Cendula et al., 2019). Interestingly, this decrease was gender specific, present only in men, suggesting that Orai1 expression might represent a possible mechanism of cardioprotective effects of estrogens (Cendula et al., 2019). By contrast, the fibroblasts from end-stage human left failing patients have increased collagen secretion capacity, which was related to increased SOCE and enhanced expression of Orai1 (Ross et al., 2017).

## *In vitro* Functional Studies

In NRVMs, non-selective inhibitors of SOC, such as glucosamine or SKF-96365, prevented the increase of NFAT nuclear translocation and cellular hypertrophy after a 48-h treatment with hypertrophic stressors (AngII or PE)

(Hunton et al., 2002). Furthermore, in the same model, SOCE inhibition by R02959 or by Orai1 KD prevented pro-hypertrophic signaling such as the nuclear localization of NFAT, the Gq-protein conveyed activation of the CaMKII/ERK1/2 signaling pathway, and CaN activation (Voelkers et al., 2010; Zheng et al., 2017). In PE-induced hypertrophy of NRVMs, in one hand, CaMKII $\delta$  inhibition by siRNA or by KN93 normalized the Orai1 protein level, as well as the hypertrophic marker. On the other hand, BTP2 treatment attenuated the hypertrophic growth and the increased CaMKII $\delta$  expression (Ji et al., 2017). The CaMKII $\delta$  upregulation might thus contribute to the PE-induced cellular hypertrophy through the overactivation of SOCE and/or conversely the enhanced SOCE induced by PE led to overexpression and activation of CaMKII $\delta$  in the cardiomyocytes.

In a mouse model and cultured cardiomyocyte model treated with AngII or PE, gatrodine, a polyphenol with anti-inflammatory properties used in traditional Chinese medicine, is protective against the development of cellular and cardiac hypertrophy by attenuating the SOCE and reducing the expression of STIM1 and Orai1 (Zheng et al., 2017).

In hECS-CMs, Orai1 inhibition by the use of Orai1-siRNAs or a dominant-negative construct Orai1<sup>G98A</sup> or by nitric oxide (NO) *via* activation of PKG prevented PE-induced cellular hypertrophy (Wang et al., 2015). Of note, the anti-hypertrophic effects of NO, cGMP, and PKG were lost when Orai1 was mutated on serine 34. Indeed, Ser34 can be phosphorylated by PKG, which decreases Orai1-mediated SOCE and therefore inhibits the development of cellular hypertrophy. These results provided novel mechanistic insights into the action of cGMP-PKG-related anti-hypertrophic agents, such as Sildenafil. More recently, AngII-induced cellular hypertrophy was blunted in embryonic cardiomyocytes from cardiomyocyte-specific Orai1-KO mice (Segin et al., 2020).

Of note, the pharmacology of Orai1 channels is poor and lack of specificity. Indeed, 2-APB was originally described as an inhibitor of the IP<sub>3</sub>R. BTP2 was known to inhibit TRPC channels and activate TRPM4. SKF-96365 has been shown to block voltage-gated Ca<sup>2+</sup> channels, K<sup>+</sup> channels, and TRP family members (Prakriya and Lewis, 2015; Bird and Putney, 2018). To avoid misinterpretation of the pathophysiological role of Orai1, it is thus essential to use KD or KO strategies in addition to the pharmacological tools.

All of these *in vitro* studies demonstrate the involvement of Orai1-mediated SOCE in hypertrophic development induced by neurohormonal stimulation. The neurohormonal-induced hypertrophy pathways imply an increase in the activity of pro-hypertrophic signaling such as CaN/NFAT, CaMKII, and ERK1/2 *via* enhanced Orai1 expression and activity.

## In vivo Functional Studies

In pressure overload-induced cardiac adaptive hypertrophy in mice, overexpression of SARAF in the heart prevented Orai1 upregulation and attenuated the cardiac hypertrophy. In addition, overexpression of SARAF also attenuated AngII-induced upregulation of Orai1 and hypertrophy of cultured cardiomyocytes (Dai et al., 2018). In similar pathological model in cats, BTP2 did not prevent the Ca<sup>2+</sup> alterations

observed in enlarged adult feline cardiomyocytes, namely the decrease in the amplitude and the prolongation of Ca<sup>2+</sup> transients and the prolongation of contraction. However, it prevented the shortening of sarcomeres in diastole; the increase in the APD as well as the Ca<sup>2+</sup> sparks frequency (Troupes et al., 2017). Overexpression of STIM1 in cultured adult feline ventricular myocytes also increased the SR Ca<sup>2+</sup> load, the diastolic spark rate, and prolonged APD and activated CaMKII. STIM1 effects were eliminated by either BTP2 or by coexpression of a dominant negative Orai1<sup>E106Q</sup> mutant (Troupes et al., 2017). These results supported the idea that, during hypertrophic stress, STIM1/Orai1 produced an exacerbated Ca<sup>2+</sup> influx that can prolong the APD and load sufficiently the SR for each cycle of contraction. However, in the long term, it can induce Ca<sup>2+</sup> leak from the SR through an alteration of the CaMKII-dependent phosphorylation state of RyR and likely contributed to the altered electromechanical properties of the hypertrophied heart (Troupes et al., 2017).

Long-term administration of pyridostigmine, an acetylcholinesterase inhibitor, alleviated pressure overload-induced cardiac hypertrophy as well as associated fibrosis (Lu et al., 2017). This beneficial effect was related to the inhibition of the CaN/NFAT3/GATA4 pathway and suppression of the interaction of Orai1/STIM1.

We also found that after chronic pressure overload, cardiomyocyte-specific dn-Orai1<sup>R91W</sup> mice (C-dnO1), or *in vivo* JPIII-treated (a new selective Orai1 inhibitor) mice were protected from left ventricular systolic dysfunction and from interstitial fibrosis deposition, even if increased cardiac hypertrophy was observed. This was correlated with a protection from pressure overload-induced cellular Ca<sup>2+</sup> signaling alterations (increased SOCE, decreased [Ca<sup>2+</sup>]<sub>i</sub> transients amplitude and decay rate, lower SR Ca<sup>2+</sup> load, and depressed cellular contractility), SERCA2a downregulation, and Pyk2/MEK/ERK overactivation (Bartoli et al., 2020). We observed an increased CRAC-like current, associated with longer APD, higher and faster [Ca<sup>2+</sup>]<sub>i</sub> transients, and increased SR Ca<sup>2+</sup> content and cell contractility in the right ventricular hypertrophy secondary to pulmonary hypertension (Sabourin et al., 2018). Pharmacological inhibition of Orai1 channels by BTP2 in hypertrophied RV cardiomyocytes normalized the [Ca<sup>2+</sup>]<sub>i</sub> transients amplitude, the SR Ca<sup>2+</sup> content and cell contractility to control levels (Sabourin et al., 2018). These new findings demonstrated that the Orai1-dependent Ca<sup>2+</sup> current participated in cardiac Ca<sup>2+</sup> remodeling in the right ventricular hypertrophy secondary to pulmonary hypertension.

All these studies seem contradictory with the results obtained with global heterozygous Orai1<sup>+/-</sup> (Horton et al., 2014). These mice subjected to pressure overload have reduced survival and develop more rapid dilated cardiomyopathy with greater loss of function than control littermates. The loss of Orai1 thus accelerated the development of dilated cardiomyopathy and HF. The cardiac hypertrophy level was similar, however, Orai1<sup>+/-</sup> mice were no longer able to compensate the chronic pressure overload, resulting in the development of a more severe systolic dysfunction. This can

be explained by significant apoptosis without differences in hypertrophic and fibrotic markers, although this was not clearly demonstrated (Horton et al., 2014). Similarly, cardiomyocyte-specific deletion of Orai1 in adult mice (Orai1CM-KO) did not protect them from AngII-induced cardiac dysfunction (Segin et al., 2020). Despite disparity in echocardiographic data, Orai1CM-KO mice presented a slight decrease in systolic function with an accumulated fibrosis compared with control mice suggesting a transition to a maladaptive hypertrophy.

Despite discrepancies between all the *in vitro* and *in vivo* studies certainly due to the different biomechanical stresses and the cardiac phenotype induced, all the published results so far support the idea that Orai1 is a critical mediator for  $\text{Ca}^{2+}$  entry and cardiac remodeling.

## PHARMACOLOGICAL OPPORTUNITIES OF ORAI1 IN CARDIAC DISEASES

HF, the end stage of almost all heart diseases, is a major health problem in the world today, affecting over 26 million persons worldwide with increased prevalence. Current treatment is mainly correlated with medications, diet, interventions, devices, and heart transplants (Seferovic et al., 2019). Whereas the outcome of HF has improved significantly in the last quarter century, the mortality still remains high, with nearly half of the patients with HF dying within 5 years after diagnosis.

Current pharmacological therapies for HF with reduced ejection fraction are largely either repurposed anti-hypertensives that blunt overactivation of the neurohormonal system or diuretics that decrease congestion. They do not address the decrease in cardiac systolic function, a central factor in HF that results in reduction in cardiac output and reserve. Numerous attempts have been made to develop and test positive cardiac inotropes that improve cardiac hemodynamics, but adverse effects inherent to their mechanism of benefit limit their uses. Intravenous positive inotropic drugs including phosphodiesterase (PDE)-3 inhibitors (e.g., milrinone),  $\beta$ -adrenergic receptor agonists (e.g., dobutamine),  $\text{Ca}^{2+}$ -sensitizing agents (e.g., levosimendan), and digoxin are indicated for acute systolic HF patients with decreased cardiac contractility and evidence of end-organ hypoperfusion (Tariq and Aronow, 2015). However, the use of positive inotropic drugs has been plagued by serious concerns regarding increased morbidity and mortality. Problems include increased atrial or ventricular arrhythmias, induced myocardial ischemia, and in some cases, arterial hypotension (Ahmad et al., 2019). Moreover, long-term use of conventional inotropic agents has been associated with no improvement in overall mortality (Ahmad et al., 2019). There is a possibility that the adverse effects of inotropic agents could promote pump failure as well as arrhythmias *via* dysfunctional  $\text{Ca}^{2+}$  cycling.

This uncomfortable dilemma has led to expand new and far more powerful methods of preventing and treating HF. Currently, HF drug treatment research focuses on interrupting intracellular signaling pathways that are injurious to

cardiovascular tissue and on stimulating signaling pathways that protect cardiovascular tissues.

There is an arsenal of pharmacological selective inhibitors that modulate Orai1 function, and several have now advanced into human clinical trials for psoriasis, pancreatitis, asthma, or Hodgkins lymphoma (Stauderman, 2018). Consequently, there has been considerable interest in identifying Orai1 modulators, excluding immune diseases, as therapeutics for more conditions.

Over the past few years, as described herein, STIM1/Orai1-mediated SOCE has emerged as a promising target to treat HF. Here arises a question of which STIM1 and/or Orai1 should be targeted since both molecules operate in the same pathway. From a safety or toxicological perspective, Orai1 may be a more attractive target than STIM1. Firstly, compared with STIM1, Orai1 appears to be more restricted in its function of mediating SOCE. STIM1 appears to be involved in the activity of other proteins than Orai1, such as Cav1.2 (Wang et al., 2010; Dionisio et al., 2015) and TRPC channels (Yuan et al., 2007; Bodnar et al., 2017). STIM1 is also connected to the universal cAMP/PKA signaling pathway by regulating plasma membrane adenylate cyclases isoforms (Lefkimmatis et al., 2009; Spirli et al., 2017; Motiani et al., 2018). As a result, drugs targeting STIM1 might lead to a poor benefit-to-risk ratio. Secondly, as exemplified in channelopathy caused by GOF mutations in Orai1 resulting in constitutive or increased SOCE independent of STIM1 (Lacruz and Feske, 2015), therapeutic targeting of STIM1 might not be as efficient, taking into account that reduction of STIM1 might accelerate transition to HF (Benard et al., 2016). Taken together, pharmacological targeting on Orai1 may produce less side effects.

According to the study conducted in our lab (Bartoli et al., 2020), under physiological conditions, cardiomyocyte-specific functional inhibition of Orai1 channels in C-dnO1 mice or systemic *in vivo* pharmacological Orai1 small-molecule inhibition by JPIII have little impact on  $\text{Ca}^{2+}$  homeostasis related to ECC and left ventricular systolic performance. After chronic pressure overload, JPIII markedly improves the left ventricular systolic function and  $\text{Ca}^{2+}$  handling by preventing the  $\text{Ca}^{2+}$  cycling mishandling, SERCA2a downregulation and fibrosis, without causing adverse effect. Our findings suggest that Orai1 inhibition has a potential favorable hemodynamic value to protect the heart from maladaptive hypertrophy and might represent a new inotropic support to help to relieve systolic dysfunction. This plausible therapeutic intervention need to be extended to other pathological models (Benitah et al., 2020). In addition, since Orai1 regulated cellular function in many tissues, concerns might raise about the safety and/or toxicity of Orai1 inhibitor due to potential chronic immunosuppression. In humans, the lack of function of Orai1 is dominated clinically by immunodeficiency with mostly normal overall T, B, and NK cell counts. In pilot studies, we have demonstrated that systemic chronic JPIII infusion for 28 days in mice did not induce any adverse effects, did not compromise the immune system, and did not promote susceptibility to develop infections (Bartoli et al., 2020). Currently, no adverse effect has been reported in clinical trials with selective Orai1 inhibitors such as AnCoA4, CM2489, CM4620, and Auxora (Stauderman, 2018; Miller et al., 2020). Nonetheless, given the

important functional role of Orai1 in the immune system, it is important to properly understand the risks of potential adverse effects for a therapeutic approach moving forward.

In conclusion, although the Orai1 function in adult cardiac physiology remains elusive, converged experimental results pointed out a detrimental effect of Orai1 upregulation in hypertrophy and HF, including fibrosis, ventricular contractility, and pro-hypertrophic  $\text{Ca}^{2+}$ -responsive signaling pathways. This pathological importance of Orai1 echoed its role during the embryonic and neonatal phase of cardiac development since hypertrophic cardiac remodeling is characterized by reactivation of the fetal gene program. Hence, Orai1-mediated SOCE may be a novel therapeutic target to consider in heart disease.

## REFERENCES

- Ahmad, T., Miller, P. E., McCullough, M., Desai, N. R., Riello, R., Psotka, M., et al. (2019). Why has positive inotropy failed in chronic heart failure? Lessons from prior inotrope trials. *Eur. J. Heart Fail.* 21, 1064–1078. doi: 10.1002/ehf.1557
- Bartoli, F., Bailey, M. A., Rode, B., Mateo, P., Antigny, F., Bedouet, K., et al. (2020). Orai1 channel inhibition preserves left ventricular systolic function and normal  $\text{Ca}^{2+}$  handling after pressure overload. *Circulation* 141, 199–216. doi: 10.1161/circulationaha.118.038891
- Bartoli, F., Moradi Bachiller, S., Antigny, F., Bedouet, K., Gerbaud, P., Sabourin, J., et al. (2019). Specific upregulation of TRPC1 and TRPC5 channels by mineralocorticoid pathway in adult rat ventricular cardiomyocytes. *Cells* 9:47. doi: 10.3390/cells9010047
- Benard, L., Oh, J. G., Cacheux, M., Lee, A., Nonnenmacher, M., Matasic, D. S., et al. (2016). Cardiac Stim1 silencing impairs adaptive hypertrophy and promotes heart failure through inactivation of mTORC2/Akt signaling. *Circulation* 133, 1458–1471.
- Benitah, J. P., Beech, D. J., and Sabourin, J. (2020). Response by Benitah et al to letter regarding article, “Orai1 channel inhibition preserves left ventricular systolic function and normal  $\text{Ca}^{2+}$  handling after Pressure Overload”. *Circulation* 141, e839–e840.
- Bird, G. S., and Putney, J. W., Jr (2018). “Pharmacology of Store-Operated Calcium Entry Channels,” in *Calcium Entry Channels in Non-Excitable Cells*, eds J. A. Kozak, and J. W., Jr Putney (Boca Raton (FL): CRC Press), 311–324. doi: 10.1201/9781315152592-16
- Bodnar, D., Chung, W. Y., Yang, D., Hong, J. H., Jha, A., and Muallem, S. (2017). STIM-TRP pathways and microdomain organization:  $\text{Ca}^{2+}$  influx channels: the Orai-STIM1-TRPC complexes. *Adv. Exp. Med. Biol.* 993, 139–157. doi: 10.1007/978-3-319-57732-6\_8
- Bonilla, I. M., Belevych, A. E., Baine, S., Stepanov, A., Mezache, L., Bodnar, T., et al. (2019). Enhancement of Cardiac Store Operated Calcium Entry (SOCE) within Novel Intercalated disk microdomains in arrhythmic disease. *Sci. Rep.* 9:10179.
- Cendula, R., Dragun, M., Gazova, A., Kyselovic, J., Hulman, M., and Matus, M. (2019). Changes in STIM isoforms expression and gender-specific alterations in Orai expression in human heart failure. *Physiol. Res.* 68, S165–S172.
- Che, H., Li, G., Sun, H. Y., Xiao, G. S., Wang, Y., and Li, G. R. (2015). Roles of store-operated  $\text{Ca}^{2+}$  channels in regulating cell cycling and migration of human cardiac c-kit+ progenitor cells. *Am. J. Physiol. Heart Circ. Physiol.* 309, H1772–H1781.
- Collins, H. E., He, L., Zou, L., Qu, J., Zhou, L., Litovsky, S. H., et al. (2014). Stromal interaction molecule 1 is essential for normal cardiac homeostasis through modulation of ER and mitochondrial function. *Am. J. Physiol. Heart Circ. Physiol.* 306, H1231–H1239.
- Correll, R. N., Goonasekera, S. A., Burr, A. R., Accornero, F., Zhang, H., Makarewich, C. A., et al. (2015). STIM1 elevation in the heart results in aberrant  $\text{Ca}^{2+}$  handling and cardiomyopathy. *J. Mol. Cell Cardiol.* 87, 38–47. doi: 10.1016/j.yjmcc.2015.07.032
- Dai, F., Zhang, Y., Wang, Q., Li, D., Yang, Y., Ma, S., et al. (2018). Overexpression of SARAF Ameliorates Pressure overload-induced cardiac hypertrophy through suppressing STIM1-Orai1 in mice. *Cell Physiol. Biochem.* 47, 817–826. doi: 10.1159/000490036
- Dionisio, N., Smani, T., Woodard, G. E., Castellano, A., Salido, G. M., and Rosado, J. A. (2015). Homer proteins mediate the interaction between STIM1 and Cav1.2 channels. *Biochim Biophys Acta* 1853, 1145–1153. doi: 10.1016/j.bbamer.2015.02.014
- Dominguez-Rodriguez, A., Diaz, I., Hmadcha, A., Castellano, A., Rosado, J. A., Benitah, J. P., et al. (2018). Urocortin-2 prevents dysregulation of  $\text{Ca}^{2+}$  homeostasis and improves early cardiac remodeling after ischemia and reperfusion. *Front. Physiol.* 9:813. doi: 10.3389/fphys.2018.00813
- Dominguez-Rodriguez, A., Ruiz-Hurtado, G., Sabourin, J., Gomez, A. M., Alvarez, J. L., and Benitah, J. P. (2015). Proarrhythmic effect of sustained EPAC activation on TRPC3/4 in rat ventricular cardiomyocytes. *J. Mol. Cell Cardiol.* 87, 74–78. doi: 10.1016/j.yjmcc.2015.07.002
- Feske, S. (2019). CRAC channels and disease - From human CRAC channelopathies and animal models to novel drugs. *Cell Calcium* 80, 112–116. doi: 10.1016/j.ceca.2019.03.004
- Feske, S., Gwack, Y., Prakriya, M., Srikanth, S., Puppel, S. H., Tanasa, B., et al. (2006). A mutation in Orai1 causes immune deficiency by abrogating CRAC channel function. *Nature* 441, 179–185.
- Gallo, S., Vitacolonna, A., Bonzano, A., Comoglio, P., and Crepaldi, T. (2019). ERK: a key player in the pathophysiology of cardiac hypertrophy. *Int. J. Mol. Sci.* 20:2163.
- Gross, S. A., Wissenbach, U., Philipp, S. E., Freichel, M., Cavalie, A., and Flockerzi, V. (2007). Murine ORAI2 splice variants form functional  $\text{Ca}^{2+}$  release-activated  $\text{Ca}^{2+}$  (CRAC) channels. *J. Biol. Chem.* 282, 19375–19384. doi: 10.1074/jbc.m701962200
- Guzman, R., Valente, E. G., Pretorius, J., Pacheco, E., Qi, M., Bennett, B. D., et al. (2014). Expression of ORAI1, a plasma membrane resident subunit of the CRAC channel, in rodent and non-rodent species. *J. Histochem. Cytochem.* 62, 864–878. doi: 10.1369/0022155414554926
- Horton, J. S., Buckley, C. L., Alvarez, E. M., Schorlemmer, A., and Stokes, A. J. (2014). The calcium release-activated calcium channel Orai1 represents a crucial component in hypertrophic compensation and the development of dilated cardiomyopathy. *Channels* 8, 35–48. doi: 10.4161/chan.26581
- Hoth, M., and Penner, R. (1992). Depletion of intracellular calcium stores activates a calcium current in mast cells. *Nature* 355, 353–356. doi: 10.1038/355353a0
- Hou, X., Pedi, L., Diver, M. M., and Long, S. B. (2012). Crystal structure of the calcium release-activated calcium channel Orai. *Science* 338, 1308–1313. doi: 10.1126/science.1228757
- Hunton, D. L., Lucchesi, P. A., Pang, Y., Cheng, X., Dell'Italia, L. J., and Marchase, R. B. (2002). Capacitative calcium entry contributes to nuclear factor of activated T-cells nuclear translocation and hypertrophy in cardiomyocytes. *J. Biol. Chem.* 277, 14266–14273. doi: 10.1074/jbc.m107167200
- Hunton, D. L., Zou, L., Pang, Y., and Marchase, R. B. (2004). Adult rat cardiomyocytes exhibit capacitative calcium entry. *Am. J. Physiol. Heart Circ. Physiol.* 286, H1124–H1132.

## AUTHOR CONTRIBUTIONS

RL drafted the manuscript under the supervision of J-PB and JS. J-PB, JS, and A-MG edited the manuscript. All authors contributed to the article and approved the submitted version.

## FUNDING

This work was supported by the research grants from INSERM, National Funding Agency for Research (ANR) (ANR-15-CE14 and ANR-19-CE14-0031-1). RL was a recipient of the CSC (Chinese Science Council) doctoral fellowship.

- Ji, Y., Guo, X., Zhang, Z., Huang, Z., Zhu, J., Chen, Q. H., et al. (2017). CaMKII $\delta$  mediates phenylephrine induced cardiomyocyte hypertrophy through store-operated Ca(2+) entry. *Cardiovasc. Pathol.* 27, 9–17. doi: 10.1016/j.carpath.2016.11.004
- Lacruz, R. S., and Feske, S. (2015). Diseases caused by mutations in ORAI1 and STIM1. *Ann. N.Y. Acad. Sci.* 1356, 45–79.
- Lee, S. H., Hadipour-Lakmeisari, S., Miyake, T., and Gramolini, A. O. (2018). Three-dimensional imaging reveals endo(sarco)plasmic reticulum-containing invaginations within the nucleoplasm of muscle. *Am. J. Physiol. Cell Physiol.* 314, C257–C267.
- Lefkimmiatis, K., Srikanthan, M., Maiellaro, I., Moyer, M. P., Curci, S., and Hofer, A. M. (2009). Store-operated cyclic AMP signalling mediated by STIM1. *Nat. Cell Biol.* 11, 433–442. doi: 10.1038/ncb1850
- Li, S., Wang, Y., Zhao, H., He, Y., Li, J., Jiang, G., et al. (2017). NF-kappaB-mediated inflammation correlates with calcium overload under arsenic trioxide-induced myocardial damage in Gallus gallus. *Chemosphere* 185, 618–627. doi: 10.1016/j.chemosphere.2017.07.055
- Liu, J., Xin, L., Benson, V. L., Allen, D. G., and Ju, Y. K. (2015). Store-operated calcium entry and the localization of STIM1 and Orai1 proteins in isolated mouse sinoatrial node cells. *Front. Physiol.* 6:69. doi: 10.3389/fphys.2015.00069
- Lu, Y., Zhao, M., Liu, J. J., He, X., Yu, X. J., Liu, L. Z., et al. (2017). Long-term administration of pyridostigmine attenuates pressure overload-induced cardiac hypertrophy by inhibiting calcineurin signalling. *J. Cell. Mol. Med.* 21, 2106–2116. doi: 10.1111/jcmm.13133
- Ma, G., Wei, M., He, L., Liu, C., Wu, B., Zhang, S. L., et al. (2015). Inside-out Ca(2+) signalling prompted by STIM1 conformational switch. *Nat. Commun.* 6:7826.
- Malette, J., Degrandmaison, J., Giguere, H., Berthiaume, J., Frappier, M., and Parent, J. L. (2019). MURC/CAVIN-4 facilitates store-operated calcium entry in neonatal cardiomyocytes. *Biochim. Biophys. Acta Mol. Cell Res.* 1866, 1249–1259. doi: 10.1016/j.bbamer.2019.03.017
- Maruyama, Y., Ogura, T., Mio, K., Kato, K., Kaneko, T., Kiyonaka, S., et al. (2009). Tetrameric Orai1 is a teardrop-shaped molecule with a long, tapered cytoplasmic domain. *J. Biol. Chem.* 284, 13676–13685. doi: 10.1074/jbc.M900812200
- Mattiazzi, A., Bassani, R. A., Escobar, A. L., Palomeque, J., Valverde, C. A., Vila Petroff, M., et al. (2015). Chasing cardiac physiology and pathology down the CaMKII cascade. *Am. J. Physiol. Heart Circ. Physiol.* 308, H1177–H1191.
- Maus, M., Cuk, M., Patel, B., Lian, J., Ouimet, M., Kaufmann, U., et al. (2017). Store-Operated Ca(2+) Entry Controls Induction of Lipolysis and the Transcriptional Reprogramming to Lipid Metabolism. *Cell Metab.* 25, 698–712. doi: 10.1016/j.cmet.2016.12.021
- Miller, J., Bruen, C., Schnaus, M., Zhang, J., Ali, S., Lind, A., et al. (2020). Auxora versus standard of care for the treatment of severe or critical COVID-19 pneumonia: results from a randomized controlled trial. *Crit. Care* 24:502.
- Motiani, R. K., Tanwar, J., Raja, D. A., Vashisht, A., Khanna, S., Sharma, S., et al. (2018). STIM1 activation of adenylyl cyclase 6 connects Ca(2+) and cAMP signaling during melanogenesis. *EMBO J.* 37:e97597.
- Nakipova, O. V., Averin, A. S., Evdokimovskii, E. V., Pimenov, O. Y., Kosarski, L., Anufriev, A., et al. (2017). Store-operated Ca2+ entry supports contractile function in hearts of hibernators. *PLoS One* 12:e0177469. doi: 10.1371/journal.pone.0177469
- Penna, A., Demuro, A., Yeromin, A. V., Zhang, S. L., Safrina, O., Parker, I., et al. (2008). The CRAC channel consists of a tetramer formed by Stim-induced dimerization of Orai dimers. *Nature* 456, 116–120. doi: 10.1038/nature07338
- Petersen, C. E., Wolf, M. J., and Smyth, J. T. (2020). Suppression of store-operated calcium entry causes dilated cardiomyopathy of the Drosophila heart. *Biol. Open* 9:bio049999. doi: 10.1242/bio.049999
- Prakriya, M., and Lewis, R. S. (2015). Store-operated calcium channels. *Physiol. Rev.* 95, 1383–1436.
- Putney, J. W. Jr. (1986). Identification of cellular activation mechanisms associated with salivary secretion. *Annu. Rev. Physiol.* 48, 75–88. doi: 10.1146/annurev.ph.48.030186.000451
- Putney, J. W. Jr. (1990). Capacitative calcium entry revisited. *Cell Calc.* 11, 611–624. doi: 10.1016/0143-4160(90)90016-n
- Rosado, J. A., Diez, R., Smani, T., and Jardin, I. (2015). STIM and orai1 variants in store-operated calcium entry. *Front Pharmacol* 6:325. doi: 10.3389/fphar.2015.00325
- Ross, G. R., Bajwa, T. Jr., Edwards, S., Emelyanova, L., Rizvi, F., Holmuhamedov, E. L., (2017). Jahangir, enhanced store-operated Ca(2+) influx and ORAI1 expression in ventricular fibroblasts from human failing heart. *Biol. Open* 6, 326–332. doi: 10.1242/bio.022632
- Sabourin, J., Bartoli, F., Antigny, F., Gomez, A. M., and Benitah, J. P. (2016). Transient Receptor Potential Canonical (TRPC)/Orai1-dependent Store-operated Ca2+ Channels: new targets of aldosterone in cardiomyocytes. *J. Biol. Chem.* 291, 13394–13409. doi: 10.1074/jbc.M115.693911
- Sabourin, J., Boet, A., Lambert, M., Gomez, A. M., Benitah, J. P., Perros, F., et al. (2018). Ca(2+) handling remodeling and STIM1L/Orai1/TRPC1/TRPC4 upregulation in monocrotaline-induced right ventricular hypertrophy. *J. Mol. Cell Cardiol.* 118, 208–224. doi: 10.1016/j.jymcc.2018.04.003
- Saliba, Y., Keck, M., Marchand, A., Atassi, F., Ouille, A., Cazorla, O., et al. (2015). Emergence of Orai3 activity during cardiac hypertrophy. *Cardiovasc. Res.* 105, 248–259. doi: 10.1093/cvr/cvu207
- Seferovic, P. M., Ponikowski, P., Anker, S. D., Bauersachs, J., Chioncel, O., Cleland, J. G. F., et al. (2019). Clinical practice update on heart failure 2019: pharmacotherapy, procedures, devices and patient management. An expert consensus meeting report of the Heart Failure Association of the European Society of Cardiology. *Eur J Heart Fail* 21, 1169–1186. doi: 10.1002/ehf.1531
- Segin, S., Berlin, M., Richter, C. R., Flockerzi, M. V., Worley, P., Freichel, M., et al. (2020). Cardiomyocyte-specific deletion of orai1 reveals its protective role in angiotensin-II-induced pathological cardiac remodeling. *Cells* 9:1092. doi: 10.3390/cells9051092
- Shiou, Y. L., Lin, H. T., Ke, L. Y., Wu, B. N., Shin, S. J., Chen, C. H., et al. (2019). Very low-density lipoproteins of metabolic syndrome modulates STIM1, suppresses store-operated calcium entry, and deranges myofilament proteins in Atrial Myocytes. *J. Clin. Med.* 8:881. doi: 10.3390/jcm8060881
- Spirli, C., Mariotti, V., Villani, A., Fabris, L., Fiorotto, R., and Strazzabosco, M. (2017). Adenylyl cyclase 5 links changes in calcium homeostasis to cAMP-dependent cyst growth in polycystic liver disease. *J. Hepatol.* 66, 571–580. doi: 10.1016/j.jhep.2016.10.032
- Stauderman, K. A. (2018). CRAC channels as targets for drug discovery and development. *Cell Calcium* 74, 147–159. doi: 10.1016/j.ceca.2018.07.005
- Takahashi, Y., Murakami, M., Watanabe, H., Hasegawa, H., Ohba, T., Munehisa, Y., et al. (2007). Essential role of the N-terminus of murine Orai1 in store-operated Ca2+ entry. *Biochem. Biophys. Res. Commun.* 356, 45–52. doi: 10.1016/j.bbrc.2007.02.107
- Tariq, S., and Aronow, W. S. (2015). Use of inotropic agents in treatment of systolic heart failure. *Int. J. Mol. Sci.* 16, 29060–29068. doi: 10.3390/ijms161226147
- Touchberry, C. D., Elmore, C. J., Nguyen, T. M., Andresen, J. J., Zhao, X., Orange, M., et al. (2011). Store-operated calcium entry is present in HL-1 cardiomyocytes and contributes to resting calcium. *Biochem. Biophys. Res. Commun.* 416, 45–50. doi: 10.1016/j.bbrc.2011.10.133
- Troupes, C. D., Wallner, M., Borghetti, G., Zhang, C., Mohsin, S., Berretta, R. M., et al. (2017). Role of STIM1 (Stromal Interaction Molecule 1) in hypertrophy-related contractile dysfunction. *Circ. Res.* 121, 125–136. doi: 10.1161/circresaha.117.311094
- Uehara, A., Yasukochi, M., Imanaga, I., Nishi, M., and Takeshima, H. (2002). Store-operated Ca2+ entry uncoupled with ryanodine receptor and junctional membrane complex in heart muscle cells. *Cell Calcium* 31, 89–96. doi: 10.1054/ceca.2001.0257
- Vig, M., DeHaven, W. I., Bird, G. S., Billingsley, J. M., Wang, H., Rao, P. E., et al. (2008). Defective mast cell effector functions in mice lacking the CRACM1 pore subunit of store-operated calcium release-activated calcium channels. *Nat. Immunol.* 9, 89–96. doi: 10.1038/ni1550
- Vig, M., Peinelt, C., Beck, A., Koomoa, D. L., Rabah, D., Kraft, S., et al. (2006). CRACM1 is a plasma membrane protein essential for store-operated Ca2+ entry. *Science* 312, 1220–1223. doi: 10.1126/science.1127883
- Voelkers, M., Salz, M., Herzog, N., Frank, D., Dolatabadi, N., Frey, N., et al. (2010). Orai1 and Stim1 regulate normal and hypertrophic growth in cardiomyocytes. *J. Mol. Cell Cardiol.* 48, 1329–1334. doi: 10.1016/j.jymcc.2010.01.020

- Volkers, M., Dolatabadi, N., Gude, N., Most, P., Sussman, M. A., and Hassel, D. (2012). Orai1 deficiency leads to heart failure and skeletal myopathy in zebrafish. *J. Cell Sci.* 125, 287–294. doi: 10.1242/jcs.090464
- Wang, P., Umeda, P. K., Sharifov, O. F., Halloran, B. A., Tabengwa, E., Grenett, H. E., et al. (2012). Evidence that 2-aminoethoxydiphenyl borate provokes fibrillation in perfused rat hearts via voltage-independent calcium channels. *Eur. J. Pharmacol.* 681, 60–67. doi: 10.1016/j.ejphar.2012.01.045
- Wang, Y., Deng, X., Mancarella, S., Hendron, E., Eguchi, S., Soboloff, J., et al. (2010). The calcium store sensor, STIM1, reciprocally controls Orai and CaV1.2 channels. *Science* 330, 105–109. doi: 10.1126/science.1191086
- Wang, Y., Li, Z. C., Zhang, P., Poon, E., Kong, C. W., Boheler, K. R., et al. (2015). Nitric oxide-cGMP-PKG pathway acts on orai1 to inhibit the hypertrophy of human embryonic stem cell-derived cardiomyocytes. *Stem Cells* 33, 2973–2984. doi: 10.1002/stem.2118
- Wilkins, B. J., Dai, Y. S., Bueno, O. F., Parsons, S. A., Xu, J., Plank, D. M., et al. (2004). Calcineurin/NFAT coupling participates in pathological, but not physiological, cardiac hypertrophy. *Circ. Res.* 94, 110–118. doi: 10.1161/01.res.0000109415.17511.18
- Wolkowicz, P. E., Huang, J., Umeda, P. K., Sharifov, O. F., Tabengwa, E., Halloran, B. A., et al. (2011). Pharmacological evidence for Orai channel activation as a source of cardiac abnormal automaticity. *Eur. J. Pharmacol.* 668, 208–216. doi: 10.1016/j.ejphar.2011.06.025
- Yuan, J. P., Zeng, W., Huang, G. N., Worley, P. F., and Muallem, S. (2007). STIM1 heteromultimerizes TRPC channels to determine their function as store-operated channels. *Nat. Cell Biol.* 9, 636–645. doi: 10.1038/ncb1590
- Zhang, H., Sun, A. Y., Kim, J. J., Graham, V., Finch, E. A., Nepliouev, I., et al. (2015). STIM1-Ca<sup>2+</sup> signaling modulates automaticity of the mouse sinoatrial node. *Proc. Natl. Acad. Sci. U.S.A.* 112, E5618–E5627. doi: 10.1073/pnas.1503847112
- Zhang, Y. H., Wu, H. J., Che, H., Sun, H. Y., Cheng, L. C., Li, X., et al. (2013). Functional transient receptor potential canonical type 1 channels in human atrial myocytes. *Pflugers. Arch.* 465, 1439–1449. doi: 10.1007/s00424-013-1291-3
- Zheng, C., Lo, C. Y., Meng, Z., Li, Z., Zhong, M., Zhang, P., et al. (2017). Gastrodin inhibits store-operated Ca(2+) entry and alleviates cardiac hypertrophy. *Front Pharmacol* 8:222. doi: 10.3389/fphar.2017.00222
- Zhu-Mauldin, X., Marsh, S. A., Zou, L., Marchase, R. B., and Chatham, J. C. (2012). Modification of STIM1 by O-linked N-acetylglucosamine (O-GlcNAc) attenuates store-operated calcium entry in neonatal cardiomyocytes. *J. Biol. Chem.* 287, 39094–39106. doi: 10.1074/jbc.m112.383778

**Conflict of Interest:** The authors declare that the research was conducted in the absence of any commercial or financial relationships that could be construed as a potential conflict of interest.

Copyright © 2020 Luo, Gomez, Benitah and Sabourin. This is an open-access article distributed under the terms of the Creative Commons Attribution License (CC BY). The use, distribution or reproduction in other forums is permitted, provided the original author(s) and the copyright owner(s) are credited and that the original publication in this journal is cited, in accordance with accepted academic practice. No use, distribution or reproduction is permitted which does not comply with these terms.



# Calcium Channels in Adult Brain Neural Stem Cells and in Glioblastoma Stem Cells

Valérie Coronas\*, Elodie Terrié, Nadine Déliot, Patricia Arnault and Bruno Constantin

Laboratoire STIM, Université de Poitiers-CNRS ERL 7003, Poitiers, France

## OPEN ACCESS

### Edited by:

Francisco Javier Martin-Romero,  
University of Extremadura, Spain

### Reviewed by:

Alejandro Berna,  
University of Extremadura, Spain  
Artur Paasz,  
Medical University of Silesia, Poland

### \*Correspondence:

Valérie Coronas  
valerie.coronas@univ-poitiers.fr

### Specialty section:

This article was submitted to  
Cellular Neuropathology,  
a section of the journal  
Frontiers in Cellular Neuroscience

**Received:** 28 August 2020

**Accepted:** 06 October 2020

**Published:** 13 November 2020

### Citation:

Coronas V, Terrié E, Déliot N,  
Arnault P and Constantin B  
(2020) Calcium Channels in Adult  
Brain Neural Stem Cells and in  
Glioblastoma Stem Cells.  
*Front. Cell. Neurosci.* 14:600018.  
doi: 10.3389/fncel.2020.600018

The brain of adult mammals, including humans, contains neural stem cells (NSCs) located within specific niches of which the ventricular-subventricular zone (V-SVZ) is the largest one. Under physiological conditions, NSCs proliferate, self-renew and produce new neurons and glial cells. Several recent studies established that oncogenic mutations in adult NSCs of the V-SVZ are responsible for the emergence of malignant primary brain tumors called glioblastoma. These aggressive tumors contain a small subpopulation of cells, the glioblastoma stem cells (GSCs), that are endowed with proliferative and self-renewal abilities like NSCs from which they may arise. GSCs are thus considered as the cells that initiate and sustain tumor growth and, because of their resistance to current treatments, provoke tumor relapse. A growing body of studies supports that  $\text{Ca}^{2+}$  signaling controls a variety of processes in NSCs and GSCs.  $\text{Ca}^{2+}$  is a ubiquitous second messenger whose fluctuations of its intracellular concentrations are handled by channels, pumps, exchangers, and  $\text{Ca}^{2+}$  binding proteins. The concerted action of the  $\text{Ca}^{2+}$  toolkit components encodes specific  $\text{Ca}^{2+}$  signals with defined spatio-temporal characteristics that determine the cellular responses. In this review, after a general overview of the adult brain NSCs and GSCs, we focus on the multiple roles of the  $\text{Ca}^{2+}$  toolkit in NSCs

**Abbreviations:** AMPA,  $\alpha$ -amino-3-hydroxy-5-méthylisooazol-4-propionate; CaBP,  $\text{Ca}^{2+}$  binding protein; CaMK,  $\text{Ca}^{2+}$ /calmodulin-dependent protein kinase; CRAC,  $\text{Ca}^{2+}$  release activated  $\text{Ca}^{2+}$  channel; DAG, diacylglycerol; EGF, epidermal growth factor; ER, endoplasmic reticulum; GABA, gamma-aminobutyric acid; GFAP, glial fibrillary acidic protein; GPCR, G protein-coupled receptor; GSC, glioblastoma stem cell; IP3, inositol triphosphate; HDAC, histone deacetylase; IP3R, IP3 receptor; LGIC, ligand-gated ion channel; MCU, mitochondrial  $\text{Ca}^{2+}$  uniporter; nAChR, ionotropic cholinergic nicotinic receptors; NCX,  $\text{Na}^+/\text{Ca}^{2+}$  exchanger; NFAT, nuclear factor activated T-cells; NMDA, N-methyl-D-aspartate; NSC, neural stem cell; NTDPase, nucleoside triphosphate diphosphohydrolase; P2X, P2Y receptors, purinergic receptors; PIP2, Phosphatidylinositol 4, 5-bisphosphate; PLC, phospholipase C; PMCA, plasma membrane  $\text{Ca}^{2+}$  ATPase; RCAS-TVA, replication-competent avian sarcoma-leukosis virus (RCAS) and its receptor the tumor virus A (TVA); ROC, receptor-operated channel; ROCE, receptor-operated  $\text{Ca}^{2+}$  entry; RTK, receptor tyrosine kinases; RYR, ryanodine receptor; SDF1, stromal cell-derived factor 1; SERCA, sarco/endoplasmic reticulum  $\text{Ca}^{2+}$ -ATPase; SOC, store-operated channel; SOCE, store-operated  $\text{Ca}^{2+}$  entry; STIM, stromal interaction molecule; TAP, transient amplifying progenitors; TRPC, transient receptor potential-canonical; TRPV, transient receptor potential vanilloid; VGCC, voltage-gated  $\text{Ca}^{2+}$  channels; V-SVZ, ventricular-subventricular zone.

and discuss how GSCs hijack these mechanisms to promote tumor growth. Extensive knowledge of the role of the  $\text{Ca}^{2+}$  toolkit in the management of essential functions in healthy and pathological stem cells of the adult brain should help to identify promising targets for clinical applications.

**Keywords:** store-operated channel, calcium toolkit, neural stem cells, brain, glioma, glioblastoma, cancer stem cell, calcium channel

## INTRODUCTION

In the brain of adult mammals, including humans, neural stem cells (NSCs) reside within two major regions: the ventricular-subventricular zone (V-SVZ, also called the subependymal zone or subventricular zone) lining the lateral brain ventricles and the subgranular zone of the dentate gyrus in the hippocampus. Within these niches, NSCs sustain lifelong neurogenesis and gliogenesis (Lim and Alvarez-Buylla, 2016; Lledo and Valley, 2016; Obernier and Alvarez-Buylla, 2019). In this review, we focus primarily on the V-SVZ that is the largest germinal region of the adult brain. Within this neurogenic area, quiescent and activated NSCs coexist. Upon activation, NSCs divide to produce transient amplifying progenitors that engender neuroblasts that in turn, replenish the olfactory bulb population of interneurons. Adult NSCs in the V-SVZ also generate astrocytes and oligodendrocytes that disperse within the brain parenchyma (Lim and Alvarez-Buylla, 2016; Lledo and Valley, 2016; Obernier and Alvarez-Buylla, 2019).

While NSCs are mobilized by brain injuries and contribute to attempts of brain repair, recent studies have consistently established that oncogenic mutations in NSCs from the V-SVZ, unfortunately, lead to the development of glioblastoma, one of the deadliest cancers in adults (Recht et al., 2003; Barami, 2007; Quiñones-Hinojosa and Chaichana, 2007; Lee et al., 2018). These malignant tissues contain a subpopulation of cells, called glioblastoma stem cells (GSCs) that share several properties with NSCs from which they may derive (Recht et al., 2003; Zarco et al., 2019). Because of their growth properties and ability to resist the current treatments, GSCs are considered responsible for tumor initiation, growth, and relapse (Galli et al., 2004; Singh et al., 2004).

NSCs and GSCs are controlled by multiple extracellular signals, numbers of which recruit  $\text{Ca}^{2+}$  signaling actors to transduce their effects.  $\text{Ca}^{2+}$  is a ubiquitous second messenger that shapes a wide range of cellular functions including proliferation, migration, and cell differentiation in various cell types (Berridge et al., 2003). Increases of intracellular  $\text{Ca}^{2+}$  concentration are triggered by a variety of channels, transporters, and  $\text{Ca}^{2+}$ -binding proteins (CaBP). These  $\text{Ca}^{2+}$  toolkit components encode specific  $\text{Ca}^{2+}$  signals that are defined by their spatio-temporal profile and their magnitude (Berridge, 1990; Berridge et al., 2003).

A growing bulk of evidence has pointed to a major role of  $\text{Ca}^{2+}$  in NSCs of the adult brain and in their pathological counterparts, namely GSCs. After a general overview of NSCs of the adult brain and on GSCs, we will review the progress that has been achieved on how  $\text{Ca}^{2+}$  signals regulate specific functions and properties of

these cells. When appropriate, we put the data of the literature into the perspective of the development of treatments to combat brain diseases.

## ADULT BRAIN NEURAL STEM CELLS, NEUROGENESIS, AND PATHOLOGY

### The Discovery of Neurogenesis and Neural Stem Cells in the Adult Brain

Most adult organs retain a population of somatic stem cells that ensure tissue homeostasis and repair by producing new cells in response to physiological conditions or injury. The brain has long been considered an exception to this rule: it was widely assumed that neurogenesis occurred only during embryogenesis and early postnatal life and that only glial cells could be produced in adulthood. This dogma was first challenged in the 1960s by Joseph Altman who reported addition of new neurons in the olfactory bulb and hippocampus of adult rats, but experimental evidence obtained with the tools available at that time was not robust enough to counter the dogma stating that neurogenesis does not occur in adults (Altman, 1963, 1969; Altman and Das, 1965). With the emergence of new tools to label proliferating cells, the persistence of neurogenesis throughout life was then directly demonstrated in the brain of adult songbirds (Nottebohm, 1985), rodents (Luskin, 1993; Lois and Alvarez-Buylla, 1994), and non-human primates. In these latter, incorporation of new neurons was described not only in the hippocampus (Gould et al., 1998, 1999; Kornack and Rakic, 1999) and olfactory bulb (Kornack and Rakic, 2001) but also amygdala (Bernier et al., 2002). Since then, neurogenesis has been identified in other brain areas like the hypothalamus of rodent and sheep brains (Kokoeva et al., 2005; Migaud et al., 2010; Yoo and Blackshaw, 2018) and the dorsal vagal complex in rodents (Bauer et al., 2005). In 1998, the analysis of brain tissue obtained post-mortem from patients, who had been injected with the nucleotide analog bromodeoxyuridine (BrdU) for diagnostic purposes during their cancer treatment, established that new neurons are generated throughout the lifespan from dividing progenitor cells in the dentate gyrus of adult humans (Eriksson et al., 1998). This discovery settled the relevance of adult neurogenesis for humans and attracted interest in the field. A neurogenic activity in the human hippocampus and olfactory bulb as well as in the striatum, a structure adjacent to V-SVZ, has thereafter been confirmed by several studies, although some controversy persists concerning the addition of new neurons in the adult human brain (Bédard and Parent, 2004; Sanai et al., 2004; Spalding et al., 2013; Ernst et al., 2014; Boldrini et al., 2018; Kempermann et al., 2018; Sorrells et al., 2018).

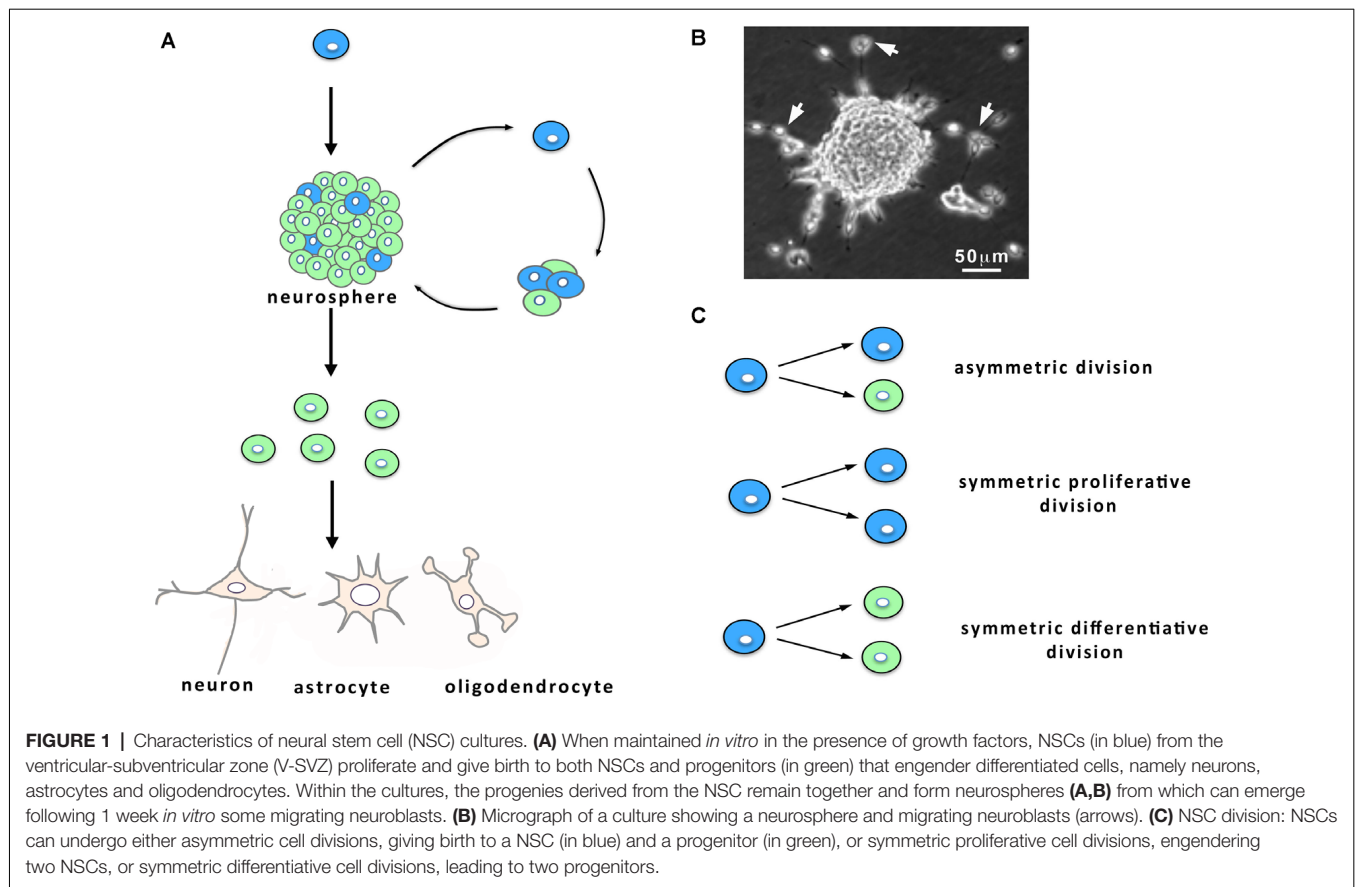
In parallel to the discovery of neurogenesis in the brain of adult mammals, cells with NSC properties were isolated by Reynolds et al. (1992) from adult mice brain and propagated *in vitro*. When placed in appropriate cell culture conditions, NSCs proliferate, forming structures called neurospheres, self-renew, and subsequently give birth to neurons and glial cells (**Figures 1A,B**). Since this seminal work, NSCs have been obtained from a few adult rodent brain regions (including the hippocampus and the area postrema) of which the V-SVZ lining the brain lateral ventricles (LVs) contains the largest pool of dividing cells with defining characteristics of NSCs (Reynolds et al., 1992; Weiss et al., 1996; Palmer et al., 1997; Charrier et al., 2006). A decade later, Sanai et al. (2004) showed that V-SVZ harvested on post-mortem human brain contains multipotent NSCs that can be amplified *in vitro* and that retain the capacity to produce neurons and glial cells. Fueling considerable hope for stem cell-based brain therapies, these studies have been implemented by the demonstration of the possibility to harvest NSCs by endoscopy from human V-SVZ (Westerlund et al., 2005), which opens the opportunity to autologous cell transplantation and could help to circumvent the problems associated with the rejection of heterologous cell grafts.

## The V-SVZ Structure and Function

The V-SVZ is a thin layer of cells extending along the walls of the LVs (**Figures 2A,B**). Combined immunocytochemical and ultrastructural characterization of the adult rodent V-SVZ enabled to recognize four main cell types within this germinal region: neuroblasts (Type A cells), SVZ astrocytes (Types B1 and B2 cells), immature precursors (Type C cells), and ependymal cells (Type E cells; Doetsch et al., 1997; **Figure 2B**). Ependymal cells form a single multiciliated layer that borders the LV and that contributes to the circulation of the cerebrospinal fluid flow. Type B cells possess ultrastructural and immunocytochemical staining characteristics of astrocytes, for example, GFAP (glial fibrillary acidic protein)-immunoreactivity, and express markers of immature cells such as SOX2 (Doetsch et al., 1997). Type B cells have been further subdivided into type B1 and type B2 cells based on their localization within the V-SVZ and cellular properties. Multiple lineage-tracing studies consistently identified type B1 cells as the NSC population (Doetsch et al., 1999a; Imura et al., 2003; Garcia et al., 2004). These cells display a radial morphology, have a short apical process with a single primary cilium sent into the LV, and extend a long basal process ending on blood vessels (Mirzadeh et al., 2008). The primary cilium, which is exquisitely poised to sense molecular signals and the mechanical flow of the cerebrospinal fluid, contributes to controlling NSC activation (Tong et al., 2014). In adult mice, there are roughly 6,000 B1 cells on the lateral wall of the LVs (Mirzadeh et al., 2008). NSCs can shuttle between activity (B1a) and quiescence (B1q), a process that is regulated by the signals arriving on NSCs. When activated, type B1 cells divide slowly, self-renew and give rise to type C cells that act as transient amplifying progenitors and express immature markers like nestin (Doetsch et al., 1999b; **Figure 2D**). For cell proliferation, NSCs can undergo three modes of division (**Figure 1C**): asymmetric

divisions produce both a stem cell and a progenitor and thus couple NSC pool maintenance to neurogenic activity, symmetric proliferative divisions engender two NSCs, and symmetric differentiative divisions generate two progenitor cells. Analysis of NSC mode of division established that they mostly divide by symmetric divisions to either self-renew or produce differentiated progenies, indicating that neurogenesis and self-renewal might be independently regulated in the V-SVZ (Obernier et al., 2018). Type B2 cells have been poorly studied but a recent publication proposed that they may be produced by type B1 cells and serve as a reserve population of NSCs (Obernier et al., 2018). Type C cells divide rapidly and generate neuroblasts (type A cells; **Figures 2B,D**) that also undergo one or two rounds of cell division to further amplify the number of new neurons engendered (Ponti et al., 2013). Neuroblasts produced in the V-SVZ migrate for a long distance in aggregates forming tangentially oriented chains that coalesce into a defined pathway, the so-called rostral migratory stream (RMS; **Figure 2A**; Lois and Alvarez-Buylla, 1994; Lois et al., 1996). After about 5 days, neuroblasts reach the core of the olfactory bulb, detach from the chains and start to migrate radially towards their final location within the olfactory bulb (Petreanu and Alvarez-Buylla, 2002). Then, they differentiate as local interneurons that integrate the pre-existing neuronal network and contribute to olfactory processing and memory (Gheusi et al., 2000; Petreanu and Alvarez-Buylla, 2002; Tepavčević et al., 2011; Alonso et al., 2012; Gheusi and Lledo, 2014). In young adult mice, it has been estimated that NSCs produce approximately 10,000 young migrating neuroblasts every day (Doetsch et al., 1999b). NSCs also generate oligodendrocytes that join neighboring corpus callosum, striatum, and fimbria-fornix both in physiological conditions and after demyelination (Menn et al., 2006; Nait-Oumesmar et al., 2007; Ortega et al., 2013; Capilla-Gonzalez et al., 2014b). Although NSCs sustain lifelong neurogenesis and gliogenesis, it remains unknown whether individual NSCs are multipotent *in vivo* or whether neurons and glia arise from distinct NSCs (Menn et al., 2006; Capilla-Gonzalez et al., 2013; Ortega et al., 2013; Sohn et al., 2015).

The V-SVZ of adult humans is mainly similar to the V-SVZ of rodents described above but differs by its organization in four layers (Quiñones-Hinojosa et al., 2006; **Figure 2C**). Layer I is a monolayer of ependymal cells that border the ventricular lumen. This layer is followed by a hypocellular layer (Layer II), heavily populated with processes of astrocytes that are joined to each other by gap junctions and large desmosomes (Quiñones-Hinojosa et al., 2006). A dense ribbon of cell bodies, many of which belong to astrocytes form layer III, lies next to layer II. Some of these astrocytes proliferate and behave as multipotent stem cells (type B cells) when placed *in vitro* (Sanai et al., 2004; Quiñones-Hinojosa et al., 2006). Some isolated neuroblasts (type A cells) are also found within this layer as well as in layers II and IV, the latter being a transition layer with the brain parenchyma (Sanai et al., 2004; Macas et al., 2006; Curtis et al., 2007; Wang et al., 2011). The V-SVZ of children younger than 18 months of age harbors many neuroblasts migrating along specific pathways to integrate as neurons not



only into the olfactory bulb but also into the ventral medial prefrontal cortex or the frontal lobe (Sanai et al., 2011; Paredes et al., 2016). This process has been reported to decline sharply during infancy (Sanai et al., 2011; Paredes et al., 2016). By adulthood, the existence of migrating neuroblasts along a RMS and incorporation of new neurons in the human olfactory bulb seems nearly extinct although there are conflicting results providing evidence of a maintenance neurogenic activity in the V-SVZ of the adult human brain (Curtis et al., 2007; Sanai et al., 2011; Wang et al., 2011; Paredes et al., 2016). One of the major hurdles when examining neurogenesis on post-mortem human brains is the possibility of labeling newly born cells. To circumvent this setback, the group led by Frisen measured  $^{14}\text{C}$  incorporated in neurons of post-mortem human brains to evaluate the numbers of newly incorporated cells in the adult brain. These studies are based on the fact that nuclear bomb testing during the Cold War in the 1950s produced elevated levels of  $^{14}\text{C}$  in the atmosphere, which entered the biotope and thereby, was incorporated in human molecules, including nucleotides forming DNA. It is assumed that the level of  $^{14}\text{C}$  in DNA mirrors the level of  $^{14}\text{C}$  at any given time, allowing the birthdate of cells in the human body to be determined retrospectively. This approach combined with histological studies showed that, in the adult human brain, V-SVZ neuroblasts robustly supply the adjacent striatum with new interneurons and also, generate new oligodendrocytes

(Bergmann et al., 2012; Ernst et al., 2014). Altogether, these data support that the V-SVZ of the adult human brain contains NSCs whose implication in neurogenesis and gliogenesis *in vivo* requires further investigation in humans.

The NSCs and their activity are substantially affected by aging. Concretely, shrinkage of the pool of the V-SVZ NSCs occurs with age (Maslov et al., 2004; Shook et al., 2012; Kalamakis et al., 2019). This smaller stem cell reservoir seems to display a decreased proliferative activity (Bouab et al., 2011; Capilla-Gonzalez et al., 2014a; Kalamakis et al., 2019), although some reports indicated the opposite (Ahlenius et al., 2009; Shook et al., 2012). A recent study based on fluorescence-activated cell sorting (FACS) analysis and injury-induced regeneration experiments in mice nicely demonstrated that quiescent NSCs in the old brain are resistant to activation but, when activated, NSCs exhibit similar behavior in the brains of young and old mice (Kalamakis et al., 2019). This increase in quiescence during aging would allow protecting the stem cell reservoir from full depletion but makes old NSCs more resistant to regenerate the injured brain. Despite age-induced quiescence in NSCs, an increase in the number of progenitors has been reported in the aged adult human forebrain following ischemia, suggesting that NSCs, at least the active subpopulation of NSCs, might be recruited by injuries in the elderly (Macas et al., 2006). In addition to inducing a state of quiescence, aging also modifies the fate

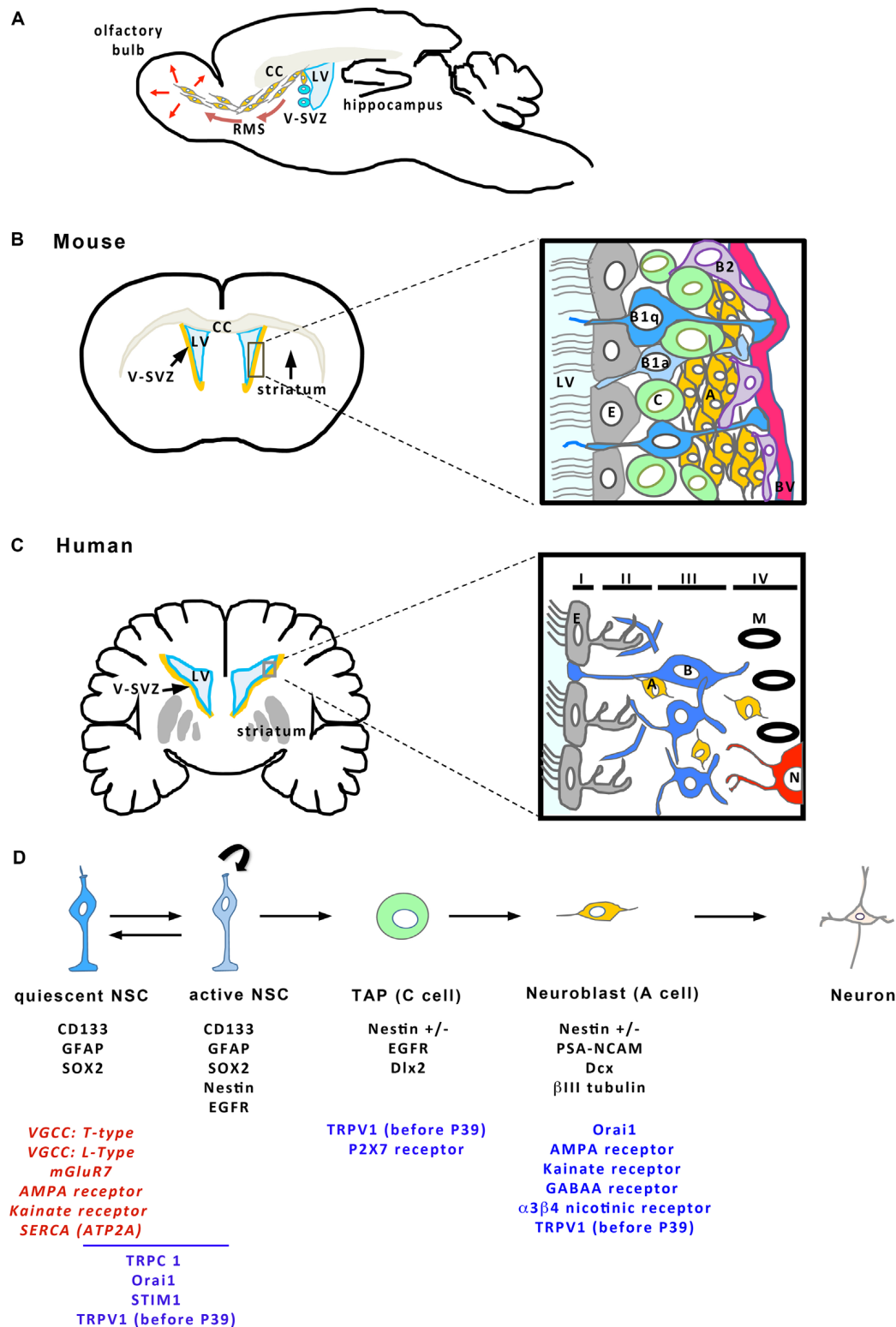


**FIGURE 2 |** Cellular organization of the V-SVZ. **(A)** Sagittal view of the mouse brain showing the V-SVZ that borders the brain lateral ventricle (LV). The V-SVZ contains NSCs (in blue) producing neuroblasts (in orange) that migrate tangentially along the rostral migratory stream (RMS) to join the olfactory bulb where they integrate the existing network. CC, Corpus callosum. Frontal sections (on the left) of the mouse **(B)** and the human **(C)** brains represent the V-SVZ that borders the LVs. The square delineates the zone enlarged illustrating a schema of the organization of the V-SVZ (on the right). **(B)** (mouse brain) Ependymal cells (E, in gray) (Continued)

**FIGURE 2 | Continued**

border the LV. NSCs (B1 cells in blue; B1a: active B1 cells; B1q: quiescent B1 cells) are located just beneath the ependymal layer and extend a cilium in the LV and a process that contacts a blood vessel (BV, in red). B1 cells can give birth to B2 cells (purple) that may act as NSC reserve cells. B1 cells engender transient amplifying progenitors (C cells, in green) that give birth to neuroblasts (A cells, in orange), then differentiating as neurons in the olfactory bulb. **(C)** In human brain, the V-SVZ is organized in four layers. Layer I is formed of ependymal cells (E, in gray). Layer II is a hypocellular layer with mainly processes. Layer III contains the cell bodies of astrocytes, part of which are NSCs (B cells, in blue). Layer IV is a transition layer with the parenchyma where myelin (M in black) and neurons (N, in red) can also be found. NSCs produce some neuroblasts (A cells, in orange) that are found across layers II to IV. **(D)** The different stages of adult neurogenesis from B cells to differentiated neurons. B cells (in blue) are NSCs that can shuttle between a quiescent and an active state. Neurogenesis occurs when B cells give birth to C cells that engender A cells migrating towards the olfactory bulb and then, differentiating as neurons. On the schema, characteristic markers expressed by the different cell types of the SVZ are indicated in black below each cell. The different components of the  $\text{Ca}^{2+}$  toolkit expressed within each of the cells are given below the corresponding cell. For B cells, some transcriptomic studies have highlighted the expression of specific components in quiescent cells. When the only information available concerns RNA expression, the corresponding actors are written in red, otherwise they are in blue. This figure has been elaborated according to the following references: Nguyen et al. (2003), Platel et al. (2008), Khodosevich et al. (2009), Young et al. (2010), Daynac et al. (2013), Sharma (2013), Khatri et al. (2014), Somasundaram et al. (2014), Stock et al. (2014), Domenichini et al. (2018), and Leeson et al. (2018).

of the cells generated by NSCs, with a substantial reduction in the production of new neurons, whereas the genesis of oligodendroglial cells is unaffected in the aged brain (Ahlenius et al., 2009; Shook et al., 2012; Capilla-Gonzalez et al., 2013, 2015). Although the consequences of these alterations need further exploration, several reports suggest that impaired NSC activity may be associated with age-related diseases (Demars et al., 2010; Lazarov and Marr, 2013).

## Recruitment of Adult Brain Neural Stem Cells by Brain Pathologies

In addition to maintaining tissue homeostasis, somatic stem cells are defined by their ability to respond to lesions. In this regard, several studies disclosed that NSCs from the V-SVZ are recruited by various brain lesions including stroke and brain trauma, or by degenerative diseases (Gonzalez-Perez, 2012; Beckervordersandforth and Rolando, 2019; Bacigaluppi et al., 2020). To illustrate this concept, we chose to focus on two specific brain injuries: stroke, that is the second leading cause of death and the third leading cause of disability according to the World Health Organization, and multiple sclerosis, that is one of the most widespread disabling neurological condition of young adults around the world.

A stroke occurs when the blood flow to the brain is disrupted because of occlusion or rupture of a cerebral artery. Ischemia, caused by blockage of an artery, is the most common form of stroke. It leads to irreversible injury in the core region and partially reversible damage in the surrounding penumbra zone that has been deprived of blood supply. Stroke induction by

transient middle cerebral artery occlusion, the most common model used for research in rodents, has been reported to boost cell proliferation in the V-SVZ by triggering NSC activation and to provoke the migration of neuroblasts from the V-SVZ towards the damaged areas (Arvidsson et al., 2002; Parent et al., 2002; Jin et al., 2003; Zhang et al., 2004). In the injured striatum, the neuroblasts arising from the V-SVZ differentiated as mature neurons, but 80% of the stroke-generated striatal neurons died during the first 2 weeks after their formation, which resulted in a very weak replacement of the striatal neuronal population lost due to the injury (Arvidsson et al., 2002). Although disappointing from a clinical perspective, these data point to the fact that NSCs contribute to attempts at brain repair. Furthermore, the fact that specific ablation of migrating neuroblasts in transgenic mice models resulted in increased infarct size and worsened functional recovery strongly suggests that stroke-recruited neuroblasts may help brain healing through mechanisms that are still elusive (Jin et al., 2010; Sun et al., 2012). It may be interesting to mention here that recent demonstrations of the ability of NSCs and neuroblasts to remove dead cell debris through phagocytosis raise a possible role of these cells in clearing the diseased environment, although this hypothesis needs to be experimentally challenged (Lu et al., 2011; Ginisty et al., 2015). Besides, NSC activation and an increase in the number of neuroblasts close to the lateral ventricular walls have also been described in brains of patients with ischemia, even those of advanced age (up to 80 years; Jin et al., 2006; Macas et al., 2006; Martí-Fàbregas et al., 2010). These results suggest that, in humans, the adult brain NSCs retain a capacity to respond to ischemic injuries and that this capacity is maintained in old age.

Multiple sclerosis is a chronic, autoimmune, and demyelinating disease that affects the central nervous system, especially among young individuals. In this pathology, most patients initially develop a clinical pattern with periodic relapses followed by remissions that ultimately end in permanent neurological disability. Experimental rodent models of demyelination displayed increased cell proliferation and migration of V-SVZ progenitors into the injured white matter where many of the mobilized cells differentiated as oligodendrocytes, in response to demyelination (Picard-Riera et al., 2002). Consecutive lineage tracing studies confirmed that V-SVZ cells, in addition to resident parenchymal oligodendroglial precursors, efficiently produce new oligodendrocytes with robust capacities of remyelination (Xing et al., 2014; Brousse et al., 2015). However, a recent study reported that selective ablation of V-SVZ cells although resulting in lowered oligodendrogenesis in mice models with multiple sclerosis, did not impact the ensuing remyelination but enhanced axonal loss (Butti et al., 2019), suggesting that NSCs may exert their beneficial effects either through oligodendrocyte replacement, or by providing trophic support, or both. In the human brain, NSC recruitment and oligodendrogenesis were also found in post-mortem brains of patients with multiple sclerosis and, importantly, were shown to occur in the brains of elderly patients (Nait-Oumesmar et al., 2007; Snethen et al., 2008). Interestingly, the olfactory dysfunction observed in mice

models of multiple sclerosis and related to the reduced supply of olfactory bulb neurons was also described in patients, suggesting that at least part of the mechanisms identified in mice may occur in humans (Tepavčević et al., 2011).

## Adult Neural Stem Cell Relationship With Cancer Stem Cells in Brain Tumors

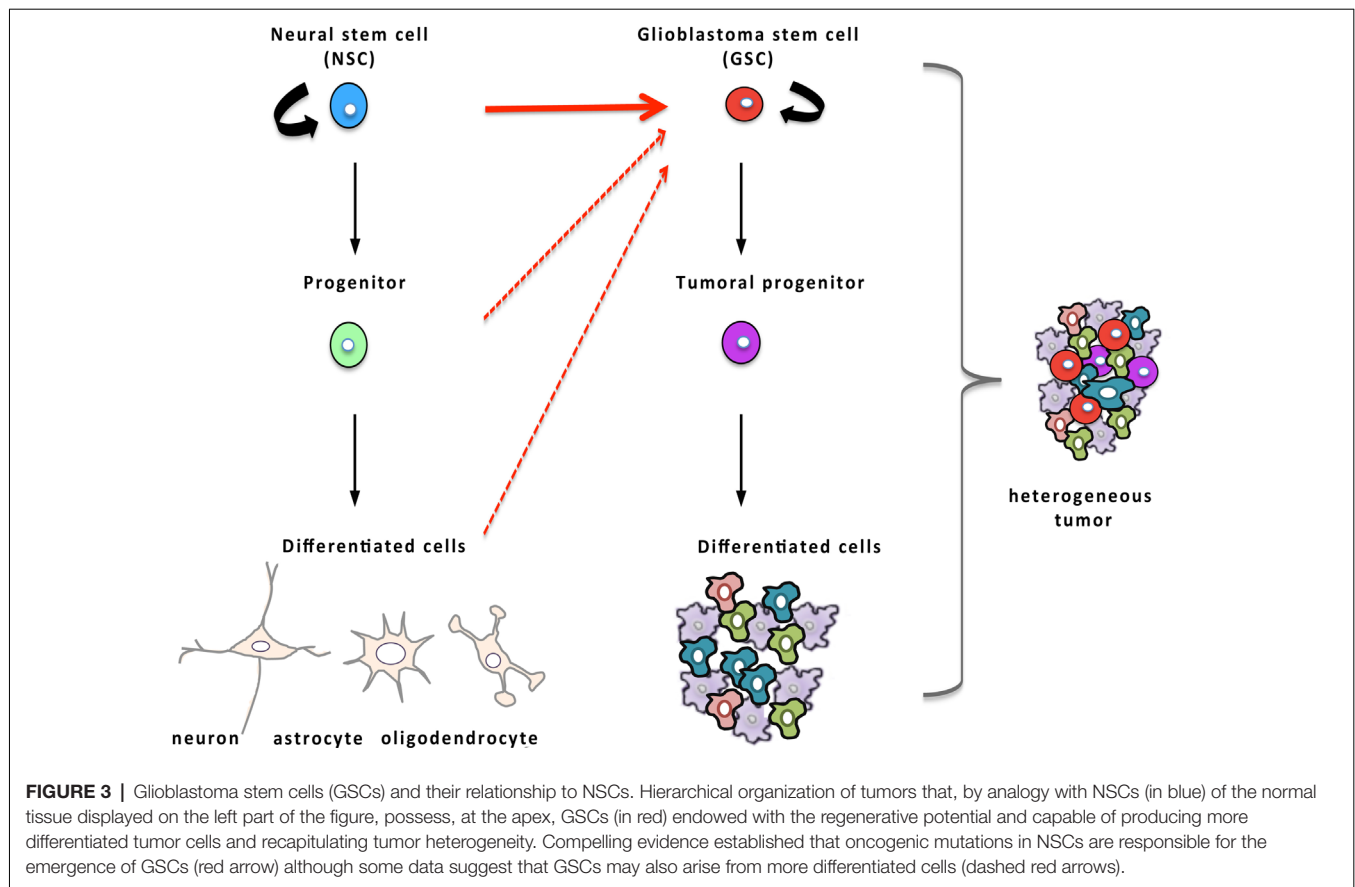
Glioblastoma is the most frequent of primary brain tumors and among the most refractory of malignancies. Standard treatment includes gross total surgical resection followed by concurrent radiotherapy and chemotherapy with the drug temozolomide (Stupp et al., 2005). Because of the resistance of glioblastoma to the current treatments, the median survival of patients hardly reaches 15 months from the time of the diagnosis (Stupp et al., 2005). Thus, new means of eliminating these tumoral cells are keenly awaited. In the process of improving the understanding of glioblastoma growth and recurrence, a subpopulation of tumor cells, called GSCs, was identified as the cause of tumor initiation, resistance to current therapies, and thus, disease recurrence (Singh et al., 2004; Bao et al., 2006; Chen et al., 2012; Chesnelong et al., 2019). The cancer stem cell hypothesis states that tumors mimic normal tissues with hierarchically arranged populations of cells, with cancer stem cells at the apex that are endowed with regenerative potential and with the ability to provide all the functional diversity of the original tumor (Figure 3). As they are more quiescent than the other tumoral cells, cancer stem cells survive the current treatments that target highly proliferative cancer cells, and then, rebuild the tumor after the treatment, provoking cancer relapse in the patient.

Because GSCs share several properties with NSCs, the hypothesis that they may derive from NSCs has been explored (Figure 3). In the 1960s, it was reported that the offspring of pregnant rats, exposed to a single injection of the mutagenic molecule *N*-Ethyl-*N*-Nitrosourea during late gestation, developed spontaneous glioblastoma when they were 4-months-old. These animals displayed early neoplasia in the V-SVZ several weeks before macroscopic tumors were noted, suggesting that glioblastoma may originate in the V-SVZ germinal niche (Recht et al., 2003). The advent of genetic tools to specifically transfer oncogenes or to inhibit tumor-suppressors *in vivo* in NSCs of transgenic mice made it possible to assess and substantiate the idea that NSCs represent possible cells of origin of glioblastoma. To selectively infect NSCs, Holland and colleagues took advantage of the RCAS-TVA viral system to target nestin-positive stem cells *in vivo*. In this approach, the gene coding for avian retrovirus receptor TVA is placed under the control of the nestin promoter which leads to an expression of TVA selectively in nestin-positive cells in the transgenic mice, allowing thereafter transduction of dividing nestin-positive cells with the avian retrovirus RCAS through its receptor TVA. The introduction of an RCAS viral vector containing the oncogenic forms of both Ras and Akt in these transgenic neonatal mice resulted in the spontaneous onset of high-grade glioma (Holland et al., 2000). About a decade later, Marumoto et al. (2009) confirmed that targeting oncogenic mutations in NSCs of the V-SVZ leads

to the development of glioblastoma. To this end, they took advantage of the cre/lox system to drive the expression of oncogenic Ras or Akt specifically in GFAP-expressing cells of the V-SVZ. For that purpose, they injected lentiviral vectors encoding of oncogenic Ras or Akt with expression controlled by cre recombinase in the V-SVZ of adult immunocompetent mice, heterozygous for p53 and genetically engineered to have a GFAP-driven expression of the recombinase cre. In these mice, the cre-induced expression of oncogenic Ras or Akt in GFAP-positive cells of the V-SVZ provoked the development of high-grade glioma (Marumoto et al., 2009). This study moreover underlined that infection of as few as 60 GFAP-expressing cells in the V-SVZ was sufficient to induce the emergence of a full-blown tumor containing GSCs whereas glioblastoma rarely developed when GFAP-expressing non-stem cells from the cortex were transduced (Marumoto et al., 2009). Concomitant studies corroborated that introduction of glioblastoma-specific oncogenic mutations in NSCs of the V-SVZ lead to a spontaneous tumoral development with a 100% penetrance (Alcantara Llaguno et al., 2009; Jacques et al., 2010). Altogether, these data consistently support that high-grade glioma originates from NSCs of the V-SVZ that have undergone malignant transformation although a few reports have identified more differentiated cells as an alternative source of cells at the origin of glioblastoma (Lindberg et al., 2009; Liu et al., 2011; Friedmann-Morvinski et al., 2012).

Recently, a study based on deep-sequencing analysis of brain tissues provided evidence that oncogenic mutations in the V-SVZ are responsible for the development of high-grade glioma in humans (Lee et al., 2018). The publication reports that, in more than half of the human brains examined, normal SVZ tissue away from the tumor contained low-level cancer-deriving mutations in genes such as TP53, PTEN, EGFR, and TERT promoter, that were similar to those found in their matching tumors (Lee et al., 2018; Matarredona and Pastor, 2019). Furthermore, the authors described that NSCs from the V-SVZ carrying driver mutations were able to migrate from the SVZ and to form high-grade malignant gliomas in distant brain regions, clearly suggesting an ontogenetic link between NSCs from the V-SVZ and glioblastoma that has been confirmed by other studies (Garcia and Dhermain, 2018; Lee et al., 2018; Tejada Neyra et al., 2018). Accordingly, it is currently admitted that cell-autonomous changes in NSCs of the V-SVZ germinal zone are most likely responsible for the emergence of glioblastoma and that NSCs could represent the cells of origin of GSCs, which matches actual demographic data on glioma incidence in the human population (Bauer et al., 2014).

In addition to this ontogenetical relationship between NSCs and GSCs, direct interactions between NSCs and the tumor have been found. It was discovered in experimental mice models of glioma that NSCs are endowed with a tumor tropism that allows them to track tumor cells and circumscribe the tumor mass, overall leading to an oncostatic effect and improved survival of mice bearing the tumor (Glass et al., 2005). This innate tumor tropism of NSCs for glioblastoma is currently exploited in clinical trials using genetically engineered therapeutic NSCs to deliver



cytotoxic drugs specifically to the tumor site (Portnow et al., 2017; Gutova et al., 2019).

## THE CALCIUM TOOLKIT

NSCs and GSCs, like the other cells of the organism, evolve in specific microenvironments whose signals shape their activities in response to the physiological demand or the pathological growth. Numerous microenvironmental signals transduce their effects through transitory rises of intracellular concentration of  $\text{Ca}^{2+}$  with specific durations and magnitudes, either in discrete cellular microdomains or throughout the whole cell (Berridge et al., 2003). Because of its wide repertoire of spatio-temporal variations in its intracellular concentrations, the  $\text{Ca}^{2+}$  signal is ideally poised to determine cellular processes in response to extracellular signals. Consequently, strict handling of  $\text{Ca}^{2+}$  is required to maintain optimized cellular functions.  $\text{Ca}^{2+}$  fluctuations are managed by different molecules that can be subdivided as follows:  $\text{Ca}^{2+}$  permeable channels that flux  $\text{Ca}^{2+}$  into the cell through the plasma membrane or that release  $\text{Ca}^{2+}$  from internal stores of the endoplasmic reticulum (ER) and mitochondria,  $\text{Ca}^{2+}$  pumps and exchangers that replenish  $\text{Ca}^{2+}$  stores or that extrude  $\text{Ca}^{2+}$  from the cell, and CaBP that buffer cytosolic free  $\text{Ca}^{2+}$  or act as effectors. The coordinated action of the  $\text{Ca}^{2+}$  toolkit components maintains low resting levels of

cytosolic free  $\text{Ca}^{2+}$  and encodes specific  $\text{Ca}^{2+}$  signals that trigger selective cellular activities in response to extracellular signals (Berridge et al., 2003). While the  $\text{Ca}^{2+}$  signal is ubiquitously used to transduce extracellular signals, the proteins that control  $\text{Ca}^{2+}$  transport display cell type-specific expression, allowing selective cellular responses. Compelling evidence suggests that  $\text{Ca}^{2+}$  channels play a pivotal role in tumor biology, display aberrant expression or localization and that they are hijacked to promote tumor growth and resistance to treatment (Déliot and Constantin, 2015; Prevarskaya et al., 2018; Terrié et al., 2019). **Figure 4** shows an overview of the key components of the  $\text{Ca}^{2+}$  toolkit. Here below, we provide a short description of this toolkit.

### Plasma Membrane Channels

At rest, the cytosolic concentration of  $\text{Ca}^{2+}$  is maintained at very low levels (50–100 nmol/L), which is about 10,000-fold less than those of the extracellular medium. Thus, the opening of any  $\text{Ca}^{2+}$  channel located in the plasma membrane leads to a pronounced  $\text{Ca}^{2+}$  influx that sharply raises the intracellular  $\text{Ca}^{2+}$  concentration, that in turn, affects the activity of nearby proteins and elicits biological responses (Samanta and Parekh, 2017).  $\text{Ca}^{2+}$  inflow from the external milieu is controlled by a variety of transmembrane proteins, of which  $\text{Ca}^{2+}$  channels mediate  $\text{Ca}^{2+}$  entry from an extracellular compartment in response to diverse stimuli: membrane depolarization, extracellular agonists,

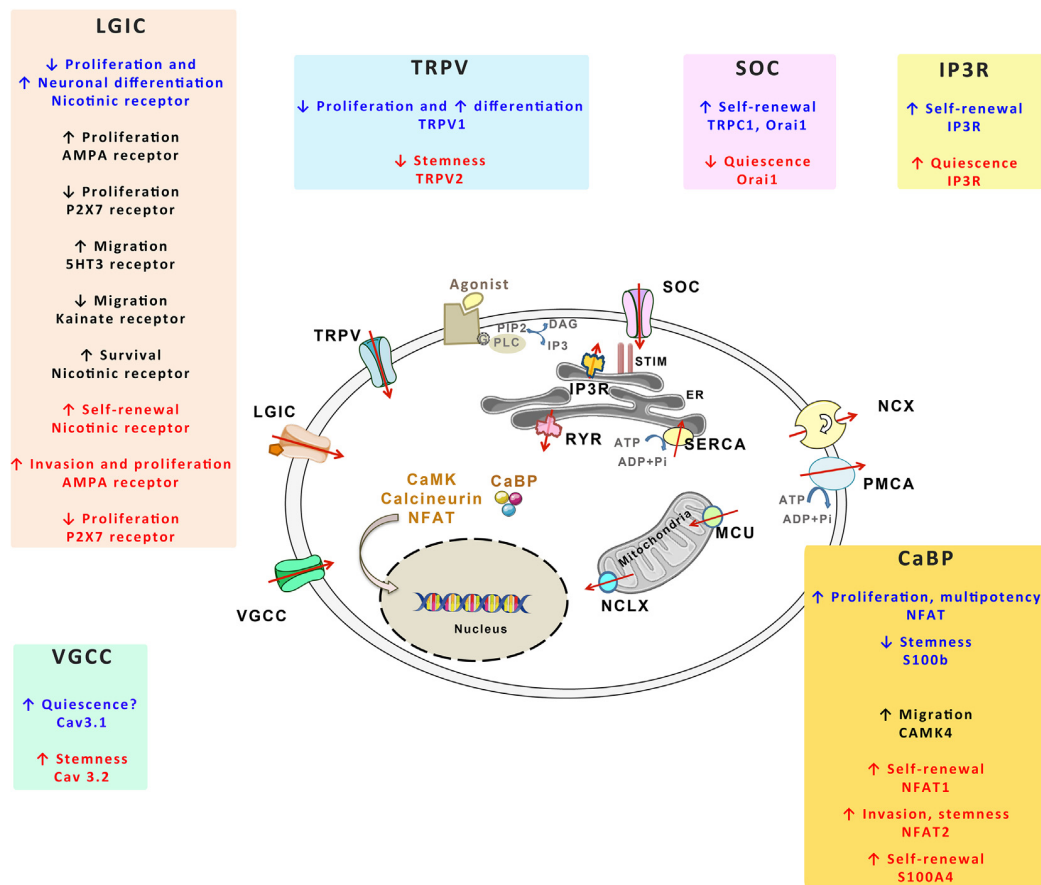


**FIGURE 4 |** The  $\text{Ca}^{2+}$  toolkit in NSCs and GSCs. The figure summarizes the different components of the  $\text{Ca}^{2+}$  toolkit. The red arrows represent the  $\text{Ca}^{2+}$  flux. Plasma membrane channels include voltage-gated  $\text{Ca}^{2+}$  channels (VGCCs), ligand-gated ion channels (LGICs), transient receptor potential vanilloids (TRPVs) and store-operated channels (SOCs). Plasma membrane also contains  $\text{Ca}^{2+}$ -extruding mechanisms, namely  $\text{Na}^{+}/\text{Ca}^{2+}$  exchanger (NCX) and plasma membrane  $\text{Ca}^{2+}$  ATPase (PMCA). Within the endoplasmic reticulum (ER), both IP3 receptor (IP3R) and ryanodine receptor (RYR) allow  $\text{Ca}^{2+}$  release in the cytosol whereas sarco/endoplasmic reticulum  $\text{Ca}^{2+}$ -ATPase (SERCA) replenishes ER  $\text{Ca}^{2+}$  stores. STIM1 detects ER  $\text{Ca}^{2+}$  concentrations that activate SOC. Mitochondria release or take up  $\text{Ca}^{2+}$  respectively through mitochondrial  $\text{Na}^{+}/\text{Ca}^{2+}$  exchanger (NCLX) and mitochondrial  $\text{Ca}^{2+}$  uniporter (MCU). The cells also contain  $\text{Ca}^{2+}$  binding protein (CaBP) that act as  $\text{Ca}^{2+}$  buffers or that transduce  $\text{Ca}^{2+}$  signals (calcineurin, NFAT, CaMK). GPCR corresponds to G protein coupled receptors, PLC to phospholipase C. For each of these  $\text{Ca}^{2+}$  actors, their effects on NSCs (written in blue), on the progenies of NSCs (written in black) and on GSCs (written in red) are provided within the specific insets.

intracellular messengers, mechanical stretch, or depletion of intracellular  $\text{Ca}^{2+}$  stores (Berridge et al., 2003).

### Voltage-Gated Calcium Channels (VGCCs)

VGCCs also called voltage-operated calcium channels (VOCC) mediate  $\text{Ca}^{2+}$  influx in cells in response to membrane depolarization. An initial increase of the membrane potential is required for the activation of the intrinsic voltage sensor and subsequent pore opening. VGCCs comprises ten members, based on the expression of a specific pore-forming  $\alpha_1$ -subunit containing the voltage sensor of the Cav family channels. This family has been subdivided into three phylogenetic subfamilies according to the characteristics of the currents they mediate: Cav1 subfamily channels that give rise to L-Type currents, Cav2 subfamily channels that produce to P/Q-, N-, and R-type currents, and Cav3 subfamily channels that mediate T-type currents (Catterall et al., 2005; Catterall, 2011). L-type and

T-type Cav subfamilies are expressed in many cell types while N, P/Q, and R-type channels are predominantly expressed in neurons. VGCCs have been first studied in electrically excitable cells, but it is now clear that they are functionally expressed in non-excitable cells including various cancer cell types (Prevarskaya et al., 2010, 2018).

### Receptor-Operated Channels (ROCs) and Store-Operated Channels (SOCs)

#### ROCs

ROCs are switched on *via* ligand-mediated activation of receptors coupled to the phospholipase C (PLC) that breaks down PIP2 to produce diacylglycerol (DAG) and inositol 1,4,5-trisphosphate (IP3). DAG activates plasma membrane channels from the TRPC (Transient receptor potential canonical) subfamily, leading to a cationic current ( $\text{Na}^{+}$  and  $\text{Ca}^{2+}$ ), a

process referred to as receptor-operated  $\text{Ca}^{2+}$  entry (ROCE; Vazquez et al., 2001; Dietrich et al., 2005). Because DAG is a second messenger, this channel type can be also called Secondary Messenger-Operated Channels (SMOCs). Among the seven TRPC identified, homotetrameric TRPC3, TRPC6 or TRPC7 channels and heterotetrameric TRPC1–TRPC3 and TRPC3–TRPC4 channels can open in response to DAG application, resulting in  $\text{Ca}^{2+}$  influx (Hofmann et al., 1999; Lintschinger et al., 2000; Liu et al., 2005a; Poteser et al., 2006). In contrast, homomeric TRPC1, -4, and -5, which are also activated by receptor-induced PLC, are completely unresponsive to DAG (Hofmann et al., 1999; Venkatachalam et al., 2003).

### SOCs

Also known as capacitive  $\text{Ca}^{2+}$  entry, store-operated  $\text{Ca}^{2+}$  entry (SOCE) represents a widespread type of  $\text{Ca}^{2+}$  entry that is triggered upon IP<sub>3</sub>-dependent depletion of ER  $\text{Ca}^{2+}$  stores (Parekh and Putney, 2005). The ER transmembrane protein Stromal Interaction Molecule 1 (STIM1) senses  $\text{Ca}^{2+}$  decrease in the ER and opens SOC to replenish intracellular  $\text{Ca}^{2+}$  stores through SERCA (Sarco/endoplasmic reticulum  $\text{Ca}^{2+}$ -ATPase) and elicit cellular responses (Parekh and Putney, 2005). Initially identified as CRAC ( $\text{Ca}^{2+}$  Release-Activated Channels) in T cells, Orai1 homopolymers form the core component of SOC. Although Orai1 is the ubiquitous SOC protein, Orai2 and Orai3 mediate SOCE in certain specific tissues (Motiani et al., 2010; Wang et al., 2017c). Depending on the cell type and on the STIM1/TRPC channel ratio (Lee et al., 2010), SOCE and  $I_{\text{SOCE}}$  (the current produced by SOCE) can also be supported by TRPC tetrameric channels (Lopez et al., 2020), which can be formed of TRPC1 and TRPC4 (Sabourin et al., 2009, 2012; Antigny et al., 2017), that interact directly with STIM1 (Huang et al., 2006; Yuan et al., 2007). SOCE and cationic  $I_{\text{SOCE}}$  can also be the result of functional cooperation between TRPC1 with Orai1 (Huang et al., 2006; Jardin et al., 2008; Desai et al., 2015; Shin et al., 2016; Ambudkar et al., 2017). SOCE has been recognized as an essential mechanism for  $\text{Ca}^{2+}$  uptake in non-excitabile cells that, in addition to restoring ER  $\text{Ca}^{2+}$  stores, elicits  $\text{Ca}^{2+}$ -dependent intracellular signaling cascades involved in cell proliferation, migration, and differentiation.

Further, Orai3 can form a heteromultimeric channel with Orai1 to build-up arachidonic acid-regulated  $\text{Ca}^{2+}$  channels (ARC) or arachidonic acid metabolite Leukotriene C<sub>4</sub> (LTC<sub>4</sub>)-regulated  $\text{Ca}^{2+}$  channels (LRC; Shuttleworth, 2009; González-Cobos et al., 2013). Different works suggest that Orai3 regulates breast, prostate, lung, and gastrointestinal cancers by either forming SOC or ARC/LRC channels in the cancerous cells but not in healthy tissue (Tanwar et al., 2020). Additionally, a recent study reinforces the idea that native CRAC channel is formed by heteromultimerization of Orai1 with Orai2 and/or Orai3, in which Orai2 and Orai3 may act as Orai1 negative regulators (Yoast et al., 2020). Their role would be therefore critical to adapt  $\text{Ca}^{2+}$  signals to agonist strengths as proposed for Orai2 in T cells (Vaeth et al., 2017).

### Ligand-Gated Ion Channels (LGICs)

LGICs also commonly referred to as ionotropic receptors, are ion channels whose gating is ligand-dependent. Neurotransmitters

serve as ligands for ionotropic receptors. LGICs are opened, or gated, by the binding of a neurotransmitter that triggers a conformational change and results in the conducting state. The LGICs comprise the excitatory, cation-selective, nicotinic acetylcholine- (nAChR; Millar and Gotti, 2009), 5-HT<sub>3</sub> serotonin- (Barnes et al., 2009), ionotropic glutamate- (Lodge, 2009), the inhibitory, anion-selective, GABA<sub>A</sub>- (Olsen and Sieghart, 2008) and glycine receptors (Lynch, 2009) as well as P2X receptors (Jarvis and Khakh, 2009) gated by extracellular adenosine 5'-triphosphate (ATP; North, 2016). In the central nervous system, activation of P2X receptors supports  $\text{Ca}^{2+}$  entry into neurons and modulates neuron responses. It is also well known that extracellular ATP is abundant in the tumor microenvironment, and since ATP may be leaked by damaged cells, stimulation of P2X channels may be prevalent upon traumatic or ischemic injury (Puchaowicz et al., 2014).

### TRPV (Transient Receptor Potential Vanilloid) Channels

TRPVs are  $\text{Ca}^{2+}$  permeable channels of the TRP family (Pedersen and Nilius, 2007) that respond to various signals from the microenvironment such as exogenous chemical ligands, noxious heat, or mechanical stretch. Because of these properties, various channels of the TRPV family, that contains six mammalian members, are known to be involved in nociception (Patapoutian et al., 2009), taste perception (Nilius and Appendino, 2013), thermosensation (Tominaga, 2007) or mechano and osmolarity sensing (Guilak et al., 2010). While heat-activated TRPV1–TRPV4 channels that also function as chemosensors are nonselective for cations and modestly permeable to  $\text{Ca}^{2+}$ , TRPV5 and TRPV6 are highly  $\text{Ca}^{2+}$  selective channels with low-temperature sensitivity. Among TRPV channels, TRPV2 is a growth factor-regulated cation channel that was shown to be up-regulated in some cancer cell types, suggesting an oncogenic role, while down-regulated in other tumor cells, suggesting an opposite tumor suppression role (Liberati et al., 2014).

### Intracellular $\text{Ca}^{2+}$ Handling and $\text{Ca}^{2+}$ Signaling Pathways

$\text{Ca}^{2+}$  handling by intracellular reservoirs and transporters may also impact cellular activity. The major  $\text{Ca}^{2+}$  store is the ER that releases  $\text{Ca}^{2+}$  to the cytoplasm, through two related  $\text{Ca}^{2+}$  release channels, namely the ryanodine receptors (RYRs) and inositol 1,4,5-trisphosphate receptors (IP<sub>3</sub>Rs) in response to multiple factors that include free  $\text{Ca}^{2+}$  ion. Three different isoforms of RYRs (RYR1, RYR2, RYR3), each encoded by a different gene, have been identified (Santulli et al., 2018). More widely expressed in most non-excitabile cells than RYRs, IP<sub>3</sub>Rs, displaying three IP<sub>3</sub>R subtypes, are activated by IP<sub>3</sub> produced in response to receptors in the plasma membrane that stimulate phospholipase C (PLC; Mikoshiba, 2015; Berridge, 2016). Specifically, the cell-surface receptors responsible for IP<sub>3</sub> formation belong to two main classes, the G protein-coupled receptors (GPCRs) protein and the receptor tyrosine kinases (RTKs) that are coupled to different PLC isoforms (the PLC $\beta$  and PLC- $\gamma$  isoforms respectively). During the transduction process, the precursor lipid PIP<sub>2</sub> is hydrolyzed by PLC to produce

both IP<sub>3</sub> and DAG. The IP<sub>3</sub> released from the membrane diffuses into the cytosol where it binds the IP<sub>3</sub>Rs, which open and releases Ca<sup>2+</sup> from the ER. The subsequent Ca<sup>2+</sup> release through IP<sub>3</sub>Rs as well as the propagation of the Ca<sup>2+</sup> signal occurs in a wide range of cells. The Ca<sup>2+</sup>-mobilizing function of IP<sub>3</sub> is terminated through the metabolism of IP<sub>3</sub>.

Ca<sup>2+</sup> entry and/or Ca<sup>2+</sup> release through the various channels leads to an increase of cytosolic free Ca<sup>2+</sup> concentration whose spatio-temporal pattern and magnitude differentially activate specific signaling pathways (Samanta and Parekh, 2017). These latter rely on various CaBP of the cytosol, such as calmodulin, calcineurin, PKC, S100 proteins, parvalbumin (Yáñez et al., 2012). While some of them, like parvalbumin or S100, buffer free Ca<sup>2+</sup>, most of CaBP decode the Ca<sup>2+</sup> signal by selectively turning on specific intracellular signaling cascades (Schwaller, 2010; Yáñez et al., 2012). For instance, the Ca<sup>2+</sup> sensor calmodulin modifies its interaction with many effectors upon binding to Ca<sup>2+</sup>, that in turn, trigger distinct signaling pathways such as mitogen-activated protein kinase/extracellular signal-regulated kinase (MEK/ERK), Nuclear factor of activated T-cells (NFAT) or Ca<sup>2+</sup>/calmodulin-dependent protein kinase (CAMK) pathways (Hogan et al., 2003). A characteristic feature of the IP<sub>3</sub> signaling pathway is that it usually generates a brief transient Ca<sup>2+</sup> release that can be repeated to give oscillations over a longer period (Berridge, 1990; Fewtrell, 1993). Many functions, such as gland secretion or differential gene transcription, are controlled by frequency coding of Ca<sup>2+</sup> oscillations that, in turn, differentially regulate CaBPs. For instance, the transcription factor nuclear factor kappa B

(NFκB) was shown to be preferentially activated by low frequency repeated Ca<sup>2+</sup> transients, whereas NFAT activation needs higher frequencies and a long duration Ca<sup>2+</sup> signals (Dolmetsch et al., 1998). The activity of the CAMK II was also reported to be dependent on the frequency of Ca<sup>2+</sup> oscillations (De Koninck and Schulman, 1998).

## PHYSIOLOGICAL ROLES OF Ca<sup>2+</sup> IN NSCs AND THEIR PROGENIES

NSCs are subjected to a wide range of extracellular cues, each of which contributes to regulate NSC activity. Analysis of the transcriptome of purified adult NSCs highlighted the importance of Ca<sup>2+</sup>-dependent signaling pathways in these cells (Beckervordersandforth et al., 2010). In parallel, Ca<sup>2+</sup> imaging experiments unveiled the existence in NSCs, of intercellular Ca<sup>2+</sup> waves that are propagated through gap junctions and that are used by NSCs to communicate with each other and with neighboring niche astrocytes both under physiological conditions (Lacar et al., 2011) and pathological conditions (Kraft et al., 2017). Live cell Ca<sup>2+</sup> imaging has also allowed to observe spontaneous Ca<sup>2+</sup> oscillations in NSC/progenitors from the V-SVZ (Domenichini et al., 2018) as well as spontaneous high-frequency transients in migrating neuroblasts (Maslyukov et al., 2018). Along with the prominence of transcripts related to the Ca<sup>2+</sup> pathway in NSCs, these data lend support to the essential role of Ca<sup>2+</sup> in NSCs and their progeny. In the subsequent sections, we will review and discuss the involvement of the Ca<sup>2+</sup> toolkit in NSC physiology by analyzing first the implication of plasma membrane channels and then, the function

**TABLE 1 |** Effects of the Ca<sup>2+</sup> toolkit components on neural stem cells (NSCs) and Glioblastoma stem cells (GSCs).

	Neural stem cells	Glioblastoma stem cells
VGCC	Maintain quiescence (T-type, L-type) induced by GABA? <sup>(1, 2)</sup>	Increase stemness and survival (T-type) <sup>(18, 19)</sup>
SOC	Increase proliferation and self-renewal (TRPC1, Orai1) <sup>(3, 4)</sup>	Increase proliferation <sup>(20)</sup>
TRPV	Decrease proliferation and increase neuronal differentiation (TRPV1) <sup>(5)</sup>	Increase cell death (TRPV1) <sup>(21)</sup> Decrease stemness (TRPV2) <sup>(22)</sup>
LGIC	Nicotinic receptors: decrease proliferation and increase neuronal differentiation <sup>(6, 7)</sup> NMDA receptors : increase oligodendroglial differentiation, increase neuroblast survival <sup>(8, 9)</sup> AMPA receptors : increase neuroblast proliferation <sup>(10)</sup> Kainate receptors : decrease neuroblast migration <sup>(11)</sup> 5HT3: increase neuroblast migration <sup>(12)</sup> P2X7 receptors: decrease transient amplifying progenitor (C cell) proliferation <sup>(13)</sup>	Nicotinic receptors: increase stemness and clonogenicity <sup>(23)</sup> AMPA receptors: increase proliferation and invasion <sup>(24, 25)</sup> P2X7 receptors: decrease proliferation <sup>(26)</sup>
IP3R	Increase self-renewal <sup>(14)</sup> Increase cell death <sup>(15)</sup>	Increase quiescence <sup>(27)</sup>
CaBP	NFAT: Increase proliferation <sup>(16)</sup> S100B : decrease stemness <sup>(17)</sup>	NFAT1 : increase self-renewal and stemness <sup>(28)</sup> NFAT2 : increase clonogenicity <sup>(29)</sup> S100A4 : increase self-renewal <sup>(30)</sup>

The table summarizes the major effects reported for Ca<sup>2+</sup> toolkit actors in NSCs and their progenies and in GSCs according to the following references: 1. Young et al. (2010); 2. Daynac et al. (2013); 3. Somasundaram et al. (2014); 4. Domenichini et al. (2018); 5. Stock et al. (2014); 6. Narla et al. (2013); 7. Wang et al. (2017b); 8. Cavaliere et al. (2012); 9. Platel et al. (2010); 10. Song et al. (2017); 11. Platel et al. (2008); 12. Garcia-González et al. (2017); 13. Leeson et al. (2018); 14. Kraft et al. (2017); 15. Shi et al. (2005); 16. Serrano-Pérez et al. (2015); 17. Raponi et al. (2007); 18. Niklasson et al. (2017); 19. Zhang et al. (2017); 20. Aulestia et al. (2018); 21. Stock et al. (2014); 22. Morelli et al. (2012); 23. Spina et al. (2016); 24. Venkataramani et al. (2019); 25. Venkatesh et al. (2019); 26. D'Alimonte et al. (2015); 27. Zeniou et al. (2015); 28. Jiang et al. (2019); 29. Song et al. (2020); 30. Chow et al. (2017).

of intracellular  $\text{Ca}^{2+}$  handling and signaling pathways. An overview of the  $\text{Ca}^{2+}$  proteins expressed in NSCs and their functions are summarized in **Table 1** and in **Figures 2D, 4**.

## Plasma Membrane Channels

### Voltage-Gated Calcium Channels (VGCCs)

Both the L-type  $\text{Ca}_v1.2$  and the T-type  $\text{Ca}_v3.1$  channels have been detected by RT-PCR in V-SVZ cell cultures that are formed of NSCs and their progenies (Kong et al., 2008). Subsequent analysis of prospectively purified NSCs by flow cytometry disclosed that quiescent NSCs display high expression levels of ion channels among which T- and L-type voltage-gated channels (Khatri et al., 2014). Indeed, electrophysiological recordings combined with pharmacology identified in NSCs (B cells), L- and T-type currents that could be physiologically evoked by GABA (Young et al., 2010). Constitutively present in the germinal niche, GABA that is produced by neuroblasts, tonically activates  $\text{GABA}_A$  receptors expressed by NSCs to maintain a quiescent state (Liu et al., 2005b; Daynac et al., 2013; Khatri et al., 2014).  $\text{GABA}_A$  receptors are ionotropic receptors that upon interaction with their neurotransmitter activate a depolarizing chloride current in NSCs whose resting membrane potential is close to  $-80$  mV. It was shown that the depolarization elicited by GABA opens VGCCs, which provokes a  $\text{Ca}^{2+}$  flux, and that this  $\text{Ca}^{2+}$  inflow can be suppressed by the L-Type channel blocker nifedipine or the T-type inhibitor mibefradil (Young et al., 2010). Thus,  $\text{Ca}_v$  channels whose expression is enriched in quiescent NSCs (Khatri et al., 2014) could be key players in preventing NSC activation and in preserving their quiescent state in response to the ambient GABA of the V-SVZ. Although this hypothesis requires formal demonstration, the above data suggest that  $\text{Ca}_v$ , by acting on NSC quiescence, would prevent excessive activation of NSCs and avoid NSC exhaustion.

In addition to NSCs, neuroblasts within the olfactory bulb also have been found to possess L-type channels that induce  $\text{Ca}^{2+}$  transients whose functions are yet undefined (Darcy and Isaacson, 2009).

### Store-Operated Channels (SOCs)

In the V-SVZ, both *Orai1* and *TRPC1* have been detected along with *STIM1* in NSCs and also in some neuroblasts (Skibinska-Kijek et al., 2009; Somasundaram et al., 2014; Domenichini et al., 2018). In these cells, SOCE could be triggered by various extracellular signals such as EGF that are used for cultures of NSCs (Reynolds et al., 1992; Somasundaram et al., 2014) or *SDF1* that controls the tumor tropism of NSCs to glioblastoma (Zhao et al., 2008; Somasundaram et al., 2014). The cholinergic agonist muscarine that stimulates NSC self-renewal could also elicit an intracellular  $\text{Ca}^{2+}$  spike followed by a plateau phase that was dependent on SOCE (Domenichini et al., 2018). Conversely, SOCE was significantly but not totally reduced following the *Orai1* knock-out (Somasundaram et al., 2014), indicating that *Orai1* and other actors, possibly *TRPC1*, build-up functional SOCs in mouse NSCs. The pharmacological blockade of SOC or genetic deletion of *Orai1* resulted in decreased cell proliferation in the V-SVZ without affecting cell death (Somasundaram et al., 2014; Domenichini et al., 2018). Importantly, recruitment

of SOC by glutamate or muscarine (Giorgi-Gerevini et al., 2005; Domenichini et al., 2018) promoted NSC self-renewal while SOCE inhibition shifted the mode of NSC division from symmetric proliferative to asymmetric, suggesting that SOCs are required to maintain or expand the pool of NSCs (Domenichini et al., 2018). How SOCs control the mode of cell division is yet unknown and could rely on the ability of SOCE to mobilize specific  $\text{Ca}^{2+}$  actors or depend on the capacity of *STIM* and *Orai* to localize at the cleavage furrow (Chan et al., 2016).

The importance of SOCs in NSCs is further underscored by a recent study showing that SOCE is required for the transduction of mechanical information due to cerebrospinal fluid flow (Petrik et al., 2018). Specifically, the authors of that study reported that the epithelium sodium channel (ENaC) that is located in the primary cilium of NSCs acts as a mechanosensor and requires a subsequent SOCE to control cell proliferation in V-SVZ in response to cerebrospinal fluid flow (Petrik et al., 2018). Altogether, these data highlight that SOCs play a pivotal role in linking NSC activity to extracellular cues. Of interest, it has been shown in neurons, that after store depletion, *STIM1* suppresses the activity of  $\text{Ca}_v1.2$  and  $\text{Ca}_v3.1$  VGCCs, both of which are expressed in quiescent NSCs and may contribute to maintaining a quiescent state (Harraz and Altier, 2014). Furthermore, it has been shown in muscle cells that SOC and  $\text{Ca}_v$  can be found in complexes, which would facilitate the switch for recruitment of either SOC or  $\text{Ca}_v$  (Ávila-Medina et al., 2016). If *STIM1* holds a similar function in NSCs, this observation raises the assumption that *STIM1* may orchestrate the shuttling between activity and quiescence of NSCs, by acting both on SOCs to trigger self-renewal and  $\text{Ca}_v$  channels to release NSCs from the quiescent state constitutively induced by ambient GABA.

### Ligand-Gated Ion Channels (LGICs)

Because NSC activities are tightly controlled by neurotransmitters, several  $\text{Ca}^{2+}$ -coupled LGICs have been identified as NSC regulators. For instance, NSCs possess, in addition to cholinergic muscarinic receptors that yield transient  $\text{Ca}^{2+}$  signals partly through SOCs (Somasundaram et al., 2014; Domenichini et al., 2018), ionotropic nAChRs of the  $\alpha3$  and  $\alpha4$  subtype (Paez-Gonzalez et al., 2014). Also, several studies indicate that other nAChR, namely  $\alpha7$  receptors are also expressed in V-SVZ and that neuroblasts, as well as possibly transient amplifying progenitors, display nAChR (Narla et al., 2013; Sharma, 2013). These receptors are physiologically exposed to acetylcholine in the V-SVZ niche that comes from innervation by cholinergic fibers from the basal forebrain (Calzà et al., 2003; Cooper-Kuhn et al., 2004) and that is also released by a small population of cholinergic neurons residing within the rodent V-SVZ (Paez-Gonzalez et al., 2014). Activation of the local cholinergic neurons or acute infusion of nicotine significantly promoted neurogenesis *in vivo* (Mudò et al., 2007; Paez-Gonzalez et al., 2014). Conversely, the destruction of basal forebrain cholinergic neurons impeded the production of new neurons (Calzà et al., 2003; Cooper-Kuhn et al., 2004), indicating that ligand-gated cholinergic receptors favor neurogenesis. The use of selective pharmacological and genetic tools identified that

$\alpha 7$  nicotinic receptors while promoting neuronal differentiation, inhibit proliferation of V-SVZ cells under both physiological conditions or in response to ischemia whereas the  $\beta 2$ -nAChR subunit control cell survival of newborn neurons (Narla et al., 2013; Wang et al., 2017a,b). Collectively, these studies lend support to a regulatory role of nicotinic receptors in the neurogenic activity of the healthy and diseased brain, albeit the pharmacology of these effects would merit further investigation.

NSCs and neuroblasts also express ionotropic glutamate receptors of the N-methyl-D-aspartate (NMDA),  $\alpha$ -amino-3-hydroxy-5-methylisoxazol-4-propionate (AMPA), and kainate subtypes (Platel et al., 2008, 2010; Khatri et al., 2014). Although little is known about the functional roles of glutamate receptors in NSCs, kainate and AMPA receptors that trigger  $\text{Ca}^{2+}$  influx have been found in neuroblasts where they, respectively, reduce the speed of the migration along the LV (Platel et al., 2008) or boost proliferation as well as promote the ability of these cells to improve brain repair following stroke (Song et al., 2017). In contrast, NMDA receptors seem critical for neuroblast survival during their journey in the RMS before entering the olfactory bulb synaptic network (Platel et al., 2010). Physiologically, the glutamate supply that activates the migrating neuroblasts is secreted by astrocytes, suggesting that astrocytes use glutamate signaling to control the number of adult-born neurons reaching their final destination (Platel et al., 2010). NMDA receptors have also been shown to stimulate oligodendrocyte differentiation in V-SVZ stem/progenitor cells (Cavaliere et al., 2012). Furthermore, AMPA receptors have been detected in oligodendroglial progenitors derived from the V-SVZ during the regeneration process occurring after the demyelination of the corpus callosum (Etxeberria et al., 2010). Collectively, these data indicate that glutamate, through the activation of specific subsets of ligand-gated receptors, controls multiple steps of neurogenesis and gliogenesis in the adult brain.

The V-SVZ also harbors serotonergic receptors that support large rhythmic  $\text{Ca}^{2+}$  oscillations in neuroblasts (García-González et al., 2017). Knock-out of the 5HT3A receptor severely reduced  $\text{Ca}^{2+}$  spikes, indicating that 5HT3A receptors represent a major gate for  $\text{Ca}^{2+}$  entry in migrating neuroblasts. Indeed, the speed of migration of neuroblasts was enhanced following optogenetic activation of serotonergic fibers while it was disrupted by loss-of-function mutation of 5HT3A receptors (García-González et al., 2017), implying that serotonergic innervation arising from the raphe nuclei governs neuroblast migration through  $\text{Ca}^{2+}$  inflow mediated by ionotropic 5HT3A receptors (García-González et al., 2017).

In addition to neurotransmitters, V-SVZ cells mobilize  $\text{Ca}^{2+}$  in response to extracellular nucleotides whose concentrations increase following brain injury because of their leakage by damaged cells. In addition to their roles in pathological states, nucleotides may also control constitutively the neurogenic niche where high levels of NTDPase2, the enzyme that hydrolyzes nucleotides, have been detected (Braun et al., 2003). Knock-out of NTDPase2 resulted in increased numbers of intermediate progenitors in the V-SVZ, suggesting that increased levels of extracellular nucleotides favor proliferation in the V-SVZ (Braun et al., 2003). Extracellular nucleotides mediate their

effects through metabotropic G-protein-coupled P2Y purinergic receptors and ionotropic purinergic P2X receptors, both of which are expressed in the V-SVZ and induce  $\text{Ca}^{2+}$  transients (Stafford et al., 2007; Messemer et al., 2013). Specifically, the P2X7R subtype that has been detected in ependymal (E) is also expressed in transient amplifying progenitors (C cells) where it plays a dual role: in the absence of the ligand, P2X7R functions as a scavenger receptor involved in phagocytosis and following its activation by ATP, the P2X7R reduces proliferation of C cells (Genzen et al., 2009; Messemer et al., 2013; Leeson et al., 2018). It should be mentioned here that although these data appear contradictory with the fact that increased levels of extracellular nucleotides favor cell proliferation, ATP also acts on other receptors among which the metabotropic P2Y1R receptors that foster expansion of the C cell population (Suyama et al., 2012). The multiplicity of receptors targeted by extracellular nucleotides shapes a unique and selective response to these ligands.

### TRPV (Transient Receptor Potential Vanilloid) Channels

Among the TRPV channels, TRPV1 has been detected within the V-SVZ in 20% of NSCs, in transient amplifying progenitors and in neuroblasts during the early postnatal period (Stock et al., 2014). TRPV1 expression then declines in 1 month old mice along with the diminution of neurogenesis, although radioautography figures published by Roberts et al. (2004) show some binding sites of TRPV1 in the V-SVZ of adult mice brain stained with radiolabeled TRPV1 ligands (Roberts et al., 2004; Stock et al., 2014). Interestingly, TRPV1 expression could be up-regulated in adulthood by physiological situations known to promote neurogenesis (Stock et al., 2014). In mice, deletion of TRPV1 conducted to a substantial rise in proliferating cells, but lesser differentiation to neurons or glia in the neurogenic niches of the postnatal brain. Thus, the loss of TRPV1 in neural stem/progenitor cells disturbs differentiation and the growth potential of V-SVZ stem cells, suggesting that TRPV1 coordinates the coupling between proliferation and differentiation of neural precursors (Stock et al., 2014).

### Intracellular $\text{Ca}^{2+}$ Handling and $\text{Ca}^{2+}$ Signaling Pathways

Several studies have underlined that maintenance of NSCs and of their activity requires an appropriate handling of the ER  $\text{Ca}^{2+}$  reservoir. For instance, the  $\text{Ca}^{2+}$  waves that promote NSC self-renewal following injury are IP3-dependent (Kraft et al., 2017). Conversely, activation of the  $\text{Ca}^{2+}$  efflux from the ER by the pro-apoptotic protein Bax increased cell death, which was substantially hampered by siRNA-mediated suppression of IP3R expression (Shi et al., 2005). These data underscore the necessity of a strict handling of  $\text{Ca}^{2+}$  for keeping the NSC population.

CaBP also play essential roles in modulation of NSC activity. Among these, NFAT, especially the NFATc1 and NFATc3 isoforms, is expressed in newborn rodent V-SVZ cell cultures (Serrano-Pérez et al., 2015). Interestingly, the recruitment of NFAT occurred only in response to local  $\text{Ca}^{2+}$  signals obtained following SOC activation but not global  $\text{Ca}^{2+}$  transients, illustrating that specific  $\text{Ca}^{2+}$  patterns are required

for selective responses (Somasundaram et al., 2014). Analysis of NFAT function showed that the NFAT inhibitor VIVIT slowed cell cycle in NSCs and reduced their ability to differentiate (Serrano-Pérez et al., 2015). Yet, a possible involvement of NFAT for keeping a multipotential stem cell state, that has been observed in embryonic stem cells (MacDougall et al., 2019), remains to be investigated. Noteworthy,  $\text{Ca}^{2+}$  buffering proteins may also control stemness as it has been shown that S100B expression is associated with a loss of NSC potential of GFAP-expressing cells (Raponi et al., 2007).

In addition, a wide transcriptomic study in migrating neuroblasts isolated from the RMS identified the calmodulin signaling network as one of the four up-regulated networks in these cells (Khodosevich et al., 2009). Silencing *in vivo* the expression of specific genes of this network, namely calmodulin (*calm1*) and CamKinase (*CamK4*), conducted to a decrease in the numbers of neuroblasts that reached the olfactory bulb, indicating that calmodulin and its effector are essential players for neuroblast migration (Khodosevich et al., 2009).

## PHYSIOPATHOLOGICAL ROLES OF $\text{Ca}^{2+}$ IN GSCs

Alterations in the  $\text{Ca}^{2+}$  toolkit have been reported in human tissues resected from glioblastoma, with increased expressions of TRPC (C1, C6) and TRPV (V1, V2) channels as compared to normal tissue (Alptekin et al., 2015). Transcriptomic analysis of GSCs unveiled that  $\text{Ca}^{2+}$  channels and signaling pathways, that elicit vital cell functions in response to extracellular cues, are enriched in GSCs, as compared to more mature non-stem glioblastoma cells that express more  $\text{Ca}^{2+}$  buffers (Wee et al., 2014). Such alterations most likely lead to modified  $\text{Ca}^{2+}$  homeostasis and  $\text{Ca}^{2+}$  codes that subsequently, may trigger tumorigenic behavior. In accordance, the epigenetic drugs that increase stemness of GSCs modify the  $\text{Ca}^{2+}$  signaling pathway (Wang et al., 2018). Interestingly, a screen of a chemical library of 72 ion channel blockers identified that 10 drugs among the 12 drugs capable of reducing GSC viability act on  $\text{Ca}^{2+}$ -related signaling networks, supporting that  $\text{Ca}^{2+}$  channels or transporters may be appealing targets in GSCs (Niklasson et al., 2017).

In the following sections, we will examine the involvement of the  $\text{Ca}^{2+}$  toolkit in GSCs by reviewing first the implication of plasma membrane channels and then, the function of intracellular  $\text{Ca}^{2+}$  handling and signaling pathways. An overview of the  $\text{Ca}^{2+}$  proteins expressed and their functions in GSCs is provided in **Figure 4** and summarized in **Table 1**.

## Plasma Membrane Channels

### Voltage-Gated Calcium Channels (VGCCs)

T-type voltage-gated  $\text{Ca}^{2+}$  channels ( $\text{Cav}3.2$ ) whose overexpression has been associated with a worse prognosis, have been found enriched in GSCs of glioblastoma as compared to either non-GSC-tumor cells or normal tissue (Wee et al., 2014; Zhang et al., 2017). Hypoxia, known to promote resistance to anticancer therapies, increased expression of the  $\text{Cav}3.2$  VGCC in GSCs. Conversely, treatment with

mibefradil, a FDA-approved inhibitor of  $\text{Cav}3.2$  that is used to treat hypertension, substantially reduced the GSC population by promoting their differentiation and reducing their viability (Niklasson et al., 2017; Zhang et al., 2017). This effect was mimicked by RNAi-mediated attenuation of  $\text{Cav}3.2$  expression (Zhang et al., 2017). Because resistance to treatments represents a major hurdle in current oncology, the fact that oral administration of mibefradil in mice xenografted with GSCs sensitized them to temozolomide treatment and prolonged survival of mice, opens new perspectives to improve the therapies against glioblastoma (Zhang et al., 2017). Among the mechanisms that may underpin these effects, it has been proposed that T-Type blockers compromise GSC survival by blocking the  $\text{Ca}^{2+}$  influx required to recruit  $\text{Ca}^{2+}$ -dependent  $\text{K}^{+}$  channels (KCa) whose activity is mandatory for the maintenance of cell polarity. This induces cell depolarization, thereby precluding the  $\text{Na}^{+}$ -dependent transport of nutrients and ultimately leading to starvation (Niklasson et al., 2017).

### Store-Operated Channels (SOCs)

SOCE is a ubiquitous  $\text{Ca}^{2+}$  influx that occurs in a wide range of cells, in response to numerous extracellular signals. During a characterization of the set of genes involved in  $\text{Ca}^{2+}$  signal generation differentially expressed in brain tumors and normal tissue, genes related to SOCE were found to be strongly perturbed, and one of the major actors of SOC, Orai 1, was disclosed as one of the genes whose expression is up-regulated in glioblastoma tissues and in GSCs (Robil et al., 2015). Already involved in promoting invasion capacities of glioblastoma cells (Motiani et al., 2013), Orai1 and/or SOC that are highly expressed in GSCs, could preserve or expand the population of GSCs. Indeed, inhibition of SOC channels with SKF-96365 reduced cell proliferation of GSCs and induced a quiescent transcriptomic signature in these cells (Aulestia et al., 2018). Altogether, these data suggest that SOCs may be pivotal for glioblastoma initiation, expansion, infiltration of the normal tissue and tumor relapse.

### Ligand-Gated Ion Channels (LGICs)

As for NSCs, AMPA receptors have been detected at high concentrations in GSCs, as compared to the differentiated non-stem tumor cells (Oh et al., 2012; Wee et al., 2014). Two elegant studies recently established that AMPA receptors expressed by human glioma cells, cultured in stem cell conditions, mediate tumor cell interactions with surrounding neurons through authentic neuron-glioma glutamatergic synapses. It was shown that neuronal activity-mediated release of glutamate drives glioma progression by promoting glioma growth and invasion through  $\text{Ca}^{2+}$ -dependent mechanisms involving AMPA receptors (Venkataramani et al., 2019; Venkatesh et al., 2019).

A screen of chemical libraries identified the nicotinic receptor antagonist, atracurium besylate, as a small molecule that effectively inhibits the clonogenic capacity and induces astroglial differentiation of patient-derived GSCs. Conversely, a nicotinic receptor agonist prevented atracurium besylate ability to reduce GSC self-renewal. Furthermore, this study showed that the survival of mice xenotransplanted with GSCs pretreated with atracurium besylate was significantly improved, suggesting that

blockade of nicotinic cholinergic receptors may reduce GSC stemness and/or cell population (Spina et al., 2016).

Extracellular nucleotides found in the microenvironment also contribute to defining GSC activity. Indeed, it has been shown that as compared to more differentiated tumoral cells, GSCs release tenfold more extracellular adenosine (Torres et al., 2019) that may act as autocrine/paracrine ligand to activate G-protein-coupled P2Y1R purinergic receptors or ionotropic purinergic P2X7R receptors to respectively promote or restrain GSC proliferation (D'Alimonte et al., 2015).

### TRPV Channels

Analysis of TRPV1 and TRPV2 expression showed that they are up-regulated in glioblastoma as compared to normal tissue (Alptekin et al., 2015). Studies of their possible functions demonstrated that the vanilloid receptor TRPV1 triggers tumor cell death in glioblastoma cells. Of interest it was shown that endovanilloids (TRPV1 ligands) are secreted by the NSCs that migrate to the tumor mass, and that the oncostatic effect that NSCs exert on the tumor involves the release of endovanilloids (Stock et al., 2014). TRPV2 on the other hand, reduces GSC stemness. Indeed, overexpression of TRPV2 was found to diminish GSC proliferation and promote their differentiation as glial cells both *in vitro* and *in vivo* in mice xenografted with TRPV2-overexpressing GSCs (Morelli et al., 2012).

### Intracellular Ca<sup>2+</sup> Handling and Ca<sup>2+</sup> Signaling Pathways

Ca<sup>2+</sup> stores of intracellular organelles, the ER and mitochondria, seem also involved in modulating GSC properties, particularly in the acquisition of a quiescent phenotype, which allows GSCs to escape from current anti-cancer therapies. The involvement of IP3R has been found following the discovery of a selective cytotoxic agent called bisacodyl that was picked out during the screening of the chemical Prestwick library for its power of eradication of quiescent GSCs (Zenou et al., 2015). Consecutive studies disclosed that this drug acts on IP3R to block Ca<sup>2+</sup> efflux from the ER (Dong et al., 2017). Thus, the maintenance of the quiescence in GSCs and resistance to chemotherapies may rely on a specific handling of Ca<sup>2+</sup> from the ER. In addition to ER, mitochondrial management of Ca<sup>2+</sup> may be involved in the control of GSC stem cell state. In support of this hypothesis, transcriptomic analysis of the Ca<sup>2+</sup> toolbox underlined an up-regulated expression of the mitochondrial Ca<sup>2+</sup> transporter MCU and of the Ca<sup>2+</sup>/Na<sup>+</sup> exchanger SLC8A3 in GSCs (Robil et al., 2015). Subsequently, it was described that proliferating cells have more sustained Ca<sup>2+</sup> signals than quiescent GSCs and that these changes in Ca<sup>2+</sup> responses are associated with mitochondrial remodeling, suggesting that mitochondrial Ca<sup>2+</sup> might control quiescence of GSCs although this hypothesis needs to be experimentally challenged (Aulestia et al., 2018).

CaBP have also been involved in GSC stemness. Specifically, the levels of S100A4 expression have been identified as an independent prognostic indicator of glioma patient survival, the worse prognosis being associated with up-regulated S100A4 expression in patients with glioblastoma of the

mesenchymal molecular subgroup (Chow et al., 2017). Further analysis showed that S100A4-expressing cells are enriched with GSCs and are required for GSC self-renewal and survival. Selective ablation of the S100A4-expressing cells in genetically engineered mice that form spontaneous gliomas was sufficient to compromise tumor growth (Chow et al., 2017).

Ca<sup>2+</sup>-dependent signaling pathways also contribute to GSC stemness or activity. Indeed, a recent study showed that NFAT1 expression is upregulated in GSCs as compared to more differentiated glioma cells. NFAT1 knockdown compromised GSC viability, impaired their self-renewal and migration abilities *in vitro*, and inhibited tumorigenesis *in vivo*. Conversely, NFAT1 overexpression promoted glioma growth through a mechanism involving the neurodevelopment protein 1-like 1 (NDEL1) that with NFAT1, controlled the maintenance of a naive stem cell state in GSCs (Jiang et al., 2019). In addition, NFAT2 may also represents a possible regulator of GSCs, especially of the mesenchymal glioblastoma subtype where it drives invasion and clonogenicity and promotes tumor growth through the regulation of HDAC1 (Song et al., 2020).

### CONCLUDING REMARKS

Our review highlights a central role of Ca<sup>2+</sup> in both NSCs and GSCs, which is correlated to prominence of Ca<sup>2+</sup>-related transcripts in both cell types. Indeed, NSCs and GSCs possess, each, a specific Ca<sup>2+</sup> toolkit that allows to maintain Ca<sup>2+</sup> homeostasis and to encode specific Ca<sup>2+</sup> signals in response to the numerous signals from their microenvironment. Several functions of specific Ca<sup>2+</sup> components in NSCs and GSCs have been unveiled. Current available data underpins that stemness is controlled by VGCCs, SOCs and IP3Rs in NSCs while it is regulated by VGCCs, nicotinic receptors, TRPVs and NFAT in GSCs, indicating that there might be cell type specific effects of Ca<sup>2+</sup> toolkit components. Such differences may rely on either a differential expression of Ca<sup>2+</sup> toolkit elements that, in turn, generates differential responses, or on yet unexplored functions of specific Ca<sup>2+</sup> components in GSCs and NSCs, or both. It should also be kept in mind that the Ca<sup>2+</sup> signals produced in a cell not only depend on Ca<sup>2+</sup> release in the cytoplasm but also on its extrusion, a process that influences the spatial and temporal extent of the Ca<sup>2+</sup> signal. Concerning the pumps, whose activity shapes the Ca<sup>2+</sup> responses, little is known on their expression and functions in either NSCs or GSCs.

*In vivo*, cells evolve in microenvironments with multiple extracellular cues, many of which elicit Ca<sup>2+</sup> signals and control cellular activities. Thus, it will be of importance to understand how the different signals are integrated and conduct to a specific Ca<sup>2+</sup> signal within each cell type. Along with this latter question, the downstream effectors recruited by the different Ca<sup>2+</sup> signals will require further investigation in order to understand how the specific spatio-temporal and magnitude profiles of Ca<sup>2+</sup> signals select a cellular response. Reciprocally, it will be essential to understand the impact of the microenvironment and of pathological states on the remodeling of the Ca<sup>2+</sup> toolkit of

NSCs and GSCs, as it has been observed for endothelial cells (Lodola et al., 2012; Moccia et al., 2020).

An in-depth knowledge of the  $\text{Ca}^{2+}$  toolkit in both NSCs and GSCs will contribute to understand the impact of  $\text{Ca}^{2+}$  alterations or dysregulation during aging and disease and will help to develop pharmacological strategies to combat brain diseases. Indeed, the remodeling of intracellular  $\text{Ca}^{2+}$  homeostasis is considered as a cellular and molecular hallmark of brain aging (Kumar et al., 2009; Gheorghe et al., 2014; Mattson and Arumugam, 2018) and represents one of the earliest abnormalities in both the familial and sporadic forms of Alzheimer's disease (Alzheimer's Association Calcium Hypothesis Workgroup, 2017; Popugaeva et al., 2018). However, age-related changes of the  $\text{Ca}^{2+}$  toolkit have not been explored in the V-SVZ so far. Yet, some molecules targeting the  $\text{Ca}^{2+}$  toolkit are already being tested in clinical trials for the treatment of glioblastoma. Among them, carboxyamidotriazole that inhibits non-VGCCs and disrupts  $\text{Ca}^{2+}$ -mediated signal transduction, showed some promising results in a recent multicenter phase IB trial when

used in combination with temozolomide, prompting further deciphering of the roles of  $\text{Ca}^{2+}$  channels in GSCs and NSCs (Omuro et al., 2018).

## AUTHOR CONTRIBUTIONS

VC wrote the initial manuscript draft. VC, ET, ND, PA and BC revised and approved the manuscript. All authors contributed to the article and approved the submitted version.

## FUNDING

This work was funded by La Ligue Contre le Cancer Grand Ouest, Comités de la Vienne et des Deux Sèvres.

## ACKNOWLEDGMENTS

We thank La Ligue Contre le Cancer Grand Ouest, Comités de la Vienne et des Deux Sèvres for financial support.

## REFERENCES

- Ahlenius, H., Visan, V., Kokaia, M., Lindvall, O., and Kokaia, Z. (2009). Neural stem and progenitor cells retain their potential for proliferation and differentiation into functional neurons despite lower number in aged brain. *J. Neurosci.* 29, 4408–4419. doi: 10.1523/JNEUROSCI.6003-08.2009
- Alcantara Llaguno, S., Chen, J., Kwon, C.-H., Jackson, E. L., Li, Y., Burns, D. K., et al. (2009). Malignant astrocytomas originate from neural stem/progenitor cells in a somatic tumor suppressor mouse model. *Cancer Cell* 15, 45–56. doi: 10.1016/j.ccr.2008.12.006
- Alonso, M., Lepousez, G., Sebastien, W., Bardy, C., Gabellec, M.-M., Torquet, N., et al. (2012). Activation of adult-born neurons facilitates learning and memory. *Nat. Neurosci.* 15, 897–904. doi: 10.1038/nn.3108
- Alptekin, M., Eroglu, S., Tutar, E., Sencan, S., Geyik, M. A., Ulasli, M., et al. (2015). Gene expressions of TRP channels in glioblastoma multiforme and relation with survival. *Tumour Biol.* 36, 9209–9213. doi: 10.1007/s13277-015-3577-x
- Altman, J. (1963). Autoradiographic investigation of cell proliferation in the brains of rats and cats. *Anat. Rec.* 145, 573–591. doi: 10.1002/ar.1091450409
- Altman, J. (1969). Autoradiographic and histological studies of postnatal neurogenesis. IV. Cell proliferation and migration in the anterior forebrain, with special reference to persisting neurogenesis in the olfactory bulb. *J. Comp. Neurol.* 137, 433–457. doi: 10.1002/cne.901370404
- Altman, J., and Das, G. D. (1965). Autoradiographic and histological evidence of postnatal hippocampal neurogenesis in rats. *J. Comp. Neurol.* 124, 319–335. doi: 10.1002/cne.901240303
- Alzheimer's Association Calcium Hypothesis Workgroup. (2017). Calcium Hypothesis of Alzheimer's disease and brain aging: a framework for integrating new evidence into a comprehensive theory of pathogenesis. *Alzheimers Dement.* 13, 178.e17–182.e17. doi: 10.1016/j.jalz.2016.12.006
- Ambudkar, I. S., de Souza, L. B., and Ong, H. L. (2017). TRPC1, Orail, and STIM1 in SOCE: friends in tight spaces. *Cell Calcium* 63, 33–39. doi: 10.1016/j.ceca.2016.12.009
- Antigny, F., Sabourin, J., Saüch, S., Bernheim, L., Koenig, S., and Frieden, M. (2017). TRPC1 and TRPC4 channels functionally interact with STIM1L to promote myogenesis and maintain fast repetitive  $\text{Ca}^{2+}$  release in human myotubes. *Biochim. Biophys. Acta Mol. Cell Res.* 1864, 806–813. doi: 10.1016/j.bbamcr.2017.02.003
- Arvidsson, A., Collin, T., Kirik, D., Kokaia, Z., and Lindvall, O. (2002). Neuronal replacement from endogenous precursors in the adult brain after stroke. *Nat. Med.* 8, 963–970. doi: 10.1038/nm747
- Aulestia, F. J., Néant, I., Dong, J., Haiech, J., Kilhoffer, M.-C., Moreau, M., et al. (2018). Quiescence status of glioblastoma stem-like cells involves remodelling of  $\text{Ca}^{2+}$  signalling and mitochondrial shape. *Sci. Rep.* 8:9731. doi: 10.1038/s41598-018-28157-8
- Ávila-Medina, J., Calderón-Sánchez, E., González-Rodríguez, P., Monje-Quiroga, F., Rosado, J. A., Castellano, A., et al. (2016). Orail and TRPC1 proteins co-localize with CaV1.2 channels to form a signal complex in vascular smooth muscle cells. *J. Biol. Chem.* 291, 21148–21159. doi: 10.1074/jbc.M116.742171
- Bacigaluppi, M., Sferruzza, G., Butti, E., Ottoboni, L., and Martino, G. (2020). Endogenous neural precursor cells in health and disease. *Brain Res.* 1730:146619. doi: 10.1016/j.brainres.2019.146619
- Bao, S., Wu, Q., McLendon, R. E., Hao, Y., Shi, Q., Hjelmeland, A. B., et al. (2006). Glioma stem cells promote radioresistance by preferential activation of the DNA damage response. *Nature* 444, 756–760. doi: 10.1038/nature05236
- Barami, K. (2007). Biology of the subventricular zone in relation to gliomagenesis. *J. Clin. Neurosci.* 14, 1143–1149. doi: 10.1016/j.jocn.2007.04.009
- Barnes, N. M., Hales, T. G., Lummis, S. C. R., and Peters, J. A. (2009). The 5-HT3 receptor—the relationship between structure and function. *Neuropharmacology* 56, 273–284. doi: 10.1016/j.neuropharm.2008.08.003
- Bauer, R., Kaiser, M., and Stoll, E. (2014). A computational model incorporating neural stem cell dynamics reproduces glioma incidence across the lifespan in the human population. *PLoS One* 9:e111219. doi: 10.1371/journal.pone.0111219
- Bauer, S., Hay, M., Amilhon, B., Jean, A., and Moyse, E. (2005). *In vivo* neurogenesis in the dorsal vagal complex of the adult rat brainstem. *Neuroscience* 130, 75–90. doi: 10.1016/j.neuroscience.2004.08.047
- Beckervordersandforth, R., and Rolando, C. (2019). Untangling human neurogenesis to understand counteract brain disorders. *Curr. Opin. Pharmacol.* 50, 67–73. doi: 10.1016/j.coph.2019.12.002
- Beckervordersandforth, R., Tripathi, P., Ninkovic, J., Bayam, E., Lepier, A., Stempfhuber, B., et al. (2010). *in vivo* fate mapping and expression analysis reveals molecular hallmarks of prospectively isolated adult neural stem cells. *Cell Stem Cell* 7, 744–758. doi: 10.1016/j.stem.2010.11.017
- Bédard, A., and Parent, A. (2004). Evidence of newly generated neurons in the human olfactory bulb. *Dev. Brain Res.* 151, 159–168. doi: 10.1016/j.devbrainres.2004.03.021
- Bergmann, O., Liebl, J., Bernard, S., Alkass, K., Yeung, M. S. Y., Steier, P., et al. (2012). The age of olfactory bulb neurons in humans. *Neuron* 74, 634–639. doi: 10.1016/j.neuron.2012.03.030
- Bernier, P. J., Bédard, A., Vinet, J., Lévesque, M., and Parent, A. (2002). Newly generated neurons in the amygdala and adjoining cortex of adult primates. *Proc. Natl. Acad. Sci. U S A* 99, 11464–11469. doi: 10.1073/pnas.172403999

- Berridge, M. J. (1990). Calcium oscillations. *J. Biol. Chem.* 265, 9583–9586.
- Berridge, M. J. (2016). The inositol trisphosphate/calcium signaling pathway in health and disease. *Physiol. Rev.* 96, 1261–1296. doi: 10.1152/physrev.00006.2016
- Berridge, M. J., Bootman, M. D., and Roderick, H. L. (2003). Calcium signalling: dynamics, homeostasis and remodelling. *Nat. Rev. Mol. Cell Biol.* 4, 517–529. doi: 10.1038/nrm1155
- Boldrini, M., Fulmore, C. A., Tartt, A. N., Simeon, L. R., Pavlova, I., Poposka, V., et al. (2018). Human hippocampal neurogenesis persists throughout aging. *Cell Stem Cell* 22, 589.e5–599.e5. doi: 10.1016/j.stem.2018.03.015
- Bouab, M., Paliouras, G. N., Aumont, A., Forest-Bérard, K., and Fernandes, K. J. L. (2011). Aging of the subventricular zone neural stem cell niche: evidence for quiescence-associated changes between early and mid-adulthood. *Neuroscience* 173, 135–149. doi: 10.1016/j.neuroscience.2010.11.032
- Braun, N., Sévigny, J., Mishra, S. K., Robson, S. C., Barth, S. W., Gerstberger, R., et al. (2003). Expression of the ecto-ATPase NTPDase2 in the germinal zones of the developing and adult rat brain. *Eur. J. Neurosci.* 17, 1355–1364. doi: 10.1046/j.1460-9568.2003.02567.x
- Brousse, B., Magalon, K., Durbec, P., and Cayre, M. (2015). Region and dynamic specificities of adult neural stem cells and oligodendrocyte precursors in myelin regeneration in the mouse brain. *Biol. Open* 4, 980–992. doi: 10.1242/bio.012773
- Butti, E., Bacigaluppi, M., Chaabane, L., Ruffini, F., Brambilla, E., Berera, G., et al. (2019). Neural stem cells of the subventricular zone contribute to neuroprotection of the corpus callosum after cuprizone-induced demyelination. *J. Neurosci.* 39, 5481–5492. doi: 10.1523/JNEUROSCI.0227-18.2019
- Calzà, L., Giuliani, A., Fernandez, M., Pirondi, S., D'Intino, G., Aloe, L., et al. (2003). Neural stem cells and cholinergic neurons: regulation by immunolesion and treatment with mitogens, retinoic acid and nerve growth factor. *Proc. Natl. Acad. Sci. U S A* 100, 7325–7330. doi: 10.1016/j.neulet.2020.135403
- Capilla-Gonzalez, V., Cebrian-Silla, A., Guerrero-Cazares, H., Garcia-Verdugo, J. M., and Quiñones-Hinojosa, A. (2013). The generation of oligodendroglial cells is preserved in the rostral migratory stream during aging. *Front. Cell. Neurosci.* 7:147. doi: 10.3389/fncel.2013.00147
- Capilla-Gonzalez, V., Cebrian-Silla, A., Guerrero-Cazares, H., Garcia-Verdugo, J. M., and Quiñones-Hinojosa, A. (2014a). Age-related changes in astrocytic and ependymal cells of the subventricular zone. *Glia* 62, 790–803. doi: 10.1002/glia.22642
- Capilla-Gonzalez, V., Guerrero-Cazares, H., Bonsu, J. M., Gonzalez-Perez, O., Achanta, P., Wong, J., et al. (2014b). The subventricular zone is able to respond to a demyelinating lesion after localized radiation. *Stem Cells* 32, 59–69. doi: 10.1002/stem.1519
- Capilla-Gonzalez, V., Herranz-Pérez, V., and García-Verdugo, J. M. (2015). The aged brain: genesis and fate of residual progenitor cells in the subventricular zone. *Front. Cell. Neurosci.* 9:365. doi: 10.3389/fncel.2015.00365
- Catterall, W. A. (2011). Voltage-gated calcium channels. *Cold Spring Harb. Perspect. Biol.* 3:a003947. doi: 10.1101/cshperspect.a003947
- Catterall, W. A., Perez-Reyes, E., Snutch, T. P., and Striessnig, J. (2005). International union of pharmacology. XLVIII. Nomenclature and structure-function relationships of voltage-gated calcium channels. *Pharmacol. Rev.* 57, 411–425. doi: 10.1124/pr.57.4.5
- Cavaliere, F., Urra, O., Alberdi, E., and Matute, C. (2012). Oligodendrocyte differentiation from adult multipotent stem cells is modulated by glutamate. *Cell Death Dis.* 3:e268. doi: 10.1038/cddis.2011.144
- Chan, C. M., Aw, J. T. M., Webb, S. E., and Miller, A. L. (2016). SOCE proteins, STIM1 and Orai1, are localized to the cleavage furrow during cytokinesis of the first and second cell division cycles in zebrafish embryos. *Zygote* 24, 880–889. doi: 10.1017/S0967199416000216
- Charrier, C., Coronas, V., Fombonne, J., Roger, M., Jean, A., Krantic, S., et al. (2006). Characterization of neural stem cells in the dorsal vagal complex of adult rat by *in vivo* proliferation labeling and *in vitro* neurosphere assay. *Neuroscience* 138, 5–16. doi: 10.1016/j.neuroscience.2005.10.046
- Chen, J., Li, Y., Yu, T.-S., McKay, R. M., Burns, D. K., Kernie, S. G., et al. (2012). A restricted cell population propagates glioblastoma growth following chemotherapy. *Nature* 488, 522–526. doi: 10.1038/nature11287
- Chesnelong, C., Restall, I., and Weiss, S. (2019). Isolation and culture of glioblastoma brain tumor stem cells. *Methods Mol. Biol.* 1869, 11–21. doi: 10.1007/978-1-4939-8805-1\_2
- Chow, K.-H., Park, H. J., George, J., Yamamoto, K., Gallup, A. D., Graber, J. H., et al. (2017). S100A4 is a biomarker and regulator of glioma stem cells that is critical for mesenchymal transition in glioblastoma. *Cancer Res.* 77, 5360–5373. doi: 10.1158/0008-5472.CAN-17-1294
- Cooper-Kuhn, C. M., Winkler, J., and Kuhn, H. G. (2004). Decreased neurogenesis after cholinergic forebrain lesion in the adult rat. *J. Neurosci. Res.* 77, 155–165. doi: 10.1002/jnr.20116
- Curtis, M. A., Kam, M., Nannmark, U., Anderson, M. F., Axell, M. Z., Wikkelso, C., et al. (2007). Human neuroblasts migrate to the olfactory bulb via a lateral ventricular extension. *Science* 315, 1243–1249. doi: 10.1126/science.1136281
- D'Alimonte, I., Nargi, E., Zuccarini, M., Lanuti, P., Di Iorio, P., Giuliani, P., et al. (2015). Potentiation of temozolomide antitumor effect by purine receptor ligands able to restrain the *in vitro* growth of human glioblastoma stem cells. *Purinergic Signal.* 11, 331–346. doi: 10.1007/s11302-015-9454-7
- Darcy, D. P., and Isaacson, J. S. (2009). L-type calcium channels govern calcium signaling in migrating newborn neurons in the postnatal olfactory bulb. *J. Neurosci.* 29, 2510–2518. doi: 10.1523/JNEUROSCI.5333-08.2009
- Daynac, M., Chicheportiche, A., Pineda, J. R., Gauthier, L. R., Boussin, F. D., and Mouthon, M.-A. (2013). Quiescent neural stem cells exit dormancy upon alteration of GABAAR signaling following radiation damage. *Stem Cell Res.* 11, 516–528. doi: 10.1016/j.scr.2013.02.008
- De Koninck, P., and Schulman, H. (1998). Sensitivity of CaM kinase II to the frequency of Ca<sup>2+</sup> oscillations. *Science* 279, 227–230. doi: 10.1126/science.279.5348.227
- Déliot, N., and Constantin, B. (2015). Plasma membrane calcium channels in cancer: alterations and consequences for cell proliferation and migration. *Biochim. Biophys. Acta* 1848, 2512–2522. doi: 10.1016/j.bbamem.2015.06.009
- Demars, M., Hu, Y.-S., Gadadhar, A., and Lazarov, O. (2010). Impaired neurogenesis is an early event in the etiology of familial Alzheimer's disease in transgenic mice. *J. Neurosci. Res.* 88, 2103–2117. doi: 10.1002/jnr.22387
- Desai, P. N., Zhang, X., Wu, S., Janoshazi, A., Bolimuntha, S., Putney, J. W., et al. (2015). Multiple types of calcium channels arising from alternative translation initiation of the Orai1 message. *Sci. Signal.* 8:ra74. doi: 10.1126/scisignal.aaa8323
- Dietrich, A., Kalwa, H., Rost, B. R., and Gudermann, T. (2005). The diacylglycerol-sensitive TRPC3/6/7 subfamily of cation channels: functional characterization and physiological relevance. *Pflugers Arch.* 451, 72–80. doi: 10.1007/s00424-005-1460-0
- Doetsch, F., Caillé, I., Lim, D. A., García-Verdugo, J. M., and Alvarez-Buylla, A. (1999a). Subventricular zone astrocytes are neural stem cells in the adult mammalian brain. *Cell* 97, 703–716. doi: 10.1016/s0092-8674(00)80783-7
- Doetsch, F., García-Verdugo, J. M., and Alvarez-Buylla, A. (1999b). Regeneration of a germinal layer in the adult mammalian brain. *Proc. Natl. Acad. Sci. U S A* 96, 11619–11624. doi: 10.1073/pnas.96.20.11619
- Doetsch, F., García-Verdugo, J. M., and Alvarez-Buylla, A. (1997). Cellular composition and three-dimensional organization of the subventricular germinal zone in the adult mammalian brain. *J. Neurosci.* 17, 5046–5061. doi: 10.1523/JNEUROSCI.17-13-05046.1997
- Dolmetsch, R. E., Xu, K., and Lewis, R. S. (1998). Calcium oscillations increase the efficiency and specificity of gene expression. *Nature* 392, 933–936. doi: 10.1038/31960
- Domenichini, F., Terrié, E., Arnault, P., Harnois, T., Magaud, C., Bois, P., et al. (2018). Store-operated calcium entries control neural stem cell self-renewal in the adult brain subventricular zone. *Stem Cells* 36, 761–774. doi: 10.1002/stem.2786
- Dong, J., Aulestia, F. J., Assad Kahn, S., Zeniou, M., Dubois, L. G., El-Habr, E. A., et al. (2017). Bisacodyl and its cytotoxic activity on human glioblastoma stem-like cells. Implication of inositol 1,4,5-trisphosphate receptor dependent calcium signaling. *Biochim. Biophys. Acta Mol. Cell Res.* 1864, 1018–1027. doi: 10.1016/j.bbamcr.2017.01.010
- Eriksson, P. S., Perfilieva, E., Björk-Eriksson, T., Alborn, A. M., Nordborg, C., Peterson, D. A., et al. (1998). Neurogenesis in the adult human hippocampus. *Nat. Med.* 4, 1313–1317. doi: 10.1038/3305

- Ernst, A., Alkass, K., Bernard, S., Salehpour, M., Perl, S., Tisdale, J., et al. (2014). Neurogenesis in the striatum of the adult human brain. *Cell* 156, 1072–1083. doi: 10.1016/j.cell.2014.01.044
- Etxeberria, A., Mangin, J.-M., Aguirre, A., and Gallo, V. (2010). Adult-born SVZ progenitors receive transient glutamatergic synapses during remyelination of the corpus callosum. *Nat. Neurosci.* 13, 287–289. doi: 10.1038/nn.2500
- Fewtrell, C. (1993).  $\text{Ca}^{2+}$  oscillations in non-excitable cells. *Annu. Rev. Physiol.* 55, 427–454. doi: 10.1146/annurev.ph.55.030193.002235
- Friedmann-Morvinski, D., Bushong, E. A., Ke, E., Soda, Y., Marumoto, T., Singer, O., et al. (2012). Dedifferentiation of neurons and astrocytes by oncogenes can induce gliomas in mice. *Science* 338, 1080–1084. doi: 10.1126/science.1226929
- Galli, R., Binda, E., Orfanelli, U., Cipelletti, B., Gritti, A., De Vitis, S., et al. (2004). Isolation and characterization of tumorigenic, stem-like neural precursors from human glioblastoma. *Cancer Res.* 64, 7011–7021. doi: 10.1158/0008-5472.CAN-04-1364
- García, G. C. T., and Dhermain, F. G. (2018). The subventricular zone concept: ready for therapeutic implications? *Neurooncology* 20, 1423–1424. doi: 10.1093/neuonc/noy147
- García, A. D. R., Doan, N. B., Imura, T., Bush, T. G., and Sofroniew, M. V. (2004). GFAP-expressing progenitors are the principal source of constitutive neurogenesis in adult mouse forebrain. *Nat. Neurosci.* 7, 1233–1241. doi: 10.1038/nn1340
- García-González, D., Khodosevich, K., Watanabe, Y., Rollenhagen, A., Lübke, J. H. R., and Monyer, H. (2017). Serotonergic projections govern postnatal neuroblast migration. *Neuron* 94, 534.e9–549.e9. doi: 10.29252/ibj.24.5.263
- Genzen, J. R., Platel, J.-C., Rubio, M. E., and Bordey, A. (2009). Ependymal cells along the lateral ventricle express functional P2X(7) receptors. *Purinergic Signal.* 5, 299–307. doi: 10.1007/s11302-009-9143-5
- Gheorghe, M., Snoeck, M., Emmerich, M., Bäck, T., Goeman, J. J., and Raz, V. (2014). Major aging-associated RNA expressions change at two distinct age-positions. *BMC Genomics* 15:132. doi: 10.1186/1471-2164-15-132
- Gheusi, G., Cremer, H., McLean, H., Chazal, G., Vincent, J. D., and Lledo, P. M. (2000). Importance of newly generated neurons in the adult olfactory bulb for odor discrimination. *Proc. Natl. Acad. Sci. U S A* 97, 1823–1828. doi: 10.1073/pnas.97.4.1823
- Gheusi, G., and Lledo, P.-M. (2014). Adult neurogenesis in the olfactory system shapes odor memory and perception. *Prog. Brain Res.* 208, 157–175. doi: 10.1016/B978-0-444-63350-7.00006-1
- Ginisty, A., Gély-Pernot, A., Abaamrane, L., Morel, F., Arnault, P., Coronas, V., et al. (2015). Evidence for a subventricular zone neural stem cell phagocytic activity stimulated by the vitamin K-dependent factor protein S. *Stem Cells* 33, 515–525. doi: 10.1002/stem.1862
- Giorgi-Gerevini, V. D., Melchiorri, D., Battaglia, G., Ricci-Vitiani, L., Ciceroni, C., Busceti, C. L., et al. (2005). Endogenous activation of metabotropic glutamate receptors supports the proliferation and survival of neural progenitor cells. *Cell Death Differ.* 12, 1124–1133. doi: 10.1038/sj.cdd.4401639
- Glass, R., Synowitz, M., Kronenberg, G., Walzlein, J.-H., Markovic, D. S., Wang, L.-P., et al. (2005). Glioblastoma-induced attraction of endogenous neural precursor cells is associated with improved survival. *J. Neurosci.* 25, 2637–2646. doi: 10.1523/JNEUROSCI.5118-04.2005
- González-Cobos, J. C., Zhang, X., Zhang, W., Ruhle, B., Motiani, R. K., Schindl, R., et al. (2013). Store-independent Orai1/3 channels activated by intracrine leukotriene C4: role in neonatal hyperplasia. *Circ. Res.* 112, 1013–1025. doi: 10.1016/j.ejogrb.2020.06.039
- Gonzalez-Perez, O. (2012). Neural stem cells in the adult human brain. *Biol. Biomed. Rep.* 2, 59–69.
- Gould, E., Reeves, A. J., Fallah, M., Tanapat, P., Gross, C. G., and Fuchs, E. (1999). Hippocampal neurogenesis in adult Old World primates. *Proc. Natl. Acad. Sci. U S A* 96, 5263–5267. doi: 10.1073/pnas.96.9.5263
- Gould, E., Tanapat, P., McEwen, B. S., Flügge, G., and Fuchs, E. (1998). Proliferation of granule cell precursors in the dentate gyrus of adult monkeys is diminished by stress. *Proc. Natl. Acad. Sci. U S A* 95, 3168–3171. doi: 10.1073/pnas.95.6.3168
- Guilak, F., Leddy, H. A., and Liedtke, W. (2010). Transient receptor potential vanilloid 4: the sixth sense of the musculoskeletal system? *Ann. N. Y. Acad. Sci.* 1192, 404–409. doi: 10.1111/j.1749-6632.2010.05389.x
- Gutova, M., Flores, L., Adhikarla, V., Tsaturyan, L., Tirughana, R., Aramburo, S., et al. (2019). Quantitative evaluation of intraventricular delivery of therapeutic neural stem cells to orthotopic glioma. *Front. Oncol.* 9:68. doi: 10.3389/fonc.2019.00068
- Harraz, O. F., and Altier, C. (2014). STIM1-mediated bidirectional regulation of  $\text{Ca}^{2+}$  entry through voltage-gated calcium channels (VGCC) and calcium-release activated channels (CRAC). *Front. Cell. Neurosci.* 8:43. doi: 10.3389/fncel.2014.00043
- Hofmann, T., Obukhov, A. G., Schaefer, M., Harteneck, C., Gudermann, T., and Schultz, G. (1999). Direct activation of human TRPC6 and TRPC3 channels by diacylglycerol. *Nature* 397, 259–263. doi: 10.1038/16711
- Hogan, P. G., Chen, L., Nardone, J., and Rao, A. (2003). Transcriptional regulation by calcium, calcineurin and NFAT. *Genes Dev.* 17, 2205–2232. doi: 10.1101/gad.1102703
- Holland, E. C., Celestino, J., Dai, C., Schaefer, L., Sawaya, R. E., and Fuller, G. N. (2000). Combined activation of Ras and Akt in neural progenitors induces glioblastoma formation in mice. *Nat. Genet.* 25, 55–57. doi: 10.1038/75596
- Huang, G. N., Zeng, W., Kim, J. Y., Yuan, J. P., Han, L., Muallem, S., et al. (2006). STIM1 carboxyl-terminus activates native SOC,  $\text{I}_{\text{Crac}}$  and TRPC1 channels. *Nat. Cell Biol.* 8, 1003–1010. doi: 10.1038/ncb1454
- Imura, T., Kornblum, H. I., and Sofroniew, M. V. (2003). The predominant neural stem cell isolated from postnatal and adult forebrain but not early embryonic forebrain expresses GFAP. *J. Neurosci.* 23, 2824–2832. doi: 10.1523/JNEUROSCI.23-07-02824.2003
- Jacques, T. S., Swales, A., Brzozowski, M. J., Henriquez, N. V., Linehan, J. M., Mirzadeh, Z., et al. (2010). Combinations of genetic mutations in the adult neural stem cell compartment determine brain tumour phenotypes. *EMBO J.* 29, 222–235. doi: 10.1038/emboj.2009.327
- Jardin, I., Lopez, J. J., Salido, G. M., and Rosado, J. A. (2008). Orai1 mediates the interaction between STIM1 and hTRPC1 and regulates the mode of activation of hTRPC1-forming  $\text{Ca}^{2+}$  channels. *J. Biol. Chem.* 283, 25296–25304. doi: 10.1074/jbc.M802904200
- Jarvis, M. F., and Khakh, B. S. (2009). ATP-gated P2X cation-channels. *Neuropharmacology* 56, 208–215. doi: 10.1016/j.neuropharm.2008.06.067
- Jiang, Y., Song, Y., Wang, R., Hu, T., Zhang, D., Wang, Z., et al. (2019). NFAT1-mediated regulation of NDEL1 promotes growth and invasion of glioma stem-like cells. *Cancer Res.* 79, 2593–2603. doi: 10.1158/0008-5472.CAN-18-3297
- Jin, K., Sun, Y., Xie, L., Peel, A., Mao, X. O., Bateau, S., et al. (2003). Directed migration of neuronal precursors into the ischemic cerebral cortex and striatum. *Mol. Cell. Neurosci.* 24, 171–189. doi: 10.1016/s1044-7431(03)00159-3
- Jin, K., Wang, X., Xie, L., Mao, X. O., and Greenberg, D. A. (2010). Transgenic ablation of doublecortin-expressing cells suppresses adult neurogenesis and worsens stroke outcome in mice. *Proc. Natl. Acad. Sci. U S A* 107, 7993–7998. doi: 10.1073/pnas.1000154107
- Jin, K., Wang, X., Xie, L., Mao, X. O., Zhu, W., Wang, Y., et al. (2006). Evidence for stroke-induced neurogenesis in the human brain. *Proc. Natl. Acad. Sci. U S A* 103, 13198–13202. doi: 10.1073/pnas.0603512103
- Kalamakis, G., Brüne, D., Ravichandran, S., Bolz, J., Fan, W., Ziebell, F., et al. (2019). Quiescence modulates stem cell maintenance and regenerative capacity in the aging brain. *Cell* 176, 1407–1419. doi: 10.1016/j.cell.2019.01.040
- Kempermann, G., Gage, F. H., Aigner, L., Song, H., Curtis, M., Thuret, S., et al. (2018). Human adult neurogenesis: evidence and remaining questions. *Cell Stem Cell* 23, 25–30. doi: 10.1016/j.stem.2018.04.004
- Khatri, P., Obernier, K., Simeonova, I. K., Hellwig, A., Hözl-Wenig, G., Mandl, C., et al. (2014). Proliferation and cilia dynamics in neural stem cells prospectively isolated from the SEZ. *Sci. Rep.* 4:3803. doi: 10.1038/srep03803
- Khodosevich, K., Seeburg, P. H., and Monyer, H. (2009). Major signaling pathways in migrating neuroblasts. *Front. Mol. Neurosci.* 2:7. doi: 10.3389/fncel.2014.00043
- Kokoeva, M. V., Yin, H., and Flier, J. S. (2005). Neurogenesis in the hypothalamus of adult mice: potential role in energy balance. *Science* 310, 679–683. doi: 10.1126/science.1115360
- Kong, H., Fan, Y., Xie, J., Ding, J., Sha, L., Shi, X., et al. (2008). AQP4 knockout impairs proliferation, migration and neuronal differentiation of adult neural stem cells. *J. Cell. Sci.* 121, 4029–4036. doi: 10.1242/jcs.035758

- Kornack, D. R., and Rakic, P. (1999). Continuation of neurogenesis in the hippocampus of the adult macaque monkey. *Proc. Natl. Acad. Sci. U S A* 96, 5768–5773. doi: 10.1073/pnas.96.10.5768
- Kornack, D. R., and Rakic, P. (2001). The generation, migration and differentiation of olfactory neurons in the adult primate brain. *Proc. Natl. Acad. Sci. U S A* 98, 4752–4757. doi: 10.1073/pnas.081074998
- Kraft, A., Jubal, E. R., von Laer, R., Döring, C., Rocha, A., Grebbin, M., et al. (2017). Astrocytic calcium waves signal brain injury to neural stem and progenitor cells. *Stem Cell Rep.* 8, 701–714. doi: 10.1016/j.stemcr.2017.01.009
- Kumar, A., Bodhinathan, K., and Foster, T. C. (2009). Susceptibility to calcium dysregulation during brain aging. *Front. Aging Neurosci.* 1:2. doi: 10.3389/neuro.24.002.2009
- Lacar, B., Young, S. Z., Platel, J.-C., and Bordey, A. (2011). Gap junction-mediated calcium waves define communication networks among murine postnatal neural progenitor cells. *Eur. J. Neurosci.* 34, 1895–1905. doi: 10.1111/j.1460-9568.2011.07901.x
- Lazarov, O., and Marr, R. A. (2013). Of mice and men: neurogenesis, cognition and Alzheimer's disease. *Front. Aging Neurosci.* 5:43. doi: 10.3389/fnagi.2013.00043
- Lee, J. H., Lee, J. E., Kahng, J. Y., Kim, S. H., Park, J. S., Yoon, S. J., et al. (2018). Human glioblastoma arises from subventricular zone cells with low-level driver mutations. *Nature* 560, 243–247. doi: 10.1038/s41586-018-0389-3
- Lee, K. P., Yuan, J. P., So, I., Worley, P. F., and Muallem, S. (2010). STIM1-dependent and STIM1-independent function of transient receptor potential canonical (TRPC) channels tunes their store-operated mode. *J. Biol. Chem.* 285, 38666–38673. doi: 10.1074/jbc.M110.155036
- Leeson, H. C., Kasherman, M. A., Chan-Ling, T., Lovelace, M. D., Brownlie, J. C., Toppinen, K. M., et al. (2018). P2X7 receptors regulate phagocytosis and proliferation in adult hippocampal and SVZ neural progenitor cells: implications for inflammation in neurogenesis. *Stem Cells* 36, 1764–1777. doi: 10.1002/stem.2894
- Liberati, S., Morelli, M. B., Amantini, C., Santoni, M., Nabissi, M., Cardinali, C., et al. (2014). Advances in transient receptor potential vanilloid-2 channel expression and function in tumor growth and progression. *Curr. Protein Pept. Sci.* 15, 732–737. doi: 10.2174/1389203715666140704115913
- Lim, D. A., and Alvarez-Buylla, A. (2016). The adult ventricular-subventricular zone (V-SVZ) and olfactory bulb (OB) neurogenesis. *Cold Spring. Harb. Perspect. Biol.* 8:a018820. doi: 10.1101/cshperspect.a018820
- Lindberg, N., Kastemar, M., Olofsson, T., Smits, A., and Uhrbom, L. (2009). Oligodendrocyte progenitor cells can act as cell of origin for experimental glioma. *Oncogene* 28, 2266–2275. doi: 10.1038/onc.2009.76
- Lintschinger, B., Balzer-Geldsetzer, M., Baskaran, T., Graier, W. F., Romanin, C., Zhu, M. X., et al. (2000). Coassembly of Trp1 and Trp3 proteins generates diacylglycerol- and Ca<sup>2+</sup>-sensitive cation channels. *J. Biol. Chem.* 275, 27799–27805. doi: 10.1074/jbc.M002705200
- Liu, C., Sage, J. C., Miller, M. R., Verhaak, R. G. W., Hippenmeyer, S., Vogel, H., et al. (2011). Mosaic analysis with double markers reveals tumor cell of origin in glioma. *Cell* 146, 209–221. doi: 10.1016/j.cell.2011.06.014
- Liu, X., Bandyopadhyay, B. C., Singh, B. B., Groschner, K., and Ambudkar, I. S. (2005a). Molecular analysis of a store-operated and 2-acetyl-sn-glycerol-sensitive non-selective cation channel. Heteromeric assembly of TRPC1-TRPC3. *J. Biol. Chem.* 280, 21600–21606. doi: 10.1074/jbc.C400492200
- Liu, X., Wang, Q., Haydar, T. F., and Bordey, A. (2005b). Nonsynaptic GABA signaling in postnatal subventricular zone controls proliferation of GFAP-expressing progenitors. *Nat. Neurosci.* 8, 1179–1187. doi: 10.1038/nn1522
- Lledo, P.-M., and Valley, M. (2016). Adult olfactory bulb neurogenesis. *Cold Spring Harb. Perspect. Biol.* 8:a018945. doi: 10.1101/cshperspect.a018945
- Lodge, D. (2009). The history of the pharmacology and cloning of ionotropic glutamate receptors and the development of idiosyncratic nomenclature. *Neuropharmacology* 56, 6–21. doi: 10.1016/j.neuropharm.2008.08.006
- Lodola, F., Laforenza, U., Bonetti, E., Lim, D., Dragoni, S., Bottino, C., et al. (2012). Store-operated Ca<sup>2+</sup> entry is remodelled and controls *in vitro* angiogenesis in endothelial progenitor cells isolated from tumoral patients. *PLoS One* 7:e42541. doi: 10.1371/journal.pone.0042541
- Lois, C., and Alvarez-Buylla, A. (1994). Long-distance neuronal migration in the adult mammalian brain. *Science* 264, 1145–1148. doi: 10.1126/science.8178174
- Lois, C., García-Verdugo, J. M., and Alvarez-Buylla, A. (1996). Chain migration of neuronal precursors. *Science* 271, 978–981. doi: 10.1126/science.271.5251.978
- Lopez, J. J., Jardin, I., Sanchez-Collado, J., Salido, G. M., Smani, T., and Rosado, J. A. (2020). TRPC Channels in the SOCE Scenario. *Cells* 9:126. doi: 10.3390/cells9010126
- Lu, Z., Elliott, M. R., Chen, Y., Walsh, J. T., Klibanov, A. L., Ravichandran, K. S., et al. (2011). Phagocytic activity of neuronal progenitors regulates adult neurogenesis. *Nat. Cell Biol.* 13, 1076–1083. doi: 10.1038/ncb2299
- Luskin, M. B. (1993). Restricted proliferation and migration of postnatally generated neurons derived from the forebrain subventricular zone. *Neuron* 11, 173–189. doi: 10.1016/0896-6273(93)90281-u
- Lynch, J. W. (2009). Native glycine receptor subtypes and their physiological roles. *Neuropharmacology* 56, 303–309. doi: 10.1016/j.neuropharm.2008.07.034
- Macas, J., Nern, C., Plate, K. H., and Momma, S. (2006). Increased generation of neuronal progenitors after ischemic injury in the aged adult human forebrain. *J. Neurosci.* 26, 13114–13119. doi: 10.1523/JNEUROSCI.4667-06.2006
- MacDougall, M. S., Clarke, R., and Merrill, B. J. (2019). Intracellular Ca<sup>2+</sup> homeostasis and nuclear export mediate exit from naive pluripotency. *Cell Stem Cell* 25, 210.e6–224.e6. doi: 10.1016/j.stem.2019.04.015
- Martí-Fàbregas, J., Romaguera-Ros, M., Gómez-Pinedo, U., Martínez-Ramírez, S., Jiménez-Xarrié, E., Marín, R., et al. (2010). Proliferation in the human ipsilateral subventricular zone after ischemic stroke. *Neurology* 74, 357–365. doi: 10.2215/CJN.09330819
- Marumoto, T., Tashiro, A., Friedmann-Morvinski, D., Scadeng, M., Soda, Y., Gage, F. H., et al. (2009). Development of a novel mouse glioma model using lentiviral vectors. *Nat. Med.* 15, 110–116. doi: 10.1038/nm.1863
- Maslov, A. Y., Barone, T. A., Plunkett, R. J., and Pruitt, S. C. (2004). Neural stem cell detection, characterization, and age-related changes in the subventricular zone of mice. *J. Neurosci.* 24, 1726–1733. doi: 10.1523/JNEUROSCI.4608-03.2004
- Masyukov, A., Li, K., Su, X., Kovalchuk, Y., and Garaschuk, O. (2018). Spontaneous calcium transients in the immature adult-born neurons of the olfactory bulb. *Cell Calcium* 74, 43–52. doi: 10.1016/j.ceca.2018.06.001
- Matarredona, E. R., and Pastor, A. M. (2019). Neural stem cells of the subventricular zone as the origin of human glioblastoma stem cells. Therapeutic implications. *Front. Oncol.* 9:779. doi: 10.3389/fonc.2019.00779
- Mattson, M. P., and Arumugam, T. V. (2018). Hallmarks of brain aging: adaptive and pathological modification by metabolic states. *Cell Metab.* 27, 1176–1199. doi: 10.1016/j.cmet.2018.05.011
- Menn, B., García-Verdugo, J. M., Yashine, C., Gonzalez-Perez, O., Rowitch, D., and Alvarez-Buylla, A. (2006). Origin of oligodendrocytes in the subventricular zone of the adult brain. *J. Neurosci.* 26, 7907–7918. doi: 10.1523/JNEUROSCI.1299-06.2006
- Messemer, N., Kunert, C., Grohmann, M., Sobottka, H., Nieber, K., Zimmermann, H., et al. (2013). P2X7 receptors at adult neural progenitor cells of the mouse subventricular zone. *Neuropharmacology* 73, 122–137. doi: 10.1016/j.neuropharm.2013.05.017
- Migaud, M., Batailler, M., Segura, S., Duittoz, A., Franceschini, I., and Pillon, D. (2010). Emerging new sites for adult neurogenesis in the mammalian brain: a comparative study between the hypothalamus and the classical neurogenic zones. *Eur. J. Neurosci.* 32, 2042–2052. doi: 10.1111/j.1460-9568.2010.07521.x
- Mikoshiba, K. (2015). Role of IP3 receptor signaling in cell functions and diseases. *Adv. Biol. Regul.* 57, 217–227. doi: 10.1016/j.jbior.2014.10.001
- Millar, N. S., and Gotti, C. (2009). Diversity of vertebrate nicotinic acetylcholine receptors. *Neuropharmacology* 56, 237–246. doi: 10.1016/j.neuropharm.2008.07.041
- Mirzadeh, Z., Merkle, F. T., Soriano-Navarro, M., García-Verdugo, J. M., and Alvarez-Buylla, A. (2008). Neural stem cells confer unique pinwheel architecture to the ventricular surface in neurogenic regions of the adult brain. *Cell Stem Cell* 3, 265–278. doi: 10.1016/j.stem.2008.07.004
- Moccia, F., Negri, S., Faris, P., and Berra-Romani, R. (2020). Targeting the endothelial Ca<sup>2+</sup> toolkit to rescue endothelial dysfunction in obesity associated-hypertension. *Curr. Med. Chem.* 27, 240–257. doi: 10.2174/0929867326666190905142135
- Morelli, M. B., Nabissi, M., Amantini, C., Farfariello, V., Ricci-Vitiani, L., di Martino, S., et al. (2012). The transient receptor potential vanilloid-2 cation channel impairs glioblastoma stem-like cell proliferation and promotes differentiation. *Int. J. Cancer* 131, E1067–E1077. doi: 10.1002/ijc.27588

- Motiani, R. K., Abdullaev, I. F., and Trebak, M. (2010). A novel native store-operated calcium channel encoded by Orai3: selective requirement of Orai3 versus Orai1 in estrogen receptor-positive versus estrogen receptor-negative breast cancer cells. *J. Biol. Chem.* 285, 19173–19183. doi: 10.1074/jbc.M110.102582
- Motiani, R. K., Hyzinski-García, M. C., Zhang, X., Henkel, M. M., Abdullaev, I. F., Kuo, Y.-H., et al. (2013). STIM1 and Orai1 mediate CRAC channel activity and are essential for human glioblastoma invasion. *Pflugers Arch.* 465, 1249–1260. doi: 10.1007/s00424-013-1254-8
- Mudò, G., Belluardo, N., Mauro, A., and Fuxe, K. (2007). Acute intermittent nicotine treatment induces fibroblast growth factor-2 in the subventricular zone of the adult rat brain and enhances neuronal precursor cell proliferation. *Neuroscience* 145, 470–483. doi: 10.1016/j.neuroscience.2006.12.012
- Nait-Oumesmar, B., Picard-Riera, N., Kerninon, C., Decker, L., Seilhean, D., Höglinger, G. U., et al. (2007). Activation of the subventricular zone in multiple sclerosis: evidence for early glial progenitors. *Proc. Natl. Acad. Sci. U S A* 104, 4694–4699. doi: 10.1073/pnas.0606835104
- Narla, S. T., Klejbor, I., Birkaya, B., Lee, Y.-W., Morys, J., Stachowiak, E. K., et al. (2013). Activation of developmental nuclear fibroblast growth factor receptor 1 signaling and neurogenesis in adult brain by  $\alpha 7$  nicotinic receptor agonist. *Stem Cells Transl. Med.* 2, 776–788. doi: 10.5966/sctm.2012-0103
- Niklasson, M., Maddalo, G., Sramkova, Z., Mutlu, E., Wee, S., Sekyrova, P., et al. (2017). Membrane-depolarizing channel blockers induce selective glioma cell death by impairing nutrient transport and unfolded protein/amino acid responses. *Cancer Res.* 77, 1741–1752. doi: 10.1158/0008-5472.CAN-16-2274
- Nilius, B., and Appendino, G. (2013). Spices: the savory and beneficial science of pungency. *Rev. Physiol. Biochem. Pharmacol.* 164, 1–76. doi: 10.1007/112\_2013\_11
- Nguyen, L., Malgrange, B., Breuskin, I., Bettendorff, L., Moonen, G., Belachew, S., et al. (2003). Autocrine/paracrine activation of the GABA<sub>A</sub> receptor inhibits the proliferation of neurogenic polysialylated neural cell adhesion molecule-positive (PSA-NCAM+) precursor cells from postnatal striatum. *J. Neurosci.* 23, 3278–3294. doi: 10.1523/JNEUROSCI.23-08-03278.2003
- North, R. A. (2016). P2X receptors. *Philos. Trans. R. Soc. Lond. B Biol. Sci.* 371:20150427. doi: 10.1098/rstb.2015.0427
- Nottebohm, F. (1985). Neuronal replacement in adulthood. *Ann. N Y Acad. Sci.* 457, 143–161. doi: 10.1111/j.1749-6632.1985.tb20803.x
- Obernier, K., and Alvarez-Buylla, A. (2019). Neural stem cells: origin, heterogeneity and regulation in the adult mammalian brain. *Development* 146:dev156059. doi: 10.1242/dev.156059
- Obernier, K., Cebrian-Silla, A., Thomson, M., Parraguez, J. I., Anderson, R., Guinto, C., et al. (2018). Adult neurogenesis is sustained by symmetric self-renewal and differentiation. *Cell Stem Cell* 22, 221.e8–234.e8. doi: 10.1016/j.stem.2018.01.003
- Oh, M. C., Kim, J. M., Safaei, M., Kaur, G., Sun, M. Z., Kaur, R., et al. (2012). Overexpression of calcium-permeable glutamate receptors in glioblastoma derived brain tumor initiating cells. *PLoS One* 7:e47846. doi: 10.1371/journal.pone.0047846
- Olsen, R. W., and Sieghart, W. (2008). International Union of Pharmacology. LXX. Subtypes of gamma-aminobutyric acid(A) receptors: classification on the basis of subunit composition, pharmacology, and function. Update. *Pharmacol. Rev.* 60, 243–260. doi: 10.1124/pr.108.00505
- Omuro, A., Beal, K., McNeill, K., Young, R. J., Thomas, A., Lin, X., et al. (2018). Multicenter phase IB trial of carboxyamidotriazole orotate and temozolomide for recurrent and newly diagnosed glioblastoma and other anaplastic gliomas. *J. Clin. Oncol.* 36, 1702–1709. doi: 10.1200/JCO.2017.76.9992
- Ortega, F., Gascón, S., Masserdotti, G., Deshpande, A., Simon, C., Fischer, J., et al. (2013). Oligodendroglial and neurogenic adult subependymal zone neural stem cells constitute distinct lineages and exhibit differential responsiveness to Wnt signalling. *Nat. Cell Biol.* 15, 602–613. doi: 10.1038/ncb2736
- Paez-Gonzalez, P., Asrican, B., Rodriguez, E., and Kuo, C. T. (2014). Identification of distinct ChAT<sup>+</sup> neurons and activity-dependent control of postnatal SVZ neurogenesis. *Nat. Neurosci.* 17, 934–942. doi: 10.1038/nn.3734
- Palmer, T. D., Takahashi, J., and Gage, F. H. (1997). The adult rat hippocampus contains primordial neural stem cells. *Mol. Cell. Neurosci.* 8, 389–404. doi: 10.1006/mcne.1996.0595
- Paredes, M. F., James, D., Gil-Perotin, S., Kim, H., Cotter, J. A., Ng, C., et al. (2016). Extensive migration of young neurons into the infant human frontal lobe. *Science* 354:aaf7073. doi: 10.1126/science.aaf7073
- Parekh, A. B., and Putney, J. W. (2005). Store-operated calcium channels. *Physiol. Rev.* 85, 757–810. doi: 10.1152/physrev.00057.2003
- Parent, J. M., Vexler, Z. S., Gong, C., Derugin, N., and Ferriero, D. M. (2002). Rat forebrain neurogenesis and striatal neuron replacement after focal stroke. *Ann. Neurol.* 52, 802–813. doi: 10.1002/ana.10393
- Patapoutian, A., Tate, S., and Woolf, C. J. (2009). Transient receptor potential channels: targeting pain at the source. *Nat. Rev. Drug Discov.* 8, 55–68. doi: 10.1038/nrd2757
- Pedersen, S. F., and Nilius, B. (2007). Transient receptor potential channels in mechanosensing and cell volume regulation. *Methods Enzymol.* 428, 183–207. doi: 10.1016/S0076-6879(07)28010-3
- Peteanu, L., and Alvarez-Buylla, A. (2002). Maturation and death of adult-born olfactory bulb granule neurons: role of olfaction. *J. Neurosci.* 22, 6106–6113. doi: 10.1523/JNEUROSCI.22-14-06106.2002
- Petrić, D., Myoga, M. H., Grade, S., Gerkau, N. J., Pusch, M., Rose, C. R., et al. (2018). Epithelial sodium channel regulates adult neural stem cell proliferation in a flow-dependent manner. *Cell Stem Cell* 22, 865.e8–878.e8. doi: 10.1016/j.stem.2018.04.016
- Picard-Riera, N., Decker, L., Delarasse, C., Goude, K., Nait-Oumesmar, B., Liblau, R., et al. (2002). Experimental autoimmune encephalomyelitis mobilizes neural progenitors from the subventricular zone to undergo oligodendrogenesis in adult mice. *Proc. Natl. Acad. Sci. U S A* 99, 13211–13216. doi: 10.1073/pnas.192314199
- Platel, J. C., Dave, K. A., and Bordey, A. (2008). Control of neuroblast production and migration by converging GABA and glutamate signals in the postnatal forebrain. *J. Physiol.* 586, 3739–3743. doi: 10.1113/jphysiol.2008.155325
- Platel, J.-C., Dave, K. A., Gordon, V., Lacar, B., Rubio, M. E., and Bordey, A. (2010). NMDA receptors activated by subventricular zone astrocytic glutamate are critical for neuroblast survival prior to entering a synaptic network. *Neuron* 65, 859–872. doi: 10.1016/j.neuron.2010.03.009
- Ponti, G., Obernier, K., Guinto, C., Jose, L., Bonfanti, L., and Alvarez-Buylla, A. (2013). Cell cycle and lineage progression of neural progenitors in the ventricular-subventricular zones of adult mice. *Proc. Natl. Acad. Sci. U S A* 110, E1045–E1054. doi: 10.1073/pnas.1219563110
- Popugaeva, E., Pchitskaya, E., and Bezprozvanny, I. (2018). Dysregulation of intracellular calcium signaling in Alzheimer's disease. *Antioxid. Redox Signal.* 29, 1176–1188. doi: 10.1089/ars.2018.7506
- Portnow, J., Synold, T. W., Badie, B., Tirughana, R., Lacey, S. F., D'Apuzzo, M., et al. (2017). Neural stem cell-based anticancer gene therapy: a first-in-human study in recurrent high-grade glioma patients. *Clin. Cancer Res.* 23, 2951–2960. doi: 10.1158/1078-0432.CCR-16-1518
- Poteser, M., Graziani, A., Rosker, C., Eder, P., Derler, I., Kahr, H., et al. (2006). TRPC3 and TRPC4 associate to form a redox-sensitive cation channel. Evidence for expression of native TRPC3-TRPC4 heteromeric channels in endothelial cells. *J. Biol. Chem.* 281, 13588–13595. doi: 10.1074/jbc.M512205200
- Prevorskaya, N., Skryma, R., and Shuba, Y. (2010). Ion channels and the hallmarks of cancer. *Trends Mol. Med.* 16, 107–121. doi: 10.1016/j.molmed.2010.01.005
- Prevorskaya, N., Skryma, R., and Shuba, Y. (2018). Ion channels in cancer: are cancer hallmarks oncochannelopathies? *Physiol. Rev.* 98, 559–621. doi: 10.1152/physrev.00044.2016
- Puchaowicz, K., Tarnowski, M., Baranowska-Bosiacka, I., Chlubek, D., and Dziedzicko, V. (2014). P2X and P2Y receptors—role in the pathophysiology of the nervous system. *Int. J. Mol. Sci.* 15, 23672–23704. doi: 10.22203/eCM.v037a04
- Quiñones-Hinojosa, A., and Chaichana, K. (2007). The human subventricular zone: a source of new cells and a potential source of brain tumors. *Exp. Neurol.* 205, 313–324. doi: 10.1016/j.expneurol.2007.03.016
- Quiñones-Hinojosa, A., Sanai, N., Soriano-Navarro, M., Gonzalez-Perez, O., Mirzadeh, Z., Gil-Perotin, S., et al. (2006). Cellular composition and cytoarchitecture of the adult human subventricular zone: a niche of neural stem cells. *J. Comp. Neurol.* 494, 415–434. doi: 10.1039/d0cp04354k
- Raponi, E., Agenes, F., Delphin, C., Assard, N., Baudier, J., Legraverend, C., et al. (2007). S100B expression defines a state in which GFAP-expressing cells lose

- their neural stem cell potential and acquire a more mature developmental stage. *Glia* 55, 165–177. doi: 10.1002/glia.20445
- Recht, L., Jang, T., Savarese, T., and Litofsky, N. S. (2003). Neural stem cells and neuro-oncology: quo vadis? *J. Cell. Biochem.* 88, 11–19. doi: 10.1002/jcb.10208
- Reynolds, B. A., Tetzlaff, W., and Weiss, S. (1992). A multipotent EGF-responsive striatal embryonic progenitor cell produces neurons and astrocytes. *J. Neurosci.* 12, 4565–4574. doi: 10.1523/JNEUROSCI.12-11-04565.1992
- Roberts, J. C., Davis, J. B., and Benham, C. D. (2004). [3H]Resiniferatoxin autoradiography in the CNS of wild-type and TRPV1 null mice defines TRPV1 (VR-1) protein distribution. *Brain Res.* 995, 176–183. doi: 10.1016/j.brainres.2003.10.001
- Robil, N., Petel, F., Kilhoffer, M.-C., and Haiech, J. (2015). Glioblastoma and calcium signaling—analysis of calcium toolbox expression. *Int. J. Dev. Biol.* 59, 407–415. doi: 10.1387/ijdb.150200jh
- Sabourin, J., Harissh, R., Harnois, T., Magaud, C., Bourmeyster, N., Déliot, N., et al. (2012). Dystrophin/ $\alpha$ 1-syntrophin scaffold regulated PLC/PKC-dependent store-operated calcium entry in myotubes. *Cell Calcium* 52, 445–456. doi: 10.1016/j.ceca.2012.08.003
- Sabourin, J., Lamiche, C., Vandebrout, A., Magaud, C., Rivet, J., Cognard, C., et al. (2009). Regulation of TRPC1 and TRPC4 cation channels requires an  $\alpha$ 1-syntrophin-dependent complex in skeletal mouse myotubes. *J. Biol. Chem.* 284, 36248–36261. doi: 10.1074/jbc.M109.012872
- Samanta, K., and Parekh, A. B. (2017). Spatial  $\text{Ca}^{2+}$  profiling: decrypting the universal cytosolic  $\text{Ca}^{2+}$  oscillation. *J. Physiol.* 595, 3053–3062. doi: 10.1113/JP272860
- Sanai, N., Nguyen, T., Ihrie, R. A., Mirzadeh, Z., Tsai, H.-H., Wong, M., et al. (2011). Corridors of migrating neurons in human brain and their decline during infancy. *Nature* 478, 382–386. doi: 10.1038/nature10487
- Sanai, N., Tramontin, A. D., Quiñones-Hinojosa, A., Barbaro, N. M., Gupta, N., Kunwar, S., et al. (2004). Unique astrocyte ribbon in adult human brain contains neural stem cells but lacks chain migration. *Nature* 427, 740–744. doi: 10.1038/nature02301
- Santulli, G., Lewis, D., des Georges, A., Marks, A. R., and Frank, J. (2018). Ryanodine receptor structure and function in health and disease. *Subcell. Biochem.* 87, 329–352. doi: 10.1007/978-981-10-7757-9\_11
- Schwaller, B. (2010). Cytosolic  $\text{Ca}^{2+}$  buffers. *Cold Spring Harb. Perspect. Biol.* 2:a004051. doi: 10.1101/cshperspect.a004051
- Serrano-Pérez, M. C., Fernández, M., Neria, F., Berjón-Otero, M., Doncel-Pérez, E., Cano, E., et al. (2015). NFAT transcription factors regulate survival, proliferation, migration and differentiation of neural precursor cells. *Glia* 63, 987–1004. doi: 10.1097/QAD.00000000000002728
- Sharma, G. (2013). The dominant functional nicotinic receptor in progenitor cells in the rostral migratory stream is the  $\alpha$ 3 $\beta$ 4 subtype. *J. Neurophysiol.* 109, 867–872. doi: 10.1152/jn.00886.2012
- Shi, J., Parada, L. F., and Kernie, S. G. (2005). Bax limits adult neural stem cell persistence through caspase and IP3 receptor activation. *Cell Death Differ.* 12, 1601–1612. doi: 10.1038/sj.cdd.4401676
- Shin, D. M., Son, A., Park, S., Kim, M. S., Ahuja, M., and Muallem, S. (2016). The TRPCs, Orais and STIMs in ER/PM junctions. *Adv. Exp. Med. Biol.* 898, 47–66. doi: 10.1007/978-3-319-26974-0\_3
- Shook, B. A., Manz, D. H., Peters, J. J., Kang, S., and Conover, J. C. (2012). Spatiotemporal changes to the subventricular zone stem cell pool through aging. *J. Neurosci.* 32, 6947–6956. doi: 10.1523/JNEUROSCI.5987-11.2012
- Shuttleworth, T. J. (2009). Arachidonic acid, ARC channels and Orai proteins. *Cell Calcium* 45, 602–610. doi: 10.1016/j.ceca.2009.02.001
- Singh, S. K., Hawkins, C., Clarke, I. D., Squire, J. A., Bayani, J., Hide, T., et al. (2004). Identification of human brain tumour initiating cells. *Nature* 432, 396–401. doi: 10.1038/nature03128
- Skibinska-Kijek, A., Wisniewska, M. B., Gruszczynska-Biegala, J., Methner, A., and Kuznicki, J. (2009). Immunolocalization of STIM1 in the mouse brain. *Acta Neurobiol. Exp.* 69, 413–428.
- Snethen, H., Love, S., and Scolding, N. (2008). Disease-responsive neural precursor cells are present in multiple sclerosis lesions. *Regener. Med.* 3, 835–847. doi: 10.2217/17460751.3.6.835
- Sohn, J., Orosco, L., Guo, F., Chung, S.-H., Bannerman, P., Mills Ko, E., et al. (2015). The subventricular zone continues to generate corpus callosum and rostral migratory stream astroglia in normal adult mice. *J. Neurosci.* 35, 3756–3763. doi: 10.1523/JNEUROSCI.3454-14.2015
- Somasundaram, A., Shum, A. K., McBride, H. J., Kessler, J. A., Feske, S., Miller, R. J., et al. (2014). Store-operated CRAC channels regulate gene expression and proliferation in neural progenitor cells. *J. Neurosci.* 34, 9107–9123. doi: 10.1523/JNEUROSCI.0263-14.2014
- Song, Y., Jiang, Y., Tao, D., Wang, Z., Wang, R., Wang, M., et al. (2020). NFAT2-HDAC1 signaling contributes to the malignant phenotype of glioblastoma. *Neuro Oncol.* 22, 46–57. doi: 10.1093/neuonc/noz136
- Song, M., Yu, S. P., Mohamad, O., Cao, W., Wei, Z. Z., Gu, X., et al. (2017). Optogenetic stimulation of glutamatergic neuronal activity in the striatum enhances neurogenesis in the subventricular zone of normal and stroke mice. *Neurobiol. Dis.* 98, 9–24. doi: 10.1016/j.nbd.2016.11.005
- Sorrells, S. F., Paredes, M. F., Cebrian-Silla, A., Sandoval, K., Qi, D., Kelley, K. W., et al. (2018). Human hippocampal neurogenesis drops sharply in children to undetectable levels in adults. *Nature* 555, 377–381. doi: 10.1038/nature25975
- Spalding, K. L., Bergmann, O., Alkass, K., Bernard, S., Salehpour, M., Huttner, H. B., et al. (2013). Dynamics of hippocampal neurogenesis in adult humans. *Cell* 153, 1219–1227. doi: 10.1016/j.cell.2013.05.002
- Spina, R., Voss, D. M., Asnaghi, L., Sloan, A., and Bar, E. E. (2016). Atracurium Besylate and other neuromuscular blocking agents promote astroglial differentiation and deplete glioblastoma stem cells. *Oncotarget* 7, 459–472. doi: 10.18632/oncotarget.6314
- Stafford, M. R., Bartlett, P. F., and Adams, D. J. (2007). Purinergic receptor activation inhibits mitogen-stimulated proliferation in primary neurospheres from the adult mouse subventricular zone. *Mol. Cell. Neurosci.* 35, 535–548. doi: 10.1016/j.mcn.2007.04.013
- Stock, K., Garthe, A., de Sassi, F. A., Glass, R., Wolf, S. A., and Kettenmann, H. (2014). The capsaicin receptor TRPV1 as a novel modulator of neural precursor cell proliferation. *Stem Cells* 32, 3183–3195. doi: 10.1002/stem.1805
- Stupp, R., Mason, W. P., van den Bent, M. J., Weller, M., Fisher, B., Taphoorn, M. J. B., et al. (2005). Radiotherapy plus concomitant and adjuvant temozolomide for glioblastoma. *N. Eng. J. Med.* 352, 987–996. doi: 10.1056/NEJMoa043330
- Sun, F., Wang, X., Mao, X., Xie, L., and Jin, K. (2012). Ablation of neurogenesis attenuates recovery of motor function after focal cerebral ischemia in middle-aged mice. *PLoS One* 7:e46326. doi: 10.1371/journal.pone.0046326
- Suyama, S., Sunabori, T., Kanki, H., Sawamoto, K., Gachet, C., Koizumi, S., et al. (2012). Purinergic signaling promotes proliferation of adult mouse subventricular zone cells. *J. Neurosci.* 32, 9238–9247. doi: 10.1523/JNEUROSCI.4001-11.2012
- Tanwar, J., Arora, S., and Motiani, R. K. (2020). Orai3: Oncochannel with therapeutic potential. *Cell Calcium* 90:102247. doi: 10.1016/j.ceca.2020.102247
- Tejada Neyra, M. A., Neuberger, U., Reinhardt, A., Brugnara, G., Bonekamp, D., Sill, M., et al. (2018). Voxel-wise radiogenomic mapping of tumor location with key molecular alterations in patients with glioma. *Neuro Oncol.* 20, 1517–1524. doi: 10.1093/neuonc/noy134
- Tepavčević, V., Lazarini, F., Alfaro-Cervello, C., Kerninon, C., Yoshikawa, K., García-Verdugo, J. M., et al. (2011). Inflammation-induced subventricular zone dysfunction leads to olfactory deficits in a targeted mouse model of multiple sclerosis. *J. Clin. Invest.* 121, 4722–4734. doi: 10.1016/j.healthpol.2012.03.004
- Terri, E., Coronas, V., and Constantin, B. (2019). Role of the calcium toolkit in cancer stem cells. *Cell Calcium* 80, 141–151. doi: 10.1016/j.ceca.2019.05.001
- Tominaga, M. (2007). “The role of TRP channels in thermosensation,” in *TRP Ion Channel Function in Sensory Transduction and Cellular Signaling Cascades*, eds. W. B. Liedtke and S. Heller (Boca Raton, FL: CRC Press/Taylor and Francis). Available online at: <http://www.ncbi.nlm.nih.gov/books/NBK5244/>. Accessed August 19, 2020.
- Tong, C. K., Han, Y.-G., Shah, J. K., Obernier, K., Guinto, C. D., and Alvarez-Buylla, A. (2014). Primary cilia are required in a unique subpopulation of neural progenitors. *Proc. Natl. Acad. Sci. U S A* 111, 12438–12443. doi: 10.1073/pnas.1321425111
- Torres, Á., Erices, J. I., Sanchez, F., Ehrenfeld, P., Turchi, L., Virolle, T., et al. (2019). Extracellular adenosine promotes cell migration/invasion of glioblastoma stem-like cells through A3 adenosine receptor activation under hypoxia. *Cancer Lett.* 446, 112–122. doi: 10.1016/j.canlet.2019.01.004

- Vaeth, M., Yang, J., Yamashita, M., Zee, I., Eckstein, M., Knosp, C., et al. (2017). ORAI2 modulates store-operated calcium entry and T cell-mediated immunity. *Nat. Commun.* 8:14714. doi: 10.1038/ncomms14714
- Vazquez, G., Lievreumont, J. P., St J Bird, G., and Putney, J. W. (2001). Human Trp3 forms both inositol trisphosphate receptor-dependent and receptor-independent store-operated cation channels in DT40 avian B lymphocytes. *Proc. Natl. Acad. Sci. U S A* 98, 11777–11782. doi: 10.1073/pnas.201238198
- Venkatachalam, K., Zheng, F., and Gill, D. L. (2003). Regulation of canonical transient receptor potential (TRPC) channel function by diacylglycerol and protein kinase C. *J. Biol. Chem.* 278, 29031–29040. doi: 10.1074/jbc.M302751200
- Venkataramani, V., Tanev, D. I., Strahle, C., Studier-Fischer, A., Fankhauser, L., Kessler, T., et al. (2019). Glutamatergic synaptic input to glioma cells drives brain tumour progression. *Nature* 573, 532–538. doi: 10.1038/s41586-019-1564-x
- Venkatesh, H. S., Morishita, W., Geraghty, A. C., Silverbush, D., Gillespie, S. M., Arzt, M., et al. (2019). Electrical and synaptic integration of glioma into neural circuits. *Nature* 573, 539–545. doi: 10.1038/s41586-019-1563-y
- Wang, C., Liu, F., Liu, Y.-Y., Zhao, C.-H., You, Y., Wang, L., et al. (2011). Identification and characterization of neuroblasts in the subventricular zone and rostral migratory stream of the adult human brain. *Cell Res.* 21, 1534–1550. doi: 10.1038/cr.2011.83
- Wang, F., Wang, A. Y., Chesnelong, C., Yang, Y., Nabbi, A., Thalappilly, S., et al. (2018). ING5 activity in self-renewal of glioblastoma stem cells via calcium and follicle stimulating hormone pathways. *Oncogene* 37, 286–301. doi: 10.1038/onc.2017.324
- Wang, J., Fu, X., Zhang, D., Yu, L., Li, N., Lu, Z., et al. (2017a). ChAT-positive neurons participate in subventricular zone neurogenesis after middle cerebral artery occlusion in mice. *Behav. Brain Res.* 316, 145–151. doi: 10.1016/j.bbr.2016.09.007
- Wang, J., Lu, Z., Fu, X., Zhang, D., Yu, L., Li, N., et al. (2017b). Alpha-7 nicotinic receptor signaling pathway participates in the neurogenesis induced by ChAT-positive neurons in the subventricular zone. *Transl. Stroke Res.* doi: 10.1007/s12975-017-0541-7 [Epub ahead of print].
- Wang, J., Xu, C., Zheng, Q., Yang, K., Lai, N., Wang, T., et al. (2017c). Orai1, 2, 3 and STIM1 promote store-operated calcium entry in pulmonary arterial smooth muscle cells. *Cell Death Discov.* 3:17074. doi: 10.1038/cddiscovery.2017.74
- Wee, S., Niklasson, M., Marinescu, V. D., Segerman, A., Schmidt, L., Hermansson, A., et al. (2014). Selective calcium sensitivity in immature glioma cancer stem cells. *PLoS One* 9:e115698. doi: 10.1371/journal.pone.0115698
- Weiss, S., Dunne, C., Hewson, J., Wohl, C., Wheatley, M., Peterson, A. C., et al. (1996). Multipotent CNS stem cells are present in the adult mammalian spinal cord and ventricular neuroaxis. *J. Neurosci.* 16, 7599–7609. doi: 10.1523/JNEUROSCI.16-23-07599.1996
- Westerlund, U., Svensson, M., Moe, M. C., Varghese, M., Gustavsson, B., Wallstedt, L., et al. (2005). Endoscopically harvested stem cells: a putative method in future autotransplantation. *Neurosurgery* 57, 779–784.
- Xing, Y. L., Röth, P. T., Stratton, J. A. S., Chuang, B. H. A., Danne, J., Ellis, S. L., et al. (2014). Adult neural precursor cells from the subventricular zone contribute significantly to oligodendrocyte regeneration and remyelination. *J. Neurosci.* 34, 14128–14146. doi: 10.1523/JNEUROSCI.3491-13.2014
- Yáñez, M., Gil-Longo, J., and Campos-Toimil, M. (2012). Calcium binding proteins. *Adv. Exp. Med. Biol.* 740, 461–482. doi: 10.1007/978-94-007-2888-2\_19
- Yeast, R. E., Emrich, S. M., Zhang, X., Xin, P., Johnson, M. T., Fike, A. J., et al. (2020). The native ORAI channel trio underlies the diversity of  $\text{Ca}^{2+}$  signaling events. *Nat. Commun.* 11:2444. doi: 10.1038/s41467-020-16232-6
- Yoo, S., and Blackshaw, S. (2018). Regulation and function of neurogenesis in the adult mammalian hypothalamus. *Prog. Neurobiol.* 170, 53–66. doi: 10.1016/j.pneurobio.2018.04.001
- Young, S. Z., Platel, J.-C., Nielsen, J. V., Jensen, N. A., and Bordey, A. (2010). GABA<sub>A</sub> increases calcium in subventricular zone astrocyte-like cells through L- and T-type voltage-gated calcium channels. *Front. Cell. Neurosci.* 4:8. doi: 10.3389/fncel.2010.00008
- Yuan, J. P., Zeng, W., Huang, G. N., Worley, P. F., and Muallem, S. (2007). STIM1 heteromultimerizes TRPC channels to determine their function as store-operated channels. *Nat. Cell Biol.* 9, 636–645. doi: 10.1038/ncb1590
- Zarco, N., Norton, E., Quiñones-Hinojosa, A., and Guerrero-Cázares, H. (2019). Overlapping migratory mechanisms between neural progenitor cells and brain tumor stem cells. *Cell. Mol. Life Sci.* 76, 3553–3570. doi: 10.1007/s00018-019-03149-7
- Zeniou, M., Fève, M., Mameri, S., Dong, J., Salomé, C., Chen, W., et al. (2015). Chemical library screening and structure-function relationship studies identify bisacodyl as a potent and selective cytotoxic agent towards quiescent human glioblastoma tumor stem-like cells. *PLoS One* 10:e0134793. doi: 10.1371/journal.pone.0134793
- Zhang, Y., Cruickshanks, N., Yuan, F., Wang, B., Pahuski, M., Wulfkühle, J., et al. (2017). Targetable T-type calcium channels drive glioblastoma. *Cancer Res.* 77, 3479–3490. doi: 10.1158/0008-5472.CAN-16-2347
- Zhang, R., Zhang, Z., Wang, L., Wang, Y., Goussev, A., Zhang, L., et al. (2004). Activated neural stem cells contribute to stroke-induced neurogenesis and neuroblast migration toward the infarct boundary in adult rats. *J. Cereb. Blood Flow Metab.* 24, 441–448. doi: 10.1097/00004647-200404000-00009
- Zhao, D., Najbauer, J., Garcia, E., Metz, M. Z., Gutova, M., Glackin, C. A., et al. (2008). Neural stem cell tropism to glioma: critical role of tumor hypoxia. *Mol. Cancer Res.* 6, 1819–1829. doi: 10.1158/1541-7786.MCR-08-0146

**Conflict of Interest:** The authors declare that the research was conducted in the absence of any commercial or financial relationships that could be construed as a potential conflict of interest.

Copyright © 2020 Coronas, Terrié, Déliot, Arnault and Constantin. This is an open-access article distributed under the terms of the Creative Commons Attribution License (CC BY). The use, distribution or reproduction in other forums is permitted, provided the original author(s) and the copyright owner(s) are credited and that the original publication in this journal is cited, in accordance with accepted academic practice. No use, distribution or reproduction is permitted which does not comply with these terms.



# Store-Operated Calcium Channels in Physiological and Pathological States of the Nervous System

Isis Zhang and Huijuan Hu\*

Department of Anesthesiology, Rutgers New Jersey Medical School, Rutgers, The State University of New Jersey, Newark, NJ, United States

## OPEN ACCESS

### Edited by:

Francisco Javier Martin-Romero,  
University of Extremadura, Spain

### Reviewed by:

Lucia Nuñez,  
University of Valladolid, Spain  
Robert Kraft,  
Leipzig University, Germany

### \*Correspondence:

Huijuan Hu  
hh480@njms.rutgers.edu

### Specialty section:

This article was submitted to  
Cellular Neuropathology,  
a section of the journal  
Frontiers in Cellular Neuroscience

**Received:** 31 August 2020

**Accepted:** 03 November 2020

**Published:** 26 November 2020

### Citation:

Zhang I and Hu H (2020)  
Store-Operated Calcium Channels  
in Physiological and Pathological  
States of the Nervous System.  
*Front. Cell. Neurosci.* 14:600758.  
doi: 10.3389/fncel.2020.600758

Store-operated calcium channels (SOCs) are widely expressed in excitatory and non-excitatory cells where they mediate significant store-operated calcium entry (SOCE), an important pathway for calcium signaling throughout the body. While the activity of SOCs has been well studied in non-excitatory cells, attention has turned to their role in neurons and glia in recent years. In particular, the role of SOCs in the nervous system has been extensively investigated, with links to their dysregulation found in a wide variety of neurological diseases from Alzheimer's disease (AD) to pain. In this review, we provide an overview of their molecular components, expression, and physiological role in the nervous system and describe how the dysregulation of those roles could potentially lead to various neurological disorders. Although further studies are still needed to understand how SOCs are activated under physiological conditions and how they are linked to pathological states, growing evidence indicates that SOCs are important players in neurological disorders and could be potential new targets for therapies. While the role of SOCE in the nervous system continues to be multifaceted and controversial, the study of SOCs provides a potentially fruitful avenue into better understanding the nervous system and its pathologies.

**Keywords:** store-operated calcium channels, STIM, Orai1, nervous system, neuron, glia, Alzheimer's disease, pain

## INTRODUCTION

Store-operated calcium channels (SOCs) are calcium-selective cation channels that represent a major pathway for calcium signaling throughout the body. Due to their physical and functional connection to the endoplasmic reticulum (ER), SOCs play an important role in maintaining calcium homeostasis by inducing calcium entry after  $\text{Ca}^{2+}$  store depletion in the ER (Putney, 1986). This store-operated calcium entry (SOCE) drives a multitude of biological processes, including gene transcription, exocytosis, cell metabolism, and motility (Lewis, 2007). SOCs are composed of stromal interaction molecules (STIM1/2 proteins), which act as ER  $\text{Ca}^{2+}$  sensors, and Orai1/2/3 proteins, which form the structure of calcium release-activated calcium (CRAC) channels in the plasma membrane (Liou et al., 2005; Zhang et al., 2005; Gross et al., 2007; Wissenbach et al., 2007). Upon depletion of  $\text{Ca}^{2+}$  stores, STIM and Orai proteins migrate from their positions in the ER and PM, respectively, to form ER-PM junctions (Baba et al., 2003; Mercer et al., 2006). These junctions allow STIMs to bind to Orais, opening the channel to permit calcium entry. Reuptake of  $\text{Ca}^{2+}$  by sarco/ER  $\text{Ca}^{2+}$  ATPase (SERCA) leads to the end of SOCE, and STIMs and Orais return to their original locations (Alonso et al., 2012; Prakriya and Lewis, 2015). STIM2 also acts as a regulator in

this mechanism, sensing a small drop of  $\text{Ca}^{2+}$  concentration in the cell and regulating basal cytosol and ER calcium level (Berna-Erro et al., 2009).

Neurons possess a variety of ion channels, receptors, transporters, and plasma membrane  $\text{Ca}^{2+}$  ATPase that work together to maintain  $\text{Ca}^{2+}$  homeostasis. In neurons, voltage-gated calcium channels (VGCCs) and ligand-gated cation channels were thought to be the primary channels involved in  $\text{Ca}^{2+}$  homeostasis. While SOCs are well recognized as the principal route of  $\text{Ca}^{2+}$  entry in non-excitable cells, SOCE was considered as a residual calcium entry in neurons and its function was neglected. Some early studies show that SOCs are not involved in  $[\text{Ca}^{2+}]_i$  homeostasis/oscillations (Friel and Tsien, 1992; Nuñez et al., 1996). However, a growing body of evidence indicates that SOCs are also important in mediating  $\text{Ca}^{2+}$  influx in neurons from different brain regions, spinal cord, and dorsal root ganglion neurons (Emptage et al., 2001; Klejman et al., 2009; Gruszczynska-Biegala et al., 2011; Gao et al., 2013; Gruszczynska-Biegala and Kuznicki, 2013; Xia et al., 2014; Wei et al., 2017).

While Orais have been identified as key components of CRAC channels, the transient receptor potential (TRP) channels have also been suggested to be constituents of CRAC channels, in particular canonical TRP channel 1 (TRPC1) (Zhu et al., 1996; Zitt et al., 1996; Brough et al., 2001; Kim et al., 2009). TRPC1 has been shown to complex with STIM1 and Orai1 and have a role in the activation of SOCE (Ong et al., 2007; Cheng et al., 2008; Jardin et al., 2008; Nascimento Da Conceicao et al., 2019). However, TRPC channels' role in calcium entry is controversial. For example, while some studies show TRPC1 contributing to SOCE, the TRPC1 mediated currents did not resemble  $I_{\text{CRAC}}$  and did not reproduce the biophysical properties of  $I_{\text{CRAC}}$  (Ambudkar et al., 2017; Lopez et al., 2020). As such, while much of the research focusing on SOCE studies the interaction between STIM1, Orai1, and TRPC isoforms, the true contribution of these channels to calcium entry remains contested. Furthermore, the closely related subfamilies TRPV (vanilloid) and TRPM (melastatin) have also recently been shown to have involvement in calcium influx via SOCE (Authi, 2007; Ma et al., 2011; Harisseh et al., 2013; Liu X. et al., 2017; Bastián-Eugenio et al., 2019). Interestingly, a recent study showed TRPM7 channel kinase modulated SOCE, which suggests that while the activity of the channels helps maintain calcium homeostasis at rest, it is smaller domains within the channel that truly control calcium flux (Faouzi et al., 2017).

STIM and Orai proteins are widely expressed throughout the body, having important roles in various physiological processes and involvement in the pathological conditions of the major organ systems (McCarl et al., 2009; Kiviluoto et al., 2011; Selvaraj et al., 2012; Collins et al., 2013; Sun S. et al., 2014; Lacruz and Feske, 2015; Avila-Medina et al., 2018; Zhang et al., 2020). SOCs have been well studied in non-excitable cells. In recent years, attention has turned to their role in neurons and glia. All homologs of STIM and Orai are present in murine and human brain tissues (Gross et al., 2007; Berna-Erro et al., 2009; Skibinska-Kijek et al., 2009; Gruszczynska-Biegala et al., 2011). STIM1 and STIM2 are differentially expressed among mouse and human brain regions (Lein et al., 2007). Regional distribution of Orai mRNAs in the brain has only been done in mice. In

whole murine brain tissue, all three Orai family members are expressed, and Orai1 mRNA is less abundant than Orai2 and Orai3 mRNA (Gross et al., 2007; Lein et al., 2007; Takahashi et al., 2007). Orai2 is highly expressed in the spinal cord and DRG while Orai1 and Orai3 are expressed at a moderate and low level in the spinal cord and DRG, respectively (Xia et al., 2014; Wei et al., 2017; Dou et al., 2018). Orai1 protein is uniformly distributed throughout the human and rodent brain (Guzman et al., 2014). SOCs are functional in neurons and glia from different regions in the nervous system (Hartmann et al., 2014; Gao et al., 2016; Korkotian et al., 2017; Dou et al., 2018; Chen-Engerer et al., 2019; Stegner et al., 2019). Growing evidence shows that SOCs play an important role in neuronal signaling and plasticity, and have been implicated in neurological disorders (Kraft, 2015; Majewski and Kuznicki, 2015; Lu and Fivaz, 2016; Bollimuntha et al., 2017; Wu H. E. et al., 2018; Alvarez et al., 2020). In this review, we summarize the current understanding of the physiological role of SOCs in the nervous system by outlining their expression, molecular components, and functions in neurons from different brain regions and glial cells. We will also describe the multitude of pathologies that have been linked to dysregulation of SOCE in different types of nervous cells and discuss future directions of research.

## SOCS IN THE CEREBRAL CORTEX

### SOC Components and Functions in Cortical Neurons

The mouse cortex and cortical neurons express both STIM mRNAs with STIM2 being the predominant isoform (Lein et al., 2007; Chauvet et al., 2016). In the human cortex, STIM1 protein was found in medium level in the cerebral cortex (Uhlén et al., 2015). The mRNA expression of Orais is controversial. Chauvet et al. (2016) have reported that Orai2 is highly expressed in the mouse cortical neurons while Orai1 and Orai3 mRNA levels are low or undetectable. Conversely, González-Sánchez et al. (2017) have shown that all three Orai isoforms are expressed in cortical neurons with Orai1 being the predominant isoform. Orai1 mRNA and protein expression in cortical neurons was also demonstrated in cortical neurons by other groups (Gruszczynska-Biegala and Kuznicki, 2013; Secondo et al., 2019). A recent study has further confirmed the expression of three *Orai* genes (Bouron, 2020). Orai3 is the major isoform expressed at the embryonic days 11 (E11) stage and remains constant during corticogenesis. Going from E11 to post-natal day 1 (PN1), Orai2 is upregulated the most, becoming the most expressed Orai gene at the end of corticogenesis and postnatally. Interestingly, Orai1 has the lowest rate of expression throughout corticogenesis (Bouron, 2020).

Both STIM proteins are involved in calcium homeostasis in cortical neurons, STIM1 mainly activates SOCE, whereas STIM2 regulates resting  $\text{Ca}^{2+}$  levels (Gruszczynska-Biegala and Kuznicki, 2013). Cortical SOCE induced by thapsigargin (TG), a  $\text{Ca}^{2+}$ -ATPase inhibitor, is sensitive to Orai blockers, but not TRPC inhibitors (Chauvet et al., 2016), suggesting Orais mediate cortical SOCE. A recent study further confirmed that Orai2 is

a major contributor to neuronal SOCE in the cortex (Stegner et al., 2019). STIM2 and Orai1 form hetero-complexes in rat cortical neurons in response to a low extracellular calcium level, which implies that these proteins regulate basal intracellular calcium levels in these neurons (Gruszczynska-Biegala and Kuznicki, 2013). Furthermore, calcium homeostasis is key to normal cortical neuron functions (Ma et al., 2016; Wegierski and Kuznicki, 2018). SOCE has been found to regulate neuronal calcium homeostasis during cortical development (Guner et al., 2017). Moreover, previous studies have shown that STIM1 is engaged by metabotropic glutamate receptors (mGluR) and is a key regulator of mGluR1 related  $\text{Ca}^{2+}$  signaling (Hou et al., 2015; González-Sánchez et al., 2017). As such, the regulation of long term depression of cortical neurons has been linked to SOCE (González-Sánchez et al., 2017).

### SOCs in Acquired Brain Injury

$\text{Ca}^{2+}$  homeostasis alteration has been shown to contribute to secondary neuronal damage and altered physiology after traumatic brain injury (Weber, 2012). Given that cortical SOC components mediate  $\text{Ca}^{2+}$  entry and regulate calcium homeostasis, they may play a role in brain injury. A previous study has reported that STIM1 expression is significantly increased at both mRNA and protein levels following traumatic brain injury, and downregulation of STIM1 leads to increased preservation of neuronal viability and inhibition of apoptosis (Hou et al., 2015). Furthermore, STIM1 expression is increased in neurons in the early stages post diffuse axonal injury, indicating that abnormal SOCE may participate in  $\text{Ca}^{2+}$  overload of neurons (Li Y. et al., 2013). However, Rao et al. (2015) found that the expression of STIM2 but not STIM1 is increased in traumatic neuronal injury, and that downregulation of STIM2 but not STIM1 improved neuronal survival and preserved neurological function both *in vitro* and *in vivo*. The latter is consistent with a previous study that STIM2-deficient mice are protected from cerebral damage after ischemic stroke (Berna-Erro et al., 2009). More research into roles of STIMs in traumatic brain injury is therefore warranted.

Interestingly, in a rat model of ischemic stroke, Secondo et al. reported that STIM1 and Orai1 proteins were significantly decreased in the ipsilesional cortex. Similarly, STIM1 and Orai1 transcripts and proteins were also reduced after exposure of rat cortical neurons to oxygen and glucose deprivation for 3 h, leading to decreases in SOCE and CRAC currents (Secondo et al., 2019; La Russa et al., 2020). Silencing of STIM1 or Orai1 negated the effect of ischemic preconditioning, which would normally induce increased tolerance for ischemia, and lead to ER stress and increased neuronal death (Secondo et al., 2019), suggesting that Orai1-mediated SOCE is required for ischemic preconditioning. As such, STIM1 and Orai1 play a neuroprotective role post neural ischemic injury. In contrast to these findings, Stegner et al. (2019) found that Orai2 deficiency reduces  $\text{Ca}^{2+}$  accumulation and neuron death after exposure to oxygen and glucose deprivation and had a protective effect in a mouse model of ischemic stroke, indicating that disruption of this normal calcium response lowers calcium overload and thereby reduces neuronal damage in ischemic stroke. Although

both Orai1 and Orai2 contribute to SOCE, they play distinct roles in ischemic stroke. As such, further research into the mechanisms and effects of calcium flux in cortical neurons is essential in understanding their roles in stroke.

## SOCS IN THE HIPPOCAMPUS

### SOC Components and Functions in Hippocampal Neurons

The hippocampus has high STIM2 expression and low STIM1 level. Both STIM1 and STIM2 mediate SOCE in hippocampal neurons (Zhang et al., 2014, 2015; Ryazantseva et al., 2018). In hippocampal CA1 tissue, all three Orai homologs are expressed while Orai2 is expressed at the highest level (Chen-Engerer et al., 2019). Orai2 is selectively involved in  $\text{IP}_3$  sensitive calcium stores in the soma of CA1 pyramidal neurons (Chen-Engerer et al., 2019), suggesting an important role of Orai2 in neuronal SOCE in the CA1 region. Interestingly, Orai1 was found in a large proportion of dendritic spines while Orai2 was detected mainly in dendritic shafts but to a lesser extent in spines (Korkotian et al., 2017; Tshuva et al., 2017). The different spatial distribution of Orai1 and Orai2 may indicate distinct roles in hippocampal function.

Store-operated calcium entry is an important  $\text{Ca}^{2+}$  influx pathway and plays an important role in basic neuronal functions and  $\text{Ca}^{2+}$  homeostasis in hippocampal neurons (Emptage et al., 2001; Baba et al., 2003). Samtleben et al. (2015) found that free ER and cytosolic calcium in hippocampal neurons was lost continuously across the plasma membrane under transiently calcium-free conditions. Interestingly, when SOCE was inhibited, an immediate decline in ER calcium was observed, suggesting that SOC components counteract continuous loss of ER and cytosolic calcium and maintain basal  $\text{Ca}^{2+}$  levels in hippocampal neurons (Samtleben et al., 2015). In addition, Orai1 is preferentially localized in spines and helps regulate spine plasticity (Korkotian et al., 2014; Segal and Korkotian, 2016). This finding aligns with data that Orai1 plays a key role in synapse formation, maturation, and plasticity (Korkotian et al., 2017; Tshuva et al., 2017). Furthermore, STIM2 facilitates synaptic delivery and regulates activity-dependent changes in synaptic strength (Yap et al., 2017).

### SOCs in Epilepsy and Alzheimer's Disease

Due to their important role in  $\text{Ca}^{2+}$  signaling and neuronal plasticity, SOC components have been implicated in diseases related to hippocampal dysfunction. Steinbeck et al. (2011) found that STIM1 and STIM2 expression was increased in a rat model of chronic epilepsy. In hippocampal specimens from medial temporal lobe epilepsy patients, STIM1 and STIM2 were also elevated (Steinbeck et al., 2011). Pharmacologic inhibition of SOCE suppressed interictal spikes and rhythmizing epileptic burst activity (Steinbeck et al., 2011). Interestingly, Orai1 overexpression has also been found to cause seizure like events in aged female mice, suggesting that SOC dysfunction on its own

is a potential etiology for seizure and epilepsy (Maciag et al., 2019; Majewski et al., 2019).

Alzheimer's disease (AD) is a chronic neurodegenerative disease and the most common cause of dementia worldwide (Lane et al., 2018). AD has been linked to dysregulation of SOCs in hippocampal neurons (Raza et al., 2007; Popugava et al., 2015b). In long-term cultures reflecting aging neurons, there is remodeling of  $\text{Ca}^{2+}$  influx and efflux with downregulation of STIM1 and Orai1, increased expression of the mitochondrial  $\text{Ca}^{2+}$  uniporter and  $\text{Ca}^{2+}$  stores in these neurons, and enhanced  $\text{Ca}^{2+}$  release (Calvo-Rodríguez et al., 2016; Calvo-Rodríguez et al., 2020). Reduction in STIM1 expression has also been found in brain tissues of pathologically confirmed AD patients (Pascual-Caro et al., 2018). Furthermore, neuronal SOCE in postsynaptic spines plays a key role in stability of mushroom shaped "memory spines," the loss of which are indicative of a deficiency in synaptic communication (Sun S. et al., 2014; Ryskamp et al., 2019). This aligns with data that show in a murine model of AD, overexpression of STIM2 attenuates A $\beta$ 42 oligomers-induced mushroom spine loss *in vitro* and *in vivo* through maintenance of normal SOCE (Popugava et al., 2015a; Zhang et al., 2015, 2016). Presenilin 1 and presenilin 2 have been associated with Familial AD, another form of AD (Lanoiselée et al., 2017). Interestingly, in the PSEN1 $\Delta$ E9 mutation model of Familial AD, there is an increase in SOCE in postsynaptic spines in primary hippocampal cultures. Pharmacologic inhibition of SOCE rescued mushroom spine loss in hippocampal neurons (Chernyuk et al., 2019). These studies suggest that SOCs play a distinct role in different forms of AD.

## SOCS IN THE STRIATUM

### SOC Components and Functions in Striatal Medium Spiny Neurons (MSNs)

Western blot analysis revealed that the SOC proteins are expressed in medium spiny neurons (MSNs) (Wu J. et al., 2018). The molecular composition of SOCs in MSNs has not been well established. Kikuta et al. (2019) found strong expression of Orai2, moderate expression of Orai3, and sparse expression of Orai1 in striatal GABAergic neurons with strong expression of both STIM1 and STIM2. Interestingly, knockdown of STIM1, Orai1, or TRPC1 proteins leads to dramatic reduction of SOCE in MSNs (Vigont et al., 2015), indicating STIM1, Orai1, and TRPC1 mediate SOCE in MSNs. Additionally, a recent study demonstrates that deletion of TRPC1 largely reduced SOCE in MSNs (Wu J. et al., 2018), further indicating an important role of TRPC1 in MSN SOCE. In addition, SKF96365, a SOC and TRPC channel inhibitor, was found to reduce the frequency of spontaneous slow  $\text{Ca}^{2+}$  oscillations in these neurons, indicating the SOCE has a role in  $\text{Ca}^{2+}$  signaling in MSNs (Kikuta et al., 2019).

### SOCS in Huntington's Disease (HD)

Huntington's disease (HD) is the most common monogenic neurodegenerative disease (Ghosh and Tabrizi, 2018). Patients

develop motor, cognitive, and psychiatric symptoms in middle age, with continuous neurodegeneration until the end of their lives (Ghosh and Tabrizi, 2018; McColgan and Tabrizi, 2018). Mutant Huntingtin (mHtt) protein causes striatal neuron dysfunction, synaptic loss, and ultimately neurodegeneration in HD (McColgan and Tabrizi, 2018). Neuronal cells expressing mHtt show inhibition of the SOC pathway through binding of mHtt to the type 1 inositol (1,4,5)-trisphosphate receptor (InsP $_3$ R1), which increases the receptor's sensitivity to activation by InsP $_3$  (Wu et al., 2011; Vigont et al., 2014). The overactivity of this pathway is also in part because STIM2 expression is elevated in these neurons, which leads to further dysregulation of SOCE and spine loss in MSNs (Wu et al., 2016). Additionally, knockdown of TRPC1, TRPC6, Orai1, or Orai2 also shows protective effects on medium spiny neuron spines in HD model mice (Wu J. et al., 2018). As such, SOCs have been studied as a potential therapeutic target for HD, with the effect of the potential anti-HD drug EVP4593 on calcium regulation via these channels being investigated in recent years (Wu et al., 2016; Vigont et al., 2018).

## SOCS IN THE SUBSTANTIA NIGRA

### SOC Components and Functions in Dopaminergic (DA) Neurons

The protein expression of STIM1, Orai1, and several TRPC channels was observed and robust SOCE and SOC currents were recorded in dopaminergic (DA) neurons (Selvaraj et al., 2012; Sun et al., 2018). While the molecular identity of SOCE has not been conclusively identified in DA neurons, it has been reported that downregulation of STIM1 or TRPC1 leads to the loss of SOCE (Selvaraj et al., 2012; Sun et al., 2018), suggesting that SOCE is mediated by STIM1 and TRPC1 in DA neurons in the substantia nigra (Selvaraj et al., 2012).

### SOCS in Parkinson's Disease

Parkinson's disease is defined by death of DA neurons in the substantia nigra, which leads to the degeneration of motor skills and memory that is characteristic of the disease (Reich and Savitt, 2019).  $\text{Ca}^{2+}$  entry is crucial in regulation of mitochondrial oxidative phosphorylation in DA neurons (Surmeier et al., 2017). Interestingly,  $\text{Ca}^{2+}$  entry also drives basal mitochondrial oxidant stress in these neurons (Surmeier et al., 2017). SOCE in DA neurons regulates  $\text{Ca}^{2+}$  entry and activates the AKT/mTOR pathway, a known neuroprotective pathway in Parkinson's disease (Selvaraj et al., 2012). Additionally, in normal conditions, pacemaking activity in DA neurons is inhibited by the TRPC1-STIM1 complex (Sun et al., 2017). When neurotoxins mimicking Parkinson's disease were introduced in DA neurons, TRPC1 expression was targeted, increasing activity of L-type  $\text{Ca}^{2+}$  channels and caspases, leading to neurodegeneration (Sun et al., 2017). Furthermore, postmortem substantia nigra samples from Parkinson's disease individuals also showed decreased TRPC1 expression in the substantia nigra pars compacta region compared to non-Parkinson's disease individuals (Selvaraj et al., 2012).

## SOCs IN THE CEREBELLUM

### SOC Components and Functions in Purkinje and Granule Neurons

The mouse cerebellum expresses the highest level of STIM1 among all brain regions (Lein et al., 2007; Hartmann et al., 2014). In a human brain tissue study, STIM1 protein expression was found to be relatively high in the cerebellum (Uhlén et al., 2015). In mouse Purkinje neurons, STIM1 expression was more robust than that of STIM2 (Hartmann et al., 2014). All three Orai isoforms are detectable in the cerebellum and in Purkinje neurons, with Orai2 as the dominant isoform in Purkinje neurons (Hartmann et al., 2014). Interestingly, research has focused on STIM1 and Orai1 proteins, which appear to mediate SOCE in Purkinje neurons (Klejman et al., 2009). In Purkinje neurons, STIM1 controls glutamate receptor-dependent synaptic transmission and motor learning in mice (Hartmann et al., 2014). Ryu et al. (2017) found deletion of STIM1 delayed clearance of cytosolic  $\text{Ca}^{2+}$  during ongoing neuronal firing, reduced Purkinje neuronal excitability, and impaired intrinsic plasticity without affecting long term synaptic plasticity. Cerebellar granule cells also express STIM1 and SOC proteins are functional in these neurons (Singaravelu et al., 2008; Klejman et al., 2009). Although essential components of the SOCE pathway are not well characterized in granule cells, expression and pharmacological studies suggest that STIM1 and Orai1 may mediate granule SOCE (Singaravelu et al., 2008; Klejman et al., 2009).

### SOC in Motor Memory Consolidation

As discussed above, SOC proteins are important for maintaining cellular function in Purkinje cells. Defects in intrinsic plasticity of Purkinje neurons can lead to formation of aberrant neural plasticity in vestibular nucleus neurons, and thereby inhibition of SOCE can affect long-term storage of motor memory and lead to deficits in motor skills (Jang et al., 2020). Furthermore, STIM1 knockout mice showed severe memory consolidation deficiency in vestibulo-ocular reflex memory (Ryu et al., 2017). As intrinsic plasticity emerges as an important factor in information processing and memory formation, especially in Purkinje neurons, SOCE and its modulation of intrinsic plasticity may elucidate potential etiologies for motor abnormalities and memory loss (Shim et al., 2018). For example, given that impaired intrinsic plasticity or degeneration of Purkinje neurons is associated with ataxia and STIM1 knockdown is linked to impaired intrinsic plasticity (Ryu et al., 2017; Ady et al., 2018; Hoxha et al., 2018), deficiency of STIM1-mediated SOCE could be a potential cause of ataxia.

## SOCs IN THE DRG AND SPINAL CORD

### SOC Components and Functions in Spinal Cord Dorsal Horn and DRG Neurons

The spinal cord dorsal horn and dorsal root ganglia (DRG) act together to relay sensory information from the periphery to

the CNS (Cho, 2015). We and others have demonstrated that Orai1/2/3 and STIM1/2 are expressed in dorsal horn neurons, with STIM1, STIM2, and Orai1 acting as key mediators of SOCE (Guzman et al., 2014; Xia et al., 2014). In addition, we have shown that activation of Orai1 increases neuronal excitability and reduces A-type potassium channels in dorsal horn neurons (Dou et al., 2018).

We and others have also shown that the SOC proteins are also expressed in DRG (Gemes et al., 2011; Wei et al., 2017). STIM1, STIM2, Orai1, and Orai3 mediate SOCE in DRG neurons, with small and medium sized DRG neurons exhibiting more robust SOCE after  $\text{Ca}^{2+}$  depletion by TG (Wei et al., 2017). In particular, nociceptors including TRPV1-, TRPA1-, TRPM8-, and IB4-positive DRG neurons displayed greater SOCE than non-nociceptive neurons. In addition, in nociceptive DRG neurons, activation of SOC proteins by TG increases neuronal excitability while Orai1 and Orai3 double knock down abolished such effect (Wei et al., 2017), suggesting SOCE is an important  $\text{Ca}^{2+}$  influx pathway for nociceptors.

### SOCs in Pain

While the role of SOC proteins in pain is not completely understood, there is strong evidence that SOC proteins play an important role in modulating nociception and chronic pain (Gao et al., 2013, 2015; Qi et al., 2016). We have reported that pretreatment with YM-58483, a potent SOC inhibitor, reduced acute pain and prevented the development of CFA- or collagen-induced inflammatory pain. YM-58483 also attenuated thermal and mechanical hypersensitivity after inflammatory pain was established (Gao et al., 2013, 2015). Moreover, administration of YM-58483 diminished neuropathic pain induced by spared nerve injury, a well-established neuropathic pain model (Gao et al., 2013). Consistent with the pharmacological results, Orai1 deficiency significantly decreased acute pain induced by noxious stimuli, reduced intraplantar carrageenan injection-induced pain, and abolished the increase in neuronal excitability induced by TG (*in vitro*) and intraplantar carrageenan injection (recorded in spinal cord slices) (Dou et al., 2018). These data suggest that SOCE is an important player in nociception and inflammatory pain, and could potentially be used as a novel target for chronic pain.

## SOCs IN GLIAL CELLS

Glial cells play essential roles in brain homeostasis. There are three main types of glia in the CNS: astrocytes, microglia, and oligodendrocytes; all play distinct roles supporting neurons and their interconnections (Jessen, 2004). For astrocytes and microglia, the regulation of their activities is in part controlled by  $\text{Ca}^{2+}$  signaling and their own calcium homeostasis (Kettenmann et al., 2011; Shigetomi et al., 2019). The various immune pathways mediated by SOCE in astrocytes and microglia point to the importance of SOC proteins in modulating inflammation and CNS defense, as well as identify dysfunction of SOC proteins as potential causes for diseases of abnormal immunity and inflammation in the CNS.

## SOC Components and Functions in Astrocytes

The expression of STIM1/2 and Orai1/2/3 in astrocytes has been demonstrated by multiple groups (Jung et al., 2000; Lo et al., 2002; Singaravelu et al., 2006; Moreno et al., 2012; Gao et al., 2016; Kwon et al., 2017). It is well documented that SOCE can be induced in astrocytes in the central nervous system. In hippocampal astrocytes, CRAC channels regulate astrocyte  $\text{Ca}^{2+}$  signaling, gliotransmitter release, and astrocyte-mediated tonic inhibition of CA1 pyramidal neurons (Toth et al., 2019). In cortical astrocytes, STIM1 in combination with Orai1 and Orai3 mediates SOCE in a majority of cells (Moreno et al., 2012; Kwon et al., 2017). Similarly, in spinal astrocytes, STIM1, STIM2, and Orai1 were identified as primary mediators of SOCE (Gao et al., 2016). Retinal Müller glia also express STIMs and OraIs (Molnar et al., 2016). Double labeling results show that STIM1 (not STIM2) is predominantly found in Müller glia. Interestingly, SOCE is mediated by synergistic activation of TRPC and Orai channels in these cells (Molnar et al., 2016). Furthermore, a group developed a mathematical model for calcium flux in astrocytes, and reported that while  $\text{Ca}^{2+}$  influx levels through SOC in astrocytes are low, sustained calcium oscillations require SOC activation (Handy et al., 2017). As the intrinsic frequency of calcium oscillations is theorized to be important in regulating activities such as gliotransmission, SOC could be used as a potential modulator of these activities (De Pittà et al., 2009; Handy et al., 2017).

## SOC Components and Functions in Microglia

Microglial SOCE was first reported in mice (Toescu et al., 1998). Later studies have reported that SOCE is present in human microglia (Wang et al., 1999; McLarnon et al., 2000; Khoo et al., 2001; Hong et al., 2006). Multiple studies have demonstrated STIM1/2 and Orai1/2/3 are expressed and SOCE occurs in these cells (Kraft, 2015; Michaelis et al., 2015; Gilbert et al., 2016). STIM1 and Orai1 play a major role in microglial SOCE and SOC currents while STIM2 is less effective to activate SOCE than STIM1 (Michaelis et al., 2015; Lim et al., 2017). Functionally, SOC inhibition or ablation of STIM1, STIM2, or Orai1 has been shown to inhibit migration, phagocytosis, cytokine secretion, and NFAT1 activity (Ikeda et al., 2013; Heo et al., 2015; Michaelis et al., 2015; Lim et al., 2017).

## Glia SOC in CNS Diseases

Reactive astrocytes have been implicated in many CNS disorders, such as epilepsy, Alzheimer disease, Parkinson's disease, and multiple sclerosis (Glass et al., 2010; Brambilla et al., 2013; Devinsky et al., 2013). Spinal astrocytes have been recognized as active participants in chronic pain conditions (Ji et al., 2006; McMahon and Malcangio, 2009). We have shown that activation of SOC increases TNF- $\alpha$  and IL-6 production, while knockdown of STIM1 or Orai1 greatly attenuates cytokine production (Gao et al., 2016). Furthermore, knockdown of STIM2 and Orai1 decreases lipopolysaccharide-induced TNF- $\alpha$  and IL-6 production without altering viability of astrocytes

(Gao et al., 2016). These data suggest that SOC may represent potential therapeutic targets for neuroinflammation.

Store-operated calcium entry has been linked to the pathogenesis of glioblastoma multiforme (GBM), the highest grade glioma and most malignant astrocytoma (Motiani et al., 2013). In human glioblastoma cells, SOC function is largely enhanced compared to normal astrocytes (Kovacs et al., 2005). Multiple groups have found STIM1 and Orai1 knockdown lead to a dramatic decrease in cell invasion in GBM, as such STIM1 has been proposed as a potential target in GBM treatment (Liu et al., 2011; Li G. et al., 2013; Motiani et al., 2013). Interestingly, in a recent study, induction of SOCE suppressed GBM growth via inhibition of Hippo pathway transcriptional coactivators YAP/TAZ (Liu et al., 2019). Hence, more research is warranted to establish the role of SOC in GBM. Astrocyte  $\text{Ca}^{2+}$  activity also plays an important role in Rett syndrome disease progression. Dong et al. (2018) reported that spontaneous calcium activity is abnormal in RTT astrocytes *in vitro* and *in vivo*, which is caused by abnormal SOCE partially associated with elevated expression of TRPC4.

Microglial SOCE has been implicated in a variety of nervous system disorders as well. For example, AD microglia have significantly higher basal  $\text{Ca}^{2+}$  relative to microglia from non-AD people, and ATP- and PAF-induced SOCE is markedly reduced (McLarnon et al., 2005), indicating that microglia from AD patients have significant abnormalities in  $\text{Ca}^{2+}$  mediated signal transduction. Microglial SOC may also play a role in PD. Lu et al. (2019) used 1-methyl-4-phenylpyridinium (MPP), a metabolite of 1-Methyl-4-phenyl-1,2,3,6-tetrahydropyridine (MPTP, a mouse model of PD), to induce microgliosis and neuroinflammation and observed time-dependent upregulation of Orai1 and an increase of SOCE. A recent report suggests that microglial SOC are also involved in brain trauma. In a mouse model of brain trauma, inhibition of SOC decreases lesion size, brain hemorrhage, and improves neurological deficits associated with decreased microglial activation, and expression levels of iNOS, Orai1 and STIM1 (Mizuma et al., 2019). Moreover, in a model of helminth infection, there was negative regulation of TRPC1 and Orai1 mediated SOCE, which lead to inhibition of NF- $\kappa$ B and MAPK pathways in microglia (Sun Y. et al., 2014).

## DEVELOPMENT OF POTENTIAL THERAPIES

Store-operated calcium channels have been proposed as therapeutic drug targets for cancer, autoimmune, and inflammatory disorders (Stauderman, 2018; Feske, 2019; Khan et al., 2020). Great efforts have been made to identify potent and selective Orai1 inhibitors. Several compounds have entered clinical trials (Stauderman, 2018). However, challenges have been encountered in developing CRAC channel blockers that have high selectivity and low side effects due to their expression profile across major organ systems (Liu S. et al., 2017). While preclinical studies continue to identify more potent and selective compounds, new chemical scaffolds that target different components or new pharmacophores in the

SOC complex may offer great opportunities to develop better therapeutics. Drug development is even more challenging for treatments of CNS diseases because of the nervous system's complex and poor translation from animal models to human disease. As such, drug discovery of SOC inhibitors for CNS disorders is still in the early phase of target validation. To validate SOC as therapeutic targets for these diseases, we should also consider whether existing therapies modulate SOC. It has been reported that non-steroidal anti-inflammatory drugs (NSAIDs) sulindac, salicylate, and other NSAIDs including ibuprofen and indomethacin have been found to inhibit SOCE in colon cancer cells and in vascular smooth muscle cells (Muñoz et al., 2011; Hernández-Morales et al., 2017; Villalobos et al., 2019). It would be worthy to investigate whether these existing drugs can treat CNS disorders associated with neuroinflammation. Elucidating how these treatments interact with SOC can lend evidence to SOC modulators as potential treatments in these pathologies.

## DISCUSSION

Store-operated calcium channels are functional throughout the nervous system and regulate a wide variety of physiological processes (Table 1). While STIMs and Orais have been shown to have significant expression in many regions of the nervous system, interestingly their expression levels and distribution patterns vary during developmental phases and in different

regions of the nervous system. *Stim1* is robustly expressed in Purkinje neurons (Hartmann et al., 2014), but *Stim2* is more abundant in hippocampal neurons (Berna-Erro et al., 2009). STIM1 mainly activates SOCE, whereas STIM2 is more involved in regulation of basal intracellular calcium levels (Gruszczynska-Biegala and Kuznicki, 2013; Xia et al., 2014). *Orais* are differentially expressed in different cell types from the nervous system with *Orai2* being the predominant isoform. *Orai2* has been reported to contribute to neuronal SOCE in the cortex and hippocampus while *Orai1* is the major functional components responsible for SOCE in most cell types. In contrast, *Orai3* appears to play a less important role. Furthermore, the various interplays of the TRP family with STIM and Orai proteins complicate the picture. As such, it is not surprising that while SOCE has been implicated in many neuronal processes from developmental signaling to pain transmission, its role in each of these actions is not consistent. Thus, it is also not surprising that loss- and gain-of-SOCE and thereby disruption of calcium homeostasis is implicated in such a wide range of neurological diseases (Figure 1). Further research into the specific expression and factors influencing SOCE in each of the aforementioned nervous system cells is warranted to elucidate their true roles in these physiological and pathological processes and to clarify whether their putative potential as treatments in these pathologies is valid.

As the field of SOC in neurological diseases is relatively nascent, data are limited and understanding of the role of

**TABLE 1** | A summary table of the various nervous cells demonstrating SOCE and their SOCE-related physiological functions.

Cell	SOCE-related physiological functions	References
Cortical neurons	Ca <sup>2+</sup> homeostasis during cortical development and in developed neurons Long term depression Long term potentiation	Gruszczynska-Biegala and Kuznicki, 2013; Garcia-Alvarez et al., 2015; Hou et al., 2015; González-Sánchez et al., 2017; Guner et al., 2017; Bouron, 2020
Hippocampal neurons	Counteract continuous loss of Ca <sup>2+</sup> across the plasma membrane to maintain basal Ca <sup>2+</sup> homeostasis Synapse formation, maturation, and plasticity	Samtleben et al., 2015; Segal and Korkotian, 2016; Korkotian et al., 2017; Yap et al., 2017
Striatal medium spiny neurons	Involvement in spontaneous slow Ca <sup>2+</sup> oscillations	Kikuta et al., 2019
Dopaminergic neurons	Regulation of mitochondrial oxidative phosphorylation Activation of AKT/mTOR pathway	Selvaraj et al., 2012; Sun et al., 2017; Surmeier et al., 2017
Purkinje neurons	Clearance of cytosolic Ca <sup>2+</sup> during neuronal firing Modulation of neuronal excitability and intrinsic plasticity Refilling of calcium stores required for TRPC3 function Regulation of mGluR1/TRPC3-dependent slow excitatory synaptic potentials Cerebellar motor function	Hartmann et al., 2014; Ryu et al., 2017; Shim et al., 2018; Jang et al., 2020
Cerebellar granule cells	Involvement in spontaneous Ca <sup>2+</sup> oscillations	Singaravelu et al., 2008
Spinal cord dorsal horn	Regulation of resting calcium homeostasis, A type potassium channels, and neuronal excitability	Xia et al., 2014
Dorsal root ganglion neurons	Modulation of neuronal excitability	Wei et al., 2017
Astrocytes	Glutamate release/gliotransmission Tonic inhibition of CA1 pyramidal neurons Cytokine secretion	Handy et al., 2017; Toth et al., 2019
Müller glia	Depletion dependent Ca <sup>2+</sup> homeostasis	Molnar et al., 2016
Microglia	Cellular migration Phagocytosis Cytokine secretion NFAT1 activity	Ikedo et al., 2013; Heo et al., 2015; Michaelis et al., 2015; Lim et al., 2017

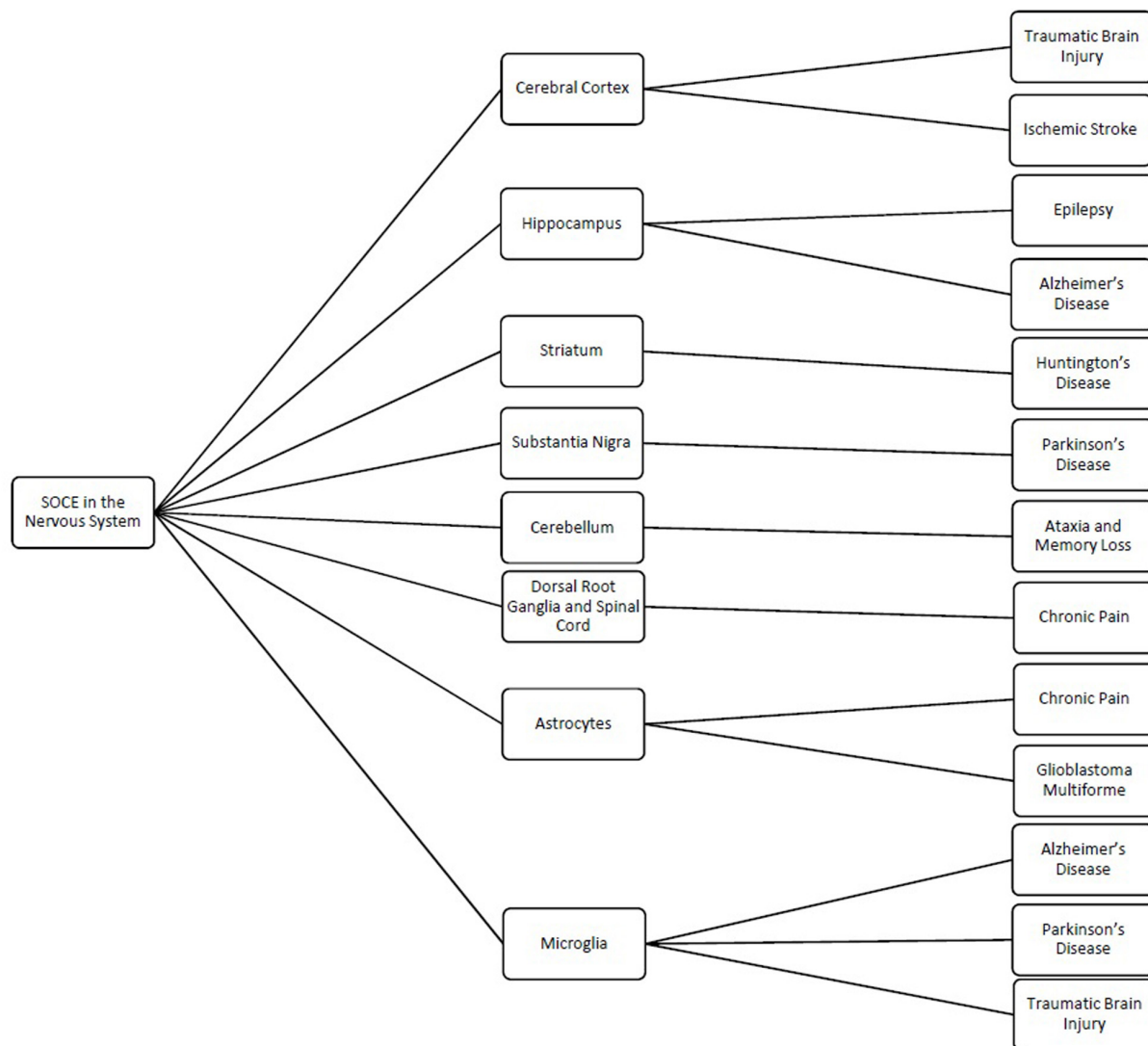


**FIGURE 1 |** Schematic showing the different regions and cells of the nervous system where store-operated calcium entry (SOCE) has been shown to regulated cellular processes and the related pathologies linked to dysfunction of SOCE in these regions.

SOCs in excitable cells is continuously evolving. While there are data exhibiting SOC function and activation, many of these experiments have employed the use of exogenous chemicals to activate or inhibit these channels (Chen et al., 2013; Gao et al., 2015; Qi et al., 2016; González-Sánchez et al., 2017; Domenichini et al., 2018). Moreover, these channels are often studied *in vitro*. When placed in a physiologic setting without these exogenous chemicals, SOC may not act as expected, which could complicate our understanding of their physiological role. As there is limited data on how SOC are activated under physiological conditions and how they affect pathological conditions *in vivo*, further studies must be done to address these questions using animal models and genetic tools.

Given the importance of  $\text{Ca}^{2+}$  homeostasis and  $\text{Ca}^{2+}$  signaling throughout the nervous system, it is understandable that SOC show connections to the wide variety of neurological

disorders discussed throughout this review. Again, as data on SOC in neurons and glial cells are limited, our understanding of where SOC fit into the pathophysiology of dementia, pain, and other neurological disorders is ever evolving. In addition, SOC are often discussed as potential novel targets for these neurological diseases (Wu et al., 2011; Gao et al., 2013; Cui et al., 2017; Stegner et al., 2019; Waldron et al., 2019). While data of modulating SOC function in animal models of diseases are promising, they cannot be taken in isolation. With STIM1/2 and Orai1/2/3 expressed widely throughout all body systems, potential therapies based on SOC modulation must take into account systemic effects when evaluating efficacy and safety. Furthermore, with data showing upregulation or maintenance is beneficial in certain disease states but deleterious or even causative in others, it is important to consider potential therapies in context of other diseases during development.

In short, the study of SOCs has yielded a new perspective by which researchers can examine the nervous system and its pathologies. Although the molecular components of SOCE and their functional significance in the nervous system are still controversial and multifaceted, it is clear that SOCs play an important role in neuronal development, homeostasis, signaling, neuronal excitability, and synapse formation. Increasing evidence indicates that dysfunction of SOCs is linked to brain injury, epilepsy, AD, HD, and pain. Furthermore, by elucidating new modalities by which neurological pathologies arise, the study of SOCs will provide additional avenues for developing therapies for difficult to treat or incurable neurological disorders. While understanding of SOCs is still developing, there is tremendous potential for

discovery and advancement of neuroscience through continued research in SOCs.

## AUTHOR CONTRIBUTIONS

IZ prepared the manuscript. Both authors edited and approved the final manuscript.

## FUNDING

This work was supported by NIH Grants R21NS077330 and R01NS087033 (to HJH).

## REFERENCES

- Ady, V., Toscano-Márquez, B., Nath, M., Chang, P. K., Hui, J., and Cook, A. (2018). Altered synaptic and firing properties of cerebellar Purkinje cells in a mouse model of ARSACS. *J. Physiol.* 596, 4253–4267. doi: 10.1113/jp275902
- Alonso, M. T., Manjarrés, I. M., and García-Sancho, J. (2012). Privileged coupling between Ca(2+) entry through plasma membrane store-operated Ca(2+) channels and the endoplasmic reticulum Ca(2+) pump. *Mol. Cell. Endocrinol.* 353, 37–44. doi: 10.1016/j.mce.2011.08.021
- Alvarez, J., Alvarez-Illera, P., García-Casas, P., Fonteriz, R. I., and Montero, M. (2020). The role of Ca(2+) Signaling in aging and neurodegeneration: insights from *Caenorhabditis elegans* models. *Cells* 9:204. doi: 10.3390/cells9010204
- Ambudkar, I. S., de Souza, L. B., and Ong, H. L. (2017). TRPC1, Orai1, and STIM1 in SOCE: friends in tight spaces. *Cell Calcium* 63, 33–39. doi: 10.1016/j.ceca.2016.12.009
- Authi, K. S. (2007). TRP channels in platelet function. *Handb. Exp. Pharmacol.* 179, 425–443. doi: 10.1007/978-3-540-34891-7\_25
- Avila-Medina, J., Mayoral-Gonzalez, I., Dominguez-Rodriguez, A., Gallardo-Castillo, I., Ribas, J., and Ordoñez, A. (2018). The complex role of store operated calcium entry pathways and related proteins in the function of cardiac, skeletal and vascular smooth muscle cells. *Front. Physiol.* 9:257.
- Baba, A., Yasui, T., Fujisawa, S., Yamada, R. X., Yamada, M. K., and Nishiyama, N. (2003). Activity-evoked capacitative Ca2+ entry: implications in synaptic plasticity. *J. Neurosci.* 23, 7737–7741. doi: 10.1523/jneurosci.23-21-07737.2003
- Bastián-Eugenio, C. E., Bohórquez-Hernández, A., Pacheco, J., Sampieri, A., Asanov, A., and Ocelotl-Oviedo, J. P. (2019). Heterologous calcium-dependent inactivation of Orai1 by neighboring TRPV1 channels modulates cell migration and wound healing. *Commun. Biol.* 2:88.
- Berna-Erro, A., Braun, A., Kraft, R., Kleinschnitz, C., Schuhmann, M. K., and Stegner, D. (2009). STIM2 regulates capacitive Ca2+ entry in neurons and plays a key role in hypoxic neuronal cell death. *Sci. Signal.* 2:ra67. doi: 10.1126/scisignal.2000522
- Bollimuntha, S., Pani, B., and Singh, B. B. (2017). Neurological and motor disorders: neuronal store-operated Ca(2+) signaling: an overview and its function. *Adv. Exp. Med. Biol.* 993, 535–556. doi: 10.1007/978-3-319-57732-6\_27
- Bouron, A. (2020). Transcriptomic profiling of Ca2+ transport systems during the formation of the cerebral cortex in mice. *Cells* 9:1800. doi: 10.3390/cells9081800
- Brambilla, L., Martorana, F., and Rossi, D. (2013). Astrocyte signaling and neurodegeneration: new insights into CNS disorders. *Prion* 7, 28–36. doi: 10.4161/pri.22512
- Brough, G. H., Wu, S., Cioffi, D., Moore, T. M., Li, M., Dean, N., et al. (2001). Contribution of endogenously expressed Trp1 to a Ca2+-selective, store-operated Ca2+ entry pathway. *FASEB J.* 15, 1727–1738.
- Calvo-Rodríguez, M., García-Durillo, M., Villalobos, C., and Núñez, M. (2016). In vitro aging promotes endoplasmic reticulum (ER)-mitochondria Ca(2+) cross talk and loss of store-operated Ca(2+) entry (SOCE) in rat hippocampal neurons. *Biochim. Biophys. Acta* 1863, 2637–2649. doi: 10.1016/j.bbamer.2016.08.001
- Calvo-Rodríguez, M., Hernando-Pérez, E., López-Vázquez, S., Núñez, J., Villalobos, C., and Núñez, L. (2020). Remodeling of intracellular Ca(2+) homeostasis in rat hippocampal neurons aged in vitro. *Int. J. Mol. Sci.* 21:1549. doi: 10.3390/ijms21041549
- Chauvet, S., Jarvis, L., Chevallet, M., Shrestha, N., Groschner, K., and Bouron, A. (2016). Pharmacological characterization of the native store-operated calcium channels of cortical neurons from embryonic mouse brain. *Front. Pharmacol.* 7:486.
- Chen, G., Panicker, S., Lau, K. Y., Apparsundaram, S., Patel, V. A., and Chen, S. L. (2013). Characterization of a novel CRAC inhibitor that potently blocks human T cell activation and effector functions. *Mol. Immunol.* 54, 355–367. doi: 10.1016/j.molimm.2012.12.011
- Chen-Engerer, H. J., Hartmann, J., Karl, R. M., Yang, J., Feske, S., and Konnerth, A. (2019). Two types of functionally distinct Ca(2+) stores in hippocampal neurons. *Nat. Commun.* 10:3223.
- Cheng, K. T., Liu, X., Ong, H. L., and Ambudkar, I. S. (2008). Functional requirement for Orai1 in store-operated TRPC1-STIM1 channels. *J. Biol. Chem.* 283, 12935–12940. doi: 10.1074/jbc.c800008200
- Chernyuk, D., Zernov, N., Kabirowa, M., Bezprozvanny, I., and Popugaeva, E. (2019). Antagonist of neuronal store-operated calcium entry exerts beneficial effects in neurons expressing PSEN1ΔE9 mutant linked to familial Alzheimer disease. *Neuroscience* 410, 118–127. doi: 10.1016/j.neuroscience.2019.04.043
- Cho, T. A. (2015). Spinal cord functional anatomy. *Continuum* 21, 13–35. doi: 10.1007/978-981-10-7033-4\_2
- Collins, H. E., Zhu-Mauldin, X., Marchase, R. B., and Chatham, J. C. (2013). STIM1/Orai1-mediated SOCE: current perspectives and potential roles in cardiac function and pathology. *Am. J. Physiol. Heart Circ. Physiol.* 305, H446–H458.
- Cui, C., Merritt, R., Fu, L., and Pan, Z. (2017). Targeting calcium signaling in cancer therapy. *Acta Pharm. Sin. B* 7, 3–17. doi: 10.1016/j.apsb.2016.11.001
- De Pittà, M., Goldberg, M., Volman, V., Berry, H., and Ben-Jacob, E. (2009). Glutamate regulation of calcium and IP3 oscillating and pulsating dynamics in astrocytes. *J. Biological. Physics* 35, 383–411. doi: 10.1007/s10867-009-9155-y
- Devinsky, O., Vezzani, A., Najjar, S., De Lanerolle, N. C., and Rogawski, M. A. (2013). Glia and epilepsy: excitability and inflammation. *Trends Neurosci.* 36, 174–184. doi: 10.1016/j.tins.2012.11.008
- Domenichini, F., Terrié, E., Arnault, P., Harnois, T., Magaud, C., Bois, P., et al. (2018). Store-operated calcium entries control neural stem cell self-renewal in the adult brain subventricular zone. *Stem Cells* 36, 761–774. doi: 10.1002/stem.2786
- Dong, Q., Liu, Q., Li, R., Wang, A., Bu, Q., Wang, K. H., et al. (2018). Mechanism and consequence of abnormal calcium homeostasis in rett syndrome astrocytes. *eLife* 7:e33417. doi: 10.7554/elife.33417
- Dou, Y., Xia, J., Gao, R., Gao, X., Munoz, F. M., and Wei, D. (2018). Orai1 plays a crucial role in central sensitization by modulating neuronal excitability. *J. Neurosci.* 38, 887–900. doi: 10.1523/jneurosci.3007-17.2017
- Emptage, N. J., Reid, C. A., and Fine, A. (2001). Calcium stores in hippocampal synaptic boutons mediate short-term plasticity, store-operated Ca2+ entry, and

- spontaneous transmitter release. *Neuron* 29, 197–208. doi: 10.1016/s0896-6273(01)00190-8
- Faouzi, M., Kilch, T., Horgen, F. D., Fleig, A., and Penner, R. (2017). The TRPM7 channel kinase regulates store-operated calcium entry. *J. Physiol.* 595, 3165–3180. doi: 10.1113/jp274006
- Feske, S. (2019). CRAC channels and disease - From human CRAC channelopathies and animal models to novel drugs. *Cell Calcium* 80, 112–116. doi: 10.1016/j.ccca.2019.03.004
- Friel, D. D., and Tsien, R. W. (1992). A caffeine- and ryanodine-sensitive Ca<sup>2+</sup> store in bullfrog sympathetic neurones modulates effects of Ca<sup>2+</sup> entry on [Ca<sup>2+</sup>]<sub>i</sub>. *J. Physiol.* 450, 217–246. doi: 10.1113/jphysiol.1992.sp019125
- Gao, R., Gao, X., Xia, J., Tian, Y., Barrett, J. E., Dai, Y., et al. (2013). Potent analgesic effects of a store-operated calcium channel inhibitor. *Pain* 154, 2034–2044. doi: 10.1016/j.pain.2013.06.017
- Gao, X. H., Gao, R., Tian, Y. Z., McGonigle, P., Barrett, J. E., Dai, Y., et al. (2015). A store-operated calcium channel inhibitor attenuates collagen-induced arthritis. *Br. J. Pharmacol.* 172, 2991–3002. doi: 10.1111/bph.13104
- Gao, X., Xia, J., Munoz, F. M., Manners, M. T., Pan, R., Meucci, O., et al. (2016). STIMs and Orai1 regulate cytokine production in spinal astrocytes. *J. Neuroinflammation* 13:126.
- García-Alvarez, G., Shetty, M. S., Lu, B., Yap, K. A., Oh-Hora, M., Sajikumar, S., et al. (2015). Impaired spatial memory and enhanced long-term potentiation in mice with forebrain-specific ablation of the Stim genes. *Front. Behav. Neurosci.* 9:180.
- Gemes, G., Bangaru, M. L., Wu, H. E., Tang, Q., Weihrauch, D., and Koopmeiners, A. S. (2011). Store-operated Ca<sup>2+</sup> entry in sensory neurons: functional role and the effect of painful nerve injury. *J. Neurosci.* 31, 3536–3549. doi: 10.1523/jneurosci.5053-10.2011
- Ghosh, R., and Tabrizi, S. J. (2018). Clinical features of huntington's disease. *Adv. Exp. Med. Biol.* 1049, 1–28.
- Gilbert, D. F., Stebbing, M. J., Kuenzel, K., Murphy, R. M., Zacharewicz, E., and Buttgeriet, A. (2016). Store-operated Ca(2+) entry (SOCE) and purinergic receptor-mediated Ca(2+) homeostasis in Murine bv2 Microglia cells: early cellular responses to ATP-mediated microglia activation. *Front. Mol. Neurosci.* 9:111.
- Glass, C. K., Saijo, K., Winner, B., Marchetto, M. C., and Gage, F. H. (2010). Mechanisms underlying inflammation in neurodegeneration. *Cell* 140, 918–934. doi: 10.1016/j.cell.2010.02.016
- González-Sánchez, P., Del Arco, A., Esteban, J. A., and Satrustegui, J. (2017). Store-operated calcium entry is required for mglur-dependent long term depression in cortical neurons. *Front. Cell Neurosci.* 11:363.
- Gross, S. A., Wissenbach, U., Philipp, S. E., Freichel, M., Cavalie, A., and Flockerzi, V. (2007). Murine ORAI2 splice variants form functional Ca<sup>2+</sup> release-activated Ca<sup>2+</sup> (CRAC) channels. *J. Biol. Chem.* 282, 19375–19384. doi: 10.1074/jbc.m701962200
- Gruszczynska-Biegala, J., and Kuznicki, J. (2013). Native STIM2 and ORAI1 proteins form a calcium-sensitive and thapsigargin-insensitive complex in cortical neurons. *J. Neurochem.* 126, 727–738. doi: 10.1111/jnc.12320
- Gruszczynska-Biegala, J., Pomorski, P., Wisniewska, M. B., and Kuznicki, J. (2011). Differential roles for STIM1 and STIM2 in store-operated calcium entry in rat neurons. *PLoS One* 6:e19285. doi: 10.1371/journal.pone.0019285
- Guner, G., Guzelsoy, G., Isleyen, F. S., Sahin, G. S., Akkaya, C., and Bayam, E. (2017). NEUROD2 regulates stim1 expression and store-operated calcium entry in cortical neurons. *eNeuro* 4, ENEURO.255–216.
- Guzman, R., Valente, E. G., Pretorius, J., Pacheco, E., Qi, M., and Bennett, B. D. (2014). Expression of ORAI1, a plasma membrane resident subunit of the CRAC channel, in rodent and non-rodent species. *J. Histochem. Cytochem.* 62, 864–878. doi: 10.1369/0022155414554926
- Handy, G., Taheri, M., White, J. A., and Borisyuk, A. (2017). Mathematical investigation of IP(3)-dependent calcium dynamics in astrocytes. *J. Comput. Neurosci.* 42, 257–273. doi: 10.1007/s10827-017-0640-1
- Harisseh, R., Chatelier, A., Magaud, C., Déliot, N., and Constantin, B. (2013). Involvement of TRPV2 and SOCE in calcium influx disorder in DMD primary human myotubes with a specific contribution of  $\alpha$ 1-syntrophin and PLC/PKC in SOCE regulation. *Am. J. Physiol. Cell Physiol.* 304, C881–C894.
- Hartmann, J., Karl, R. M., Alexander, R. P., Adelsberger, H., Brill, M. S., and Ruhlmann, C. (2014). STIM1 controls neuronal Ca(2+)(+) signaling, mGluR1-dependent synaptic transmission, and cerebellar motor behavior. *Neuron* 82, 635–644. doi: 10.1016/j.neuron.2014.03.027
- Heo, D. K., Lim, H. M., Nam, J. H., Lee, M. G., and Kim, J. Y. (2015). Regulation of phagocytosis and cytokine secretion by store-operated calcium entry in primary isolated murine microglia. *Cell. Signal.* 27, 177–186. doi: 10.1016/j.cellsig.2014.11.003
- Hernández-Morales, M., Sobradillo, D., Valero, R. A., Muñoz, E., Ubierna, D., and Moyer, M. P. (2017). Mitochondria sustain store-operated currents in colon cancer cells but not in normal colonic cells: reversal by non-steroidal anti-inflammatory drugs. *Oncotarget* 8, 55332–55352. doi: 10.18632/oncotarget.19430
- Hong, S. H., Choi, H. B., Kim, S. U., and McLarnon, J. G. (2006). Mitochondrial ligand inhibits store-operated calcium influx and COX-2 production in human microglia. *J. Neurosci. Res.* 83, 1293–1298. doi: 10.1002/jnr.20829
- Hou, P. F., Liu, Z. H., Li, N., Cheng, W. J., and Guo, S. W. (2015). Knockdown of STIM1 improves neuronal survival after traumatic neuronal injury through regulating mGluR1-dependent Ca(2+) signaling in mouse cortical neurons. *Cell Mol. Neurobiol.* 35, 283–292. doi: 10.1007/s10571-014-0123-0
- Hoxha, E., Balbo, I., Miniaci, M. C., and Tempia, F. (2018). Purkinje cell signaling deficits in animal models of ataxia. *Front. Synaptic Neurosci.* 10:6.
- Ikeda, M., Tsuno, S., Sugiyama, T., Hashimoto, A., Yamoto, K., and Takeuchi, K. (2013). Ca(2+) spiking activity caused by the activation of store-operated Ca(2+) channels mediates TNF- $\alpha$  release from microglial cells under chronic purinergic stimulation. *Biochim. Biophys. Acta* 1833, 2573–2585. doi: 10.1016/j.bbamcr.2013.06.022
- Jang, D. C., Shim, H. G., and Kim, S. J. (2020). Intrinsic plasticity of cerebellar purkinje cells contributes to motor memory consolidation. *J. Neurosci.* 40:4145. doi: 10.1523/jneurosci.1651-19.2020
- Jardin, I., Lopez, J. J., Salido, G. M., and Rosado, J. A. (2008). Orai1 mediates the interaction between STIM1 and hTRPC1 and regulates the mode of activation of hTRPC1-forming Ca<sup>2+</sup> channels. *J. Biol. Chem.* 283, 25296–25304. doi: 10.1074/jbc.m802904200
- Jessen, K. R. (2004). Glial cells. *Int. J. Biochem. Cell Biol.* 36, 1861–1867.
- Ji, R. R., Kawasaki, Y., Zhuang, Z. Y., Wen, Y. R., and Decosterd, I. (2006). Possible role of spinal astrocytes in maintaining chronic pain sensitization: review of current evidence with focus on bFGF/JNK pathway. *Neuron Glia Biol.* 2, 259–269. doi: 10.1017/s1740925x07000403
- Jung, S., Pfeiffer, F., and Deitmer, J. W. (2000). Histamine-induced calcium entry in rat cerebellar astrocytes: evidence for capacitative and non-capacitative mechanisms. *J. Physiol.* 3(Pt 3), 549–561. doi: 10.1111/j.1469-7793.2000.00549.x
- Kettenmann, H., Hanisch, U. K., Noda, M., and Verkhratsky, A. (2011). Physiology of microglia. *Physiol. Rev.* 91, 461–553.
- Khan, H. Y., Mpilla, G. B., Sexton, R., Viswanadha, S., Penmetsa, K. V., and Aboukameel, A. (2020). Calcium release-activated calcium (CRAC) channel inhibition suppresses pancreatic ductal adenocarcinoma cell proliferation and patient-derived tumor growth. *Cancers* 12:750. doi: 10.3390/cancers12030750
- Khoo, C., Helm, J., Choi, H. B., Kim, S. U., and McLarnon, J. G. (2001). Inhibition of store-operated Ca(2+) influx by acidic extracellular pH in cultured human microglia. *Glia* 36, 22–30. doi: 10.1002/glia.1092
- Kikuta, S., Iguchi, Y., Kakizaki, T., Kobayashi, K., Yanagawa, Y., Takada, M., et al. (2019). Store-operated calcium channels are involved in spontaneous slow calcium oscillations in striatal neurons. *Front. Cell Neurosci.* 13:547.
- Kim, M. S., Zeng, W., Yuan, J. P., Shin, D. M., Worley, P. F., and Muallem, S. (2009). Native store-operated Ca<sup>2+</sup> Influx requires the channel function of orai1 and TRPC1. *J. Biol. Chem.* 284, 9733–9741. doi: 10.1074/jbc.m808097200
- Kiviluoto, S., Decuyper, J. P., De Smedt, H., Missiaen, L., Parys, J. B., and Bultynck, G. (2011). STIM1 as a key regulator for Ca<sup>2+</sup> homeostasis in skeletal-muscle development and function. *Skelet. Muscle* 1:16. doi: 10.1186/2044-5040-1-16
- Klejman, M. E., Gruszczynska-Biegala, J., Skibinska-Kijek, A., Wisniewska, M. B., Misztal, K., Blazejczyk, M., et al. (2009). Expression of STIM1 in brain and puncta-like co-localization of STIM1 and ORAI1 upon depletion of Ca(2+) store in neurons. *Neurochem. Int.* 54, 49–55. doi: 10.1016/j.neuint.2008.10.005
- Korkotian, E., Frotscher, M., and Segal, M. (2014). Synaptotagmin regulates spine plasticity: mediation by calcium stores. *J. Neurosci.* 34, 11641–11651. doi: 10.1523/jneurosci.0381-14.2014
- Korkotian, E., Oni-Biton, E., and Segal, M. (2017). The role of the store-operated calcium entry channel Orai1 in cultured rat hippocampal synapse

- formation and plasticity. *J. Physiol.* 595, 125–140. doi: 10.1113/jp272645
- Kovacs, G. G., Zsembery, A., Anderson, S. J., Komlosi, P., Gillespie, G. Y., Bell, P. D., et al. (2005). Changes in intracellular  $\text{Ca}^{2+}$  and pH in response to thapsigargin in human glioblastoma cells and normal astrocytes. *Am. J. Physiol. Cell Physiol.* 289, C361–C371.
- Kraft, R. (2015). STIM and ORAI proteins in the nervous system. *Channels* 9, 245–252. doi: 10.1080/19336950.2015.1071747
- Kwon, J., An, H., Sa, M., Won, J., Shin, J. I., and Lee, C. J. (2017). Orai1 and Orai3 in combination with stim1 mediate the majority of store-operated calcium entry in astrocytes. *Exp. Neurobiol.* 26, 42–54. doi: 10.5607/en.2017.26.1.42
- La Russa, D., Frisina, M., Secondo, A., Bagetta, G., and Amantea, D. (2020). Modulation of cerebral store-operated calcium entry-regulatory factor (saraf) and peripheral orai1 following focal cerebral ischemia and preconditioning in mice. *Neuroscience* 441, 8–21. doi: 10.1016/j.neuroscience.2020.06.014
- Lacruz, R. S., and Feske, S. (2015). Diseases caused by mutations in ORAI1 and STIM1. *Ann. N. Y. Acad. Sci.* 1356, 45–79.
- Lane, C. A., Hardy, J., and Schott, J. M. (2018). Alzheimer's disease. *Eur. J. Neurol.* 25, 59–70.
- Lanoiselée, H. M., Nicolas, G., Wallon, D., Rovelet-Lecrux, A., Lacour, M., and Rousseau, S. (2017). APP, PSEN1, and PSEN2 mutations in early-onset Alzheimer disease: a genetic screening study of familial and sporadic cases. *PLoS Med.* 14:e1002270. doi: 10.1371/journal.pmed.1002270
- Lein, E. S., Hawrylycz, M. J., Ao, N., Ayres, M., Bensinger, A., and Bernard, A. (2007). Genome-wide atlas of gene expression in the adult mouse brain. *Nature* 445, 168–176.
- Lewis, R. S. (2007). The molecular choreography of a store-operated calcium channel. *Nature* 446, 284–287. doi: 10.1038/nature05637
- Li, G., Zhang, Z., Wang, R., Ma, W., Yang, Y., Wei, J., et al. (2013). Suppression of STIM1 inhibits human glioblastoma cell proliferation and induces G0/G1 phase arrest. *J. Exp. Clin. Cancer Res.* 32:20. doi: 10.1186/1756-9966-32-20
- Li, Y., Song, J., Liu, X., Zhang, M., An, J., Sun, P., et al. (2013). High expression of STIM1 in the early stages of diffuse axonal injury. *Brain Res.* 1495, 95–102. doi: 10.1016/j.brainres.2012.12.005
- Lim, H. M., Woon, H., Han, J. W., Baba, Y., Kurosaki, T., and Lee, M. G. (2017). UDP-induced phagocytosis and atp-stimulated chemotactic migration are impaired in stim1(-/-) microglia in vitro and in vivo. *Mediators Inflamm.* 2017:8158514.
- Liou, J., Kim, M. L., Heo, W. D., Jones, J. T., Myers, J. W., Ferrell, J. E., et al. (2005). STIM is a  $\text{Ca}^{2+}$  sensor essential for  $\text{Ca}^{2+}$ -store-depletion-triggered  $\text{Ca}^{2+}$  influx. *Curr. Biol.* 15, 1235–1241. doi: 10.1016/j.cub.2005.05.055
- Liu, H., Hughes, J. D., Rollins, S., Chen, B., and Perkins, E. (2011). Calcium entry via ORAI1 regulates glioblastoma cell proliferation and apoptosis. *Exp. Mol. Pathol.* 91, 753–760. doi: 10.1016/j.yexmp.2011.09.005
- Liu, S., Hasegawa, H., Takemasa, E., Suzuki, Y., Oka, K., and Kiyoi, T. (2017). Efficiency and safety of CRAC inhibitors in human rheumatoid arthritis xenograft models. *J. Immunol.* 199, 1584–1595. doi: 10.4049/jimmunol.1700192
- Liu, X., Gong, B., de Souza, L. B., Ong, H. L., Subedi, K. P., and Cheng, K. T. (2017). Radiation inhibits salivary gland function by promoting STIM1 cleavage by caspase-3 and loss of SOCE through a TRPM2-dependent pathway. *Sci. Signal.* 10:eal4064. doi: 10.1126/scisignal.aal4064
- Liu, Z., Wei, Y., Zhang, L., Yee, P. P., Johnson, M., and Zhang, X. (2019). Induction of store-operated calcium entry (SOCE) suppresses glioblastoma growth by inhibiting the Hippo pathway transcriptional coactivators YAP/TAZ. *Oncogene* 38, 120–139. doi: 10.1038/s41388-018-0425-7
- Lo, K.-J., Luk, H.-N., Chin, T.-Y., and Chueh, S.-H. (2002). Store depletion-induced calcium influx in rat cerebellar astrocytes. *Br. J. Pharmacol.* 135, 1383–1392. doi: 10.1038/sj.bjp.0704594
- Lopez, J. J., Jardin, I., Sanchez-Collado, J., Salido, G. M., Smani, T., and Rosado, J. A. (2020). TRPC channels in the SOCE scenario. *Cells* 9:126. doi: 10.3390/cells9010126
- Lu, B., and Fivaz, M. (2016). Neuronal SOCE: myth or reality? *Trends Cell Biol.* 26, 890–893. doi: 10.1016/j.tcb.2016.09.008
- Lu, J., Dou, F., and Yu, Z. (2019). The potassium channel  $\text{KCa}3.1$  represents a valid pharmacological target for microglia-induced neuronal impairment in a mouse model of Parkinson's disease. *J. Neuroinflammation* 16:273.
- Ma, X., Cheng, K. T., Wong, C. O., O'Neil, R. G., Birnbaumer, L., Ambudkar, I. S., et al. (2011). Heteromeric TRPV4-C1 channels contribute to store-operated  $\text{Ca}^{2+}$  entry in vascular endothelial cells. *Cell Calcium* 50, 502–509. doi: 10.1016/j.ceca.2011.08.006
- Ma, Z., Tanis, J. E., Taruno, A., and Foskett, J. K. (2016). Calcium homeostasis modulator (CALHM) ion channels. *Pflugers. Arch.* 468, 395–403. doi: 10.1007/s00424-015-1757-6
- Maciąg, F., Majewski, L., Boguszewski, P. M., Gupta, R. K., Wasilewska, I., Wojtaś, B., et al. (2019). Behavioral and electrophysiological changes in female mice overexpressing ORAI1 in neurons. *Biochim. Biophys. Acta Mol. Cell Res.* 1866, 1137–1150. doi: 10.1016/j.bbamcr.2019.01.007
- Majewski, L., and Kuznicki, J. (2015). SOCE in neurons: signaling or just refilling? *Biochim. Biophys. Acta* 1853, 1940–1952.
- Majewski, L., Wojtas, B., Maciąg, F., and Kuznicki, J. (2019). Changes in calcium homeostasis and gene expression implicated in epilepsy in hippocampi of mice overexpressing ORAI1. *Int. J. Mol. Sci.* 20:5539. doi: 10.3390/ijms20225539
- McCarl, C.-A., Picard, C., Khalil, S., Kawasaki, T., Röther, J., and Papolos, A. (2009). ORAI1 deficiency and lack of store-operated  $\text{Ca}^{2+}$  entry cause immunodeficiency, myopathy, and ectodermal dysplasia. *J. Allergy Clin. Immunol.* 124, 1311–1318.e7.
- McColgan, P., and Tabrizi, S. J. (2018). Huntington's disease: a clinical review. *Eur. J. Neurol.* 25, 24–34.
- McLarnon, J. G., Choi, H. B., Lue, L. F., Walker, D. G., and Kim, S. U. (2005). Perturbations in calcium-mediated signal transduction in microglia from Alzheimer's disease patients. *J. Neurosci. Res.* 81, 426–435. doi: 10.1002/jnr.20487
- McLarnon, J. G., Helm, J., Goghari, V., Franciosi, S., Choi, H. B., Nagai, A., et al. (2000). Anion channels modulate store-operated calcium influx in human microglia. *Cell Calcium* 28, 261–268. doi: 10.1054/ceca.2000.0150
- McMahon, S. B., and Malcangio, M. (2009). Current challenges in glia-pain biology. *Neuron* 64, 46–54. doi: 10.1016/j.neuron.2009.09.033
- Mercer, J. C., Dehaven, W. I., Smyth, J. T., Wedel, B., Boyles, R. R., Bird, G. S., et al. (2006). Large store-operated calcium selective currents due to co-expression of Orai1 or Orai2 with the intracellular calcium sensor, Stim1. *J. Biol. Chem.* 281, 24979–24990. doi: 10.1074/jbc.m604589200
- Michaelis, M., Nieswandt, B., Stegner, D., Eilers, J., and Kraft, R. (2015). STIM1, STIM2, and Orai1 regulate store-operated calcium entry and purinergic activation of microglia. *Glia* 63, 652–663. doi: 10.1002/glia.22775
- Mizuma, A., Kim, J. Y., Kacimi, R., Stauderman, K., Dunn, M., Hebbbar, S., et al. (2019). Microglial calcium release-activated calcium channel inhibition improves outcome from experimental traumatic brain injury and microglia-induced neuronal death. *J. Neurotrauma* 36, 996–1007. doi: 10.1089/neu.2018.5856
- Molnar, T., Yarishkin, O., Iuso, A., Barabas, P., Jones, B., Marc, R. E., et al. (2016). Store-Operated calcium entry in muller glia is controlled by synergistic activation of TRPC and Orai channels. *J. Neurosci.* 36, 3184–3198. doi: 10.1523/jneurosci.4069-15.2016
- Moreno, C., Sampieri, A., Vivas, O., Peña-Segura, C., and Vaca, L. (2012). STIM1 and Orai1 mediate thrombin-induced  $\text{Ca}^{2+}$  influx in rat cortical astrocytes. *Cell Calcium* 52, 457–467. doi: 10.1016/j.ceca.2012.08.004
- Motiani, R. K., Hyzinski-García, M. C., Zhang, X., Henkel, M. M., Abdullaev, I. F., Kuo, Y. H., et al. (2013). STIM1 and Orai1 mediate CRAC channel activity and are essential for human glioblastoma invasion. *Pflugers. Arch.* 465, 1249–1260. doi: 10.1007/s00424-013-1254-8
- Muñoz, E., Valero, R. A., Quintana, A., Hoth, M., Núñez, L., and Villalobos, C. (2011). Nonsteroidal anti-inflammatory drugs inhibit vascular smooth muscle cell proliferation by enabling the  $\text{Ca}^{2+}$ -dependent inactivation of calcium release-activated calcium/orai channels normally prevented by mitochondria. *J. Biol. Chem.* 286, 16186–16196. doi: 10.1074/jbc.m110.198952
- Nascimento Da Conceicao, V., Sun, Y., Zboril, E. K., De la Chapa, J. J., and Singh, B. B. (2019). Loss of  $\text{Ca}^{2+}$  entry via Orai-TRPC1 induces ER stress, initiating immune activation in macrophages. *J. Cell Sci.* 133:jcs237610. doi: 10.1242/jcs.237610
- Núñez, L., Sanchez, A., Fonteriz, R. I., and Garcia-Sancho, J. (1996). Mechanisms for synchronous calcium oscillations in cultured rat cerebellar neurons. *Eur. J. Neurosci.* 8, 192–201. doi: 10.1111/j.1460-9568.1996.tb01180.x
- Ong, H. L., Cheng, K. T., Liu, X., Bandyopadhyay, B. C., Paria, B. C., Soboloff, J., et al. (2007). Dynamic assembly of TRPC1-STIM1-Orai1 ternary complex

- is involved in store-operated calcium influx: evidence for similarities in store-operated and calcium release-activated calcium channel components. *J. Biol. Chem.* 282, 9105–9116. doi: 10.1074/jbc.m608942200
- Pascual-Caro, C., Berrocal, M., Lopez-Guerrero, A. M., Alvarez-Barrientos, A., and Pozo-Guisado, E. (2018). STIM1 deficiency is linked to Alzheimer's disease and triggers cell death in SH-SY5Y cells by upregulation of L-type voltage-operated Ca(2+) entry. *J. Mol. Med.* 96, 1061–1079. doi: 10.1007/s00109-018-1677-y
- Popugaeva, E., Pchitskaya, E., Speshilova, A., Alexandrov, S., Zhang, H., Vlasova, O., et al. (2015a). STIM2 protects hippocampal mushroom spines from amyloid synaptotoxicity. *Mol. Neurodegener.* 10:37.
- Popugaeva, E., Vlasova, O. L., and Bezprozvanny, I. (2015b). Restoring calcium homeostasis to treat Alzheimer's disease: a future perspective. *Neurodegener. Dis. Manag.* 5, 395–398. doi: 10.2217/nmt.15.36
- Prakriya, M., and Lewis, R. S. (2015). Store-operated calcium channels. *Physiol. Rev.* 95, 1383–1436.
- Putney, J. W. Jr. (1986). A model for receptor-regulated calcium entry. *Cell Calcium* 7, 1–12. doi: 10.1016/0143-4160(86)90026-6
- Qi, Z., Wang, Y., Zhou, H., Liang, N., Yang, L., Liu, L., et al. (2016). The central analgesic mechanism of YM-58483 in attenuating neuropathic pain in rats. *Cell Mol. Neurobiol.* 36, 1035–1043. doi: 10.1007/s10571-015-0292-5
- Rao, W., Zhang, L., Peng, C., Hui, H., Wang, K., and Su, N. (2015). Downregulation of STIM2 improves neuronal survival after traumatic brain injury by alleviating calcium overload and mitochondrial dysfunction. *Biochim. Biophys. Acta* 1852, 2402–2413. doi: 10.1016/j.bbdis.2015.08.014
- Raza, M., Deshpande, L. S., Blair, R. E., Carter, D. S., Sombati, S., and DeLorenzo, R. J. (2007). Aging is associated with elevated intracellular calcium levels and altered calcium homeostatic mechanisms in hippocampal neurons. *Neurosci. Lett.* 418, 77–81. doi: 10.1016/j.neulet.2007.03.005
- Reich, S. G., and Savitt, J. M. (2019). Parkinson's disease. *Med. Clin. North Am.* 103, 337–350.
- Ryazantseva, M., Goncharova, A., Skobeleva, K., Erokhin, M., Methner, A., Georgiev, P., et al. (2018). Presenilin-1 Delta E9 mutant induces STIM1-driven store-operated calcium channel hyperactivation in hippocampal neurons. *Mol. Neurobiol.* 55, 4667–4680. doi: 10.1007/s12035-017-0674-4
- Ryskamp, D., Wu, L., Wu, J., Kim, D., Rammes, G., Geva, M., et al. (2019). Pridopidine stabilizes mushroom spines in mouse models of Alzheimer's disease by acting on the sigma-1 receptor. *Neurobiol. Dis.* 124, 489–504. doi: 10.1016/j.nbd.2018.12.022
- Ryu, C., Jang, D. C., Jung, D., Kim, Y. G., Shim, H. G., and Ryu, H.-H. (2017). STIM1 regulates somatic Ca(2+) signals and intrinsic firing properties of cerebellar purkinje neurons. *J. Neurosci.* 37, 8876–8894. doi: 10.1523/jneurosci.3973-16.2017
- Samtleben, S., Wachter, B., and Blum, R. (2015). Store-operated calcium entry compensates fast ER calcium loss in resting hippocampal neurons. *Cell Calcium* 58, 147–159. doi: 10.1016/j.ceca.2015.04.002
- Secondo, A., Petrozziello, T., Tedeschi, V., Boscia, F., Vinciguerra, A., and Ciccone, R. (2019). ORAI1/STIM1 interaction intervenes in stroke and in neuroprotection induced by ischemic preconditioning through store-operated calcium entry. *Stroke* 50, 1240–1249. doi: 10.1161/strokeaha.118.024115
- Segal, M., and Korkotian, E. (2016). Roles of calcium stores and store-operated channels in plasticity of dendritic spines. *Neuroscientist* 22, 477–485. doi: 10.1177/1073858415613277
- Selvaraj, S., Sun, Y., Watt, J. A., Wang, S., Lei, S., Birnbaumer, L., et al. (2012). Neurotoxin-induced ER stress in mouse dopaminergic neurons involves downregulation of TRPC1 and inhibition of AKT/mTOR signaling. *J. Clin. Invest.* 122, 1354–1367. doi: 10.1172/jci61332
- Shigetomi, E., Saito, K., Sano, F., and Koizumi, S. (2019). Aberrant calcium signals in reactive astrocytes: a key process in neurological disorders. *Int. J. Mol. Sci.* 20:996. doi: 10.3390/ijms20040996
- Shim, H. G., Lee, Y. S., and Kim, S. J. (2018). The emerging concept of intrinsic plasticity: activity-dependent modulation of intrinsic excitability in cerebellar purkinje cells and motor learning. *Exp. Neurobiol.* 27, 139–154. doi: 10.5607/en.2018.27.3.139
- Singaravelu, K., Lohr, C., and Deitmer, J. W. (2006). Regulation of store-operated calcium entry by calcium-independent phospholipase A2 in rat cerebellar astrocytes. *J. Soc. Neurosci.* 26, 9579–9592. doi: 10.1523/jneurosci.2604-06.2006
- Singaravelu, K., Lohr, C., and Deitmer, J. W. (2008). Calcium-independent phospholipase A2 mediates store-operated calcium entry in rat cerebellar granule cells. *Cerebellum* 7, 467–481. doi: 10.1007/s12311-008-0050-z
- Skibinska-Kijek, A., Wisniewska, M. B., Gruszczynska-Biegala, J., Methner, A., and Kuznicki, J. (2009). Immunolocalization of STIM1 in the mouse brain. *Acta Neurobiol. Exp.* 69, 413–428.
- Stauderman, K. A. (2018). CRAC channels as targets for drug discovery and development. *Cell Calcium* 74, 147–159. doi: 10.1016/j.ceca.2018.07.005
- Stegner, D., Hofmann, S., Schuhmann, M. K., Kraft, P., Herrmann, A. M., and Popp, S. (2019). Loss of Orai2-mediated capacitative Ca(2+) entry is neuroprotective in acute ischemic stroke. *Stroke* 50, 3238–3245. doi: 10.1161/jexpneurol.2011.08.022
- Steinbeck, J. A., Henke, N., Opatz, J., Gruszczynska-Biegala, J., Schneider, L., and Theiss, S. (2011). Store-operated calcium entry modulates neuronal network activity in a model of chronic epilepsy. *Exp. Neurol.* 232, 185–194. doi: 10.1016/j.expneurol.2011.08.022
- Sun, S., Zhang, H., Liu, J., Popugaeva, E., Xu, N.-J., Feske, S., et al. (2014). Reduced synaptic STIM2 expression and impaired store-operated calcium entry cause destabilization of mature spines in mutant presenilin mice. *Neuron* 82, 79–93. doi: 10.1016/j.neuron.2014.02.019
- Sun, Y., Chauhan, A., Sukumaran, P., Sharma, J., Singh, B. B., and Mishra, B. B. (2014). Inhibition of store-operated calcium entry in microglia by helminth factors: implications for immune suppression in neurocysticercosis. *J. Neuroinflammation* 11:210.
- Sun, Y., Selvaraj, S., Pandey, S., Humphrey, K. M., Foster, J. D., Wu, M., et al. (2018). MPP(+) decreases store-operated calcium entry and TRPC1 expression in Mesenchymal Stem Cell derived dopaminergic neurons. *Sci. Rep.* 8:11715.
- Sun, Y., Zhang, H., Selvaraj, S., Sukumaran, P., Lei, S., Birnbaumer, L., et al. (2017). Inhibition of L-Type Ca(2+) channels by TRPC1-STIM1 complex is essential for the protection of dopaminergic neurons. *J. Neurosci.* 37, 3364–3377. doi: 10.1523/jneurosci.3010-16.2017
- Surmeier, D. J., Schumacker, P. T., Guzman, J. D., Ilijic, E., Yang, B., and Zampese, E. (2017). Calcium and Parkinson's disease. *Biochem. Biophys. Res. Commun.* 483, 1013–1019.
- Takahashi, Y., Murakami, M., Watanabe, H., Hasegawa, H., Ohba, T., and Munehisa, Y. (2007). Essential role of the N-terminus of murine Orai1 in store-operated Ca2+ entry. *Biochem. Biophys. Res. Commun.* 356, 45–52. doi: 10.1016/j.bbrc.2007.02.107
- Toescu, E. C., Möller, T., Kettenmann, H., and Verkhratsky, A. (1998). Long-term activation of capacitative Ca2+ entry in mouse microglial cells. *Neuroscience* 86, 925–935. doi: 10.1016/s0306-4522(98)00123-7
- Toth, A. B., Hori, K., Novakovic, M. M., Bernstein, N. G., Lambot, L., and Prakriya, M. (2019). CRAC channels regulate astrocyte Ca(2+) signaling and gliotransmitter release to modulate hippocampal GABAergic transmission. *Sci. Signal.* 12:eaw5450. doi: 10.1126/scisignal.aaw5450
- Tshuva, R. Y., Korkotian, E., and Segal, M. (2017). ORAI1-dependent synaptic plasticity in rat hippocampal neurons. *Neurobiol. Learn. Mem.* 140, 1–10. doi: 10.1016/j.nlm.2016.12.024
- Uhlén, M., Fagerberg, L., Hallström, B. M., Lindskog, C., Oksvold, P., and Mardinoglu, A. (2015). Proteomics. Tissue-based map of the human proteome. *Science* 347:1260419.
- Vigont, V. A., Zimina, O. A., Glushankova, L. N., Kolobkova, J. A., Ryazantseva, M. A., Mozhayeva, G. N., et al. (2014). STIM1 protein activates store-operated calcium channels in cellular model of huntington's disease. *Acta Nat.* 6, 40–47. doi: 10.32607/20758251-2014-6-4-40-47
- Vigont, V., Kolobkova, Y., Skopin, A., Zimina, O., Zenin, V., Glushankova, L., et al. (2015). Both orai1 and TRPC1 are involved in excessive store-operated calcium entry in striatal neurons expressing mutant huntingtin exon 1. *Front. Physiol.* 6:337.
- Vigont, V., Nekrasov, E., Shalygin, A., Gusev, K., Klushnikov, S., Illarionovskii, S., et al. (2018). Patient-specific iPSC-based models of huntington's disease as a tool to study store-operated calcium entry drug targeting. *Front. Pharmacol.* 9:696.
- Villalobos, C., Hernández-Morales, M., Gutiérrez, L. G., and Núñez, L. (2019). TRPC1 and ORAI1 channels in colon cancer. *Cell Calcium* 81, 59–66. doi: 10.1016/j.ceca.2019.06.003
- Waldron, R. T., Chen, Y., Pham, H., Go, A., Su, H. Y., and Hu, C. (2019). The Orai Ca(2+) channel inhibitor CM4620 targets both parenchymal and immune cells to reduce inflammation in experimental acute pancreatitis. *J. Physiol.* 597, 3085–3105. doi: 10.1113/jp277856

- Wang, X., Bae, J. H., Kim, S. U., and McLarnon, J. G. (1999). Platelet-activating factor induced Ca(2+) signaling in human microglia. *Brain Res.* 842, 159–165. doi: 10.1016/S0006-8993(99)01849-1
- Weber, J. T. (2012). Altered calcium signaling following traumatic brain injury. *Front. Pharmacol.* 3:60.
- Wegierski, T., and Kuznicki, J. (2018). Neuronal calcium signaling via store-operated channels in health and disease. *Cell Calcium* 74, 102–111. doi: 10.1016/j.ceca.2018.07.001
- Wei, D., Mei, Y., Xia, J., and Hu, H. (2017). Orai1 and Orai3 mediate store-operated calcium entry contributing to neuronal excitability in dorsal root ganglion neurons. *Front. Cell Neurosci.* 11:400.
- Wissenbach, U., Philipp, S. E., Gross, S. A., Cavalié, A., and Flockerzi, V. (2007). Primary structure, chromosomal localization and expression in immune cells of the murine ORAI and STIM genes. *Cell Calcium* 42, 439–446. doi: 10.1016/j.ceca.2007.05.014
- Wu, H. E., Gemes, G., and Hogan, Q. H. (2018). Recording SOCE activity in neurons by patch-clamp electrophysiology and microfluorometric calcium imaging. *Methods Mol. Biol.* 1843, 41–53. doi: 10.1007/978-1-4939-8704-7\_3
- Wu, J., Ryskamp, D. A., Liang, X., Egorova, P., Zakharova, O., Hung, G., et al. (2016). Enhanced store-operated calcium entry leads to striatal synaptic loss in a huntington's disease mouse model. *J. Neurosci.* 36:125.
- Wu, J., Ryskamp, D., Birnbaumer, L., and Bezprozvanny, I. (2018). Inhibition of TRPC1-dependent store-operated calcium entry improves synaptic stability and motor performance in a mouse model of huntington's disease. *J. Huntingtons Dis.* 7, 35–50. doi: 10.3233/jhd-170266
- Wu, J., Shih, H. P., Vigont, V., Hrdlicka, L., Diggins, L., and Singh, C. (2011). Neuronal store-operated calcium entry pathway as a novel therapeutic target for Huntington's disease treatment. *Chem. Biol.* 18, 777–793. doi: 10.1016/j.chembiol.2011.04.012
- Xia, J., Pan, R., Gao, X., Meucci, O., and Hu, H. (2014). Native store-operated calcium channels are functionally expressed in mouse spinal cord dorsal horn neurons and regulate resting calcium homeostasis. *J. Physiol.* 592, 3443–3461. doi: 10.1113/jphysiol.2014.275065
- Yap, K. A., Shetty, M. S., Garcia-Alvarez, G., Lu, B., Alagappan, D., Oh-Hora, M., et al. (2017). STIM2 regulates AMPA receptor trafficking and plasticity at hippocampal synapses. *Neurobiol. Learn. Mem.* 138, 54–61. doi: 10.1016/j.nlm.2016.08.007
- Zhang, H., Bryson, V., Luo, N., Sun, A. Y., and Rosenberg, P. (2020). STIM1-Ca(2+) signaling in coronary sinus cardiomyocytes contributes to interatrial conduction. *Cell Calcium* 87:102163. doi: 10.1016/j.ceca.2020.102163
- Zhang, H., Sun, S., Wu, L., Pchitskaya, E., Zakharova, O., Fon Tacer, K., et al. (2016). Store-operated calcium channel complex in postsynaptic spines: a new therapeutic target for alzheimer's disease treatment. *J. Neurosci.* 36, 11837–11850. doi: 10.1523/jneurosci.1188-16.2016
- Zhang, H., Wu, L., Pchitskaya, E., Zakharova, O., Saito, T., Saido, T., et al. (2015). Neuronal store-operated calcium entry and mushroom spine loss in amyloid precursor protein knock-in mouse model of alzheimer's disease. *J. Neurosci.* 35:13275.
- Zhang, M., Song, J. N., Wu, Y., Zhao, Y. L., Pang, H. G., Fu, Z. F., et al. (2014). Suppression of STIM1 in the early stage after global ischemia attenuates the injury of delayed neuronal death by inhibiting store-operated calcium entry-induced apoptosis in rats. *Neuroreport* 25, 507–513.
- Zhang, S. L., Yu, Y., Roos, J., Kozak, J. A., Deerinck, T. J., Ellisman, M. H., et al. (2005). STIM1 is a Ca2+ sensor that activates CRAC channels and migrates from the Ca2+ store to the plasma membrane. *Nature* 437, 902–905. doi: 10.1038/nature04147
- Zhu, X., Jiang, M., Peyton, M., Boulay, G., Hurst, R., Stefani, E., et al. (1996). trp, a novel mammalian gene family essential for agonist-activated capacitative Ca2+ entry. *Cell* 85, 661–671. doi: 10.1016/S0092-8674(00)81233-7
- Zitt, C., Zobel, A., Obukhov, A. G., Harteneck, C., Kalkbrenner, F., Lückhoff, A., et al. (1996). Cloning and functional expression of a human Ca2+-permeable cation channel activated by calcium store depletion. *Neuron* 16, 1189–1196. doi: 10.1016/S0896-6273(00)80145-2

**Conflict of Interest:** The authors declare that the research was conducted in the absence of any commercial or financial relationships that could be construed as a potential conflict of interest.

Copyright © 2020 Zhang and Hu. This is an open-access article distributed under the terms of the Creative Commons Attribution License (CC BY). The use, distribution or reproduction in other forums is permitted, provided the original author(s) and the copyright owner(s) are credited and that the original publication in this journal is cited, in accordance with accepted academic practice. No use, distribution or reproduction is permitted which does not comply with these terms.



# Target Molecules of STIM Proteins in the Central Nervous System

Karolina Serwach and Joanna Gruszczynska-Biegala\*

Molecular Biology Unit, Mossakowski Medical Research Centre, Polish Academy of Sciences, Warsaw, Poland

## OPEN ACCESS

### Edited by:

Daniele Dell'Orco,  
University of Verona, Italy

### Reviewed by:

Rodrigo Portes Ureshino,  
Federal University of São Paulo, Brazil  
Francesco Moccia,  
University of Pavia, Italy

### \*Correspondence:

Joanna Gruszczynska-Biegala  
jgruszczynska@imdik.pan.pl

**Received:** 14 October 2020

**Accepted:** 02 December 2020

**Published:** 23 December 2020

### Citation:

Serwach K and  
Gruszczynska-Biegala J (2020) Target  
Molecules of STIM Proteins in the  
Central Nervous System.  
*Front. Mol. Neurosci.* 13:617422.  
doi: 10.3389/fnmol.2020.617422

Stromal interaction molecules (STIMs), including STIM1 and STIM2, are single-pass transmembrane proteins that are located predominantly in the endoplasmic reticulum (ER). They serve as calcium ion ( $\text{Ca}^{2+}$ ) sensors within the ER. In the central nervous system (CNS), they are involved mainly in Orai-mediated store-operated  $\text{Ca}^{2+}$  entry (SOCE). The key molecular components of the SOCE pathway are well-characterized, but the molecular mechanisms that underlie the regulation of this pathway need further investigation. Numerous intracellular target proteins that are located in the plasma membrane, ER, cytoskeleton, and cytoplasm have been reported to play essential roles in concert with STIMs, such as conformational changes in STIMs, their translocation, the stabilization of their interactions with Orai, and the activation of other channels. The present review focuses on numerous regulators, such as Homer, SOCE-associated regulatory factor (SARAF), septin, synaptopodin, golli proteins, partner of STIM1 (POST), and transcription factors and proteasome inhibitors that regulate STIM-Orai interactions in the CNS. Further we describe novel roles of STIMs in mediating  $\text{Ca}^{2+}$  influx via other than Orai pathways, including TRPC channels, VGCCs, AMPA and NMDA receptors, and group I metabotropic glutamate receptors. This review also summarizes recent findings on additional molecular targets of STIM proteins including SERCA,  $\text{IP}_3$ Rs, end-binding proteins (EB), presenilin, and CaMKII. Dysregulation of the SOCE-associated toolkit, including STIMs, contributes to the development of neurodegenerative disorders (e.g., Alzheimer's disease, Parkinson's disease, and Huntington's disease), traumatic brain injury, epilepsy, and stroke. Emerging evidence points to the role of STIM proteins and several of their molecular effectors and regulators in neuronal and glial physiology and pathology, suggesting their potential application for future therapeutic strategies.

**Keywords:** STIM, SOCE components, glutamate receptors,  $\text{Ca}^{2+}$  channels, calcium signaling, STIM regulators and effectors, store-operated calcium entry (SOCE), central nervous system

## INTRODUCTION

Calcium ion ( $\text{Ca}^{2+}$ ) is a second messenger of crucial importance to neurons as it participates in the transmission of the depolarizing signals and contributes to synaptic activity and apoptosis. Cytoplasmic  $\text{Ca}^{2+}$  level in neurons is regulated in a comprehensive way via the components localized in the plasma membrane (PM) such as ion channels, exchangers, and pumps, as well as the components localized in the mitochondria, endoplasmic reticulum (ER), Golgi apparatus, and nucleus (Brini et al., 2014).

Plasma membrane  $\text{Ca}^{2+}$  channels in neurons are divided into three major groups according to their mechanism of action: voltage-gated  $\text{Ca}^{2+}$  channels (VGCC),

receptor-operated  $\text{Ca}^{2+}$  channels (ROC:  $\alpha$ -amino-3-hydroxy-5-methyl-4-isoxazole propionic acid receptors [AMPA] and *N*-methyl-D-aspartate receptors [NMDARs]), and store-operated channels (SOC; Orai, transient receptor potential cation [TRPC] channels, arachidonate-regulated  $\text{Ca}^{2+}$  [ARC] channels) (Brini et al., 2014). In neurons,  $\text{Ca}^{2+}$  entry from the extracellular space is mediated via VGCCs and glutamate receptors (ionotropic: AMPAR, NMDAR, and metabotropic: mGluR) and is complemented by store-operated  $\text{Ca}^{2+}$  entry (SOCE) (Brini et al., 2014). Noteworthy, SOCE is the main  $\text{Ca}^{2+}$  source in resting neurons, while after depolarization  $\text{Ca}^{2+}$  influx is mediated mainly via VGCC, NMDAR and AMPAR (Brini et al., 2014). mGluR mediates both rapid transient depolarization and prolonged depolarization (Brini et al., 2014). Two systems responsible for  $\text{Ca}^{2+}$  extrusion from the cytoplasm to the extracellular milieu are PM  $\text{Ca}^{2+}$  adenosine triphosphatase (PMCA) and PM  $\text{Na}^+/\text{Ca}^{2+}$  exchanger (NCX). While NCX affinity to  $\text{Ca}^{2+}$  is low, its capacity is high. Contrary, PMCA is characterized by opposite properties (Blaustein et al., 2002; Brini and Carafoli, 2011; Brini et al., 2014).

Mitochondria are also essential components of neuronal  $\text{Ca}^{2+}$  toolkit. They modulate intensity and duration of  $\text{Ca}^{2+}$  signals following extracellular stimuli (Duszyński et al., 2006). Since they have the ability to accumulate  $\text{Ca}^{2+}$ , they function as  $\text{Ca}^{2+}$  buffers. Mitochondria localized in close proximity to  $\text{Ca}^{2+}$  channels are exposed to high  $\text{Ca}^{2+}$  level and can accumulate  $\text{Ca}^{2+}$  efficiently. This decreases local  $\text{Ca}^{2+}$  level and results in depletion of ER  $\text{Ca}^{2+}$  stores and activation of SOCE (Duszyński et al., 2006; Spät and Szanda, 2017). Special communication between mitochondria and the ER also enables  $\text{Ca}^{2+}$  release from the ER to mitochondria and its accumulation in the mitochondrial matrix. Increased  $\text{Ca}^{2+}$  concentration in the mitochondrial matrix stimulates the energy metabolism and boosts the activity of the tricarboxylic acid cycle enzymes, providing reducing equivalents to the respiratory chain and thus influencing the production of ATP (Brini et al., 2014). Calcium influx during SOCE results in mitochondrial  $\text{Ca}^{2+}$

uptake, which in turn boosts mitochondrial energy metabolism. If  $\text{Ca}^{2+}$  overload appears, it may cause cell apoptosis (Spät and Szanda, 2017). Thus, mitochondria link cell metabolism with  $\text{Ca}^{2+}$  signaling and homeostasis (Duszyński et al., 2006).

Neuronal  $\text{Ca}^{2+}$  signaling also appears to be pivotal in the nucleus. Cell depolarization propagates  $\text{Ca}^{2+}$  to the nucleus where they target the CREB transcription factor and DREAM transcriptional repressor, thereby affecting the transcription of many genes (Dick and Bading, 2010).

In neurons, the ER constitutes a vital  $\text{Ca}^{2+}$  storage organelle. Release of  $\text{Ca}^{2+}$  from the ER occurs via ryanodine receptor (RyR) and inositol-1,4,5-trisphosphate 3 ( $\text{IP}_3$ ) receptor ( $\text{IP}_3\text{R}$ ).  $\text{Ca}^{2+}$  release through  $\text{IP}_3\text{R}$  occurs in response to mGluR activation in the PM. In turn, an elevated level of cytoplasmic  $\text{Ca}^{2+}$  is the major trigger for  $\text{Ca}^{2+}$  release via RyR in the mechanism known as  $\text{Ca}^{2+}$ -induced  $\text{Ca}^{2+}$  release (CICR) (Brini et al., 2014). The decreased  $\text{Ca}^{2+}$  level in the ER is refilled by SOCE.

SOCE is based on the influx of  $\text{Ca}^{2+}$  from the extracellular environment through channels of the PM and the replenishment of these ions in the ER when their levels decrease because of release into the cytoplasm (Blaustein and Golovina, 2001; Putney, 2003). The depletion of ER  $\text{Ca}^{2+}$  stores is detected by stromal interaction molecules (STIMs), including STIM1 and STIM2 proteins, that are sensors of  $\text{Ca}^{2+}$  levels in the ER (Liou et al., 2005; Roos et al., 2005; Zhang et al., 2005). After the activation of  $\text{IP}_3\text{Rs}$ , the drop in  $\text{Ca}^{2+}$  concentration in the ER (Berridge et al., 2000) causes the oligomerization of STIM proteins and their movement toward ER-PM junctions (Liou et al., 2005; Zhang et al., 2005; Wu et al., 2006; Serwach and Gruszczynska-Biegala, 2019). At these junctions, STIM proteins form complexes with proteins of  $\text{Ca}^{2+}$  release-activated channels (CRACs) that are formed by Orais or SOCs that consist of Orais and TRPC channels, leading to the activation of these channels (Liou et al., 2005; Mercer et al., 2006; Soboloff et al., 2006c; Liao et al., 2008; Salido et al., 2009; Saul et al., 2014; Albarran et al., 2016). Two types of  $\text{Ca}^{2+}$  currents are caused by  $\text{Ca}^{2+}$  store depletion:  $\text{I}_{\text{CRAC}}$  (mediated by the activation of Orai1 and STIM1) and  $\text{I}_{\text{SOC}}$  (involving Orai1, TRPC1, and STIM1; Desai et al., 2015). Channel activation results in  $\text{Ca}^{2+}$  influx from the extracellular milieu to the cytoplasm (Prakriya et al., 2006), and then  $\text{Ca}^{2+}$  is taken to the ER by sarco/endoplasmic reticulum  $\text{Ca}^{2+}$ -adenosine triphosphatase (SERCA) pump.

The interaction between STIM proteins and Orai1 is widely known to be essential for the proper function of SOCE in non-excitable cells. SOCE is a ubiquitous cell signaling pathway that is also present in many other tissues, including the rodent and human brain (Moccia et al., 2015) where it is involved in the regulation of intracellular ionic equilibrium and determines the excitability of neurons (Emptage et al., 2001; Gemes et al., 2011; Sun et al., 2014; Majewski and Kuznicki, 2015).

STIM proteins were originally described in non-excitable cells. They are now known to be present in most cells, including excitable cells, such as neurons, where STIM2 protein is predominantly expressed (Berna-Erro et al., 2009; Skibinska-Kijek et al., 2009; Gruszczynska-Biegala et al., 2011; Steinbeck et al., 2011). The primary function of STIM2 in neurons was suggested to be the regulation of resting levels of  $\text{Ca}^{2+}$  in

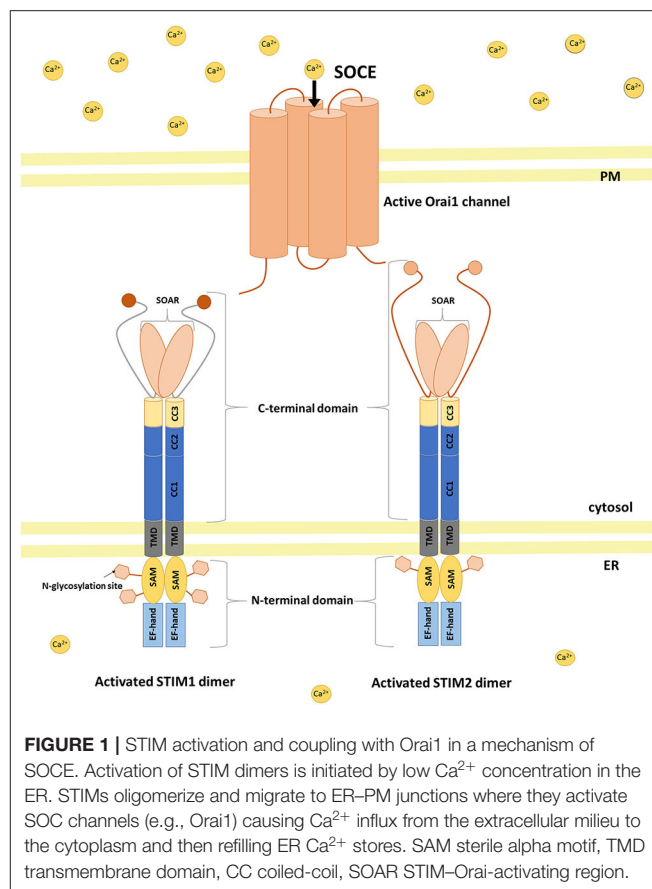
**Abbreviations:** AD, Alzheimer's disease; AMPAR,  $\alpha$ -amino-3-hydroxy-5-methyl-4-isoxazolepropionic acid receptor; APP, amyloid- $\beta$  precursor protein;  $\text{Ca}^{2+}$ , calcium ion; CaMKII,  $\text{Ca}^{2+}$ /calmodulin-dependent protein kinase II; CNS, central nervous system; CRAC,  $\text{Ca}^{2+}$  release-activated channel; DNs, dopaminergic neurons; dSTIM1, *Drosophila* STIM1; EB, end-binding protein; ER, endoplasmic reticulum; FAD, Familial Alzheimer's disease; HD, Huntington's disease;  $\text{IP}_3$ , inositol-1,4,5-trisphosphate 3;  $\text{IP}_3\text{R}$ ,  $\text{IP}_3$  receptor; KI, knockin; KO, knockout; LTD, long-term depression; LTP, long-term potentiation; MBP, myelin basic protein; mGluR, metabotropic glutamate receptor; MT, microtubule; NEUROD2, Neurogenic differentiation factor 2; NMDAR, *N*-methyl-D-aspartate receptor; nNOS, neuronal nitric oxide synthase; NPC, neural progenitor cell; OASE, Orai1-activating small fragment; OPC, oligodendrocyte progenitor cell; PD, Parkinson's disease; PLA, proximity ligation assay; PLC, phospholipase C; PM, plasma membrane; PMCA, plasma membrane  $\text{Ca}^{2+}$  adenosine triphosphatase; PN, Purkinje neuron; POST, partner of STIM1; PS, presenilin; PSD, post-synaptic density; SARA, SOCE-associated regulatory factor; SERCA, sarco/endoplasmic reticulum  $\text{Ca}^{2+}$ -adenosine triphosphatase; siRNA, small-interfering RNA; SOAR, STIM-Orai-activating region; SOC, store-operated channel; SOCE, store-operated  $\text{Ca}^{2+}$  entry; SP, synaptopodin; STIM, stromal interaction molecule; TRPC, transient receptor potential cation channel subfamily C; TRPM, transient receptor potential cation channel subfamily M; VGCC, voltage-gated  $\text{Ca}^{2+}$  channel; WT, wildtype.

the ER and  $\text{Ca}^{2+}$  leakage (Gruszczynska-Biegala et al., 2011; Gruszczynska-Biegala and Kuznicki, 2013). The main function of STIM1 in neurons appears to involve the activation of SOCE (Gruszczynska-Biegala et al., 2011). Various studies have also identified STIM proteins in neuroglial cells, such as astroglia, tumor cells of astroglial origin, oligodendrocyte progenitor cells (OPCs), and microglia (Kettenmann and Bruce, 2013; Verkhatsky and Parpura, 2014; Kraft, 2015; Molnár et al., 2016). Although both STIM1 and STIM2 are expressed in astroglia, STIM1 is thought to be the more abundant isoform in these cells (Gruszczynska-Biegala et al., 2011; Kraft, 2015). Gruszczynska-Biegala et al. showed that *Stim1* mRNA levels in both astroglial and neuronal cortical cultures were similar (Gruszczynska-Biegala et al., 2011).

In addition to interactions with and gating Orai, STIMs were found to recognize numerous interaction partners other than Orai. Thus, the present review focuses on the most important highly divergent target molecules of STIM proteins including positive and negative effectors and regulators in the central nervous system (CNS), mainly in neurons and glia. Recent data revealed a key role for STIM in several physiological and pathological conditions, including hypoxic/ischemic neuronal injury, traumatic brain injury (TBI), epilepsy, Alzheimer's disease (AD), Parkinson's disease (PD), and Huntington's disease (HD; Berna-Erro et al., 2009; Gemes et al., 2011; Steinbeck et al., 2011; Sun et al., 2014; Zhang et al., 2014, 2015; Popugaeva et al., 2015; Rao et al., 2015; Vigont et al., 2015; Tong et al., 2016; Czeredys et al., 2018; Serwach and Gruszczynska-Biegala, 2019). Therefore, studies of SOCE and STIM proteins may elucidate pathogenic mechanisms that are involved in the development of these diseases. Consequently, positive and negative modulators of STIM protein function or translocation may have many potential therapeutic applications. Thus, we also briefly discuss the pathophysiological significance of STIM protein interactions with their target proteins.

## STIM PROTEIN STRUCTURE

STIM1 and STIM2 proteins are encoded by the *STIM1* and *STIM2* genes, respectively, in humans (Williams et al., 2001). They are type 1 transmembrane proteins that are localized in the ER, although STIM1 was also found in the PM (Williams et al., 2001; Liou et al., 2005; Roos et al., 2005; Keil et al., 2010). Both isoforms contain luminal and cytosolic domains (Figure 1; Soboloff et al., 2012; Moccia et al., 2015). The ER luminal N-terminal domain consists of a conserved cysteine pair, a  $\text{Ca}^{2+}$ -binding canonical EF-hand (cEF) domain, a non- $\text{Ca}^{2+}$ -binding hidden EF-hand (hEF) domain, a sterile  $\alpha$ -motif (SAM) with one (for STIM2) or two (for STIM1) N-glycosylation sites, and a transmembrane domain (TMD). The cytosolic C-terminus includes three coiled-coil regions (CC1, CC2, and CC3) with a STIM–Orai-activating region (SOAR). The SOAR contains four  $\alpha$ -helices ( $\alpha$ 1,  $\alpha$ 2,  $\alpha$ 3, and  $\alpha$ 4) and a KIKKKR sequence, which is required for the activation of Orai1 (Yuan et al., 2009; Yang et al., 2012). The CRAC activation domain (CAD) and Orai1-activating small fragment (OASF) are both larger than the SOAR, contain a CC1 region, and activate Orai1 (Muik et al., 2009; Park et al., 2009). SOAR function is inhibited by



an inhibitory helix that is localized in  $\alpha$ 3 (Yang et al., 2012). Downstream of SOAR is an acidic inhibitory domain (ID) that also mediates the fast  $\text{Ca}^{2+}$ -dependent inactivation of Orai1 (Lee et al., 2009). The C-terminus tail of STIM proteins also contains a proline/serine-rich (PS) domain, a microtubule-interacting domain, and a polybasic lysine-rich domain that is responsible for phospholipid interaction in the PM (Soboloff et al., 2012).

STIM1 and STIM2 proteins diverge significantly within the C-terminus (Figure 1). Strong evidence indicates that STIM proteins associate *in vivo*, and these interactions may be mediated by an association between CC regions of C-terminal ends of these proteins (Soboloff et al., 2006a). Notably, STIM2 has lower affinity for  $\text{Ca}^{2+}$  sensing compared with STIM1 because of three amino acid substitutions in cEF that allow STIM2 to detect smaller decreases in  $\text{Ca}^{2+}$  inside the ER lumen (Brandman et al., 2007; Hoth and Niemeyer, 2013).

## STIM PROTEINS IN THE PHYSIOLOGY OF NEURONS, AUTOPHAGY, AND NEURODEGENERATIVE DISEASES

### Physiology

By activating neuronal SOCE, STIM proteins play a pivotal role in the physiology of neurons (Serwach and Gruszczynska-Biegala, 2019). In neurons deprived of STIM2, the amount of mushroom dendritic spines, which are vital for memory storage, was decreased (Sun et al., 2014; Garcia-Alvarez et al., 2015; Yap

et al., 2017). STIM2 also co-localizes with  $\text{Ca}^{2+}$ /calmodulin-dependent protein kinase II (CaMKII) in dendritic spines and regulates its phosphorylation (Yap et al., 2017). STIM2-mediated SOCE sustained CaMKII activation and thus is important in the maintenance of dendritic spines. STIM2-Orai2-TRPC6 complexes regulate SOCE in mice hippocampal synapses and thus influence the number of dendritic spines. Orai-STIM2 complexes play an essential role in the formation of new synapses (Korkotian et al., 2017). All these studies demonstrate a vital role of STIM-mediated SOCE in both formation and maintenance of mushroom spines, and suggest its role in synaptic plasticity. Neuronal SOCE indeed takes part in long-term potentiation (LTP) and long-term depression (LTD), processes responsible for memory and learning (Serwach and Gruszczynska-Biegala, 2019). In Purkinje neurons (PNs), slow excitatory post-synaptic currents (EPSCs) were the result of TRPC3 activity. Lack of STIM1 resulted in no ER  $\text{Ca}^{2+}$  release and slow EPSCs (Hartmann et al., 2014). Thus, STIM1 is considered to refill the dendritic ER  $\text{Ca}^{2+}$  stores only under resting conditions. In resting cells, STIM1-mediated SOCE also caused an ubiquitination and degradation of Sp4 transcription factor (Lalonde et al., 2014). These results underlie an essential homeostatic function of STIM1-mediated SOCE in resting neurons.

## Autophagy

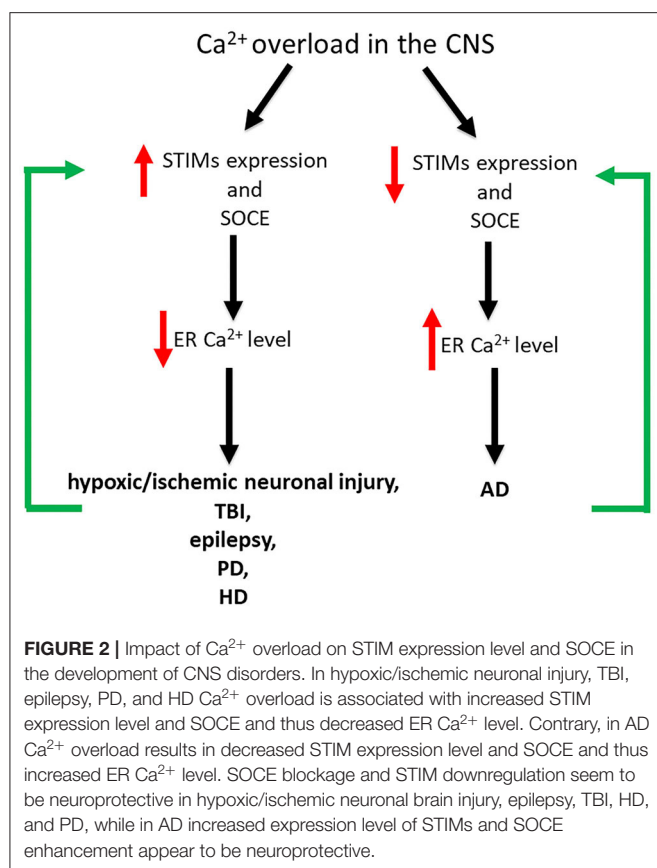
Autophagy is stimulated in response to various types of cellular stress, including ER stress, oxidative stress, starvation of nutrients and growth factors, hypoxia and mitochondrial damage (Kroemer et al., 2010). Moderate ER stress can improve the ability of the ER to process unfolded or misfolded proteins and maintain cell survival. However, if the stress is prolonged or extensive, homeostasis within the cell is disrupted leading to apoptosis, which is primarily mediated by  $\text{Ca}^{2+}$  overload, or autophagy (Berridge et al., 2000; Bernales et al., 2006; Ding et al., 2007; Høyer-Hansen and Jäättelä, 2007). Autophagy, e.g., caused by oxygen and glucose deprivation and reoxygenation, may maintain cellular homeostasis, but its excessive level may lead to autophagic neuronal necrosis and apoptosis (Ahsan et al., 2019; Zhou et al., 2019). Differences in cytosolic  $\text{Ca}^{2+}$  levels associated with autophagy and apoptosis have been demonstrated in several cell lines. Calcium is mostly considered as an activator of autophagy, but there are some reports that  $\text{Ca}^{2+}$  suppresses autophagy (Høyer-Hansen et al., 2007; Cárdenas et al., 2010; Law et al., 2010; Parys et al., 2012; Wong et al., 2013).

However, the role of STIM1/Orai1 in autophagy and apoptosis in the CNS is still unclear, and there is not much work on the subject, thus underscoring the need for further research in this field. Proteasome inhibitors MG-132 and LA promoted the autophagy-mediated degradation of STIM1 and STIM2 and thus reduced SOCE in neurons (Kuang et al., 2016). The opposite is true in HEK293 cells where the stability of STIM1 was not affected by proteasome inhibitors, although thapsigargin-induced surface levels of STIM1 and SOCE were increased in cells pretreated with MG-132 (Keil et al., 2010). These differences are likely to be due to the different conditions for treating cells with protease inhibitors and may also exist

depending on the type of cells used. Further, Kondratskyi et al. demonstrated that, in prostate cancer cells, SOCE inhibitor (ML-9) stimulates autophagosome formation and inhibits autophagosome degradation independent of SOCE and STIM1 (Kondratskyi et al., 2014). On the other hand, in prostate cancer cells (DU145 and PC3), resveratrol has been proposed to induce autophagy by regulating the function of STIM1 and then SOCE. Indeed, STIM1 overexpression restores resveratrol-induced reduction of SOCE as well as autophagic cell death induced by ER stress (Selvaraj et al., 2016). In line with this, STIM1 and SOCE have been shown to positively regulate oxidized low-density lipoprotein-induced autophagy in endothelial progenitor cells (Yang et al., 2017). Recently, hypoxia-induced  $\text{Ca}^{2+}$  release from the ER in neuron-like PC12 cells was modulated by STIM1/Orai1 (Hu et al., 2020). In addition, STIM1/Orai1 signaling induced by  $\alpha 2$ -adrenergic receptor agonist, dexmedetomidine, following hypoxia was mediated by a decrease of  $[\text{Ca}^{2+}]_i$ , leading to a reduction of autophagy. The results suggest that dexmedetomidine may have neuroprotective effects against oxidative stress, autophagy, and neuronal apoptosis after oxygen-glucose deprivation and reoxygenation injury through modulation of  $\text{Ca}^{2+}$ -STIM1/Orai1 signaling (Hu et al., 2020). In turn, STIM1 has been shown to be not essential in hypoxia-mediated autophagy in both SHSY-5Y and HSG cells (Sukumaran et al., 2015). The available data suggest that STIMs influence autophagy differently depending on cell type and triggers of autophagy.

## Neurodegenerative Diseases

Dysregulation of neuronal SOCE and changes in STIM expression levels are associated with various pathological conditions of the CNS such as hypoxic/ischemic neuronal injury, TBI, epilepsy, AD, PD and HD (Figure 2; Serwach and Gruszczynska-Biegala, 2019). Many studies have demonstrated the role of STIM2 in hypoxic/ischemic neuronal injury (Soboloff et al., 2006b; Vig et al., 2006; Berna-Erro et al., 2009). Hippocampal neurons, both in slices and in culture, showed reduced ER  $\text{Ca}^{2+}$  level during hypoxia, and STIM2 reduced  $\text{Ca}^{2+}$  overload during ischemic challenge (Berna-Erro et al., 2009). *Stim2* knockout (KO) mice were better protected against cerebral ischemia (Berna-Erro et al., 2009). Thus, it seems that the absence of STIM2 may potentially constitute a protective strategy against stroke. STIM1 and STIM2 have also been implicated in epilepsy as they are up-regulated both in CA1 and CA3 regions of chronic epileptic mice (Steinbeck et al., 2011). Non-selective SOCE inhibitors rhythimized epileptic burst activity in epileptic hippocampal slices, suggesting that SOCE blockage may potentially bring positive effect in patients with epilepsy. STIM2 has also been shown to be overexpressed after TBI (Rao et al., 2015). The downregulation of STIM2 improved neuronal survival in models of TBI, decreasing neuronal apoptosis and preserving neurological function by alleviating mitochondrial dysfunction and  $\text{Ca}^{2+}$  overload. STIM2 downregulation not only decreased  $\text{Ca}^{2+}$  release from the ER, but also reduced SOCE and dropped mitochondrial  $\text{Ca}^{2+}$  level, restoring its morphology and function. Downregulation of STIM2 has a neuroprotective effect and may be a target in TBI treatment (Rao et al., 2015). Dysregulation of SOCE also contributes to



PD. A neurotoxin, which mimics PD *in vitro*, decreased level of TRPC1 and its interaction with STIM1, thus increasing neuronal death. Pharmacological inhibition of SOCE appears to be neuroprotective representing a potential target for PD drug discovery (Pchitskaya et al., 2018). In HD transgenic mice, over-activation of synaptic SOCE and enhancement of STIM2 expression resulted in the disruption of dendritic spines. STIM2 knockdown has been shown to normalize SOCE and prevent loss of dendritic spines. It seems that pharmacological modulation of SOCE and its components have neuroprotective effects in HD patients. On the other hand, in mice models of AD, impairment of SOCE and reduction of synaptic STIM2 proteins contributed to the destabilization of dendritic spines (Sun et al., 2014; Zhang et al., 2016). Since stabilization of dendritic spines is considered to prevent memory loss in AD patients, the modification of STIM proteins and SOCE may be a potential therapeutic target in the treatment of memory loss in these patients.

Changes in neuronal SOCE may vary among pathological states of the CNS. SOCE blockage and STIM downregulation seem to be neuroprotective in hypoxic/ischemic neuronal brain injury, epilepsy, TBI, HD and PD, while in AD STIMs and SOCE appear to be neuroprotective (Figure 2).

Misfolded proteins and the associated ER stress are common features of some neurodegenerative diseases such as PD, AD and HD. These properties can further induce autophagy or apoptosis in neurons (Ghavami et al., 2014; Remondelli and Renna, 2017). Given the high sensitivity of neurons to ER  $\text{Ca}^{2+}$  store disturbances, STIM and SOCE have been proposed

as potential targets for neuroprotection by reversing ER and mitochondrial stress-induced damage. Interestingly, blockade of SOCE reduced apoptosis mediated by oxidative stress in hippocampal neuronal HT-22 cells (Rao et al., 2013). Hawkins et al. demonstrated that in lymphocyte cells oxidative stress favors STIM1 trafficking and puncta formation, which confirms that STIM1 is regulated by the redox state (Hawkins et al., 2010). In turn, the formation of the STIM1 puncta, their translocation to the PM and the subsequent SOCE in HEK cells were disrupted by mitochondrial depolarization in mitofusin 2 dependent manner. These effects have been shown to be overcome by overexpression of STIM1 (Singaravelu et al., 2011). Consequently, STIM1 in 401L neuroblastoma cells provided protection against ER stress and mitochondrial oxidative stress causing cell death (Zhang and Thomas, 2016). Experiments performed on embryonic fibroblasts also reported that STIM1 rescue protected from oxidative stress and enabled cell survival by impairing the translocation of the apoptosis-inducing factor into the nucleus (Henke et al., 2012). All these findings suggest that STIM may indeed provide protection against cell death mediated by the ER and oxidative stress, which often precede neurodegeneration.

## STIM-BINDING $\text{Ca}^{2+}$ CHANNELS

According to the current state of knowledge, neuronal STIM proteins regulate both CRAC and SOC. Other channel proteins, such as L-type voltage-gated  $\text{Ca}^{2+}$  channels (VGCCs;  $\text{Ca}_v1.2$ ,  $\text{Ca}_v1.3$ ) and receptor/ligand-activated  $\text{Ca}^{2+}$  channels (AMPA receptors and NMDARs), couple or engage in an interplay with STIMs in the CNS in a modulatory way as part of SOCE signaling (Figure 3).

## Orai

As mentioned above, emptying ER  $\text{Ca}^{2+}$  stores causes STIM protein oligomerization and translocation of the oligomers toward the PM where they form complexes, known as puncta, with an  $\text{Ca}^{2+}$  selective ion channel protein, Orai1. We previously showed that the depletion of  $\text{Ca}^{2+}$  from the ER by thapsigargin, a selective SERCA inhibitor, increased the number of puncta-like structures with Yellow Fluorescence Protein (YFP)-STIM1 and Orai1 but not those with YFP-STIM2 and Orai1 (Klejman et al., 2009; Gruszczynska-Biegala et al., 2011). In contrast, a reduction of extracellular  $\text{Ca}^{2+}$  levels with ethylene glycol-bis( $\beta$ -aminoethyl ether)- $N,N,N',N'$ -tetraacetic acid (EGTA) triggered the puncta formation of both YFP-STIM1/Orai1 and YFP-STIM2/Orai1. Other results showed that endogenous STIM1 and STIM2 can interact with Orai1, which was observed in a co-immunoprecipitation assay and *in situ* proximity ligation assay (PLA; Gruszczynska-Biegala and Kuznicki, 2013). The higher association between endogenous STIM2 and Orai1 in cortical neurons occurred in the presence of BAPTA-AM, membrane permeable  $\text{Ca}^{2+}$  chelator, and in a low- $\text{Ca}^{2+}$  medium but not in the presence of thapsigargin. When SOCE was induced, the greatest number of PLA signals that corresponded to integrated STIM1 and Orai1 puncta was visible. The interaction between them was quantified and correlated well with the number of exogenous complexes that formed under

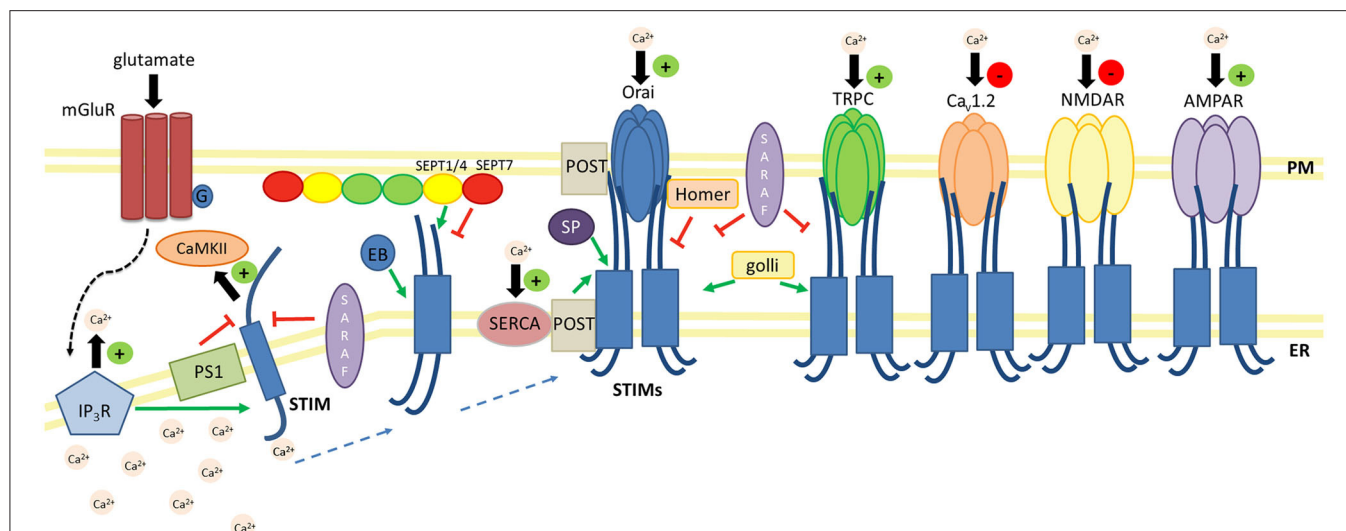


**FIGURE 3 |** Schematic overview of key regulators and effectors of STIM proteins in the CNS. Negative regulators (—|): SARAF prevents STIM1 activation and inhibits the STIM1-Orai1 association. SARAF silencing increases TRPC1-mediated  $\text{Ca}^{2+}$  entry. The PS1- $\gamma$ -secretase complex cleaves the STIM1 transmembrane domain. Homer1a dissociates the STIM1-Orai1 complex. Lower dSEPT7 expression increases the amount of dSTIM-dOrai clusters. Positive regulators (→): The glutamate-mediated activation of mGluRs results in  $\text{Ca}^{2+}$  release from ER stores via  $\text{IP}_3\text{Rs}$  and activates STIM-Orai coupling. EB3 forms complexes with STIM2, which promotes the formation of mushroom spines in hippocampal neurons. SEPT1/4 regulates the number of ER-PM junctions and enhances STIM1-Orai1 interactions. The STIM1-POST complex binds to SERCA and promotes ER  $\text{Ca}^{2+}$  refilling. Golgi proteins interact with STIM1 and TRPC1 and thus enhance SOCE. SP interacts with STIM and Orai and determines synaptic plasticity. Positive effectors (+): STIM proteins increase  $\text{Ca}^{2+}$  influx via Orai, TRPC, and AMPARs. STIM2-mediated SOCE activates CaMKII and thus stabilizes mushroom spines. Negative effectors (—): STIM proteins decrease  $\text{Ca}^{2+}$  influx via L-type VGCCs and NMDARs.

the same conditions (Klejman et al., 2009; Gruszczynska-Biegala et al., 2011; Gruszczynska-Biegala and Kuznicki, 2013).

We can conclude that STIM1 and STIM2 can activate Orai1 channels and play different roles in neuronal SOCE (Berna-Erro et al., 2009; Klejman et al., 2009; Keil et al., 2010; Gruszczynska-Biegala et al., 2011; Gruszczynska-Biegala and Kuznicki, 2013; Sun et al., 2014; Majewski and Kuznicki, 2015). In rat cortical neurons, STIM1 mainly forms complexes with Orai1 and activates SOCE only after  $\text{Ca}^{2+}$  is completely emptied from the ER. This demonstrates its role in maintaining the level of  $\text{Ca}^{2+}$  in the ER. In contrast, STIM2 forms a hetero-complex with Orai1 to allow the regulation of resting intracellular  $\text{Ca}^{2+}$  levels and activation of constitutive  $\text{Ca}^{2+}$  influx after a slight decrease in  $\text{Ca}^{2+}$  levels in the ER.

In the rat cortex, SOCE is mainly mediated by Orai1-STIM1 complexes. In the mouse brain, in contrast, it is triggered either by Orai2 and STIM2 (cortex and hippocampus; Berna-Erro et al., 2009; Sun et al., 2014) or by Orai2 and STIM1 (cerebellum; Hartmann et al., 2014). Likewise, STIM2-gated SOC channels in dendritic mushroom spines are formed by a complex of Orai2 and TRPC6 (Zhang et al., 2016; Popugaeva et al., 2020). In turn, both STIM1 and STIM2 are involved in SOCE in sensory neurons in dorsal root ganglia. Moreover, both Orai1 and Orai3 contribute to SOCE in these neurons, where they may form homomultimers to mediate SOCE (Wei et al., 2017).

In addition to a canonical function as an ER  $\text{Ca}^{2+}$  level refilling toolkit, STIM1-Orai1-mediated SOCE was also shown to regulate gene expression and proliferation in mouse and human neural progenitor cells (NPCs) and thus is thought

to be a key regulator of neurogenesis in mammalian cells (Somasundaram et al., 2014; Gopurappilly et al., 2018). The knockdown of Orai1 or STIM1 diminishes SOCE in NPCs. SOCE is not observed in NPCs from transgenic mice that lack Orai1 or STIM1 or in knock-in (KI) mice that express a Orai1 mutant. The deletion or suppression of STIM1 and Orai1 diminishes the proliferation of embryonic and adult NPCs both *in vitro* and *in vivo* in the subventricular zone (SVZ) in the adult mouse brain (Somasundaram et al., 2014). Domenichini et al. showed that SOCE in SVZ cells is mediated not only by STIM1 and Orai1 but also by TRPC1 (Domenichini et al., 2018). The pharmacological blockade of this process in mouse SVZ cells decreases proliferation and impairs self-renewal by shifting the type of cell division from symmetric to asymmetric, thereby reducing stem cell population (Domenichini et al., 2018). In human NPCs, SOCE has been shown to be significantly attenuated by the short-hairpin RNA/micro RNA targeting of STIM1 (Gopurappilly et al., 2018). Gopurappilly et al. investigated global gene expression in human NPCs with STIM1 knockdown and showed that signaling pathways that are associated with DNA replication and cell proliferation were downregulated, whereas post-synaptic cell signaling was upregulated in these cells (Gopurappilly et al., 2018). To understand the functional relevance of these gene expression alterations, these authors also measured the self-renewal capacity of NPCs with STIM1 knockdown and found a substantially smaller neurosphere size and number and a decrease in differentiation toward cells with a neuronal lineage. These findings demonstrate that STIM1-mediated SOCE in human

NPCs regulates gene expression alterations, which is likely to modulate the differentiation and self-renewal of NPCs (Gopurappilly et al., 2018).

STIM1 and ORAI1 have been shown to be involved in  $\text{Ca}^{2+}$  signaling in both astroglia and glioblastoma cells. The knockdown of both STIM1 and Orai1 or Orai1 alone resulted in a reduction of SOCE in rat astrocytes (Moreno et al., 2012). The silencing of STIM1 or Orai1 was shown to reduce SOCE and CRAC currents in human glioblastoma cells (Motiani et al., 2013). Surprisingly, Ronco et al. found that Orai3 but not Orai1 is a dominant Orai homolog in astroglia (Ronco et al., 2014). Recent studies ascribed a role to STIM1, Orai1, and Orai3 in astroglial SOCE (Gao et al., 2016; Kwon et al., 2017). Additionally, the activation of SOCE in spinal astroglia promotes the production of proinflammatory cytokines, such as tumor necrosis factor  $\alpha$  (TNF- $\alpha$ ) and interleukin-6 (IL-6). The production of TNF- $\alpha$  and IL-6 was decreased by the knockdown of Orai1 or STIM1 (Gao et al., 2016). Interestingly, Orai1 and STIM2 knockdown minimized lipopolysaccharide (LPS)-induced TNF- $\alpha$  and IL-6 production (Gao et al., 2016). This research may provide a basis for assessing SOCE and its components for the treatment of chronic pain and other neurological diseases that are associated with astroglial overactivation.

Studies that focused on the optic nerve in mice identified Orai1 and STIM1 but not STIM2 in astrocytes, whereas Orai1, STIM1, and STIM2 in oligodendrocytes suggested that STIM1 may be localized in the cell soma, and STIM2 may be localized in myelin (Papanikolaou et al., 2017).

In cultured rat microglia, SOCE is mediated by Orai channels rather than TRPC channels (Ohana et al., 2009). Siddiqui et al. identified high levels of Orai1 and STIM1 in microglial podosomes, structures that are responsible for cell motility (Siddiqui et al., 2012). Another research group confirmed the expression of STIM1, Orai1, Orai2, and Orai3 in cultured mouse microglia and showed that the downregulation of STIM1 and Orai1 reduced SOCE in these cells (Heo et al., 2015). Michaelis et al. studied the role of Orai1 and STIM proteins in microglia using cells that were obtained from knockout mice (Michaelis et al., 2015). The results showed that SOCE was reduced in the absence of Orai1 or STIM proteins. SOCE was nearly absent in *Stim1*<sup>-/-</sup> microglia and substantially reduced in *Orai1*<sup>-/-</sup> microglia, whereas a less pronounced effect was observed in *Stim2*<sup>-/-</sup> microglia (Michaelis et al., 2015). Orai1 and STIM1 appear to be major components of microglial SOCE, and STIM2 is also a constituent of this signaling pathway in these cells (Kraft, 2015). Interestingly, recent studies showed that STIM1- and Orai1-mediated SOCE regulate phagocytic activity and cytokine release in primary murine microglia (Heo et al., 2015). Phagocytic activity, as well as LPS stimulation-mediated proinflammatory cytokine release (e.g., TNF- $\alpha$  and IL-6), was inhibited by SOCE inhibitors and STIM1 and Orai1 knockdown (Heo et al., 2015). This research suggests that STIM1 may be a new regulatory target for the prevention of an excessive proinflammatory response of microglia in neurodegenerative disorders.

## TRPC Channels

In addition to Orai activation, STIM proteins may cause  $\text{Ca}^{2+}$  influx via TRPC channels, which are found in cells from all regions of the brain and spinal cord, with high TRPV (TRP channel subfamily V), TRPC, and TRPM (TRP channel subfamily M) expression (Verkhatsky et al., 2014). Nevertheless, TRPC1 and Orai1 activation is mediated by different STIM1 domains. TRPC1 is involved in SOCE, but like the other TRPC channels, it is unable to generate a current that resembles  $\text{Ca}^{2+}$ -selective  $\text{I}_{\text{CRAC}}$  (Albarrán et al., 2016). TRPC1 function depends on Orai1-mediated  $\text{Ca}^{2+}$  influx, which triggers the recruitment of TRPC1 into the PM, where it is activated by STIM1. TRPC1 is thought to modify the initial  $\text{Ca}^{2+}$  signal that is caused by Orai1 activation (Ambudkar et al., 2017).

TRPC1-mediated SOCE is essential for neuronal survival (Wang and Poo, 2005; Bollimuntha et al., 2006; Selvaraj et al., 2012). The STIM1-TRPC1 interaction is thought to be neuroprotective in both *in vitro* and *in vivo* models of PD (Selvaraj et al., 2012; Sun et al., 2017, 2018). In the human SH-SY5Y neuroblastoma cell line, SOCE mainly depends on the activation of TRPC1. A neurotoxin that caused the selective loss of dopaminergic neurons (DNs) in the substantia nigra pars compacta (SNpc) decreases TRPC1 expression, the TRPC1-STIM1 interaction, and SOCE but not Orai expression (Selvaraj et al., 2012). TRPC1 overexpression prevents the neurotoxin-mediated loss of SOCE and decreases ER  $\text{Ca}^{2+}$  levels and the unfolded protein response (UPR). Additionally, TRPC1-mediated  $\text{Ca}^{2+}$  entry activates the neuroprotective AKT pathway. STIM1 or TRPC1 but not TRPC3 silencing increases the UPR. Consistent with these results, *Trpc1*<sup>-/-</sup> mice have a higher UPR and lower number of DNs, similar to PD patients. The overexpression of TRPC1 in mice increased DN survival after neurotoxin treatment.

STIM1 was also shown to inactivate  $\text{Ca}^{2+}$  entry via VGCCs, which is detrimental to DNs. Thus, the STIM1-TRPC1 interaction was thought to inhibit  $\text{Ca}^{2+}$  influx via VGCC channels, thereby protecting DNs (Selvaraj et al., 2012). Subsequent research showed that TRPC1 regulates L-type VGCCs in SNpc neurons (Sun et al., 2017). The STIM1-TRPC1 interaction after store depletion reduced DN activity in wildtype (WT) but not *Trpc1*<sup>-/-</sup> mice. In *Trpc1*<sup>-/-</sup> SNpc neurons, L-type VGCC  $\text{Ca}^{2+}$  currents increased, STIM1- $\text{Ca}_v1.3$  interactions were attenuated, and the number of DNs decreased. After TRPC1 activation, L-type  $\text{Ca}^{2+}$  currents and  $\text{Ca}_v1.3$  opening probability decreased, whereas they increased after STIM1/TRPC1 silencing. Additionally, store depletion increased the  $\text{Ca}_v1.3$ -TRPC1-STIM1 association. TRPC1 appears to suppress  $\text{Ca}_v1.3$  activation proving that STIM1 is essential for DN survival (Sun et al., 2017).

Sun et al. showed that mesenchymal stem cell (MSC)-derived DNs, similar to native neurons, utilize TRPC1-mediated SOCE (Sun et al., 2018). Similar to SH-SY5Y cells, neurotoxin treatment in MSC-derived DNs decreased TRPC1 expression and SOCE. TRPC inhibition alleviated dopamine release and MSC-derived DN viability. These results indicate that ER  $\text{Ca}^{2+}$  levels that are maintained by TRPC1-mediated SOCE are neuroprotective.

Neurotoxin exposure may cause alterations of SOCE and TRPC1-mediated  $\text{Ca}^{2+}$  homeostasis that may further induce ER stress and the UPR, leading to neurodegeneration. These results demonstrate that MSC-derived DNPs are similar to native DNPs, which potentially broadens the prospect of their usage for regenerative therapy in PD patients (Sun et al., 2018).

STIM1 and TRPC have also been shown to be involved in SOCE in astroglia. Antisense oligonucleotides that targeted the *Trpc1* gene reduced SOCE in murine astrocytes (Golovina, 2005). An anti-TRPC1 antibody lessened SOCE in rat astrocytes (Malarkey et al., 2008). In spinal astrocytes, SOCE was predominantly subserved by TRPC3 (Miyano et al., 2010). Some studies ascribed these differences between Orai- and TRPC-mediated SOCE to the stage of astroglial development, suggesting that SOCE in immature and maturing astroglia is predominantly mediated by Orai, whereas SOCE in mature cells is predominantly mediated by TRPC1 (Kettenmann and Bruce, 2013; Verkhratsky and Papura, 2014). Another study speculated that Orai1 and Orai3 are expressed in astroglial cells with abundant SOCE, whereas TRPC1 is restricted to astroglia where this process is attenuated (Kwon et al., 2017). STIM proteins, Orai1, and TRPM3 were identified as constituents of SOCE in astrocytes and oligodendrocytes of the mouse optic nerve (Papanikolaou et al., 2017). The developmental downregulation of Orai1 is consistent with TRPC channels as major components of mature astrocytes and oligodendrocytes, suggesting a potential role for Orai/STIM SOCE in immature glia and TRPM3 in mature glia (Verkhratsky et al., 2014).

Müller glia, a type of retinal glial cell, expresses STIM1 and requires the synergistic activation of both TRPC1 and Orai channels. The precise mechanism by which Orai and TRPC1 are activated by STIM1 has not been ascertained in these cells (Molnár et al., 2016).

## VGCCs

VGCCs are  $\text{Ca}^{2+}$  channels that are present primarily in electrically excitable cells (as neurons), known as transducers of electrical activity that enable  $\text{Ca}^{2+}$  influx in response to subthreshold depolarizing stimuli or action potentials (Harraz and Altier, 2014). They are assembled from the pore-forming  $\alpha 1$  subunit and accessory  $\beta$  and  $\alpha 2\delta$ -like subunits (Heine et al., 2020). Various isoforms of the  $\alpha 1$  subunit differ in voltage and  $\text{Ca}^{2+}$  sensitivity, which defines the specific kinetic properties of the channel. Thus, VGCCs are classified into low and high voltage-activated. The accessory  $\beta$  and  $\alpha 2\delta$ -like subunits play a role in membrane trafficking and the modulation of kinetic properties of high voltage-activated  $\text{Ca}^{2+}$  channels (Campiglio and Flucher, 2015; Brockhaus et al., 2018).  $\alpha 2\delta$ -like subunit and chemotaxis receptor domain containing 1 (Cachd1) alter the kinetic properties and surface expression of VGCCs (Cottrell et al., 2018; Dahimene et al., 2018). Cachd1 also impacts the gating and trafficking of low voltage-activated  $\text{Ca}^{2+}$  channels (Cottrell et al., 2018).

In excitable cells, VGCCs are the main route of  $\text{Ca}^{2+}$  entry in response to depolarizing stimuli. The main VGCC subtype that is present in neuronal, cardiac, and smooth muscle cells is  $\text{Ca}_v1.2$ , whereas  $\text{Ca}_v1.3$  is the predominant subtype in DNPs

(Sun et al., 2017). Both VGCC subtypes were shown to be suppressed by STIM1 (Park et al., 2010; Wang et al., 2010; Harraz and Altier, 2014; Sun et al., 2017, 2018). Two independent studies of excitable cells showed that ER  $\text{Ca}^{2+}$  store depletion alleviates depolarization-mediated  $\text{Ca}_v1.2$  activity, whereas the  $\text{Ca}_v1.2$  response increases after functional impairments in STIM1 (Park et al., 2010; Wang et al., 2010). STIM1- $\text{Ca}_v1.2$  interactions are directly mediated by the SOAR domain (i.e., the same domain that activates SOCcs) of STIM1 and C-terminus of the  $\text{Ca}_v1.2$   $\alpha 1$  subunit (Harraz and Altier, 2014; Pascual-Caro et al., 2018). The influence of STIM1 on VGCCs is also associated with an increase in channel internalization from the PM. Despite reporting similar results, two studies suggested different inhibitory mechanisms. Park et al. proposed a mechanism that involves the attenuation of VGCC expression, whereas Wang et al. suggested a potential role for Orai1 in the inhibitory STIM1- $\text{Ca}_v1.2$  interaction because the simultaneous inhibition of both Orai1 and STIM1 was necessary to suppress  $\text{Ca}_v1.2$  activity (Park et al., 2010; Wang et al., 2010).

The ability of STIM1 to regulate Orai1 and  $\text{Ca}_v1.2$  is tissue specific. STIM1 appears to stimulate SOCE in non-excitable cells and inhibit VGCCs in excitable cells (Harraz and Altier, 2014). STIM1 was also shown to control the plasticity of L-type VGCC-dependent dendritic spines (Dittmer et al., 2017; Sather and Dittmer, 2019). The activation of neuronal STIM1 induces changes in the ER structure, which depends on L-type VGCCs. The NMDAR activation of L-type VGCCs triggers  $\text{Ca}^{2+}$  release from the ER, which in turn causes STIM1 aggregation and its coupling with L-type VGCCs and then inhibits the activation of this channel, thus increasing ER spine content and stabilizing mushroom spines (Dittmer et al., 2017). STIM1 deficiency is associated with AD and triggers SH-SY5Y cell death by upregulating  $\text{Ca}_v1.2$  (Pascual-Caro et al., 2018). Thus, STIM1 KO cells may constitute an *in vitro* model to study the pathogenesis of AD and may be useful for understanding the role of STIM1 in neurodegeneration. In turn, as mentioned in section TRPC Channels above, TRPC1 in DNPs facilitates STIM1- $\text{Ca}_v1.3$  interactions to suppress  $\text{Ca}_v1.3$  activity, thereby reducing apoptosis and protecting DNPs against neurotoxin-induced insults that lead to PD (Sun et al., 2017).

## AMPA Receptors

AMPA receptors belong to the family of ionotropic glutamate receptors. They are thought to be the most significant mediators of excitatory neurotransmission in the CNS (Rogawski, 2011). They are assembled from four subunits (GluA1-4) and are mainly permeable to  $\text{Na}^+$  and  $\text{K}^+$  and to  $\text{Ca}^{2+}$  to a lesser extent. The subunit composition of AMPARs varies depending on the stage of development, region, and cell type (Song and Haganir, 2002). Phosphorylation of the GluA1 C-terminal tail regulates activity-dependent synaptic transport and channel features of the receptor (Esteban et al., 2003). Ser-831 and Ser-845 are two phosphorylation sites of GluA1 that have been well-characterized. Phosphorylation at Ser-831 by CaMKII and protein kinase C (PKC) regulates channel conductance, whereas cyclic adenosine monophosphate (cAMP)/protein kinase A (PKA)-dependent phosphorylation at Ser-845 enhances channel open probability and promotes AMPAR internalization (Derkach

et al., 1999). The PKA-dependent phosphorylation of GluA1 depends on the PKA scaffold AKAP150, which places PKA in proximity to its synaptic targets (Garcia-Alvarez et al., 2015) and cAMP-mediated dissociation of the regulatory subunit (rPKA) from the catalytic subunit (cPKA; Garcia-Alvarez et al., 2015). Both Ser-845 and Ser-831 phosphorylation sites play a role in LTP and LTD, forms of synaptic plasticity that are responsible for learning and memory (Esteban et al., 2003; Makino and Malinow, 2011).

Interestingly, STIM2 was shown to interact with AMPARs through a mechanism that is not associated with SOCE (Garcia-Alvarez et al., 2015). Recent research showed that STIM2 induces the cAMP/PKA-dependent delivery of GluA1 to the PM (Garcia-Alvarez et al., 2015). These authors suggested that STIM2 couples PKA to AMPARs and promotes the phosphorylation of GluA1 at Ser-845. They revealed a strong interaction between STIM2 and cPKA and weak STIM2 binding to rPKA and AKAP150, which may clarify the mechanism of interaction. Surprisingly, STIM2 and the phosphorylation of GluA1 at Ser-831 are negatively correlated. In STIM2-silenced neurons, phosphorylation at Ser-831 is enhanced. These findings indicate that STIM2 regulates the phosphorylation of GluA1 at both Ser-845 and Ser-831 but in a different manner. In turn, STIM1 overexpression was shown to increase GluA1 phosphorylation at Ser-845 in hippocampal synaptoneurosome (Majewski et al., 2017).

Our previous study found that STIM proteins in primary rat cortical neurons may also interact with AMPARs in a SOCE-dependent manner, meaning that when ER  $\text{Ca}^{2+}$  stores are depleted,  $\text{Ca}^{2+}$  may enter through Orais, TRPC channels, and AMPARs (Gruszczyńska-Biegala et al., 2016). The SOCE inhibitors ML-9 and SKF96365 decreased AMPA-induced  $\text{Ca}^{2+}$  influx, and the competitive AMPAR antagonists CNQX and NBQX inhibited SOCE. The induction of SOCE by thapsigargin resulted in AMPAR activation either directly through the recruitment of AMPARs to the PM or indirectly through unknown mechanisms. We also confirmed that both STIM1 and STIM2 proteins directly interacted with the GluA1 and GluA2 subunits of AMPARs. Moreover, STIM-AMPA complexes appear to be located in ER-PM junctions (Gruszczyńska-Biegala et al., 2016).

## NMDA Receptors

NMDARs are ligand-gated ion channels that mediate  $\text{Ca}^{2+}$  influx when activated by glutamate, the main excitatory neurotransmitter in the mammalian CNS. NMDARs are tetramers that are composed of two glycine-binding NR1 (GluN1) and two glutamate-binding NR2 (GluN2) subunits (Cull-Candy and Leszkiewicz, 2004). Synaptic NMDARs consist mainly of NR1-NR2A or NR1-NR2A-NR2B receptors, and somatic NMDARs consist mainly of NR1-NR2B (Cull-Candy and Leszkiewicz, 2004).  $\text{Ca}^{2+}$  influx through NMDARs plays an important role in neuronal development, the formation of basal excitatory synaptic transmission, cell survival, and different forms of synaptic plasticity, such as LTP and LTD (Malenka and Bear, 2004; Nakazawa et al., 2004; Kerchner and Nicoll, 2008).

Pathologically high levels of glutamate and NMDA cause excitotoxicity by allowing high levels of  $\text{Ca}^{2+}$  to enter the cell (Sattler and Tymianski, 2000). Excessive NMDAR stimulation and prolonged increases in intracellular  $\text{Ca}^{2+}$  concentrations cause  $\text{Ca}^{2+}$  overload, which is considered a main cause of neuronal death in various neurodegenerative diseases that are associated with excitotoxicity, such as HD and AD (Marambaud et al., 2009; Pchitskaya et al., 2018; Serwach and Gruszczyńska-Biegala, 2019). Attenuating intracellular  $\text{Ca}^{2+}$  overload is thus essential for limiting neuronal cell death under neuropathological conditions.

In hippocampal pyramidal neurons, SOCE can be activated by synaptic NMDAR stimulation, thus demonstrating its involvement in synaptic plasticity, such as LTP (Baba et al., 2003; Dittmer et al., 2017). Interestingly, glutamate release from neuronal terminals and NMDAR activation also induce SOCE in the PM of adjacent astrocytes possibly involving astrocytic mGluR5 (Lim et al., 2018). We recently reported that NMDARs contribute to  $\text{Ca}^{2+}$  influx in SOCE in rat cortical neurons (Gruszczyńska-Biegala et al., 2020). The glutamate depolarization of neurons activates  $\text{Ca}^{2+}$  influx through NMDARs and L-type VGCCs, releases  $\text{Ca}^{2+}$  from the ER (Simpson et al., 1995; Emptage et al., 1999, 2001; Dittmer et al., 2017), and aggregates and activates STIM1, which then triggers SOCE (Rae et al., 2000; Emptage et al., 2001; Dittmer et al., 2017). In recent work, we found that endogenous STIM1 and STIM2 interact *in situ* and *in vitro* and co-localize with endogenous NMDAR subunits in rat cortical neurons. Emptying  $\text{Ca}^{2+}$  from ER stores induces a decrease in the physical association between endogenous STIM1 and NR2B and between STIM2 and NR2A (Gruszczyńska-Biegala et al., 2020). Additionally, STIMs were shown to modulate NMDA-evoked intracellular  $\text{Ca}^{2+}$  levels by interacting with them. These data suggest that STIM1 and STIM2 are negative regulators of NMDA-induced intracellular  $\text{Ca}^{2+}$  elevations in cortical neurons (Gruszczyńska-Biegala et al., 2020), in which they have been shown to inhibit the activity of L-type VGCCs (Park et al., 2010; Wang et al., 2010; Dittmer et al., 2017).

## STIM INTERACTING PROTEINS

Most of the aforementioned studies on STIM function in the CNS focused on its canonical function in ER  $\text{Ca}^{2+}$  store refilling that results from the activation of SOCE. Recently, an increasing number of proteins have been reported to play a vital role in the regulation of Orai1-, TRPC-, and STIM1-associated  $\text{Ca}^{2+}$  signaling in both a SOCE-dependent and SOCE-independent manner in the CNS. This section focuses on several of the most important partners of STIM proteins that may also contribute to essential molecular processes in the CNS (Figure 3).

### mGluRs

Group I metabotropic glutamate receptors (mGluRs) are widely distributed in the CNS and play a key role in synaptic transmission and plasticity. Excessive mGluR activation was shown in acute and chronic neurodegenerative disorders such as PD, AD, and HD (Crupi et al., 2019). The stimulation of

group I mGluRs activates two signaling pathways (Hartmann et al., 2014). The first signaling pathway activates phospholipase C (PLC), thus inducing the formation of IP<sub>3</sub>, which interacts with IP<sub>3</sub>Rs to release Ca<sup>2+</sup> from ER stores (Hartmann et al., 2014). The second signaling pathway involves the formation of slow excitatory post-synaptic potentials (EPSPs; Batchelor et al., 1994) and is mediated by TRPC3 (Hartmann et al., 2008).

STIM proteins also interact with TRPC3, and the STIM-mGluR association has been widely investigated. Hartman et al. showed that following mGluR1 activation, STIM1 proteins oligomerize and evoke SOCE through TRPC3 channels (Hartmann et al., 2008, 2014). Consistent with this, Ng et al. found that the activation of group I mGluRs with 3,5-dihydroxyphenylglycine (DHPG) in hippocampal neurons stimulated STIM1 oligomerization and its transport to the PM (Ng et al., 2011). Another research group showed that STIM1 in cerebellar PNs participates in mGluR1-dependent synaptic transmission and thus regulates cerebellar motor behavior (Hartmann et al., 2014). In mice with the PN-specific deletion of STIM1, mGluR1-dependent signaling was eliminated, and both IP<sub>3</sub>-dependent Ca<sup>2+</sup> release from the ER and TRPC3-mediated EPSCs were attenuated. The disruption of these two pathways abolished cerebellar motor behavior (Hartmann et al., 2014). The role of STIM1 in synaptic plasticity was also investigated in hippocampal slices from adult transgenic Tg(STIM1)Ibd mice. STIM1 overexpression appears to disrupt mGluR LTD that is induced by DHPG (Majewski et al., 2017).

A recent analysis by Tellios et al. showed that in the absence of neuronal nitric oxide synthase (nNOS)-derived NO signaling along with the higher expression of mGluR1, STIM1 expression and cluster density are elevated in PNs (Tellios et al., 2020). These authors suggested that the overactivation of mGluR1 results in ER Ca<sup>2+</sup> depletion and chronic STIM1 oligomerization. Because of the unlimited opening of TRPC3 channels, Ca<sup>2+</sup> entry through STIM1-gated TRPC3 channels may be elevated, further leading to a reduction of dendritic spine integrity in PNs (Tellios et al., 2020). In contrast, under physiological conditions, nNOS/NO signaling maintains Ca<sup>2+</sup> homeostasis in neurons by reducing its influx through mGluR1 and inducing the S-nitrosylation of STIM1. As STIMs and Ora1s as well as NMDARs and mGluRs are expressed in the microvascular endothelial cells of the brain (LeMaistre et al., 2012; Negri et al., 2020), we can suspect that these endothelial receptors may also be regulated by STIMs. Especially since the Ca<sup>2+</sup> response to glutamate by activating mGluR1 and mGluR5 is initiated by endogenous Ca<sup>2+</sup> release from the ER through IP<sub>3</sub>R<sub>3</sub> and sustained by SOCE, resulting in a rapid NO release (Negri et al., 2020).

## Homer Family Proteins

Homer family proteins are post-synaptic scaffolding proteins that regulate glutamatergic signaling and intracellular Ca<sup>2+</sup> concentrations in neurons (Chen et al., 2012). Homer was reported in neurological disorders, including AD, TBI, and schizophrenia (Luo et al., 2012). These proteins are divided into two major groups: short-form Homer1a proteins and long-form Homer1b/c, Homer2, and Homer3 proteins. Both groups have N-terminal EVH1 domain that is involved in protein

interactions, and long-form proteins also have a C-terminal coiled-coil domain that is involved in self-association (Chen et al., 2012). Homer1b/c has been shown to alter SOCE through an association with STIM1 and Ora1 in human platelets. This interaction between STIM1, Homer1b/c, and Ora1 is enhanced by thapsigargin (Jardin et al., 2012). Thapsigargin also induces Homer1, STIM1, and L-type VGCC associations in HEK-293 cells (Dionisio et al., 2015).

In the CNS, SOCE antagonists and STIM1-targeted small-interfering RNA (siRNA) increase the expression of *Homer1a* mRNA and the amount of Homer1a protein (Li et al., 2013). The knockdown of Homer1a expression partially reverses this effect. Moreover, SOCE inhibition appears to protect neurons against oxidative stress through the upregulation of Homer1a expression (Li et al., 2013). SOCE inhibitors also prevented mitochondrial dysfunction and activation of mitochondrial apoptotic factors after MPP<sup>+</sup> injury. Since mitochondrial dysfunction is thought to play a crucial role in PD, it seems that SOCE may be a potential target in the treatment of PD patients (Li et al., 2013).

Homer1a affects STIM1-Ora1 associations, inhibits SOCE, and alleviates glutamate-induced cell death after oxidative stress injury (Rao et al., 2016). Both thapsigargin-induced and glutamate-mediated STIM1-Ora1 associations are attenuated by Homer1a overexpression. After thapsigargin-induced ER Ca<sup>2+</sup> store depletion, the association between STIM1 and Homer1a decreases, whereas no change occurs in the Homer1a-Ora1 association. These interactions between STIM1, Homer1a, and Ora1 are similar to interactions between STIM1 and Homer1b/c or STIM1, Homer1b/c, and Ora1 (Jardin et al., 2012; Dionisio et al., 2015; Rao et al., 2016). Therefore, Homer1a might dissociate STIM1-Ora1 complexes and downregulate SOCE through negative competition with Homer1b/c (Rao et al., 2016). The regulation of Homer1a and SOCE inhibition may be a potential therapeutic target for the treatment of neurological disorders, the etiology of which is associated with oxidative stress.

## SARAF

SOCE-associated regulatory factor (SARAF) is a 339-amino-acid type I transmembrane protein that has exceptionally high transcript levels in neuronal tissues (Palty et al., 2012). It is assembled from a single N-terminal transmembrane domain and a C-terminal domain that is located in the ER or PM (Palty et al., 2012; Albarran et al., 2016). The activation of SARAF involves the intraluminal region, whereas the interaction with SARAF engages the cytosolic region (Jha et al., 2013). Gene product of TMEM66, SARAF was identified as a biomarker linked to AD (Twine et al., 2011).

SARAF modulates STIM1-regulated Ca<sup>2+</sup> entry, which includes both SOCE and Ca<sup>2+</sup> influx through ARC channels (Palty et al., 2012; Albarran et al., 2016). SARAF prevents the spontaneous activation of STIM1, regulates STIM1-Ora1-mediated SOCE, facilitates the slow Ca<sup>2+</sup>-dependent inactivation of SOCE, and promotes STIM1 deoligomerization after Ca<sup>2+</sup> store refilling (Palty et al., 2012; Jha et al., 2013). SARAF was also reported to modulate cytosolic and ER Ca<sup>2+</sup> levels (Palty et al., 2012). The molecular mechanism of action of SARAF was described by Jha et al., who showed that SARAF interacts

with the C-terminal inhibitory domain (CTID) of STIM1 to mediate the slow  $\text{Ca}^{2+}$ -dependent inactivation (SCDI) of Orai1-forming CRAC (Jha et al., 2013). Under resting conditions, when intracellular  $\text{Ca}^{2+}$  stores are filled with  $\text{Ca}^{2+}$ , CTID facilitates the access of SARAF to the SOAR to keep STIM1 in an inactive state, resulting in the inhibition of STIM1-Orai communication. Upon  $\text{Ca}^{2+}$  store depletion, SARAF dissociates from STIM1 to allow the activation of STIM1-Orai complexes at ER-PM junctions, thereby leading to SOCE (Jha et al., 2013).

SARAF is constitutively expressed in the PM. It was also shown to modulate  $\text{Ca}^{2+}$  entry through ARC channels in the SH-SY5Y neuroblastoma cell line (Albarran et al., 2016). ARC channels are heteropentameric complexes that consist of three Orai1 and two Orai3 subunits and PM-resident STIM1. The overexpression of SARAF in neuroblastoma cells attenuated the arachidonic acid (AA)-induced  $\text{Ca}^{2+}$  response, and the transfection of SARAF siRNA enhanced AA-stimulated  $\text{Ca}^{2+}$  influx via ARC channels. The results suggest that SARAF is a negative regulator of AA-induced  $\text{Ca}^{2+}$  signaling (Albarran et al., 2016).

SARAF was also shown to interact with TRPC1 in a STIM1-independent manner in both STIM1-deficient NG115-401L and endogenous STIM1-expressing SH-SY5Y neuroblastoma cells (Albarrán et al., 2016). The silencing of SARAF expression in STIM1-deficient cells increased TRPC1-mediated  $\text{Ca}^{2+}$  entry. In cells that endogenously expressed STIM1, the interaction between SARAF and TRPC1 was not associated with STIM1. This regulation of  $\text{Ca}^{2+}$  entry is thought to protect the cell from  $\text{Ca}^{2+}$  overload and adjust the influx of  $\text{Ca}^{2+}$ , which was previously reported for the regulation of SOCE and ARC channels (Albarran et al., 2016). The silencing of SARAF expression did not influence TRPC6-mediated  $\text{Ca}^{2+}$  entry, in contrast to TRPC1, meaning that SARAF is unlikely to regulate the TRPC6 function. SARAF appears to play a negative regulatory role in both STIM1-Orai1- and STIM1-TRPC1-mediated  $\text{Ca}^{2+}$  entry by destabilizing STIM1/Orai1 complexes (Palty et al., 2012). Notably, a recent study reported a reduction of the expression of STIM1 and SARAF in the ischemic cortex, indicating that SARAF may be a new neuroprotective target for the treatment of stroke (La Russa et al., 2020).

## Septins

Septins are a class of evolutionary conserved GTPases that are assembled into hexameric or octameric complexes organized into linear filaments or other higher-order structures. They function as diffusion barriers and intracellular scaffolds in cells during various cellular processes (Mostowy and Cossart, 2012). The altered septin function may contribute to synaptic dysfunction in neurodegenerative diseases (Marttinen et al., 2015).

Septins were shown to regulate SOCE in both non-excitable mammalian cells (Sharma et al., 2013) and *Drosophila* neurons (Deb and Hasan, 2016, 2019; Deb et al., 2016, 2020). In *Drosophila*, septins are classified into several groups: dSEPT1, dSEPT2, dSEPT4, dSEPT5 and dSEPT7. The dSEPT7, dSEPT1, and dSEPT4 groups form linear hexamers. dSEPT1 and dSEPT4 occupy the central position, and dSEPT7 is localized in terminal positions of the hexamer. These hexamers are then linked

and form linear septin filaments (Mostowy and Cossart, 2012; Mavrakakis et al., 2014). The molecular mechanism of SOCE regulation and contribution of different subgroups of septins to the regulation of SOCE is complex.

The simultaneous knockdown of dSEPT1 and dSEPT4 reduced SOCE in *Drosophila* flight circuit neurons (Deb et al., 2016). The knockdown of these subgroups results in the loss of septin filaments and loss of the diffusion barrier, which has a negative influence on Orai activation by STIM (Deb and Hasan, 2016). dSEPT1 and dSEPT4 appear to function as positive regulators of SOCE in *Drosophila* neurons (Deb et al., 2016; Deb and Hasan, 2019). On the other hand, reduction of dSEPT7 had no significant influence on SOCE in *Drosophila* neurons. Nevertheless, the reduction of dSEPT7 in primary neurons that had low levels of *Drosophila* STIM1 (dSTIM1) improved SOCE (Deb et al., 2016). Additionally, STIM1 is necessary for SOCE through Orai channels also in SEPT7 knockdown human neural progenitor cells (hNPCs; Deb et al., 2020). In resting neurons with low dSEPT7 expression, the intensity of dSTIM and resulting dSTIM-dOrai clusters that are observed near the ER-PM region increased (Deb et al., 2016, 2020). Similar STIM1 and Orai1 reorganization was shown at the cell surface in SEPT7 knockdown neurons that were differentiated from hNPCs (Deb et al., 2020). Deb et al. suggested that the partial reduction of dSEPT7 leaves hexameric complexes intact but results in the formation of smaller septin filaments because filament elongation requires dSEPT7 (Deb et al., 2016). Shorter SEPT7 filaments support dSTIM migration to the peripheral ER in resting neurons, promoting Orai channel opening independently from either ER- $\text{Ca}^{2+}$  store depletion or  $\text{Ca}^{2+}$  release through  $\text{IP}_3\text{Rs}$ . Similarly, SEPT4 regulates the number of the ER-PM junctions and enhances STIM1-Orai1 interactions within junctions in human cells (Katz et al., 2019). Store-independent dOrai  $\text{Ca}^{2+}$  influx results in higher cytosolic  $\text{Ca}^{2+}$  concentrations in resting neurons (Deb and Hasan, 2016). The loss of dSEPT7 influences the constitutive activation of Orai channels in resting neurons by uncoupling septin heteromers from ER-PM junctions, thus allowing the STIM interaction with Orai (Deb et al., 2016, 2020).

Septins (e.g., dSEPT1, dSEPT4, and SEPT7) appear to perform antagonistic rather than synergistic functions in Orai channel activation by STIM. This discrepancy may be caused by a different assembly of septins during complex formation and by differences in subsequent filament structure (Deb and Hasan, 2019). Altogether, these results could link alterations of septin expression to impairments in STIM1-dependent SOCE in human neurodegenerative diseases.

## Golli Proteins

Golli proteins are isoforms of myelin basic protein (MBP) that are abundantly expressed in immune cells and the CNS (Paez et al., 2011). It is upregulated in adult OPCs and microglia in multiple sclerosis lesions (Filipovic et al., 2002). Myelin abnormalities have been implicated in neurodegenerative and neuropsychiatric diseases and Golli-MBP expression was increased in the aging brains (Siu et al., 2015). Golli proteins were shown to be components of remyelination that is caused by treatment with

taxol in demyelinating transgenic mice, thus demonstrating their role in early stages of OPC proliferation and migration (Moscarello et al., 2002). Although no evidence suggests the occurrence of SOCE in oligodendroglia cells, this process was detected in OPCs and brain slices and shown to be mediated by STIM1 and TRPC1. Additionally, SOCE in these cells is positively modified by golgi proteins that interact with STIM1 and TRPC1 (Paez et al., 2011). Changes in golgi protein expression alter VGCCs and SOC to mediate the migration and proliferation in OPCs that influence their maturation and survival (Paez et al., 2009a,b; Paez et al., 2007). Another study showed that golgi protein overexpression increases the mitogen-stimulated proliferation of OPCs through the activation of SOCE, which is essential for cell division (Paez et al., 2009a). In OPCs, the proliferation of golgi protein-KO cells was less robust, and the duration of the cell cycle increased. Golgi proteins were also reported to increase apoptotic cell death, which was associated with an increase in  $\text{Ca}^{2+}$  influx through VGCCs (Paez et al., 2009a). Notably, the C-terminus of STIM1 was also shown to bind to MBP in a brain extract in a pull-down assay, which is likely an epitope that is shared with golgi protein (Walsh et al., 2010).

## POST and SERCA

Several molecular mechanisms are responsible for the increase in cytosolic  $\text{Ca}^{2+}$  concentrations after cell depolarization, including SERCA, PMCA, NCX, and mitochondrial  $\text{Ca}^{2+}$  uptake. Among these mechanisms, SERCA and PMCA are regulated by STIM1, combined with an adaptor protein called partner of STIM1 (POST; Krapivinsky et al., 2011). After ER  $\text{Ca}^{2+}$  store depletion, the STIM1-POST complex binds to SERCA and keeps it close to  $\text{Ca}^{2+}$  entry sites on the PM to promote the refilling of ER  $\text{Ca}^{2+}$  stores (Krapivinsky et al., 2011). The STIM1-POST complex also inhibits PMCA activity, which is associated with  $\text{Ca}^{2+}$  outflow from the cytoplasm to the extracellular space (Ritchie et al., 2012). STIM1 appears to play opposing roles at the same time. However, SERCA contributes more to cytosolic  $\text{Ca}^{2+}$  clearance than PMCA, especially in PNs (Fierro et al., 1998). Thus, after PM depolarization, STIM1 reduces cytoplasmic  $\text{Ca}^{2+}$  concentrations. Additionally, Ryu et al. showed that STIM1 contributes to SERCA-dependent cytosolic  $\text{Ca}^{2+}$  clearance in the soma of firing PNs (Ryu et al., 2017). These authors proposed that the STIM1-POST complex may pull SERCA into the vicinity of VGCCs. If so, then SERCA could buffer  $\text{Ca}^{2+}$  influx more rapidly after depolarization, which can optimize the  $\text{Ca}^{2+}$ -clearing and -buffering function of SERCA and prevent excessive cytosolic  $\text{Ca}^{2+}$  concentrations during repetitive firing (Ryu et al., 2017).

STIM1 mediates the sequestration of cytosolic  $\text{Ca}^{2+}$  ions by SERCA. It may also regulate neuronal excitability. Nevertheless, still unknown is whether this occurs only with high-firing neurons, such as PNs, or also with slow-firing neurons, such as pyramidal and cortical neurons (Ryu et al., 2017).

In this context it is worth noting that the function of SERCA can be also regulated by ER lumen residents calreticulin and ERp57 oxidoreductase (Li and Camacho, 2004). Thus, we suspect that these proteins may interact with STIM in neurons, especially since they are expressed therein (Coe and

Michalak, 2010). ERp57 and STIM1 formed complexes *in vivo* and *in vitro* to inhibit STIM oligomerization and SOCE in mouse embryonic fibroblasts (Prins et al., 2011). Interestingly, in megakaryocytes from healthy individuals, calreticulin regulated SOCE activation through interaction with ERp57 and STIM1. In megakaryocytes from patients with mutated calreticulin, destabilization of the complex between calreticulin, ERp57 and STIM1 was observed, leading to enhanced SOCE and thus to abnormal cell proliferation (Di Buduo et al., 2020). ERp57 is associated not only with myeloproliferative neoplasms, but also with many disease states of CNS, such as prion disorders and AD, where ERp57 and calreticulin have been shown to prevent amyloid aggregation (Coe and Michalak, 2010). Similarly, SERCA-mediated  $\text{Ca}^{2+}$  dysregulation is associated with neuropathological conditions, such as affective disorders and neurodegenerative diseases (Britzolaki et al., 2020).

## IP<sub>3</sub>Rs

Receptors that activate PLC cause the formation of IP<sub>3</sub>, which triggers both  $\text{Ca}^{2+}$  release from ER stores through IP<sub>3</sub>Rs and  $\text{Ca}^{2+}$  influx from the extracellular milieu, which is mediated by SOCE. IP<sub>3</sub>Rs are thought to regulate SOCE by mediating ER  $\text{Ca}^{2+}$  release. Under physiological conditions, store depletion causes STIM and IP<sub>3</sub>R accumulation near the PM, an association between STIM and Orai, and the activation of SOCE. In *Drosophila* neurons with mutant IP<sub>3</sub>Rs, SOCE was attenuated (Chakraborty et al., 2016; Deb et al., 2016) and this attenuation was reversed by STIM and Orai overexpression. The authors speculated that after ER  $\text{Ca}^{2+}$  store depletion in *Drosophila* neurons, IP<sub>3</sub>R translocation to the ER-PM junction triggers the coupling of STIM to Orai, leading to the activation of SOCE (Chakraborty et al., 2016).

The same research group also reported the enhancement of spontaneous  $\text{Ca}^{2+}$  influx from the extracellular milieu and loss of SOCE in *Drosophila* pupal neurons with mutant IP<sub>3</sub>Rs (Chakraborty and Hasan, 2017). Both spontaneous  $\text{Ca}^{2+}$  influx and the attenuation of SOCE were reversed by dOrai and dSTIM overexpression. Additionally, the expression of VGCCs decreased, and the expression of *trp* mRNAs and TRPC protein increased in mutant neurons, suggesting that these channels might be associated with the increase in spontaneous  $\text{Ca}^{2+}$  influx. Spontaneous  $\text{Ca}^{2+}$  influx likely compensates for the loss of SOCE in *Drosophila* IP<sub>3</sub>R mutant neurons and maintains intercellular  $\text{Ca}^{2+}$  homeostasis (Chakraborty and Hasan, 2017). The overexpression of dSTIM in insulin-producing neurons and aminergic neurons also improves SOCE and restores flight in a flightless *Drosophila* IP<sub>3</sub>R mutant (Agrawal et al., 2010). These authors suggested that IP<sub>3</sub>R-mediated  $\text{Ca}^{2+}$  release couples to SOCE via dSTIM/dOrai in *Drosophila* flight circuit neurons, thereby allowing dSTIM to compensate for impairments in IP<sub>3</sub>R function (Agrawal et al., 2010).

No evidence has been reported that the contribution of IP<sub>3</sub>R to SOCE in *Drosophila* occurs in mammalian neurons. However, in some mammalian cells, IP<sub>3</sub>Rs have been shown to co-localize with Orai1 (Lur et al., 2011) and interact with STIM1, Orai1, and TRPCs (Hong et al., 2011). The expression of IP<sub>3</sub>R isoform (IP<sub>3</sub>R<sub>3</sub>) was shown to be significantly lower in STIM1-deficient

SH-SY5Y cells, meaning that STIM1 is a positive regulator of *ITPR3* gene expression in these cells (Pascual-Caro et al., 2020).  $IP_3R_3$  is a  $Ca^{2+}$  channel that is localized mainly at the ER-mitochondrion junction, which transfers  $Ca^{2+}$  from the ER to mitochondria (Ivanova et al., 2014). Thus, STIM1 deficiency leads to a decrease in mitochondrial  $Ca^{2+}$  concentrations, leading to cell death. The overexpression of  $IP_3R_3$  restores mitochondrial  $Ca^{2+}$  homeostasis and bioenergetics, ATP production, and cell survival in STIM1-KO neuronal-like cells (Pascual-Caro et al., 2020). These results provide evidence of a novel STIM1- $IP_3R_3$ -mediated pathway of mitochondrial  $Ca^{2+}$  levels, the dysregulation of which contributes to neurodegeneration. Mitochondria from AD patients have lower  $Ca^{2+}$  uptake (Kumar et al., 1994), which is attributed to lower  $IP_3R_3$  and STIM1 levels (Pascual-Caro et al., 2020).

## EB1 and EB3

The dynamic structure of dendritic spines is preserved mainly by actin filaments, and microtubules (MTs) are cytoskeleton-organizing components localized in dendrites and axons (Majewski and Kuznicki, 2015; Wu et al., 2017). Microtubules have been shown to enter dendritic spines and trigger spine head enlargement (Gu et al., 2008; Hu et al., 2008). This transport of MTs into dendritic spines appears to be involved in mechanisms of synaptic plasticity. Microtubule plus-ends contain end-binding (EB) proteins, which are divided into three types: EB1, EB2, and EB3 and have been shown to interact with STIM1 (Akhmanova and Steinmetz, 2010).

EB1/EB3-STIM1 complexes mediate ER movement in non-excitable cells (Grigoriev et al., 2008; Honnappa et al., 2009; Asanov et al., 2013). The STIM1-EB association sequesters STIM1 in MTs and prevents the excessive activation of SOCE (Chang et al., 2018). STIM1 regulates the dynamics of EB1/EB3, coupling the ER to MTs within filopodia and thus controlling growth cones in the nascent nervous system (Pavez et al., 2019). Additionally, recent research demonstrated that EB3 forms complexes with STIM2 that promote the formation of mushroom spines in hippocampal neurons, and the disintegration of these complexes results in the loss of mushroom spines (Pchitskaya et al., 2017). The overexpression of EB3 increases the proportion of mushroom spines and rescues their deficiency in hippocampal neurons in an AD mouse model. EB3 overexpression also rescues the loss of mushroom spines after STIM2 knockdown, whereas STIM2 overexpression does not restore mushroom spines after EB3 depletion. Neither STIM2 overexpression nor the activation of hippocampal TRPC6 increases spine neuronal SOC or the proportion of mushroom spines in WT neurons. EB3 recruits various proteins to dendritic spines during synaptic plasticity, and STIM2 may be one of these cargo proteins (Pchitskaya et al., 2017). EB3 is involved in the regulation of dendritic spine morphology partly through its association with STIM2. Therefore, targeting EB3-STIM2 complexes may stabilize dendritic spines in AD patients (Pchitskaya et al., 2017).

## Synaptopodin

In cultured neurons, STIM1 interacts with anchoring proteins in the dendritic spine apparatus that consists of laminar smooth

ER stacks. Synaptopodin (SP) is localized between ER stacks of the spine apparatus. This cytosolic actin and  $\alpha$ -actinin-binding protein has been shown to be essential for the formation of this organelle (Deller et al., 2003). Synaptopodin is more common in spines with large-volume spine heads, where it regulates synaptic plasticity by controlling spine head enlargement during LTP in the CA1 region of the hippocampus and enhances glutamate-induced  $Ca^{2+}$  release in dendritic spines of cultured hippocampal neurons (Deller et al., 2003; Vlachos et al., 2009; Korkotian et al., 2014). Synaptopodin deficiency alleviated the AD symptoms in the 3xTg mice and restores normal synaptic plasticity (Aloni et al., 2019).

Synaptopodin was recently shown to regulate activity-dependent  $Ca^{2+}$  signaling by recruiting STIM1 to the post-synaptic density (PSD; Korkotian et al., 2014; Segal and Korkotian, 2014). In primary hippocampal neurons, SP co-localizes with STIM1 (Korkotian et al., 2014). The localization of STIM1 in spines depended on SP, in which this protein preferentially located STIM1 to mushroom spines, where this association was especially evident (Korkotian et al., 2014). These results indicate that SP interacts with STIM and Orai and thus may regulate the functionality of  $Ca^{2+}$  stores and determine synaptic plasticity.

As SP belongs to actin-binding proteins, it would be interesting to investigate whether STIM could also directly interact with actin in dendritic spines. It is worth mentioning the regulatory role of actin in spine morphogenesis and stabilization that is necessary for memory formation, the role in mechanisms related to synaptic plasticity and the contribution to AD pathology (Basu and Lamprecht, 2018; Pelucchi et al., 2020). Previous research has demonstrated that STIM1 may interact with actin, and actin remodeling was required to move STIM to the PM after store depletion in human platelets. Furthermore, the polymerization of actin filaments was necessary for association of STIM1 with TRPC1 (López et al., 2006). Similarly, actin fibers were shown to be involved in an alternatively spliced long variant of STIM1 oligomerization that precedes activation of Orai1 in myoblasts (Darbellay et al., 2011). Notably, Trebak's group reported that STIM1 controls formation of actin stress fibers, independently of Orai1 and  $Ca^{2+}$ , thus thrombin-mediated disruption of endothelial barrier function (Shinde et al., 2013).

## Presenilins and CaMKII

Familial Alzheimer's disease (FAD) is caused by a dominant inherited mutation of presenilins (PSs; PS1 and PS2) and amyloid- $\beta$  ( $A\beta$ ) precursor protein (APP; Chakraborty and Stutzmann, 2014). Presenilins constitute catalytic components of the  $\gamma$ -secretase complex, which cleaves transmembrane APP to produce  $A\beta$ . PS1 mutations have been shown to change APP cleavage in favor of producing  $A\beta$ . This peptide accumulates, causing neuronal death in the cerebral cortex and hippocampal neurons, contributing to cognitive impairment and other pathological hallmarks of AD (Chakraborty and Stutzmann, 2014).

Endogenous PS1 and STIM1 have been shown to interact in human SH-SY5Y neuroblastoma cells and mouse primary cortical neurons (Tong et al., 2016). Tong et al. defined

STIM1 as a new substrate of  $\gamma$ -secretase in a PS model of AD. The PS1-associated  $\gamma$ -secretase complex cleaves the STIM1 transmembrane domain, reducing ORAI activation and diminishing SOCE (Tong et al., 2016). Dendritic spines in hippocampal neurons with mutant PS1 are destabilized, which is reversed by both a  $\gamma$ -secretase inhibitor and STIM1 overexpression. Although, the cleavage of STIM2 has not yet been established, its structural similarity to STIM1 suggests that it may also be a target of  $\gamma$ -secretase. Ryazantseva et al. reported the enhancement of SOCE in hippocampal neurons with a PS1  $\Delta$ E9 mutation (Ryazantseva et al., 2018). This PS1 mutation excludes 28 amino acids from the proteolytic cleavage site, resulting in the accumulation of uncleaved proteins. STIM1 accumulation results in its enhanced relocation to the PM, increasing the Orai1-TRPC association and enhancing SOCE (Ryazantseva et al., 2018). In turn, SOCE was attenuated directly in neurons from transgenic mice expressing human mutant PS1 A246E (Herms et al., 2003). The effect of PS1 on STIM1 appears to differ depending on the type of mutation. Greotti et al. reported that both PS1 and PS2 in SH-SY5Y cells reduce SOCE by reducing STIM1 expression levels (Greotti et al., 2019). However, this reduction does not depend on  $\gamma$ -secretase activity. Lower amounts of STIM1 protein were also found in FAD PS-expressing cells that were treated with a  $\gamma$ -secretase inhibitor. Moreover, chronic ER  $\text{Ca}^{2+}$  depletion or alterations of STIM1 expression levels did not affect SOCE under resting conditions (Greotti et al., 2019). These results may be considered an adaptive consequence of a prolonged reduction of ER  $\text{Ca}^{2+}$  levels.

Interestingly, A $\beta$  itself decreases both STIM1 and STIM2 expression. Several studies have reported a link between A $\beta$ -mediated STIM2 downregulation and the loss of synapses in animal models of AD (Bojarski et al., 2009; Fonseca et al., 2015; Popugaeva et al., 2015; Sanati et al., 2019). STIM2 protects mushroom spines from toxic effects of amyloid oligomers *in vitro* and *in vivo* in models of amyloid synaptotoxicity (Popugaeva et al., 2015). Sanati et al. reported that gold nanoparticles (AuNPs) reversed deteriorations of memory and spatial learning in A $\beta$ -treated rat hippocampal neurons (Sanati et al., 2019). AuNPs delay the elongation of A $\beta$  and dissociate existing A $\beta$  to less toxic form, enhanced the expression of STIM protein, and potentiated the cAMP/PKA signaling cascade that modulates synaptic plasticity and influences learning and memory (Waltereit and Weller, 2003; Sanati et al., 2019). Additionally, AuNPs may directly increase cAMP levels and consequently recruit STIM2 and PKA to potentiate GluR1-dependent synaptic plasticity (Sanati et al., 2019).

In PS1 KI neurons, STIM2-mediated SOCE activates CaMKII and thus stabilizes mushroom spines (Sun et al., 2014). STIM2 is abundantly expressed in dendritic spines of hippocampal neurons, where it co-localizes with CaMKII. STIM2 overexpression rescues SOCE, restores CaMKII activity, and prevents dendritic spine loss. The conditional deletion of STIM2 reduced synaptic SOCE, thereby causing the loss of mushroom spines and eventually leading to the death of hippocampal neurons in mice that expressed FAD-associated PS1 variants (Sun et al., 2014). On the other hand, STIM2 was

reported to inhibit  $\text{I}_{\text{CRAC}}$  and SOCE amplitude and enhance intracellular  $\text{Ca}^{2+}$  stores through PS1 M146V mutant expression in a cellular model of AD (Ryazantseva et al., 2013). Mushroom spine loss also occurred in an APP-KI mouse model of AD, which was reported to be attributable to the accumulation of A $\beta$  in the medium of APP-KI neurons (Zhang et al., 2015). A $\beta$  overactivates mGluR5, leading to higher ER  $\text{Ca}^{2+}$  levels, the downregulation of STIM2 expression, impairments in synaptic SOCE, and lower CaMKII activity (Sun et al., 2014; Popugaeva et al., 2015; Zhang et al., 2015). The pharmacological inhibition of mGluR5 or overexpression of STIM2 restores synaptic SOCE and prevents mushroom spine loss. Downregulation of the synaptic STIM2–SOCE–CaMKII pathway causes the loss of mushroom spines in both PS1-KI and APP-KI models of AD. Moreover, TRPC6 and Orai2 have been shown to form complexes with STIM2 in hippocampal dendritic spines (Zhang et al., 2016). Thus, TRPC6 activation, STIM2 overexpression, and SOCE positive modulators can rescue mushroom spine loss in hippocampal neurons from both PS-KI and APP-KI mouse models of AD (Sun et al., 2014; Zhang et al., 2016).

## OTHER STIM-INTERACTING MOLECULES

Recent studies have shown other regulators of STIM proteins, such as transcription factors and proteasome inhibitors that may negatively modulate their function. Here, we describe three such regulators.

### NEUROD2

Neurogenic differentiation factor 2 (NEUROD2) is one of the most important neurogenic transcription factors in the CNS (Guner et al., 2017), which mutation is associated with schizophrenia (Dennis et al., 2019). Contrary to previous research that showed that NEUROD2 is a transcriptional activator (Fong et al., 2012; Bayam et al., 2015), a recent study suggested that it may also limit *Stim1* expression in cortical neurons and consequently regulate  $\text{Ca}^{2+}$  influx in SOCE (Guner et al., 2017). Using a chromatin immunoprecipitation and sequencing approach in mouse postnatal cerebral cortical tissue, NEUROD2 was found to bind to an intronic element within the *Stim1* gene. The knockdown of *Neurod2* expression in cortical neurons increased STIM1 protein expression and resulted in the upregulation of SOCE, whereas its overexpression decreased SOCE. NEUROD2 activity is induced by  $\text{Ca}^{2+}$  influx via VGCCs, and depolarization-mediated  $\text{Ca}^{2+}$  influx via VGCCs appears to activate NEUROD2, which in turn fine-tunes the expression of STIM1 and SOCE and results in the STIM1-dependent inhibition of L-type VGCCs (Guner et al., 2017).

### Sp4

Sp4 is a transcription factor that regulates neuronal morphogenesis and function. Its stability depends on membrane potential. Sp4 level was increased in the brains of AD patients and reduced in the brains of bipolar disorder patients (Boutillier et al., 2007; Pinacho et al., 2011). A recent study reported that the maximal activation of SOCE under resting conditions promotes the degradation of Sp4 in cerebellar granule neurons

*in vitro* (Lalonde et al., 2014). The lowering of extracellular  $K^+$  levels reduces neuronal excitability and stimulates the depletion of ER  $Ca^{2+}$  stores, resulting in STIM1 migration to the ER-PM junction and SOCE activation. SOCE inhibitors prevent the ubiquitination and degradation of Sp4 during low extracellular  $K^+$  levels. STIM1 knockdown also inhibits the degradation of Sp4, whereas a constitutively active STIM1 mutant (STIM1D76A) decreased Sp4 protein levels after depolarization (Lalonde et al., 2014). Neurons that were transfected with STIM1D76A were less likely to show immunopositive nuclei with Sp4 than WT STIM1. These findings suggest that STIM1 regulates Sp4 protein, meaning that Sp4 is a downstream effector of STIM1 and STIM1-mediated SOCE. We can assume that dysregulation of STIM1-mediated SOCE may induce abnormal Sp4 expression and promote the development of disorders such as bipolar disorder or AD.

### Proteasome Inhibitors

A recent study showed that sub-lethal doses of proteasome inhibitors, such as MG-132 and clasto-lactacystin- $\beta$ -lactone (LA), decreased STIM1 and STIM2 levels in primary rat cortical neurons but did not affect either Orai1 or TRPC1 (Kuang et al., 2016). The loss of STIM1 and STIM2 proteins was also observed in SH-SY5Y neuroblastoma cells that had low levels of the proteasome subunit  $\beta$  type 5. Additionally, MG-132 and LA promoted autophagy and STIM1/STIM2 mobilization to lysosomes. Thus, inhibition of the ubiquitin-proteasome system, common in neurodegenerative disorders, may disrupt  $Ca^{2+}$  homeostasis by suppressing SOCE.

### CONCLUDING REMARKS

Calcium homeostasis in the CNS is vital for cell maintenance. As a second messenger,  $Ca^{2+}$  participates in plenty physiological processes and its level is regulated in a comprehensive way via the components localized in the PM (ion channels, exchangers, and pumps), as well as the components localized in the mitochondria, ER, Golgi apparatus, and nucleus. Under pathological conditions,  $Ca^{2+}$  homeostasis is dysregulated, with increased cytoplasm, mitochondrial, and changed ER  $Ca^{2+}$  concentration leading to apoptosis (Ureshino et al., 2019). Since the increasing evidence of the relevance of  $Ca^{2+}$  homeostasis in neuroprotection, we focused on the expression and function of  $Ca^{2+}$  signaling-related proteins, STIM partners and effectors, in terms of the effects on  $Ca^{2+}$  regulation and its potential use in the alleviation of the symptoms of neurodegenerative diseases.

Since the discovery of STIM and Orai proteins 15 years ago, they have been found to be the main components of SOCE but not the only components. Experimental evidence that was reviewed herein clearly demonstrates that STIM-Orai-mediated SOCE in the CNS is influenced by several regulators and STIMs have several effectors. We summarized the existing knowledge of target molecules of STIM proteins (Table 1 and Figure 3).

We can distinguish both positive (SEPT1, SEPT4, golgi proteins, SP, POST, and EB) and negative (Homer, SARAF,

SEPT7, PS1, NEUROD2, and proteasome inhibitors) regulators of STIM that affect STIM expression and structure and its movement to the PM or activation of Orai channels (Table 1). The majority of these regulators have an impact on STIM-Orai interactions, but both golgi proteins and SARAF also influence STIM-TRPC associations. Interestingly, some of the regulators appear to function in two ways. SEPT1 and SEPT4 increase STIM-Orai-dependent SOCE, whereas SEPT7 inhibits STIM migration to ER-PM junctions and Orai activation. In turn, EB3 can restore the loss of mushroom spines after knocking down STIM2 (i.e., a regulator of STIM). Conversely, the dynamics of EB1/EB3 are regulated by STIM1 (i.e., an effector of STIM). Notably, in contrast to golgi proteins in immune cells where it negatively regulates STIM-dependent SOCE, golgi proteins in the brain appear to have a positive regulatory action on SOCE activity that is mediated by STIM1. We assume that the action of golgi proteins differs depending on the type of cell tested. However, the exact molecular mechanisms that underlie the STIM1-golgi protein interaction have not yet been defined.

The main effectors of STIM proteins are Orai and TRPC, which together constitute molecular components of SOCE. The evidence gathered in this review suggests that disturbances of the STIM-Orai- and STIM-TRPC-mediated SOCE pathway contribute to the pathogenesis of diverse neurodegenerative diseases. The STIM-Orai association is also vital for the regulation of neurogenesis in mammalian cells and production of proinflammatory cytokines in astroglia and murine microglia. In turn, the STIM-TRPC interaction is essential for the survival of DNs in animal models of PD. In addition to Orai and TRPC, STIM proteins can also control  $Ca^{2+}$  influx via other molecular channels, including L-type VGCCs, and receptors, such as AMPARs, NMDARs, mGluR1, and mGluR5. The interaction between STIM proteins and their molecular targets can both increase and decrease  $Ca^{2+}$  influx from the extracellular milieu to the cytoplasm. Associations between STIMs and Orai, TRPC, AMPARs, mGluR1, and mGluR5 elevate  $Ca^{2+}$  influx, whereas  $Ca^{2+}$  influx via L-type VGCCs and NMDARs is inhibited by STIMs. Interestingly, maximal SOCE activation occurs under resting conditions, whereas VGCC and NMDAR activation requires cell membrane depolarization. Depolarization activates  $Ca^{2+}$  influx via both NMDARs and L-type VGCCs and decreases  $Ca^{2+}$  content in the ER, thereby enhancing STIM1-mediated SOCE and decreasing  $Ca^{2+}$  influx via VGCCs and NMDARs. Thus, STIM proteins in neurons may regulate  $Ca^{2+}$  influx under both resting and action potential.

The relationship between STIM proteins and glutamate receptors is essential for different forms of synaptic plasticity. In primary rat hippocampal neurons, STIM2 promotes the phosphorylation and surface delivery of AMPARs, contributing to LTP. SOCE can be activated by synaptic NMDARs, thus also influencing LTP. Additionally, STIM1 was shown to control the plasticity of L-type VGCC-dependent dendritic spines in PNs and strengthen mGluR1-dependent synaptic transmission, thereby regulating cerebellar motor behavior. Other STIM

**TABLE 1 |** STIM target molecules.

Interacting protein	Identity of binding protein	Subcellular location	Function	STIM isoform
Orai	Ca <sup>2+</sup> channel	PM	Positive effector	STIM1 STIM2
TRP	Ca <sup>2+</sup> channel	PM	Positive effector	STIM1
VGCC	Ca <sup>2+</sup> channel	PM	Negative effector	STIM1
AMPA	Ionotropic receptor	PM	Positive effector	STIM1 STIM2
NMDAR	Ionotropic receptor	PM	Negative effector	STIM1 STIM2
mGluR1	Metabotropic receptor	PM	Positive regulator	STIM1
septin	GTPase	PM lipids (cytoskeleton)	Positive/negative regulator	dSTIM
Homer	Scaffolding protein	PSD (cytoskeleton)	Negative regulator	STIM1
SP	Actin-binding protein	PSD (cytoskeleton)	Positive regulator	STIM1
CaMKII	Kinase	PSD (cytoskeleton)	Positive effector	STIM2
EB1, EB3	Microtubule-binding protein	Cytoplasm (cytoskeleton)	Positive effector/regulator	STIM1 STIM2
Golli proteins	Myelin basic protein	Cytoplasm	Positive regulator	STIM1
SARAF	Transmembrane regulatory factor	ER (predominant), PM	Negative regulator	STIM1
POST	Transmembrane protein	ER (predominant), PM	Positive regulator	STIM1
SERCA	Ca <sup>2+</sup> -ATPase	ER	Positive effector	STIM1
IP <sub>3</sub> R	Ca <sup>2+</sup> channel	ER	Positive regulator/effector	dSTIM STIM1
PS1	Ca <sup>2+</sup> -leak channel, endoprotease	ER	Negative regulator	STIM1 STIM2
NEUROD2	Transcription factor	Nucleus	Negative regulator	STIM1
Sp4	Transcription factor	Nucleus	Negative effector	STIM1
MG-132/LA	Proteasome inhibitors	Cytoplasm/nucleus	Negative regulator	STIM1 STIM2

PM, plasma membrane; ER, endoplasmic reticulum; PSD, post-synaptic density.

protein effectors and regulators that reside outside the PM also contribute to synaptic plasticity. Synaptopodin recruits STIM1 to the PSD and regulates the function of Ca<sup>2+</sup> stores and plasticity of spine heads during LTP. After cell depolarization, the STIM1-POST complex binds to SERCA and keeps it in close proximity to L-type VGCCs to promote ER Ca<sup>2+</sup> replenishment during repetitive firing, regulating neuronal excitability and plasticity. The STIM1-POST complex appears to prevent excessive Ca<sup>2+</sup> concentrations in the cytoplasm. In turn, the STIM1-IP<sub>3</sub>R<sub>3</sub> interaction regulates basal Ca<sup>2+</sup> levels in mitochondria. Interestingly, the dysregulation of both cytosolic and mitochondrial Ca<sup>2+</sup> levels contributes to neurodegeneration in AD. In turn, the STIM2-EB3 and STIM2-CaMKII complexes promote the formation of mushroom spines and stabilize them. Targeting these complexes could be a novel way of stabilizing dendritic spines and thus improve memory in AD patients.

Studying STIM proteins and their partners in different subcellular compartments enables us to understand a wide range of processes that are regulated by these proteins.

Future studies should examine the ways in which these regulators act in concert to modulate STIM activity during Ca<sup>2+</sup> influx into the cell. The precise molecular mechanisms of action of STIMs together with these all regulators (e.g., in the activation/inactivation of Orai channels) also remain to be explored. Such studies will help to elucidate the pathological mechanisms that are involved in the development of various neurodegenerative diseases (e.g., AD, PD, and HD), affective disorders (schizophrenia, bipolar disorder), chronic pain, oxidative trauma, brain trauma, stroke, and epilepsy. Therefore, it appears that STIM proteins and their modulators/effectors may have potential therapeutic applications for the treatment of these diseases.

## AUTHOR CONTRIBUTIONS

KS wrote and commented on the manuscript and prepared the figures. JG-B designed the manuscript, contributed to writing it, and prepared the final version. All authors contributed to the article and approved the submitted version.

## FUNDING

This study was supported by funds from the National Science Centre (research project no. 2017/26/E/NZ3/01144 to JG-B).

## ACKNOWLEDGMENTS

We thank Prof. Barbara Zabłocka and Dr. Magdalena Czeredys for critically reading the manuscript.

## REFERENCES

- Agrawal, N., Venkiteswaran, G., Sadaf, S., Padmanabhan, N., Banerjee, S., and Hasan, G. (2010). Inositol 1,4,5-trisphosphate receptor and dSTIM function in *Drosophila* insulin-producing neurons regulates systemic intracellular calcium homeostasis and flight. *J. Neurosci.* 30, 1301–1313. doi: 10.1523/JNEUROSCI.3668-09.2010
- Ahsan, A., Zheng, Y. R., Wu, X. L., Tang, W. D., Liu, M. R., Ma, S. J., et al. (2019). Urolithin A-activated autophagy but not mitophagy protects against ischemic neuronal injury by inhibiting ER stress *in vitro* and *in vivo*. *CNS Neurosci. Ther.* 25, 976–986. doi: 10.1111/cns.13136
- Akhmanova, A., and Steinmetz, M. O. (2010). Microtubule +TIPs at a glance. *J. Cell Sci.* 123, 3415–3419. doi: 10.1242/jcs.062414
- Albarrán, L., López, J. J., Gómez, L. J., Salido, G. M., and Rosado, J. A. (2016). SARAF modulates TRPC1, but not TRPC6, channel function in a STIM1-independent manner. *Biochem. J.* 473, 3581–3595. doi: 10.1042/BCJ20160348
- Albarran, L., Lopez, J. J., Woodard, G. E., Salido, G. M., and Rosado, J. A. (2016). Store-operated  $\text{Ca}^{2+}$  entry-associated regulatory factor (SARAF) plays an important role in the regulation of arachidonate-regulated  $\text{Ca}^{2+}$  (ARC) channels. *J. Biol. Chem.* 291, 6982–6988. doi: 10.1074/jbc.M115.704940
- Aloni, E., Oni-Biton, E., Tsoory, M., Moallem, D. H., and Segal, M. (2019). Synaptopodin deficiency ameliorates symptoms in the 3xTg mouse model of Alzheimer's disease. *J. Neurosci.* 39, 3983–3992. doi: 10.1523/JNEUROSCI.2920-18.2019
- Ambudkar, I. S., de Souza, L. B., and Ong, H. L. (2017). TRPC1, Orai1, and STIM1 in SOCE: friends in tight spaces. *Cell Calcium* 63, 33–39. doi: 10.1016/j.ceca.2016.12.009
- Asanov, A., Sherry, R., Sampieri, A., and Vaca, L. (2013). A relay mechanism between EB1 and APC facilitate STIM1 puncta assembly at endoplasmic reticulum-plasma membrane junctions. *Cell Calcium* 54, 246–256. doi: 10.1016/j.ceca.2013.06.008
- Baba, A., Yasui, T., Fujisawa, S., Yamada, R. X., Yamada, M. K., Nishiyama, N., et al. (2003). Activity-evoked capacitive  $\text{Ca}^{2+}$  entry: implications in synaptic plasticity. *J. Neurosci.* 23, 7737–7741. doi: 10.1523/JNEUROSCI.23-21-07737.2003
- Basu, S., and Lamprecht, R. (2018). The role of actin cytoskeleton in dendritic spines in the maintenance of long-term memory. *Front. Mol. Neurosci.* 11, 143. doi: 10.3389/fnmol.2018.00143
- Batchelor, A. M., Madge, D. J., and Garthwaite, J. (1994). Synaptic activation of metabotropic glutamate receptors in the parallel fibre-Purkinje cell pathway in rat cerebellar slices. *Neuroscience* 63, 911–915. doi: 10.1016/0306-4522(94)90558-4
- Bayam, E., Sahin, G. S., Guzelsoy, G., Guner, G., Kabakcioglu, A., and Ince-Dunn, G. (2015). Genome-wide target analysis of NEUROD2 provides new insights into regulation of cortical projection neuron migration and differentiation. *BMC Genomics* 16:681. doi: 10.1186/s12864-015-1882-9
- Berna-Erro, A., Braun, A., Kraft, R., Kleinschmitz, C., Schuhmann, M. K., Stegner, D., et al. (2009). STIM2 regulates capacitive  $\text{Ca}^{2+}$  entry in neurons and plays a key role in hypoxic neuronal cell death. *Sci. Signal.* 2: ra67. doi: 10.1126/scisignal.2000522
- Bernales, S., McDonald, K. L., and Walter, P. (2006). Autophagy counterbalances endoplasmic reticulum expansion during the unfolded protein response. *PLoS Biol.* 4: e423. doi: 10.1371/journal.pbio.0040423
- Berridge, M. J., Lipp, P., and Bootman, M. D. (2000). The versatility and universality of calcium signalling. *Nat. Rev. Mol. Cell Biol.* 1, 11–21. doi: 10.1038/35036035
- Blaustein, M. P., and Golovina, V. A. (2001). Structural complexity and functional diversity of endoplasmic reticulum  $\text{Ca}^{2+}$  stores. *Trends Neurosci.* 24, 602–608. doi: 10.1016/S0166-2236(00)01891-9
- Blaustein, M. P., Juhaszova, M., Golovina, V. A., Church, P. J., and Stanley, E. F. (2002). Na/Ca exchanger and PMCA localization in neurons and astrocytes: functional implications. *Ann. N. Y. Acad. Sci.* 976, 356–366. doi: 10.1111/j.1749-6632.2002.tb04762.x
- Bojarski, L., Pomorski, P., Szybinska, A., Drab, M., Skibinska-Kijek, A., Gruszczynska-Biegala, J., et al. (2009). Presenilin-dependent expression of STIM proteins and dysregulation of capacitative  $\text{Ca}^{2+}$  entry in familial Alzheimer's disease. *Biochim. Biophys. Acta* 1793, 1050–1057. doi: 10.1016/j.bbamer.2008.11.008
- Bollimuntha, S., Ebadi, M., and Singh, B. B. (2006). TRPC1 protects human SH-SY5Y cells against salsolinol-induced cytotoxicity by inhibiting apoptosis. *Brain Res.* 1099, 141–149. doi: 10.1016/j.brainres.2006.04.104
- Boutillier, S., Lannes, B., Buée, L., Delacourte, A., Rouaux, C., Mohr, M., et al. (2007). Sp3 and sp4 transcription factor levels are increased in brains of patients with Alzheimer's disease. *Neurodegener. Dis.* 4, 413–423. doi: 10.1159/000107701
- Brandman, O., Liou, J., Park, W. S., and Meyer, T. (2007). STIM2 is a feedback regulator that stabilizes basal cytosolic and endoplasmic reticulum  $\text{Ca}^{2+}$  levels. *Cell* 131, 1327–1339. doi: 10.1016/j.cell.2007.11.039
- Brini, M., Calì, T., Ottolini, D., and Carafoli, E. (2014). Neuronal calcium signaling: function and dysfunction. *Cell. Mol. Life Sci.* 71, 2787–2814. doi: 10.1007/s00018-013-1550-7
- Brini, M., and Carafoli, E. (2011). The plasma membrane  $\text{Ca}^{2+}$  ATPase and the plasma membrane sodium calcium exchanger cooperate in the regulation of cell calcium. *Cold. Spring Harb. Perspect. Biol.* 3:a004168. doi: 10.1101/cshperspect.a004168
- Britzolaki, A., Saurine, J., Klocke, B., and Pitychoutis, P. M. (2020). A role for SERCA pumps in the neurobiology of neuropsychiatric and neurodegenerative disorders. *Adv. Exp. Med. Biol.* 1131, 131–161. doi: 10.1007/978-3-030-12457-1\_6
- Brockhaus, J., Schreitmüller, M., Repetto, D., Klatt, O., Reissner, C., Elmslie, K., et al. (2018).  $\alpha$ -neurexins together with  $\alpha 2\delta$ -1 auxiliary subunits regulate  $\text{Ca}^{2+}$  influx through  $\text{Ca}_v$  2.1 channels. *J. Neurosci.* 38, 8277–8294. doi: 10.1523/JNEUROSCI.0511-18.2018
- Campiglio, M., and Flucher, B. E. (2015). The role of auxiliary subunits for the functional diversity of voltage-gated calcium channels. *J. Cell. Physiol.* 230, 2019–2031. doi: 10.1002/jcp.24998
- Cárdenas, C., Miller, R. A., Smith, I., Bui, T., Molgó, J., Müller, M., et al. (2010). Essential regulation of cell bioenergetics by constitutive InsP3 receptor  $\text{Ca}^{2+}$  transfer to mitochondria. *Cell* 142, 270–283. doi: 10.1016/j.cell.2010.06.007
- Chakraborty, S., Deb, B. K., Chorna, T., Konieczny, V., Taylor, C. W., and Hasan, G. (2016). Mutant IP3 receptors attenuate store-operated  $\text{Ca}^{2+}$  entry by destabilizing STIM-Orai interactions in *Drosophila* neurons. *J. Cell Sci.* 129, 3903–3910. doi: 10.1242/jcs.191585
- Chakraborty, S., and Hasan, G. (2017). Spontaneous  $\text{Ca}^{2+}$  influx in *drosophila* pupal neurons is modulated by IP3-receptor function and influences maturation of the flight circuit. *Front. Mol. Neurosci.* 10:111. doi: 10.3389/fnmol.2017.00111

- Chakraborty, S., and Stutzmann, G. E. (2014). Calcium channelopathies and Alzheimer's disease: insight into therapeutic success and failures. *Eur. J. Pharmacol.* 739, 83–95. doi: 10.1016/j.ejphar.2013.11.012
- Chang, C. L., Chen, Y. J., Quintanilla, C. G., Hsieh, T. S., and Liou, J. (2018). EB1 binding restricts STIM1 translocation to ER-PM junctions and regulates store-operated Ca entry. *J. Cell Biol.* 217, 2047–2058. doi: 10.1083/jcb.201711151
- Chen, T., Fei, F., Jiang, X. F., Zhang, L., Qu, Y., Huo, K., et al. (2012). Down-regulation of Homer1b/c attenuates glutamate-mediated excitotoxicity through endoplasmic reticulum and mitochondria pathways in rat cortical neurons. *Free Radic. Biol. Med.* 52, 208–217. doi: 10.1016/j.freeradbiomed.2011.10.451
- Coe, H., and Michalak, M. (2010). ERp57, a multifunctional endoplasmic reticulum resident oxidoreductase. *Int. J. Biochem. Cell Biol.* 42, 796–799. doi: 10.1016/j.bbocel.2010.01.009
- Cottrell, G. S., Soubrane, C. H., Hounshell, J. A., Lin, H., Owenson, V., Rigby, M., et al. (2018). CACHD1 is an  $\alpha 2\delta$ -like protein that modulates Ca V 3 voltage-gated calcium channel activity. *J. Neurosci.* 38, 9186–9201. doi: 10.1523/JNEUROSCI.3572-15.2018
- Crupi, R., Impellizzeri, D., and Cuzzocrea, S. (2019). Role of metabotropic glutamate receptors in neurological disorders. *Front. Mol. Neurosci.* 12:20. doi: 10.3389/fnmol.2019.00020
- Cull-Candy, S. G., and Leszkiewicz, D. N. (2004). Role of distinct NMDA receptor subtypes at central synapses. *Sci. STKE* 2004: re16. doi: 10.1126/stke.2552004re16
- Czeredys, M., Vigont, V. A., Boeva, V. A., Mikoshiba, K., Kaznacheyeva, E. V., and Kuznicki, J. (2018). Huntingtin-associated protein 1A regulates store-operated calcium entry in medium spiny neurons from transgenic YAC128 mice, a model of Huntington's disease. *Front. Cell. Neurosci.* 12:381. doi: 10.3389/fncel.2018.00381
- Dahimene, S., Page, K. M., Kadirin, I., Ferron, L., Ho, D. Y., Powell, G. T., et al. (2018). The  $\alpha 2\delta$ -like protein carchd1 increases N-type calcium currents and cell surface expression and competes with  $\alpha 2\delta$ -1. *Cell Rep.* 25, 1610.e5–1621.e5. doi: 10.1016/j.celrep.2018.10.033
- Darbellay, B., Arnaudeau, S., Bader, C. R., König, S., and Bernheim, L. (2011). STIM1L is a new actin-binding splice variant involved in fast repetitive  $\text{Ca}^{2+}$  release. *J. Cell Biol.* 194, 335–346. doi: 10.1083/jcb.201012157
- Deb, B. K., Chakraborty, P., Gopurappilly, R., and Hasan, G. (2020). SEPT7 regulates  $\text{Ca}^{2+}$  entry through Orai channels in human neural progenitor cells and neurons. *Cell Calcium* 90:102252. doi: 10.1016/j.ceca.2020.102252
- Deb, B. K., and Hasan, G. (2016). Regulation of store-operated  $\text{Ca}^{2+}$  entry by septins. *Front. Cell Dev. Biol.* 4:142. doi: 10.3389/fcell.2016.00142
- Deb, B. K., and Hasan, G. (2019). SEPT7-mediated regulation of  $\text{Ca}^{2+}$  entry through Orai channels requires other septin subunits. *Cytoskeleton* 76, 104–114. doi: 10.1002/cm.21476
- Deb, B. K., Pathak, T., and Hasan, G. (2016). Store-independent modulation of  $\text{Ca}^{2+}$  entry through Orai by Septin 7. *Nat. Commun.* 7:11751. doi: 10.1038/ncomms11751
- Deller, T., Korte, M., Chabanis, S., Drakew, A., Schwegler, H., Stefani, G. G., et al. (2003). Synaptopodin-deficient mice lack a spine apparatus and show deficits in synaptic plasticity. *Proc. Natl. Acad. Sci. U.S.A.* 100, 10494–10499. doi: 10.1073/pnas.1832384100
- Dennis, D. J., Han, S., and Schuurmans, C. (2019). bHLH transcription factors in neural development, disease, and reprogramming. *Brain Res.* 1705, 48–65. doi: 10.1016/j.brainres.2018.03.013
- Derkach, V., Barria, A., and Soderling, T. R. (1999).  $\text{Ca}^{2+}$ /calmodulin-kinase II enhances channel conductance of  $\alpha$ -amino-3-hydroxy-5-methyl-4-isoxazolepropionate type glutamate receptors. *Proc. Natl. Acad. Sci. U.S.A.* 96, 3269–3274. doi: 10.1073/pnas.96.6.3269
- Desai, P. N., Zhang, X., Wu, S., Janoshazi, A., Bolimuntha, S., Putney, J. W., et al. (2015). Multiple types of calcium channels arising from alternative translation initiation of the Orai1 message. *Sci. Signal.* 8: ra74. doi: 10.1126/scisignal.aaa8323
- Di Buduo, C. A., Abbonante, V., Marty, C., Moccia, F., Rumi, E., Pietra, D., et al. (2020). Defective interaction of mutant calreticulin and SOCE in megakaryocytes from patients with myeloproliferative neoplasms. *Blood* 135, 133–144. doi: 10.1182/blood.2019001103
- Dick, O., and Bading, H. (2010). Synaptic activity and nuclear calcium signaling protect hippocampal neurons from death signal-associated nuclear translocation of FoxO3a induced by extrasynaptic N-methyl-D-aspartate receptors. *J. Biol. Chem.* 285, 19354–19361. doi: 10.1074/jbc.M110.127654
- Ding, W. X., Ni, H. M., Gao, W., Hou, Y. F., Melan, M. A., Chen, X., et al. (2007). Differential effects of endoplasmic reticulum stress-induced autophagy on cell survival. *J. Biol. Chem.* 282, 4702–4710. doi: 10.1074/jbc.M609267200
- Dionisio, N., Smani, T., Woodard, G. E., Castellano, A., Salido, G. M., and Rosado, J. A. (2015). Homer proteins mediate the interaction between STIM1 and Cav1.2 channels. *Biochim. Biophys. Acta* 1853, 1145–1153. doi: 10.1016/j.bbamcr.2015.02.014
- Dittmer, P. J., Wild, A. R., Dell'Acqua, M. L., and Sather, W. A. (2017). STIM1  $\text{Ca}^{2+}$  sensor control of L-type  $\text{Ca}^{2+}$ -channel-dependent dendritic spine structural plasticity and nuclear signaling. *Cell Rep.* 19, 321–334. doi: 10.1016/j.celrep.2017.03.056
- Domenichini, F., Terrié, E., Arnault, P., Harnois, T., Magaud, C., Bois, P., et al. (2018). Store-operated calcium entries control neural stem cell self-renewal in the adult brain subventricular zone. *Stem Cells* 36, 761–774. doi: 10.1002/stem.2786
- Duszyński, J., Kozieł, R., Brutkowski, W., Szczepanowska, J., and Zabłocki, K. (2006). The regulatory role of mitochondria in capacitative calcium entry. *Biochim. Biophys. Acta* 1757, 380–387. doi: 10.1016/j.bbabi.2006.04.017
- Emptage, N., Bliss, T. V., and Fine, A. (1999). Single synaptic events evoke NMDA receptor-mediated release of calcium from internal stores in hippocampal dendritic spines. *Neuron* 22, 115–124. doi: 10.1016/S0896-6273(00)80683-2
- Emptage, N. J., Reid, C. A., and Fine, A. (2001). Calcium stores in hippocampal synaptic boutons mediate short-term plasticity, store-operated  $\text{Ca}^{2+}$  entry, and spontaneous transmitter release. *Neuron* 29, 197–208. doi: 10.1016/S0896-6273(01)00190-8
- Esteban, J. A., Shi, S. H., Wilson, C., Nuriya, M., Haganir, R. L., and Malinow, R. (2003). PKA phosphorylation of AMPA receptor subunits controls synaptic trafficking underlying plasticity. *Nat. Neurosci.* 6, 136–143. doi: 10.1038/nn997
- Fierro, L., DiPolo, R., and Llano, I. (1998). Intracellular calcium clearance in Purkinje cell somata from rat cerebellar slices. *J. Physiol.* 510 (Pt 2), 499–512. doi: 10.1111/j.1469-7793.1998.499bk.x
- Filipovic, R., Rakic, S., and Zecevic, N. (2002). Expression of Golgi proteins in adult human brain and multiple sclerosis lesions. *J. Neuroimmunol.* 127, 1–12. doi: 10.1016/S0165-5728(02)00070-X
- Fong, A. P., Yao, Z., Zhong, J. W., Cao, Y., Ruzzo, W. L., Gentleman, R. C., et al. (2012). Genetic and epigenetic determinants of neurogenesis and myogenesis. *Dev. Cell* 22, 721–735. doi: 10.1016/j.devcel.2012.01.015
- Fonseca, A. C., Moreira, P. I., Oliveira, C. R., Cardoso, S. M., Pinton, P., and Pereira, C. F. (2015). Amyloid-beta disrupts calcium and redox homeostasis in brain endothelial cells. *Mol. Neurobiol.* 51, 610–622. doi: 10.1007/s12035-014-8740-7
- Gao, X., Xia, J., Munoz, F. M., Mannens, M. T., Pan, R., Meucci, O., et al. (2016). STIMs and Orail regulate cytokine production in spinal astrocytes. *J. Neuroinflammation* 13:126. doi: 10.1186/s12974-016-0594-7
- García-Alvarez, G., Lu, B., Yap, K. A., Wong, L. C., Thevathasan, J. V., Lim, L., et al. (2015). STIM2 regulates PKA-dependent phosphorylation and trafficking of AMPARs. *Mol. Biol. Cell* 26, 1141–1159. doi: 10.1091/mbc.E14-07-1222
- Gemes, G., Bangaru, M. L., Wu, H. E., Tang, Q., Weihrauch, D., Koopmeiners, A. S., et al. (2011). Store-operated  $\text{Ca}^{2+}$  entry in sensory neurons: functional role and the effect of painful nerve injury. *J. Neurosci.* 31, 3536–3549. doi: 10.1523/JNEUROSCI.5053-10.2011
- Ghavami, S., Shojaei, S., Yeganeh, B., Ande, S. R., Jangamreddy, J. R., Mehrpour, M., et al. (2014). Autophagy and apoptosis dysfunction in neurodegenerative disorders. *Prog. Neurobiol.* 112, 24–49. doi: 10.1016/j.pneurobio.2013.10.004
- Golovina, V. A. (2005). Visualization of localized store-operated calcium entry in mouse astrocytes. Close proximity to the endoplasmic reticulum. *J. Physiol.* 564, 737–749. doi: 10.1113/jphysiol.2005.085035
- Gopurappilly, R., Deb, B. K., Chakraborty, P., and Hasan, G. (2018). Stable STIM1 knockdown in self-renewing human neural precursors promotes premature neural differentiation. *Front. Mol. Neurosci.* 11:178. doi: 10.3389/fnmol.2018.00178
- Greotti, E., Capitanio, P., Wong, A., Pozzan, T., Pizzo, P., and Pendin, D. (2019). Familial Alzheimer's disease-linked presenilin mutants and intracellular  $\text{Ca}^{2+}$  handling: a single-organelle, FRET-based analysis. *Cell Calcium* 79, 44–56. doi: 10.1016/j.ceca.2019.02.005

- Grigoriev, I., Gouveia, S. M., van der Vaart, B., Demmers, J., Smyth, J. T., Honnappa, S., et al. (2008). STIM1 is a MT-plus-end-tracking protein involved in remodeling of the ER. *Curr. Biol.* 18, 177–182. doi: 10.1016/j.cub.2007.12.050
- Gruszczynska-Biegala, J., and Kuznicki, J. (2013). Native STIM2 and ORAI1 proteins form a calcium-sensitive and thapsigargin-insensitive complex in cortical neurons. *J. Neurochem.* 126, 727–738. doi: 10.1111/jnc.12320
- Gruszczynska-Biegala, J., Pomorski, P., Wisniewska, M. B., and Kuznicki, J. (2011). Differential roles for STIM1 and STIM2 in store-operated calcium entry in rat neurons. *PLoS ONE* 6: e19285. doi: 10.1371/journal.pone.0019285
- Gruszczynska-Biegala, J., Sladowska, M., and Kuznicki, J. (2016). AMPA receptors are involved in store-operated calcium entry and interact with STIM proteins in rat primary cortical neurons. *Front. Cell. Neurosci.* 10:251. doi: 10.3389/fncel.2016.00251
- Gruszczynska-Biegala, J., Strucinska, K., Maciag, F., Majewski, L., Sladowska, M., and Kuznicki, J. (2020). STIM Protein-NMDA2 receptor interaction decreases NMDA-dependent calcium levels in cortical neurons. *Cells* 9:160. doi: 10.3390/cells9010160
- Gu, J., Firestein, B. L., and Zheng, J. Q. (2008). Microtubules in dendritic spine development. *J. Neurosci.* 28, 12120–12124. doi: 10.1523/JNEUROSCI.2509-08.2008
- Guner, G., Guzelsoy, G., Isleyen, F. S., Sahin, G. S., Akkaya, C., Bayam, E., et al. (2017). NEUROD2 regulates stim1 expression and store-operated calcium entry in cortical neurons. *eNeuro* 4, 1–17. doi: 10.1523/ENEURO.0255-16.2017
- Harras, O. F., and Altier, C. (2014). STIM1-mediated bidirectional regulation of Ca(2+) entry through voltage-gated calcium channels (VGCC) and calcium-release activated channels (CRAC). *Front. Cell. Neurosci.* 8:43. doi: 10.3389/fncel.2014.00043
- Hartmann, J., Dragicevic, E., Adelsberger, H., Henning, H. A., Sumser, M., Abramowitz, J., et al. (2008). TRPC3 channels are required for synaptic transmission and motor coordination. *Neuron* 59, 392–398. doi: 10.1016/j.neuron.2008.06.009
- Hartmann, J., Karl, R. M., Alexander, R. P., Adelsberger, H., Brill, M. S., Rühlmann, C., et al. (2014). STIM1 controls neuronal Ca<sup>2+</sup> signaling, mGluR1-dependent synaptic transmission, and cerebellar motor behavior. *Neuron* 82, 635–644. doi: 10.1016/j.neuron.2014.03.027
- Hawkins, B. J., Irrinki, K. M., Mallilankaraman, K., Lien, Y. C., Wang, Y., Bhanumathy, C. D., et al. (2010). S-glutathionylation activates STIM1 and alters mitochondrial homeostasis. *J. Cell Biol.* 190, 391–405. doi: 10.1083/jcb.201004152
- Heine, M., Heck, J., Ciurasciewicz, A., and Bikbaev, A. (2020). Dynamic compartmentalization of calcium channel signalling in neurons. *Neuropharmacology* 169:107556. doi: 10.1016/j.neuropharm.2019.02.038
- Henke, N., Albrecht, P., Pfeiffer, A., Tautzaris, D., Zanger, K., and Methner, A. (2012). Stromal interaction molecule 1 (STIM1) is involved in the regulation of mitochondrial shape and bioenergetics and plays a role in oxidative stress. *J. Biol. Chem.* 287, 42042–42052. doi: 10.1074/jbc.M112.417212
- Heo, D. K., Lim, H. M., Nam, J. H., Lee, M. G., and Kim, J. Y. (2015). Regulation of phagocytosis and cytokine secretion by store-operated calcium entry in primary isolated murine microglia. *Cell. Signal.* 27, 177–186. doi: 10.1016/j.cellsig.2014.11.003
- Hermes, J., Schneider, I., Dewachter, I., Caluwaerts, N., Kretschmar, H., and Van Leuven, F. (2003). Capacitive calcium entry is directly attenuated by mutant presenilin-1, independent of the expression of the amyloid precursor protein. *J. Biol. Chem.* 278, 2484–2489. doi: 10.1074/jbc.M206769200
- Hong, J. H., Li, Q., Kim, M. S., Shin, D. M., Feske, S., Birnbaumer, L., et al. (2011). Polarized but differential localization and recruitment of STIM1, Orai1 and TRPC channels in secretory cells. *Traffic* 12, 232–245. doi: 10.1111/j.1600-0854.2010.01138.x
- Honnappa, S., Gouveia, S. M., Weisbrich, A., Damberger, F. F., Bhavesh, N. S., Jawhari, H., et al. (2009). An EB1-binding motif acts as a microtubule tip localization signal. *Cell* 138, 366–376. doi: 10.1016/j.cell.2009.04.065
- Hoth, M., and Niemeyer, B. A. (2013). The neglected CRAC proteins: Orai2, Orai3, and STIM2. *Curr. Top. Membr.* 71, 237–271. doi: 10.1016/B978-0-12-407870-3.00010-X
- Høyer-Hansen, M., Bastholm, L., Szyniarowski, P., Campanella, M., Szabadkai, G., Farkas, T., et al. (2007). Control of macroautophagy by calcium, calmodulin-dependent kinase kinase-beta, and Bcl-2. *Mol. Cell* 25, 193–205. doi: 10.1016/j.molcel.2006.12.009
- Høyer-Hansen, M., and Jäättelä, M. (2007). Connecting endoplasmic reticulum stress to autophagy by unfolded protein response and calcium. *Cell Death Differ.* 14, 1576–1582. doi: 10.1038/sj.cdd.4402200
- Hu, X., Viesselmann, C., Nam, S., Merriam, E., and Dent, E. W. (2008). Activity-dependent dynamic microtubule invasion of dendritic spines. *J. Neurosci.* 28, 13094–13105. doi: 10.1523/JNEUROSCI.3074-08.2008
- Hu, Y. D., Tang, C. L., Jiang, J. Z., Lv, H. Y., Wu, Y. B., Qin, X. D., et al. (2020). Neuroprotective effects of dexmedetomidine preconditioning on oxygen-glucose deprivation-reoxygenation injury in PC12 cells via regulation of Ca<sup>2+</sup>-STIM1/Orai1 signaling. *Curr. Med. Sci.* 40, 699–707. doi: 10.1007/s11596-020-2201-5
- Ivanova, H., Vervliet, T., Missiaen, L., Parys, J. B., De Smedt, H., and Bultynck, G. (2014). Inositol 1,4,5-trisphosphate receptor-isoform diversity in cell death and survival. *Biochim. Biophys. Acta* 1843, 2164–2183. doi: 10.1016/j.bbamcr.2014.03.007
- Jardin, I., Albarrán, L., Bermejo, N., Salido, G. M., and Rosado, J. A. (2012). Homers regulate calcium entry and aggregation in human platelets: a role for Homers in the association between STIM1 and Orai1. *Biochem. J.* 445, 29–38. doi: 10.1042/BJ20120471
- Jha, A., Ahuja, M., Maléth, J., Moreno, C. M., Yuan, J. P., Kim, M. S., et al. (2013). The STIM1 CTID domain determines access of SARAF to SOAR to regulate Orai1 channel function. *J. Cell Biol.* 202, 71–79. doi: 10.1083/jcb.201301148
- Katz, Z. B., Zhang, C., Quintana, A., Lillemeier, B. F., and Hogan, P. G. (2019). Septins organize endoplasmic reticulum-plasma membrane junctions for STIM1-Orai1 calcium signalling. *Sci. Rep.* 9:10839. doi: 10.1038/s41598-019-46862-w
- Keil, J. M., Shen, Z., Briggs, S. P., and Patrick, G. N. (2010). Regulation of STIM1 and SOCE by the ubiquitin-proteasome system (UPS). *PLoS ONE* 5:e13465. doi: 10.1371/journal.pone.0013465
- Kerchner, G. A., and Nicoll, R. A. (2008). Silent synapses and the emergence of a postsynaptic mechanism for LTP. *Nat. Rev. Neurosci.* 9, 813–825. doi: 10.1038/nrn2501
- Kettenmann, H. R., and Bruce, R. (2013). *Neuroglia*. Oxford: Oxford University Press. doi: 10.1093/med/9780199794591.001.0001
- Klejman, M. E., Gruszczynska-Biegala, J., Skibinska-Kijek, A., Wisniewska, M. B., Misztal, K., Blazejczyk, M., et al. (2009). Expression of STIM1 in brain and puncta-like co-localization of STIM1 and Orai1 upon depletion of Ca(2+) store in neurons. *Neurochem. Int.* 54, 49–55. doi: 10.1016/j.neuint.2008.10.005
- Kondratskyi, A., Yassine, M., Slomianny, C., Kondratska, K., Gordienko, D., Dewailly, E., et al. (2014). Identification of ML-9 as a lysosomotropic agent targeting autophagy and cell death. *Cell Death Dis.* 5:e1193. doi: 10.1038/cddis.2014.156
- Korkotian, E., Frotscher, M., and Segal, M. (2014). Synaptopodin regulates spine plasticity: mediation by calcium stores. *J. Neurosci.* 34, 11641–11651. doi: 10.1523/JNEUROSCI.0381-14.2014
- Korkotian, E., Oni-Biton, E., and Segal, M. (2017). The role of the store-operated calcium entry channel Orai1 in cultured rat hippocampal synapse formation and plasticity. *J. Physiol.* 595, 125–140. doi: 10.1113/JP272645
- Kraft, R. (2015). STIM and Orai proteins in the nervous system. *Channels* 9, 245–252. doi: 10.1080/19336950.2015.1071747
- Krapivinsky, G., Krapivinsky, L., Stotz, S. C., Manasian, Y., and Clapham, D. E. (2011). POST, partner of stromal interaction molecule 1 (STIM1), targets STIM1 to multiple transporters. *Proc. Natl. Acad. Sci. U.S.A.* 108, 19234–19239. doi: 10.1073/pnas.1117231108
- Kroemer, G., Mariño, G., and Levine, B. (2010). Autophagy and the integrated stress response. *Mol. Cell* 40, 280–293. doi: 10.1016/j.molcel.2010.09.023
- Kuang, X. L., Liu, Y., Chang, Y., Zhou, J., Zhang, H., Li, Y., et al. (2016). Inhibition of store-operated calcium entry by sub-lethal levels of proteasome inhibition is associated with STIM1/STIM2 degradation. *Cell Calcium* 59, 172–180. doi: 10.1016/j.ceca.2016.01.007
- Kumar, U., Dunlop, D. M., and Richardson, J. S. (1994). Mitochondria from Alzheimer's fibroblasts show decreased uptake of calcium and increased sensitivity to free radicals. *Life Sci.* 54, 1855–1860. doi: 10.1016/0024-3205(94)90142-2
- Kwon, J., An, H., Sa, M., Won, J., Shin, J. I., and Lee, C. J. (2017). Orai1 and Orai3 in combination with stim1 mediate the majority of store-operated calcium entry in astrocytes. *Exp. Neurobiol.* 26, 42–54. doi: 10.5607/en.2017.26.1.42

- La Russa, D., Frisina, M., Secondo, A., Bagetta, G., and Amantea, D. (2020). Modulation of cerebral store-operated calcium entry-regulatory factor (SARAF) and peripheral Orai1 following focal cerebral ischemia and preconditioning in mice. *Neuroscience* 441, 8–21. doi: 10.1016/j.neuroscience.2020.06.014
- Lalonde, J., Saia, G., and Gill, G. (2014). Store-operated calcium entry promotes the degradation of the transcription factor Sp4 in resting neurons. *Sci. Signal.* 7: ra51. doi: 10.1126/scisignal.2005242
- Law, B. Y., Wang, M., Ma, D. L., Al-Mousa, F., Michelangeli, F., Cheng, S. H., et al. (2010). Alisol, B., a novel inhibitor of the sarcoplasmic/endoplasmic reticulum Ca(2+) ATPase pump, induces autophagy, endoplasmic reticulum stress, and apoptosis. *Mol. Cancer Ther.* 9, 718–730. doi: 10.1158/1535-7163.MCT-09-0700
- Lee, K. P., Yuan, J. P., Zeng, W., So, I., Worley, P. F., and Muallem, S. (2009). Molecular determinants of fast Ca<sup>2+</sup>-dependent inactivation and gating of the Orai channels. *Proc. Natl. Acad. Sci. U.S.A.* 106, 14687–14692. doi: 10.1073/pnas.0904664106
- LeMaistre, J. L., Sanders, S. A., Stobart, M. J., Lu, L., Knox, J. D., Anderson, H. D., et al. (2012). Coactivation of NMDA receptors by glutamate and D-serine induces dilation of isolated middle cerebral arteries. *J. Cereb. Blood Flow Metab.* 32, 537–547. doi: 10.1038/jcbfm.2011.161
- Li, X., Chen, W., Zhang, L., Liu, W. B., and Fei, Z. (2013). Inhibition of store-operated calcium entry attenuates MPP(+)-induced oxidative stress via preservation of mitochondrial function in PC12 cells: involvement of Homer1a. *PLoS ONE* 8: e83638. doi: 10.1371/journal.pone.0083638
- Li, Y., and Camacho, P. (2004). Ca<sup>2+</sup>-dependent redox modulation of SERCA 2b by ERp57. *J. Cell Biol.* 164, 35–46. doi: 10.1083/jcb.200307010
- Liao, Y., Erxleben, C., Abramowitz, J., Flockerzi, V., Zhu, M. X., Armstrong, D. L., et al. (2008). Functional interactions among Orai1, TRPCs, and STIM1 suggest a STIM-regulated heteromeric Orai/TRPC model for SOCE/Icrac channels. *Proc. Natl. Acad. Sci. U.S.A.* 105, 2895–2900. doi: 10.1073/pnas.0712288105
- Lim, D., Mapelli, L., Canonico, P. L., Moccia, F., and Genazzani, A. A. (2018). Neuronal activity-dependent activation of astroglial calcineurin in mouse primary hippocampal cultures. *Int. J. Mol. Sci.* 19:2997. doi: 10.3390/ijms19102997
- Liou, J., Kim, M. L., Heo, W. D., Jones, J. T., Myers, J. W., Ferrell, J. E., et al. (2005). STIM is a Ca<sup>2+</sup> sensor essential for Ca<sup>2+</sup>-store-depletion-triggered Ca<sup>2+</sup> influx. *Curr. Biol.* 15, 1235–1241. doi: 10.1016/j.cub.2005.05.055
- López, J. J., Salido, G. M., Pariente, J. A., and Rosado, J. A. (2006). Interaction of STIM1 with endogenously expressed human canonical TRP1 upon depletion of intracellular Ca<sup>2+</sup> stores. *J. Biol. Chem.* 281, 28254–28264. doi: 10.1074/jbc.M604272200
- Luo, P., Li, X., Fei, Z., and Poon, W. (2012). Scaffold protein Homer 1: implications for neurological diseases. *Neurochem. Int.* 61, 731–738. doi: 10.1016/j.neuint.2012.06.014
- Lur, G., Sherwood, M. W., Ebisui, E., Haynes, L., Feske, S., Sutton, R., et al. (2011). InsP3 receptors and Orai channels in pancreatic acinar cells: co-localization and its consequences. *Biochem. J.* 436, 231–239. doi: 10.1042/BJ20110083
- Majewski, L., and Kuznicki, J. (2015). SOCE in neurons: Signaling or just refilling? *Biochim. Biophys. Acta* 1853, 1940–1952. doi: 10.1016/j.bbamcr.2015.01.019
- Majewski, L., Maciag, F., Boguszewski, P. M., Wasilewska, I., Wiera, G., Wójtowicz, T., et al. (2017). Overexpression of STIM1 in neurons in mouse brain improves contextual learning and impairs long-term depression. *Biochim. Biophys. Acta Mol. Cell Res.* 1864, 1071–1087. doi: 10.1016/j.bbamcr.2016.11.025
- Makino, H., and Malinow, R. (2011). Compartmentalized versus global synaptic plasticity on dendrites controlled by experience. *Neuron* 72, 1001–1011. doi: 10.1016/j.neuron.2011.09.036
- Malarkey, E. B., Ni, Y., and Pappas, V. (2008). Ca<sup>2+</sup> entry through TRPC1 channels contributes to intracellular Ca<sup>2+</sup> dynamics and consequent glutamate release from rat astrocytes. *Glia* 56, 821–835. doi: 10.1002/glia.20656
- Malenka, R. C., and Bear, M. F. (2004). LTP and LTD: an embarrassment of riches. *Neuron* 44, 5–21. doi: 10.1016/j.neuron.2004.09.012
- Marambaud, P., Dreses-Werringloer, U., and Vingtdoux, V. (2009). Calcium signaling in neurodegeneration. *Mol. Neurodegener.* 4:20. doi: 10.1186/1750-1326-4-20
- Martinen, M., Kurkinen, K. M., Soininen, H., Haapasalo, A., and Hiltunen, M. (2015). Synaptic dysfunction and septin protein family members in neurodegenerative diseases. *Mol. Neurodegener.* 10:16. doi: 10.1186/s13024-015-0013-z
- Mavrikakis, M., Azou-Gros, Y., Tsai, F. C., Alvarado, J., Bertin, A., Iv, F., et al. (2014). Septins promote F-actin ring formation by crosslinking actin filaments into curved bundles. *Nat. Cell Biol.* 16, 322–334. doi: 10.1038/ncb2921
- Mercer, J. C., Dehaven, W. I., Smyth, J. T., Wedel, B., Boyles, R. R., Bird, G. S., et al. (2006). Large store-operated calcium selective currents due to co-expression of Orai1 or Orai2 with the intracellular calcium sensor, Stim1. *J. Biol. Chem.* 281, 24979–24990. doi: 10.1074/jbc.M604589200
- Michaelis, M., Nieswandt, B., Stegner, D., Eilers, J., and Kraft, R. (2015). STIM1, STIM2, and Orai1 regulate store-operated calcium entry and purinergic activation of microglia. *Glia* 63, 652–663. doi: 10.1002/glia.22775
- Miyano, K., Morioka, N., Sugimoto, T., Shiraishi, S., Uezono, Y., and Nakata, Y. (2010). Activation of the neurokinin-1 receptor in rat spinal astrocytes induces Ca<sup>2+</sup> release from IP3-sensitive Ca<sup>2+</sup> stores and extracellular Ca<sup>2+</sup> influx through TRPC3. *Neurochem. Int.* 57, 923–934. doi: 10.1016/j.neuint.2010.09.012
- Moccia, F., Zuccolo, E., Soda, T., Tanzi, F., Guerra, G., Mapelli, L., et al. (2015). Stim and Orai proteins in neuronal Ca(2+) signaling and excitability. *Front. Cell Neurosci.* 9:153. doi: 10.3389/fncel.2015.00153
- Molnár, T., Yarishkin, O., Iuso, A., Barabas, P., Jones, B., Marc, R. E., et al. (2016). Store-operated calcium entry in Müller Glia is controlled by synergistic activation of TRPC and orai channels. *J. Neurosci.* 36, 3184–3198. doi: 10.1523/JNEUROSCI.4069-15.2016
- Moreno, C., Sampieri, A., Vivas, O., Peña-Segura, C., and Vaca, L. (2012). STIM1 and Orai1 mediate thrombin-induced Ca(2+) influx in rat cortical astrocytes. *Cell Calcium* 52, 457–467. doi: 10.1016/j.ceca.2012.08.004
- Moscarello, M. A., Mak, B., Nguyen, T. A., Wood, D. D., Mastronardi, F., and Ludwin, S. K. (2002). Paclitaxel (Taxol) attenuates clinical disease in a spontaneously demyelinating transgenic mouse and induces remyelination. *Mult. Scler.* 8, 130–138. doi: 10.1191/1352458502ms7760a
- Mostowy, S., and Cossart, P. (2012). Septins: the fourth component of the cytoskeleton. *Nat. Rev. Mol. Cell Biol.* 13, 183–194. doi: 10.1038/nrm3284
- Motiani, R. K., Hyzinski-García, M. C., Zhang, X., Henkel, M. M., Abdullaev, I. F., Kuo, Y. H., et al. (2013). STIM1 and Orai1 mediate CRAC channel activity and are essential for human glioblastoma invasion. *Pflugers Arch.* 465, 1249–1260. doi: 10.1007/s00424-013-1254-8
- Muik, M., Fahrner, M., Derler, I., Schindl, R., Bergsmann, J., Frischauf, I., et al. (2009). A cytosolic homomerization and a modulatory domain within STIM1 C terminus determine coupling to Orai1 channels. *J. Biol. Chem.* 284, 8421–8426. doi: 10.1074/jbc.C800229200
- Nakazawa, K., McHugh, T. J., Wilson, M. A., and Tonegawa, S. (2004). NMDA receptors, place cells and hippocampal spatial memory. *Nat. Rev. Neurosci.* 5, 361–372. doi: 10.1038/nrn1385
- Negri, S., Faris, P., Pellavio, G., Botta, L., Orgiu, M., Forcaia, G., et al. (2020). Group 1 metabotropic glutamate receptors trigger glutamate-induced intracellular Ca<sup>2+</sup> signals and nitric oxide release in human brain microvascular endothelial cells. *Cell. Mol. Life Sci.* 77, 2235–2253. doi: 10.1007/s00018-019-03284-1
- Ng, A. N., Krogh, M., and Toresson, H. (2011). Dendritic EGFP-STIM1 activation after type I metabotropic glutamate and muscarinic acetylcholine receptor stimulation in hippocampal neuron. *J. Neurosci. Res.* 89, 1235–1244. doi: 10.1002/jnr.22648
- Ohana, L., Newell, E. W., Stanley, E. F., and Schlichter, L. C. (2009). The Ca<sup>2+</sup> release-activated Ca<sup>2+</sup> current (I(CRAC)) mediates store-operated Ca<sup>2+</sup> entry in rat microglia. *Channels* 3, 129–139. doi: 10.4161/chan.3.2.8609
- Paez, P. M., Fulton, D., Colwell, C. S., and Campagnoni, A. T. (2009b). Voltage-operated Ca(2+) and Na(+) channels in the oligodendrocyte lineage. *J. Neurosci. Res.* 87, 3259–3266. doi: 10.1002/jnr.21938
- Paez, P. M., Fulton, D., Spreuer, V., Handley, V., and Campagnoni, A. T. (2011). Modulation of canonical transient receptor potential channel 1 in the proliferation of oligodendrocyte precursor cells by the golli products of the myelin basic protein gene. *J. Neurosci.* 31, 3625–3637. doi: 10.1523/JNEUROSCI.4424-10.2011
- Paez, P. M., Fulton, D. J., Spreuer, V., Handley, V., Campagnoni, C. W., and Campagnoni, A. T. (2009a). Regulation of store-operated and voltage-operated Ca<sup>2+</sup> channels in the proliferation and death of oligodendrocyte precursor cells by golli proteins. *ASN Neuro* 1.e00003. doi: 10.1042/AN20090003
- Paez, P. M., Spreuer, V., Handley, V., Feng, J. M., Campagnoni, C., and Campagnoni, A. T. (2007). Increased expression of golli myelin basic

- proteins enhances calcium influx into oligodendroglial cells. *J. Neurosci.* 27, 12690–12699. doi: 10.1523/JNEUROSCI.2381-07.2007
- Palty, R., Raveh, A., Kaminsky, I., Meller, R., and Reuveny, E. (2012). SARAF inactivates the store operated calcium entry machinery to prevent excess calcium refilling. *Cell* 149, 425–438. doi: 10.1016/j.cell.2012.01.055
- Papanikolaou, M., Lewis, A., and Butt, A. M. (2017). Store-operated calcium entry is essential for glial calcium signalling in CNS white matter. *Brain Struct. Funct.* 222, 2993–3005. doi: 10.1007/s00429-017-1380-8
- Park, C. Y., Hoover, P. J., Mullins, F. M., Bachhawat, P., Covington, E. D., Raunser, S., et al. (2009). STIM1 clusters and activates CRAC channels via direct binding of a cytosolic domain to Orai1. *Cell* 136, 876–890. doi: 10.1016/j.cell.2009.02.014
- Park, C. Y., Shcheglovitov, A., and Dolmetsch, R. (2010). The CRAC channel activator STIM1 binds and inhibits L-type voltage-gated calcium channels. *Science* 330, 101–105. doi: 10.1126/science.1191027
- Parys, J. B., Decuyper, J. P., and Bultynck, G. (2012). Role of the inositol 1,4,5-trisphosphate receptor/ $\text{Ca}^{2+}$ -release channel in autophagy. *Cell Commun. Signal.* 10:17. doi: 10.1186/1478-811X-10-17
- Pascual-Caro, C., Berrocal, M., Lopez-Guerrero, A. M., Alvarez-Barrientos, A., Pozo-Guisado, E., Gutierrez-Merino, C., et al. (2018). STIM1 deficiency is linked to Alzheimer's disease and triggers cell death in SH-SY5Y cells by upregulation of L-type voltage-operated  $\text{Ca}^{2+}$ . *J. Mol. Med.* 96, 1061–1079. doi: 10.1007/s00109-018-1677-y
- Pascual-Caro, C., Orantós-Aguilera, Y., Sanchez-Lopez, I., de Juan-Sanz, J., Parys, J. B., Area-Gomez, E., et al. (2020). STIM1 deficiency leads to specific down-regulation of ITPR3 in SH-SY5Y cells. *Int. J. Mol. Sci.* 21:6598. doi: 10.3390/ijms21186598
- Pavez, M., Thompson, A. C., Arnott, H. J., Mitchell, C. B., D'Atri, L., Don, E. K., et al. (2019). STIM1 is required for remodeling of the endoplasmic reticulum and microtubule cytoskeleton in steering growth cones. *J. Neurosci.* 39, 5095–5114. doi: 10.1523/JNEUROSCI.2496-18.2019
- Pchitskaya, E., Kraskovskaya, N., Chernyuk, D., Popugaeva, E., Zhang, H., Vlasova, O., et al. (2017). Stim2-Eb3 association and morphology of dendritic spines in hippocampal neurons. *Sci. Rep.* 7:17625. doi: 10.1038/s41598-017-17762-8
- Pchitskaya, E., Popugaeva, E., and Bezprozvanny, I. (2018). Calcium signaling and molecular mechanisms underlying neurodegenerative diseases. *Cell Calcium* 70, 87–94. doi: 10.1016/j.ceca.2017.06.008
- Pelucchi, S., Stringhi, R., and Marcello, E. (2020). Dendritic spines in alzheimer's disease: how the actin cytoskeleton contributes to synaptic failure. *Int. J. Mol. Sci.* 21:908. doi: 10.3390/ijms21030908
- Pinacho, R., Villalmanzo, N., Lalonde, J., Haro, J. M., Meana, J. J., Gill, G., et al. (2011). The transcription factor SP4 is reduced in postmortem cerebellum of bipolar disorder subjects: control by depolarization and lithium. *Bipolar Disord.* 13, 474–485. doi: 10.1111/j.1399-5618.2011.00941.x
- Popugaeva, E., Chernyuk, D., and Bezprozvanny, I. (2020). Reversal of calcium dysregulation as potential approach for treating Alzheimer's disease. *Curr. Alzheimer Res.* 17, 344–354. doi: 10.2174/1567205017666200528162046
- Popugaeva, E., Pchitskaya, E., Sheshilova, A., Alexandrov, S., Zhang, H., Vlasova, O., et al. (2015). STIM2 protects hippocampal mushroom spines from amyloid synaptotoxicity. *Mol. Neurodegener.* 10:37. doi: 10.1186/s13024-015-0034-7
- Prakriya, M., Feske, S., Gwack, Y., Srikanth, S., Rao, A., and Hogan, P. G. (2006). Orai1 is an essential pore subunit of the CRAC channel. *Nature* 443, 230–233. doi: 10.1038/nature05122
- Prins, D., Groenendyk, J., Touret, N., and Michalak, M. (2011). Modulation of STIM1 and capacitative  $\text{Ca}^{2+}$  entry by the endoplasmic reticulum luminal oxidoreductase ERp57. *EMBO Rep.* 12, 1182–1188. doi: 10.1038/embor.2011.173
- Putney, J. W. (2003). Capacitative calcium entry in the nervous system. *Cell Calcium* 34, 339–344. doi: 10.1016/S0143-4160(03)00143-X
- Rae, M. G., Martin, D. J., Collingridge, G. L., and Irving, A. J. (2000). Role of  $\text{Ca}^{2+}$  stores in metabotropic L-glutamate receptor-mediated supralinear  $\text{Ca}^{2+}$  signaling in rat hippocampal neurons. *J. Neurosci.* 20, 8628–8636. doi: 10.1523/JNEUROSCI.20-23-08628.2000
- Rao, W., Peng, C., Zhang, L., Su, N., Wang, K., Hui, H., et al. (2016). Homer1a attenuates glutamate-induced oxidative injury in HT-22 cells through regulation of store-operated calcium entry. *Sci. Rep.* 6:33975. doi: 10.1038/srep33975
- Rao, W., Zhang, L., Peng, C., Hui, H., Wang, K., Su, N., et al. (2015). Downregulation of STIM2 improves neuronal survival after traumatic brain injury by alleviating calcium overload and mitochondrial dysfunction. *Biochim. Biophys. Acta* 1852, 2402–2413. doi: 10.1016/j.bbdis.2015.08.014
- Rao, W., Zhang, L., Su, N., Wang, K., Hui, H., Wang, L., et al. (2013). Blockade of SOCE protects HT22 cells from hydrogen peroxide-induced apoptosis. *Biochem. Biophys. Res. Commun.* 441, 351–356. doi: 10.1016/j.bbrc.2013.10.054
- Remondelli, P., and Renna, M. (2017). The endoplasmic reticulum unfolded protein response in neurodegenerative disorders and its potential therapeutic significance. *Front. Mol. Neurosci.* 10:187. doi: 10.3389/fnmol.2017.00187
- Ritchie, M. F., Samakai, E., and Soboloff, J. (2012). STIM1 is required for attenuation of PMCA-mediated  $\text{Ca}^{2+}$  clearance during T-cell activation. *EMBO J.* 31, 1123–1133. doi: 10.1038/emboj.2011.495
- Rogawski, M. A. (2011). Revisiting AMPA receptors as an antiepileptic drug target. *Epilepsy Curr.* 11, 56–63. doi: 10.5698/1535-7511.11.2.56
- Ronco, V., Grolla, A. A., Glasnov, T. N., Canonico, P. L., Verkhratsky, A., Genazzani, A. A., et al. (2014). Differential deregulation of astrocytic calcium signalling by amyloid- $\beta$ , TNF $\alpha$ , IL-1 $\beta$  and LPS. *Cell Calcium* 55, 219–229. doi: 10.1016/j.ceca.2014.02.016
- Roos, J., DiGregorio, P. J., Yeromin, A. V., Ohlsen, K., Lioudyno, M., Zhang, S., et al. (2005). STIM1, an essential and conserved component of store-operated  $\text{Ca}^{2+}$  channel function. *J. Cell Biol.* 169, 435–445. doi: 10.1083/jcb.200502019
- Ryazantseva, M., Goncharova, A., Skobeleva, K., Erokhin, M., Methner, A., Georgiev, P., et al. (2018). Presenilin-1 delta E9 mutant induces STIM1-driven store-operated calcium channel hyperactivation in hippocampal neurons. *Mol. Neurobiol.* 55, 4667–4680. doi: 10.1007/s12035-017-0674-4
- Ryazantseva, M., Skobeleva, K., and Kaznacheeva, E. (2013). Familial Alzheimer's disease-linked presenilin-1 mutation M146V affects store-operated calcium entry: does gain look like loss? *Biochimie* 95, 1506–1509. doi: 10.1016/j.biochi.2013.04.009
- Ryu, C., Jang, D. C., Jung, D., Kim, Y. G., Shim, H. G., Ryu, H. H., et al. (2017). STIM1 regulates somatic  $\text{Ca}^{2+}$  signals and intrinsic firing properties of cerebellar purkinje neurons. *J. Neurosci.* 37, 8876–8894. doi: 10.1523/JNEUROSCI.3973-16.2017
- Salido, G. M., Sage, S. O., and Rosado, J. A. (2009). TRPC channels and store-operated  $\text{Ca}^{2+}$  entry. *Biochim. Biophys. Acta* 1793, 223–230. doi: 10.1016/j.bbamcr.2008.11.001
- Sanati, M., Khodagholi, F., Aminiavari, S., Ghasemi, F., Gholami, M., Kebriaeezadeh, A., et al. (2019). Impact of Gold Nanoparticles on amyloid  $\beta$ -induced Alzheimer's disease in a rat animal model: involvement of STIM proteins. *ACS Chem. Neurosci.* 10, 2299–2309. doi: 10.1021/acschemneuro.8b00622
- Sather, W. A., and Dittmer, P. J. (2019). Regulation of voltage-gated calcium channels by the ER calcium sensor STIM1. *Curr. Opin. Neurobiol.* 57, 186–191. doi: 10.1016/j.conb.2019.01.019
- Sattler, R., and Tymianski, M. (2000). Molecular mechanisms of calcium-dependent excitotoxicity. *J. Mol. Med.* 78, 3–13. doi: 10.1007/s001090000077
- Saul, S., Stanisiz, H., Backes, C. S., Schwarz, E. C., and Hoth, M. (2014). How ORAI and TRP channels interfere with each other: interaction models and examples from the immune system and the skin. *Eur. J. Pharmacol.* 739, 49–59. doi: 10.1016/j.ejphar.2013.10.071
- Segal, M., and Korkotian, E. (2014). Endoplasmic reticulum calcium stores in dendritic spines. *Front. Neuroanat.* 8:64. doi: 10.3389/fnana.2014.00064
- Selvaraj, S., Sun, Y., Sukumaran, P., and Singh, B. B. (2016). Resveratrol activates autophagic cell death in prostate cancer cells via downregulation of STIM1 and the mTOR pathway. *Mol. Carcinog.* 55, 818–831. doi: 10.1002/mc.22324
- Selvaraj, S., Sun, Y., Watt, J. A., Wang, S., Lei, S., Birnbaumer, L., et al. (2012). Neurotoxin-induced ER stress in mouse dopaminergic neurons involves downregulation of TRPC1 and inhibition of AKT/mTOR signaling. *J. Clin. Invest.* 122, 1354–1367. doi: 10.1172/JCI61332
- Serwach, K., and Gruszczyńska-Biegala, J. (2019). STIM proteins and glutamate receptors in neurons: role in neuronal physiology and neurodegenerative diseases. *Int. J. Mol. Sci.* 20:2289. doi: 10.3390/ijms20092289
- Sharma, S., Quintana, A., Findlay, G. M., Mettlen, M., Baust, B., Jain, M., et al. (2013). An siRNA screen for NFAT activation identifies septins as coordinators of store-operated  $\text{Ca}^{2+}$  entry. *Nature* 499, 238–242. doi: 10.1038/nature12229
- Shinde, A. V., Motiani, R. K., Zhang, X., Abdullaev, I. F., Adam, A. P., González-Cobos, J. C., et al. (2013). STIM1 controls endothelial barrier

- function independently of Orai1 and  $\text{Ca}^{2+}$  entry. *Sci. Signal.* 6: ra18. doi: 10.1126/scisignal.2003425
- Siddiqui, T. A., Lively, S., Vincent, C., and Schlichter, L. C. (2012). Regulation of podosome formation, microglial migration and invasion by  $\text{Ca}^{2+}$ -signaling molecules expressed in podosomes. *J. Neuroinflammation* 9:250. doi: 10.1186/1742-2094-9-250
- Simpson, P. B., Challiss, R. A., and Nahorski, S. R. (1995). Neuronal  $\text{Ca}^{2+}$  stores: activation and function. *Trends Neurosci.* 18, 299–306. doi: 10.1016/0166-2236(95)93919-O
- Singaravelu, K., Nelson, C., Bakowski, D., de Brito, O. M., Ng, S. W., Di Capite, J., et al. (2011). Mitofusin 2 regulates STIM1 migration from the  $\text{Ca}^{2+}$  store to the plasma membrane in cells with depolarized mitochondria. *J. Biol. Chem.* 286, 12189–12201. doi: 10.1074/jbc.M110.174029
- Siu, C. R., Balsor, J. L., Jones, D. G., and Murphy, K. M. (2015). Classic and Golgi Myelin Basic Protein have distinct developmental trajectories in human visual cortex. *Front. Neurosci.* 9:138. doi: 10.3389/fnins.2015.00138
- Skibinska-Kijek, A., Wisniewska, M. B., Gruszczynska-Biegala, J., Methner, A., and Kuznicki, J. (2009). Immunolocalization of STIM1 in the mouse brain. *Acta Neurobiol. Exp.* 69, 413–428.
- Soboloff, J., Rothberg, B. S., Madesh, M., and Gill, D. L. (2012). STIM proteins: dynamic calcium signal transducers. *Nat. Rev. Mol. Cell Biol.* 13, 549–565. doi: 10.1038/nrm3414
- Soboloff, J., Spassova, M. A., Dziadek, M. A., and Gill, D. L. (2006a). Calcium signals mediated by STIM and Orai proteins—a new paradigm in inter-organelle communication. *Biochim. Biophys. Acta* 1763, 1161–1168. doi: 10.1016/j.bbamer.2006.09.023
- Soboloff, J., Spassova, M. A., Hewavitharana, T., He, L. P., Xu, W., Johnstone, L. S., et al. (2006b). STIM2 is an inhibitor of STIM1-mediated store-operated  $\text{Ca}^{2+}$  entry. *Curr. Biol.* 16, 1465–1470. doi: 10.1016/j.cub.2006.05.051
- Soboloff, J., Spassova, M. A., Tang, X. D., Hewavitharana, T., Xu, W., and Gill, D. L. (2006c). Orai1 and STIM1 reconstitute store-operated calcium channel function. *J. Biol. Chem.* 281, 20661–20665. doi: 10.1074/jbc.C600126200
- Somasundaram, A., Shum, A. K., McBride, H. J., Kessler, J. A., Feske, S., Miller, R. J., et al. (2014). Store-operated CRAC channels regulate gene expression and proliferation in neural progenitor cells. *J. Neurosci.* 34, 9107–9123. doi: 10.1523/JNEUROSCI.0263-14.2014
- Song, I., and Hagan, R. L. (2002). Regulation of AMPA receptors during synaptic plasticity. *Trends Neurosci.* 25, 578–588. doi: 10.1016/S0166-2236(02)02270-1
- Spät, A., and Szanda, G. (2017). The role of mitochondria in the activation/maintenance of SOCE: store-operated  $\text{Ca}^{2+}$  entry and mitochondria. *Adv. Exp. Med. Biol.* 993, 257–275. doi: 10.1007/978-3-319-57732-6\_14
- Steinbeck, J., Nadine, H., Opatz, J., Gruszczynska-Biegala, J., Schneider, L., Theiss, S., et al. (2011). Store-operated calcium entry modulates neuronal network activity in a model of chronic epilepsy. *Exp. Neurol.* 232, 185–194. doi: 10.1016/j.expneurol.2011.08.022
- Sukumaran, P., Sun, Y., Vyas, M., and Singh, B. B. (2015). TRPC1-mediated  $\text{Ca}^{2+}$  entry is essential for the regulation of hypoxia and nutrient depletion-dependent autophagy. *Cell Death Dis.* 6: e1674. doi: 10.1038/cddis.2015.7
- Sun, S., Zhang, H., Liu, J., Popugayeva, E., Xu, N. J., Feske, S., et al. (2014). Reduced synaptic STIM2 expression and impaired store-operated calcium entry cause destabilization of mature spines in mutant presenilin mice. *Neuron* 82, 79–93. doi: 10.1016/j.neuron.2014.02.019
- Sun, Y., Selvaraj, S., Pandey, S., Humphrey, K. M., Foster, J. D., Wu, M., et al. (2018). MPP+ decreases store-operated calcium entry and TRPC1 expression in Mesenchymal Stem Cell derived dopaminergic neurons. *Sci. Rep.* 8:11715. doi: 10.1038/s41598-018-29528-x
- Sun, Y., Zhang, H., Selvaraj, S., Sukumaran, P., Lei, S., Birnbaumer, L., et al. (2017). Inhibition of L-type  $\text{Ca}^{2+}$  channels by TRPC1-STIM1 complex is essential for the protection of dopaminergic neurons. *J. Neurosci.* 37, 3364–3377. doi: 10.1523/JNEUROSCI.3010-16.2017
- Tellios, V., Maksoud, M. J. E., Xiang, Y. Y., and Lu, W. Y. (2020). Nitric oxide critically regulates purkinje neuron dendritic development through a metabotropic glutamate receptor type 1-mediated mechanism. *Cerebellum* 19, 510–526. doi: 10.1007/s12311-020-01125-7
- Tong, B. C., Lee, C. S., Cheng, W. H., Lai, K. O., Foskett, J. K., and Cheung, K. H. (2016). Familial Alzheimer's disease-associated presenilin 1 mutants promote  $\gamma$ -secretase cleavage of STIM1 to impair store-operated  $\text{Ca}^{2+}$  entry. *Sci. Signal.* 9: ra89. doi: 10.1126/scisignal.aaf1371
- Twine, N. A., Janitz, K., Wilkins, M. R., and Janitz, M. (2011). Whole transcriptome sequencing reveals gene expression and splicing differences in brain regions affected by Alzheimer's disease. *PLoS ONE* 6:e16266. doi: 10.1371/journal.pone.0016266
- Ureshino, R. P., Erustes, A. G., Bassani, T. B., Wachilewski, P., Guarache, G. C., Nascimento, A. C., et al. (2019). The Interplay between  $\text{Ca}^{2+}$  signaling pathways and neurodegeneration. *Int. J. Mol. Sci.* 20:6004. doi: 10.3390/ijms20236004
- Verkhratsky, A., and Parpura, V. (2014). Store-operated calcium entry in neuroglia. *Neurosci. Bull.* 30, 125–133. doi: 10.1007/s12264-013-1343-x
- Verkhratsky, A., Reyes, R. C., and Parpura, V. (2014). TRP channels coordinate ion signalling in astroglia. *Rev. Physiol. Biochem. Pharmacol.* 166, 1–22. doi: 10.1007/112\_2013\_15
- Vig, M., Peinelt, C., Beck, A., Koomoa, D. L., Rabah, D., Koblan-Huberson, M., et al. (2006). CRACM1 is a plasma membrane protein essential for store-operated  $\text{Ca}^{2+}$  entry. *Science* 312, 1220–1223. doi: 10.1126/science.1127883
- Vigont, V., Kolobkova, Y., Skopin, A., Zimina, O., Zenin, V., Glushankova, L., et al. (2015). Both Orai1 and TRPC1 are involved in excessive store-operated calcium entry in striatal neurons expressing mutant huntingtin exon 1. *Front. Physiol.* 6:337. doi: 10.3389/fphys.2015.00337
- Vlachos, A., Korkotian, E., Schonfeld, E., Copanaki, E., Deller, T., and Segal, M. (2009). Synaptotagmin regulates plasticity of dendritic spines in hippocampal neurons. *J. Neurosci.* 29, 1017–1033. doi: 10.1523/JNEUROSCI.5528-08.2009
- Walsh, C. M., Doherty, M. K., Tepikin, A. V., and Burgoyne, R. D. (2010). Evidence for an interaction between Golgi and STIM1 in store-operated calcium entry. *Biochem. J.* 430, 453–460. doi: 10.1042/BJ20100650
- Waltereit, R., and Weller, M. (2003). Signaling from cAMP/PKA to MAPK and synaptic plasticity. *Mol. Neurobiol.* 27, 99–106. doi: 10.1385/MN:27:1:99
- Wang, G. X., and Poo, M. M. (2005). Requirement of TRPC channels in netrin-1-induced chemotropic turning of nerve growth cones. *Nature* 434, 898–904. doi: 10.1038/nature03478
- Wang, Y., Deng, X., Mancarella, S., Hendron, E., Eguchi, S., Soboloff, J., et al. (2010). The calcium store sensor, STIM1, reciprocally controls Orai and  $\text{CaV}1.2$  channels. *Science* 330, 105–109. doi: 10.1126/science.1191086
- Wei, D., Mei, Y., Xia, J., and Hu, H. (2017). Orai1 and Orai3 mediate store-operated calcium entry contributing to neuronal excitability in dorsal root ganglion neurons. *Front. Cell. Neurosci.* 11:400. doi: 10.3389/fncel.2017.00400
- Williams, R. T., Manji, S. S., Parker, N. J., Hancock, M. S., Van Stekelenburg, L., Eid, J. P., et al. (2001). Identification and characterization of the STIM (stromal interaction molecule) gene family: coding for a novel class of transmembrane proteins. *Biochem. J.* 357, 673–685. doi: 10.1042/0264-6021:3570673
- Wong, A., Grubb, D. R., Cooley, N., Luo, J., and Woodcock, E. A. (2013). Regulation of autophagy in cardiomyocytes by  $\text{Ins}(1,4,5)\text{P}(3)$  and  $\text{IP}(3)$ -receptors. *J. Mol. Cell Cardiol.* 54, 19–24. doi: 10.1016/j.yjmcc.2012.10.014
- Wu, M. M., Buchanan, J., Luik, R. M., and Lewis, R. S. (2006).  $\text{Ca}^{2+}$  store depletion causes STIM1 to accumulate in ER regions closely associated with the plasma membrane. *J. Cell Biol.* 174, 803–813. doi: 10.1083/jcb.200604014
- Wu, Y., Whiteus, C., Xu, C. S., Hayworth, K. J., Weinberg, R. J., Hess, H. F., et al. (2017). Contacts between the endoplasmic reticulum and other membranes in neurons. *Proc. Natl. Acad. Sci. U.S.A.* 114, E4859–E4867. doi: 10.1073/pnas.1701078114
- Yang, J., Yu, J., Li, D., Yu, S., Ke, J., Wang, L., et al. (2017). Store-operated calcium entry-activated autophagy protects EPC proliferation via the CAMKK2-MTOR pathway in ox-LDL exposure. *Autophagy* 13, 82–98. doi: 10.1080/15548627.2016.1245261
- Yang, X., Jin, H., Cai, X., Li, S., and Shen, Y. (2012). Structural and mechanistic insights into the activation of Stromal interaction molecule 1 (STIM1). *Proc. Natl. Acad. Sci. U.S.A.* 109, 5657–5662. doi: 10.1073/pnas.1118947109
- Yap, K. A., Shetty, M. S., Garcia-Alvarez, G., Lu, B., Alagappan, D., Oh-Hora, M., et al. (2017). STIM2 regulates AMPA receptor trafficking and plasticity at hippocampal synapses. *Neurobiol. Learn. Mem.* 138, 54–61. doi: 10.1016/j.nlm.2016.08.007
- Yuan, J. P., Zeng, W., Dorwart, M. R., Choi, Y. J., Worley, P. F., and Muallem, S. (2009). SOAR and the polybasic STIM1 domains gate and regulate Orai channels. *Nat. Cell Biol.* 11, 337–343. doi: 10.1038/ncb1842

- Zhang, C., and Thomas, D. W. (2016). Stromal Interaction Molecule 1 rescues store-operated calcium entry and protects NG115-401L cells against cell death induced by endoplasmic reticulum and mitochondrial oxidative stress. *Neurochem. Int.* 97, 137–145. doi: 10.1016/j.neuint.2016.04.002
- Zhang, H., Sun, S., Wu, L., Pchitskaya, E., Zakharova, O., Fon Tacer, K., et al. (2016). Store-operated calcium channel complex in postsynaptic spines: a new therapeutic target for Alzheimer's disease treatment. *J. Neurosci.* 36, 11837–11850. doi: 10.1523/JNEUROSCI.1188-16.2016
- Zhang, H., Wu, L., Pchitskaya, E., Zakharova, O., Saito, T., Saido, T., et al. (2015). Neuronal store-operated calcium entry and mushroom spine loss in amyloid precursor protein knock-in mouse model of Alzheimer's disease. *J. Neurosci.* 35, 13275–13286. doi: 10.1523/JNEUROSCI.1034-15.2015
- Zhang, M., Song, J. N., Wu, Y., Zhao, Y. L., Pang, H. G., Fu, Z. F., et al. (2014). Suppression of STIM1 in the early stage after global ischemia attenuates the injury of delayed neuronal death by inhibiting store-operated calcium entry-induced apoptosis in rats. *Neuroreport* 25, 507–513. doi: 10.1097/WNR.0000000000000127
- Zhang, S. L., Yu, Y., Roos, J., Kozak, J. A., Deerinck, T. J., Ellisman, M. H., et al. (2005). STIM1 is a  $\text{Ca}^{2+}$  sensor that activates CRAC channels and migrates from the  $\text{Ca}^{2+}$  store to the plasma membrane. *Nature* 437, 902–905. doi: 10.1038/nature04147
- Zhou, Z., Xu, H., Liu, B., Dun, L., Lu, C., Cai, Y., et al. (2019). Suppression of lncRNA RMRP ameliorates oxygen-glucose deprivation/re-oxygenation-induced neural cells injury by inhibiting autophagy and PI3K/Akt/mTOR-mediated apoptosis. *Biosci. Rep.* 39:BSR20181367. doi: 10.1042/BSR20181367
- Conflict of Interest:** The authors declare that the research was conducted in the absence of any commercial or financial relationships that could be construed as a potential conflict of interest.

Copyright © 2020 Serwach and Gruszczynska-Biegala. This is an open-access article distributed under the terms of the Creative Commons Attribution License (CC BY). The use, distribution or reproduction in other forums is permitted, provided the original author(s) and the copyright owner(s) are credited and that the original publication in this journal is cited, in accordance with accepted academic practice. No use, distribution or reproduction is permitted which does not comply with these terms.



# Dysregulation of Neuronal Calcium Signaling via Store-Operated Channels in Huntington's Disease

Magdalena Czeredys\*

Laboratory of Neurodegeneration, International Institute of Molecular and Cell Biology in Warsaw, Warsaw, Poland

## OPEN ACCESS

### Edited by:

Agnese Secondo,  
University of Naples Federico II, Italy

### Reviewed by:

Emanuele Giurisato,  
University of Siena, Italy  
Rosely Oliveira Godinho,  
Federal University of São Paulo, Brazil

### \*Correspondence:

Magdalena Czeredys  
mczeredys@iimcb.gov.pl

### Specialty section:

This article was submitted to  
Signaling,  
a section of the journal  
Frontiers in Cell and Developmental  
Biology

**Received:** 29 September 2020

**Accepted:** 01 December 2020

**Published:** 23 December 2020

### Citation:

Czeredys M (2020) Dysregulation of  
Neuronal Calcium Signaling via  
Store-Operated Channels in  
Huntington's Disease.  
Front. Cell Dev. Biol. 8:611735.  
doi: 10.3389/fcell.2020.611735

Huntington's disease (HD) is a progressive neurodegenerative disorder that is characterized by motor, cognitive, and psychiatric problems. It is caused by a polyglutamine expansion in the huntingtin protein that leads to striatal degeneration via the transcriptional dysregulation of several genes, including genes that are involved in the calcium ( $\text{Ca}^{2+}$ ) signalosome. Recent research has shown that one of the major  $\text{Ca}^{2+}$  signaling pathways, store-operated  $\text{Ca}^{2+}$  entry (SOCE), is significantly elevated in HD. SOCE refers to  $\text{Ca}^{2+}$  flow into cells in response to the depletion of endoplasmic reticulum  $\text{Ca}^{2+}$  stores. The dysregulation of  $\text{Ca}^{2+}$  homeostasis is postulated to be a cause of HD progression because the SOCE pathway is indirectly and abnormally activated by mutant huntingtin (HTT) in  $\gamma$ -aminobutyric acid (GABA)ergic medium spiny neurons (MSNs) from the striatum in HD models before the first symptoms of the disease appear. The present review summarizes recent studies that revealed a relationship between HD pathology and elevations of SOCE in different models of HD, including YAC128 mice (a transgenic model of HD), cellular HD models, and induced pluripotent stem cell (iPSC)-based GABAergic medium spiny neurons (MSNs) that are obtained from adult HD patient fibroblasts. SOCE in MSNs was shown to be mediated by currents through at least two different channel groups,  $\text{Ca}^{2+}$  release-activated  $\text{Ca}^{2+}$  current ( $I_{\text{CRAC}}$ ) and store-operated  $\text{Ca}^{2+}$  current ( $I_{\text{SOC}}$ ), which are composed of stromal interaction molecule (STIM) proteins and Orai or transient receptor potential channel (TRPC) channels. Their role under physiological and pathological conditions in HD are discussed. The role of Huntingtin-associated protein 1 isoform A in elevations of SOCE in HD MSNs and potential compounds that may stabilize elevations of SOCE in HD are also summarized. Evidence is presented that shows that the dysregulation of molecular components of SOCE or pathways upstream of SOCE in HD MSN neurons is a hallmark of HD, and these changes could lead to HD pathology, making them potential therapeutic targets.

**Keywords:** Huntington disease, huntingtin,  $\text{Ca}^{2+}$  signaling, neuronal store-operated  $\text{Ca}^{2+}$  channels, neuronal store-operated  $\text{Ca}^{2+}$  entry, medium spiny neurons, spines, huntingtin-associated protein 1 isoform A

## INTRODUCTION

Calcium ( $\text{Ca}^{2+}$ ) ions are important universal second messengers that regulate numerous cellular processes.  $\text{Ca}^{2+}$  concentrations are strictly regulated by multiple  $\text{Ca}^{2+}$  channels, pumps, exchangers, and protein buffers. Under resting conditions, intracellular  $\text{Ca}^{2+}$  levels oscillate within the range of 100–300 nM. Upon cell activation, an increase in cytosolic  $\text{Ca}^{2+}$  concentrations in the range of 50–100  $\mu\text{M}$  can occur in the form of microdomains by both the influx of  $\text{Ca}^{2+}$  ions through the plasma membrane (PM) or  $\text{Ca}^{2+}$  release from intracellular stores, such as the endoplasmic reticulum (ER) (Targos et al., 2005; Kiselyov et al., 2006; McCarron et al., 2006; Majewski and Kuznicki, 2015). Store-operated  $\text{Ca}^{2+}$  entry (SOCE) is the main  $\text{Ca}^{2+}$  entry pathway in non-excitable cells (Parekh and Putney, 2005; Prakriya and Lewis, 2015; Putney et al., 2017), which was characterized in detail in immune cells (Parekh and Penner, 1997; Feske et al., 2001, 2005; Feske, 2011). Initially, the SOCE process was known as capacitative  $\text{Ca}^{2+}$  entry (Putney, 1986). SOCE is described as  $\text{Ca}^{2+}$  flow into cells through PM  $\text{Ca}^{2+}$  channels in response to the depletion of ER  $\text{Ca}^{2+}$  stores.  $\text{Ca}^{2+}$  is released from the ER upon the activation of inositol-1,4,5-triphosphate receptors (IP3Rs) (Berridge, 2002, 2009; Bezprozvanny, 2005; Mikoshiba, 2007) and ryanodine receptors (RyRs) (Rossi and Sorrentino, 2002; Amador et al., 2013) and through passive leakage (van Coppenolle et al., 2004; Tu et al., 2006; Supnet and Bezprozvanny, 2011). The  $\text{Ca}^{2+}$  response via IP3Rs is known as IP3-induced  $\text{Ca}^{2+}$  release (IICR) (Miyazaki et al., 1993;

Mikoshiba, 2007), whereas RyRs act according to  $\text{Ca}^{2+}$ -induced  $\text{Ca}^{2+}$  release (CICR) (Berridge, 1998, 2002; Verkhratsky, 2005).  $\text{Ca}^{2+}$  release by IICR is often amplified by CICR (Berridge, 2002; Chen et al., 2011). RyRs are stimulated to transport  $\text{Ca}^{2+}$  into the cytoplasm by recognizing  $\text{Ca}^{2+}$  on its cytoplasmic side, thus creating a positive feedback mechanism (Santulli and Marks, 2015).  $\text{Ca}^{2+}$  concentrations in the ER are detected by two stromal interaction molecule (STIM) isoforms, STIM1, and STIM2 (Liou et al., 2005; Roos et al., 2005; Zhang et al., 2005). They are localized in ER membranes and function as sensors of  $\text{Ca}^{2+}$  concentrations. Upon a decrease in  $\text{Ca}^{2+}$  in the ER, STIM proteins oligomerize, and migrate to ER-PM junctions where they interact with highly selective  $\text{Ca}^{2+}$  channels, Orai1-3, at the PM (Feske et al., 2006; Peinelt et al., 2006; Prakriya et al., 2006; Vig et al., 2006) and form large complexes that are visible as puncta under a microscope (Potier and Trebak, 2008; Klejman et al., 2009; Gruszczynska-Biegala and Kuznicki, 2013; Shim et al., 2015). This interaction causes the SOCE process, specifically  $\text{Ca}^{2+}$  flow from the extracellular space into the cytoplasm (Liou et al., 2005; Cahalan, 2009). To refill ER stores, the sarco-endoplasmic reticulum  $\text{Ca}^{2+}$  adenosine triphosphatase (SERCA) pump transports  $\text{Ca}^{2+}$  ions to the ER (Berridge, 2002; Periasamy and Kalyanasundaram, 2007; Brini et al., 2013a; Majewski and Kuznicki, 2015). SOCE is mediated by two different currents. One of them is  $\text{Ca}^{2+}$  release-activated  $\text{Ca}^{2+}$  current ( $I_{\text{CRAC}}$ ), which is highly selective for  $\text{Ca}^{2+}$ , non-voltage activated, and inwardly rectifying (Hoth and Penner, 1993; Lewis and Cahalan, 1995). The second is store-operated  $\text{Ca}^{2+}$  current ( $I_{\text{SOC}}$ ), which is characterized by non-selective outward current with distinct biophysical features, including greater conductance than  $I_{\text{CRAC}}$  (Golovina et al., 2001; Trepakova et al., 2001; Strübing et al., 2003; Ma et al., 2015; Lopez et al., 2016, 2020). STIM-regulated Orai channels contribute to  $I_{\text{CRAC}}$ -mediated SOCE, whereas STIM operated transient receptor potential channel 1 (TRPC1) activity mediates  $I_{\text{SOC}}$  (Majewski and Kuznicki, 2015; Moccia et al., 2015; Secondo et al., 2018).

$\text{Ca}^{2+}$  signaling regulates multiple cellular processes (Brini et al., 2013b). Its dysregulation is the postulated underlying mechanism of many disorders, including neurodegenerative diseases, such as Alzheimer's disease, Parkinson's disease, amyotrophic lateral sclerosis (Pchitskaya et al., 2018; Secondo et al., 2018), and Huntington's disease (HD) (Raymond, 2017; Pchitskaya et al., 2018).

Huntington's disease is a progressive neurodegenerative disorder with autosomal-dominant heritability that is caused by CAG trinucleotide repeat expansion in the huntingtin gene (*HTT*) (MacDonald et al., 1993). The *HTT* gene encodes huntingtin protein (HTT), which is around 350 kDa in size and ubiquitously expressed in the cytoplasm of all cell types (MacDonald et al., 1993). Mutant HTT (mHTT) contains an expansion of polyglutamine residues (polyQ) in its amino-terminal part (Ross, 2002). Expansion longer than 35 repeats in mHTT results in a polyglutamine tract that leads to mHTT aggregation and earlier HD onset (DiFiglia et al., 1997; Krobisch and Lindquist, 2000; Langbehn et al., 2004; Gusella and MacDonald, 2006). CAG repeats in mHTT between 40 and 60 cause the onset of HD at 30–50 years of age. The

**Abbreviations:** AMPARs,  $\alpha$ -amino-3-hydroxy-5-methyl-4-isoxazolepropionic acid receptors; 2-APB, 2-aminoethoxydiphenyl borate; ASOs, antisense oligonucleotides; BDNF, brain-derived neurotrophic factor; BIP, binding immunoglobulin protein; CacyBP/SIP, calcyclin binding protein and Siah-1 interacting protein; CaMKII,  $\text{Ca}^{2+}$ /calmodulin-dependent protein kinase II; cAMP, cyclic adenosine monophosphate;  $\text{Ca}_v2.2$ , N-type voltage-gated calcium channel; Cdc42, cell division cycle 42;  $\text{C}_{20}\text{H}_{22}\text{BrClN}_2$ , 6-bromo-*N*-(2-phenylethyl)-2,3,4,9-tetrahydro-1*H*-carbazol-1-aminehydrochloride; CICR,  $\text{Ca}^{2+}$ -induced  $\text{Ca}^{2+}$  release; CMC, 4-chloro-*m*-cresol; CNS, central nervous system; CPA, cyclopiazonic acid; CRACs,  $\text{Ca}^{2+}$  release-activated  $\text{Ca}^{2+}$  channels; CRISPR-Cas9, clustered regularly interspaced short palindromic repeats/CRISPR-associated protein 9; DAG, diacylglycerol; DHBP, 1,1'-diheptyl-4,4'-bipyridinium dibromide; DHPG, (S)-3,5-dihydroxyphenylglycine; ER, endoplasmic reticulum; EVP4593, 6-amino-4-(4-phenoxyphenethyl-amino)quinazoline; FKBP12, FK506-binding protein 12; HAP1, huntingtin-associated protein 1; HD, Huntington's disease; hESCs, human embryonic stem cells; HTT, huntingtin; mHTT, mutant huntingtin;  $I_{\text{CRAC}}$ ,  $\text{Ca}^{2+}$  release-activated  $\text{Ca}^{2+}$  current; IICR, IP3-induced  $\text{Ca}^{2+}$  release; IP3, inositol trisphosphate; IP3Rs, inositol-1,4,5-triphosphate receptors; iPSCs, induced pluripotent stem cells;  $I_{\text{SOC}}$ , store-operated  $\text{Ca}^{2+}$  current; LTP, long-term potentiation; MAM, mitochondria-associated membrane; mGluR1/5, metabotropic glutamate receptors 1/5; MPTPs, mitochondrial permeability transition pores; MSNs,  $\gamma$ -aminobutyric acid (GABA)ergic medium spiny neurons; NMDARs, *N*-methyl-D-aspartate receptors; NPCs, neural progenitor cells; nSOCE, neuronal store-operated calcium entry; nSOCs, neuronal store-operated calcium channels; PKA, protein kinase A; PKC, protein kinase C;  $\text{PI}_{(4,5)}\text{P}_{(2)}$ , phosphatidylinositol 4,5-bisphosphate; PLC, phospholipase C; PM, plasma membrane; polyQ, polyglutamine residues; 3-PPP, R(+)-3-(3-hydroxyphenyl)-*N*-propylpiperidine; PS1, presenilin 1; PSD95, PDZ-domain scaffold protein post-synaptic density 95; Rab4, Ras-related protein Rab4; RyRs, ryanodine receptors; SERCA, sarco-endoplasmic reticulum calcium-adenosine triphosphatase; SOCE, store-operated calcium entry; S1Rs, sigma-1 receptors; STIM, stromal interaction molecule; TrkB, tropomyosin receptor kinase B; TRPCs, transient receptor potential channels; VGCCs, voltage-gated calcium channels.

onset of HD before the age of 21 and CAG repeats over 60 are characteristic of the juvenile form of HD (Quigley, 2017), which resembles a neurodevelopmental disorder (Switońska et al., 2018; Wiatr et al., 2018). The most affected cells in HD are  $\gamma$ -aminobutyric acid (GABA)ergic medium spiny neurons (MSNs) in the striatum (Vonsattel and DiFiglia, 1998; Zoghbi and Orr, 2000). The clinical manifestations of HD include chorea, dementia, and mood and cognitive impairments (Zoghbi and Orr, 2000; Bates et al., 2015). Juvenile HD patients often present with rigidity, dystonia, seizures, cognitive alterations, and psychiatric symptoms (Quigley, 2017). No effective treatments have been developed for HD. The available medications only delay progression of the disease or alleviate its symptoms. Therefore, identification of the molecular mechanisms of HD and potential treatment targets are needed. In HD, the cascade of neurodegenerative processes was suggested to be caused by disturbances in  $\text{Ca}^{2+}$  signaling (Pchitskaya et al., 2018) that appear to be related to HTT function. Although its function remains unclear, the highest levels of wildtype HTT are found in the brain. Mutant HTT forms aggregates in neuronal nuclei. mHTT inhibits the function of various proteins, such as key transcription factors and  $\text{Ca}^{2+}$  signaling components, thereby affecting  $\text{Ca}^{2+}$  homeostasis (Giacomello et al., 2013). Disturbances in the  $\text{Ca}^{2+}$  signalosome were found in HD models and post-mortem samples from HD patients (Hodges et al., 2006; Wu et al., 2011, 2016; Czeredys et al., 2013). Abnormal  $\text{Ca}^{2+}$  signaling is considered an early event in HD pathology (Pchitskaya et al., 2018), particularly the SOCE pathway that is elevated in HD (Wu et al., 2011, 2016, 2018; Czeredys et al., 2013).

The present review provides an overview of  $\text{Ca}^{2+}$  signaling via store-operated  $\text{Ca}^{2+}$  channels under physiological conditions in neurons and under pathological conditions, namely HD. The distribution of STIM, Orai, and TRPC proteins in neurons and their functions in both the maintenance of ER  $\text{Ca}^{2+}$  concentrations and the activity of SOCE are discussed. The dysregulation of neuronal SOCE channels (nSOCs) has been implicated in HD pathology, especially affecting dendritic spines. The role of SOCE and SOCE components in the formation and maturation of dendritic spines and their contribution to synaptic plasticity under physiological conditions are also discussed. Finally, recent findings are presented that support the role of molecular components of neuronal SOCE (nSOCE) and upstream pathways that regulate these processes in dendritic spine pathology in HD. Potential drug candidates are proposed that may restore normal SOCE in HD. An argument is made that nSOCE may be a novel therapeutic target for HD.

## NEURONAL $\text{Ca}^{2+}$ SIGNALING VIA STORE-OPERATED $\text{Ca}^{2+}$ CHANNELS UNDER PHYSIOLOGICAL CONDITIONS

The role of SOCE as the main  $\text{Ca}^{2+}$  entry pathway in non-excitable cells is well-established. An important role for SOCE in excitable cells in the central nervous system (CNS), such as cortical pyramidal neurons (Klejman et al., 2009; Gruszczynska-Biegala et al., 2011), dorsal root ganglion neurons (Gemes et al., 2011), striatal MSNs (Wu et al., 2011, 2016; Czeredys

et al., 2017), hippocampal pyramidal neurons (Emptage et al., 2001; Baba et al., 2003; Samtleben et al., 2015), and cerebellar Purkinje neurons (Hartmann et al., 2014), has also been recently demonstrated. Moreover, growing evidence suggests the existence of synaptic nSOCE (Sun et al., 2014; Wu et al., 2016, 2018; Ryskamp D. et al., 2019). The presence of molecular components of SOCE in both the neuronal cell body (Klejman et al., 2009; Gruszczynska-Biegala and Kuznicki, 2013) and dendritic spines (Garcia-Alvarez et al., 2015; Korkotian et al., 2017) has been reported. Additionally, the ER was shown to extend over the entire neuron, including numerous spines that encrust the dendrites (Berridge, 2002). Both STIM isoforms, STIM1 and STIM2, are broadly but differentially expressed in the CNS. STIM1 is the predominant isoform in the cerebellum (Klejman et al., 2009; Skibinska-Kijek et al., 2009; Hartmann et al., 2014). STIM2 is most prominent in the hippocampus (Berna-Erro et al., 2009; Skibinska-Kijek et al., 2009) and cortex (Skibinska-Kijek et al., 2009; Kraft, 2015). In immune cells, STIM2.1 and STIM2.2 isoforms were identified, which have different properties in the regulation of SOCE. STIM2.1 is a negative regulator of SOCE, and STIM2.2 is the counterpart of STIM2 (Miederer et al., 2015). Both isoforms are equally expressed in MSNs (Czeredys et al., 2018), but their functions in the regulation of SOCE in neurons are unknown.

STIM1 has high affinity for  $\text{Ca}^{2+}$  and requires the higher depletion of  $\text{Ca}^{2+}$  from the ER during SOCE. STIM2 is characterized by slower aggregation kinetics, and the weaker depletion of ER  $\text{Ca}^{2+}$  stores is sufficient to activate it (Brandman et al., 2007; Parvez et al., 2008; Stathopoulos et al., 2009; Gruszczynska-Biegala et al., 2011; Gruszczynska-Biegala and Kuznicki, 2013). STIM2 was found to stabilize basal  $\text{Ca}^{2+}$  levels in rat neuronal cortical cultures and cell lines of peripheral origin (Brandman et al., 2007; Gruszczynska-Biegala et al., 2011; Gruszczynska-Biegala and Kuznicki, 2013). The interaction between STIM2 and Orai1 is weak and causes poor channel activation, whereas STIM2 was found to trigger remodeling of the STIM1 C-terminus and facilitate STIM1/Orai1 coupling and the enhancement of Orai1 function when alterations of  $\text{Ca}^{2+}$  levels in the ER are not sufficiently low to initiate STIM1 responses (Subedi et al., 2018).

Three members of the Orai channel family have been identified: Orai1, Orai2, and Orai3. They all interact with STIM1 but have different inactivation and permeability properties (DeHaven et al., 2007; Lis et al., 2007). Orairs are known as  $\text{Ca}^{2+}$  release-activated  $\text{Ca}^{2+}$  channels (CRACs) (Prakriya et al., 2006). Among them, Orai1 is a crucial pore subunit of the CRAC channel (Prakriya et al., 2006) that mediates higher currents compared with the other isoforms (Putney et al., 2017). The Orai1 channel functions as a hexamer (Hou et al., 2012; Cai et al., 2016; Yen et al., 2016). Orai1 is the dominant form in immune cells (Vaeth et al., 2017), but the highest expression levels of the Orai2 isoform were detected in the brain (Chen-Engerer et al., 2019). Orai3 is highly expressed in cancer cells (Vashisht et al., 2018). Apart from STIM-regulated Orai channels that contribute to  $\text{Ca}^{2+}$  release-activated  $\text{Ca}^{2+}$  current ( $I_{\text{CRAC}}$ )-mediated SOCE, recent studies indicated that STIM-operated TRPC1 activity mediates  $I_{\text{SOC}}$  (Liu et al., 2003; Ambudkar et al., 2017). Among

six known TRPC proteins, TRPC1, TRPC3, and TRPC4 are SOCE partners that are activated by the depletion of  $\text{Ca}^{2+}$  from stores, whereas the operation of TRPC5, TRPC6, and TRPC7 is store-independent (Ambudkar et al., 2007; Liu et al., 2007; Venkatachalam and Montell, 2007; Trebak et al., 2009; Putney and Tomita, 2012). Phospholipase C (PLC)-mediated phosphatidylinositol 4,5-bisphosphate ( $\text{PI}_{(4,5)}\text{P}_2$ ) hydrolysis upon the (S)-3,5-dihydroxyphenylglycine (DHPG)-induced activation of metabotropic glutamate receptor 1/5 (mGluR1/5) may activate TRPCs in a store-independent manner with diacylglycerol (DAG) (Itsuki et al., 2014). TRPC1 is recruited to the PM by Rab4-dependent recycling, which is critical for TRPC1-STIM1 clustering within ER-PM junctions (de Souza et al., 2015). TRPC1 function depends on Orai1-mediated  $\text{Ca}^{2+}$  entry, which enables TRPC1 recruitment to the PM where it is subsequently activated by STIM1 (Ambudkar et al., 2017). TRPC proteins may form different heteromeric structures that are involved in SOCE (Goel et al., 2002; Hofmann et al., 2002; Strübing et al., 2003; Wu et al., 2004; Liu et al., 2005; Zagranichnaya et al., 2005; Sundivakkam et al., 2012). The most prevalent TRPC channels in the mammalian brain are TRPC1, TRPC4, and TRPC5, which are mainly expressed in the hippocampus, prefrontal cortex, and lateral septum (Fowler et al., 2007, 2012), whereas TRPC3 is highly expressed in cerebellar Purkinje cells (Hartmann et al., 2014).

In the CNS,  $\text{Ca}^{2+}$  influx is mainly controlled by voltage-gated  $\text{Ca}^{2+}$  channels (VGCCs) and ionotropic glutamate receptors, such as glutamate-sensitive *N*-methyl-D-aspartate receptors (NMDARs) and  $\alpha$ -amino-3-hydroxy-5-methyl-4-isoxazolepropionic acid receptors (AMPA) (Catterall, 2011; Paoletti et al., 2013; Henley and Wilkinson, 2016), whereas the SOCE pathway is activated under resting conditions to refill ER stores and governs spontaneous neurotransmitter release (Emptage et al., 2001; Baba et al., 2003; Gruszczynska-Biegala and Kuznicki, 2013; Moccia et al., 2015; Wegierski and Kuznicki, 2018). In Purkinje neurons, STIM1-mediated SOCE replenishes intracellular  $\text{Ca}^{2+}$  levels when VGCC activity is low (Hartmann et al., 2014). Recent data suggest that SOCE may play a role in synaptic plasticity in the CNS and participate in regulating spine morphogenesis, neuronal excitability, and gene expression (Moccia et al., 2015). The role of STIM2 in maintaining post-synaptic mushroom spines in hippocampal neurons was also reported (Sun et al., 2014; Kraft, 2015).  $\text{Ca}^{2+}$  influx via STIM2-mediated SOCE regulates  $\text{Ca}^{2+}$ /calmodulin-dependent protein kinase II (CaMKII) and stabilizes mushroom spines that play a role in memory storage (Sun et al., 2014). STIM2 also regulates AMPAR trafficking and plasticity at hippocampal synapses (Yap et al., 2017). Garcia-Alvarez et al. showed that STIM2 localizes to dendritic spines, is enriched in the post-synaptic density, and is required for regular synaptic activity. STIM2 mediates cyclic adenosine monophosphate (cAMP)-dependent phosphorylation and trafficking of the GluA1 subunit of AMPARs to PM-ER junctions independently from SOCE (Garcia-Alvarez et al., 2015). The role of STIM2 in synaptic plasticity has been established (Moccia et al., 2015), but the roles of STIM1 and Orai1 in spine architecture are just emerging. Korkotian et al. recently reported the role of Orai1 in the formation, maturation,

and plasticity of dendritic spines in developing hippocampal neurons (Korkotian et al., 2017). These authors found that upon store depletion, STIM2 co-localized with Orai1 in spines, and STIM1 was less mobile in moving to spines than STIM2. Furthermore, the presence of clusters of Orai1 correlated with the emergence of nascent spines on dendrites following the transient elevation of extracellular  $\text{Ca}^{2+}$  concentrations (Korkotian et al., 2017). The role of STIM1 in regulating the structural plasticity of L-type VGCC-dependent dendritic spines was reported (Dittmer et al., 2017). The NMDAR activation of L-type VGCCs was proposed to release  $\text{Ca}^{2+}$  from the ER, which consequently causes STIM1 aggregation, inhibits L-type VGCCs, enhances ER spine content, and stabilizes mushroom spines (Dittmer et al., 2017). These findings were consistent with previous studies by two independent research groups that found a direct interaction between STIM1 protein and L-type VGCCs and the role of STIM1 in inhibiting the depolarization-mediated opening of L-type VGCC depolarization (Park et al., 2010; Wang et al., 2010). The role of STIM proteins in synaptic plasticity is further supported by findings by our group that STIMs can interact with and induce  $\text{Ca}^{2+}$  influx through AMPARs (Gruszczynska-Biegala et al., 2016). Additionally, the role of STIM proteins as potential negative regulators of NMDA-stimulated  $\text{Ca}^{2+}$  signaling was shown in cortical neurons (Gruszczynska-Biegala et al., 2020). The overexpression of STIM1 in brain neurons in transgenic mice improved contextual learning and impaired long-term depression (Majewski et al., 2017). Furthermore, STIM1 protein is responsible for mGluR1-dependent synaptic transmission in cerebellar Purkinje neurons (Hartmann et al., 2014). Accumulating evidence indicates a role for STIM1 in neurogenesis (Somasundaram et al., 2014) and the proliferation and early differentiation of neural progenitor cells (NPCs) (Somasundaram et al., 2014; Gopurappilly et al., 2018). The knockdown of both STIM isoforms reduced SOCE and inhibited the entry of mouse embryonic stem cells into a neural lineage (Hao et al., 2014). In human embryonic stem cells (hESCs), SOCE but not VGCC-mediated  $\text{Ca}^{2+}$  entry was observed, thus confirming that SOCE could play an essential role in  $\text{Ca}^{2+}$  signaling that is important for the self-renewal and differentiation of hESCs (Huang et al., 2017) and supporting the role of molecular components of SOCE in brain development.

Neuronal  $\text{Ca}^{2+}$  signaling is a complex process that involves  $\text{Ca}^{2+}$  inflow from the extracellular space and  $\text{Ca}^{2+}$  discharge from ER. Apart from the main molecular components of SOCE and PM receptors, several other molecules regulate  $\text{Ca}^{2+}$  signaling in neurons (**Figure 1**). The list of  $\text{Ca}^{2+}$  signalosomes directly or indirectly regulating  $\text{Ca}^{2+}$  signaling in neurons and their main physiological function were listed in **Table 1**. One of them is HTT binding partner, Huntingtin-associated protein-1 (HAP1), which facilitates functional effects of HTT on IP3R1 in planar lipid bilayers (Tang et al., 2004). In neurons, both HTT and HAP1 are involved in cytoskeleton regulation (Ma et al., 2011) and intracellular trafficking (Caviston and Holzbaaur, 2009; Wu and Zhou, 2009). Another  $\text{Ca}^{2+}$  signalosome that does not directly regulate  $\text{Ca}^{2+}$  signaling is calcyclin binding protein and Siah-1 interacting protein (CacyBP/SIP), which

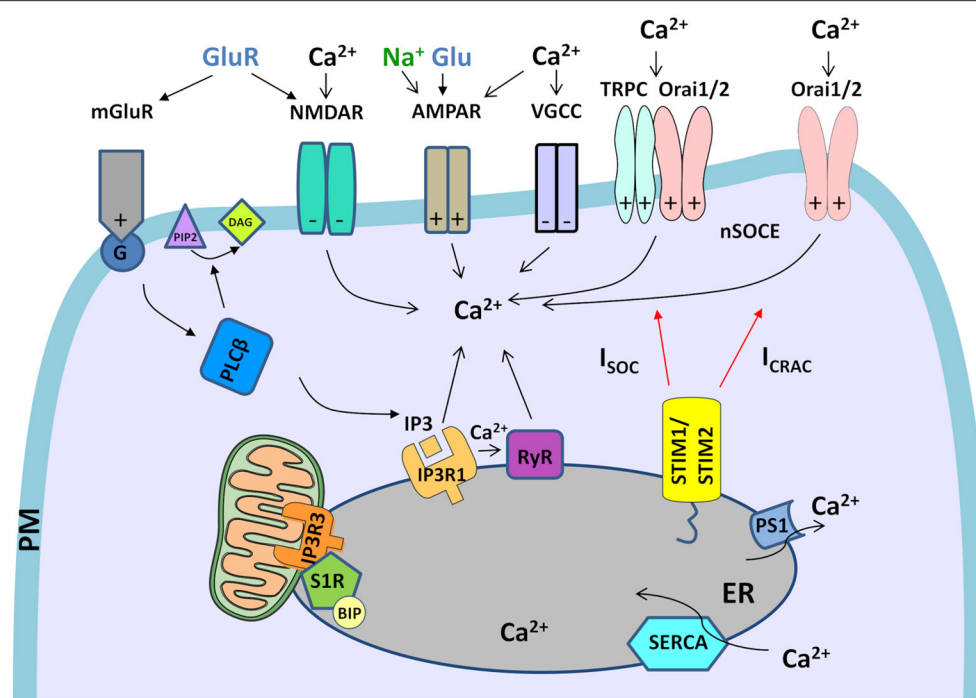


**FIGURE 1 |** Neuronal  $\text{Ca}^{2+}$  signalosomes in physiology. Neuronal  $\text{Ca}^{2+}$  signaling is a complex process that involves  $\text{Ca}^{2+}$  influx from the extracellular space and  $\text{Ca}^{2+}$  release from ER, which contains the largest endogenous  $\text{Ca}^{2+}$  pool. Glutamate (Glu) is released from presynaptic neuronal terminals, which leads to stimulation of glutamate receptors (NMDARs, AMPARs, and mGluR1s), which are present in post-synaptic terminals of the excitatory synapses. Activation of  $\text{Ca}^{2+}$  efflux by NMDAR and VGCCs requires the excitatory post-synaptic potential that arises as a result of AMPAR activity that gates  $\text{Na}^{+}$  entry. VGCCs are activated only by depolarized membrane potential. In NMDAR activation excitatory post-synaptic potential removes the  $\text{Mg}^{2+}$  block from the channel what allows its opening in response to Glu stimulation and mediates  $\text{Ca}^{2+}$  influx. mGluR is activated by Glu and coupled to trimeric G-protein, which activates a membrane-associated enzyme, PLC $\beta$ , that mediates the hydrolysis of  $\text{PI}_{(4,5)}\text{P}_2$  phospholipid to diacylglycerol (DAG) and signaling molecule, IP3. Then, IP3 interacts with IP3R receptors in the ER what causes the release of  $\text{Ca}^{2+}$  from ER stores. Further,  $\text{Ca}^{2+}$  release from the ER is exaggerated by RyR receptors in the ER, which are activated by  $\text{Ca}^{2+}$  release via IP3Rs through a mechanism called  $\text{Ca}^{2+}$ -induced  $\text{Ca}^{2+}$  release (CICR). The activation of RyRs via NMDARs or VGCCs in the plasma membrane (PM) could also be involved in CICR (not shown in the figure). Upon depletion of ER  $\text{Ca}^{2+}$  stores,  $\text{Ca}^{2+}$  influx from extracellular space is caused by neuronal store-operated  $\text{Ca}^{2+}$  entry (nSOCE), which is mediated by the interaction between the ER  $\text{Ca}^{2+}$ -sensors, Stim1 and Stim2, and the  $\text{Ca}^{2+}$ -permeable channels, consisting of Orai1 and Orai2 and/or Orai and TRPC channels. These interactions mediate two types of currents,  $I_{\text{CRAC}}$  and  $I_{\text{SOC}}$ . To refill ER  $\text{Ca}^{2+}$  stores SERCA pumps  $\text{Ca}^{2+}$  from the cytosol to the ER, while presenilin 1 (PS1) causes  $\text{Ca}^{2+}$  leak from the ER. Crosstalk between STIM proteins and receptors/channels in PM that was observed in neurons is marked on each receptor/channel as “+”-positive regulator/effector of STIM or “-”-negative effector of STIM. The only mGluR is the regulator of STIM. Within mitochondria-associated membranes (MAMs), the S1R receptor interacts with binding immunoglobulin protein (BiP), thereby regulates lipid dynamics and chaperones IP3R3 to the MAMs and facilitates  $\text{Ca}^{2+}$  flux from the ER to mitochondria. Filled black and red arrows represent interaction mechanisms. Open black arrows represent  $\text{Ca}^{2+}$ /Na $^{+}$  flux. Parts of the **Figures 1–3** were drawn by using pictures from Servier Medical Art (<http://smart.servier.com/>), licensed under a Creative Commons Attribution 3.0 Unported License (<https://creativecommons.org/licenses/by/3.0/>).

interacts with  $\text{Ca}^{2+}$  binding protein calyculin (Filipek et al., 2002), and its role was found, among others, in the cytoskeleton regulation (Jurewicz et al., 2013). There are several important signaling molecules in the ER that include presenilin 1 (PS1), which is a  $\text{Ca}^{2+}$  leak channel in the ER (Tu et al., 2006), the sigma-1 receptor (S1R), which is an ER-resident transmembrane protein regulating ER  $\text{Ca}^{2+}$  homeostasis (Su et al., 2010), and binding immunoglobulin protein (BiP), a chaperone protein, which maintains high  $\text{Ca}^{2+}$  levels in the ER (Hendershot, 2004). S1R interacts with BiP and prolong  $\text{Ca}^{2+}$  signaling from ER into mitochondria by stabilizing IP3R3s at the mitochondria-associated membranes (MAMs) (Hayashi and Su, 2007). It also blocks the inhibitory actions of ankyrin on IP3R3 (Wu and Bowen, 2008). In MSNs, where IP3R1 is a predominant neuronal isoform (Czeredys et al., 2018) S1R resisting in MAMs and stabilizes IP3R3 (Ryskamp D. A. et al., 2019). The S1R directly binds to IP3R1 and leads

to the stimulation of protein kinase C (PKC) activity and suppression of IP3 synthesis in hepatocytes (Abou-Lovergne et al., 2011).

Besides the molecules that regulate SOCE, these processes might be regulated by rearrangement in cytoskeleton proteins. The role of the cytoskeleton in SOCE regulation through the modulation of the interaction between their main molecular components was demonstrated by several groups (Smyth et al., 2007; Grigoriev et al., 2008; Vaca, 2010; Galán et al., 2011; Giurisato et al., 2014). Septins are one of the cytoskeletal components that have been shown to facilitate interactions between STIM1 and Orai1 proteins (Sharma et al., 2013). In *Drosophila* neurons it was shown that dSEPT7 prevents dOrai-mediated spontaneous  $\text{Ca}^{2+}$  entry. Lower dSEPT7 levels lead to  $\text{Ca}^{2+}$  store-independent constitutive opening of dOrai channels and higher cytosolic  $\text{Ca}^{2+}$  in resting neurons, while dSEPT7 overexpression resulted in lower SOCE (Deb et al.,

**TABLE 1** | Ca<sup>2+</sup> signalosome directly or indirectly regulating Ca<sup>2+</sup> signaling in neurons.

Ca <sup>2+</sup> signalosome	Identity	Subcellular location	Physiological function	References
<b>AMPAR</b>	Ionotropic receptor	PM	Glutamate receptor and cation channel; involved in synaptic plasticity; positive effector of STIM1 and STIM2	Gruszczynska-Biegala et al., 2016; Henley and Wilkinson, 2016
<b>BIP</b>	Chaperone protein	ER	Maintain high Ca <sup>2+</sup> levels in the ER; interacts with S1R what stabilize IP3R3 in MAMs; senses stress and activate unfolded protein response	Hendershot, 2004; Hayashi and Su, 2007
<b>CacyBP/SIP</b>	Phosphatase	Cytosol/nucleus	Interact with Ca <sup>2+</sup> binding protein calyculin; a modulator of the cytoskeleton	Filipek et al., 2002; Jurewicz et al., 2013
<b>CaMKII</b>	Kinase	PSD (cytoskeleton)	Activated by Ca <sup>2+</sup> influx via STIM2 stabilizes mushroom spines by regulation of PSD95 and Cdc42	Sun et al., 2014
<b>DAG</b>	Second messenger signaling lipid	PM	Activates TRPC in a store-independent manner	Itsuki et al., 2014
<b>HAP1</b>	Interacting protein	Cytosol	Facilitates effects of HTT on IP3R1; involved in intracellular trafficking	Tang et al., 2004; Wu and Zhou, 2009
<b>HTT</b>	Interacting protein	Cytosol/nucleus	Activates IP3R1; involved in intracellular trafficking	Tang et al., 2004; Caviston and Holzbaur, 2009
<b>IP3</b>	Second messenger signaling molecule	Cytosol	Activates IP3R1	Bezprozvanny, 2005; Mikoshiba, 2007
<b>IP3R</b>	Ca <sup>2+</sup> channel	ER	Releases Ca <sup>2+</sup> from the ER	Bezprozvanny, 2005; Mikoshiba, 2007
<b>mGluR1/5</b>	Metabotropic glutamate receptor	PM	Glutamate receptor; modulates activation of other receptors; induces a biochemical cascade of IP3 production; positive regulator of STIM1	Tang et al., 2005; Hartmann et al., 2014
<b>NMDAR</b>	Ionotropic receptor	PM	Glutamate receptor and cation channel; involved in synaptic plasticity; negative effector of STIM1 and STIM2	Paoletti et al., 2013; Gruszczynska-Biegala et al., 2020
<b>Orai</b>	Ca <sup>2+</sup> channel	PM	Ca <sup>2+</sup> channel; positive effector of STIM1	Feske et al., 2006; Peinelt et al., 2006; Prakriya et al., 2006
<b>PI<sub>(4,5)</sub>P<sub>2</sub></b>	Phospholipid	PM	Substrate for hydrolysis of IP3 and DAG by PLC	Itsuki et al., 2014
<b>PLC</b>	Membrane-associated enzyme	PM	Mediates PI <sub>(4,5)</sub> P <sub>2</sub> hydrolysis to DAG and IP3	Itsuki et al., 2014
<b>PS1</b>	Ca <sup>2+</sup> -leak channel	ER	Ca <sup>2+</sup> leak channels in the ER	Tu et al., 2006
<b>RyR</b>	Ca <sup>2+</sup> channel	ER	Releases Ca <sup>2+</sup> from the ER	Rossi and Sorrentino, 2002; Amador et al., 2013
<b>SERCA</b>	Ca <sup>2+</sup> -ATPase	ER	Refill ER Ca <sup>2+</sup> stores	Periasamy and Kalyanasundaram, 2007; Brini et al., 2013a
<b>S1R</b>	Chaperone protein	ER	In MAMs regulates lipid dynamics and Ca <sup>2+</sup> flux from the ER to mitochondria	Hayashi and Su, 2003, 2007; Su et al., 2010; Ryskamp D. A. et al., 2019
<b>STIMs</b>	Ca <sup>2+</sup> sensor	ER	Ca <sup>2+</sup> sensors in the ER	Liou et al., 2005; Roos et al., 2005; Zhang et al., 2005
<b>TRPC</b>	Ca <sup>2+</sup> channel	PM	Ca <sup>2+</sup> channel; positive effector of STIM1	Liu et al., 2003; Ambudkar et al., 2017
<b>VGCC</b>	Ca <sup>2+</sup> channel	PM	Ca <sup>2+</sup> channel activated at depolarized membrane potential; causes excitation of neurons; negative effector of STIM1	Park et al., 2010; Wang et al., 2010; Catterall, 2011; Dittmer et al., 2017

2016). Furthermore, it was shown in *Drosophila* neurons that microtubule stabilization by expression of a dominant-negative variant of the microtubule-severing protein spastin reduces SOCE, and decreases ER Ca<sup>2+</sup> content. These effects were restored upon the application of a drug that stabilized microtubules (Vajente et al., 2019).

## DYSREGULATION OF SOCE CAUSES SYNAPTIC LOSS IN HD MODELS

Elevations of SOCE have been reported in several models of HD, including YAC128 MSNs (Wu et al., 2011, 2016; Czeredys et al., 2017). In YAC128 MSNs, an increase in STIM2 expression

was observed in both YAC128 MSN cultures and 12-month-old YAC128 mice compared with controls. Increases in STIM2 expression elevated synaptic nSOCE, which likely was involved in synaptic loss in MSNs (Wu et al., 2016), whereas STIM1 expression was unchanged in HD MSNs. Indeed the CRISPR-Cas9-mediated knockdown of STIM2 caused the stabilization of dendritic spines in YAC128 MSNs. A key role for TRPC1 channels in supporting the SOC pathway was also shown in an HD model. The RNA interference (RNAi)-mediated knockdown of TRPC1 in YAC128 mouse MSNs exerted a significant protective effect against glutamate-induced apoptosis (Wu et al., 2011). Patch-clamp experiments in SK-N-SH cells transfected with full-length mutant HTT with 138Q (HTT-138Q) revealed that the current-voltage relationship of  $I_{SOC}$  currents was consistent with the involvement of TRP channels, and TRPC1 knockdown significantly reduced the magnitude of  $I_{SOC}$  currents in these cells (Wu et al., 2011). Additionally, crossing YAC128 mice with TRPC1 knockout mice improved motor performance and rescued MSN spines *in vitro* and *in vivo* (Wu et al., 2018). The RNAi-mediated knockdown of channels that are involved in SOCE other than TRPC1, such as TRPC6, Orai1, and Orai2, and knockout of the ER  $Ca^{2+}$  sensor STIM2 (Wu et al., 2016, 2018) resulted in the stabilization of spines and suppressed abnormal nSOCE in YAC128 MSNs. These results indicate that the molecular composition of the SOCE pathway in HD is complex and suggest the involvement of other players beyond STIM2 and TRPC1.

Apart from YAC128 transgenic mice, elevations of SOCE have also been described in a cellular model of HD (Wu et al., 2011; Vigont et al., 2014, 2015). In human neuroblastoma cells, expression of the N-terminal fragment of mHTT (exon-1 HTT with 138Q) increased STIM1-mediated SOCE (Vigont et al., 2014). Similar findings were reported in mouse neuroblastoma cells and primary cultures of mouse MSNs upon the lentiviral expression of N-terminal mHTT. Elevations of SOCE through actions of the sensor STIM1 and both TRPC1 and Orai1 subunits that comprise a heteromeric channel were found in these *in vitro* cultures (Vigont et al., 2015). Recent studies found that iPSC-based GABAergic MSNs from HD patient fibroblasts, which recapitulate some aspects of HD pathology, were characterized by elevations of SOC currents *in vitro* (Nekrasov et al., 2016). The SOCE of iPSC-based GABAergic HD MSNs was shown to be mediated by currents through at least two different channel groups,  $I_{CRAC}$  and  $I_{SOC}$ . These currents were upregulated compared with wildtype iPSC-based GABAergic MSNs. Thapsigargin-induced intracellular  $Ca^{2+}$  store depletion in iPSC-based GABAergic MSNs resulted in the simultaneous activation of both  $I_{CRAC}$  and  $I_{SOC}$  (Vigont et al., 2018).

## **Ca<sup>2+</sup> SIGNALING PATHWAYS THAT MAY AFFECT SOCE AND CAUSE SYNAPTIC LOSS IN HD**

Previous studies demonstrated that mHTT affects  $Ca^{2+}$  signaling in MSNs by increasing the sensitivity of IP3R1 to IP3 (Tang et al., 2003), facilitating  $Ca^{2+}$  release from internal  $Ca^{2+}$  stores

( $Ca^{2+}$  leakage) through RyRs (Suzuki et al., 2012), stimulating the activity of NR1/NR2B NMDARs (Chen et al., 1999; Sun et al., 2001; Zeron et al., 2002, 2004; Tang et al., 2005; Fan et al., 2007; Milnerwood and Raymond, 2007; Zhang et al., 2008), and disturbing mitochondrial  $Ca^{2+}$  handling (Panov et al., 2002; Choo et al., 2004; Oliveira et al., 2007). The increase in SOC pathway activity in HD may be caused directly by an increase in STIM2 expression in the presence of mHTT (Wu et al., 2016) or may result from a compensatory response of cells to the destabilization of  $Ca^{2+}$  signaling, such as an increase in the activity of IP3R1 by mHTT in YAC128 mice (Tang et al., 2003, 2004; Wu et al., 2016) or the modulation of SOC channels by receptors in the ER, such as S1Rs (Su et al., 2010).

A physiological mechanism that is responsible for activating SOCE results from the stimulation of G-protein-coupled receptors that are associated with the IP3 and PLC cascade, resulting in the release of  $Ca^{2+}$  from the ER via the IP3Rs (Streb et al., 1983). IP3R1 signaling is one of the pathways that act upstream of SOCE. Upon the release of  $Ca^{2+}$  from the ER via IP3R1, STIMs activate channels in the PM and cause  $Ca^{2+}$  influx to the cytosol. IP3R1 is abnormally activated in HD models that dysregulate ER  $Ca^{2+}$  dynamics. IP3R1 is the main IP3R isoform that is expressed in the striatum (Czeredys et al., 2018), and its activity is elevated in YAC128 MSNs (Wu et al., 2016). In MSNs, the overexpression of HTT-138Q activates IP3R1 more strongly compared with HTT that contains only 82Q repeats (Tang et al., 2003). Wu et al. reported that mHTT caused supranormal IP3R1 activity, which reduced ER  $Ca^{2+}$  levels (Wu et al., 2016). The depletion of ER  $Ca^{2+}$  leads to an increase in the activation of nSOCE in YAC128 MSN spines. Wu et al. showed that the inhibition of IP3R1 expression attenuated abnormal nSOCE and rescued spine loss in YAC128 MSNs (Wu et al., 2016), supporting the role of IP3R1 in neurite development (Fiedler and Nathanson, 2011). To inhibit IP3R1 activity, antisense oligonucleotides were applied, which resulted in the normalization of nSOCE and rescued spine loss in YAC128 MSNs (Wu et al., 2016). In summary, the role of IP3R1 that acts upstream of SOCE was established in synaptic loss in HD, in addition to known components of  $I_{SOC}$ , including STIM2 and TRPC1 (Wu et al., 2016).

In our previous studies, we observed several abnormalities of  $Ca^{2+}$  signaling in YAC128 mice, such as the upregulation of some members of  $Ca^{2+}$  signalosomes in the striatum, including HAP1 and CacyBP/SIP (Czeredys et al., 2013). Their role has been recently established in neurodegenerative or neurodevelopmental diseases (Wasik et al., 2013; Xiang et al., 2017; Wang et al., 2019; Bohush and Filipek, 2020; Liu et al., 2020). Our group also observed the elevation of SOCE and an increase in IP3R1 activity in YAC128 MSNs (Czeredys et al., 2017). Our recent research focused on regulatory mechanisms of elevations of SOCE in MSNs from YAC128 mice (Czeredys et al., 2018). We found that the HAP1A isoform was responsible for the increase in SOC channel activity when it was overexpressed in MSNs from YAC128 mice. The HAP1B isoform differs from HAP1A in its C-terminal part and cannot interact with IP3R1

(Tang et al., 2003). HAP1B did not affect SOCE (Czeredys et al., 2018). We also observed a decrease in SOC channel activity when HAP1 protein was silenced. Upon HAP1A overexpression, an increase in IP3R1 activity and a decrease in the ionomycin-sensitive ER  $\text{Ca}^{2+}$  pool were observed. When the IP3R1 inhibitor IP3 sponge (Uchiyama et al., 2002) was applied via lentiviruses in YAC128 MSN cultures that overexpressed HAP1A, the increase in the release of  $\text{Ca}^{2+}$  from the ER and consequently the elevation of SOCE were both restored to wildtype levels. These experiments revealed that HAP1A elevates SOCE in the HD model through its interaction with mHTT and facilitation of the effects of mHTT on IP3R1 (Tang et al., 2003, 2004). To unravel the role of HAP1A in SOCE dysregulation in HD, we also used a cellular model of HD, SK-N-SH cells that express HTT138Q. We found that HAP1A overexpression constitutively activated SOC channels and upregulated STIM2 protein (Czeredys et al., 2018). Therefore, STIM2 may also be involved in the activation of DHPG-induced SOCE in YAC128 MSN cultures that overexpress HAP1A. The upregulation of STIM2 and hyperactivity of IP3R1 may underlie the constitutive activity of SOC channels in SK-N-SH-HTT-138Q-overexpressing HAP1A. Overall, our data indicate that HAP1A causes the aberrant activation of SOC channels in HD models. Thus, HAP1A appears to be an important player in HD pathology. Published data indicate that HAP1A dysregulates IP3R1 and upregulates STIM2. Therefore, we predict that elevations of SOCE in HD models may also underlie synaptic loss and neurodegeneration in HD.

In addition to IP3R1 signaling, which contributes to elevations of SOCE in HD models, another mechanism that involves S1Rs was recently reported (Ryskamp et al., 2017). The striatal upregulation of S1R was detected in aged YAC128 transgenic mice and HD patients, which caused ER  $\text{Ca}^{2+}$  dysregulation by IP3R1 modulation, an increase in SOCE, and abnormal dendritic spine morphology (Ryskamp et al., 2017). It was previously reported that upon ER  $\text{Ca}^{2+}$  depletion or ER stress or at high concentrations of S1R agonists, S1R is released from BIP, dislocates beyond the MAM domain (Su et al., 2010), and modulates additional targets, including IP3R1, STIM1, and ion channels and receptors on the PM (Kourrich et al., 2012; Ryskamp D. A. et al., 2019). The S1R was also reported to have functions in neuromodulation (Maurice et al., 2006) and neuroplasticity (Takebayashi et al., 2004; Tsai et al., 2009; Kourrich et al., 2012). The CRISPR/Cas9-mediated deletion of S1Rs resulted in MSN spine loss in wildtype corticostriatal co-cultures, thus indicating an essential role for S1Rs in the development or maintenance of synaptic connections between cortical and striatal neurons (Ryskamp et al., 2017).

Concentrations of  $\text{Ca}^{2+}$  in the ER are a determinant of the magnitude of  $\text{Ca}^{2+}$  signaling through IP3R and RyR channels. In HD models, the dysregulation of  $\text{Ca}^{2+}$  release from the ER by RyR signaling was also observed. Abnormal  $\text{Ca}^{2+}$  leakage by RyRs was detected in striatal and cortical neurons from an R6/2 mouse model of HD that overexpresses exon-1 mHTT (Suzuki et al., 2012). The involvement of RyRs in mHTT-induced neuronal death was also shown in R6/2 HD mice (Suzuki et al.,

2012) and YAC128 mice (Chen et al., 2011). The association between SOCE and IP3R-gated  $\text{Ca}^{2+}$  stores has been thoroughly examined, but the role of RyR-gated stores in SOCE is less well-known. RyRs might play a role in synaptic plasticity (Baker et al., 2013; Johnenning et al., 2015). A study that used an Orai1 dominant-negative mutant revealed the role of Orai1 in dendritic spine formation following the chemical induction of long-term potentiation (LTP) (Tshuva et al., 2017). This finding was attributable to the release of  $\text{Ca}^{2+}$  from RyR-associated ER stores. Spine formation in control neurons was reduced by the RyR antagonist dantrolene (Zucchi and Ronca-Testoni, 1997). Tshuva et al. postulated that  $\text{Ca}^{2+}$  stores are important for the formation of new dendritic spines. Under conditions of Orai1 deficiency, there is less  $\text{Ca}^{2+}$  in the stores, and  $\text{Ca}^{2+}$  release decreases, leading to decreases in LTP and spine formation (Tshuva et al., 2017).

The activation of SOCE by RyRs has been intensively studied in different cell types. RyR2-gated  $\text{Ca}^{2+}$  stores were shown to contribute to SOCE in pulmonary artery smooth muscle cells. However, depletion of RyR-sensitive  $\text{Ca}^{2+}$  store with caffeine was insufficient to activate  $\text{Ca}^{2+}$  entry but required a particular RyR conformation that was modified by ryanodine binding (Lin et al., 2016). Additionally, in primary human T cells, the RyR is related to CRAC machinery such that SOCE triggers RyR activation via a CICR mechanism following the attenuation of  $\text{Ca}^{2+}$  concentrations within the ER lumen in the proximity of STIM1, thereby facilitating SOCE by diminishing store-dependent CRAC inhibition (Thakur et al., 2012). Moreover, the RyR agonist 4-chloro-3-ethylphenol blocked Orai store-operated channels in rat L6 myoblasts and HEK293 cells (Zeng et al., 2014).

Apart from the effect of an increase in SOCE or its upstream pathways on the dysregulation of spines in HD, other pathways that involve disturbances in  $\text{Ca}^{2+}$  signaling have been proposed to be involved in HD pathology (Tang et al., 2005). One of them is the dysregulation of neurotransmitter release in synapses of HD neurons. A few recent studies found that mHTT can modulate N-type VGCCs ( $\text{Ca}_v2.2$ ), which are essential for presynaptic neurotransmitter release. In young BACHD mice that expressed full-length mHTT, an increase in striatal glutamate release was found, which was reduced to wildtype levels by  $\text{Ca}_v2.2$  inhibition.  $\text{Ca}_v2.2$   $\text{Ca}^{2+}$  current density and PM expression also increased in these mice, which could be responsible for the elevation of glutamate release (Silva et al., 2017). The increases in synaptic vesicle release and elevations of  $\text{Ca}^{2+}$  influx at presynaptic terminals in primary cortical neurons were also found in a knock-in mouse model of HD (zQ175) (Chen et al., 2018). Moreover, under experimental conditions, the application of glutamate *in vitro* resulted in the apoptosis of YAC128 MSNs but not wildtype MSNs (Tang et al., 2005). Tang et al. found that abnormal glutamate release from corticostriatal projection neurons stimulated NR1/NR2B NMDARs and mGluR1/5 in YAC128 MSNs (Tang et al., 2005). Activation of NR1/NR2B NMDAR leads to  $\text{Ca}^{2+}$  influx and activation of mGluR5 receptors, leading to the production of IP3, which caused the subsequent activation of  $\text{Ca}^{2+}$  release via IP3R1. The stimulation of glutamate receptors results in supranormal  $\text{Ca}^{2+}$  responses in HD MSNs, which contributes to cytosolic  $\text{Ca}^{2+}$  overload

and consequently exceeds mitochondrial  $\text{Ca}^{2+}$  storage capacity. This, in turn, guides the opening of mitochondrial permeability transition pores (MPTPs), release of cytochrome *c* into the cytosol, and activation of caspases 9 and 3 and apoptosis (Zeron et al., 2004; Tang et al., 2005). Although, the effect of the abnormal glutamate stimulation of NMDARs on dendritic spines of YAC128 MSNs have not been examined (Tang et al., 2005), these receptors may contribute to dendritic spine pathology in HD. Accumulating evidence suggests crosstalk between NMDARs and STIMs (Dittmer et al., 2017; Gruszczynska-Biegala et al., 2020). STIM1 was shown to regulate the structural plasticity of L-type VGCC-dependent dendritic spines. The NMDAR activation of L-type  $\text{Ca}^{2+}$  channels triggers  $\text{Ca}^{2+}$  release from the ER, which then regulates STIM1 aggregation, downregulates L-type channels, and enhances ER spine content and the stabilization of mushroom spines (Dittmer et al., 2017). The activation of NMDARs in pyramidal neurons causes the recruitment of IP3 through interactions with IP3R, leading to  $\text{Ca}^{2+}$  release from ER stores and SOCE stimulation. SOCE inhibitors reduced NMDA-dependent  $\text{Ca}^{2+}$  influx and synaptic plasticity in the hippocampus (Baba et al., 2003).

A few recent studies reported the role of AMPARs in HD pathology. In the striatum in HTTQ111/+ HD knock-in mice, synaptic dysfunction and disturbances in AMPAR-mediated signaling were observed. In the striatum in these mice, a decrease in synapse density, an increase in post-synaptic density thickness, and an increase in synaptic cleft width were observed. Acute slice electrophysiology showed alterations of spontaneous AMPAR-mediated post-synaptic currents, an increase in evoked NMDAR-mediated excitatory post-synaptic currents, and elevations of extrasynaptic NMDAR currents (Kovalenko et al., 2018). Cognitive impairments in rodent models of HD are linked to the improper diffusion of AMPARs in dendritic spines of hippocampal neurons through the dysregulation of brain-derived neurotrophic factor (BDNF)-TrkB-CaMKII signaling (Zhang et al., 2018). Moreover, in YAC128 mice, the AMPAR-dependent formation of new synapses through BDNF signaling is also disturbed (Smith-Dijk et al., 2019).  $\text{Ca}^{2+}$  influx via STIM2-mediated SOCE regulates CaMKII and stabilizes mushroom spines (Sun et al., 2014), but we cannot exclude the possible effects of other players of SOCE on abnormal AMPAR diffusion in spines in HD that were shown to act through BDNF-TrkB-CaMKII signaling (Zhang et al., 2018). Recent studies in rat cortical pyramidal neurons suggested that  $\text{Ca}^{2+}$  influx through AMPARs is induced by STIMs, which might confirm the relationship between SOCE and AMPARs (Gruszczynska-Biegala et al., 2016). These authors found that AMPAR antagonists inhibited SOCE, SOCE inhibitors decreased AMPA-induced  $\text{Ca}^{2+}$  influx, and both STIM1 and STIM2 proteins cooperated with GluA1 and GluA2 subunits of AMPARs (Gruszczynska-Biegala et al., 2016). However, other studies showed that STIM2 protein can interact with AMPARs in a SOCE-independent manner (Garcia-Alvarez et al., 2015). It was found that STIM2 regulated the phosphorylation of GluA1 at both Ser845 and Ser831, which promoted the cAMP/protein kinase A (PKA)-dependent surface delivery of GluA1 via exocytosis and endocytosis (Garcia-Alvarez et al., 2015).

## POTENTIAL THERAPEUTIC STRATEGIES TO STABILIZE SOCE IN HD

In the striatum in HD transgenic mice, elevations of synaptic nSOCE were suggested to underlie post-synaptic dendritic spines loss in MSNs in aged corticostriatal co-cultures that were established from YAC128 mice (Wu et al., 2016). Several studies postulated that early neuropathological features of HD include perturbances of corticostriatal synaptic function and connectivity (Milnerwood and Raymond, 2007, 2010; Miller and Bezprozvanny, 2010; Orth et al., 2010; Murmu et al., 2013) and might lead to the accelerated neurodegeneration of MSNs in the striatum (Myers et al., 1988; Vonsattel and DiFiglia, 1998). Disturbances in the stability of synaptic spines have been suggested to underlie the development of HD symptoms (Bezprozvanny and Hiesinger, 2013; Murmu et al., 2013). The pharmacological inhibition of nSOCE that is abnormally elevated in HD could be a potential way to block neurodegeneration. A few SOCE inhibitors have been tested in HD models to date. One of these inhibitors is 6-amino-4-(4-phenoxyphenethyl-amino)quinazoline (EVP4593), which is a specific inhibitor of nSOC entry (Wu et al., 2011). A screen of a library of quinazoline-derived compounds was performed in HD flies that developed a progressive motor phenotype upon the induction of HTT-128Q transgene expression in the nervous system. In these flies, the HD phenotype was quantified using an automated climbing assay that automatically monitors motor functions. The application of EVP4593 normalized motor behavior in this fly model of HD and exerted neuroprotective effects in a glutamate toxicity assay in YAC128 MSN cultures, whereas its inactive analog EVP14808 failed to inhibit the SOC pathway in HD models (Wu et al., 2011). Further research revealed that EVP4593 reduces synaptic nSOCE and recovers abnormal spines in YAC128 MSNs. The intraventricular administration of EVP4593 in YAC128 mice *in vivo* rescued age-dependent striatal spine loss (Wu et al., 2016). Additionally, EVP4593 reduced SOCE to normal levels in MSNs that expressed exon-1 HTT with 138Q (Vigont et al., 2015). This compound also potently stabilized SOC entry in HD iPSC-based GABAergic MSNs (Nekrasov et al., 2016), thus confirming its specificity in neurons that were reprogrammed from fibroblasts from HD patients. The molecular target of EVP4593 is still unknown, but recent data showed that EVP4593 equally affected different SOC channels in HD iPSC-based GABAergic MSNs, suggesting that this compound could target SOCE regulatory proteins that are involved in both  $\text{I}_{\text{CRAC}}$  and  $\text{I}_{\text{SOC}}$  (e.g., STIM proteins) (Vigont et al., 2018). Huntington's disease iPSC-based GABAergic MSNs that were characterized by both excessive SOCE and progressive HD pathology (Nekrasov et al., 2016) were recently proposed to serve as a platform for personal drug screening in HD (Bezprozvanny and Kiselev, 2017; Vigont et al., 2018).

The stabilization of SOCE by tetrahydrocarbazoles was reported by our group in MSNs from YAC128 mice (Czeredys et al., 2017). We previously showed that these compounds decreased carbachol-induced  $\text{Ca}^{2+}$  efflux from the ER in HEK293-PS1-M146L cells, a cellular model of familial Alzheimer's disease (Honarnejad et al., 2014). Among seven

selected tetrahydrocarbazoles, the most active compound in the HD model was 6-bromo-*N*-(2-phenylethyl)-2,3,4,9-tetrahydro-1*H*-carbazol-1-aminehydrochloride ( $C_{20}H_{22}BrClN_2$ ). This compound was able to restore disturbances in  $Ca^{2+}$  homeostasis and stabilize both DHPG- and CPA-induced SOCE in YAC128 MSN cultures.  $C_{20}H_{22}BrClN_2$  was added just 5 min before the measurements, and we concluded that it acts through the post-translational modification of proteins that are involved in SOCE, stabilization of the cytoskeleton, or the inhibition of SOCE or ER  $Ca^{2+}$  release channels. However, the effect of this tetrahydrocarbazole on the increase in  $Ca^{2+}$  release from the ER was not statistically significant, in contrast to its effect on SOCE. It specifically attenuated SOCE in YAC128 MSNs and did not affect SOCE in wildtype MSNs. We also found beneficial effects of this tetrahydrocarbazole on the function of mitochondria from YAC128 MSNs (Czeredys et al., 2017), which was consistent with its protective effects in the Alzheimer's disease model (Honarnejad et al., 2014). Our recent studies showed that the SOCE stabilizer  $C_{20}H_{22}BrClN_2$  reversed the elevation of SOCE in YAC128 MSN cultures that overexpressed HAP1A (Czeredys et al., 2018). In conclusion, this tetrahydrocarbazole stabilized SOCE in MSNs from YAC128 mice and might be a promising compound for the treatment of HD.

Synaptic nSOCE is suggested to underlie spines loss in YAC128 MSNs. Therefore, compounds that can inhibit elevations of SOCE could be beneficial for synapse maintenance in HD and possibly attenuating HD pathology. The effects of EVP4593 have already been established in the restoration of spines in HD models (Wu et al., 2016), but the effects of tetrahydrocarbazoles require further studies. Potential drugs that may inhibit elevations of SOCE and consequently attenuate spine abnormalities in HD neurons are summarized in **Table 2**.

## POTENTIAL THERAPEUTIC STRATEGIES TO STABILIZE $Ca^{2+}$ SIGNALING IN HD

There are several points of mHTT interference with MSN  $Ca^{2+}$  signaling that are upstream of the SOCE pathway (**Figure 2**), and their dysregulation may cause elevations of SOCE in HD models, such as IP3R1 (Wu et al., 2016; Czeredys et al., 2018) and S1R (Ryskamp et al., 2017) signaling. Therefore, inhibitors of these pathways may also be promising drug candidates in HD.

One such drug is pridopidine, which was postulated to be a “dopamine stabilizer.” It has been shown to improve motor symptoms in clinical trials of HD (Lundin et al., 2010; de Yebenes et al., 2011; Esmaeilzadeh et al., 2011; Kiebert et al., 2013). In previous studies, pridopidine improved motor functions and prolonged the survival in R6/2 HD mice, and exerted neuroprotective effects in a mouse striatal knock-in (STHdh111/111) model of HD (Squitieri et al., 2015). Further research has shown that the pharmacological activation of S1Rs with pridopidine and the chemically similar S1R agonist R(+)-3-(3-hydroxyphenyl)-*N*-propylpiperidine (3-PPP) prevents MSN spine loss in aging YAC128 co-cultures through the normalization of IP3R1 hyperactivity, suppression of abnormal ER  $Ca^{2+}$  release, restoration of ER  $Ca^{2+}$  levels,

and reduction of excessive nSOCE in spines (Ryskamp et al., 2017). Pridopidine normalized ER  $Ca^{2+}$  levels, but its actions were prevented by S1R deletion. To evaluate the long-term effects of pridopidine, the expression profiles of  $Ca^{2+}$  signaling genes were analyzed. Pridopidine elevated the striatal expression of proteins that regulate  $Ca^{2+}$ , such as calbindin and homer1a, whereas their striatal expression decreased in aged Q175KI and YAC128 HD mouse models compared with wildtype mice. Both pridopidine and 3-PPP restored  $Ca^{2+}$  dysregulation and synaptic loss in corticostriatal co-cultures from YAC128 mice (Ryskamp et al., 2017). Moreover, another S1R agonist, PRE-084, exerted neuroprotective effects in PC6.3 cells that expressed N-terminal mHTT (Hyrskyluoto et al., 2013).

An RyR antagonist and the clinically relevant intracellular  $Ca^{2+}$  stabilizer dantrolene was shown to protect cultured YAC128 MSNs against glutamate-induced apoptosis. Feeding dantrolene to YAC128 mice significantly attenuated age-dependent motor deficiency and decreased both the death of NeuN-positive striatal neurons and nuclear aggregation of mHTT (Chen et al., 2011). These results indicate that inhibiting RyR-mediated CICR may be a possible therapeutic approach for the treatment of HD, and dantrolene could be a potent compound that can be applied as an HD medication. An increase in  $Ca^{2+}$  leakage was observed in striatal and cortical neurons from R6/2 HD mice that overexpressed exon-1 mHTT. The application of RyR inhibitors, such as dantrolene, ryanodine, 1,1'-diheptyl-4,4'-bipyridinium dibromide (DHBp), and ruthenium red, suppressed cell death in cortical neurons that overexpressed the N-terminal fragment of mHTT, whereas the addition of the potent RyR activator 4-chloro-*m*-cresol (CMC) increased mHTT toxicity. In contrast, 2-aminoethoxydiphenyl borate (2-APB), an inhibitor of IP3Rs, failed to protect these neurons (Suzuki et al., 2012). These results suggest that the inhibition of  $Ca^{2+}$  release from RyRs but not IP3Rs alleviates neuronal death that is induced by exon-1 mHTT. Additionally, intracellular  $Ca^{2+}$  imaging revealed that exon-1 mHTT caused excessive basal  $Ca^{2+}$  release ( $Ca^{2+}$  leakage) through RyRs, leading to the depletion of internal  $Ca^{2+}$  stores. Moreover, the expression of FK506-binding protein 12 (FKBP12), which interacts and stabilizes RyR1 by decreasing channel open permeability (Brillantes et al., 1994), suppressed both  $Ca^{2+}$  leakage and cell death. These results provide evidence of the role of RyRs in neuronal cell death and suggest that the stabilization of RyRs might be beneficial for the treatment of HD (Suzuki et al., 2012).

Apart from small-molecule compounds that have been proposed for the treatment of HD, antisense oligonucleotides (ASOs) may also target mHTT in HD patients (Skotte et al., 2014; van Roon-Mom et al., 2018; Barker et al., 2020). Antisense oligonucleotides are short, synthetic, single-stranded oligodeoxynucleotides that can alter mRNA expression through various mechanisms and modify protein expression (Rinaldi and Wood, 2018). In addition to the ability of ASOs to decrease mHTT levels, other strategies to normalize the dysregulation of  $Ca^{2+}$  signaling have been proposed. The knockdown of IP3R1 by ASOs (536178-2) stabilized the supranormal steady-state activity of IP3R1 in YAC128 MSNs in corticostriatal co-cultures (Wu et al., 2016). Abnormal IP3R1 activation is a major cause

**TABLE 2** | Potential strategies to stabilize SOCE in HD models.

Potential treatment	Target	Effect on pathological mechanism in HD	References
<b>EVP4593</b>			
<i>In vitro</i> (30–300 nM)	nSOCE inhibitor	<ul style="list-style-type: none"> <li>Stabilizes SOCE in YAC128 MSNs cultures</li> </ul>	Wu et al., 2011
<i>In vivo</i> delivery (0.25 mg/ml via osmotic minipumps; Alzet)		<ul style="list-style-type: none"> <li>Normalizes motor behavior in a fly model of HD</li> <li>Exerts neuroprotective effects in a glutamate toxicity assay in YAC128 MSN cultures</li> <li>Reduces SOCE in MSNs that express exon-1 HTT-138Q</li> <li>Stabilizes synaptic nSOC and rescues spine loss in YAC128 MSNs</li> <li>Rescues age-dependent striatal spine loss in YAC128 mice <i>in vivo</i></li> <li>Stabilizes elevated <math>I_{SOC}</math> and <math>I_{CRAC}</math> currents in HD iPSC-based GABAergic MSNs</li> </ul>	Vigont et al., 2015 Wu et al., 2016 Vigont et al., 2018
<b>C<sub>20</sub>H<sub>22</sub>BrCIN<sub>2</sub></b> (10 $\mu$ M)	SOCE stabilizer	<ul style="list-style-type: none"> <li>Stabilizes both DHPG- and CPA-induced SOCE in YAC128 MSN cultures</li> <li>Increases mitochondrial membrane potential in YAC128 MSNs</li> <li>Reverses the elevation of SOCE in YAC128 MSN cultures that overexpress HAP1A</li> </ul>	Czeredys et al., 2017 Czeredys et al., 2018

of elevations of ER  $Ca^{2+}$  leakage that consequently leads to abnormal nSOCE in HD MSNs. Treatment with ASOs against IP3R1 rescued YAC128 MSN spines, increasing their numbers to the same levels as in wildtype cultures (Wu et al., 2016). Therefore, the ASO-mediated suppression of IP3R1 expression was sufficient to prevent spine loss in YAC128 MSNs, presumably through the stabilization of  $Ca^{2+}$  levels in the ER and nSOCE in neuronal spines. Wu et al. proposed that ASOs may be a promising treatment for HD because they can modify IP3R1 levels (Wu et al., 2016).

Moreover, IP3R1 sponge that was delivered using a lentivirus system *in vitro* into YAC128 MSNs that overexpressed HAP1A restored abnormal SOCE. IP3R1 sponge, through its ability to inhibit IP3R1 activity, attenuated the effects of mHTT and HAP1A on this receptor, which led to the normalization of SOCE in an HD model (Czeredys et al., 2018). Mutant HTT was previously shown to specifically bind to the C-terminal cytosolic region of IP3R1 (a 122-amino acid-long IC10 fragment) (Tang et al., 2003). These findings led Tang et al. to propose a novel therapy for HD, who introduced IC10 peptide into HD MSNs *in trans* to disrupt the pathogenic association between IP3R1 and mHTT to normalize neuronal  $Ca^{2+}$  signaling and prevent the cell death of HD MSNs. Indeed, infection with lenti-GFP-IC10 virus stabilized  $Ca^{2+}$  signaling in YAC128 MSNs *in vitro* and protected these neurons from glutamate-induced apoptosis. Intrastriatal injections of AAV1-GFP-IC10 attenuated motor deficits and diminished MSN loss and shrinkage in YAC128 mice *in vivo* (Tang et al., 2009). These results demonstrated the importance of IP3R1 and mHTT in the pathogenesis of HD and suggested that IC10 peptide may be useful for HD treatment. Additionally, IC10 peptide was shown to reduce mHTT aggregation and nuclear accumulation, which may suggest a novel protective

mechanism of IC10 that works jointly with its stabilizing effects on  $Ca^{2+}$  signaling (Tang et al., 2009). Additionally, the IP3R blocker 2-APB (Maruyama et al., 1997) protected YAC128 MSNs from glutamate-induced apoptosis (Tang et al., 2005). Furthermore, low-molecular-weight heparin sulfate Enoxaparin inhibited IP3R1 activity and protected YAC128 MSNs from glutamate-induced apoptosis (Tang et al., 2005).

In summary, potential strategies to stabilize elevations of  $Ca^{2+}$  signaling pathways in the ER might be beneficial for HD patients because they may prevent abnormal SOCE and dendritic spine abnormalities. Possible treatment options that target  $Ca^{2+}$  signaling receptors in the ER, which may restore spine pathology in HD, are summarized in **Table 3**.

One of the causes of MSN degeneration in HD is dysregulation of the glutamate/ $Ca^{2+}$  signaling pathway. Antagonists of glutamate signaling pathways might have beneficial effects for the treatment of HD, especially because crosstalk between glutamate receptors and neuronal SOCE was recently reported (Serwach and Gruszczynska-Biegala, 2019). The non-competitive NMDAR antagonist memantine (Lipton, 2006) protected YAC128 MSNs from glutamate-induced cell death. Furthermore, another antagonist of glutamate signaling pathways, riluzole, which acts on the inhibition of glutamate release, was also protective against glutamate-induced cell death, although it was less potent than memantine (Wu et al., 2006). Memantine was also examined in a 2-year-long human clinical study of HD. Memantine retarded the progression of HD in patients in motor, functional, and behavioral tests (Beister et al., 2004). Neuroprotective effects of the NMDAR antagonist (+)MK801 and NR2B-specific NMDAR antagonist ifenprodil were also found in a glutamate-induced cell death assay in YAC128 MSNs (Tang et al., 2005). Tang et al. found that mGluR1/5 inhibition by a combination of MPEP and

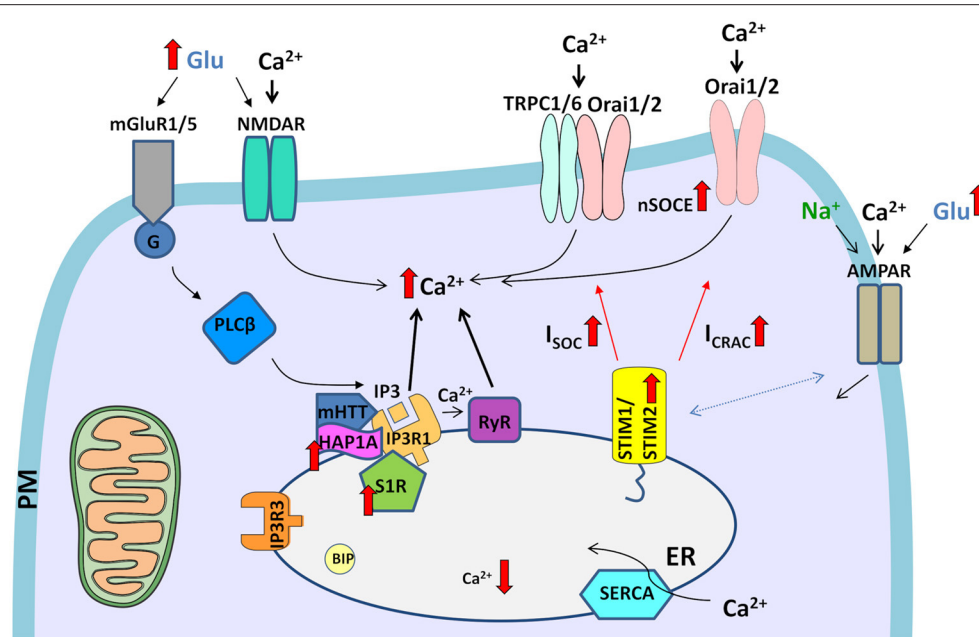


**FIGURE 2 |** Dysregulation of  $\text{Ca}^{2+}$  signaling pathways in HD neurons. The elevation of glutamate (Glu) release from presynaptic neuronal terminals leads to the excessive stimulation of glutamate receptors (e.g., NMDARs and mGluR1/5) in post-synaptic terminals. The overactivation of NMDARs results in excessive  $\text{Ca}^{2+}$  influx. In turn, mGluRs couple to G-protein, which activates PLC $\beta$  and induces the formation of IP $_3$ , which interacts with IP $_3$ R and causes the release of  $\text{Ca}^{2+}$  from ER stores. HAP1A interacts with mHTT and exaggerates the effect of mHTT on IP $_3$ R1, which leads to the greater sensitivity of IP $_3$ R1 to IP $_3$  and an increase in the release of  $\text{Ca}^{2+}$  from the ER, resulting in the attenuation of ER  $\text{Ca}^{2+}$  levels. Additionally,  $\text{Ca}^{2+}$  release from the ER is exaggerated by RyRs, which are activated by abnormal  $\text{Ca}^{2+}$  release via IP $_3$ R. Activated S1Rs via several processes, such as ER stress,  $\text{Ca}^{2+}$  release from the ER, or ligands, dissociate from binding immunoglobulin protein (BIP), thereby disconnecting from IP $_3$ R3 in mitochondria-associated membranes. Subsequently, upregulated S1R interacts with IP $_3$ R1. Upon the abnormal depletion of ER  $\text{Ca}^{2+}$  stores, upregulated STIM2 senses ER  $\text{Ca}^{2+}$  content and activates SOC channels in the plasma membrane (PM), which mediate two currents,  $I_{\text{SOC}}$  and  $I_{\text{CRAC}}$ . Elevations of neuronal SOCE (nSOCE) contribute to  $\text{Ca}^{2+}$  overload. The surface distribution of AMPARs is disturbed in HD neurons. Crosstalk that was observed between AMPARs and STIMs in wildtype neurons might contribute to abnormal  $\mathcal{C}\mathcal{a}^{2+}$  influx through AMPARs in HD pathology in the presence of upregulated STIM2. Filled black and red arrows represent interaction mechanisms. Open black arrows represent  $\text{Ca}^{2+}$ /Na $^{+}$  flux. Thick red arrows represent an increase or decrease in expression/concentration. Dashed arrows represent suspected interactions.

CPCCOEt reduced the glutamate-induced apoptosis of YAC128 MSNs to wildtype MSN levels, and a mixture of mGluR1/5 and NMDAR blockers [MPEP, CPCCOEt, and (+)MK801] abolished glutamate-dependent cell death in both wildtype and YAC128 MSNs (Tang et al., 2005).

Although crosstalk between AMPARs and SOCE has been shown (Serwach and Gruszczynska-Biegala, 2019), an inhibitor of AMPARs, the antidepressant tianeptine ([3-chloro-6-methyl-5,5-dioxo-6,11-dihydro-(c,f)-dibenzo-(1,2-thiazepine)-11-yl)amino]-7 heptanoic acid) restored synaptic deficits in HD models independently from the SOCE process. Tianeptine improved hippocampal synaptic and memory deficits and anxiety/depression-like behavior in HD mice, possibly through the modulation of BDNF signaling and AMPAR surface diffusion (Zhang et al., 2018). The AMPAR-dependent formation of new synapses in cortical neurons from HD mice through BDNF signaling was restored by pridopidine, a drug that enhances BDNF signaling through the stimulation of S1Rs, and the S1R agonist 3-PPP (Smith-Dijk et al., 2019). Potential strategies to stabilize glutamate receptors in the PM that might affect SOCE in HD models are presented in Table 4.

The nSOC pathway plays an important role in supporting the stability of MSN spines under physiological conditions, and this process is disturbed in HD pathology. Both SOCE players and other  $\text{Ca}^{2+}$  signaling pathways that regulate nSOCE may contribute to the synaptic dysregulation of MSNs in HD (Figure 3). Substantial evidence suggests that the pharmacological inhibition of nSOCE, its upstream pathways, and other receptors that may affect the SOCE process may be beneficial for synapse maintenance in HD models. Although SOCE inhibition in the striatum might be protective in HD patients, the same compound might be detrimental in other brain regions that contain cortical and hippocampal pyramidal neurons where SOCE is unchanged (Secondo et al., 2018).

## CONCLUDING REMARKS

The dysregulation of  $\text{Ca}^{2+}$  signaling via store-operated  $\text{Ca}^{2+}$  channels is involved in the pathogenesis of HD. Abnormal nSOCE leads to synaptic dysregulation in HD MSNs. Several SOCE components have been identified in dendritic spine pathology. Among these, STIM2 and TRPC1 deserve special attention as potential HD treatment targets. Elevations of

**TABLE 3 |** Potential strategies to stabilize  $\text{Ca}^{2+}$  signaling pathways in the ER that may prevent abnormal SOCE in HD models.

Potential treatment	Target	Effect on pathological mechanism in HD	References
<b>Pridopidine</b>			
<i>In vivo</i> (5 or 6 mg/kg, i.p.)	Dopamine stabilizer; S1R activator	• Improves motor functions and prolongs survival of R6/2 HD mice	Squitieri et al., 2015
<i>In vitro</i> (150 $\mu\text{M}$ )		• Antiapoptotic effects in knock-in cellular HD model (STHdh111/111)	Squitieri et al., 2015
<i>In vitro</i> (100 nM or 1 $\mu\text{M}$ )		• Activates S1Rs, which prevents MSN spine loss in YAC128 co-cultures; suppresses supranormal ER $\text{Ca}^{2+}$ release; restores ER calcium levels; reduces excessive synaptic nSOC	Ryskamp et al., 2017
<b>3-PPP</b>			
<i>In vitro</i> (100 nM or 1 $\mu\text{M}$ )	S1R agonist	• Activates S1Rs, which prevents MSN spine loss in YAC128 co-cultures; restores excessive synaptic nSOC	Ryskamp et al., 2017
<b>PRE-084</b>			
<i>In vitro</i> (0.3 $\mu\text{M}$ )	S1R agonist	• Neuroprotective properties in PC6.3 cells that express N-terminal mHTT	Hyrskyluoto et al., 2013
<b>ASO 536178-2 (Isis Pharmaceuticals)</b>			
<i>In vitro</i> (500 nM)	Knockdown of IP3R1	<ul style="list-style-type: none"> <li>• Stabilizes the supranormal steady-state activity of IP3R1 in YAC128 MSNs co-cultures</li> <li>• Prevents spine loss in YAC128 MSNs through the stabilization of <math>\text{Ca}^{2+}</math> levels in the ER and nSOC in neuronal spines</li> </ul>	Wu et al., 2016
<b>IP3R1 sponge</b>			
<i>In vitro</i> p49-dTomato in pUltraChili	IP3R1 inhibitor	<ul style="list-style-type: none"> <li>• Restores abnormal SOCE in YAC128 MSNs that overexpress HAP1A</li> <li>• Restores increase in <math>\text{Ca}^{2+}</math> release from the ER in YAC128 MSNs that overexpress HAP1A</li> </ul>	Czeredys et al., 2018
<b>IC10 peptide</b>			
IC10 fragment of rat IP3R1 (122 aa length)	IP3R1 inhibitor	<ul style="list-style-type: none"> <li>• Disrupts the pathogenic association between IP3R1 and mHTT</li> <li>• Stabilizes <math>\text{Ca}^{2+}</math> signaling in cultured YAC128 MSNs and protects YAC128 MSNs from glutamate-induced apoptosis</li> </ul>	Tang et al., 2009
<i>In vitro</i> pLenti-GFP-IC10			
<i>In vivo</i> AAV1-GFP-IC10		<ul style="list-style-type: none"> <li>• Intrastriatal injections significantly alleviate motor deficits and reduce MSN loss and shrinkage in YAC128 mice <i>in vivo</i></li> <li>• Reduces mHTT aggregation and nuclear accumulation</li> </ul>	
<b>2-APB</b>			
<i>In vitro</i> (400 $\mu\text{M}$ )	IP3R1 inhibitor	• Protects YAC128 MSNs from glutamate-induced apoptosis	Tang et al., 2005
<b>Enoxaparin (Lovenox)</b>			
<i>In vitro</i> (200 $\mu\text{g/ml}$ )	IP3R1 inhibitor	• Protects YAC128 MSNs from glutamate-induced apoptosis	Tang et al., 2005
<b>Dantrolene</b>			
<i>In vitro</i> (10–50 $\mu\text{M}$ )	RyRs antagonist	<ul style="list-style-type: none"> <li>• Protects cultured YAC128 MSNs from glutamate-induced apoptosis</li> <li>• Attenuates age-dependent motor deficits in YAC128 mice <i>in vivo</i></li> <li>• Decreases death of NeuN-positive striatal neurons and nuclear aggregation of mHTT</li> </ul>	Chen et al., 2011
<i>In vivo</i> feeding (5 mg/kg twice/week)			
<i>In vitro</i> (30 $\mu\text{M}$ )		• Suppresses cell death in cortical neurons that are transfected with N-terminal mHTT-150Q	Suzuki et al., 2012
<b>Ryanodine</b>			
<i>In vitro</i> (10 $\mu\text{M}$ )	RyR inhibitor *at nanomolar concentrations, ryanodine partially activates RyRs	• Suppresses cell death in cortical neurons that are transfected with N-terminal mHTT-150Q	Suzuki et al., 2012
<b>DHBP</b>			
<i>In vitro</i> (50 nM)	RyR inhibitor	<ul style="list-style-type: none"> <li>• Alleviates <math>\text{Ca}^{2+}</math> leakage through RyRs in cortical neurons that are transfected with N-terminal mHTT-150Q</li> <li>• Suppresses cell death in cortical neurons that are transfected with N-terminal mHTT-150Q</li> </ul>	Suzuki et al., 2012
<b>Ruthenium red</b>			
<i>In vitro</i> (10 nM)	RyR inhibitor	• Suppresses cell death in cortical neurons that are transfected with N-terminal mHTT-150Q	Suzuki et al., 2012

**TABLE 4 |** Potential strategies to stabilize receptors in the plasma membrane that may affect nSOCE in HD models.

Potential treatment	Target	Effect on pathological mechanism in HD	References
<b>Memantine</b>			
<i>In vitro</i> (10 μM)	Non-competitive NMDAR antagonist	• Protects YAC128 MSNs from glutamate-induced cell death	Wu et al., 2006
Up to 30 mg/ day in HD patients		• Retards the progression of motor, functional, and behavioral deficits in HD patients	Beister et al., 2004
<b>Riluzole</b>			
<i>In vitro</i> (10 μM)	Inhibition of glutamate release	• Protects against glutamate-induced cell death in YAC128 MSNs	Wu et al., 2006
<b>(+)MK801</b>			
<i>In vitro</i> (10 μM)	NMDAR antagonist	• Neuroprotective against glutamate-induced cell death in YAC128 MSNs	Tang et al., 2005
<b>Ifenprodil</b>			
<i>In vitro</i> (20 μM)	NR2B-specific NMDAR antagonist	• Neuroprotective against glutamate-induced cell death in YAC128 MSNs	Tang et al., 2005
Mixture of 20 μM MPEP and 50 μM CPCCOEt <i>in vitro</i>	mGluR1/5 inhibitors	• Reduces the glutamate-induced apoptosis of YAC128 MSNs	Tang et al., 2005
<b>Tianeptine</b>			
25 mg/kg (i.p., daily for 8 weeks)	AMPA inhibitor	• Improves hippocampal synaptic and memory deficits	Zhang et al., 2018
10 mg/kg (single injection)		• Reverses anxiety/depression-like behavior in HD mice by modulating BDNF signaling and AMPAR surface diffusion	
<b>Pridopidine</b>			
<i>In vitro</i> (1 μM)	S1R activator	• Restores disruption of homeostatic synaptic plasticity signaling in cortical pyramidal neurons in HD models • Restores AMPAR-dependent formation of new synapses through BDNF signaling in HD cortical neurons	Smith-Dijak et al., 2019
<b>3-PPP</b>			
<i>In vitro</i> (1 μM)	S1R agonist	• Restores disruption of homeostatic synaptic plasticity signaling in cortical neurons in HD models • Restores AMPAR-dependent formation of new synapses through BDNF signaling in HD cortical neurons	Smith-Dijak et al., 2019

SOCE in HD models also result from abnormal  $\text{Ca}^{2+}$  signaling responses at the ER. The activity of two receptors in the ER, IP3R1, and S1R, is significantly elevated in HD models, which contributes to elevations of nSOCE and consequently MSN dendritic spine pathology. Additionally, the role of HAP1A protein should be emphasized because it can exaggerate the effect of mHTT on IP3R1, which leads to an increase in the release of  $\text{Ca}^{2+}$  from the ER and consequently elevations of SOCE in HD MSNs. One function of SOCE in neurons is to refill ER  $\text{Ca}^{2+}$  that is released during cell activation to initiate specific signaling pathways. However, SOCE also triggers various other signaling pathways. Evidence suggests crosstalk in neurons between glutamate receptors and SOCE components. Elevations of SOCE in HD might also be affected by glutamate receptors that are abnormally activated, which consequently causes MSN cell death. Under physiological conditions, SOCE components appear to be crucial in several aspects of neuronal development, including the proliferation and early differentiation of NPCs. Additionally, SOCE components play a role in synaptic

formation and maturation, and they contribute to synaptic plasticity. Therefore, the dysregulation of SOCE appears to underlie dendritic spine abnormalities that have been identified in HD models. Recent findings that were reviewed herein support the role of molecular components of nSOCE and upstream pathways that regulate these processes in dendritic spine pathology in HD, and these components may be potential targets for HD treatment. Several drug candidates may restore abnormal SOCE (e.g., EVP4593 and tetrahydrocarbazoles) or other disturbances in  $\text{Ca}^{2+}$  signaling pathways, including IP3R1, RyR, and S1R. A few known compounds may prevent dendritic spine loss in HD by stabilizing abnormal nSOCE (e.g., EVP4593) and S1R activity (e.g., pridopidine and 3-PPP) or by attenuating supranormal IP3R1 activity (e.g., ASOs). The arguments that nSOC pathways could be novel therapeutic targets for HD treatment are convincing because elevations of SOCE were observed not only in transgenic and cellular HD models but also in iPSC-based GABAergic MSNs that were obtained from adult HD patient fibroblasts. However, such proposed

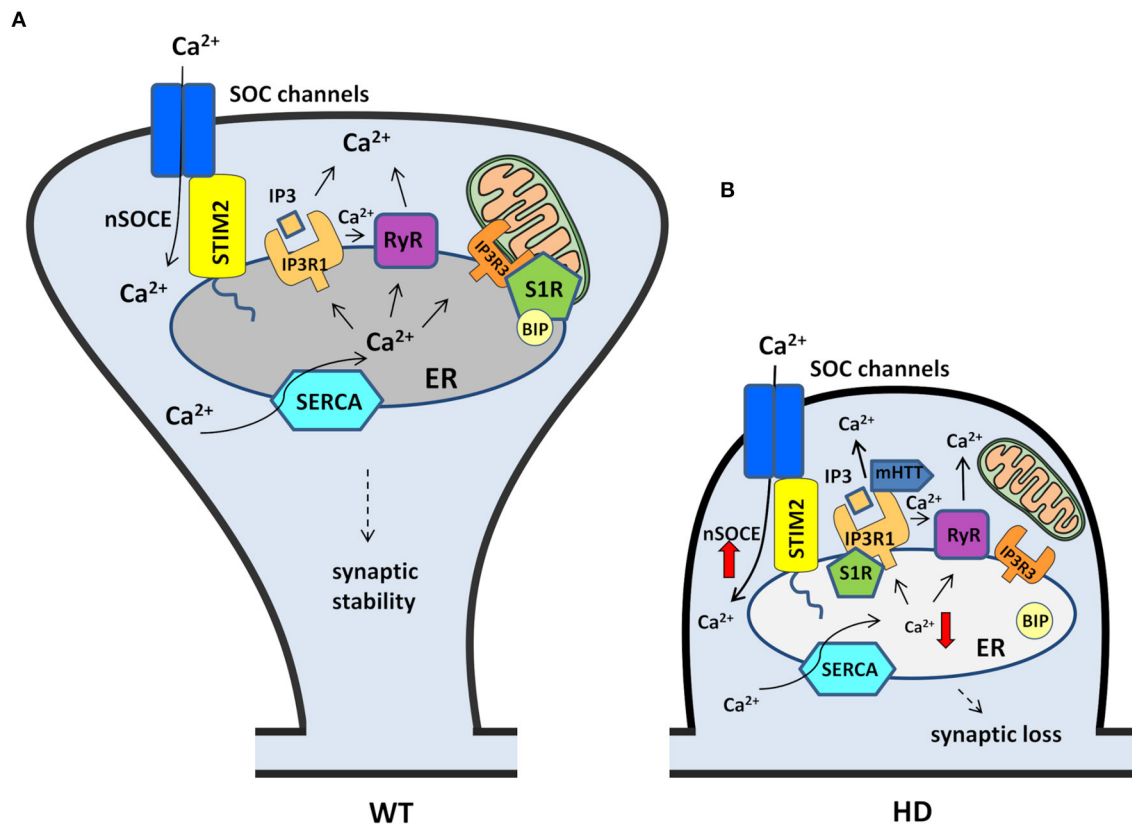


**FIGURE 3 |** Contribution of nSOCE components and  $\text{Ca}^{2+}$  signaling pathways to the dysregulation of MSN spines in HD. **(A)** In wildtypes, MSN synaptic spine stability is maintained by the nSOCE pathway. nSOCE is gated by STIM2, which regulates ER  $\text{Ca}^{2+}$  levels by activating SOC channels in the plasma membrane, and SERCA pumps  $\text{Ca}^{2+}$  from the cytosol to the ER to refill ER  $\text{Ca}^{2+}$  stores.  $\text{Ca}^{2+}$  is released from the ER to the cytosol by IP3R1 and RyRs, and S1R facilitates  $\text{Ca}^{2+}$  flux from the ER to mitochondria via IP3R3. **(B)** In HD MSNs, supranormal synaptic nSOCE causes spine loss. mHTT sensitizes IP3R1 to IP3, causing excessive  $\text{Ca}^{2+}$  leakage from the ER.  $\text{Ca}^{2+}$  release from the ER is exaggerated by RyRs that are activated by abnormal  $\text{Ca}^{2+}$  release via IP3R1. Upon activation, S1Rs redistribute to the entire ER network where they interact with additional targets, including IP3R1, to affect their function. STIM2 upregulation compensates for the abnormal depletion of  $\text{Ca}^{2+}$  from the ER and causes the aberrant activation of nSOCE. Finally, supranormal nSOCE activates pathways and effectors that destabilize spines and lead to their loss in HD MSNs. Black arrows represent  $\text{Ca}^{2+}$  flux. The thick red arrows represent an increase or decrease in  $\text{Ca}^{2+}$  concentration.

drug candidates or other therapeutic strategies that may act on SOCE components in HD deserve further scrutiny to provide clear evidence that they can successfully and specifically target these proteins to improve or reverse the dysregulation of  $\text{Ca}^{2+}$  homeostasis and signaling without causing major side effects.

## AUTHOR CONTRIBUTIONS

MC wrote the review and discussed literature data in this paper.

## REFERENCES

Abou-Lovergne, A., Collado-Hilly, M., Monnet, F. P., Koukoui, O., Prigent, S., Coquil, J. F., et al. (2011). Investigation of the role of signal-1-receptors in inositol 1,4,5-trisphosphate dependent calcium signaling in hepatocytes. *Cell Calcium* 50, 62–72. doi: 10.1016/j.ceca.2011.05.008

## FUNDING

This study was supported by the National Science Center in Poland (Grant No. 2019/33/B/NZ3/02889 and 2014/15/D/NZ3/05181 to MC).

## ACKNOWLEDGMENTS

The author thanks Prof. Jacek Kuznicki and Dr. Tomasz Wegierski for critically reading the manuscript.

Amador, F. J., Stathopoulos, P. B., Enomoto, M., and Ikura, M. (2013). Ryanodine receptor calcium release channels: lessons from structure-function studies. *FEBS J.* 280, 5456–5470. doi: 10.1111/febs.12194

Ambudkar, I. S., de Souza, L. B., and Ong, H. L. (2017). TRPC1, Orai1, and STIM1 in SOCE: Friends in tight spaces. *Cell Calcium* 63, 33–39. doi: 10.1016/j.ceca.2016.12.009

- Ambudkar, I. S., Ong, H. L., Liu, X., Bandyopadhyay, B. C., Bandyopadhyay, B., and Cheng, K. T. (2007). TRPC1: the link between functionally distinct store-operated calcium channels. *Cell Calcium* 42, 213–223. doi: 10.1016/j.ceca.2007.01.013
- Baba, A., Yasui, T., Fujisawa, S., Yamada, R. X., Yamada, M. K., Nishiyama, N., et al. (2003). Activity-evoked capacitative  $\text{Ca}^{2+}$  entry: implications in synaptic plasticity. *J. Neurosci.* 23, 7737–7741. doi: 10.1523/JNEUROSCI.23-21-07737.2003
- Baker, K. D., Edwards, T. M., and Rickard, N. S. (2013). The role of intracellular calcium stores in synaptic plasticity and memory consolidation. *Neurosci. Biobehav. Rev.* 37, 1211–1239. doi: 10.1016/j.neubiorev.2013.04.011
- Barker, R. A., Fujimaki, M., Rogers, P., and Rubinsztein, D. C. (2020). Huntingtin-lowering strategies for Huntington's disease. *Expert Opin. Investig. Drugs* 29, 1125–1132. doi: 10.1080/13543784.2020.1804552
- Bates, G. P., Dorsey, R., Gusella, J. F., Hayden, M. R., Kay, C., Leavitt, B. R., et al. (2015). Huntington disease. *Nat. Rev. Dis. Primers* 1:15005. doi: 10.1038/nrdp.2015.5
- Beister, A., Kraus, P., Kuhn, W., Dose, M., Weindl, A., and Gerlach, M. (2004). The N-methyl-D-aspartate antagonist memantine retards progression of Huntington's disease. *J. Neural Transm. Suppl.* 117–22. doi: 10.1007/978-3-7091-0579-5\_14
- Berna-Erro, A., Braun, A., Kraft, R., Kleinschmitz, C., Schuhmann, M. K., Stegner, D., et al. (2009). STIM2 regulates capacitive  $\text{Ca}^{2+}$  entry in neurons and plays a key role in hypoxic neuronal cell death. *Sci. Signal* 2:ra67. doi: 10.1126/scisignal.2000522
- Berridge, M. J. (1998). Neuronal calcium signaling. *Neuron* 21, 13–26. doi: 10.1016/S0896-6273(00)80510-3
- Berridge, M. J. (2002). The endoplasmic reticulum: a multifunctional signaling organelle. *Cell Calcium* 32, 235–249. doi: 10.1016/S0143416002001823
- Berridge, M. J. (2009). Inositol trisphosphate and calcium signalling mechanisms. *Biochim. Biophys. Acta* 1793, 933–940. doi: 10.1016/j.bbamcr.2008.10.005
- Bezprozvanny, I. (2005). The inositol 1,4,5-trisphosphate receptors. *Cell Calcium* 38, 261–272. doi: 10.1016/j.ceca.2005.06.030
- Bezprozvanny, I., and Hiesinger, P. R. (2013). The synaptic maintenance problem: membrane recycling,  $\text{Ca}^{2+}$  homeostasis and late onset degeneration. *Mol. Neurodegener.* 8:23. doi: 10.1186/1750-1326-8-23
- Bezprozvanny, I., and Kiselev, S. L. (2017). Neurons from skin mimic brain holes. *Oncotarget* 8, 8997–8998. doi: 10.18632/oncotarget.13709
- Bohush, A., and Filipek, A. (2020). HSP90 co-chaperone, CacyBP/SIP, protects  $\alpha$ -synuclein from aggregation. *Cells* 9:2254. doi: 10.3390/cells9102254
- Brandman, O., Liou, J., Park, W. S., and Meyer, T. (2007). STIM2 is a feedback regulator that stabilizes basal cytosolic and endoplasmic reticulum  $\text{Ca}^{2+}$  levels. *Cell* 131, 1327–1339. doi: 10.1016/j.cell.2007.11.039
- Brillantes, A. B., Ondrias, K., Scott, A., Kobrinsky, E., Ondriasová, E., Moschella, M. C., et al. (1994). Stabilization of calcium release channel (ryanodine receptor) function by FK506-binding protein. *Cell* 77, 513–523. doi: 10.1016/0092-8674(94)90214-3
- Brini, M., Cali, T., Ottolini, D., and Carafoli, E. (2013a). The plasma membrane calcium pump in health and disease. *FEBS J.* 280, 5385–5397. doi: 10.1111/febs.12193
- Brini, M., Cali, T., Ottolini, D., and Carafoli, E. (2013b). Intracellular calcium homeostasis and signaling. *Met. Ions Life Sci.* 12, 119–168. doi: 10.1007/978-94-007-5561-1\_5
- Cahalan, M. D. (2009). STIMulating store-operated  $\text{Ca}^{2+}$  entry. *Nat. Cell Biol.* 11, 669–677. doi: 10.1038/ncb0609-669
- Cai, X., Zhou, Y., Nwokoko, R. M., Loktionova, N. A., Wang, X., Xin, P., et al. (2016). The orai1 store-operated calcium channel functions as a Hexamer. *J. Biol. Chem.* 291, 25764–25775. doi: 10.1074/jbc.M116.758813
- Catterall, W. A. (2011). Voltage-gated calcium channels. *Cold Spring Harb. Perspect. Biol.* 3:a003947. doi: 10.1101/cshperspect.a003947
- Caviston, J. P., and Holzbaur, E. L. (2009). Huntingtin as an essential integrator of intracellular vesicular trafficking. *Trends Cell Biol.* 19, 147–155. doi: 10.1016/j.tcb.2009.01.005
- Chen, N., Luo, T., Wellington, C., Metzler, M., McCutcheon, K., Hayden, M. R., et al. (1999). Subtype-specific enhancement of NMDA receptor currents by mutant huntingtin. *J. Neurochem.* 72, 1890–1898. doi: 10.1046/j.1471-4159.1999.0721890.x
- Chen, S., Yu, C., Rong, L., Li, C. H., Qin, X., Ryu, H., et al. (2018). Altered synaptic vesicle release and  $\text{Ca}^{2+}$  influx at single presynaptic terminals of cortical neurons in a knock-in mouse model of Huntington's disease. *Front. Mol. Neurosci.* 11:478. doi: 10.3389/fnmol.2018.00478
- Chen, X., Wu, J., Lvovskaya, S., Herndon, E., Supnet, C., and Bezprozvanny, I. (2011). Dantrolene is neuroprotective in Huntington's disease transgenic mouse model. *Mol. Neurodegener.* 6:81. doi: 10.1186/1750-1326-6-81
- Chen-Engerer, H. J., Hartmann, J., Karl, R. M., Yang, J., Feske, S., and Konnerth, A. (2019). Two types of functionally distinct  $\text{Ca}^{2+}$ . *Nat. Commun.* 10:3223. doi: 10.1038/s41467-019-11207-8
- Choo, Y. S., Johnson, G. V., MacDonald, M., Detloff, P. J., and Lesort, M. (2004). Mutant huntingtin directly increases susceptibility of mitochondria to the calcium-induced permeability transition and cytochrome c release. *Hum. Mol. Genet.* 13, 1407–1420. doi: 10.1093/hmg/ddh162
- Czeredys, M., Gruszczynska-Biegala, J., Schacht, T., Methner, A., and Kuznicki, J. (2013). Expression of genes encoding the calcium signalosome in cellular and transgenic models of Huntington's disease. *Front. Mol. Neurosci.* 6:42. doi: 10.3389/fnmol.2013.00042
- Czeredys, M., Maciag, F., Methner, A., and Kuznicki, J. (2017). Tetrahydrocarbazoles decrease elevated SOCE in medium spiny neurons from transgenic YAC128 mice, a model of Huntington's disease. *Biochem. Biophys. Res. Commun.* 483, 1194–1205. doi: 10.1016/j.bbrc.2016.08.106
- Czeredys, M., Vigont, V. A., Boeva, V. A., Mikoshiba, K., Kaznacheyeva, E. V., and Kuznicki, J. (2018). Huntingtin-associated protein 1A regulates store-operated calcium entry in medium spiny neurons from transgenic YAC128 mice, a model of Huntington's disease. *Front. Cell. Neurosci.* 12:381. doi: 10.3389/fncel.2018.00381
- de Souza, L. B., Ong, H. L., Liu, X., and Ambudkar, I. S. (2015). Fast endocytic recycling determines TRPC1-STIM1 clustering in ER-PM junctions and plasma membrane function of the channel. *Biochim. Biophys. Acta* 1853, 2709–2721. doi: 10.1016/j.bbamcr.2015.07.019
- de Yebenes, J. G., Landwehrmeyer, B., Squitieri, F., Reilmann, R., Rosser, A., Barker, R. A., et al. (2011). Pridopidine for the treatment of motor function in patients with Huntington's disease (MermaiHD): a phase 3, randomised, double-blind, placebo-controlled trial. *Lancet Neurol.* 10, 1049–1057. doi: 10.1016/S1474-4422(11)70233-2
- Deb, B. K., Pathak, T., and Hasan, G. (2016). Store-independent modulation of  $\text{Ca}^{2+}$  entry through Orai by Septin 7. *Nat. Commun.* 7:11751. doi: 10.1038/ncomms11751
- DeHaven, W. I., Smyth, J. T., Boyles, R. R., and Putney, J. W. (2007). Calcium inhibition and calcium potentiation of Orai1, Orai2, and Orai3 calcium release-activated calcium channels. *J. Biol. Chem.* 282, 17548–17556. doi: 10.1074/jbc.M611374200
- DiFiglia, M., Sapp, E., Chase, K. O., Davies, S. W., Bates, G. P., Vonsattel, J. P., et al. (1997). Aggregation of huntingtin in neuronal intranuclear inclusions and dystrophic neurites in brain. *Science* 277, 1990–1993. doi: 10.1126/science.277.5334.1990
- Dittmer, P. J., Wild, A. R., Dell'Acqua, M. L., and Sather, W. A. (2017). STIM1  $\text{Ca}^{2+}$  sensor control of L-type  $\text{Ca}^{2+}$  channel-dependent dendritic spine structural plasticity and nuclear signaling. *Cell Rep.* 19, 321–334. doi: 10.1016/j.celrep.2017.03.056
- Emptage, N. J., Reid, C. A., and Fine, A. (2001). Calcium stores in hippocampal synaptic boutons mediate short-term plasticity, store-operated  $\text{Ca}^{2+}$  entry, and spontaneous transmitter release. *Neuron* 29, 197–208. doi: 10.1016/S0896-6273(01)00190-8
- Esmailzadeh, M., Kullingsjö, J., Ullman, H., Varrone, A., and Tedroff, J. (2011). Regional cerebral glucose metabolism after pridopidine (ACR16) treatment in patients with Huntington disease. *Clin. Neuropharmacol.* 34, 95–100. doi: 10.1097/WNF.0b013e31821c31d8
- Fan, M. M., Fernandes, H. B., Zhang, L. Y., Hayden, M. R., and Raymond, L. A. (2007). Altered NMDA receptor trafficking in a yeast artificial chromosome transgenic mouse model of Huntington's disease. *J. Neurosci.* 27, 3768–3779. doi: 10.1523/JNEUROSCI.4356-06.2007
- Feske, S. (2011). Immunodeficiency due to defects in store-operated calcium entry. *Ann. N. Y. Acad. Sci.* 1238, 74–90. doi: 10.1111/j.1749-6632.2011.06240.x
- Feske, S., Giltman, J., Dolmetsch, R., Staudt, L. M., and Rao, A. (2001). Gene regulation mediated by calcium signals in T lymphocytes. *Nat. Immunol.* 2, 316–324. doi: 10.1038/86318

- Feske, S., Gwack, Y., Prakriya, M., Srikanth, S., Puppel, S. H., Tanasa, B., et al. (2006). A mutation in Orai1 causes immune deficiency by abrogating CRAC channel function. *Nature* 441, 179–185. doi: 10.1038/nature04702
- Feske, S., Prakriya, M., Rao, A., and Lewis, R. S. (2005). A severe defect in CRAC Ca<sup>2+</sup> channel activation and altered K<sup>+</sup> channel gating in T cells from immunodeficient patients. *J. Exp. Med.* 202, 651–662. doi: 10.1084/jem.20050687
- Fiedler, M. J., and Nathanson, M. H. (2011). The type I inositol 1,4,5-trisphosphate receptor interacts with protein 4.1N to mediate neurite formation through intracellular Ca waves. *Neurosignals* 19, 75–85. doi: 10.1159/000324507
- Filipek, A., Jastrzebska, B., Nowotny, M., and Kuznicki, J. (2002). CacyBP/SIP, a calyculin and Slah-1-interacting protein, binds EF-hand proteins of the S100 family. *J. Biol. Chem.* 277, 28848–28852. doi: 10.1074/jbc.M203602200
- Fowler, M. A., Sidiropoulou, K., Ozkan, E. D., Phillips, C. W., and Cooper, D. C. (2007). Corticolimbic expression of TRPC4 and TRPC5 channels in the rodent brain. *PLoS ONE* 2:e573. doi: 10.1371/journal.pone.0000573
- Fowler, M. A., Varnell, A. L., Dietrich, A., Birnbaumer, L., and Cooper, D. C. (2012). Deletion of the *trpc1* gene and the effects on locomotor and conditioned place-preference responses to cocaine. *Nat. Prec.* doi: 10.1038/npre.2012.7153
- Galán, C., Dionisio, N., Smani, T., Salido, G. M., and Rosado, J. A. (2011). The cytoskeleton plays a modulatory role in the association between STIM1 and the Ca<sup>2+</sup> channel subunits Orai1 and TRPC1. *Biochem. Pharmacol.* 82, 400–410. doi: 10.1016/j.bcp.2011.05.017
- García-Alvarez, G., Lu, B., Yap, K. A., Wong, L. C., Thevathasan, J. V., Lim, L., et al. (2015). STIM2 regulates PKA-dependent phosphorylation and trafficking of AMPARs. *Mol. Biol. Cell* 26, 1141–1159. doi: 10.1091/mbc.E14-07-1222
- Gemes, G., Bangaru, M. L., Wu, H. E., Tang, Q., Weihrauch, D., Koopmeiners, A. S., et al. (2011). Store-operated Ca<sup>2+</sup> entry in sensory neurons: functional role and the effect of painful nerve injury. *J. Neurosci.* 31, 3536–3549. doi: 10.1523/JNEUROSCI.5053-10.2011
- Giacomello, M., Oliveros, J. C., Naranjo, J. R., and Carafoli, E. (2013). Neuronal Ca(2+) dyshomeostasis in Huntington disease. *Prior* 7, 76–84. doi: 10.4161/pri.23581
- Giuriso, E., Gamberucci, A., Olivieri, C., Marruganti, S., Rossi, E., Giacomello, E., et al. (2014). The KSR2-calcineurin complex regulates STIM1-ORAI1 dynamics and store-operated calcium entry (SOCE). *Mol. Biol. Cell.* 25, 1769–1781. doi: 10.1091/mbc.e13-05-0292
- Goel, M., Sinks, W. G., and Schilling, W. P. (2002). Selective association of TRPC channel subunits in rat brain synaptosomes. *J. Biol. Chem.* 277, 48303–48310. doi: 10.1074/jbc.M207882200
- Golovina, V. A., Platoshyn, O., Bailey, C. L., Wang, J., Limsuwan, A., Sweeney, M., et al. (2001). Upregulated TRP and enhanced capacitative Ca(2+) entry in human pulmonary artery myocytes during proliferation. *Am. J. Physiol. Heart Circ. Physiol.* 280, H746–H755. doi: 10.1152/ajpheart.2001.280.2.H746
- Gopurappilly, R., Deb, B. K., Chakraborty, P., and Hasan, G. (2018). Stable STIM1 knockdown in self-renewing human neural precursors promotes premature neural differentiation. *Front Mol Neurosci.* 11:178. doi: 10.3389/fnmol.2018.00178
- Grigoriev, I., Gouveia, S. M., van der Vaart, B., Demmers, J., Smyth, J. T., Honnappa, S., et al. (2008). STIM1 is a MT-plus-end-tracking protein involved in remodeling of the ER. *Curr. Biol.* 18, 177–182. doi: 10.1016/j.cub.2007.12.050
- Gruszczynska-Biegala, J., and Kuznicki, J. (2013). Native STIM2 and ORAI1 proteins form a calcium-sensitive and thapsigargin-insensitive complex in cortical neurons. *J. Neurochem.* 126, 727–738. doi: 10.1111/jnc.12320
- Gruszczynska-Biegala, J., Pomorski, P., Wisniewska, M. B., and Kuznicki, J. (2011). Differential roles for STIM1 and STIM2 in store-operated calcium entry in rat neurons. *PLoS ONE* 6:e19285. doi: 10.1371/journal.pone.0019285
- Gruszczynska-Biegala, J., Sladowska, M., and Kuznicki, J. (2016). AMPA receptors are involved in store-operated calcium entry and interact with STIM proteins in rat primary cortical neurons. *Front. Cell. Neurosci.* 10:251. doi: 10.3389/fncel.2016.00251
- Gruszczynska-Biegala, J., Strucinska, K., Maciag, F., Majewski, L., Sladowska, M., and Kuznicki, J. (2020). STIM protein-NMDA2 receptor interaction decreases NMDA-dependent calcium levels in cortical neurons. *Cells* 9:160. doi: 10.3390/cells9010160
- Gusella, J. F., and MacDonald, M. E. (2006). Huntington's disease: seeing the pathogenic process through a genetic lens. *Trends Biochem. Sci.* 31, 533–540. doi: 10.1016/j.tibs.2006.06.009
- Hao, B., Lu, Y., Wang, Q., Guo, W., Cheung, K. H., and Yue, J. (2014). Role of STIM1 in survival and neural differentiation of mouse embryonic stem cells independent of Orai1-mediated Ca<sup>2+</sup> entry. *Stem Cell Res.* 12, 452–466. doi: 10.1016/j.scr.2013.12.005
- Hartmann, J., Karl, R. M., Alexander, R. P., Adelsberger, H., Brill, M. S., Rühlmann, C., et al. (2014). STIM1 controls neuronal Ca<sup>2+</sup> signaling, mGluR1-dependent synaptic transmission, and cerebellar motor behavior. *Neuron* 82, 635–644. doi: 10.1016/j.neuron.2014.03.027
- Hayashi, T., and Su, T. P. (2003). Sigma-1 receptors (sigma(1) binding sites) form raft-like microdomains and target lipid droplets on the endoplasmic reticulum: roles in endoplasmic reticulum lipid compartmentalization and export. *J. Pharmacol. Exp. Ther.* 306, 718–725. doi: 10.1124/jpet.103.051284
- Hayashi, T., and Su, T. P. (2007). Sigma-1 receptor chaperones at the ER-mitochondrion interface regulate Ca(2+) signaling and cell survival. *Cell* 131, 596–610. doi: 10.1016/j.cell.2007.08.036
- Hendershot, L. M. (2004). The ER function BiP is a master regulator of ER function. *Mt. Sinai J. Med.* 71, 289–297.
- Henley, J. M., and Wilkinson, K. A. (2016). Synaptic AMPA receptor composition in development, plasticity and disease. *Nat. Rev. Neurosci.* 17, 337–350. doi: 10.1038/nrn.2016.37
- Hodges, A., Strand, A. D., Aragaki, A. K., Kuhn, A., Sengstag, T., Hughes, G., et al. (2006). Regional and cellular gene expression changes in human Huntington's disease brain. *Mol. Genet.* 15, 965–977. doi: 10.1093/hmg/ddl013
- Hofmann, T., Schaefer, M., Schultz, G., and Gudermann, T. (2002). Subunit composition of mammalian transient receptor potential channels in living cells. *Proc. Natl. Acad. Sci. U.S.A.* 99, 7461–7466. doi: 10.1073/pnas.102596199
- Honarnejad, K., Daschner, A., Gehring, A. P., Szybinska, A., Giese, A., Kuznicki, J., et al. (2014). Identification of tetrahydrocarbazoles as novel multifactorial drug candidates for treatment of Alzheimer's disease. *Transl. Psychiatry* 4:e489. doi: 10.1038/tp.2014.132
- Hoth, M., and Penner, R. (1993). Calcium release-activated calcium current in rat mast cells. *J. Physiol.* 465, 359–386. doi: 10.1113/jphysiol.1993.sp019681
- Hou, X., Pedi, L., Diver, M. M., and Long, S. B. (2012). Crystal structure of the calcium release-activated calcium channel Orai. *Science* 338, 1308–1313. doi: 10.1126/science.1228757
- Huang, J. J., Wang, Y. J., Zhang, M., Zhang, P., Liang, H., Bai, H. J., et al. (2017). Functional expression of the Ca<sup>2+</sup> signaling machinery in human embryonic stem cells. *Acta Pharmacol. Sin.* 38, 1663–1672. doi: 10.1038/aps.2017.29
- Hyrskyluoto, A., Pulli, I., Törnqvist, K., Ho, T. H., Korhonen, L., and Lindholm, D. (2013). Sigma-1 receptor agonist PRE084 is protective against mutant huntingtin-induced cell degeneration: involvement of calpastatin and the NF-κB pathway. *Cell Death Dis.* 4:e646. doi: 10.1038/cddis.2013.170
- Itsuki, K., Imai, Y., Hase, H., Okamura, Y., Inoue, R., and Mori, M. X. (2014). PLC-mediated PI(4,5)P<sub>2</sub> hydrolysis regulates activation and inactivation of TRPC6/7 channels. *J. Gen. Physiol.* 143, 183–201. doi: 10.1085/jgp.201311033
- Johanning, F. W., Theis, A. K., Pannasch, U., Rückl, M., Rüdiger, S., and Schmitz, D. (2015). Ryanodine receptor activation induces long-term plasticity of spine calcium dynamics. *PLoS Biol.* 13:e1002181. doi: 10.1371/journal.pbio.1002181
- Jurewicz, E., Ostrowska, Z., Jozwiak, J., Redowicz, M. J., Lesniak, W., Moraczewska, J., et al. (2013). CacyBP/SIP as a novel modulator of the thin filament. *Biochim. Biophys. Acta* 1833, 761–766. doi: 10.1016/j.bbamcr.2012.12.010
- Kiebert, K., McGarry, A., McDermott, M., Kayson, E., Harrison, M., Marder, K., et al. (2013). A randomized, double-blind, placebo-controlled trial of pridopidine in Huntington's disease. *Mov. Disord.* 28, 1407–1415. doi: 10.1002/mds.25362
- Kiselyov, K., Wang, X., Shin, D. M., Zang, W., and Muallem, S. (2006). Calcium signaling complexes in microdomains of polarized secretory cells. *Cell Calcium* 40, 451–459. doi: 10.1016/j.ceca.2006.08.009
- Klejman, M. E., Gruszczynska-Biegala, J., Skibinska-Kijek, A., Wisniewska, M. B., Misztal, K., Blazeczyk, M., et al. (2009). Expression of STIM1 in brain and puncta-like co-localization of STIM1 and ORAI1 upon depletion of Ca(2+) store in neurons. *Neurochem. Int.* 54, 49–55. doi: 10.1016/j.neuint.2008.10.005
- Korkotian, E., Oni-Biton, E., and Segal, M. (2017). The role of the store-operated calcium entry channel Orai1 in cultured rat hippocampal synapse formation and plasticity. *J. Physiol.* 595, 125–140. doi: 10.1113/JP272645
- Kourrich, S., Su, T. P., Fujimoto, M., and Bonci, A. (2012). The sigma-1 receptor: roles in neuronal plasticity and disease. *Trends Neurosci.* 35, 762–771. doi: 10.1016/j.tins.2012.09.007

- Kovalenko, M., Milnerwood, A., Giordano, J., St. Claire, J., Guide, J. R., Stromberg, M., et al. (2018). HttQ111/+ Huntington's disease knock-in mice exhibit brain region-specific morphological changes and synaptic dysfunction. *J. Huntingtons. Dis.* 7, 17–33. doi: 10.3233/JHD-170282
- Kraft, R. (2015). STIM and ORAI proteins in the nervous system. *Channels* 9, 245–252. doi: 10.1080/19336950.2015.1071747
- Krobitsch, S., and Lindquist, S. (2000). Aggregation of huntingtin in yeast varies with the length of the polyglutamine expansion and the expression of chaperone proteins. *Proc. Natl. Acad. Sci. U.S.A.* 97, 1589–1594. doi: 10.1073/pnas.97.4.1589
- Langbehn, D. R., Brinkman, R. R., Falush, D., Paulsen, J. S., Hayden, M. R., Group, I. H., et al. (2004). A new model for prediction of the age of onset and penetrance for Huntington's disease based on CAG length. *Clin. Genet.* 65, 267–277. doi: 10.1111/j.1399-0004.2004.00241.x
- Lewis, R. S., and Cahalan, M. D. (1995). Potassium and calcium channels in lymphocytes. *Annu. Rev. Immunol.* 13, 623–653. doi: 10.1146/annurev.iy.13.040195.003203
- Lin, A. H., Sun, H., Paudel, O., Lin, M. J., and Sham, J. S. (2016). Conformation of ryanodine receptor-2 gates store-operated calcium entry in rat pulmonary arterial myocytes. *Cardiovasc. Res.* 111, 94–104. doi: 10.1093/cvr/cvw067
- Liou, J., Kim, M. L., Heo, W. D., Jones, J. T., Myers, J. W., Ferrell, J. E., et al. (2005). STIM is a Ca<sup>2+</sup> sensor essential for Ca<sup>2+</sup>-store-depletion-triggered Ca<sup>2+</sup> influx. *Curr. Biol.* 15, 1235–1241. doi: 10.1016/j.cub.2005.05.055
- Lipton, S. A. (2006). Paradigm shift in neuroprotection by NMDA receptor blockade: memantine and beyond. *Nat. Rev. Drug Discov.* 5, 160–170. doi: 10.1038/nrd1958
- Lis, A., Peinelt, C., Beck, A., Parvez, S., Monteilh-Zoller, M., Fleig, A., et al. (2007). CRACM1, CRACM2, and CRACM3 are store-operated Ca<sup>2+</sup> channels with distinct functional properties. *Curr. Biol.* 17, 794–800. doi: 10.1016/j.cub.2007.03.065
- Liu, D. Y., Thilo, F., Scholze, A., Wittstock, A., Zhao, Z. G., Harteneck, C., et al. (2007). Increased store-operated and 1-oleoyl-2-acetyl-sn-glycerol-induced calcium influx in monocytes is mediated by transient receptor potential canonical channels in human essential hypertension. *J. Hypertens.* 25, 799–808. doi: 10.1097/HJH.0b013e32803cae2b
- Liu, Q., Cheng, S., Yang, H., Zhu, L., Pan, Y., Jing, L., et al. (2020). Loss of Hap1 selectively promotes striatal degeneration in Huntington disease mice. *Proc. Natl. Acad. Sci. U.S.A.* 117, 20265–20273. doi: 10.1073/pnas.2002283117
- Liu, X., Bandyopadhyay, B. C., Singh, B. B., Groschner, K., and Ambudkar, I. S. (2005). Molecular analysis of a store-operated and 2-acetyl-sn-glycerol-sensitive non-selective cation channel. Heteromeric assembly of TRPC1-TRPC3. *J. Biol. Chem.* 280, 21600–21606. doi: 10.1074/jbc.C400492200
- Liu, X., Singh, B. B., and Ambudkar, I. S. (2003). TRPC1 is required for functional store-operated Ca<sup>2+</sup> channels. Role of acidic amino acid residues in the S5-S6 region. *J. Biol. Chem.* 278, 11337–11343. doi: 10.1074/jbc.M213271200
- Lopez, J. J., Albarran, L., Gómez, L. J., Smani, T., Salido, G. M., and Rosado, J. A. (2016). Molecular modulators of store-operated calcium entry. *Biochim. Biophys. Acta* 1863, 2037–2043. doi: 10.1016/j.bbamcr.2016.04.024
- Lopez, J. J., Jardin, I., Sanchez-Collado, J., Salido, G. M., Smani, T., and Rosado, J. A. (2020). TRPC channels in the SOCE scenario. *Cells* 9:126. doi: 10.3390/cells9010126
- Lundin, A., Dietrichs, E., Haghighi, S., Göller, M. L., Heiberg, A., Loutfi, G., et al. (2010). Efficacy and safety of the dopaminergic stabilizer Pridopidine (ACR16) in patients with Huntington's disease. *Clin. Neuropharmacol.* 33, 260–264. doi: 10.1097/WNF.0b013e3181ebb285
- Ma, B., Savas, J. N., Yu, M. S., Culver, B. P., Chao, M. V., and Tanese, N. (2011). Huntingtin mediates dendritic transport of  $\beta$ -actin mRNA in rat neurons. *Sci. Rep.* 1:140. doi: 10.1038/srep00140
- Ma, G., Wei, M., He, L., Liu, C., Wu, B., Zhang, S. L., et al. (2015). Inside-out Ca<sup>2+</sup> signalling prompted by STIM1 conformational switch. *Nat. Commun.* 6:7826. doi: 10.1038/ncomms8826
- MacDonald, M. E., Ambrose, C. M., Duyao, M. P., Myers, R. H., Lin, C., Srinidhi, L. et al. (1993). A novel gene containing a trinucleotide repeat that is expanded and unstable on Huntington's disease chromosomes. The Huntington's Disease Collaborative Research Group. *Cell* 72, 971–983. doi: 10.1016/0092-8674(93)90585-E
- Majewski, L., and Kuznicki, J. (2015). SOCE in neurons: signaling or just refilling? *Biochim. Biophys. Acta* 1853, 1940–1952. doi: 10.1016/j.bbamcr.2015.01.019
- Majewski, L., Maciag, F., Boguszewski, P. M., Wasilewska, I., Wiera, G., Wójtowicz, T., et al. (2017). Overexpression of STIM1 in neurons in mouse brain improves contextual learning and impairs long-term depression. *Biochim Biophys Acta Mol Cell Res.* 1864, 1071–1087. doi: 10.1016/j.bbamcr.2016.11.025
- Maruyama, T., Kanaji, T., Nakade, S., Kanno, T., and Mikoshiba, K. (1997). 2APB, 2-aminoethoxydiphenyl borate, a membrane-penetrable modulator of Ins(1,4,5)P<sub>3</sub>-induced Ca<sup>2+</sup> release. *J. Biochem.* 122, 498–505. doi: 10.1093/oxfordjournals.jbchem.a021780
- Maurice, T., Grégoire, C., and Espallergues, J. (2006). Neuro(steroid)s actions at the neuromodulatory signal (sigma1) receptor: biochemical and physiological evidences, consequences in neuroprotection. *Pharmacol. Biochem. Behav.* 84, 581–597. doi: 10.1016/j.pbb.2006.07.009
- McCarron, J. G., Chalmers, S., Bradley, K. N., MacMillan, D., and Muir, T. C. (2006). Ca<sup>2+</sup> microdomains in smooth muscle. *Cell Calcium* 40, 461–493. doi: 10.1016/j.ceca.2006.08.010
- Miederer, A. M., Alansary, D., Schwär, G., Lee, P. H., Jung, M., Helms, V., et al. (2015). A STIM2 splice variant negatively regulates store-operated calcium entry. *Nat. Commun.* 6:6899. doi: 10.1038/ncomms7899
- Mikoshiba, K. (2007). IP<sub>3</sub> receptor/Ca<sup>2+</sup> channel: from discovery to new signaling concepts. *J. Neurochem.* 102, 1426–1446. doi: 10.1111/j.1471-4159.2007.04825.x
- Miller, B. R., and Bezprozvanny, I. (2010). Corticostriatal circuit dysfunction in Huntington's disease: intersection of glutamate, dopamine and calcium. *Future Neurol.* 5, 735–756. doi: 10.2217/fnl.10.41
- Milnerwood, A. J., and Raymond, L. A. (2007). Corticostriatal synaptic function in mouse models of Huntington's disease: early effects of huntingtin repeat length and protein load. *J. Physiol.* 585, 817–831. doi: 10.1113/jphysiol.2007.142448
- Milnerwood, A. J., and Raymond, L. A. (2010). Early synaptic pathophysiology in neurodegeneration: insights from Huntington's disease. *Trends Neurosci.* 33, 513–523. doi: 10.1016/j.tins.2010.08.002
- Miyazaki, S., Shirakawa, H., Nakada, K., and Honda, Y. (1993). Essential role of the inositol 1,4,5-trisphosphate receptor/Ca<sup>2+</sup> release channel in Ca<sup>2+</sup> waves and Ca<sup>2+</sup> oscillations at fertilization of mammalian eggs. *Dev. Biol.* 158, 62–78. doi: 10.1006/dbio.1993.1168
- Moccia, F., Zuccolo, E., Soda, T., Tanzi, F., Guerra, G., Mapelli, L., et al. (2015). Stim and Orai proteins in neuronal Ca<sup>2+</sup> signaling and excitability. *Front. Cell. Neurosci.* 9:153. doi: 10.3389/fncel.2015.00153
- Murmu, R. P., Li, W., Holtmaat, A., and Li, J. Y. (2013). Dendritic spine instability leads to progressive neocortical spine loss in a mouse model of Huntington's disease. *J. Neurosci.* 33, 12997–13009. doi: 10.1523/JNEUROSCI.5284-12.2013
- Myers, R. H., Vonsattel, J. P., Stevens, T. J., Cupples, L. A., Richardson, E. P., Martin, J. B., et al. (1988). Clinical and neuropathologic assessment of severity in Huntington's disease. *Neurology* 38, 341–347. doi: 10.1212/WNL.38.3.341
- Nekrasov, E. D., Vigont, V. A., Klyushnikov, S. A., Lebedeva, O. S., Vassina, E. M., Bogomazova, A. N., et al. (2016). Manifestation of Huntington's disease pathology in human induced pluripotent stem cell-derived neurons. *Mol. Neurodegener.* 11:27. doi: 10.1186/s13024-016-0092-5
- Oliveira, J. M., Jekabsons, M. B., Chen, S., Lin, A., Rego, A. C., Gonçalves, J., et al. (2007). Mitochondrial dysfunction in Huntington's disease: the bioenergetics of isolated and in situ mitochondria from transgenic mice. *J. Neurochem.* 101, 241–249. doi: 10.1111/j.1471-4159.2006.04361.x
- Orth, M., Schippling, S., Schneider, S. A., Bhatia, K. P., Talelli, P., Tabrizi, S. J., et al. (2010). Abnormal motor cortex plasticity in premanifest and very early manifest Huntington disease. *J. Neurol. Neurosurg. Psychiatr.* 81, 267–270. doi: 10.1136/jnnp.2009.171926
- Panov, A. V., Gutekunst, C. A., Leavitt, B. R., Hayden, M. R., Burke, J. R., Strittmatter, W. J., et al. (2002). Early mitochondrial calcium defects in Huntington's disease are a direct effect of polyglutamines. *Nat. Neurosci.* 5, 731–736. doi: 10.1038/nn884
- Paoletti, P., Bellone, C., and Zhou, Q. (2013). NMDA receptor subunit diversity: impact on receptor properties, synaptic plasticity and disease. *Nat. Rev. Neurosci.* 14, 383–400. doi: 10.1038/nrn3504
- Parekh, A. B., and Penner, R. (1997). Store depletion and calcium influx. *Physiol. Rev.* 77, 901–930. doi: 10.1152/physrev.1997.77.4.901

- Parekh, A. B., and Putney, J. W. (2005). Store-operated calcium channels. *Physiol. Rev.* 85, 757–810. doi: 10.1152/physrev.00057.2003
- Park, C. Y., Shcheglovitov, A., and Dolmetsch, R. (2010). The CRAC channel activator STIM1 binds and inhibits L-type voltage-gated calcium channels. *Science* 330, 101–105. doi: 10.1126/science.1191027
- Parvez, S., Beck, A., Peinelt, C., Soboloff, J., Lis, A., Monteilh-Zoller, M., et al. (2008). STIM2 protein mediates distinct store-dependent and store-independent modes of CRAC channel activation. *FASEB J.* 22, 752–761. doi: 10.1096/fj.07-9449com
- Pchitskaya, E., Popugaeva, E., and Bezprozvanny, I. (2018). Calcium signaling and molecular mechanisms underlying neurodegenerative diseases. *Cell Calcium* 70, 87–94. doi: 10.1016/j.ceca.2017.06.008
- Peinelt, C., Vig, M., Koomoa, D. L., Beck, A., Nadler, M. J., Koblan-Huberson, M., et al. (2006). Amplification of CRAC current by STIM1 and CRACM1 (Orai1). *Nat. Cell Biol.* 8, 771–773. doi: 10.1038/ncb1435
- Periasamy, M., and Kalyanasundaram, A. (2007). SERCA pump isoforms: their role in calcium transport and disease. *Muscle Nerve* 35, 430–442. doi: 10.1002/mus.20745
- Potier, M., and Trebak, M. (2008). New developments in the signaling mechanisms of the store-operated calcium entry pathway. *Pflügers Arch.* 457, 405–415. doi: 10.1007/s00424-008-0533-2
- Prakriya, M., Feske, S., Gwack, Y., Srikanth, S., Rao, A., and Hogan, P. G. (2006). Orai1 is an essential pore subunit of the CRAC channel. *Nature* 443, 230–233. doi: 10.1038/nature05122
- Prakriya, M., and Lewis, R. S. (2015). Store-operated calcium channels. *Physiol. Rev.* 95, 1383–1436. doi: 10.1152/physrev.00020.2014
- Putney, J. W. (1986). A model for receptor-regulated calcium entry. *Cell Calcium* 7, 1–12. doi: 10.1016/0143-4160(86)90026-6
- Putney, J. W., Steinckwich-Besançon, N., Numaga-Tomita, T., Davis, F. M., Desai, P. N., D'Agostin, D. M., et al. (2017). The functions of store-operated calcium channels. *Biochim. Biophys. Acta Mol. Cell Res.* 1864, 900–906. doi: 10.1016/j.bbamer.2016.11.028
- Putney, J. W., and Tomita, T. (2012). Phospholipase C signaling and calcium influx. *Adv. Biol. Regul.* 52, 152–164. doi: 10.1016/j.advenzreg.2011.09.005
- Quigley, J. (2017). Juvenile Huntington's disease: diagnostic and treatment considerations for the psychiatrist. *Curr. Psychiatry Rep.* 19:9. doi: 10.1007/s11920-017-0759-9
- Raymond, L. A. (2017). Striatal synaptic dysfunction and altered calcium regulation in Huntington disease. *Biochem. Biophys. Res. Commun.* 483, 1051–1062. doi: 10.1016/j.bbrc.2016.07.058
- Rinaldi, C., and Wood, M. J. A. (2018). Antisense oligonucleotides: the next frontier for treatment of neurological disorders. *Nat. Rev. Neurol.* 14, 9–21. doi: 10.1038/nrnneurol.2017.148
- Roos, J., DiGregorio, P. J., Yeromin, A. V., Ohlsen, K., Lioudyno, M., Zhang, S., et al. (2005). STIM1, an essential and conserved component of store-operated Ca<sup>2+</sup> channel function. *J. Cell Biol.* 169, 435–445. doi: 10.1083/jcb.200502019
- Ross, C. A. (2002). Polyglutamine pathogenesis: emergence of unifying mechanisms for Huntington's disease and related disorders. *Neuron* 35, 819–822. doi: 10.1016/S0896-6273(02)00872-3
- Rossi, D., and Sorrentino, V. (2002). Molecular genetics of ryanodine receptors Ca<sup>2+</sup>-release channels. *Cell Calcium* 32, 307–319. doi: 10.1016/S0143416002001987
- Ryskamp, D., Wu, J., Geva, M., Kusko, R., Grossman, I., Hayden, M., et al. (2017). The sigma-1 receptor mediates the beneficial effects of pridopidine in a mouse model of Huntington disease. *Neurobiol. Dis.* 97, 46–59. doi: 10.1016/j.nbd.2016.10.006
- Ryskamp, D., Wu, L., Wu, J., Kim, D., Rammes, G., Geva, M., et al. (2019). Pridopidine stabilizes mushroom spines in mouse models of Alzheimer's disease by acting on the sigma-1 receptor. *Neurobiol. Dis.* 124, 489–504. doi: 10.1016/j.nbd.2018.12.022
- Ryskamp, D. A., Korban, S., Zhemkov, V., Kraskovskaya, N., and Bezprozvanny, I. (2019). Neuronal Sigma-1 receptors: signaling functions and protective roles in neurodegenerative diseases. *Front. Neurosci.* 13:862. doi: 10.3389/fnins.2019.00862
- Samtleben, S., Wachter, B., and Blum, R. (2015). Store-operated calcium entry compensates fast ER calcium loss in resting hippocampal neurons. *Cell Calcium* 58, 147–159. doi: 10.1016/j.ceca.2015.04.002
- Santulli, G., and Marks, A. R. (2015). Essential roles of intracellular calcium release channels in muscle, brain, metabolism, and aging. *Curr. Mol. Pharmacol.* 8, 206–222. doi: 10.2174/1874467208666150507105105
- Secondo, A., Bagetta, G., and Amantea, D. (2018). On the role of store-operated calcium entry in acute and chronic neurodegenerative diseases. *Front. Mol. Neurosci.* 11:87. doi: 10.3389/fnmol.2018.00087
- Serwach, K., and Gruszczynska-Biegala, J. (2019). STIM proteins and glutamate receptors in neurons: role in neuronal physiology and neurodegenerative diseases. *Int. J. Mol. Sci.* 20:2289. doi: 10.3390/ijms20092289
- Sharma, S., Quintana, A., Findlay, G. M., Mettlen, M., Baust, B., Jain, M., et al. (2013). An siRNA screen for NFAT activation identifies septins as coordinators of store-operated Ca<sup>2+</sup> entry. *Nature* 499, 238–242. doi: 10.1038/nature12229
- Shim, A. H., Tirado-Lee, L., and Prakriya, M. (2015). Structural and functional mechanisms of CRAC channel regulation. *J. Mol. Biol.* 427, 77–93. doi: 10.1016/j.jmb.2014.09.021
- Silva, F. R., Miranda, A. S., Santos, R. P. M., Olmo, I. G., Zamponi, G. W., Dobransky, T., et al. (2017). N-type Ca<sup>2+</sup> channels are affected by full-length mutant huntingtin expression in a mouse model of Huntington's disease. *Neurobiol. Aging* 55, 1–10. doi: 10.1016/j.neurobiolaging.2017.03.015
- Skibinska-Kijek, A., Wisniewska, M. B., Gruszczynska-Biegala, J., Methner, A., and Kuznicki, J. (2009). Immunolocalization of STIM1 in the mouse brain. *Acta Neurobiol. Exp.* 69, 413–428.
- Skotte, N. H., Southwell, A. L., Østergaard, M. E., Carroll, J. B., Warby, S. C., Doty, C. N., et al. (2014). Allele-specific suppression of mutant huntingtin using antisense oligonucleotides: providing a therapeutic option for all Huntington disease patients. *PLoS ONE* 9:e107434. doi: 10.1371/journal.pone.0107434
- Smith-Dijak, A. I., Nassrallah, W. B., Zhang, L. Y. J., Geva, M., Hayden, M. R., and Raymond, L. A. (2019). Impairment and restoration of homeostatic plasticity in cultured cortical neurons from a mouse model of Huntington disease. *Front. Cell. Neurosci.* 13, 209. doi: 10.3389/fncel.2019.00209
- Smyth, J. T., DeHaven, W. I., Bird, G. S., and Putney, J. W. (2007). Role of the microtubule cytoskeleton in the function of the store-operated Ca<sup>2+</sup> channel activator STIM1. *J. Cell Sci.* 120, 3762–3771. doi: 10.1242/jcs.015735
- Somasundaram, A., Shum, A. K., McBride, H. J., Kessler, J. A., Feske, S., Miller, R. J., et al. (2014). Store-operated CRAC channels regulate gene expression and proliferation in neural progenitor cells. *J. Neurosci.* 34, 9107–9123. doi: 10.1523/JNEUROSCI.0263-14.2014
- Squitieri, F., Di Pardo, A., Favellato, M., Amico, E., Maglione, V., and Frati, L. (2015). Pridopidine, a dopamine stabilizer, improves motor performance and shows neuroprotective effects in Huntington disease R6/2 mouse model. *J. Cell. Mol. Med.* 19, 2540–2548. doi: 10.1111/jcmm.12604
- Stathopoulos, P. B., Zheng, L., and Ikura, M. (2009). Stromal interaction molecule (STIM) 1 and STIM2 calcium sensing regions exhibit distinct unfolding and oligomerization kinetics. *J. Biol. Chem.* 284, 728–732. doi: 10.1074/jbc.C800178200
- Streb, H., Irvine, R. F., Berridge, M. J., and Schulz, I. (1983). Release of Ca<sup>2+</sup> from a nonmitochondrial intracellular store in pancreatic acinar cells by inositol-1,4,5-trisphosphate. *Nature* 306, 67–69. doi: 10.1038/306067a0
- Strübing, C., Krapivinsky, G., Krapivinsky, L., and Clapham, D. E. (2003). Formation of novel TRPC channels by complex subunit interactions in embryonic brain. *J. Biol. Chem.* 278, 39014–39019. doi: 10.1074/jbc.M306705200
- Su, T. P., Hayashi, T., Maurice, T., Buch, S., and Ruoho, A. E. (2010). The sigma-1 receptor chaperone as an inter-organelle signaling modulator. *Trends Pharmacol. Sci.* 31, 557–566. doi: 10.1016/j.tips.2010.08.007
- Subedi, K. P., Ong, H. L., Son, G. Y., Liu, X., and Ambudkar, I. S. (2018). STIM2 induces activated conformation of STIM1 to control orail function in ER-PM junctions. *Cell Rep.* 23, 522–534. doi: 10.1016/j.celrep.2018.03.065
- Sun, S., Zhang, H., Liu, J., Popugaeva, E., Xu, N. J., Feske, S., et al. (2014). Reduced synaptic STIM2 expression and impaired store-operated calcium entry cause destabilization of mature spines in mutant presenilin mice. *Neuron* 82, 79–93. doi: 10.1016/j.neuron.2014.02.019
- Sun, Y., Savanenin, A., Reddy, P. H., and Liu, Y. F. (2001). Polyglutamine-expanded huntingtin promotes sensitization of N-methyl-D-aspartate receptors via post-synaptic density 95. *J. Biol. Chem.* 276, 24713–24718. doi: 10.1074/jbc.M103501200
- Sundivakkam, P. C., Freichel, M., Singh, V., Yuan, J. P., Vogel, S. M., Flockerzi, V., et al. (2012). The Ca(2+) sensor stromal interaction molecule 1 (STIM1)

- is necessary and sufficient for the store-operated  $\text{Ca}^{2+}$  entry function of transient receptor potential canonical (TRPC) 1 and 4 channels in endothelial cells. *Mol. Pharmacol.* 81, 510–526. doi: 10.1124/mol.111.074658
- Supnet, C., and Bezprozvanny, I. (2011). Presenilins function in ER calcium leak and Alzheimer's disease pathogenesis. *Cell Calcium* 50, 303–309. doi: 10.1016/j.ceca.2011.05.013
- Suzuki, M., Nagai, Y., Wada, K., and Koike, T. (2012). Calcium leak through ryanodine receptor is involved in neuronal death induced by mutant huntingtin. *Biochem. Biophys. Res. Commun.* 429, 18–23. doi: 10.1016/j.bbrc.2012.10.107
- Switońska, K., Szlachcic, W. J., Handschuh, L., Wojciechowski, P., Marczak, Ł., Stelmaszczyk, M., et al. (2018). Identification of altered developmental pathways in human juvenile HD iPSC with 71Q and 109Q using transcriptome profiling. *Front. Cell. Neurosci.* 12:528. doi: 10.3389/fncel.2018.00528
- Takebayashi, M., Hayashi, T., and Su, T. P. (2004). A perspective on the new mechanism of antidepressants: neuritogenesis through sigma-1 receptors. *Pharmacopsychiatry* 37 (Suppl. 3), S208–S213. doi: 10.1055/s-2004-832679
- Tang, T. S., Guo, C., Wang, H., Chen, X., and Bezprozvanny, I. (2009). Neuroprotective effects of inositol 1,4,5-trisphosphate receptor C-terminal fragment in a Huntington's disease mouse model. *J. Neurosci.* 29, 1257–1266. doi: 10.1523/JNEUROSCI.4411-08.2009
- Tang, T. S., Slow, E., Lupu, V., Stavrovskaya, I. G., Sugimori, M., Llinás, R., et al. (2005). Disturbed  $\text{Ca}^{2+}$  signaling and apoptosis of medium spiny neurons in Huntington's disease. *Proc. Natl. Acad. Sci. U.S.A.* 102, 2602–2607. doi: 10.1073/pnas.0409402102
- Tang, T. S., Tu, H., Chan, E. Y., Maximov, A., Wang, Z., Wellington, C. L., et al. (2003). Huntingtin and huntingtin-associated protein 1 influence neuronal calcium signaling mediated by inositol-(1,4,5) triphosphate receptor type 1. *Neuron* 39, 227–239. doi: 10.1016/S0896-6273(03)00366-0
- Tang, T. S., Tu, H., Orban, P. C., Chan, E. Y., Hayden, M. R., and Bezprozvanny, I. (2004). HAP1 facilitates effects of mutant huntingtin on inositol 1,4,5-trisphosphate-induced Ca release in primary culture of striatal medium spiny neurons. *Eur. J. Neurosci.* 20, 1779–1787. doi: 10.1111/j.1460-9568.2004.03633.x
- Targos, B., Barańska, J., and Pomorski, P. (2005). Store-operated calcium entry in physiology and pathology of mammalian cells. *Acta Biochim. Pol.* 52, 397–409. doi: 10.18388/abp.2005\_3452
- Thakur, P., Dadsetan, S., and Fomina, A. F. (2012). Bidirectional coupling between ryanodine receptors and  $\text{Ca}^{2+}$  release-activated  $\text{Ca}^{2+}$  (CRAC) channel machinery sustains store-operated  $\text{Ca}^{2+}$  entry in human T lymphocytes. *J. Biol. Chem.* 287, 37233–37244. doi: 10.1074/jbc.M112.398974
- Trebak, M., Lemonnier, L., DeHaven, W. I., Wedel, B. J., Bird, G. S., and Putney, J. W. (2009). Complex functions of phosphatidylinositol 4,5-bisphosphate in regulation of TRPC5 cation channels. *Pflugers Arch.* 457, 757–769. doi: 10.1007/s00424-008-0550-1
- Trepakova, E. S., Gericke, M., Hirakawa, Y., Weisbrod, R. M., Cohen, R. A., and Bolotina, V. M. (2001). Properties of a native cation channel activated by  $\text{Ca}^{2+}$  store depletion in vascular smooth muscle cells. *J. Biol. Chem.* 276, 7782–7790. doi: 10.1074/jbc.M010104200
- Tsai, S. Y., Hayashi, T., Harvey, B. K., Wang, Y., Wu, W. W., Shen, R. F., et al. (2009). Sigma-1 receptors regulate hippocampal dendritic spine formation via a free radical-sensitive mechanism involving Rac1xGTP pathway. *Proc. Natl. Acad. Sci. U.S.A.* 106, 22468–22473. doi: 10.1073/pnas.0909089106
- Tshuva, R. Y., Korkotian, E., and Segal, M. (2017). ORAI1-dependent synaptic plasticity in rat hippocampal neurons. *Neurobiol. Learn. Mem.* 140, 1–10. doi: 10.1016/j.nlm.2016.12.024
- Tu, H., Nelson, O., Bezprozvanny, A., Wang, Z., Lee, S. F., Hao, Y. H., et al. (2006). Presenilins form ER  $\text{Ca}^{2+}$  leak channels, a function disrupted by familial Alzheimer's disease-linked mutations. *Cell* 126, 981–993. doi: 10.1016/j.cell.2006.06.059
- Uchiyama, T., Yoshikawa, F., Hishida, A., Furuichi, T., and Mikoshiba, K. (2002). A novel recombinant hyperaffinity inositol 1,4,5-trisphosphate (IP(3)) absorbent traps IP(3), resulting in specific inhibition of IP(3)-mediated calcium signaling. *J. Biol. Chem.* 277, 8106–8113. doi: 10.1074/jbc.M108337200
- Vaca, L. (2010). SOCIC: the store-operated calcium influx complex. *Cell Calcium* 47, 199–209. doi: 10.1016/j.ceca.2010.01.002
- Vaeth, M., Yang, J., Yamashita, M., Zee, I., Eckstein, M., Knosp, C., et al. (2017). ORAI2 modulates store-operated calcium entry and T cell-mediated immunity. *Nat. Commun.* 8:14714. doi: 10.1038/ncomms14714
- Vajente, N., Norante, R., Redolfi, N., Daga, A., Pizzo, P., and Pendin, D. (2019). Microtubules stabilization by mutant spastin affects ER morphology and Ca. *Front. Physiol.* 10:1544. doi: 10.3389/fphys.2019.01544
- van Coppenolle, F., vanden Abeele, F., Slomianny, C., Flourakis, M., Hesketh, J., Dewailly, E., et al. (2004). Ribosome-translocon complex mediates calcium leakage from endoplasmic reticulum stores. *J. Cell Sci.* 117, 4135–4142. doi: 10.1242/jcs.01274
- van Roon-Mom, W. M. C., Roos, R. A. C., and de Bot, S. T. (2018). Dose-dependent lowering of mutant huntingtin using antisense oligonucleotides in huntington disease patients. *Nucleic Acid Ther.* 28, 59–62. doi: 10.1089/nat.2018.0720
- Vashisht, A., Tanwar, J., and Motiani, R. K. (2018). Regulation of proto-oncogene Orai3 by miR18a/b and miR34a. *Cell Calcium* 75, 101–111. doi: 10.1016/j.ceca.2018.08.006
- Venkatachalam, K., and Montell, C. (2007). TRP channels. *Annu. Rev. Biochem.* 76, 387–417. doi: 10.1146/annurev.biochem.75.103004.142819
- Verkhatsky, A. (2005). Physiology and pathophysiology of the calcium store in the endoplasmic reticulum of neurons. *Physiol. Rev.* 85, 201–279. doi: 10.1152/physrev.00004.2004
- Vig, M., Peinelt, C., Beck, A., Koormo, D. L., Rabah, D., Koblan-Huberson, M., et al. (2006). CRACM1 is a plasma membrane protein essential for store-operated  $\text{Ca}^{2+}$  entry. *Science* 312, 1220–1223. doi: 10.1126/science.1127883
- Vigont, V., Kolobkova, Y., Skopin, A., Zimina, O., Zenin, V., Glushankova, L., et al. (2015). Both orai1 and TRPC1 are involved in excessive store-operated calcium entry in striatal neurons expressing mutant huntingtin exon 1. *Front. Physiol.* 6:337. doi: 10.3389/fphys.2015.00337
- Vigont, V., Nekrasov, E., Shalygin, A., Gusev, K., Klushnikov, S., Illarionov, S., et al. (2018). Patient-specific iPSC-based models of Huntington's disease as a tool to study store-operated calcium entry drug targeting. *Front. Pharmacol.* 9:696. doi: 10.3389/fphar.2018.00696
- Vigont, V. A., Zimina, O. A., Glushankova, L. N., Kolobkova, J. A., Ryazantseva, M. A., Mozhayeva, G. N., et al. (2014). STIM1 protein activates store-operated calcium channels in cellular model of Huntington's disease. *Acta Nat.* 6, 40–47. doi: 10.32607/20758251-2014-6-4-40-47
- Vonsattel, J. P., and DiFiglia, M. (1998). Huntington disease. *J. Neuropathol. Exp. Neurol.* 57, 369–384. doi: 10.1097/00005072-199805000-00001
- Wang, T., Wang, J., Mao, L., Tang, B., Vanderklisch, P. W., Liao, X., et al. (2019). HAP1 is an *in vivo* UBE3A target that augments autophagy in a mouse model of Angelman syndrome. *Neurobiol. Dis.* 132, 104585. doi: 10.1016/j.nbd.2019.104585
- Wang, Y., Deng, X., Mancarella, S., Hendron, E., Eguchi, S., Soboloff, J., et al. (2010). The calcium store sensor, STIM1, reciprocally controls Orai and  $\text{CaV}1.2$  channels. *Science* 330, 105–109. doi: 10.1126/science.1191086
- Wasik, U., Schneider, G., Mietelska-Porowska, A., Mazurkiewicz, M., Fabczak, H., Weis, S., et al. (2013). Calcyclin binding protein and Siah-1 interacting protein in Alzheimer's disease pathology: neuronal localization and possible function. *Neurobiol. Aging* 34, 1380–1388. doi: 10.1016/j.neurobiolaging.2012.11.007
- Wegierski, T., and Kuznicki, J. (2018). Neuronal calcium signaling via store-operated channels in health and disease. *Cell Calcium* 74, 102–111. doi: 10.1016/j.ceca.2018.07.001
- Wiatr, K., Szlachcic, W. J., Trzeciak, M., Figlerowicz, M., and Figiel, M. (2018). Huntington disease as a neurodevelopmental disorder and early signs of the disease in stem cells. *Mol. Neurobiol.* 55, 3351–3371. doi: 10.1007/s12035-017-0477-7
- Wu, J., Ryskamp, D., Birnbaumer, L., and Bezprozvanny, I. (2018). Inhibition of TRPC1-dependent store-operated calcium entry improves synaptic stability and motor performance in a mouse model of Huntington's disease. *J. Huntingtons. Dis.* 7, 35–50. doi: 10.3233/JHD-170266
- Wu, J., Ryskamp, D. A., Liang, X., Egorova, P., Zakharova, O., Hung, G., et al. (2016). Enhanced store-operated calcium entry leads to striatal synaptic loss in a Huntington's disease mouse model. *J. Neurosci.* 36, 125–141. doi: 10.1523/JNEUROSCI.1038-15.2016
- Wu, J., Shih, H. P., Vigont, V., Hrdlicka, L., Diggins, L., Singh, C., et al. (2011). Neuronal store-operated calcium entry pathway as a novel therapeutic target for Huntington's disease treatment. *Chem. Biol.* 18, 777–793. doi: 10.1016/j.chembiol.2011.04.012

- Wu, J., Tang, T., and Bezprozvanny, I. (2006). Evaluation of clinically relevant glutamate pathway inhibitors in *in vitro* model of Huntington's disease. *Neurosci. Lett.* 407, 219–223. doi: 10.1016/j.neulet.2006.08.036
- Wu, L. L., and Zhou, X. F. (2009). Huntingtin associated protein 1 and its functions. *Cell Adh. Migr.* 3, 71–76. doi: 10.4161/cam.3.1.7511
- Wu, X., Zagranichnaya, T. K., Gurda, G. T., Eves, E. M., and Villereal, M. L. (2004). A TRPC1/TRPC3-mediated increase in store-operated calcium entry is required for differentiation of H19-7 hippocampal neuronal cells. *J. Biol. Chem.* 279, 43392–43402. doi: 10.1074/jbc.M408959200
- Wu, Z., and Bowen, W. D. (2008). Role of sigma-1 receptor C-terminal segment in inositol 1,4,5-trisphosphate receptor activation: constitutive enhancement of calcium signaling in MCF-7 tumor cells. *J. Biol. Chem.* 283, 28198–28215. doi: 10.1074/jbc.M802099200
- Xiang, J., Yang, S., Xin, N., Gaertig, M. A., Reeves, R. H., Li, S., et al. (2017). DYRK1A regulates Hap1-Dcaf7/WDR68 binding with implication for delayed growth in Down syndrome. *Proc. Natl. Acad. Sci. U.S.A.* 114, E1224–E1233. doi: 10.1073/pnas.1614893114
- Yap, K. A., Shetty, M. S., Garcia-Alvarez, G., Lu, B., Alagappan, D., Oh-Hora, M., et al. (2017). STIM2 regulates AMPA receptor trafficking and plasticity at hippocampal synapses. *Neurobiol. Learn. Mem.* 138, 54–61. doi: 10.1016/j.nlm.2016.08.007
- Yen, M., Lokteva, L. A., and Lewis, R. S. (2016). Functional analysis of orail concatemers supports a hexameric stoichiometry for the CRAC channel. *Biophys. J.* 111, 1897–1907. doi: 10.1016/j.bpj.2016.09.020
- Zagranichnaya, T. K., Wu, X., and Villereal, M. L. (2005). Endogenous TRPC1, TRPC3, and TRPC7 proteins combine to form native store-operated channels in HEK-293 cells. *J. Biol. Chem.* 280, 29559–29569. doi: 10.1074/jbc.M505842200
- Zeng, B., Chen, G. L., Daskoulidou, N., and Xu, S. Z. (2014). The ryanodine receptor agonist 4-chloro-3-ethylphenol blocks ORAI store-operated channels. *Br. J. Pharmacol.* 171, 1250–1259. doi: 10.1111/bph.12528
- Zeron, M. M., Fernandes, H. B., Krebs, C., Shehadeh, J., Wellington, C. L., Leavitt, B. R., et al. (2004). Potentiation of NMDA receptor-mediated excitotoxicity linked with intrinsic apoptotic pathway in YAC transgenic mouse model of Huntington's disease. *Mol. Cell. Neurosci.* 25, 469–479. doi: 10.1016/j.mcn.2003.11.014
- Zeron, M. M., Hansson, O., Chen, N., Wellington, C. L., Leavitt, B. R., Brundin, P., et al. (2002). Increased sensitivity to N-methyl-D-aspartate receptor-mediated excitotoxicity in a mouse model of Huntington's disease. *Neuron* 33, 849–860. doi: 10.1016/S0896-6273(02)00615-3
- Zhang, H., Li, Q., Graham, R. K., Slow, E., Hayden, M. R., and Bezprozvanny, I. (2008). Full length mutant huntingtin is required for altered Ca<sup>2+</sup> signaling and apoptosis of striatal neurons in the YAC mouse model of Huntington's disease. *Neurobiol. Dis.* 31, 80–88. doi: 10.1016/j.nbd.2008.03.010
- Zhang, H., Zhang, C., Vincent, J., Zala, D., Benstaali, C., Sainlos, M., et al. (2018). Modulation of AMPA receptor surface diffusion restores hippocampal plasticity and memory in Huntington's disease models. *Nat. Commun.* 9:4272. doi: 10.1038/s41467-018-06675-3
- Zhang, S. L., Yu, Y., Roos, J., Kozak, J. A., Deerinck, T. J., Ellisman, M. H., et al. (2005). STIM1 is a Ca<sup>2+</sup> sensor that activates CRAC channels and migrates from the Ca<sup>2+</sup> store to the plasma membrane. *Nature* 437, 902–905. doi: 10.1038/nature04147
- Zoghbi, H. Y., and Orr, H. T. (2000). Glutamine repeats and neurodegeneration. *Annu. Rev. Neurosci.* 23, 217–247. doi: 10.1146/annurev.neuro.23.1.217
- Zucchi, R., and Ronca-Testoni, S. (1997). The sarcoplasmic reticulum Ca<sup>2+</sup>-channel/ryanodine receptor: modulation by endogenous effectors, drugs and disease states. *Pharmacol. Rev.* 49, 1–51.

**Conflict of Interest:** The author declares that the research was conducted in the absence of any commercial or financial relationships that could be construed as a potential conflict of interest.

Copyright © 2020 Czeredys. This is an open-access article distributed under the terms of the Creative Commons Attribution License (CC BY). The use, distribution or reproduction in other forums is permitted, provided the original author(s) and the copyright owner(s) are credited and that the original publication in this journal is cited, in accordance with accepted academic practice. No use, distribution or reproduction is permitted which does not comply with these terms.



OPEN ACCESS

**Edited by:**

Joanna Gruszczynska-Biegala,  
Polish Academy of Sciences, Poland

**Reviewed by:**

Bronwen Connor,  
The University of Auckland,  
New Zealand  
Carina Weissmann,  
CONICET Institute of Physiology,  
Molecular Biology and Neurosciences  
(IFIBYNE), Argentina

**\*Correspondence:**

Elena V. Kaznacheyeva  
evkzn@incras.ru  
Maria A. Lagarkova  
lagar@rcpcm.org

<sup>†</sup>These authors have contributed  
equally to this work

**Specialty section:**

This article was submitted to  
Signaling,  
a section of the journal  
Frontiers in Cell and Developmental  
Biology

**Received:** 02 November 2020

**Accepted:** 11 January 2021

**Published:** 02 February 2021

**Citation:**

Vigont VA, Grekhnev DA,  
Lebedeva OS, Gusev KO,  
Volovikov EA, Skopin AY,  
Bogomazova AN, Shuvalova LD,  
Zubkova OA, Khomyakova EA,  
Glushankova LN, Klyushnikov SA,  
Illarioshkin SN, Lagarkova MA and  
Kaznacheyeva EV (2021) STIM2  
Mediates Excessive Store-Operated  
Calcium Entry in Patient-Specific  
iPSC-Derived Neurons Modeling a  
Juvenile Form of Huntington's  
Disease.  
Front. Cell Dev. Biol. 9:625231.  
doi: 10.3389/fcell.2021.625231

# STIM2 Mediates Excessive Store-Operated Calcium Entry in Patient-Specific iPSC-Derived Neurons Modeling a Juvenile Form of Huntington's Disease

Vladimir A. Vigont<sup>1†</sup>, Dmitriy A. Grekhnev<sup>1†</sup>, Olga S. Lebedeva<sup>2,3†</sup>, Konstantin O. Gusev<sup>1</sup>, Egor A. Volovikov<sup>2</sup>, Anton Yu. Skopin<sup>1</sup>, Alexandra N. Bogomazova<sup>2,3</sup>, Lilia D. Shuvalova<sup>2</sup>, Olga A. Zubkova<sup>2</sup>, Ekaterina A. Khomyakova<sup>2</sup>, Lyubov N. Glushankova<sup>1</sup>, Sergey A. Klyushnikov<sup>4</sup>, Sergey N. Illarioshkin<sup>4</sup>, Maria A. Lagarkova<sup>2,3\*</sup> and Elena V. Kaznacheyeva<sup>1\*</sup>

<sup>1</sup> Laboratory of Ionic Channels of Cell Membranes, Department of Molecular Physiology of the Cell, Institute of Cytology, Russian Academy of Sciences, St. Petersburg, Russia, <sup>2</sup> Laboratory of Cell Biology, Department of Cell Biology, Federal Research and Clinical Center of Physical-Chemical Medicine, Federal Medical Biological Agency, Moscow, Russia, <sup>3</sup> Center for Precision Genome Editing and Genetic Technologies for Biomedicine, Federal Research and Clinical Center of Physical-Chemical Medicine, Federal Medical Biological Agency, Moscow, Russia, <sup>4</sup> Research Center of Neurology, Moscow, Russia

Huntington's disease (HD) is a severe autosomal-dominant neurodegenerative disorder caused by a mutation within a gene, encoding huntingtin protein. Here we have used the induced pluripotent stem cell technology to produce patient-specific terminally differentiated GABA-ergic medium spiny neurons modeling a juvenile form of HD (HD76). We have shown that calcium signaling is dramatically disturbed in HD76 neurons, specifically demonstrating higher levels of store-operated and voltage-gated calcium uptakes. However, comparing the HD76 neurons with the previously described low-repeat HD models, we have demonstrated that the severity of calcium signaling alterations does not depend on the length of the polyglutamine tract of the mutant huntingtin. Here we have also observed greater expression of huntingtin and an activator of store-operated calcium channels STIM2 in HD76 neurons. Since shRNA-mediated suppression of STIM2 decreased store-operated calcium uptake, we have speculated that high expression of STIM2 underlies the excessive entry through store-operated calcium channels in HD pathology. Moreover, a previously described potential anti-HD drug EVP4593 has been found to attenuate high levels of both huntingtin and STIM2 that may contribute to its neuroprotective effect. Our results are fully supportive in favor of the crucial role of calcium signaling deregulation in the HD pathogenesis and indicate that the cornerstone of excessive calcium uptake in HD-specific neurons is a calcium sensor and store-operated calcium channels activator STIM2, which should become a molecular target for medical treatment and novel neuroprotective drug development.

**Keywords:** calcium, store-operated calcium channels, Huntington's disease, induced pluripotent stem cells, neurodegeneration, EVP4593, STIM2

## INTRODUCTION

Since neurodegenerative disorders are one of the most acute and socially significant problems facing modern medicine, adequate models for these diseases are highly demanded. New perspectives in the modeling of hereditary neurodegenerative pathologies have arisen through patient-specific induced pluripotent stem cells (iPSCs) (Ishida et al., 2016; Mungenast et al., 2016; Nekrasov et al., 2016; Naphade et al., 2019).

Huntington's disease (HD) is a severe neurodegenerative pathology characterized by motor dysfunction, cognitive decline and the presence of mental disorders. At the molecular level, HD occurs due to an increase in the number of CAG repeats in the first exon of the gene encoding the huntingtin protein. The most vulnerable cells in HD are the striatal medium spiny neurons (Vonsattel and DiFiglia, 1998).

The involvement of disturbed intracellular calcium signaling in the pathogenesis of HD and other neurodegenerative diseases is widely discussed (Bezprozvanny, 2009; Wu et al., 2011; Egorova et al., 2015; Huang et al., 2016; Nekrasov et al., 2016; Czeredys et al., 2018; Hisatsune et al., 2018). Numerous potential drugs have demonstrated a pronounced specific effect on the pathological functioning of calcium signaling (Chen et al., 2011; Wu et al., 2011, 2016; Weber et al., 2019). The mutant huntingtin deregulates calcium signaling by many ways including interactions with mitochondria membranes (Panov et al., 2002; Choo et al., 2004) and calcium-binding proteins (Bao et al., 1996), impact on NMDA receptor trafficking (Fan et al., 2007), changes in the expression of genes responsible for calcium homeostasis (Luthi-Carter et al., 2002; Czeredys et al., 2013; Nekrasov et al., 2016) modulation of voltage-gated calcium channels activity (Silva et al., 2017; Chen et al., 2018). Moreover, mutant huntingtin was shown to interact with and potentiate the receptor for inositol-1,4,5-trisphosphate (InsP3R) thereby promoting calcium leakage from endoplasmic reticulum (ER) to cytosol (Tang et al., 2003, 2005).

The store-operated calcium (SOC) entry (SOCE) is one of the most ubiquitous pathways of calcium influx in mammalian cells, including neurons. SOCE physiologically occurs as a result of the InsP3R-mediated intracellular calcium store depletion and it is controlled by stromal interacting molecules (STIM1 and STIM2) – ER calcium sensors (Dziadek and Johnstone, 2007; Shalygin et al., 2015). The accumulated evidence indicates an important physiological role for neuronal SOCE both in normal and pathogenic conditions (Wegierski and Kuznicki, 2018). Several reports showed the importance of STIM2 for these processes (Ryazantseva et al., 2013; Sun et al., 2014; Wu et al., 2016; Yap et al., 2017; Czeredys et al., 2018). Alterations in SOCE were observed in various neurodegenerative pathologies (Ryazantseva et al., 2016, 2018; Secondo et al., 2018), including

HD (Wu et al., 2011; Vigont et al., 2015, 2018; Nekrasov et al., 2016). Moreover, pharmacological inhibition of SOC channels have a neuroprotective effect in HD mice model YAC128 and improved motor functions in HD-afflicted flies (Wu et al., 2011). Also, RNAi knockdown or CRISPR/Cas9 knockout of different components of the SOC channels restore the density of spines in medium spiny neurons (MSNs) of YAC128 (Wu et al., 2018).

It has been established that the length of the polyglutamine (polyQ) tract in mutant huntingtin directly correlates with the severity of the disease and inversely correlates with the age of manifestation of the first symptoms for the vast majority of cases (Andrew et al., 1993; Illarioshkin et al., 1994). However, a few publications demonstrate some physiological cellular disturbances depending on the length of the polyQ tract (Ooi et al., 2019). In this paper, we investigated levels of store-operated and voltage-gated calcium uptakes in the newly developed patient-specific model of a juvenile form of HD (HD76) and compared this model with previously established low-repeat (40–47Q) HD models (Nekrasov et al., 2016). We also studied the role of STIM2 in SOCE alterations in HD76 neurons.

## MATERIALS AND METHODS

### Ethical Approval and Patient Information

Primary skin fibroblasts were obtained from skin biopsies of the forearm of two healthy donors and one patient with HD (76Q repeats) as described in Chestkov et al. (2014). All donors signed informed consents (available upon request). Experiments were approved by ethical committees of Research Center of Neurology, Institute of Cytology RAS and Federal Research and Clinical Center of Physical-Chemical Medicine FMBA.

### Generation of iPSCs With Lentiviruses

We produced lentiviral particles based on LeGO vectors (Weber et al., 2010) containing Oct4, Sox2, Klf4, c-Myc (OSKM). We infected human skin fibroblasts at passage 3 with lentiviruses as described in Chestkov et al. (2014). 20–25 days after infection, iPSC-like colonies were mechanically passaged to separate wells of 48-well plates coated with Matrigel (Corning, USA) and cultivated as individual clones.

### iPSC Generation With Sendai Virus

Non-integrative reprogramming of human skin fibroblasts was made with CytoTune™-iPS 2.0 Sendai Reprogramming Kit (ThermoFisher Scientific, USA) according to manufacturer's instructions.

It should be noted that different approaches of iPSCs generation had no impact on calcium measurements performed in this study (in more details please see Results section The juvenile iPSCs-based HD model demonstrates pathologically enhanced SOCE and **Supplementary Figure 1**).

### iPSC Cultivation

We grew iPSCs in Petri dishes coated with Matrigel (Corning, USA). Up to the second passage, we cultured iPSCs in mTesR1 medium (Stemcell technologies, Canada) with 50 U/ml penicillin/streptomycin (Paneco, Russia). After the second

**Abbreviations:** ER, endoplasmic reticulum; EVP4593, 4-N-[2-(4-Phenoxyphenyl)ethyl]quinazoline-4,6-diamine; HD, Huntington's disease; HD76, patient-specific neuronal model of juvenile form of Huntington's disease; HD76 STIM2(-), HD76 neurons with shRNA-mediated suppression of STIM2; iPSCs, induced pluripotent stem cells; MSNs, medium spiny neurons; polyQ, polyglutamine; SOC(E), store-operated calcium (entry); VGCC, voltage-gated calcium channels; WT, wild type.

passage, we cultured iPSCs in TesR-E8 medium (Stemcell technologies, Canada) with 50 U/ml penicillin/streptomycin (Paneco, Russia). We passaged iPSCs with 0.05% Trypsin (Hyclone, USA) and 5  $\mu$ M Y27632 (Stemgent, USA) and cryopreserved iPSCs in FBS (Hyclone, USA) with addition of 10% DMSO (Paneco, Russia) and 5  $\mu$ M Y27632 (Stemgent, USA).

In some experiments, we used iPSC-based models of HD (iPSHD22 with 47Q, iPSHD11 with 40Q, iPSHD34 with 42Q) and healthy iPSCs (UEF3B) described previously in Nekrasov et al. (2016) and Holmqvist et al. (2016).

The list of cell lines used in our study is presented in **Supplementary Table 1**.

## Embryoid Body Formation

We generated embryoid bodies (EB) from iPSCs with Aggrewell 400 system (Stemcell Technologies) according to manufacturer's protocol. After formation, EBs were transferred to Ultra-low-adhesion plates (Corning, USA) and cultured in DMEM/F12 (Paneco, Russia), 15% Knock-Out Serum Replacement (Invitrogen, USA), 5% FBS (Hyclone, USA), 0.1 mM  $\beta$ -mercaptoethanol (Sigma, USA), 1% NEAA (Hyclone, USA) and 50 U/ml penicillin-streptomycin (Paneco, Russia). The medium was changed every 2 days. Embryoid bodies were grown for 10 days, transferred to gelatin-coated Petri dishes and cultured for 15–20 days in the same medium.

## Karyotyping

We cultured iPSCs up to 80% confluency. Colcemid (0.2  $\mu$ g/ml, Sigma) was added to cells 30 min before cell harvesting. The cells were washed two times with PBS (Paneco, Russia), detached with 0.05% Trypsin (Gibco, USA) and transferred to a conical tube with addition of 10% FBS (Hyclone, USA). Then 5 volumes of 0.075M KCl were added and the cell suspension was incubated for 10 min at 42°C. The cell suspension was then washed by centrifugation with fixatives (methanol: glacial acetic acid as 6:1 and 3:1). The resulting suspension was used for preparation of metaphase chromosomes. Karyotyping was performed using GTG-banding at a resolution of 400 bands with 20 metaphases analyzed. Metaphases were scored using Metafer semi-automated system and IKAROS software (MetaSystems GmbH, Altlußheim, Germany).

## Differentiation of iPSCs Into Neurons

We trypsinized iPSCs and plated at a density of 40,000 cells/cm<sup>2</sup> in mTesR-1 medium (Stemcell technologies) in the presence of 5  $\mu$ M ROCK inhibitor Y-27632 on a Matrigel substrate (Corning). Upon reaching a density of about 80–90%, cells were transferred to a medium for neuronal differentiation composed of: DMEM/F12 (Paneco, Russia), 1% N2 supplement (Paneco, Russia), 1 mM glutamine (Gibco, USA), 50 U/ml penicillin-streptomycin (Paneco, Russia), 200 nM LDN-193189, 10  $\mu$ M SB431542 and 2  $\mu$ M dorsomorphin (all from Miltenyi Biotec, USA). The medium was changed every 2 days; cells were cultivated for 14 days. The resulting neural precursors were split with Versene solution and incubated for 10 min in a CO<sub>2</sub> incubator at 37°C. Cell suspension was centrifuged for 5 min at 300 g. Cells were plated at density of 250,000–400,000

cells per cm<sup>2</sup> in Petri dishes or multi-well plates coated with Matrigel. The next day, the medium was changed to a medium for neural precursors composed of: Neurobasal (Invitrogen), 1% N2 supplement (Paneco, Russia), 1 mM glutamine (Gibco, USA), 50 U/ml penicillin-streptomycin (Paneco, Russia), 1  $\mu$ M Purmorphamine, and 20 ng/ml FGF2 (Miltenyi Biotec, USA). The medium was changed every 2 days. Neural precursors were passaged once a week. At this stage, we had created a bank of cryopreserved neuronal progenitors. Neural precursors were cultured and frozen until the seventh passage. We reseeded neural precursors to a density of 300,000–400,000 cells per cm<sup>2</sup>. In order to obtain mature striatal-like GABAergic neurons, the cells were transferred to a medium for neuronal maturation consisting of: Neurobasal-A (Gibco, USA), 2% B27 supplement (Invitrogen, USA), 1 mM glutamine, 50 U/ml penicillin-streptomycin, 20 ng/ml BDNF, 20 ng/ml GDNF, and 2  $\mu$ M forskolin (Miltenyi Biotec, USA). The medium was changed every other day. After 2 weeks, the concentration of BDNF and GDNF was reduced to 10 ng/ml, and after another week to 5 ng/ml. One month after the cells were transferred to the maturation medium, the obtained neurons were used in the experiments.

## PCR Analysis

The PCR primers used in the study are listed in **Supplementary Table 2**.

## Immunocytochemistry

Cells were grown on Petri dishes to a desired confluency. Then medium was aspirated and cells were washed with PBS (Paneco, Russia) and fixed in 4% PFA (Sigma, USA) for 20 min. PFA was aspirated and plates were washed with PBS and incubated in 0.1% Tween 20, (PBST) with addition of 0.3% Tryton-X100 for 10 min. Plates were washed with PBST three times. Cells were then incubated for 60 min in blocking solution consisting of PBST, 5% FBS (Hyclone, USA) and 5% Goat serum (Sigma, USA). Primary antibodies were then added in desired concentrations in blocking solution; cells were incubated overnight at 4°C. Primary antibodies were aspirated and cells were washed four times with PBST; secondary antibodies in PBST were added for 60 min. Cells were then washed three times with PBST. We added DAPI in a concentration of 100 ng/ml and cells were incubated for 2 min. Then DAPI was aspirated and cells were washed with PBS and visualized under a fluorescent microscope BX43 (Olympus, Japan). The list of antibodies is presented in **Supplementary Table 3**.

## Fluorescent Calcium Imaging

Cells were grown in 96-well cell culture plates (Corning, USA). Cells were loaded with 4  $\mu$ M Fluo-4AM (Thermo Fisher Scientific) dye in the growth media and incubated at room temperature for 1 h. The cells were washed with HBSS (Hank's Balanced Salt Solution contained in mM: 130 NaCl, 2.5 KCl, 2 CaCl<sub>2</sub>, 1.2 MgCl<sub>2</sub>, 10 HEPES, and 10 glucose, pH was adjusted to 7.4 with NaOH) or HBSS without Ca<sup>2+</sup> and containing 500  $\mu$ M EGTA. The 96-well plates were then read on the FLUO star Omega Plate Reader (BMG Labtech) illuminated at 495 nm;

a fluorescence emission was recorded at 510 nm. After a 3-s baseline read, we added to the microplate 1  $\mu$ M of thapsigargin (Sigma, USA) prepared in HBSS buffer containing 2 or 4 mM  $\text{CaCl}_2$ . Fluorescence results were calculated as the ratio of the fluorescence signal over the fluorescence signal before the addition of thapsigargin.

## Electrophysiological Studies

Ion currents were recorded using the whole-cell patch-clamp technique (Hamill and Sakmann, 1981). The measurements were made with an Axopatch 200B amplifier (Axon Instruments, USA). The microelectrode resistance was 5–10 M $\Omega$ ; the series resistance was not compensated but continuously monitored throughout the experiment, with its values being in the range of 10–25 M $\Omega$ . The signal was enhanced and filtered with an internal 2-pole Bessel filter (section frequency 5,000 Hz) and digitized at 5,000 Hz using an AD converter plate (L-Card, Russia). To record currents through voltage-gated calcium channels, we maintained cells at  $-40$  mV and applied a series of 500 ms voltage steps, from  $-80$  to  $+50$  mV with an increment of 10 mV. The pipette solution contained (in mM) 125 CsCl, 10 EGTA-Cs, 10 HEPES-Cs, 4.5  $\text{CaCl}_2$ , 1.5  $\text{MgCl}_2$ , 4  $\text{Mg-ATP}$ , 0.4  $\text{Na-GTP}$  pH was adjusted to 7.3 with CsOH. The extracellular solution contained (in mM) 140 NMDG-Asp, 10  $\text{BaCl}_2$ , 10 HEPES-Cs, 10 Glucose, pH was adjusted to 7.3 with CsOH. The recorded currents were normalized relative to cell capacitance (6–20 pF).

During the recording of integral currents through SOC channels, the membrane potential initially held at  $-40$  mV. Then it was periodically (every 5 s) decreased to  $-100$  mV for 30 ms, then gradually raised to 100 mV at a rate of 1 mV/ms, and then returned to  $-40$  mV. Measurements were made at 0.5 mV intervals. The recorded currents were normalized relative to cell capacitance (6–20 pF). The traces recorded prior to current activation were used as templates for leak subtraction. Currents were evoked by the application of 1  $\mu$ M thapsigargin to the external solution. The same solutions as for voltage-gated current recordings were used with addition of 0.01 mM nifedipine into the extracellular solution. All chemicals were obtained from Sigma-Aldrich (USA).

## Electrophoresis and Western Blotting

Cells were grown in 50-mm Petri dishes. After transfection, they were lysed in 10 mM Tris-HCl buffer (pH 7.5) with 150 mM NaCl, 1% Triton X-100, 1% NP40 (Nonidet P40, non-ionic detergent nonylphenoxypolyethoxyethanol), 2 mM EDTA, 0.2 mM phenylmethanesulfonylfluoride (PMSF; serine protease inhibitor), and protease inhibitor cocktail (Roche). Proteins were resolved by electrophoresis in 8% polyacrylamide gel and transferred to a PVDF membrane, pre-treated with methanol and transfer buffer (48 mM Tris, 39 mM glycine and 5% methanol). The membrane was incubated with 5% milk for 1 h at room temperature and treated with primary monoclonal anti-huntingtin antibody (1:5,000; catalog no. ab109115, Abcam, USA), or primary polyclonal anti-STIM2 antibody (1:1,000; catalog no. 4917, Cell Signaling Technology) and peroxidase-conjugated goat anti-mouse (1:30,000; catalog no. A0168, Sigma), or anti-rabbit (1:30,000; catalog no. A0545, Sigma, USA) IgG

secondary antibody, respectively. Target proteins were visualized using the Super Signal West Femto Maximum Sensitivity Substrate (lot TH269871, Thermo Scientific, USA). All of the experiments were performed in at least three replications with different cell lysates. Monoclonal anti- $\alpha$ -tubulin antibody (1:1,000; catalog no. T6074, Sigma, USA) was used as the loading control. Relative protein content was estimated using standard software for comparing the intensity of bands in the scanned blots. The list of primary antibodies used in study is presented in **Supplementary Table 3**.

## Lentiviral Infection

Lentiviral particles were produced in HEK293T cells transfected with the plasmid for STIM2 suppression or control plasmid (described below), as well as MD2.G (AddGene no.12259, USA) and psPAX2 (AddGene no.12260, USA) packaging plasmid. The medium with lentiviral particles was harvested on the second and the third day post-transfection; viral particles were centrifuged (45,000 g) and resuspended in fresh medium. Viral particles were stored at  $-80^\circ\text{C}$ . Neuronal cultures were infected using viral titers with a high level of transfection efficiency (no <90%).

To suppress STIM2, we used a plasmid encoding the shRNA against STIM2 (Sigma no. TRCN0000150821, sequence CCGGGCTCAATTTTCAGACACTCATTCTCGAGAATGAGTGTCTGAAATTGAGCTTTTTTTG in pLKO.1 vector). A non-target shRNA (cat. no SHC002, Sigma, USA) was used as a negative control.

## Statistics

Statistical analysis was performed using Origin 8.0 (Origin Lab). The amplitudes of currents were compared using one-way ANOVA ( $p < 0.05$ ) with Bonferroni correction. The normality of the distribution and the equality of variances were evaluated using the Shapiro-Wilk and Leven tests, respectively. We used the Mann-Whitney-Wilcoxon test to compare the expression levels of the proteins.

## RESULTS

### Establishment and Characterization of Human iPSCs

Human iPSC lines were established via reprogramming of primary fibroblasts of healthy donors and a patient with a juvenile form of HD by using either the lentiviral transduction method or Sendai viruses. We characterized iPSCs by their morphology, karyotype, expression of markers of pluripotent stem cells and ability to differentiate into derivatives of all three germ layers *in vitro*.

The iPSCs from diseased and healthy individuals were similar by these characteristics; all iPSCs had a normal karyotype, expressed TRA-1-60, SSEA4, Oct-4 and formed EBs upon spontaneous differentiation (**Supplementary Figure 2**).

### Characterization of Neuronal Populations

To create a fully physiologically adequate model, we produced terminally differentiated neuronal cells (striatal MSNs). To differentiate iPSCs into GABA-ergic MSNs, we used a protocol

based on double inhibition of the SMAD cascade, followed by purmorphamine treatment directing cells into lateral ganglionic eminence progenitors (LGE) using purmorphamine, and further maturation of neurons with neurotrophic factors BDNF and GDNF. The LGE were differentiated into mature GABA MSNs during at least 20 days. Differentiated neurons had specific neuronal morphology; there were no visible differences between neurons derived from normal and mutant cells in terms of cell morphology, neurite length and viability. Differentiated neurons could be cultured for more than 3 months. Immunocytochemical analysis showed that up to 100% of the cells were specifically stained for neuronal marker MAP2 and up to 80% of MAP2-positive cells were specifically stained for DARPP-32, a known GABA MSNs specific marker (Figure 1).

## The Juvenile iPSCs-Based HD Model Demonstrates Pathologically Enhanced SOCE

Previously, we have demonstrated an augmented SOCE in 40–47 CAG repeats iPSC-based HD models. In all these described iPSCs-based models the amplitudes of SOCE were 2-fold higher compared to wild type GABA MSNs (Nekrasov et al., 2016). To address the question whether the amplitude of SOCE correlates with the length of the polyQ tract we performed the electrophysiological recordings of calcium currents in the newly established juvenile model of HD with 76Q (HD76).

To evoke store-operated calcium entry, we applied 1  $\mu$ M thapsigargin; this blocks calcium pump SERCA and passively depletes intracellular calcium stores. For analysis, we subtracted the currents recorded prior to the activation of SOC channels. This protocol is a standard and ubiquitously used for SOC channels recordings in different cells (Kaznatcheyeva et al., 2007; Wu et al., 2011; Pani et al., 2013; Czeredys et al., 2018; Lin et al., 2019) including patient-specific GABA MSNs (Nekrasov et al., 2016; Vigont et al., 2018).

We showed that the peak amplitude of thapsigargin-induced calcium currents was  $3.01 \pm 0.19$  pA/pF in HD76 neurons compared to  $1.44 \pm 0.13$  pA/pF in wild-type neurons (WT GABA MSNs) obtained from healthy donors (Figures 2A–C). Taken together with previously published data (Nekrasov et al., 2016) our results demonstrate that SOCE is significantly higher in any HD-specific cell line including the juvenile HD model compared to any control cell line. At the same time, we did not see any correlation between SOCE amplitudes and the length of the polyQ tract of mutant huntingtin (Figure 2D).

It should be noted that in neuronal differentiation we used three different iPSCs from two patients as WT neurons and two different HD76 iPSCs from one patient which were reprogrammed using either the lentiviral transduction method or Sendai viruses. Comparing the electrophysiological features of iPSCs-derived neurons did not demonstrate any differences in SOCE neither for WT lines nor for HD76 neurons (Supplementary Figures 1A,B), so we combined the data from these lines and presented it as WT and HD76, respectively.

## EVP4593 Can Attenuate Pathologically Enhanced Level of Huntingtin in HD76 Neurons

It has been repeatedly demonstrated that mutant huntingtin has many toxic functions altering intracellular calcium signaling (Bao et al., 1996; Luthi-Carter et al., 2002; Panov et al., 2002; Tang et al., 2003, 2005; Choo et al., 2004; Fan et al., 2007; Czeredys et al., 2013; Silva et al., 2017; Chen et al., 2018), in particular, improper regulation of an activity of SOC channels (Wu et al., 2011; Vigont et al., 2015, 2018; Nekrasov et al., 2016).

We checked the level of expression of huntingtin and found it to be significantly greater in HD76 compared to WT GABA MSNs. Pre-incubation of the HD76 neurons with the previously described (Wu et al., 2011) potential anti-HD drug and SOC inhibitor EVP4593 in concentration of 300 nM for 24 hours before lysis decreased expression level of huntingtin, returning it to the level comparable with control values (Figures 3A,B). Thus, EVP4593 may be involved in the neuroprotection via regulation of expression of huntingtin.

HD76 neurons are specific for the heterozygous patient. In order to address if there are any preferences for huntingtin expression from normal or mutant alleles, we resolved the expression of normal ( $\ll$ light $\gg$ ) and mutant ( $\ll$ heavy $\gg$ ) huntingtin by long electrophoresis and Western blot analysis. Our data indicated that both normal and mutant huntingtin were overexpressed in HD76 neurons compared to WT GABA MSNs (Figure 3C). Moreover, we observed the same overexpression of huntingtin protein in neurons derived from HD iPSCs with shorter polyQ tract (Supplementary Figure 3A).

## STIM2 Mediates Excessive SOCE in HD76 Neurons

Currently, STIM proteins are established as well-known activators for SOC channels. In mammals, this family is represented by two proteins: STIM1 and STIM2 (Dziadek and Johnstone, 2007). These proteins act as calcium sensors in the lumen of the ER and mediate the activity of SOC channels upon a loss of calcium binding. The STIM2 constant of calcium binding is lower than that of STIM1, so it can sense smaller changes in calcium ER content. Despite it being well-known that STIM2 is a relatively weak activator of SOCE, activation of the SOC channels by STIM2 is highly physiologically relevant. We have previously demonstrated that expression level of STIM2 was significantly higher in human neuroblastoma cells SK-N-SH modeling HD by overexpression of mutant huntingtin with 138 glutamine residues and huntingtin associated protein 1 (Czeredys et al., 2018).

We checked whether the STIM2 level is changed in HD GABA MSNs. The results of Western blot analysis demonstrated that in HD76, the level of STIM2 protein was 65% higher than in WT GABA MSNs (Figures 4A,B). Previously described low-repeat HD models also showed higher levels of STIM2 compared to WT neurons (Supplementary Figure 3B). Despite the fact that the gene encoding STIM2 has no NF- $\kappa$ B-dependent promoters or enhancers, EVP4593 surprisingly had an ability to attenuate the STIM2 level after 24 h incubation (Figures 4A,B).

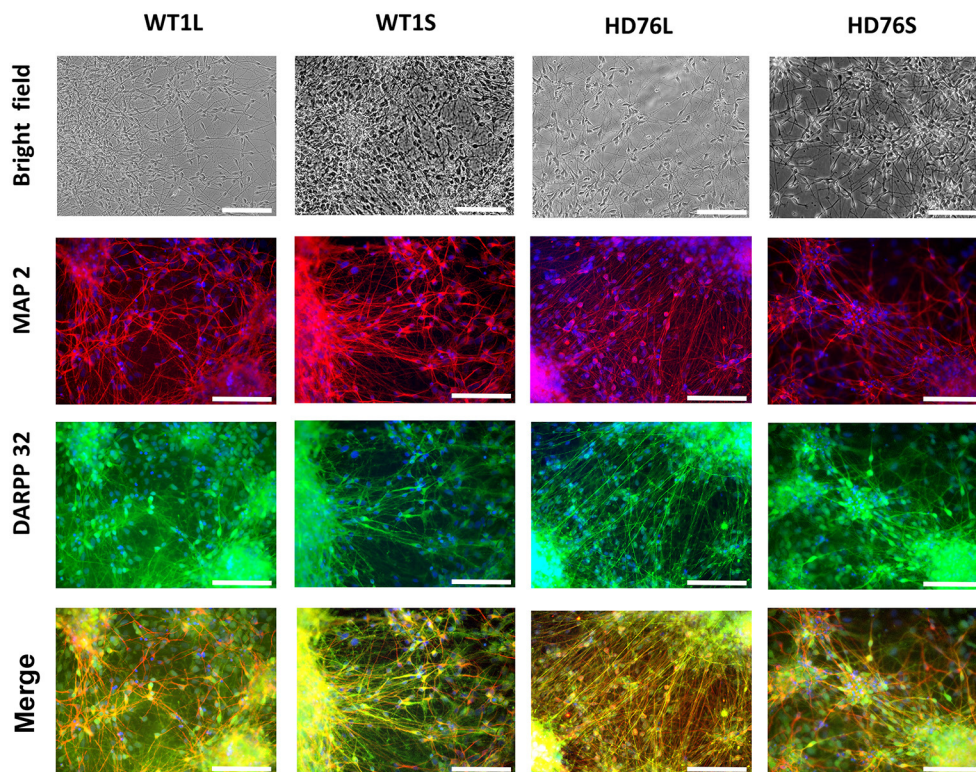


**FIGURE 1 |** HD76 and WT iPSCs-derived neurons analysis. Representative images of neurons in the bright field (photo of the cells in culture) and immunostained for MAP2 (red), DARPP-32 (green) and merge of MAP2 and DARPP32 counterstained with DAPI (blue). HD76L and HD76S – juvenile HD-specific neuronal cell lines differentiated from iPSCs obtained by lentivirus and Sendai virus approaches, respectively; WT1L and WT1S – wild type neuronal cell lines differentiated from iPSCs obtained by Lentivirus and Sendai virus approaches, respectively. The cell lines are also represented in **Supplementary Table 1**. Scale bar 100  $\mu$ m.

Our findings allowed us to speculate that the excessive expression of STIM2 may underlie pathological SOCE in HD76. To test this hypothesis, we checked whether STIM2 suppression by EVP4593 (**Figures 4A,B**) affects calcium entry through SOC channels. The amplitude of thapsigargin-induced calcium currents in HD76 neurons after 24 h incubation with 300 nM EVP4593 was  $1.32 \pm 0.21$  pA/pF (**Figures 4C,D**), demonstrating significantly lower level than in intact HD76 neurons ( $3.01 \pm 0.19$  pA/pF).

To verify the hypothesis that excessive SOCE in HD76 neurons depends on STIM2, we knocked down its expression in HD76 by lentiviral infection of shRNA against STIM2. These cells were named HD76 STIM2(–). The non-target shRNA was used as a negative control. After confirmation of STIM2 suppression by Western blot (**Supplementary Figure 4**), we registered store-operated calcium currents in HD76 STIM2(–). The amplitude of thapsigargin-induced calcium currents was  $3.06 \pm 0.37$  pA/pF in HD76 non-target shRNA compared to  $1.42 \pm 0.24$  pA/pF in HD76 STIM2(–) neurons (**Figures 4C,D**). Thus, we demonstrated that STIM2 suppression in HD76 neurons by using both shRNA-mediated knockdown and EVP4593 application leads to significant reduction of SOCE (**Figures 4C,D**). We also found that STIM2 suppression mediates SOC channels in WT

GABA MSNs resulting in about 35% attenuation of SOCE in WT STIM2(–) neurons (**Supplementary Figure 5**).

We also confirmed the decrease in SOCE in HD76 STIM2(–) by fluorescent calcium imaging with Fluo-4AM. We incubated cells in a calcium-free bath containing 0.5 mM EGTA for 40 min to deplete the intracellular calcium stores and evoke activation of SOC channels. Then we returned calcium (final concentration was 4 mM) into the bath solution and added the thapsigargin to prevent refilling the stores. The measurements demonstrated that the steady-state level of the relative fluorescence of Fluo-4 after the SOC channels activation was  $1.70 \pm 0.07$  a.u. in HD76 non-target shRNA compared to  $1.47 \pm 0.09$  a.u. HD76 STIM2(–) (**Supplementary Figure 6**); this confirmed the data obtained by electrophysiological recordings.

To further strengthen the conclusion that STIM2 drives the enhanced SOCE in HD76 neurons we performed experiments with G418, which is known to be a selective antagonist of STIM2. Electrophysiological recordings showed that application of 50  $\mu$ M of G418 decreased SOCE amplitude in HD76 neurons from  $3.27 \pm 0.53$  to  $1.23 \pm 0.36$  pA/pF (**Supplementary Figure 7**).

Altogether our data indicate that STIM2 drives pathological hyperactivity of SOC channels in HD76 neurons.

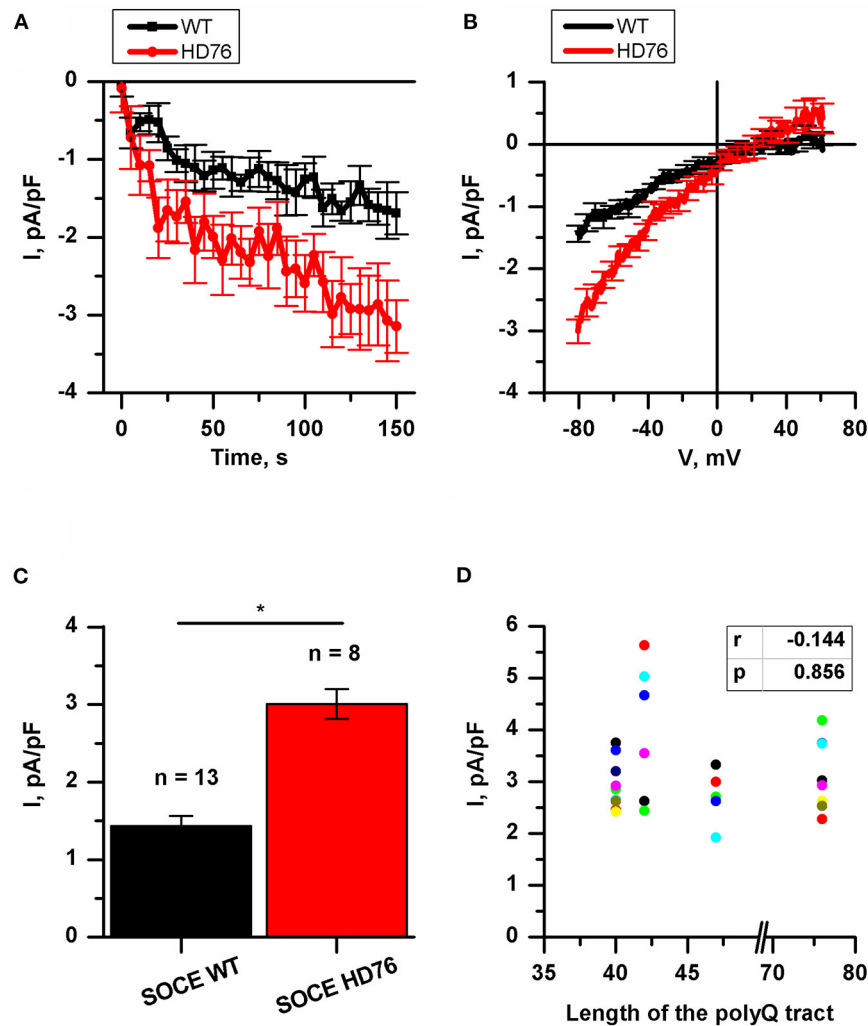


**FIGURE 2 |** Disturbance of SOCE in HD76 neurons. **(A)** Normalized SOC currents evoked by application of thapsigargin ( $1 \mu\text{M}$ ) and plotted as a function of time in HD76 (red circles), and WT (black squares) GABA MSNs. SOC currents were measured every 5 s at a test potential of  $-80 \text{ mV}$ . Each trace shows mean  $\pm$  SEM. **(B)** Average Current-Voltage relationships ( $I$ - $V$  curves) of normalized currents evoked by passive depletion of calcium stores with thapsigargin ( $1 \mu\text{M}$ ) in HD76 (red line), and WT (black line) GABA MSNs. The  $I$ - $V$  curves were plotted after the full development of the SOC currents. The number of experiments is depicted at the panel **(C)**. **(C)** Average amplitude of the normalized SOC currents determined at a test potential of  $-80 \text{ mV}$  for HD76 (red), and WT (black) GABA MSNs. The amplitudes are plotted as the mean  $\pm$  SEM ( $n$  = number of single cell experiments). The asterisks indicate that differences in amplitudes are statistically significant ( $p < 0.05$ ). **(D)** Correlation between the amplitude of SOC currents and the length of the polyglutamine tract of mutant huntingtin. The correlation coefficient ( $r$ ) and the  $p$ -value are indicated above the plot. The cell lines are represented in **Supplementary Table 1**.

## HD76 Neurons Demonstrate Upregulated Calcium Entry Through Voltage-Gated Channels

We also measured the currents through the voltage-gated calcium channels (VGCC) in HD76 neurons. The peak amplitudes of VGCC current in HD76 and WT GABA MSNs were  $1.80 \pm 0.26$  and  $0.97 \pm 0.08$  pA/pF, respectively (Figures 5A,B); This demonstrates a pathological increase of calcium entry through VGCC by  $\sim 85\%$ . Moreover, we detected analogical increase in voltage-gated calcium uptake in low-repeat HD model (Supplementary Figure 8). These currents were

partially sensitive to L-type channels blocker nifedipine (Supplementary Figure 9). As well as for SOCE, we also confirmed that amplitudes of currents through VGCC do not significantly vary in different WT and HD76 lines (Supplementary Figures 1C,D).

Then we showed that STIM2 suppression had no effect on calcium entry through VGCC. The peak amplitude of VGCC current in HD76 non-target shRNA was  $1.86 \pm 0.28$  pA/pF compared to  $1.78 \pm 0.17$  pA/pF in HD76 STIM2(-) neurons (Figures 5C,D). Thus, we concluded that the upregulation of VGCC in HD76 neurons is not associated with high STIM2 levels.

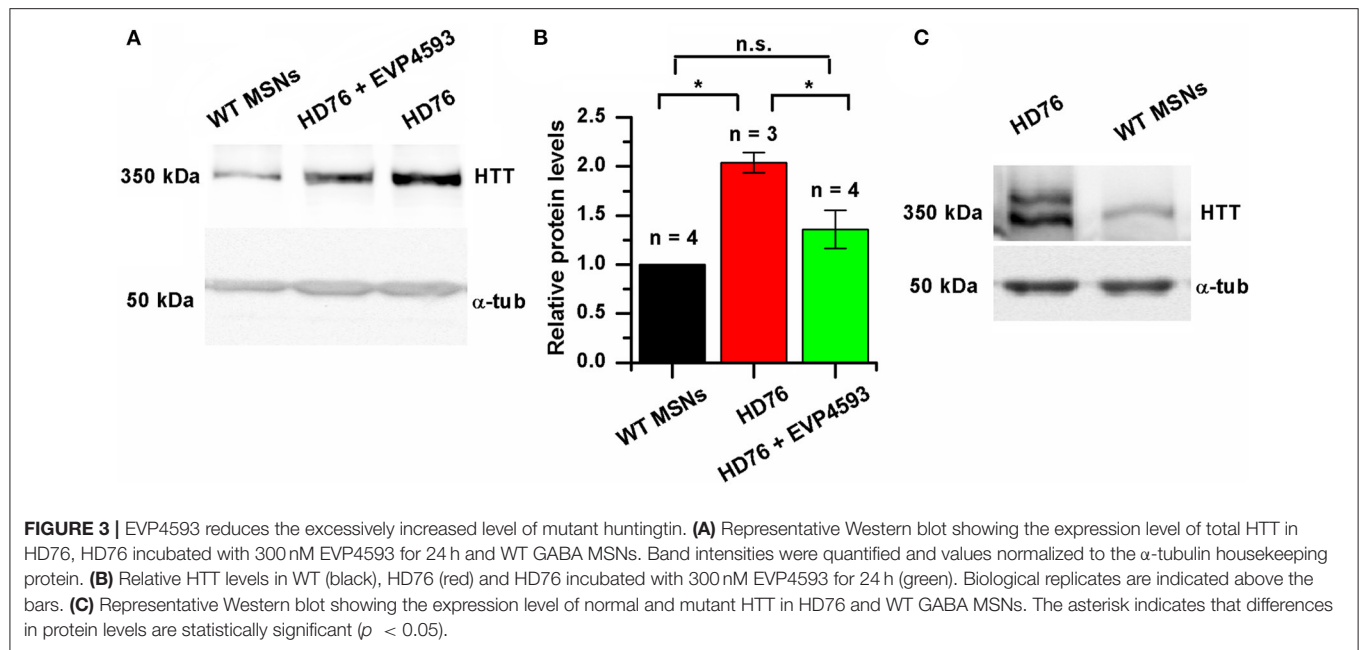


**FIGURE 3 |** EVP4593 reduces the excessively increased level of mutant huntingtin. **(A)** Representative Western blot showing the expression level of total HTT in HD76, HD76 incubated with 300 nM EVP4593 for 24 h and WT GABA MSNs. Band intensities were quantified and values normalized to the  $\alpha$ -tubulin housekeeping protein. **(B)** Relative HTT levels in WT (black), HD76 (red) and HD76 incubated with 300 nM EVP4593 for 24 h (green). Biological replicates are indicated above the bars. **(C)** Representative Western blot showing the expression level of normal and mutant HTT in HD76 and WT GABA MSNs. The asterisk indicates that differences in protein levels are statistically significant ( $p < 0.05$ ).

## DISCUSSION

Previously we have characterized iPSC-based low-repeat HD models and postulated that SOCE is dramatically upregulated in HD-specific GABA MSNs (Nekrasov et al., 2016). Here we measured SOC currents in HD76 neurons, modeling a juvenile form of HD. Since it is well-known that the severity of HD pathology highly correlates with the length of the polyQ tract of mutant huntingtin, we expected to find differences in calcium disturbances between low-repeat and juvenile models. However, our data indicate that SOCE in HD-specific GABA MSNs does not depend on the length of the polyQ tract. One possible hypothesis explaining this is that the cells have a limit to channel-forming and/or activator proteins. Indeed, in a previously described human neuroblastoma SK-N-SH HD model, we expected that overexpression of Hap1 protein (huntingtin associated protein 1) resulted in further SOCE increase, but we have not confirmed this effect since all SOC channels had already been activated upon mutant huntingtin expression (Czeredys et al., 2018). However, it has recently been found that isogenic HD-specific neural cells exhibit mitochondrial deficits and high levels of reactive oxygen species, correlating with the length of the polyQ tract (Ooi et al., 2019). Thus, we conclude that alterations in calcium signaling observed in cell models of HD are independent of the length of the polyQ tract and can be a common part of the pathogenesis of juvenile and late-onset forms of HD. However, mitochondrial impairments and high levels of reactive oxygen species can be caused by processes located downstream of calcium uptake and demonstrate a strong correlation with the length of the polyQ tract.

A number of studies of iPSC-based HD models were focused on alterations in gene expression. Mostly, the RNAseq technique is used to determine the upregulated or downregulated genes in HD-specific cells. Such investigations are highly relevant since

it provides novel candidates for medical treatment. A number of scientific groups observed differential gene expression in iPSC-based HD models (HD iPSC Consortium, 2017; Switońska et al., 2018; Ooi et al., 2019). We previously reported a gene ontology analysis in low-repeat HD models indicating that genes maintaining calcium signaling are upregulated in HD GABA MSNs compared to WT GABA MSNs (Nekrasov et al., 2016).

In this paper, we showed that huntingtin expression in HD76 neurons is significantly higher at the protein level (Figures 3A,B). One of the translation-enhancing mechanisms is triggered by association of the expanded CAG repeat to RNA binding protein MID1, which recruits 40S ribosome kinase S6K to mCAG-RNA, and stimulates enhanced translation of mutant RNA (Krauss et al., 2013).

Since HD is a monogenic disease, the only way to totally treat it is to prevent the expression of the mutant huntingtin. One of the rapidly developing therapeutic approaches is using antisense oligonucleotide technology to lower huntingtin levels in HD (Aslesh and Yokota, 2020; Marxreiter et al., 2020). However, the searching for the small molecules able to supplement and/or enhance action of antisense oligonucleotides remains highly actual. Here we found that the potential anti-HD drug EVP4593 can attenuate high expression of the mutant huntingtin, thus, suppressing its toxic functions (Figures 3A,B). This compound was initially described as an inhibitor of activation of the NF- $\kappa$ B signal pathway (Tobe et al., 2003). Then we showed that EVP4593 can attenuate SOCE (Wu et al., 2011; Vigont et al., 2015) and now it is well accepted as a SOC channels inhibitor (Nekrasov et al., 2016; Vigont et al., 2018; Chernyuk et al., 2019). This compound has been previously tested on various HD models, including patient-specific GABA MSNs, demonstrating both SOCE inhibitory activity (Wu et al., 2011; Vigont et al., 2015, 2018; Nekrasov et al., 2016) and neuroprotective effect (Wu et al., 2011, 2016; Nekrasov et al., 2016). Despite it has

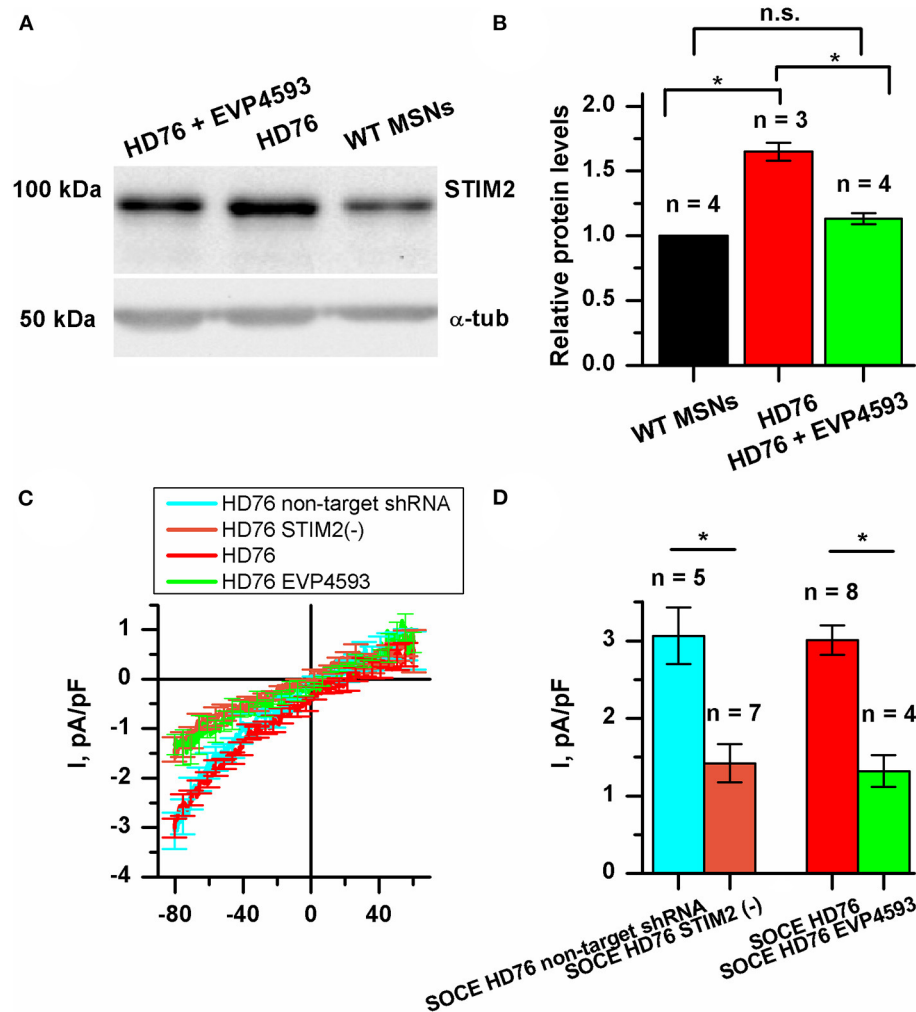


**FIGURE 4 |** STIM2 as the cornerstone of significantly increased SOCE in HD76 GABA MSNs. **(A)** Representative Western blot showing the expression level of STIM2 in HD76, HD76 incubated with 300 nM EVP4593 for 24 h and WT GABA MSNs. Band intensities were quantified and values normalized to the  $\alpha$ -tubulin housekeeping protein. **(B)** Relative STIM2 levels in HD76 (red), HD76 incubated with 300 nM EVP4593 (green) and WT GABA MSNs (black). Biological replicates are mentioned above the bars. **(C)** Average Current-Voltage relationships (I-V curves) of normalized currents evoked by passive depletion of calcium stores with thapsigargin (1  $\mu$ M) in HD76 expressing non-target shRNA (HD76 non-target shRNA, cyan line), HD76 expressing shRNA against STIM2 (HD76 STIM2(-), orange line) and intact HD76 (red line) and HD76 pre-incubated with 300 nM EVP4593 for 24 h (green line). The number of experiments is depicted at the panel **(D)**. **(D)** Average amplitude or the normalized SOC currents determined at a test potential of  $-80$  mV for HD76 expressing non-target shRNA (cyan), HD76 expressing shRNA against STIM2 (orange), intact HD76 (red) and HD76 pre-incubated with 300 nM EVP4593 for 24 h (green). The amplitudes are plotted as the mean  $\pm$  SEM ( $n$  = number of single cell experiments). The asterisk indicates that differences in amplitudes are statistically significant ( $p < 0.05$ ).

been reported that EVP4593 specifically inhibit mitochondrial complex I (Krishnathas et al., 2017), the molecular mechanisms explaining its inhibition of SOC channels and neuroprotection remain unclear.

Our data allowed us to suppose that the neuroprotective effect of EVP4593 observed in HD-specific cells can be explained by the indirect impact of EVP4593 on the mutant huntingtin expression level. The effect of EVP4593 on huntingtin level was highly estimated since the gene encoding huntingtin has an NF- $\kappa$ B-dependent promoter/enhancer (Bećanović et al., 2015).

Earlier, it has been reported the tendency to shorter life-time of mutant huntingtin compared to normal huntingtin (Tsvetkov

et al., 2013). This can explain the observed strong reduction in huntingtin level in HD76 neurons even after 24 h treatment with EVP4593 (Figures 3A,B). It has also been shown that in HD neurons derived from hESCs even 10% reduction of the mutant huntingtin level was sufficient to prevent toxicity, whereas up to 90% reduction of the wild-type huntingtin was tolerated and safe to those cells (Lu and Palacino, 2013). Hence, EVP4593-mediated attenuation of both normal and mutant huntingtin could have a potential clinical application in HD treatment.

We have demonstrated that high SOCE is a well-repeated parameter in HD-specific GABA MSNs and could be considered as a pathology marker. We also suggest that STIM2 is a promising

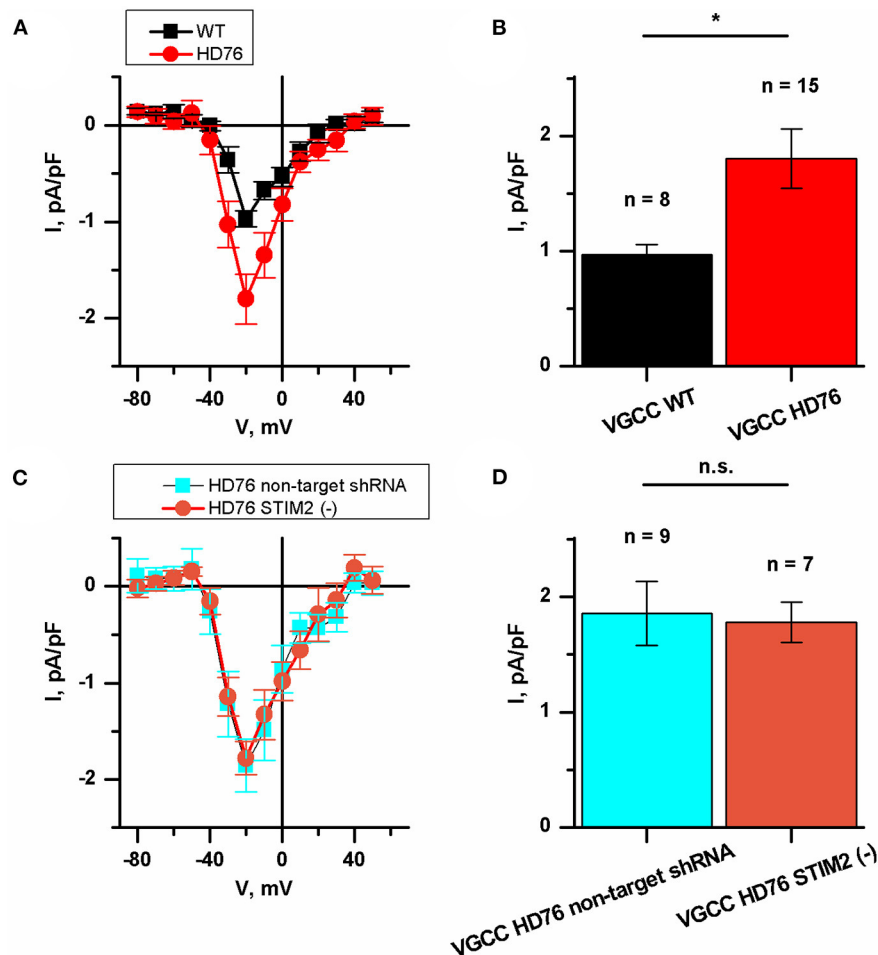


**FIGURE 5 |** Disturbance of VGCC in HD76 neurons. **(A)** Average I-V curves of normalized voltage-gated calcium currents for HD76 (red circles) and WT (black squares) GABA MSNs. The number of experiments is depicted at the panel **(B)**. **(B)** Average amplitude of VGCC currents at the potential of -20 mV for HD76 (red), and WT (black) GABA MSNs. The amplitudes are plotted as the mean  $\pm$  SEM ( $n$  = number of single cell experiments). The asterisk indicates that differences in amplitudes are statistically significant ( $p < 0.05$ ). **(C)** Average I-V curves of normalized voltage-gated calcium currents in HD76 expressing non-target shRNA (HD76 non-target shRNA, cyan squares) and HD76 expressing shRNA against STIM2 (HD76 STIM2(-), orange circles). The number of experiments is depicted at the panel **(D)**. **(D)** Average amplitude of VGCC currents at the potential of -20 mV for HD76 expressing non-target shRNA (HD76 non-target shRNA, cyan) and HD76 expressing shRNA against STIM2 (HD76 STIM2(-), orange). The amplitudes are plotted as the mean  $\pm$  SEM ( $n$  = number of single cell experiments). n.s. indicates the absence of statistically significant differences ( $p > 0.05$ ).

target for drug design. We showed that STIM2 is upregulated in HD76 neurons and the pre-incubation of HD76 neurons with EVP4593 resulted in lowering the STIM2 level (Figures 4A,B). This result correlates well with the published data, demonstrating the attenuation of both lithium-induced and normal STIM2 expression by application of another NF- $\kappa$ B antagonist wogonin (Sukkar et al., 2018). Then we hypothesized that STIM2 drives the high activity of SOC channels in HD. Our data indicated that suppression of STIM2 in HD76 neurons using both shRNA-mediated knockdown and treatment with EVP4593 results in a significant reduction of pathological SOCE (Figures 4C,D). Furthermore, application of STIM2 antagonist G418 (Parvez et al., 2008) also reduced SOCE level in HD76 neurons (Supplementary Figure 7). The major role for STIM2 in HD is also supported by the study demonstrating STIM2-mediated

dendritic spine dysregulation in neuron cultures of YAC128 HD mice (Wu et al., 2016).

Involvement of VGCC in HD pathogenesis was demonstrated in only few recent papers. They showed an important role for N-type VGCC in the increased release of synaptic vesicles at presynaptic terminals of HD cortical neurons in heterozygous zQ175 mice (Chen et al., 2018) and disease stage-dependent alterations in calcium influx in BACHD mice (Silva et al., 2017). A significant increase in L-type calcium currents in cortical neurons from BACHD mice has been also reported (Miranda et al., 2019). Here we have also shown greater calcium entry through VGCC in HD neurons. The recorded currents were partially sensitive to L-type VGCC blocker nifedipine (Supplementary Figure 7). Surprisingly we found that currents through VGCC were upregulated in HD76

under STIM2 suppression (Figures 5C,D). This result was unexpected since a reduction of STIM2 expression level may shift the balance to predominant activation of STIM1, which is known to be an inhibitor of the L-type VGCC (Park et al., 2010). Further investigations in the framework of the separate study are required to shed light on the molecular mechanisms of VGCC alterations in HD pathogenesis, their possible relation to SOCE pathway, and impacts of VGCC of different types.

In summary, the polyQ expansion within huntingtin affects neuronal calcium signaling in HD76 neurons, demonstrating high levels of calcium influx through both SOC channels and VGCC. Modulation of calcium channels and regulation of expression levels of proteins responsible for calcium uptake are perspective directions for anti-neurodegenerative drug development. We postulate that calcium sensor STIM2 drives a hyperactivity of the SOC channels in HD76 neurons, thus, establishing STIM2 as a promising molecular target for medical treatment. Further investigation will contribute to deeper insights into the molecular mechanisms of neurodegeneration. This hopefully will shed light on the key points of precision regulation of pathological intracellular signaling and contribute to patient-oriented personalized strategies in medical treatment.

## DATA AVAILABILITY STATEMENT

The original contributions presented in the study are included in the article/Supplementary Material, further inquiries can be directed to the corresponding authors.

## ETHICS STATEMENT

The studies involving human participants were reviewed and approved by the ethical committee of the Research Center of Neurology, Moscow, Russian Federation the ethical committee of the Institute of Cytology RAS, Saint-Petersburg, Russian Federation the ethical committee of the Federal Research, and Clinical Center of Physical-Chemical Medicine FMBA, Moscow, Russian Federation. The patients/participants provided their written informed consent to participate in this study.

## REFERENCES

- Andrew, S., Theilmann, J., Almqvist, E., Norremolle, A., Lucotte, G., Anvret, M., et al. (1993). DNA analysis of distinct populations suggests multiple origins for the mutation causing Huntington disease. *Clin. Genet.* 43, 286–294. doi: 10.1111/j.1399-0004.1993.tb03820.x
- Aslesh, T., and Yokota, T. (2020). Development of antisense oligonucleotide gapmers for the treatment of Huntington's disease. *Methods Mol. Biol.* 2176, 57–67. doi: 10.1007/978-1-0716-0771-8\_4
- Bao, J., Sharp, A. H., Wagster, M. V., Becher, M., Schilling, G., Ross, C. A., et al. (1996). Expansion of polyglutamine repeat in huntingtin leads to abnormal protein interactions involving calmodulin. *Proc. Natl. Acad. Sci. U. S. A.* 93, 5037–5042. doi: 10.1073/pnas.93.10.5037
- Bećanović, K., Nørremølle, A., Neal, S. J., Kay, C., Collins, J. A., Arenillas, D., et al. (2015). A SNP in the HTT promoter alters NF-κB binding and is

## AUTHOR CONTRIBUTIONS

VV: conceptualization, methodology, validation, formal analysis, investigation, writing—original draft, writing—review and editing, visualization, project administration, and funding acquisition. DG: validation, formal analysis, investigation, writing—original draft, writing—review and editing, and visualization. OL: validation, formal analysis, investigation, writing—original draft, and writing—review and editing, visualization. KG: investigation. EV: investigation. AS: investigation. AB: formal analysis, investigation, and writing—review and editing. LS: investigation. OZ: investigation. EAK: investigation. LG: investigation. SK: investigation and resources. SI: conceptualization and resources. ML: conceptualization, methodology, formal analysis, writing—review and editing, visualization, supervision, project administration, and funding acquisition. EVK: conceptualization, methodology, formal analysis, writing—review and editing, visualization, supervision, project administration, and funding acquisition. All authors have read and agreed to the published version of the manuscript.

## FUNDING

This research was funded by the Russian Science Foundation, grants number 17-74-20068 (VV, AS, DG, KG, and SK), and 19-15-00425 (ML, EV, OL, EAK, and LS); the Russian Foundation for Basic Research, grant number 17-54-80006 (EVK and AS), and the grant from the President of the Russian Federation number MK-2335.2019.4 (VV and DG). Ministry of Science and Higher Education of Russia – Research Project N 075-15-2020-795, local identifier 13.1902.21.0027 (VV, DG, KG, and EVK).

## SUPPLEMENTARY MATERIAL

The Supplementary Material for this article can be found online at: <https://www.frontiersin.org/articles/10.3389/fcell.2021.625231/full#supplementary-material>

The following are available in supplementary file: Methods: Embryoid body formation, Karyotyping, Immunocytochemistry, Fluorescent calcium imaging; Figures and Tables.

- a bidirectional genetic modifier of Huntington disease. *Nat. Neurosci.* 18, 807–816. doi: 10.1038/nn.4014
- Bezprozvanny, I. (2009). Calcium signaling and neurodegenerative diseases. *Trends Mol. Med.* 15, 89–100. doi: 10.1016/j.molmed.2009.01.001
- Chen, S., Yu, C., Rong, L., Li, C. H., Qin, X., Ryu, H., et al. (2018). Altered synaptic vesicle release and  $Ca^{2+}$  influx at single presynaptic terminals of cortical neurons in a knock-in mouse model of Huntington's disease. *Front. Mol. Neurosci.* 11:478. doi: 10.3389/fnmol.2018.00478
- Chen, X., Wu, J., Lvovskaya, S., Herndon, E., Supnet, C., and Bezprozvanny, I. (2011). Dantrolene is neuroprotective in Huntington's disease transgenic mouse model. *Mol. Neurodegener.* 6:81. doi: 10.1186/1750-1326-6-81
- Chernyuk, D., Zernov, N., Kabirova, M., Bezprozvanny, I., and Popugaeva, E. (2019). Antagonist of neuronal store-operated calcium entry exerts beneficial effects in neurons expressing PSEN1ΔE9 mutant linked to familial Alzheimer disease. *Neuroscience* 410, 118–127. doi: 10.1016/j.neuroscience.2019.04.043

- Chestkov, I. V., Vasilieva, E. A., Illarionovskii, S. N., Lagarkova, M. A., and Kiselev, S. L. (2014). Patient-specific induced pluripotent stem cells for SOD1-associated amyotrophic lateral sclerosis pathogenesis studies. *Acta Naturae* 6, 54–60. doi: 10.32607/20758251-2014-6-1-54-60
- Choo, Y. S., Johnson, G. V., MacDonald, M., Detloff, P. J., and Lesort, M. (2004). Mutant huntingtin directly increases susceptibility of mitochondria to the calcium-induced permeability transition and cytochrome c release. *Hum. Mol. Genet.* 13, 1407–1420. doi: 10.1093/hmg/ddh162
- Czeredys, M., Gruszczynska-Biegala, J., Schacht, T., Methner, A., and Kuznicki, J. (2013). Expression of genes encoding the calcium signalosome in cellular and transgenic models of Huntington's disease. *Front. Mol. Neurosci.* 6:42. doi: 10.3389/fnmol.2013.00042
- Czeredys, M., Vigont, V. A., Boeva, V. A., Mikoshiba, K., Kaznacheyeva, E. V., and Kuznicki, J. (2018). Huntingtin-associated protein 1A regulates store-operated calcium entry in medium spiny neurons from transgenic YAC128 mice, a model of Huntington's disease. *Front. Cell. Neurosci.* 12:381. doi: 10.3389/fncel.2018.00381
- Dziadek, M. A., and Johnstone, L. S. (2007). Biochemical properties and cellular localization of STIM proteins. *Cell Calcium* 42, 123–132. doi: 10.1016/j.ceca.2007.02.006
- Egorova, P., Popugayeva, E., and Bezprozvanny, I. (2015). Disturbed calcium signaling in spinocerebellar ataxias and Alzheimer's disease. *Semin. Cell Dev. Biol.* 40, 127–133. doi: 10.1016/j.semdb.2015.03.010
- Fan, M. M., Fernandes, H. B., Zhang, L. Y., Hayden, M. R., and Raymond, L. A. (2007). Altered NMDA receptor trafficking in a yeast artificial chromosome transgenic mouse model of Huntington's disease. *J. Neurosci.* 27, 3768–3779. doi: 10.1523/JNEUROSCI.4356-06.2007
- Hamill, O. P., and Sakmann, B. (1981). Multiple conductance states of single acetylcholine receptor channels in embryonic muscle cells. *Nature* 294, 462–464. doi: 10.1038/294462a0
- HD iPSC Consortium (2017). Developmental alterations in Huntington's disease neural cells and pharmacological rescue in cells and mice. *Nat. Neurosci.* 20, 648–660. doi: 10.1038/nn.4532
- Hisatsune, C., Hamada, K., and Mikoshiba, K. (2018).  $Ca^{2+}$  signaling and spinocerebellar ataxia. *Biochim. Biophys. Acta Mol. Cell Res.* 1865, 1733–1744. doi: 10.1016/j.bbamcr.2018.05.009
- Holmqvist, S., Lehtonen, Š., Chumarina, M., Puttonen, K. A., Azevedo, C., Lebedeva, O., et al. (2016). Creation of a library of induced pluripotent stem cells from Parkinsonian patients. *NPJ Parkinsons Dis.* 2:16009. doi: 10.1038/npjparkd.2016.9
- Huang, D. S., Lin, H. Y., Lee-Chen, G. J., Hsieh-Li, H. M., Wu, C. H., and Lin, J. Y. (2016). Treatment with a Ginkgo biloba extract, EGB 761, inhibits excitotoxicity in an animal model of spinocerebellar ataxia type 17. *Drug Des. Dev. Ther.* 10, 723–731. doi: 10.2147/DDDT.S98156
- Illarionovskii, S. N., Igarashi, S., Onodera, O., Markova, E. D., Nikolskaya, N. N., Tanaka, H., et al. (1994). Trinucleotide repeat length and rate of progression of Huntington's disease. *Ann. Neurol.* 36, 630–635. doi: 10.1002/ana.410360412
- Ishida, Y., Kawakami, H., Kitajima, H., Nishiyama, A., Sasai, Y., Inoue, H., et al. (2016). Vulnerability of purkinje cells generated from spinocerebellar ataxia type 6 patient-derived iPSCs. *Cell Rep.* 17, 1482–1490. doi: 10.1016/j.celrep.2016.10.026
- Kaznacheyeva, E., Glushankova, L., Bugaj, V., Zimina, O., Skopin, A., Alexeenko, V., et al. (2007). Suppression of TRPC3 leads to disappearance of store-operated channels and formation of a new type of store-independent channels in A431 cells. *J. Biol. Chem.* 282, 23655–23662. doi: 10.1074/jbc.M608378200
- Krauss, S., Griesche, N., Jastrzebska, E., Chen, C., Rutschow, D., Achmüller, C., et al. (2013). Translation of HTT mRNA with expanded CAG repeats is regulated by the MID1-PP2A protein complex. *Nat. Commun.* 4:1511. doi: 10.1038/ncomms2514
- Krishnathas, R., Bonke, E., Dröse, S., Zickermann, V., and Nasiri, H. R. (2017). Identification of 4-N-[2-(4-phenoxyphenyl)ethyl]quinazoline-4,6-diamine as a novel, highly potent and specific inhibitor of mitochondrial complex I. *Medchemcomm.* 8, 657–661. doi: 10.1039/C6MD00655H
- Lin, Y. P., Bakowski, D., Mirams, G. R., and Parekh, A. B. (2019). Selective recruitment of different  $Ca^{2+}$ -dependent transcription factors by STIM1-Orai1 channel clusters. *Nat. Commun.* 10:2516. doi: 10.1038/s41467-019-10329-3
- Lu, B., and Palacino, J. (2013). A novel human embryonic stem cell-derived Huntington's disease neuronal model exhibits mutant huntingtin (mHTT) aggregates and soluble mHTT-dependent neurodegeneration. *FASEB J.* 27, 1820–1829. doi: 10.1096/fj.12-219220
- Luthi-Carter, R., Hanson, S. A., Strand, A. D., Bergstrom, D. A., Chun, W., Peters, N. L., et al. (2002). Dysregulation of gene expression in the R6/2 model of polyglutamine disease: parallel changes in muscle and brain. *Hum. Mol. Genet.* 11, 1911–1926. doi: 10.1093/hmg/11.17.1911
- Marxreiter, F., Stemick, J., and Kohl, Z. (2020). Huntingtin lowering strategies. *Int. J. Mol. Sci.* 21:2146. doi: 10.3390/ijms21062146
- Miranda, A. S., Cardozo, P. L., Silva, F. R., de Souza, J. M., Olmo, I. G., Cruz, J. S., et al. (2019). Alterations of calcium channels in a mouse model of Huntington's disease and neuroprotection by blockage of CaV1 channels. *ASN Neuro* 11:1759091419856811. doi: 10.1177/1759091419856811
- Mungenast, A. E., Siegert, S., and Tsai, L. H. (2016). Modeling Alzheimer's disease with human induced pluripotent stem (iPS) cells. *Mol. Cell. Neurosci.* 73, 13–31. doi: 10.1016/j.mcn.2015.11.010
- Naphade, S., Tshilenge, K. T., and Ellerby, L. M. (2019). Modeling polyglutamine expansion diseases with induced pluripotent stem cells. *Neurotherapeutics* 16, 979–998. doi: 10.1007/s13311-019-00810-8
- Nekrasov, E. D., Vigont, V. A., Klyushnikov, S. A., Lebedeva, O. S., Vassina, E. M., Bogomazova, A. N., et al. (2016). Manifestation of Huntington's disease pathology in human induced pluripotent stem cell-derived neurons. *Mol. Neurodegener.* 11:27. doi: 10.1186/s13024-016-0092-5
- Ooi, J., Langley, S. R., Xu, X., Utami, K. H., Sim, B., Huang, Y., et al. (2019). Unbiased profiling of isogenic Huntington disease hPSC-derived CNS and peripheral cells reveals strong cell-type specificity of CAG length effects. *Cell Rep.* 123, 48–57. doi: 10.1016/j.celrep.2019.02.008
- Pani, B., Liu, X., Bollimuntha, S., Cheng, K. T., Niesman, I. R., Zheng, C., et al. (2013). Impairment of TRPC1-STIM1 channel assembly and AQP5 translocation compromise agonist-stimulated fluid secretion in mice lacking caveolin1. *J. Cell Sci.* 126, 667–675. doi: 10.1242/jcs.118943
- Panov, A. V., Gutekunst, C. A., Leavitt, B. R., Hayden, M. R., Burke, J. R., Strittmatter, W. J., et al. (2002). Early mitochondrial calcium defects in Huntington's disease are a direct effect of polyglutamines. *Nat. Neurosci.* 5, 731–736. doi: 10.1038/nn884
- Park, C. Y., Shcheglovitov, A., and Dolmetsch, R. (2010). The CRAC channel activator STIM1 binds and inhibits L-type voltage-gated calcium channels. *Science* 330, 101–105. doi: 10.1126/science.1191027
- Parvez, S., Beck, A., Peinelt, C., Soboloff, J., Lis, A., Monteilh-Zoller, M., et al. (2008). STIM2 protein mediates distinct store-dependent and store-independent modes of CRAC channel activation. *FASEB J.* 22, 752–761. doi: 10.1096/fj.07-9449com
- Ryazantseva, M., Goncharova, A., Skobeleva, K., Erokhin, M., Methner, A., and Georgiev, P. (2018). Presenilin-1 delta E9 mutant induces STIM1-driven store-operated calcium channel hyperactivation in hippocampal neurons. *Mol. Neurobiol.* 55, 4667–4680. doi: 10.1007/s12035-017-0674-4
- Ryazantseva, M., Skobeleva, K., Glushankova, L., and Kaznacheyeva, E. (2016). Attenuated presenilin-1 endoproteolysis enhances store-operated calcium currents in neuronal cells. *J. Neurochem.* 136, 1085–1095. doi: 10.1111/jnc.13495
- Ryazantseva, M., Skobeleva, K., and Kaznacheyeva, E. (2013). Familial Alzheimer's disease-linked presenilin-1 mutation M146V affects store-operated calcium entry: does gain look like loss? *Biochimie* 95, 1506–1509. doi: 10.1016/j.biochi.2013.04.009
- Secondo, A., Bagetta, G., and Amantea, D. (2018). On the role of store-operated calcium entry in acute and chronic neurodegenerative diseases. *Front. Mol. Neurosci.* 11:87. doi: 10.3389/fnmol.2018.00087
- Shalygin, A., Skopin, A., Kalinina, V., Zimina, O., Glushankova, L., Mozhayeva, G. N., et al. (2015). STIM1 and STIM2 proteins differently regulate endogenous store-operated channels in HEK293 cells. *J. Biol. Chem.* 290, 4717–4727. doi: 10.1074/jbc.M114.601856
- Silva, F. R., Miranda, A. S., Santos, R. P. M., Olmo, I. G., Zamponi, G. W., Dobransky, et al. (2017). N-type  $Ca^{2+}$  channels are affected by full-length mutant huntingtin expression in a mouse model of Huntington's disease. *Neurobiol. Aging* 55, 1–10. doi: 10.1016/j.neurobiolaging.2017.03.015
- Sukkar, B., Hauser, S., Pelzl, L., Hosseinzadeh, Z., Sahu, I., and Al-Maghout, T. (2018). Inhibition of Lithium sensitive Orai1/ STIM1 expression and store operated  $Ca^{2+}$  entry in chorea-acanthocytosis neurons by NF- $\kappa$ B inhibitor Wogonin. *Cell. Physiol. Biochem.* 51, 278–289. doi: 10.1159/000495229

- Sun, S., Zhang, H., Liu, J., Popugaeva, E., Xu, N. J., Feske, S., et al. (2014). Reduced synaptic STIM2 expression and impaired store-operated calcium entry cause destabilization of mature spines in mutant presenilin mice. *Neuron* 82, 79–93. doi: 10.1016/j.neuron.2014.02.019
- Switońska, K., Szlachcic, W. J., Handschuh, L., Wojciechowski, P., Marczak, Ł., Stelmaszczuk, M., et al. (2018). Identification of altered developmental pathways in human juvenile HD iPSC with 71Q and 109Q using transcriptome profiling. *Front. Cell. Neurosci.* 12:528. doi: 10.3389/fncel.2018.00528
- Tang, T. S., Slow, E., Lupu, V., Stavrovskaya, I. G., Sugimori, M., Llinás, R., et al. (2005). Disturbed  $\text{Ca}^{2+}$  signaling and apoptosis of medium spiny neurons in Huntington's disease. *Proc. Natl. Acad. Sci. U. S. A.* 102, 2602–2607. doi: 10.1073/pnas.0409402102
- Tang, T. S., Tu, H., Chan, E. Y., Maximov, A., Wang, Z., Wellington, C. L., et al. (2003). Huntingtin and huntingtin-associated protein 1 influence neuronal calcium signaling mediated by inositol-(1,4,5) triphosphate receptor type 1. *Neuron* 39, 227–239. doi: 10.1016/S0896-6273(03)00366-0
- Tobe, M., Isobe, Y., Tomizawa, H., Nagasaki, T., Takahashi, H., and Hayashi, H. (2003). A novel structural class of potent inhibitors of NF- $\kappa$ B activation: structure-activity relationships and biological effects of 6-aminoquinazoline derivatives. *Bioorg. Med. Chem.* 11, 3869–3878. doi: 10.1016/S0968-0896(03)00438-3
- Tsvetkov, A. S., Arrasate, M., Barmada, S., Ando, D. M., Sharma, P., Shaby, B. A., et al. (2013). Proteostasis of polyglutamine varies among neurons and predicts neurodegeneration. *Nat. Chem. Biol.* 9, 586–592. doi: 10.1038/nchembio.1308
- Vigont, V., Kolobkova, Y., Skopin, A., Zimina, O., Zenin, V., Glushankova, L., et al. (2015). Both Orai1 and TRPC1 are involved in excessive store-operated calcium entry in striatal neurons expressing mutant huntingtin exon 1. *Front. Physiol.* 6:337. doi: 10.3389/fphys.2015.00337
- Vigont, V., Nekrasov, E., Shalygin, A., Gusev, K., Klushnikov, S., Illarioshkin, S., et al. (2018). Patient-specific iPSC-based models of Huntington's disease as a tool to study store-operated calcium entry drug targeting. *Front. Pharmacol.* 9:696. doi: 10.3389/fphar.2018.00696
- Vonsattel, J. P., and DiFiglia, M. (1998). Huntington disease. *J. Neuropathol. Exp. Neurol.* 57, 369–384. doi: 10.1097/00005072-199805000-00001
- Weber, J. J., Clemensson, L. E., Schiöth, H. B., and Nguyen, H. P. (2019). Olesoxime in neurodegenerative diseases: scrutinising a promising drug candidate. *Biochem. Pharmacol.* 168, 305–318. doi: 10.1016/j.bcp.2019.07.002
- Weber, K., Mock, U., Petrowitz, B., Bartsch, U., and Fehse, B. (2010). Lentiviral gene ontology (LeGO) vectors equipped with novel drug-selectable fluorescent proteins: new building blocks for cell marking and multi-gene analysis. *Gene Ther.* 17, 511–520. doi: 10.1038/gt.2009.149
- Wegierski, T., and Kuznicki, J. (2018). Neuronal calcium signaling via store-operated channels in health and disease. *Cell Calcium* 74, 102–111. doi: 10.1016/j.ceca.2018.07.001
- Wu, J., Ryskamp, D., Birnbaumer, L., and Bezprozvanny, I. (2018). Inhibition of TRPC1-dependent store-operated calcium entry improves synaptic stability and motor performance in a mouse model of Huntington's disease. *J. Huntingtons. Dis.* 7, 35–50. doi: 10.3233/JHD-170266
- Wu, J., Ryskamp, D. A., Liang, X., Egorova, P., Zakharova, O., and Hung, G. (2016). Enhanced store-operated calcium entry leads to striatal synaptic loss in a Huntington's disease mouse model. *J. Neurosci.* 36, 125–141. doi: 10.1523/JNEUROSCI.1038-15.2016
- Wu, J., Shih, H. P., Vigont, V., Hrdlicka, L., Diggins, L., Singh, C., et al. (2011). Neuronal store-operated calcium entry pathway as a novel therapeutic target for Huntington's disease treatment. *Chem. Biol.* 18, 777–793. doi: 10.1016/j.chembiol.2011.04.012
- Yap, K. A., Shetty, M. S., Garcia-Alvarez, G., Lu, B., Alagappan, D., Oh-Hora, M., et al. (2017). STIM2 regulates AMPA receptor trafficking and plasticity at hippocampal synapses. *Neurobiol. Learn. Mem.* 138, 54–61. doi: 10.1016/j.nlm.2016.08.007

**Conflict of Interest:** The authors declare that the research was conducted in the absence of any commercial or financial relationships that could be construed as a potential conflict of interest.

Copyright © 2021 Vigont, Grekhnev, Lebedeva, Gusev, Volovikov, Skopin, Bogomazova, Shuvalova, Zubkova, Khomyakova, Glushankova, Klyushnikov, Illarioshkin, Lagarkova and Kaznacheyeva. This is an open-access article distributed under the terms of the Creative Commons Attribution License (CC BY). The use, distribution or reproduction in other forums is permitted, provided the original author(s) and the copyright owner(s) are credited and that the original publication in this journal is cited, in accordance with accepted academic practice. No use, distribution or reproduction is permitted which does not comply with these terms.



# Transmembrane Domain 3 (TM3) Governs Orai1 and Orai3 Pore Opening in an Isoform-Specific Manner

Adéla Tiffner<sup>†</sup>, Lena Maltan<sup>†</sup>, Marc Fahrner, Matthias Sallinger, Sarah Weiß, Herwig Grabmayr, Carmen Höglinger and Isabella Derler\*

JKU Life Science Center, Institute of Biophysics, Johannes Kepler University Linz, Linz, Austria

## OPEN ACCESS

### Edited by:

Francisco Javier Martin-Romero,  
University of Extremadura, Spain

### Reviewed by:

Yubin Zhou,  
Texas A&M University, United States  
Xuexin Zhang,  
Penn State University College of  
Medicine, United States

### \*Correspondence:

Isabella Derler  
Isabella.derler@jku.at

<sup>†</sup>These authors have contributed  
equally to this work

### Specialty section:

This article was submitted to  
Signaling,  
a section of the journal  
Frontiers in Cell and Developmental  
Biology

**Received:** 30 November 2020

**Accepted:** 21 January 2021

**Published:** 11 February 2021

### Citation:

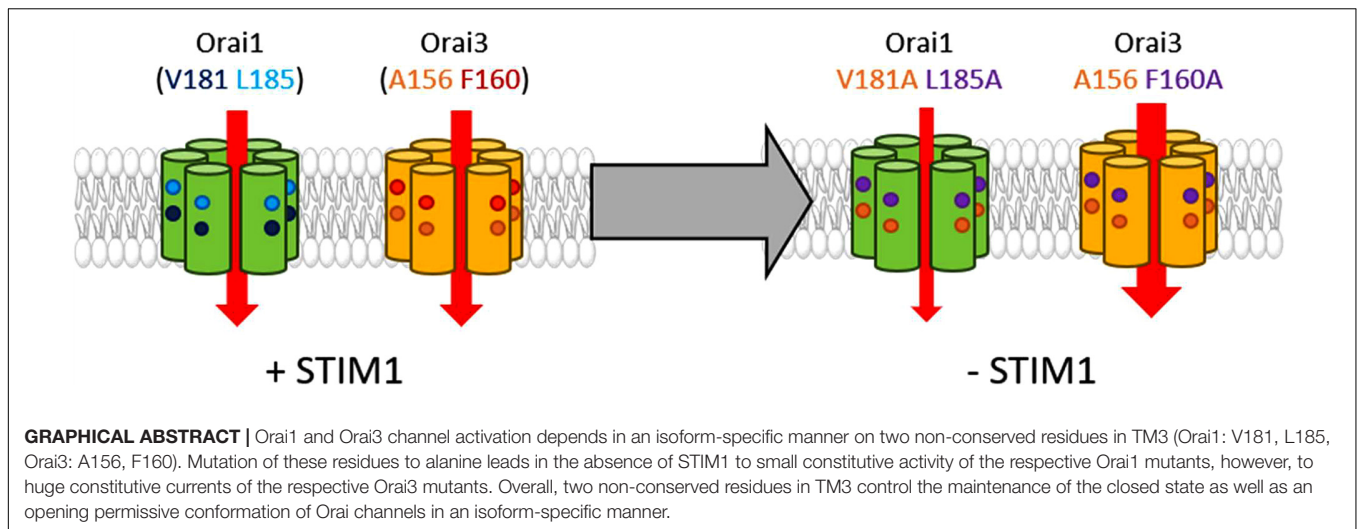
Tiffner A, Maltan L, Fahrner M,  
Sallinger M, Weiß S, Grabmayr H,  
Höglinger C and Derler I (2021)  
Transmembrane Domain 3 (TM3)  
Governs Orai1 and Orai3 Pore  
Opening in an Isoform-Specific  
Manner.  
Front. Cell Dev. Biol. 9:635705.  
doi: 10.3389/fcell.2021.635705

STIM1-mediated activation of calcium selective Orai channels is fundamental for life. The three Orai channel isoforms, Orai1-3, together with their multiple ways of interplay, ensure their highly versatile role in a variety of cellular functions and tissues in both, health and disease. While all three isoforms are activated in a store-operated manner by STIM1, they differ in diverse biophysical and structural properties. In the present study, we provide profound evidence that non-conserved residues in TM3 control together with the cytosolic loop2 region the maintenance of the closed state and the configuration of an opening-permissive channel conformation of Orai1 and Orai3 in an isoform-specific manner. Indeed, analogous amino acid substitutions of these non-conserved residues led to distinct extents of gain- (GoF) or loss-of-function (LoF). Moreover, we showed that enhanced overall hydrophobicity along TM3 correlates with an increase in GoF mutant currents. Conclusively, while the overall activation mechanisms of Orai channels appear comparable, there are considerable variations in gating checkpoints crucial for pore opening. The elucidation of regions responsible for isoform-specific functional differences provides valuable targets for drug development selective for one of the three Orai homologs.

**Keywords:** Orai1, Orai3, STIM1, isoform-specific activation, CRAC channel

## INTRODUCTION

A plethora of processes in the human body, for instance, the immune system or neuronal signaling, is triggered by elevations of cytosolic calcium ( $\text{Ca}^{2+}$ ) ion concentrations (Berridge et al., 2000, 2003; Lee et al., 2010). The  $\text{Ca}^{2+}$  release-activated  $\text{Ca}^{2+}$  (CRAC) channel represents a major pathway for  $\text{Ca}^{2+}$  transport into the cell (Feske et al., 2006; Parekh, 2008). It is activated upon the release of intracellular  $\text{Ca}^{2+}$  from the endoplasmic reticulum (ER). The link between  $\text{Ca}^{2+}$  store depletion and subsequent  $\text{Ca}^{2+}$  entry from the extracellular space into the cell is fully established by two proteins, the stromal interaction molecule 1 (STIM1) and Orai. While STIM1 is a  $\text{Ca}^{2+}$  sensing protein in the ER membrane, Orai proteins are highly  $\text{Ca}^{2+}$  selective ion channels located in the plasma membrane (PM) (Liou et al., 2005; Zhang et al., 2005, 2006; Feske et al., 2006; Mercer et al., 2006; Peinelt et al., 2006; Prakriya et al., 2006; Soboloff et al., 2006; Spassova et al., 2006; Vig et al., 2006; Wu et al., 2006; Yeromin et al., 2006; Cahalan and Chandy, 2009). ER  $\text{Ca}^{2+}$



depletion initiated via receptor-ligand binding at the plasma membrane leads to STIM1 activation, its coupling to and activation of Orai channels (Wu et al., 2006; Barr et al., 2008; Muik et al., 2008; Cahalan, 2009; Calloway et al., 2009; Park et al., 2009; Muik et al., 2011; Srikanth and Gwack, 2013; Zhou et al., 2013; Gudlur et al., 2014; Butorac et al., 2020). CRAC channels are highly  $\text{Ca}^{2+}$  selective with currents exhibiting a reversal potential in the range of +50 mV. Typical CRAC channel hallmarks further include fast  $\text{Ca}^{2+}$  dependent inactivation (FCDI), enhancement in currents in a divalent free (DVF)  $\text{Na}^{+}$ - compared to a  $\text{Ca}^{2+}$ -containing solution and inhibition by 50  $\mu\text{M}$  2-APB (Prakriya and Lewis, 2006; Yamashita et al., 2007; Derler et al., 2018; Krizova et al., 2019).

Several structures of *Drosophila melanogaster* Orai (dOrai), two in the closed state and four of constitutively open dOrai mutants, are currently available (Hou et al., 2012, 2018; Liu et al., 2019; Hou et al., 2020). These structures consistently suggest that Orai channels form hexameric complexes. Each subunit is composed of four transmembrane domains that are connected by two extracellular loop regions and a cytosolic one, and flanked by an N- and a C-terminal strand (Feske et al., 2006; Hewavitharana et al., 2007; Hou et al., 2012). The pore region in the center of the channel complex is established by six TM1 domains and is surrounded by TM2 and TM3 in a second and by TM4 in a third ring (Zhou et al., 2016, 2017). At the end of TM4, a bent region, the so-called nexus, forms the connection to the C-terminus. Orai C-termini represent the main coupling sites for STIM1 (Li et al., 2007; Muik et al., 2008; Park et al., 2009; Derler et al., 2013; McNally et al., 2013; Zheng et al., 2013; Palty and Isacoff, 2015). Other cytosolic regions are also essential for STIM1 mediated activation (Derler et al., 2013, 2018; Fahrner et al., 2018; Butorac et al., 2019), however, whether they function as direct interaction sites for STIM1 is still a matter of debate.

An arsenal of Orai1 gain- (GoF) and loss-of-function (LoF) mutants led to the hypothesis that channel activation is accompanied by interdependent TM domain motions (Yeung et al., 2018; Tiffner et al., 2020b, 2021). We recently demonstrated via a screen of double mutants, systematically combining

one GoF and one LoF mutation, that Orai1 pore opening indispensably requires global conformational changes of the channel complex and clearance of a series of gating checkpoints (Tiffner et al., 2020b). Structural resolutions together with functional studies suggest that the main conformational changes upon Orai1 activation occur along the pore-lining TM1 and at the outmost side of the channel complex (Hou et al., 2012, 2018, 2020; Liu et al., 2019). While structural alterations within the pore are well understood, the extent of structural changes at the Orai1 channel periphery is still under discussion (Butorac et al., 2020; Zhou et al., 2019). Molecular dynamic (MD) simulations suggest twist-to-open motions with counter-clockwise rotations of TM1 and dilation of the pore at the extracellular side (Dong et al., 2019). At the intracellular side, alternate Orai1 subunits either move outward or show a clockwise rotation. The most recent cryo-EM structure suggests that Orai activation is accompanied by rigid body outward movements of each subunit (Hou et al., 2020).

The Orai protein family consists of three homologs: Orai1, Orai2, and Orai3. Their commonalities include store-operated STIM1 mediated activation, high  $\text{Ca}^{2+}$  selectivity and overall structural design (Prakriya et al., 2006; Lis et al., 2007). Nevertheless, they possess several distinct functional and structural characteristics.

While TM1 is fully conserved among Orai isoforms, TM2, TM3, and TM4 have approximately 80% sequence identity. Substantial distinctions in the sequence occur in the cytosolic- and extracellular domains (Shuttleworth, 2012; Hogan and Rao, 2015; Fahrner et al., 2018; Krizova et al., 2019). These differences are responsible for a variety of functional alterations.

STIM1 mediated maximum Orai1 currents are 2–3 fold enhanced compared to that of Orai2 and Orai3 (Lis et al., 2007; Frischauf et al., 2009). This difference occurs likely due to the presence of a polybasic- and proline-rich region in the N-terminus of Orai1, but not in that of Orai2 and Orai3 (Li et al., 2007; Takahashi et al., 2007; Fahrner et al., 2009; Yuan et al., 2009). Moreover, FCDI is three times more pronounced for Orai3 compared to that of Orai1 and Orai2. Additionally,

only STIM1 mediated Orai1 currents exhibit subsequent to fast inactivation, reaching its maximum within the first 100 ms, a reactivation phase upon the application of a hyperpolarizing voltage step (Lis et al., 2007; Lee et al., 2009; Schindl et al., 2009; Derler et al., 2018; Krizova et al., 2019). The reasons for these isoform-specific inactivation profiles are variations in the cytosolic regions of Orai channels (Lee et al., 2009; Frischauf et al., 2011). Well-known enhancements of CRAC channel currents in a DVF versus a  $\text{Ca}^{2+}$  containing solution vary for Orai isoforms. The ratio of currents  $I_{\text{DVF}}:I_{\text{Ca}^{2+}}$  is lower for STIM1/Orai1 versus STIM1/Orai3, likely due to less pronounced FCDI of Orai1 compared to Orai3 (Prakriya and Lewis, 2006; Derler et al., 2018; Krizova et al., 2019). Moreover, STIM1 mediated currents of Orai isoforms respond distinctly to the well-known drug 2-aminoethylidiphenyl borate (2-APB). Fifty  $\mu\text{M}$  2-APB inhibit STIM1 induced Orai1 and Orai2 currents, while Orai3 currents independent of the presence of STIM1 display strongly enhanced, double rectifying currents (Lis et al., 2007; Derler et al., 2008; Peinelt et al., 2008; Putney, 2010; Krizova et al., 2019). Furthermore, Orai isoforms responded with distinct pharmacological profiles to the two compounds Synta66 and IA65 (Zhang et al., 2020).

Coiled-coil probability predictions revealed that this structural arrangement is 15–17 fold higher for Orai2 and Orai3 C-terminus compared to the Orai1 C-terminus (Frischauf et al., 2009). A single point mutation (L273S/D) within Orai1 C-terminus is sufficient to abolish STIM1 coupling and mediated activation. Contrary, in Orai2 and Orai3 C-termini, two point mutations are required to completely impair STIM1 mediated activation. Analogously, also within STIM1 C-terminus, a single point mutation was sufficient to abolish coupling to Orai1, while a double point mutation was required to block coupling to Orai2 and Orai3 (Li et al., 2007; Muik et al., 2008; Frischauf et al., 2009).

Furthermore, we have recently reported that the communication of the Orai1 N-terminus and the loop2 region is indispensable for Orai1 pore opening and occurs in an isoform-specific manner (Derler et al., 2013). This isoform-specific communication is especially reflected by analog Orai N-terminal truncation mutants, among which only those of Orai1 lose function, while the ones of Orai2 and Orai3 remain functional, despite the remaining N-terminal region is fully conserved. The latter is subject to distinct structural properties of the loop2, the cytosolic portion connecting TM2 and TM3 (Derler et al., 2013; Fahrner et al., 2018). In contrast to Orai3, the flexible loop2 region in Orai1 is longer and thus, forms inhibitory contacts with Orai1 N-terminus as soon as it is truncated to a certain position. Only the swap of Orai3 loop2 restores the activity of the loss-of-function Orai1 N-terminal truncation mutants (Fahrner et al., 2018).

Typically, loss of activity of constitutive Orai1 mutants due to certain N-terminal deletions can be restored by the swap of Orai3-loop2 also in the absence of STIM1 (Fahrner et al., 2018). Intriguingly, this is not the case for the constitutively active Orai1 hinge mutant, containing the substitutions  $_{261}\text{ANSGA}_{265}$  at the bent connection between TM4 and the C-terminus (Zhou et al., 2016). This constitutive channel loses its function upon its N-terminal truncation and remains non-functional

also upon the exchange of its loop2 by that of Orai3 (Butorac et al., 2020).

In the present study, we report that Orai TM3 controls the closed and the open state of Orai1 and Orai3 in an isoform-specific manner. This distinct regulation is accomplished by two non-conserved residues in TM3 (in Orai1: V181, L185; in Orai3: A156, F160) which are required for both, the maintenance of the closed state and an opening permissive conformation. Orai isoform-specific differences of TM3 together with the loop2 regions determine the extent of pore opening and  $\text{Ca}^{2+}$  ion currents.

## EXPERIMENTAL PROCEDURES

### Molecular Biology

For N-terminal fluorescence labeling of human Orai1 (Orai1; accession number NM\_032790, provided by the laboratory of A. Rao) as well as human Orai3 (Orai3; accession number NM\_152288, provided by the laboratory of L. Birnbaumer), the constructs were cloned into the pEYFP-C1 (Clontech) expression vector via *KpnI/XbaI* (Orai1) and *BamHI/XbaI* (Orai3) restriction sites, respectively. Chimeric constructs were cloned via SOEing (Splicing by Overlap Extension) into the pEYFP-C1 (Clontech) expression vector for N-terminal fluorescence labeling. Site-directed mutagenesis of all the mutants was performed using the QuikChange<sup>TM</sup> XL site-directed mutagenesis kit (Stratagene) with the corresponding Orai1, Orai3 and/or Orai1-Orai3 chimeric constructs serving as a template, respectively.

Human STIM1 (STIM1; Accession number: NM\_003156), N-terminally ECFP-tagged, was kindly provided by T. Meyer's Lab, Stanford University.

The integrity of all resulting clones was confirmed by sequence analysis (Eurofins Genomics/Microsynth).

### Cell Culture and Transfection

The transient transfection of human embryonic kidney (HEK) 293 cells was performed (Derler et al., 2006) using the TransFectin Lipid Reagent (Bio-Rad) (New England Biolabs). For each transfection, Orai1 plasmids together with STIM1 plasmids were used at a 1:1 ratio, while for Orai3 constructs together with STIM1 plasmids at a 1.5:1 ratio. Regularly, potential cell contamination with mycoplasma species was tested using VenorGem Advanced Mycoplasma Detection kit (VenorGEM).

### $\text{Ca}^{2+}$ Fluorescence Measurements

HEK293 cells, transfected with a ratio of 1:1.5 and 1.5:1.5 for the Orai1/R-Geco1.2 (purchased from Addgene, Wu et al., 2013) and Orai3/R-Geco1.2 plasmids, respectively, were grown on coverslips for 1 day. Coverslips were transferred to an extracellular solution without  $\text{Ca}^{2+}$  and mounted on an Axiovert 135 inverted microscope (Zeiss, Germany) equipped with a sCMOS-Panda digitale Scientific Grade camera 4.2 MPixel and a LedHUB LED Light-Engine light source. Excitation of R-Geco1.2 was obtained using the LED spanning 505 – 600 nm together with a Chroma filter allowing excitation

between 540 and 580 nm.  $\text{Ca}^{2+}$  measurements are shown as normalized intensities of R-Geco1.2 fluorescence in HEK293 cells. Image acquisition and intensity recordings were performed with Visiview5.0.0.0 software (Visitron Systems). A Thomas Wisa perfusion pump was used for extracellular solution exchange during the experiment. All experiments were performed on 3 days and at room temperature.

## Electrophysiology

Electrophysiological recordings that assessed the characteristics of 2–3 constructs were carried out in paired comparison on the same day. Expression patterns and levels of the various constructs were carefully monitored by fluorescence microscopy and were not significantly changed by the introduced mutations. Electrophysiological experiments were performed at 20–24°C, using the patch-clamp technique in the whole-cell recording configuration. For Orai1, Orai3, STIM1/Orai1, STIM1/Orai3 as well as STIM1/Orai1-Orai3 chimera current measurements, voltage ramps were usually applied every 5 s from a holding potential of 0 mV, covering a range of –90 to +90 mV over 1 s. Voltage step protocols were applied from a holding potential of 0 mV to –70 mV for 1.5 s to determine FCDI. The internal pipette solution for passive store-depletion contained (in mM) 3.5  $\text{MgCl}_2$ , 145 Cesium Methane Sulfonate, 8 NaCl, 10 HEPES, 20 EGTA, pH 7.2. Extracellular solution consisted of (in mM) 145 NaCl, 5 CsCl, 1  $\text{MgCl}_2$ , 10 HEPES, 10 glucose, 10  $\text{CaCl}_2$ , pH 7.4.  $\text{Na}^+$ -DVF solution contained (in mM) 150 NaCl, 10 HEPES, 10 glucose, and 10 EDTA pH 7.4. Applied voltages were not corrected for the liquid junction potential, which was determined as +12 mV. All currents were leak-corrected by subtraction of the leak current which remained following 10  $\mu\text{M}$   $\text{La}^{3+}$  application. All experiments were carried out at least on two different days.

Bar graphs in the figures display for Orai1 proteins in the absence of STIM1 the current density at  $t = 0$  s, while in the presence of STIM1 maximum current densities are shown.

## Confocal Fluorescence Microscopy

Confocal microscopy for localization experiments was performed similarly to Singh et al. (2006) and for NFAT subcellular localization studies in analogy to Schober et al. (2019). In brief, a CSU-X1 Real-Time Confocal System (Yokogawa Electric Corporation) was used for recording fluorescence images connected to two CoolSNAP HQ2 CCD cameras (Photometrics) and a dual port adapter (dichroic: 505lp; cyan emission filter: 470/24; yellow emission filter: 535/30; Chroma Technology Corp., United States). All these parts were connected to an Axio Observer Z1 inverted microscope (Carl Zeiss) with two diode lasers (445 and 515 nm, Visitron Systems) and placed on a Vision IsoStation anti-vibration table (Newport Corporation). The VisiView software package (v2.1.4, Visitron Systems) was used for controlling and image generation of the confocal system. Threshold determination and background subtraction for image correction had to be done. YFP and CFP images were recorded with an illumination-time of about 300–400 ms.

Images of Orai isoforms as well as NFAT localization were created and analyzed with a custom-made software integrated into MATLAB (v7.11.0, The MathWorks, Inc.).

ImageJ was employed for subcellular localization analysis of the NFAT transcription factors by intensity measurements of the cytosol and nucleus, distinguishing between three different populations with different nucleus/cytosol ratios: inactive ( $<0.85$ ), homogenous (0.85–1.15), and active ( $>1.15$ ).

All experiments were performed on three different days at room temperature and the resulting data are presented as mean  $\pm$  S.E.M. (standard error of the mean) for the indicated number of experiments.

## Hydrophobicity Profiles

Hydrophobicity profiles (Rose et al., 1985) were determined with a window size of nine amino acids<sup>1</sup>.

## Statistics

Results are presented as means  $\pm$  S.E.M. calculated for the indicated number of experiments. The Mann–Whitney test was performed for statistical comparison of two independent samples considering differences statistically significant at  $p < 0.05$ . For multiple independent samples, we tested for variance homogeneity by Levene Test. As variance homogeneity was not fulfilled, we performed instead of the ANOVA test, the Welch-ANOVA test. Subsequent to Welch-ANOVA we performed the Games-Howell *post hoc* test to determine the pairs which differ statistically significant ( $p < 0.05$ ). Shapiro–Wilk-Test was applied to prove the normal distribution of the respective datasets.

## RESULTS

### TM3 Maintains the Closed State of Orai1 and Orai3 in an Isoform-Specific Manner

Recently, two independent site-directed mutagenesis screens on Orai1 TM domains revealed more than a dozen GoF mutations, suggesting that these positions are critical to maintain the closed state (Yeung et al., 2018; Tiffner et al., 2020b). Comparison of these residues (Yeung et al., 2018; Tiffner et al., 2020b) with analog positions in Orai3 TM domains revealed that most of them are fully conserved, except two positions in TM3 (Table 1), which are explained in the paragraph after the next. Initially, we investigated a few conserved positions in TM2 and TM4. In TM2, the single point mutant Orai3 H109A exhibits constitutive activity, in analogy to the GoF-mutant Orai1 H134A (Frischauf et al., 2017). Both, Orai1 H134A and Orai3 H109A reached in the absence and presence of STIM1 maximal current levels similar to those of STIM1 mediated Orai1 or Orai3 currents (Figures 1A,D,E,H). In TM4, Orai3 S248C (analog of the GoF mutant Orai1 S239C) (Figures 1C,D,G,H) and Orai3 P254L (analog of the GoF mutant Orai1 P245L) (Nesin et al., 2014; Derler et al., 2018) exhibit also constitutive activity. Constitutive currents of both, Orai1 S239C as well as Orai3 S248C in the absence of STIM1 are further enhanced in the presence of STIM1 (Figures 1C–E,G,H).

Moreover, we recently discovered that among the residues which contribute to the maintenance of the closed state,

<sup>1</sup><https://web.expasy.org/protscale/>

**TABLE 1** | Comparison of analog positions in Orai1 and Orai3 known especially from Orai1 to be involved in the maintenance of the closed state and formation of an opening-permissive pore conformation (Yeung et al., 2018; Tiffner et al., 2020b).

TM1		TM2		TM3		TM4	
Orai1	Orai3	Orai1	Orai3	Orai1	Orai3	Orai1	Orai3
V107	V82	L130	L105	E190	E165	A235	Q243
V102	V77	H134	H109	F187	F162	S239	S248
F99	F74	F136	F111	<b>L185</b>	<b>F160</b>	P245	P254
G98	G73	A137	A112	<b>V181</b>	<b>A156</b>	F250	F259
S97	S72	L138	L113	W176	W151		
		S141	S116				

The main focus of the study lied on bold-marked non-conserved residues of TM3 domain.

some additionally determine an opening permissive channel conformation. This was proven via site-directed mutagenesis leading at a single position in dependence of the inserted amino acid not only to gain- but also to loss-of-function (GoF and LoF, respectively) (Frischauf et al., 2017; Yeung et al., 2018; Tiffner et al., 2020b). In analogy to Orai1 LoF mutants (Orai1 H134W, Orai1 S239W), we discovered that Orai3 H109W and Orai3 S248W are LoF mutations as well (**Supplementary Figures 1a,c,d**).

In TM3, the non-conserved residues that maintain the closed state, represent V181 and L185 in Orai1 which correspond to A156 and F160 in Orai3 (**Figure 1**, scheme and **Table 1**). Both single point mutants, Orai1 V181A and Orai1 L185A, led to small constitutive activity in the absence of STIM1, which is further enhanced in the presence of STIM1 (**Figures 1B,D**). Despite the V181A mutation mimics the analog position A156 in Orai3 wild-type, Orai3 maintains the quiescent state. This position will be focused on later in the text. Interestingly, the analog mutant of Orai1 L185A, Orai3 F160A, displays significantly enhanced constitutive activity (**Figures 1F,H**) to similar extents in the absence and presence of STIM1 in comparison to STIM1 mediated Orai3 wild-type currents. Due to the distinct extents of constitutive currents upon alanine substitutions at these non-conserved positions in TM3, we suppose that they contribute to the maintenance of the closed state in an isoform-specific manner.

Diverse other mutations of F160 led either to gain-of-function or STIM1-mediated activation (**Supplementary Figures 1h-j**), in analogy to Orai1 L185X mutants (Tiffner et al., 2020b). While Orai3 F160W showed only store-operated activation in the presence of STIM1, Orai3 F160L displayed tiny constitutive currents, which were further enhanced in the presence of STIM1. Orai3 F160S and Orai3 F160G exhibit constitutive activity similar to Orai3 F160A (**Supplementary Figures 1h-j**). We discovered no mutation of F160 in Orai3 that led to loss-of-function similar to our findings for L185 in Orai1 (Tiffner et al., 2020b).

Among different amino acid substitutions at position A156 in Orai3, it is of note that Orai3 A156K led to robust constitutive activity (**Supplementary Figures 1e,g**) similar to its analog Orai1 V181K (**Figure 1D** and Tiffner et al., 2020b). Orai3 A156G, Orai3

A156L and Orai3 A156S exhibited activation only in a store-operated manner via STIM1. Orai3 A156W is a LoF-mutant in the absence as well as the presence of STIM1 (**Supplementary Figures 1e-g**), in contrast to its analog Orai1 V181W which activated in a store-operated manner by STIM1 (Tiffner et al., 2020b). Orai3 A156F, interestingly, lost plasma membrane expression (**Supplementary Figure 2a**), contrary to its analog Orai1 V181F, representing a LoF mutant (Tiffner et al., 2020b) with maintained plasma membrane expression (**Supplementary Figure 2b**). Thus, position V181 in Orai1 and its analog A156 in Orai3 are further involved in an isoform-specific manner in the formation of an opening-permissive conformation.

To determine whether other conserved hydrophobic residues possess also an isoform-specific role on Orai function, we investigated additionally the impact of some of them along TM3, in particular, one helical turn up- (Orai1: F178; Orai3 F153) or downstream (Orai1:L188; Orai3: L163) to the two non-conserved residues (**Supplementary Figure 2**, schemes). However, only the substitution of the non-conserved residues to serine varied in their impact on activation, while the mutation of the conserved residues to serine led to a comparable behavior in both Orai isoforms (**Supplementary Figures 2c,d**).

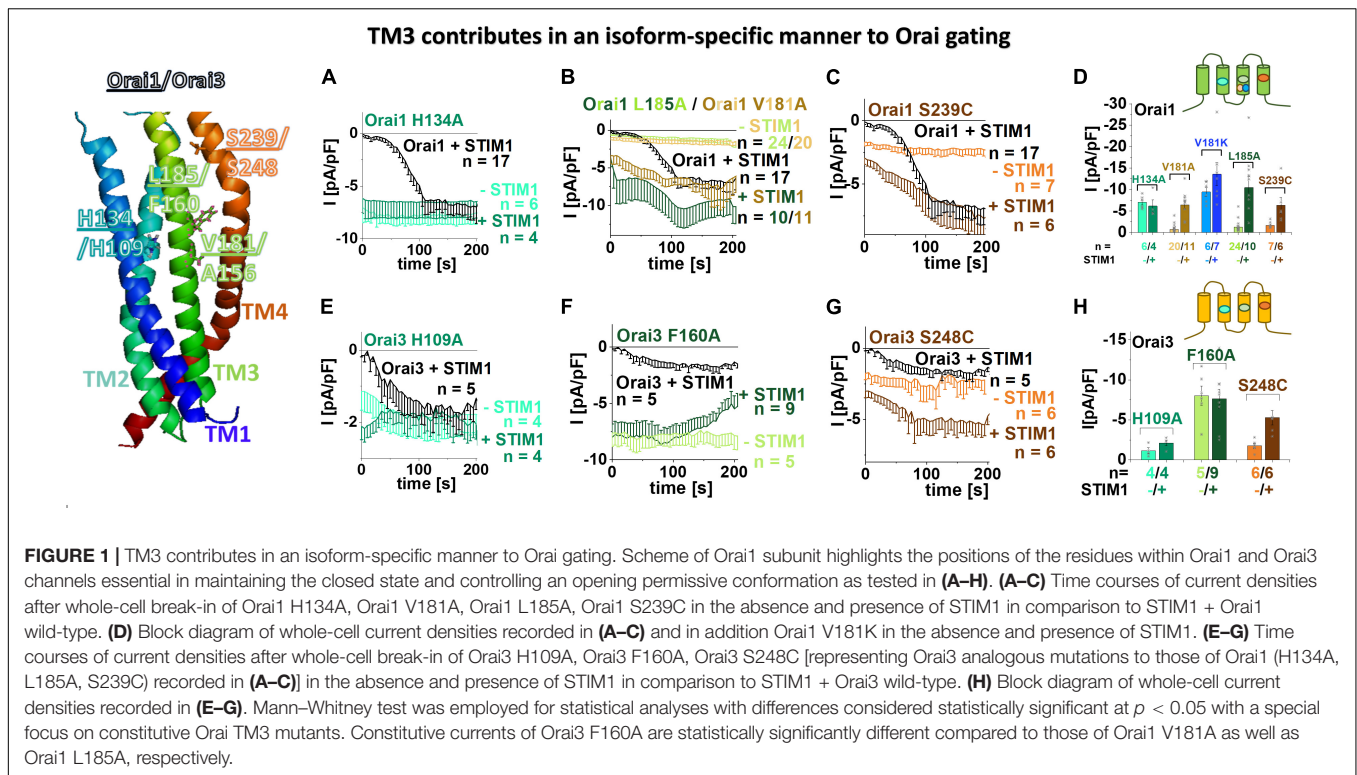
In summary, we discovered that two non-conserved positions in TM3 contribute to a distinct extent to the maintenance of the closed state of Orai channels. Indeed, diverse amino acid substitutions at the analog positions L185 in Orai1 and F160 in Orai3 led to a significant difference in constitutive currents. Additionally, in particular, V181 in Orai1 and A156 in Orai3 configure an opening permissive pore geometry in an isoform-specific manner. In fact, among diverse amino acid substitutions, only the insertion of phenylalanine at V181 in Orai1 and tryptophan at A156 in Orai3 led to loss-of-function.

## Non-conserved Residues in TM3 Modulate Orai1 and Orai3 Mediated $\text{Ca}^{2+}$ Entry and NFAT Translocation in an Isoform-Specific Manner

To corroborate our electrophysiological data on the strong difference in the extent of current densities of constitutively active Orai TM3 point mutations, we additionally examined the prominent ones via the complementary assays  $\text{Ca}^{2+}$  imaging and activation of the transcription factor NFAT (nuclear factor of activated T cells).

As expected, overexpression of Orai1 and Orai3, respectively, in HEK 293 cells yielded no enhancements in  $\text{Ca}^{2+}$  levels upon the exchange from a 0 mM  $\text{Ca}^{2+}$  to a 2 mM  $\text{Ca}^{2+}$  containing solution, as determined via fluorescence intensity of R-Geco1.2 (**Figures 2A,D**). In contrast, all point mutants Orai1 V181A, Orai1 V181K, Orai1 L185A as well as Orai3 F160A exhibited robust enhancements in  $\text{Ca}^{2+}$  levels upon the switch to a  $\text{Ca}^{2+}$  containing solution (**Figures 2A,D**). Remarkably, in accord with our electrophysiological results, Orai1 V181A and Orai1 L185A showed significantly lower  $\text{Ca}^{2+}$  entry compared to Orai1 V181K and Orai3 F160A (**Figures 2A,D**).

Furthermore, while Orai1 and Orai3 expressing cells showed no detectable NFAT translocation to the nucleus, the expression



of Orai1 V181A and Orai1 L185A led to NFAT translocation in  $\sim 60 - 70\%$  of the cells, and the presence of Orai1 V181K and Orai3 F160A triggered NFAT translocation in  $\sim 90 - 100\%$  of the cells (Figures 2B,C,E,F). These results are in accordance with the enhanced constitutive activity of Orai1 V181K and Orai3 F160A versus Orai1 V181A and Orai1 L185A (Figures 1B,D,F,H, 2A,D).

In agreement with our electrophysiological evidence, both, our  $\text{Ca}^{2+}$  imaging and NFAT translocation results, reflect the distinct activities of analog constitutive Orai1 and Orai3 point mutants. Alanine substitutions of the non-conserved residues V181 and L185 in TM3 cause only low constitutive activity. Contrary, A156 in Orai3 wild-type (analog to V181A in Orai1) maintains the closed state, while the F160A in Orai3 (analog to L185A in Orai1) induces robust constitutive activity to comparable levels as obtained with Orai1 V181K.

## Orai3 Requires Comparable Global TM Domain Motions to Enable Pore Opening as Orai1

We recently showed via a library of Orai1 double mutants, containing each one GoF and one LoF mutation that the LoF mutation acts dominant over the GoF mutations independent of their location relative to each other (Tiffner et al., 2020b). These findings suggested that Orai1 pore opening predominantly requires clearance of a set of checkpoints in and a global conformational change of all TM domains. Here we examined whether this also applies to Orai3 since TM3 maintains the closed state of Orai variants in an isoform-specific manner.

To address the latter, we tested several double mutants, each combining a LoF and a GoF mutation, one of which is closer to TM1 than the second within the middle and cytosolic extended transmembrane regions that we previously termed MTR and CETR (Tiffner et al., 2020b).

Initially, analogous to what we have shown previously in Tiffner et al. (2020b), we investigated an Orai3 double point mutant combining a LoF mutation in TM2, H109W, closer to TM1 with a GoF mutation in TM4, S248C, thus, farther apart from TM1, both within the MTR. As expected, we discovered that the H109W acts dominant over S248C (Figures 3A,B). Similarly, Orai3 H109W P254L, also with the LoF mutation closer to TM1 than the GoF mutation, exhibited loss of function (Supplementary Figure 3a).

Next, we investigated an Orai3 double point mutant with the GoF mutation (H109A in TM2) closer to the pore than the LoF mutation (S248W in TM4) within the MTR. In analogy to our findings with Orai1 (Tiffner et al., 2020b), we discovered loss-of-function for Orai3 H109A S248W (Figures 3C,D). Hence, the LoF mutations act dominant over the respective GoF mutations, independent of their location relative to each other and the pore.

Moreover, we investigated two other Orai3 LoF mutations in the CETR of TM2 and TM3, E124K (analog to E149K in Orai1) and L149D (analog to L174D in Orai1) (Supplementary Figure 3b) for their effect on the constitutively active Orai3 F160A (Figures 3E–G). Both LoF mutations act dominant over the GoF mutation, as shown via the impaired activity of Orai3 E124K F160A and Orai3 L149D F160A.

Overall, despite Orai3-TM3 exhibits distinct features than that of Orai1 in maintaining the closed state of the channel, both

## Non-conserved residues in Orai TM3 modulate $\text{Ca}^{2+}$ entry and NFAT translocation in an isoform-specific manner

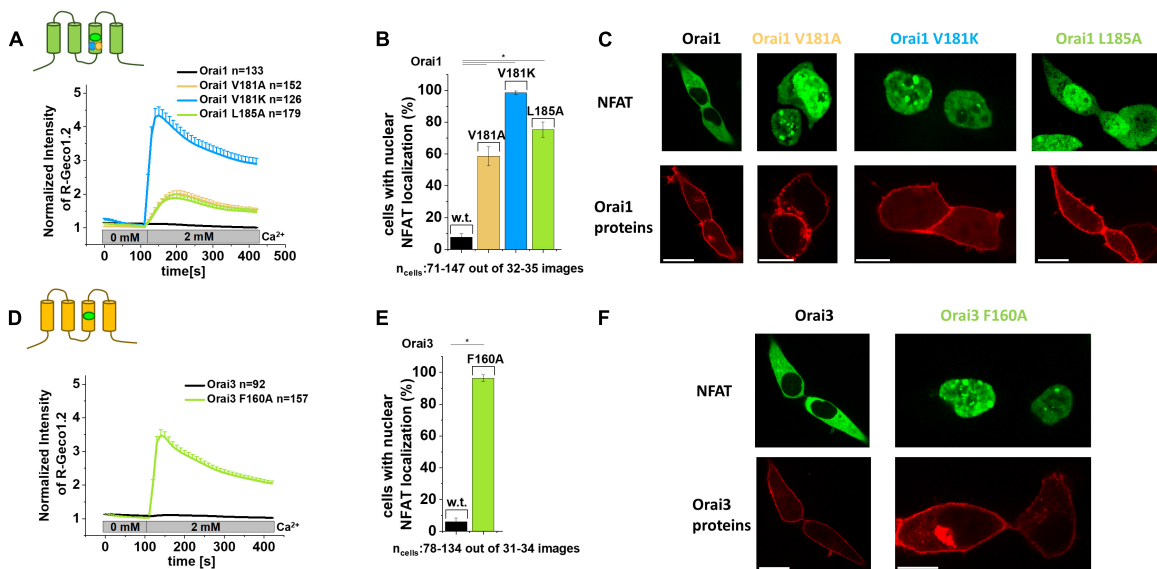


**FIGURE 2 |** Non-conserved residues in Orai TM3 modulate  $\text{Ca}^{2+}$  entry and NFAT translocation in an isoform-specific manner. **(A,D)** Cytosolic  $\text{Ca}^{2+}$  concentrations represented by the normalized intensity of overexpressed R-Geco1.2 were monitored initially in a nominally  $\text{Ca}^{2+}$  free extracellular solution, followed by a solution containing 2 mM  $\text{Ca}^{2+}$  in HEK293 cells overexpressing Orai1, Orai1 V181A, Orai1 V181K or Orai1 L185A **(A)** or Orai3 and Orai3 F160A **(D)**. **(B,E)** The average number of HEK293 cells that exhibit nuclear NFAT localization determined upon co-expression (NFAT-CFP) with Orai1 **(B)** or Orai3 **(E)** or corresponding mutants shown in **(A,D)** after 24 h in 2 mM  $\text{Ca}^{2+}$  containing media. For the analysis 31–34 images of cells containing in total 78–134 cells were used. **(C,F)** Representative images of HEK293 cells co-expressing Orai1 **(C)** or Orai3 **(F)** and corresponding mutants shown in **(A,B,D,E)**, respectively, with NFAT-CFP in the presence of 2 mM  $\text{Ca}^{2+}$  (Scale bar, 10  $\mu\text{m}$ ). In **(A,B)** Welch-ANOVA test (due to lack of variance homogeneity as determined by Levene Test) was used for statistical comparison of Orai1 mutants using the F-distribution  $F(3,252.24) = 98.15$ ,  $p < 0.001$  **(A)**;  $F(3,64.77) = 498.75$ ,  $p < 0.001$  **(B)**. Subsequent to Welch-ANOVA we performed the Games-Howell *post hoc* test to determine the pairs which differ statistically significant ( $p < 0.05$ ). Statistical significance was determined for Orai1 compared to all Orai1 GoF mutants as well as Orai1 V181A and Orai1 L185A compared to Orai1 V181K. In **(D,E)** Mann-Whitney test was employed for statistical analyses with differences considered statistically significant at  $p < 0.05$ . Statistical significance was determined for Orai3 compared to Orai3 F160A.

isoforms require a global conformational change of the channel complex to establish pore opening.

## Swapping Non-conserved Residues in TM3 Unravels Their Significance in Orai Channel Gating

To investigate whether mainly the non-conserved residues in TM3 are responsible for the isoform-specific maintenance of the closed state, we swapped the respective residues in Orai1 and Orai3 (**Figure 4**, table). Orai1 V181A, thus mimicking Orai3 A156, is constitutively active. In contrast, Orai1 L185F, thus analog to Orai3 F160, and Orai1 V181A L185F, thus representing TM3 in particular in terms of A156 and F160 in wild-type Orai3, remain both inactive in the absence of STIM1 (**Figures 4A,B**). Vice versa, Orai3 shows constitutive activity upon the F160L mutation, thus mimicking Orai1 at this site. In contrast, Orai3 A156V, which mimics Orai1 V181, and Orai3 A156V F160L, which mimics both V181 and L185 in Orai1, remain inactive in the absence of STIM1 (**Figures 4D,E**). This indicates that distinct side-chain properties at analog positions in TM3 of Orai1 and Orai3 determine isoform-specific maintenance of the closed and open state. In the presence of STIM1, all mutants show store-operated activation

typical for CRAC channels (**Figures 4B,E** and **Supplementary Figures 3c,d**).

Moreover, we performed the bioinformatic analysis by hydrophobicity profiles, particularly along TM3, employing a prediction program (see section “Materials and Methods”) based on the Rose and Lesser hydrophobicity scale. The hydrophobicity profile of Orai1 and Orai3 displayed four transmembrane domains in correlation with recent studies (Derler et al., 2009) (**Supplementary Figures 3e,f**). The mutation of the valine to alanine in Orai1 (at position 181) caused a reduction in overall hydrophobicity along TM3. In contrast, the introduction of the single point mutation L185F or the double mutations V181A L185F caused an increase in overall hydrophobicity along TM3 (**Figure 4C**). In Orai3, the mutation F160L led to a reduction, while A156V and A156V F160L caused an enhancement in the overall hydrophobicity along TM3 (**Figure 4F**). Hence, the two constitutively active Orai mutants, Orai1 V181A and Orai3 F160L, displayed the lowest overall hydrophobicity along TM3 (**Figures 4C,F**). In contrast, other mutants only active upon store-dependent, STIM1-mediated activation, display an overall hydrophobicity along TM3 comparable or even higher than that of wild-type Orai proteins.

Summarizing, we discovered that the constitutive activity of certain Orai mutants, thus, together with maintenance of the

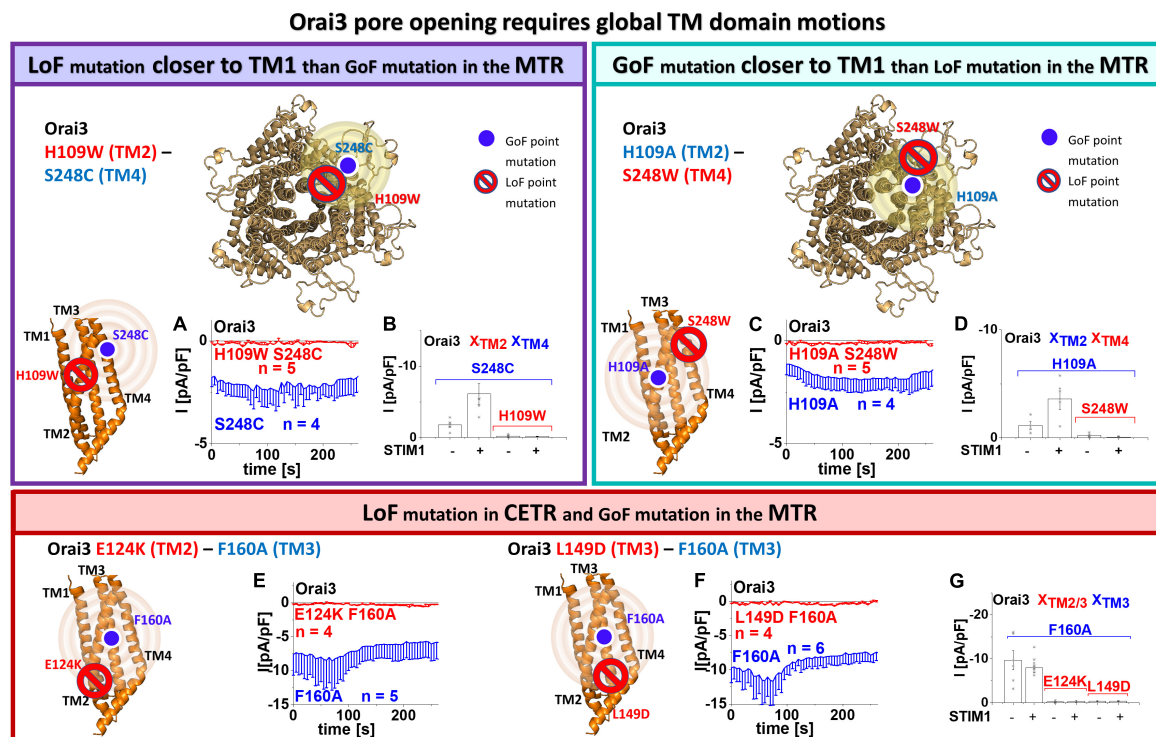


**FIGURE 3 |** Orai3 pore opening requires global TM domain motions. Schemes representing the location of the investigated residues within a single subunit (top – left, bottom left and middle) of Orai3 or the whole channel complex (top – middle), for either LoF or GoF mutation closer to the pore, respectively. The red stop sign indicates the position of the LoF mutation, while the blue circle shows the position of the GoF mutation. The yellow spheres indicate the impact of the GoF mutation on the entire subunit. Special focus was addressed to H109, F160, and S248, due to their location in TM2, thus, close to the pore, in TM3, thus, in the center of the channel complex or TM4, thus, at the periphery of the channel complex, respectively (**A–D**). Via combining a GoF and a LoF mutation at the respective position and investigating their impact on each other, we examined whether interdependent TM domain motions within the entire MTR are necessary for pore opening. (**A**) Time courses of current densities after whole-cell break-in of Orai3 S248C compared to Orai3 H109W S248C in the absence of STIM1. Constitutive currents of the MTR-GoF Orai3 S248C mutant are abolished by the additional introduction of the LoF mutation H109W. (**B**) Block diagram of whole-cell current densities of Orai3 S248C, Orai3 H109W S248C in the absence ( $t = 0$  s) and the presence (maximum current densities) of STIM1 ( $n = 4–5$  cells; values are mean  $\pm$  SEM). (**C**) Time courses of current densities after whole-cell break-in of Orai3 H109A compared to Orai3 H109A S248W in the absence of STIM1. Constitutive currents of the MTR-GoF Orai3 H109A mutant are inhibited by the additional introduction of the LoF mutation S248W. (**D**) Block diagram of whole-cell current densities of Orai3 H109A, Orai3 H109A S248W in the absence ( $t = 0$  s) and the presence (maximum current densities) of STIM1 ( $n = 4–5$  cells; values are mean  $\pm$  SEM). Next, special focus was addressed to the LoF mutations E124K, L149D in the CETR (**E–G**). Via combining a GoF in the MTR and a LoF mutation in the CETR at those respective positions and investigating their impact on each other, we examined whether interdependent TM domain motions within the entire channel complex are necessary for pore opening. (**E,F**) Time courses of current densities after whole-cell break-in of Orai3 F160A compared to Orai3 E124K F160A in the absence of STIM1 and Orai3 F160A compared to Orai3 L149D F160A, respectively. Constitutive currents of the MTR-GoF Orai3 F160A mutant are abolished by the additional introduction of the LoF mutation E124K or L149D. (**G**) Block diagram of whole-cell current densities of Orai3 F160A, Orai3 E124K F160A, Orai3 L149D F160A in the absence ( $t = 0$  s) and the presence (maximum current densities) of STIM1 ( $n = 4–6$  cells; values are mean  $\pm$  SEM). The Welch-ANOVA test (due to lack of variance homogeneity as determined by Levene Test) was used for statistical comparison of Orai3 mutants in (**B,D,G**) using the F-distribution [ $F(3,9.19) = 12.91$ ,  $p < 0.005$  (**B**),  $F(3,5.53) = 17.86$ ,  $p < 0.005$  (**D**),  $F(5,10.69) = 29.15$ ,  $p < 0.001$  (**G**)]. Subsequent to Welch-ANOVA we performed the Games-Howell *post hoc* test to determine the pairs which differ statistically significant ( $p < 0.05$ ). Statistical significance was determined for Orai3 GoF mutant currents compared to Orai3 GoF-LoF double mutant currents (**B,D,G**).

closed state of Orai channels in resting conditions, correlates with the overall hydrophobicity along TM3.

## Enhanced Hydrophobicity at A156 in Orai3 Reduces the Constitutive Activity of Orai3 F160A

In case overall hydrophobicity along TM3 determines the extent of constitutive activity, we hypothesized that enhanced hydrophobicity at position A156 in Orai3 decreases the robust, constitutive activity of Orai3 F160A. Thus, we substituted A156

in Orai3 F160A by different amino acids with an enhancing degree of hydrophobicity, in particular, by valine, leucine, phenylalanine, and tryptophan (**Figure 5**, scheme). Substitution to valine left constitutive activity of the respective double mutant, Orai3 A156V F160A, almost comparable to that of Orai3 F160A. Remarkably, Orai3 A156L F160A, Orai3 A156F F160A and Orai3 A156W F160A led with increased hydrophobicity to a decrease in constitutive activity by about 40 – 50% (**Figures 5A,B**). Intriguingly, in the presence of STIM1, all Orai3 double mutant currents were reduced compared to those in the absence of STIM1. Nevertheless, similar as in the absence

## Swapping TM3 residues in Orai1 and Orai3

### Decrease in overall hydrophobicity along TM3 facilitates pore opening

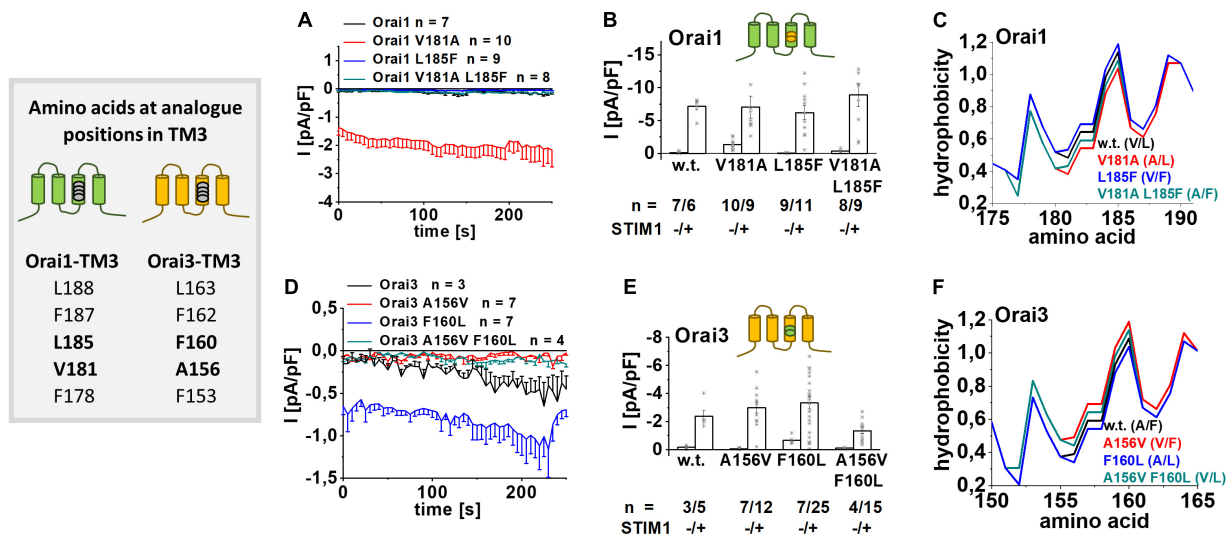


**FIGURE 4 |** Swapping TM3 residues in Orai1 and Orai3 shows that a decrease in overall hydrophobicity along TM3 facilitates pore opening. Table depicting amino acids at the analog position in TM3 in Orai1 and Orai3 (left). **(A)** Time courses of current densities after whole-cell break-in of Orai1 V181A, Orai1 L185F and Orai1 V181A L185F (thus mimicking the positions A156 and F160 in Orai3) compared to Orai1 in the absence of STIM1. **(B)** Block diagram of whole-cell current densities of Orai1, Orai1 V181A, Orai1 L185F, and Orai1 V181A L185F in the absence ( $t = 0$  s) and the presence (maximum current densities) of STIM1 ( $n = 6-11$  cells; values are mean  $\pm$  SEM). **(C)** Hydrophobicity plots of the Orai1 TM3 region (amino acid 175–190) for mutants investigated in **(A)**. **(D)** Time courses of current densities after whole-cell break-in of Orai3 A156V, Orai3 F160L and Orai3 A156V F160L (thus mimicking the positions V181 and L185 in Orai1) compared to Orai3 in the absence of STIM1. **(E)** Block diagram of whole-cell current densities of Orai3, Orai3 A156V, Orai3 F160L, and Orai3 A156V F160L in the absence ( $t = 0$  s) and the presence (maximum current densities) of STIM1 ( $n = 3-25$  cells; values are mean  $\pm$  SEM). **(F)** Hydrophobicity plots of the Orai3 TM3 region (amino acid 150–165) for mutants investigated in **(D)**. Mann-Whitney test was employed for statistical analyses with differences considered statistically significant at  $p < 0.05$ . Statistical significance was determined for different Orai channel currents, either in the absence or presence of STIM1 via pairwise comparison. Currents of Orai1 wild-type, Orai1 L185F and Orai1 V181A L185F are statistically significantly different to those of Orai1 V181A **(B)** in the absence of STIM1. Currents of Orai3 wild-type, Orai3 A156V and Orai3 A156V F160L are statistically significantly different to those of Orai3 F160L **(E)** in the absence of STIM1.

of STIM1, we observed also in the presence of STIM1 with increased hydrophobicity and side-chain size at position A156 a reduction in Orai3 double mutant compared to Orai3 F160A currents (Figure 5B).

Determination of the overall hydrophobicity along TM3 revealed the lowest level for Orai3 F160A in line with its robust constitutive activity. The exchange of A156 by amino acids with enhanced hydrophobicity, as tested in Figures 5A,B, indeed revealed a gradual increase of overall hydrophobicity along TM3 (Figure 5C), in accord with the decrease in currents.

Altogether, we discovered that overall enhancement in hydrophobicity along TM3 in dependence of the inserted amino acid at position 156 in Orai3 correlates with a decrease in constitutive activity of Orai3 F160A. Apparently, Orai3 double mutants did not lose constitutive activity, likely due to the strong impact of the F160A mutation on Orai3 pore opening.

## The Isoform-Specific Role of TM3 Is Supported by the Cytosolic Loop2 Region

In the following, we further questioned why only Orai3 F160A, but not the analog Orai1 L185A displays huge constitutive

current densities compared to STIM1 mediated Orai activation (Figures 1B,F). Intriguingly, a double point mutant Orai1 V181A L185A exhibited only small constitutive activity (Figures 6A,I), despite the side-chain properties at the mutated positions match with those of Orai3 F160A (Figure 4, table). Remarkably, Orai3 A156V F160A remained strongly constitutively active (Figures 5A,B, 6B,J), although these mutated positions in TM3 correspond to the analog ones in Orai1 L185A (Figure 4, table).

Investigation of the overall hydrophobicity of TM3 revealed for all constitutively active mutants a reduced hydrophobicity compared to their respective wild-type Orai proteins. Interestingly, Orai1 V181A L185A and Orai3 F160A reached the lowest levels for the Orai isoforms (Figures 6C,D,G,H). Thus, alterations of overall hydrophobicity along the TM3 region cannot fully explain distinct levels of current densities.

Next, we exchanged the non-conserved cysteine C195 in Orai1 by a glycine, as present at the analog positions in Orai3 (Figure 6, alignment). However, also Orai1 V181A L185A C195G showed small constitutively active currents similar to Orai1 V181A L185A (Figure 6I and Supplementary Figure 4a).

We recently reported isoform-specific functional differences of Orai1 and Orai3 due to distinct structural properties of the loop2 regions connecting TM2 and TM3 [Orai3-loop2

## Enhanced hydrophobicity at A156 in Orai3 reduces constitutive activity of Orai3 F160A

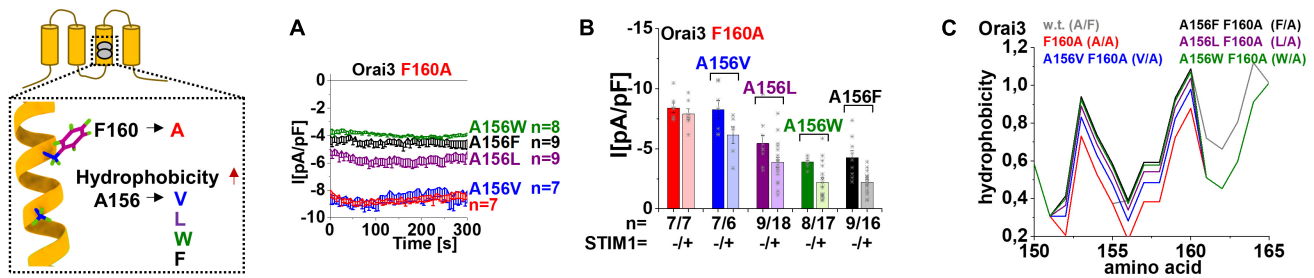


**FIGURE 5 |** Enhanced hydrophobicity at A156 in Orai3 reduces the constitutive activity of Orai3 F160A. The scheme represents Orai3 with a special focus on the two non-conserved residues in TM3 (F160 and A156). Those positions are examined by mutations at position A156 toward different hydrophobic amino acids within the background of the constitutive mutant F160A. **(A)** Time courses of constitutive current densities after whole-cell break-in of Orai3 F160A, Orai3 A156V F160A, Orai3 A156L F160A, Orai3 A156W F160A, and Orai3 A156F F160A in the absence of STIM1. **(B)** Block diagram of whole-cell current densities of Orai3 mutants tested in **(A)** in the absence ( $t = 0$  s) and the presence (maximum current densities) of STIM1 ( $n = 6-18$  cells; values are mean  $\pm$  SEM). **(C)** Hydrophobicity plots showing the Orai3 TM3 region (amino acid 150–165) for mutants investigated in **(A)** compared to Orai3 wild-type. In **(B)** the Welch-ANOVA test (due to lack of variance homogeneity as determined by Levene Test) was used for statistical comparison of Orai3 mutants using the F-distribution [ $F(9,30.65) = 31.14, p < 0.001$ ]. After Welch-ANOVA we performed the Games-Howell *post hoc* test to determine the pairs which differ statistically significant ( $p < 0.05$ ). Statistical significance was determined for Orai3 A156L F160A, Orai3 A156W F160A, and Orai3 A156F F160A compared to Orai3 F160A, both in the absence and presence of STIM1.

## Orai Loop2-TM3 segment controls the extent of pore opening

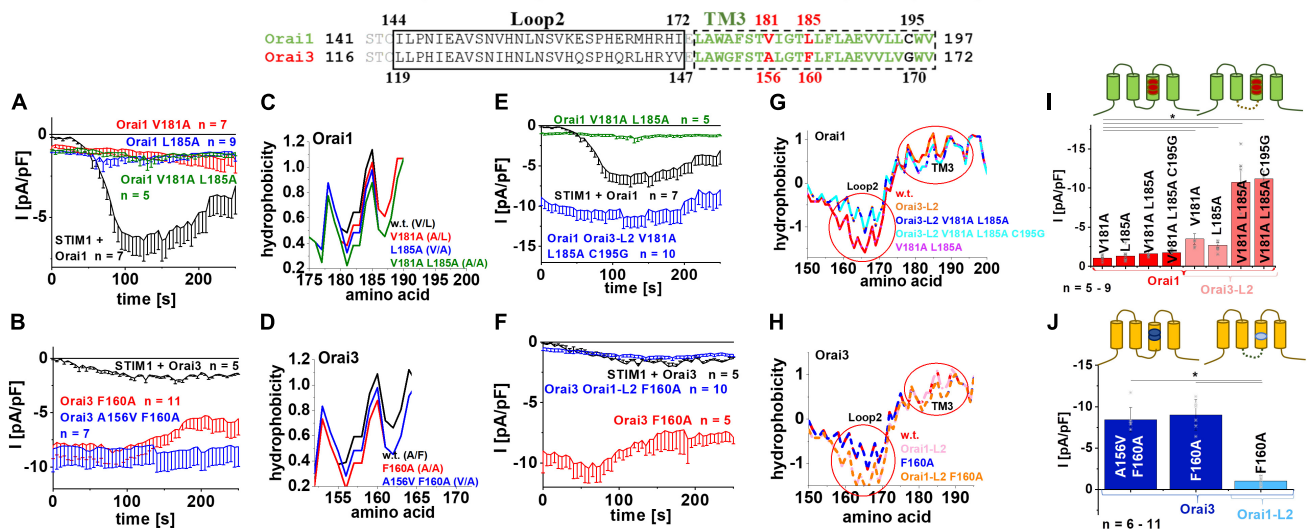
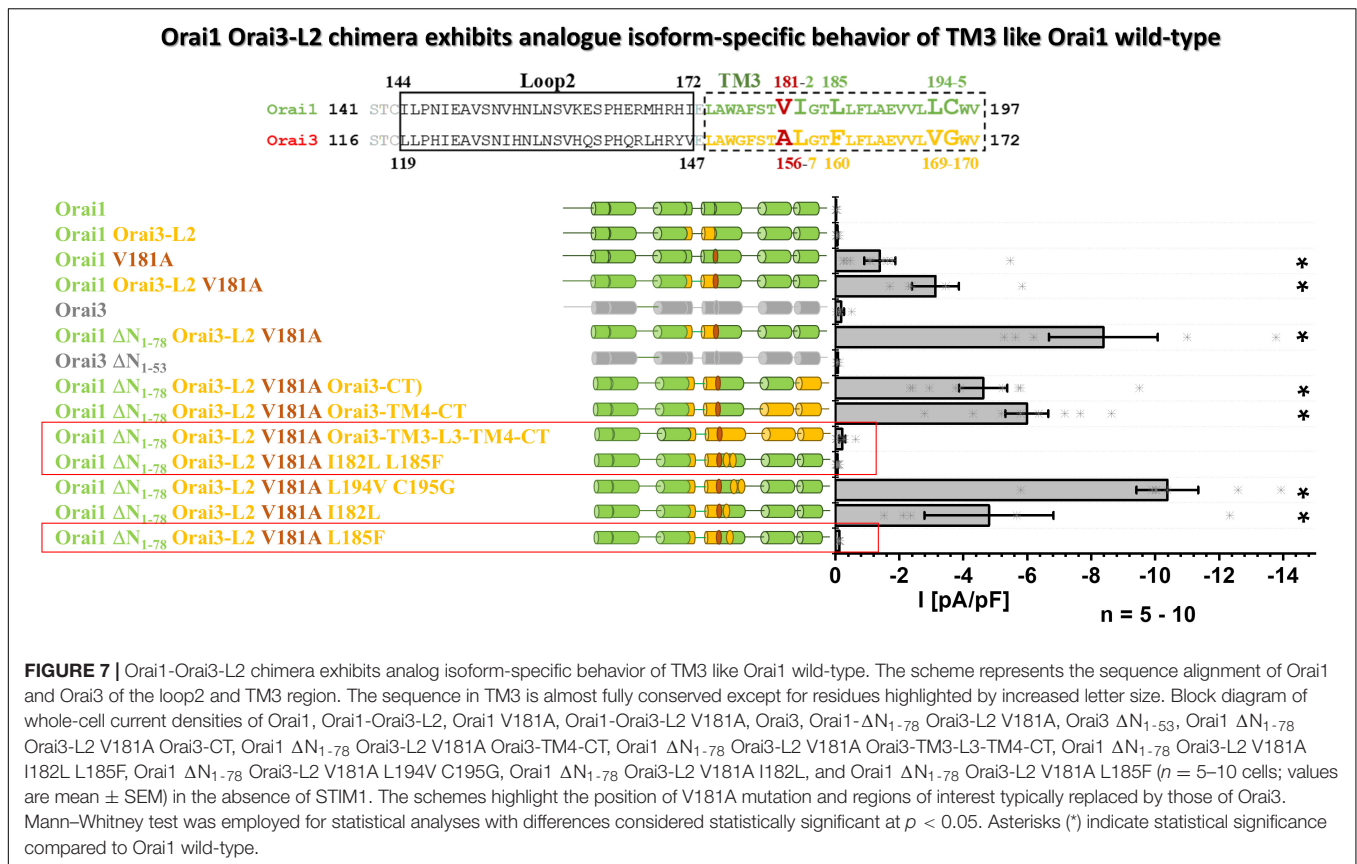


**FIGURE 6 |** Orai loop2-TM3 segment controls the extent of pore opening. The scheme represents the sequence alignment of Orai1 and Orai3 at the loop2 and TM3 region. The sequence in TM3 is almost fully conserved except three residues highlighted in red and black. **(A)** Time courses of current densities after whole-cell break-in of Orai1 V181A, Orai1 L185A and Orai1 V181A L185A in the absence of STIM1 compared to Orai1 in the presence of STIM1. **(B)** Time courses of current densities after whole-cell break-in of Orai3 F160A and Orai3 A156V F160A in the absence of STIM1 compared to Orai3 in the presence of STIM1. **(C)** Hydrophobicity plots of the Orai1 TM3 region (amino acid 175–190) for mutants investigated in **(A)** compared to Orai1 wild-type. **(D)** Hydrophobicity plots of the Orai3 TM3 region (amino acid 150–165) for Orai3 F160A and Orai3 A156V F160A compared to Orai3 wild-type. **(E)** Time courses of current densities after whole-cell break-in of Orai1 Orai1-L2 V181A L185A in the absence of STIM1 compared to Orai1 in the presence of STIM1. **(F)** Time courses of current densities after whole-cell break-in of Orai3 Orai1-L2 F160A and Orai3 F160A in the absence of STIM1 compared to Orai3 in the presence of STIM1. **(G)** Hydrophobicity plots of the Orai1-L2-TM3 region (amino acid 150–200) for Orai1 Orai1-L2, Orai1 Orai1-L2 V181A L185A, Orai1 Orai1-L2 V181A L185A C195G, and Orai1 V181A L185A compared to Orai1 wild-type. Loop2 and TM3 are highlighted by red circles. **(H)** Hydrophobicity plots of the Orai3-L2-TM3 region (amino acid 150–195) for Orai3 Orai1-L2, Orai3 F160A, and Orai3 Orai1-L2 F160A compared to Orai3 wild-type. **(I)** Block diagram of whole-cell current densities of Orai1 V181A, Orai1 L185A, Orai1 V181A L185A C195G, Orai1 V181A L185A, Orai1 Orai1-L2 V181A L185A, and Orai1 Orai1-L2 V181A L185A C195G in the absence of STIM1 ( $n = 5-9$  cells; values are mean  $\pm$  SEM). **(J)** Block diagram of whole-cell current densities of Orai3 F160A, Orai3 A156V F160A, and Orai3 Orai1-L2 F160A in the absence of STIM1 ( $n = 6-11$  cells; values are mean  $\pm$  SEM). In **(I,J)** the Welch-ANOVA test (due to lack of variance homogeneity as determined by Levene Test) was used for statistical comparison of Orai1 and Orai3 mutants using the F-distribution [ $F(6,16.86) = 14.41, p < 0.001$  **(I)**;  $F(7,22.33) = 32.11, p < 0.001$  **(J)**]. Subsequent to Welch-ANOVA we performed the Games-Howell *post hoc* test to determine the pairs which differ statistically significant ( $p < 0.05$ ). Asterisks (\*) indicates statistical significance compared to Orai1 V181A **(I)** or Orai3 Orai1-L2 F160A **(J)**, respectively.



(L2) – aa:119–147, Orai1-L2 – aa:144–172] (Fahrner et al., 2018). By applying this knowledge, we discovered that Orai1 V181A Orai3-L2 and Orai1 L185A Orai3-L2 showed slightly enhanced constitutive activity compared to the single point mutants without the swapped loop2 (Figure 6I and Supplementary Figures 4b,c). Remarkably, an additional exchange of the loop2 of Orai1 by that of Orai3 (thus mimicking Orai3 at this region; see alignment Figure 6) in Orai1 V181A L185A or also Orai1 V181A L185A C195G led to strongly enhanced constitutive currents, in analogy to Orai3 F160A (Figures 6E,I and Supplementary Figures 4d,e). Vice versa, Orai3 F160A containing the loop2 of Orai1 instead of that of Orai3, thus Orai3 Orai1-L2 (aa:144–172) F160A displayed only small constitutive currents similar to Orai1 V181A, Orai1 L185A or Orai1 V181A L185A (Figures 6F,J).

Analysis of the overall hydrophobicity of TM3 of the respective chimeric constructs revealed no difference compared to wild-type constructs. Interestingly, overall hydrophobicity along the loop2 region was distinct (Figures 6G,H, red circles). The huge constitutive activity could be only obtained upon enhanced hydrophobicity along the loop2 region and reduced hydrophobicity along TM3.

Altogether, those results provide indisputable evidence that distinct magnitudes of the constitutive Orai1- and Orai3-TM3 mutant current densities are not only determined by certain residues in TM3 but rather by the entire loop2-TM3 segments. Thus, the loop2 is not only crucial for an interplay with the Orai

N-terminus (Fahrner et al., 2018), but also determines together with TM3 isoform-specific Orai activation.

Due to rather drastic modifications of the strongly constitutively active Orai1 Orai3-L2 chimeras (e.g., Orai1 Orai3-L2 V181A L185A C195G), we still investigated whether their biophysical properties, the so-called authentic CRAC channel hallmarks, are comparable to that of Orai3 F160A (Derler et al., 2018). As shown exemplarily for Orai1 Orai3-L2 V181A L185A C195G (Supplementary Figures 4f–h), constitutive currents exhibit a strongly inward-rectifying current/voltage relationships with a reversal potential of  $\sim +50$  mV, both in the absence and presence of STIM1 (Supplementary Figure 4f). In the absence of STIM1, the I/V relationship exhibited a U-shaped form at very negative potentials between  $-85$  mV and  $-70$  mV, as we discovered also for Orai3 F160A (Derler et al., 2018) (Supplementary Figure 4f). Upon switching from a  $\text{Ca}^{2+}$ -containing to a DVF  $\text{Na}^{+}$ -solution the Orai1 Orai3-L2 V181A L185A C195G currents decreased in the absence of STIM1 and enhanced in the presence of STIM1 (Supplementary Figure 4g), in accord with our previous findings (Derler et al., 2018). Moreover, fast  $\text{Ca}^{2+}$  dependent inactivation (FCDI) was completely abolished in the absence of STIM1 and instead reversed into a robust potentiation. The presence of STIM1 fully restored FCDI as known for STIM1-Orai1 currents as well as a diversity of other constitutively active mutants (Derler et al., 2018) (Supplementary Figure 4h). Overall, this constitutive Orai1 Orai3-L2 chimeric mutant

### Non-conserved residues in TM3 as well as the loop2 region are important for the closed and open state of Orai1 and Orai3 in an isoform-specific manner

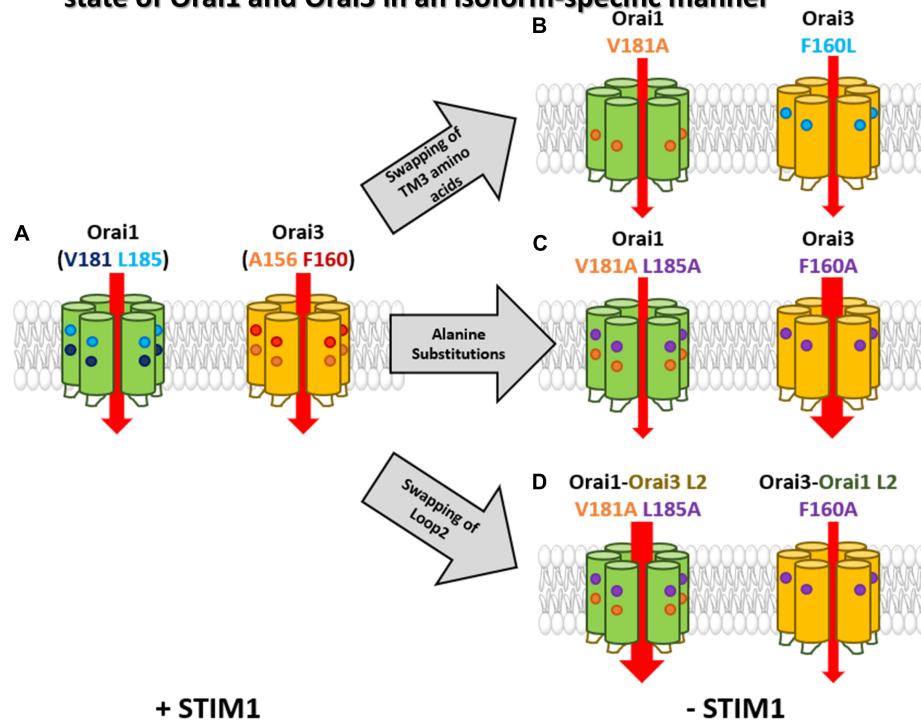


**FIGURE 8 |** Non-conserved residues in TM3 as well as the loop2 region are involved in the maintenance of the closed state and configure an opening permissive conformation of Orai1 and Orai3 in an isoform-specific manner. A simplified summary of the isoform-specific effects of TM3 of Orai1 and Orai3. **(A)** Orai1 and Orai3 are active in the presence of STIM1. The non-conserved residues in TM3 of each Orai isoform are highlighted. **(B)** Swapping of certain TM3 isoform-specific amino acids (Orai1 V181A and Orai3 F160L) leads to a constitutive activity already in the absence of STIM1. **(C)** Alanine substitutions of non-conserved residues in TM3 reveal only small constitutive currents for Orai1 V181A L185A, while Orai3 F160A displays huge currents even higher than its wild-type analog. **(D)** Additional swapping of the loop2 regions within the mutants of **(C)** also swaps the extent of constitutive activity highlighting the importance of the whole loop2-TM3 region.

shows CRAC channel characteristics similar to Orai3 F160A (Derler et al., 2018).

In summary, the maintenance of the closed state of Orai1 and Orai3 is not only governed in an isoform-specific manner by two non-conserved residues in their TM3 domains (Orai1: V181, L185; Orai3: A156, F160), but further controlled by a distinct overall conformation of the loop2-TM3 region.

### Orai1 Orai3-L2 Chimera Exhibits Analog Isoform-Specific Behavior of TM3 Like Orai1 Wild-Type

Since Orai1 Orai3-L2 V181A showed enhanced constitutive activity versus Orai1 V181A, we employed a chimeric approach to investigate whether also in this case, only the two non-conserved residues in TM3 make up the isoform-specific control of Orai channel function (Figure 7). To determine whether the different N-termini have an impact on the constitutive activity of Orai1 Orai3-L2 V181A, we deleted the first 78 residues. Nevertheless, this deletion mutant chimera (Orai1 DN<sub>1-78</sub> Orai3-L2 V181A) left constitutive activity unaffected. This is in line with other constitutively active mutants (Derler et al., 2018) and showed that the N-terminal segment 1–78

is not involved in the maintenance of constitutive currents. Next, we tested whether non-conserved residues in TM4 or even the C-terminus influence the constitutive currents of Orai1 DN<sub>1-78</sub> Orai3-L2 V181A. However, neither the swap of Orai1 C-terminal nor Orai1 TM4-C-terminal region by that of Orai3 impaired constitutive activity. Only the exchange of the region starting from TM3 till the end of the C-terminus in Orai1 by that of Orai3 led to the loss of the constitutive activity. This suggests that the sites modulating constitutive activation are located in TM3. Via site-directed mutagenesis of non-conserved residues in TM3 (Figure 7, alignment), we narrowed down the point mutation abolishing constitutive activity of Orai1 DN<sub>1-78</sub> Orai3-L2 V181A. Specifically, we introduced the following point mutations: I182L, L185F, L194V, C195G, thus, exchanging non-conserved residues in Orai1-TM3 by those of Orai3 (Figure 7, alignment). Insertion of the double mutation L194V C195G or the single mutation I182L retained constitutive activity of Orai1 DN<sub>1-78</sub> Orai3-L2 V181A. Interestingly, insertion of the double mutant I182L L185F (Orai1 DN<sub>1-78</sub> Orai3-L2 V181A I182L L185F) or L185F (Orai1 DN<sub>1-78</sub> Orai3-L2 V181A L185F) led to the loss of constitutive activity of the N-truncated chimera. This finding is in line with the resting state of the analog Orai3 N-truncation mutant, Orai3 DN<sub>1-53</sub> (Figure 7).

In accord with the results in **Figure 5**, we demonstrate in the background of the Orai3-loop2 that while a V181A substitution in Orai1 can induce constitutive activity, an additional substitution L185F brings Orai1 back into the closed state. This chimeric approach further strengthens our findings that in TM3 predominantly two non-conserved residues, V181 and L185 in Orai1 (A156 and F160 in Orai3), determine the maintenance of the closed state in an isoform-specific manner.

## DISCUSSION

In this study, we elucidated an isoform-specific function of Orai gating checkpoints in TM3 (**Figure 8**). Two non-conserved hydrophobic residues in TM3 contribute to the maintenance of the closed state and the configuration of an opening permissive conformation of Orai1 and Orai3 channels to a different degree, which is in accordance with the overall hydrophobicity along TM3. In addition, the non-conserved Orai loop2 regions contribute to isoform-specific features of Orai channel activation.

We recently demonstrated that Orai1 channel activation requires the clearance of a series of gating checkpoints within all TM domains (Tiffner et al., 2020b). Mutation of the respective checkpoints can lead either to gain- or loss-of-function in dependence of the inserted amino acid. This suggests that the particular residues are involved in both, maintenance of the closed state and the establishment of an opening permissive pore/channel conformation. Here, we showed that most of these checkpoints in TM2, TM3, and TM4 are conserved (**Table 1**). Only TM3 includes two non-conserved positions (V181, L185 in Orai1 and the analogs A156, F160 in Orai3) (**Figure 8A**). Analog substitutions of representative gating checkpoints in TM2 and TM4 of Orai1 (Tiffner et al., 2020b) and Orai3 showed comparable extents of gain- or loss-of-function relative to store-operated activation of the wild-type protein. Concerning TM3, mutation of two non-conserved residues to small amino acids, such as alanine or serine, led to distinct magnitudes of current densities,  $\text{Ca}^{2+}$  entry and NFAT translocation, suggesting that they impact the maintenance of the closed state in an isoform-specific manner (**Figure 8C**). In addition, only different amino acid substitutions at the analogous positions V181 in Orai1 and A156 in Orai3 led to loss of function (Orai1 V181F, Orai3 A156W). This indicates that this position also influences the establishment of an opening-permissive conformation differently in the respective Orai variants.

Despite these isoform-specific differences in TM3, we provide evidence that both channels necessitate a global conformational change of the channel complex for pore opening. We demonstrated this aspect via several Orai3 double point mutants each containing one LoF and one GoF mutation in the MTR and CETR. In all possible combinations, the LoF mutation acted dominant over the GoF mutation independent of their location relative to each other, leading to overall loss-of-function of Orai3 channels, both, in the absence as well as the presence of STIM1. This is conform with our recent finding on Orai1 (Tiffner et al., 2020b).

Even though global activation mechanisms of Orai channels are identical, a detailed characterization of the individual checkpoints is valuable for potential isoform-specific interferences with Orai channel functions. Our characterization of GoF mutations in TM3 revealed that Orai1 V181A and Orai1 L185A lead to small constitutive activity. Interestingly, despite the analog position of Orai1 V181A in Orai3 contains already an alanine (A156), it remains in the resting state. The reason for the latter is subject to the residue one helical turn downstream which features lower hydrophobicity in Orai1 (L185) than in Orai3 (F160). Indeed, the double mutant Orai1 V181A L185F, thus, mimicking Orai3 at the two positions, lost constitutive activity. Analogously, Orai3 F160L gained constitutive activity, in line with Orai1 V181A (**Figure 8B**). Thus, in Orai1, both, V181 and L185 contribute to the maintenance of the closed state, while in Orai3, it is predominantly the position F160. Accordingly, overall hydrophobicity along TM3 is enhanced for Orai proteins and mutants retaining the resting state and decreased for Orai mutants showing constitutive activity. Indeed, the robust constitutive activity of Orai3 F160A was reduced upon the substitution of A156 one helical turn upstream by amino acids with enhanced hydrophobicity. Also, the insertion of a strongly hydrophilic lysine at the positions A156 in Orai3 led to robust constitutive currents. Furthermore, the latter finding counteracts the potential argument that an increase in the side-chain size of different hydrophobic amino acids at position A156 in Orai3 F160A decreases constitutive activity.

Remarkably individual substitutions, as well as double point mutations of the two non-conserved residues in Orai1, led to small constitutive activity, while Orai3 F160A exhibited huge constitutive activity compared to maximum currents reached upon STIM1 mediated Orai wild-type activation (**Figure 8C**). We discovered via the swap of the loop2 region of either Orai1 or Orai3 in either of the constitutively active Orai3 F160A or Orai1 V181A L185A mutants, that currents reduced (Orai3 Orai1-L2 F160A) or enhanced (e.g., Orai1 Orai3-L2 V181A L185A), respectively (**Figure 8D**). While these chimeras exhibited comparable overall hydrophobicity along TM3, the hydrophobicity along the loop2 region enhanced for high constitutively active mutants and decreased for low constitutively active mutants. Overall, we showed that the current levels of GoF TM3 mutants are not only determined by amino acids in TM3, but also by the entire loop2 region. We identified that constitutive currents increased with reduced hydrophobicity along TM3 and enhanced hydrophobicity along the loop2 region. We recently published that the loop2 region of Orai channels exhibits isoform-specific functional and structural features in respect to a co-regulation with the Orai N-terminus. MD simulations revealed that the loop2 region in Orai1 contains a longer helical portion than that of Orai3 (Fahrner et al., 2018). Thus, it seems that the lower flexibility of the loop2 region possesses a stimulating effect on  $\text{Ca}^{2+}$  permeation. Moreover, also Orai1-Orai3 chimeras clearly revealed that the synergy of the two non-conserved residues in TM3 maintains the closed state of the respective Orai variant. Reducing the overall hydrophobicity

along TM3 by a swap of amino acids by the respective other Orai isoform leads to constitutive activity not only in Orai wild-type, but also in the Orai1-Orai3-L2 chimeras.

It is worth noting that these non-conserved hydrophobic residues in TM3 point to hydrophobic residues in TM4, suggesting that communication of TM3 and TM4 controls Orai activation (Tiffner et al., 2021). We recently reported that Orai1 F250C, located opposite L185, shows small constitutive activity (Tiffner et al., 2020a). Interestingly, while also Orai1 L185A/S show weak constitutive activity, we discovered that a double point mutant Orai1 L185A F250A exhibits strongly pronounced constitutive currents (Derler et al., 2018; Tiffner et al., 2020a). Moreover, it is known that P245L (Nesin et al., 2014; Palty et al., 2015; Derler et al., 2018), associated with the Stormorken syndrome and located at a kink in the middle of TM4, and the 261 ANSGA<sub>265</sub> mutations (Zhou et al., 2016), located at the bent connection between TM4 and C-terminus, induce GoF. Despite this knowledge on TM3 and TM4 mutations, it remains to be determined how they affect the communication of TM3 and TM4 to maintain the closed state or to induce pore opening. Currently available dOrai structures suggest that pore opening involves a pore dilation and outward rigid body movement of all TM domains especially at the cytosolic side of the channel complex (Hou et al., 2012, 2018, 2020; Liu et al., 2019). Interestingly, the crystal structures of dOrai open states further resolved a straightening of the TM4-C-terminus region, which, however, is not visible in dOrai cryo-EM structures. Thus, further studies are required to resolve which conformational changes occur physiologically at the outmost side of the channel complex to induce Orai pore opening and whether they occur in an isoform-specific manner.

Summarizing, we discovered that non-conserved gating checkpoints in TM3 of Orai1 and Orai3 control the maintenance of the closed state and an opening permissive channel conformation in an isoform-specific manner, while overall global conformational TM motions are indispensable for pore opening of both channels. The extent of current size increases with reduced overall hydrophobicity along TM3 and enhanced hydrophobicity along the loop2 region. The elucidation of isoform-specific differences provides novel targets for the development of future therapeutic interventions in an Orai-isoform-specific manner.

## REFERENCES

- Barr, V. A., Bernot, K. M., Srikanth, S., Gwack, Y., Balagopalan, L., Regan, C. K., et al. (2008). Dynamic movement of the calcium sensor STIM1 and the calcium channel Orai1 in activated T-cells: puncta and distal caps. *Mol. Biol. Cell* 19, 2802–2817. doi: 10.1091/mbc.e08-02-0146
- Berridge, M. J., Bootman, M. D., and Roderick, H. L. (2003). Calcium signalling: dynamics, homeostasis and remodelling. *Nat. Rev. Mol. Cell Biol.* 4, 517–529. doi: 10.1038/nrm1155
- Berridge, M. J., Lipp, P., and Bootman, M. D. (2000). The versatility and universality of calcium signalling. *Nat. Rev. Mol. Cell Biol.* 1, 11–21. doi: 10.1038/35036035
- Butorac, C., Krizova, A., and Derler, I. (2020). Review: structure and activation mechanisms of CRAC channels. *Adv. Exp. Med. Biol.* 1131, 547–604. doi: 10.1007/978-3-030-12457-1\_23

## DATA AVAILABILITY STATEMENT

The original contributions presented in the study are included in the article/**Supplementary Material**, further inquiries can be directed to the corresponding author/s.

## AUTHOR CONTRIBUTIONS

AT, LM, and ID conceived and coordinated the study and wrote the manuscript. ID, AT, and LM performed and analyzed the electrophysiological experiments. ID performed the Secondary Structure Assignments and Bioinformatics. MF and CH contributed to molecular biology. HG performed the confocal localization measurements for Orai mutants. MS and HG performed the NFAT studies. MS analyzed the NFAT experiments. SW performed and analyzed the Ca<sup>2+</sup> fluorescence measurements. All the authors reviewed the results and approved the final version of the manuscript.

## FUNDING

This work was supported in part by the Linz Institute of Technology project LIT-2018-05-SEE-111 and the Austrian Science Fund (FWF) projects P30567, P32851 and to ID as well as P32947 to MF. In addition, LM holds a Ph.D. scholarship of Upper Austria with the FWF 1250B20 Upper Austria DK NanoCell project. HG holds a Ph.D. scholarship of the FWF Ph.D. program W1250 NanoCell.

## ACKNOWLEDGMENTS

We thank S. Buchegger for excellent technical assistance.

## SUPPLEMENTARY MATERIAL

The Supplementary Material for this article can be found online at: <https://www.frontiersin.org/articles/10.3389/fcell.2021.635705/full#supplementary-material>

- Butorac, C., Muik, M., Derler, I., Stadlbauer, M., Lunz, V., Krizova, A., et al. (2019). A novel STIM1-Orai1 gating interface essential for CRAC channel activation. *Cell Calcium* 79, 57–67. doi: 10.1016/j.ceca.2019.02.009
- Cahalan, M. D. (2009). STIMulating store-operated Ca(2+) entry. *Nat. Cell Biol.* 11, 669–677. doi: 10.1038/ncb0609-669
- Cahalan, M. D., and Chandy, K. G. (2009). The functional network of ion channels in T lymphocytes. *Immunol. Rev.* 231, 59–87. doi: 10.1111/j.1600-065x.2009.00816.x
- Calloway, N., Vig, M., Kinet, J. P., Holowka, D., and Baird, B. (2009). Molecular clustering of STIM1 with Orai1/CRACM1 at the plasma membrane depends dynamically on depletion of Ca<sup>2+</sup> stores and on electrostatic interactions. *Mol. Biol. Cell* 20, 389–399. doi: 10.1091/mbc.e07-11-1132
- Derler, I., Butorac, C., Krizova, A., Stadlbauer, M., Muik, M., Fahrner, M., et al. (2018). Authentic CRAC channel activity requires STIM1 and the conserved

- portion of the Orai N terminus. *J. Biol. Chem.* 293, 1259–1270. doi: 10.1074/jbc.m117.812206
- Derler, I., Fahrner, M., Carugo, O., Muik, M., Bergsmann, J., Schindl, R., et al. (2009). Increased hydrophobicity at the N terminus/membrane interface impairs gating of the severe combined immunodeficiency-related ORAI1 mutant. *J. Biol. Chem.* 284, 15903–15915. doi: 10.1074/jbc.m808312200
- Derler, I., Fritsch, R., Schindl, R., and Romanin, C. (2008). CRAC inhibitors: identification and potential. *Expert Opin. Drug Discov.* 3, 787–800. doi: 10.1517/17460441.3.7.787
- Derler, I., Hofbauer, M., Kahr, H., Fritsch, R., Muik, M., Kepplinger, K., et al. (2006). Dynamic but not constitutive association of calmodulin with rat TRPV6 channels enables fine tuning of Ca<sup>2+</sup>-dependent inactivation. *J. Physiol.* 577(Pt 1), 31–44. doi: 10.1113/jphysiol.2006.118661
- Derler, I., Plenck, P., Fahrner, M., Muik, M., Jardin, I., Schindl, R., et al. (2013). The extended transmembrane Orai1 N-terminal (ETON) region combines binding interface and gate for Orai1 activation by STIM1. *J. Biol. Chem.* 288, 29025–29034. doi: 10.1074/jbc.m113.501510
- Dong, H., Zhang, Y., Song, R., Xu, J., Yuan, Y., Liu, J., et al. (2019). Toward a model for activation of orai channel. *iScience* 16, 356–367. doi: 10.1016/j.isci.2019.05.041
- Fahrner, M., Muik, M., Derler, I., Schindl, R., Fritsch, R., Frischauf, I., et al. (2009). Mechanistic view on domains mediating STIM1-Orai coupling. *Immunol. Rev.* 231, 99–112. doi: 10.1111/j.1600-065x.2009.00815.x
- Fahrner, M., Pandey, S. K., Muik, M., Traxler, L., Butorac, C., Stadlbauer, M., et al. (2018). Communication between N terminus and loop2 tunes Orai activation. *J. Biol. Chem.* 293, 1271–1285. doi: 10.1074/jbc.m117.812693
- Feske, S., Gwack, Y., Prakriya, M., Srikanth, S., Puppel, S. H., Tanasa, B., et al. (2006). A mutation in Orai1 causes immune deficiency by abrogating CRAC channel function. *Nature* 441, 179–185.
- Frischauf, I., Litvinukova, M., Schober, R., Zayats, V., Svobodova, B., Bonhenry, D., et al. (2017). Transmembrane helix connectivity in Orai1 controls two gates for calcium-dependent transcription. *Sci. Signal.* 10:eaa0358. doi: 10.1126/scisignal.aao0358
- Frischauf, I., Muik, M., Derler, I., Bergsmann, J., Fahrner, M., Schindl, R., et al. (2009). Molecular determinants of the coupling between STIM1 and Orai channels: differential activation of Orai1-3 channels by a STIM1 coiled-coil mutant. *J. Biol. Chem.* 284, 21696–21706.
- Frischauf, I., Schindl, R., Bergsmann, J., Derler, I., Fahrner, M., Muik, M., et al. (2011). Cooperativeness of Orai cytosolic domains tunes subtype-specific gating. *J. Biol. Chem.* 286, 8577–8584. doi: 10.1074/jbc.m110.187179
- Gudlur, A., Quintana, A., Zhou, Y., Hirve, N., Mahapatra, S., and Hogan, P. G. (2014). STIM1 triggers a gating rearrangement at the extracellular mouth of the ORAI1 channel. *Nat Commun.* 5:5164.
- Hewavitharana, T., Deng, X., Soboloff, J., and Gill, D. L. (2007). Role of STIM and Orai proteins in the store-operated calcium signaling pathway. *Cell Calcium* 42, 173–182. doi: 10.1016/j.ceca.2007.03.009
- Hogan, P. G., and Rao, A. (2015). Store-operated calcium entry: mechanisms and modulation. *Biochem. Biophys. Res. Commun.* 460, 40–49. doi: 10.1016/j.bbrc.2015.02.110
- Hou, X., Burstein, S. R., and Long, S. (2018). Structures reveal opening of the store-operated calcium channel Orai. *bioRxiv [Preprint]* doi: 10.1101/284034
- Hou, X., Outhwaite, I. R., Pedi, L., and Long, S. B. (2020). Cryo-EM structure of the calcium release-activated calcium channel Orai in an open conformation. *eLife* 9:e62772.
- Hou, X., Pedi, L., Diver, M. M., and Long, S. B. (2012). Crystal structure of the calcium release-activated calcium channel Orai. *Science* 338, 1308–1313. doi: 10.1126/science.1228757
- Krizova, A., Maltan, L., and Derler, I. (2019). Critical parameters maintaining authentic CRAC channel hallmarks. *Eur. Biophys. J.* 48, 425–445. doi: 10.1007/s00249-019-01355-6
- Lee, K. P., Yuan, J. P., Hong, J. H., So, I., Worley, P. F., and Muallem, S. (2010). An endoplasmic reticulum/plasma membrane junction: STIM1/Orai1/TRPCs. *FEBS Lett.* 584, 2022–2027. doi: 10.1016/j.febslet.2009.11.078
- Lee, K. P., Yuan, J. P., Zeng, W., So, I., Worley, P. F., and Muallem, S. (2009). Molecular determinants of fast Ca<sup>2+</sup>-dependent inactivation and gating of the Orai channels. *Proc. Natl. Acad. Sci. U.S.A.* 106, 14687–14692. doi: 10.1073/pnas.0904664106
- Li, Z., Lu, J., Xu, P., Xie, X., Chen, L., and Xu, T. (2007). Mapping the interacting domains of STIM1 and Orai1 in Ca<sup>2+</sup> release-activated Ca<sup>2+</sup> channel activation. *J. Biol. Chem.* 282, 29448–29456. doi: 10.1074/jbc.m703573200
- Liou, J., Kim, M. L., Heo, W. D., Jones, J. T., Myers, J. W., Ferrell, J. E. Jr., et al. (2005). STIM is a Ca<sup>2+</sup> sensor essential for Ca<sup>2+</sup>-store-depletion-triggered Ca<sup>2+</sup> influx. *Curr. Biol.* 15, 1235–1241. doi: 10.1016/j.cub.2005.05.055
- Lis, A., Peinelt, C., Beck, A., Parvez, S., Monteilh-Zoller, M., Fleig, A., et al. (2007). CRACM1, CRACM2, and CRACM3 are store-operated Ca<sup>2+</sup> channels with distinct functional properties. *Curr. Biol.* 17, 794–800. doi: 10.1016/j.cub.2007.03.065
- Liu, X., Wu, G., Yu, Y., Chen, X., Ji, R., Lu, J., et al. (2019). Molecular understanding of calcium permeation through the open Orai channel. *PLoS Biol.* 17:e3000096. doi: 10.1371/journal.pbio.3000096
- McNally, B. A., Somasundaram, A., Jairaman, A., Yamashita, M., and Prakriya, M. (2013). The C- and N-terminal STIM1 binding sites on Orai1 are required for both trapping and gating CRAC channels. *J. Physiol.* 591(Pt 11), 2833–2850. doi: 10.1113/jphysiol.2012.250456
- Mercer, J. C., Dehaven, W. I., Smyth, J. T., Wedel, B., Boyles, R. R., Bird, G. S., et al. (2006). Large store-operated calcium selective currents due to co-expression of Orai1 or Orai2 with the intracellular calcium sensor. *Stim1. J. Biol. Chem.* 281, 24979–24990. doi: 10.1074/jbc.m604589200
- Muik, M., Fahrner, M., Schindl, R., Stathopoulos, P., Frischauf, I., Derler, I., et al. (2011). STIM1 couples to ORAI1 via an intramolecular transition into an extended conformation. *EMBO J.* 30, 1678–1689. doi: 10.1038/emboj.2011.79
- Muik, M., Frischauf, I., Derler, I., Fahrner, M., Bergsmann, J., Eder, P., et al. (2008). Dynamic coupling of the putative coiled-coil domain of ORAI1 with STIM1 mediates ORAI1 channel activation. *J. Biol. Chem.* 283, 8014–8022. doi: 10.1074/jbc.m708898200
- Nesin, V., Wiley, G., Kousi, M., Ong, E. C., Lehmann, T., Nicholl, D. J., et al. (2014). Activating mutations in STIM1 and ORAI1 cause overlapping syndromes of tubular myopathy and congenital myosis. *Proc. Natl. Acad. Sci. U.S.A.* 111, 4197–4202. doi: 10.1073/pnas.1312520111
- Palty, R., and Isacoff, E. Y. (2015). Cooperative binding of stromal interaction molecule 1 (STIM1) to the N and C termini of calcium release-activated calcium modulator 1 (Orai1). *J Biol Chem.* 291, 334–341. doi: 10.1074/jbc.m115.685289
- Palty, R., Stanley, C., and Isacoff, E. Y. (2015). Critical role for Orai1 C-terminal domain and TM4 in CRAC channel gating. *Cell Res.* 25, 963–980. doi: 10.1038/cr.2015.80
- Parekh, A. B. (2008). Store-operated channels: mechanisms and function. *J. Physiol.* 586:3033. doi: 10.1113/jphysiol.2008.156885
- Park, C. Y., Hoover, P. J., Mullins, F. M., Bachhawat, P., Covington, E. D., Raunser, S., et al. (2009). STIM1 clusters and activates CRAC channels via direct binding of a cytosolic domain to Orai1. *Cell* 136, 876–890. doi: 10.1016/j.cell.2009.02.014
- Peinelt, C., Lis, A., Beck, A., Fleig, A., and Penner, R. (2008). 2-Aminoethoxydiphenyl borate directly facilitates and indirectly inhibits STIM1-dependent gating of CRAC channels. *J. Physiol.* 586, 3061–3073. doi: 10.1113/jphysiol.2008.151365
- Peinelt, C., Vig, M., Koomoa, D. L., Beck, A., Nadler, M. J., Koblan-Huberson, M., et al. (2006). Amplification of CRAC current by STIM1 and CRACM1 (Orai1). *Nat. Cell Biol.* 8, 771–773. doi: 10.1038/ncb1435
- Prakriya, M., Feske, S., Gwack, Y., Srikanth, S., Rao, A., and Hogan, P. G. (2006). Orai1 is an essential pore subunit of the CRAC channel. *Nature* 443, 230–233. doi: 10.1038/nature05122
- Prakriya, M., and Lewis, R. S. (2006). Regulation of CRAC channel activity by recruitment of silent channels to a high open-probability gating mode. *J. Gen. Physiol.* 128, 373–386. doi: 10.1085/jgp.200609588
- Putney, J. W. (2010). Pharmacology of store-operated calcium channels. *Mol Interv.* 10, 209–218.
- Rose, G. D., Geselowitz, A. R., Lesser, G. J., Lee, R. H., and Zehfus, M. H. (1985). Hydrophobicity of amino acid residues in globular proteins. *Science* 229, 834–838. doi: 10.1126/science.4023714
- Schindl, R., Frischauf, I., Bergsmann, J., Muik, M., Derler, I., Lackner, B., et al. (2009). Plasticity in Ca<sup>2+</sup> selectivity of Orai1/Orai3 heteromeric channel. *Proc. Natl. Acad. Sci. U.S.A.* 106, 19623–19628. doi: 10.1073/pnas.0907714106
- Schober, R., Bonhenry, D., Lunz, V., Zhu, J., Krizova, A., Frischauf, I., et al. (2019). Sequential activation of STIM1 links Ca(2+) with luminal domain unfolding. *Sci. Signal.* 12:eaax3194. doi: 10.1126/scisignal.aax3194

- Shuttleworth, T. J. (2012). Orai3—the 'exceptional' Orai? *J. Physiol.* 590(Pt 2), 241–257. doi: 10.1113/jphysiol.2011.220574
- Singh, A., Hamedinger, D., Hoda, J. C., Gebhart, M., Koschak, A., Romanin, C., et al. (2006). C-terminal modulator controls Ca<sup>2+</sup>-dependent gating of Ca(v)1.4 L-type Ca<sup>2+</sup> channels. *Nat. Neurosci.* 9, 1108–1116. doi: 10.1038/nn1751
- Soboloff, J., Spassova, M. A., Tang, X. D., Hewavitharana, T., Xu, W., and Gill, D. L. (2006). Orai1 and STIM1 reconstitute store-operated calcium channel function. *J. Biol. Chem.* 281, 20661–20665. doi: 10.1074/jbc.c600126200
- Spassova, M. A., Soboloff, J., He, L. P., Xu, W., Dziadek, M. A., and Gill, D. L. (2006). STIM1 has a plasma membrane role in the activation of store-operated Ca(2+) channels. *Proc. Natl. Acad. Sci. U.S.A.* 103, 4040–4045. doi: 10.1073/pnas.0510050103
- Srikanth, S., and Gwack, Y. (2013). Molecular regulation of the pore component of CRAC channels. *Orai1. Curr Top Membr.* 71, 181–207. doi: 10.1016/b978-0-12-407870-3.00008-1
- Takahashi, Y., Murakami, M., Watanabe, H., Hasegawa, H., Ohba, T., Munehisa, Y., et al. (2007). Essential role of the N-terminus of murine Orai1 in store-operated Ca<sup>2+</sup> entry. *Biochem. Biophys. Res. Commun.* 356, 45–52. doi: 10.1016/j.bbrc.2007.02.107
- Tiffner, A., Maltan, L., Weiss, S., and Derler, I. (2021). The Orai pore opening mechanism. *Int. J. Mol. Sci.* 22:E533.
- Tiffner, A., Schober, R., Hoeglenger, C., Bonhenry, D., Pandey, S., Lunz, V., et al. (2020a). CRAC channel opening is determined by a series of Orai1 gating checkpoints in the transmembrane and cytosolic regions. *J. Biol. Chem.* doi: 10.1074/jbc.RA120.015548 Online ahead of print
- Tiffner, A., Schober, R., Höglenger, C., Bonhenry, D., Pandey, S., Lunz, V., et al. (2020b). A series of Orai1 gating checkpoints in transmembrane and cytosolic regions requires clearance for CRAC channel opening: clearance and synergy of Orai1 gating checkpoints controls pore opening. *bioRxiv [Preprint]* doi: 10.1101/2020.07.16.207183
- Vig, M., Peinelt, C., Beck, A., Koomoa, D. L., Rabah, D., Koblan-Huberson, M., et al. (2006). CRACM1 is a plasma membrane protein essential for store-operated Ca<sup>2+</sup> entry. *Science* 312, 1220–1223. doi: 10.1126/science.1127883
- Wu, J., Liu, L., Matsuda, T., Zhao, Y., Rebane, A., Drobizhev, M., et al. (2013). Improved orange and red Ca(2+/-) indicators and photophysical considerations for optogenetic applications. *ACS Chem. Neurosci.* 4, 963–972. doi: 10.1021/cn400012b
- Wu, M. M., Buchanan, J., Luik, R. M., and Lewis, R. S. (2006). Ca<sup>2+</sup> store depletion causes STIM1 to accumulate in ER regions closely associated with the plasma membrane. *J. Cell Biol.* 174, 803–813. doi: 10.1083/jcb.200604014
- Yamashita, M., Navarro-Borelly, L., McNally, B. A., and Prakriya, M. (2007). Orai1 mutations alter ion permeation and Ca<sup>2+</sup>-dependent fast inactivation of CRAC channels: evidence for coupling of permeation and gating. *J. Gen. Physiol.* 130, 525–540. doi: 10.1085/jgp.200709872
- Yeromin, A. V., Zhang, S. L., Jiang, W., Yu, Y., Safrina, O., and Cahalan, M. D. (2006). Molecular identification of the CRAC channel by altered ion selectivity in a mutant of Orai. *Nature* 443, 226–229. doi: 10.1038/nature05108
- Yeung, P. S., Yamashita, M., Ing, C. E., Pomes, R., Freymann, D. M., and Prakriya, M. (2018). Mapping the functional anatomy of Orai1 transmembrane domains for CRAC channel gating. *Proc. Natl. Acad. Sci. U.S.A.* 115, E5193–E5202.
- Yuan, J. P., Zeng, W., Dorwart, M. R., Choi, Y. J., Worley, P. F., and Muallem, S. (2009). SOAR and the polybasic STIM1 domains gate and regulate Orai channels. *Nat. Cell Biol.* 11, 337–343. doi: 10.1038/ncb1842
- Zhang, S. L., Yeromin, A. V., Zhang, X. H. F., Yu, Y., Safrina, O., Penna, A., et al. (2006). Genome-wide RNAi screen of Ca<sup>2+</sup> influx identifies genes that regulate Ca<sup>2+</sup> release-activated Ca<sup>2+</sup> channel activity. *PNAS* 103, 9357–9362. doi: 10.1073/pnas.0603161103
- Zhang, S. L., Yu, Y., Roos, J., Kozak, J. A., Deerinck, T. J., Ellisman, M. H., et al. (2005). STIM1 is a Ca<sup>2+</sup> sensor that activates CRAC channels and migrates from the Ca<sup>2+</sup> store to the plasma membrane. *Nature* 437, 902–905. doi: 10.1038/nature04147
- Zhang, X., Xin, P., Yeast, R. E., Emrich, S. M., Johnson, M. T., Pathak, T., et al. (2020). Distinct pharmacological profiles of ORAI1, ORAI2, and ORAI3 channels. *Cell Calcium* 91:102281.
- Zheng, H., Zhou, M. H., Hu, C., Kuo, E., Peng, X., Hu, J., et al. (2013). Differential roles of the C and N termini of Orai1 protein in interacting with stromal interaction molecule 1 (STIM1) for Ca<sup>2+</sup> release-activated Ca<sup>2+</sup> (CRAC) channel activation. *J. Biol. Chem.* 288, 11263–11272. doi: 10.1074/jbc.m113.450254
- Zhou, Y., Cai, X., Loktionova, N. A., Wang, X., Nwokonko, R. M., Wang, X., et al. (2016). The STIM1-binding site nexus remotely controls Orai1 channel gating. *Nat. Commun.* 7:13725.
- Zhou, Y., Cai, X., Nwokonko, R. M., Loktionova, N. A., Wang, Y., and Gill, D. L. (2017). The STIM-Orai coupling interface and gating of the Orai1 channel. *Cell Calcium* 63, 8–13. doi: 10.1016/j.ceca.2017.01.001
- Zhou, Y., Nwokonko, R. M., Baraniak, J. H. Jr., Trebak, M., Lee, K. P. K., and Gill, D. L. (2019). The remote allosteric control of Orai channel gating. *PLoS Biol.* 17:e3000413. doi: 10.1371/journal.pbio.3000413
- Zhou, Y., Srinivasan, P., Razavi, S., Seymour, S., Meraner, P., Gudlur, A., et al. (2013). Initial activation of STIM1, the regulator of store-operated calcium entry. *Nat. Struct. Mol. Biol.* 20, 973–981. doi: 10.1038/nsmb.2625

**Conflict of Interest:** The authors declare that the research was conducted in the absence of any commercial or financial relationships that could be construed as a potential conflict of interest.

Copyright © 2021 Tiffner, Maltan, Fahrner, Sallinger, Weiß, Grabmayr, Höglenger and Derler. This is an open-access article distributed under the terms of the Creative Commons Attribution License (CC BY). The use, distribution or reproduction in other forums is permitted, provided the original author(s) and the copyright owner(s) are credited and that the original publication in this journal is cited, in accordance with accepted academic practice. No use, distribution or reproduction is permitted which does not comply with these terms.



# Gain-of-Function STIM1 L96V Mutation Causes Myogenesis Alteration in Muscle Cells From a Patient Affected by Tubular Aggregate Myopathy

## OPEN ACCESS

### Edited by:

Agnese Secondo,  
University of Naples Federico II, Italy

### Reviewed by:

Jose M. Eltit,  
Virginia Commonwealth University,  
United States  
Edoardo Malfatti,  
INSERM U1179 Handicap  
neuromusculaire: Physiopathologie,  
Biothérapie et Pharmacologie  
appliquées (END-ICAP), France

### \*Correspondence:

Antonella Liantonio  
antonella.liantonio@uniba.it

<sup>†</sup>These authors have contributed  
equally to this work

### Specialty section:

This article was submitted to  
Signaling,  
a section of the journal  
Frontiers in Cell and Developmental  
Biology

**Received:** 29 November 2020

**Accepted:** 02 February 2021

**Published:** 26 February 2021

### Citation:

Conte E, Pannunzio A, Imbrici P,  
Camerino GM, Maggi L, Mora M,  
Gibertini S, Cappellari O, De Luca A,  
Coluccia M and Liantonio A (2021)  
Gain-of-Function STIM1 L96V  
Mutation Causes Myogenesis  
Alteration in Muscle Cells From a  
Patient Affected by Tubular Aggregate  
Myopathy.  
Front. Cell Dev. Biol. 9:635063.  
doi: 10.3389/fcell.2021.635063

**Elena Conte<sup>1†</sup>, Alessandra Pannunzio<sup>1†</sup>, Paola Imbrici<sup>1</sup>, Giulia Maria Camerino<sup>1</sup>,  
Lorenzo Maggi<sup>2</sup>, Marina Mora<sup>2</sup>, Sara Gibertini<sup>2</sup>, Ornella Cappellari<sup>1</sup>, Annamaria De Luca<sup>1</sup>,  
Mauro Coluccia<sup>1†</sup> and Antonella Liantonio<sup>1\*†</sup>**

<sup>1</sup> Department of Pharmacy—Drug Sciences, University of Bari, Bari, Italy, <sup>2</sup> Neuromuscular Diseases and Neuroimmunology  
Unit, Foundation IRCCS Neurological Institute C. Besta, Milan, Italy

Tubular Aggregate Myopathy (TAM) is a hereditary ultra-rare muscle disorder characterized by muscle weakness and cramps or myasthenic features. Biopsies from TAM patients show the presence of tubular aggregates originated from sarcoplasmic reticulum due to altered Ca<sup>2+</sup> homeostasis. TAM is caused by gain-of-function mutations in STIM1 or ORAI1, proteins responsible for Store-Operated-Calcium-Entry (SOCE), a pivotal mechanism in Ca<sup>2+</sup> signaling. So far there is no cure for TAM and the mechanisms through which *STIM1* or *ORAI1* gene mutation lead to muscle dysfunction remain to be clarified. It has been established that post-natal myogenesis critically relies on Ca<sup>2+</sup> influx through SOCE. To explore how Ca<sup>2+</sup> homeostasis dysregulation associated with TAM impacts on muscle differentiation cascade, we here performed a functional characterization of myoblasts and myotubes deriving from patients carrying STIM1 L96V mutation by using fura-2 cytofluorimetry, high content imaging and real-time PCR. We demonstrated a higher resting Ca<sup>2+</sup> concentration and an increased SOCE in STIM1 mutant compared with control, together with a compensatory down-regulation of genes involved in Ca<sup>2+</sup> handling (*RyR1*, *Atp2a1*, *Trpc1*). Differentiating STIM1 L96V myoblasts persisted in a mononuclear state and the fewer multinucleated myotubes had distinct morphology and geometry of mitochondrial network compared to controls, indicating a defect in the late differentiation phase. The alteration in myogenic pathway was confirmed by gene expression analysis regarding early (*Myf5*, *Mef2D*) and late (*DMD*, *Tnnt3*) differentiation markers together with mitochondrial markers (*IDH3A*, *OGDH*). We provided evidences of mechanisms responsible for a defective myogenesis associated to TAM mutant and validated a reliable cellular model useful for TAM preclinical studies.

**Keywords:** STIM1, tubular aggregate myopathy, myogenesis (*in vitro*), high content imaging, calcium homeostasis

## INTRODUCTION

In its primary form, Tubular Aggregate Myopathy (TAM) is a clinically heterogeneous and very rare skeletal muscle disorder, in most cases inherited in an autosomal dominant pattern (Böhm and Laporte, 2018; Michelucci et al., 2018; Morin et al., 2020). Signs and symptoms typically begin in childhood and worsen over time. TAM patients can be characterized by asymptomatic elevated creatine kinase (CK) levels as well as by muscle weakness predominantly affecting the proximal muscles of lower limbs. Myalgia and cramps have also been described (Böhm et al., 2014; Hedberg et al., 2014; Walter et al., 2015) and in some cases the full picture of the multisystemic Stormorken syndrome develops (Morin et al., 2020). A consistent histopathological feature of TAM patients is represented by the presence of tubular aggregates (TAs) in skeletal muscle fibers. TAs are formed by regular arrays of densely packed membrane tubules, most likely originating from sarcoplasmic reticulum (SR) (Böhm et al., 2013, 2017; Endo et al., 2015; Harris et al., 2017; Böhm and Laporte, 2018). However, TAs represent a non-specific morphological alteration being present in several neuromuscular disorders associated to SR stress (Michelucci et al., 2018).

TAM can be caused by heterozygous mutations in STIM1 or ORAI1 gene (Morin et al., 2020), both encoding for  $\text{Ca}^{2+}$  homeostasis key regulators, and CASQ1 gene (Barone et al., 2017; Böhm et al., 2018), encoding for calsequestrin, the major  $\text{Ca}^{2+}$  buffering protein in skeletal muscle SR. Particularly, STIM1 and ORAI1 are key components of the calcium release-activated calcium (CRAC) channels (Prakriya, 2009), which are activated following intracellular SR or endoplasmic reticulum (ER)  $\text{Ca}^{2+}$  store depletion and allow extracellular  $\text{Ca}^{2+}$  influx through a process called store operated  $\text{Ca}^{2+}$  entry (SOCE). SOCE is therefore fundamental in a variety of cellular functions, including secretion, transcription, motility, enzyme activity,  $\text{Ca}^{2+}$  store filling-state, and muscle contraction (Kiviluoto et al., 2011; Stiber and Rosenberg, 2011; Cho et al., 2017). SOCE-dependent  $\text{Ca}^{2+}$  signaling is also crucial for the onset of skeletal muscle development (Stiber et al., 2008; Darbellay et al., 2009, 2010; Li et al., 2012; Phuong et al., 2013; Wei-Lapierre et al., 2013; Tu et al., 2016). SOCE is indeed necessary for the activity of various  $\text{Ca}^{2+}$ -dependent enzymes regulating myogenesis-associated transcription factors, as has been shown for Nuclear Factor of Activated T cells (NFAT) in murine models (Kegley et al., 2001; Armand et al., 2008), as well as for Myocyte Enhancer Factor-2 (MEF2) and Myogenin in myoblasts deriving from human biopsies (Louis et al., 2008; Darbellay et al., 2009, 2010).

STIM1 is an ER/SR transmembrane protein activated by a drop in ER/SR calcium levels. This is at the basis of the SOCE process. Indeed, following  $\text{Ca}^{2+}$  store depletion, the STIM1  $\text{Ca}^{2+}$ -sensing intraluminal EF-hands undergo a conformational switch leading to protein di- and oligomerization, to an extended active state, interacting and activating the plasma membrane  $\text{Ca}^{2+}$  channel ORAI1, thus finally leading to  $\text{Ca}^{2+}$  entry (Park et al., 2009; Cho et al., 2017; Gudlur et al., 2018).

To date, 18 distinct STIM1 mutations causing TAM have been identified, of which 15 cluster in the EF-hand domains

(Morin et al., 2020). According to the resolved STIM1 protein structure (Yang et al., 2012; Zhu et al., 2017; Lopez et al., 2020), TAM-associated STIM1 EF-hand mutations appear to affect amino acids involved in  $\text{Ca}^{2+}$  coordination or forming a hydrophobic pocket which maintains STIM1 in a folded state (Stathopoulos et al., 2008; Böhm et al., 2014). Functional impact of TAM-associated STIM1 EF-hand mutations has been investigated through their heterologous expression in murine C2C12 myoblasts (Böhm et al., 2013) as well as in other engineered cell lines (Hedberg et al., 2014; Nesin et al., 2014). All known EF-hand mutations were shown to induce STIM1 oligomerization and clustering independently from intraluminal SR/ER  $\text{Ca}^{2+}$  level, thus indicating a constitutive STIM1 and SOCE activation and a gain-of-function effect leading to intracellular  $\text{Ca}^{2+}$  accumulation (Böhm and Laporte, 2018). Importantly, only in selected cases, *i.e.*, the STIM1 A84G (Böhm et al., 2013) and G81A (Walter et al., 2015) mutations,  $\text{Ca}^{2+}$  homeostasis alteration was directly confirmed on TAM patient-derived muscle cells.

So far, there is no cure for TAM and there is little information in literature regarding a therapy or management of this disorder. Considering that symptoms generally occur at a young age and significantly reduce the quality of life of the affected people, there is an urgent need to find new treatments. The resulting aberrant  $\text{Ca}^{2+}$  homeostasis associated to TAM mutants is likely the key cellular event causing serious damage on muscle development and integrity. Thus, the investigation of cellular processes dysfunction induced by  $\text{Ca}^{2+}$  homeostasis alteration associated with TAM mutants remains a pivotal strategy to identify novel druggable targets for this rare disease.

In this study, the STIM1 L96V-associated  $\text{Ca}^{2+}$  homeostasis dysregulation has been evaluated in patient-derived skeletal muscle cells. This mutation, located in the  $\text{Ca}^{2+}$  sensing canonical EF hand (cEF-hand) of STIM1 protein, was identified in a 13 year old girl showing CK elevation and lower limb weakness and myalgia, along with a muscle histology characterized by TAs, fiber size variability and internal nuclei (Böhm et al., 2014). Functional and morphological characterization of patient derived STIM1 L96V myoblasts and myotubes has been performed by using  $\text{Ca}^{2+}$  cytofluorimetry, molecular biology and high content imaging technologies. Our results confirm the STIM1 L96V-associated  $\text{Ca}^{2+}$  homeostasis dysfunction on patient-derived cells and demonstrate, for the first time, that the STIM1 L96V mutation alters the myogenic differentiation program, particularly regarding the terminal differentiation step, thereby providing new insights in the pathogenesis of STIM1-related TAM.

## MATERIALS AND METHODS

### Cell Culture

Human muscle samples were provided by the Telethon biobank at Besta Neurological Institute in Milan. Written, informed consent was obtained from the subjects or their parents/legal guardians. Research was conducted according to protocols approved by the Institutional Review Board of the Besta Neurological Institute and University of Bari, and in compliance

with the Helsinki Declaration and local legislation. Particularly, we used myoblasts and myotubes deriving from one TAM patient's biopsy carrying STIM1 L96V mutant. The patient's mutation was found by Böhm's laboratory in 2014 (Böhm et al., 2014). Particularly, patient's cells genetic characterization was performed on DNA extracted from blood cells. Sanger-sequencing has been used for all coding exons and the adjacent splice-relevant regions of STIM1 (NM\_001277961). The mutation found in the proband was also analyzed in the parents (our patient belongs to Family 3 in Böhm et al., 2014). The patient carries a *de novo* heterozygous mutation. Mutations in DMD and lamin A/C (LMNA) were also excluded for the patient. A control muscle cell line was obtained from a patient not affected from TAM (who had no STIM, ORAI, or CASQ1 mutations) of the same age and sex of affected patients. To assess the myogenesis characteristics in control condition, gene expression analysis of genes involved in the differentiation of myoblasts to myotubes was performed both in cells deriving from a patient not affected from TAM (control) and for comparison in a control muscle cell line (HMb\_2) (see **Supplementary Material**). Myoblast derived cells were isolated from patients' biopsy, cultured using the protocol described in Zanotti et al. (2007) and used under 2 different stages of differentiation. Primary myoblasts were derived directly from biopsied material by culturing in Dulbecco's modified Eagle's medium (DMEM; Lonza Group Ltd, Basel, Switzerland) containing 20% heat-inactivated fetal bovine serum (FBS) (Gibco Life Technologies), 1% penicillin-streptomycin (Lonza), L-glutamine (Lonza), 10 µg/ml insulin (Sigma Aldrich, St. Louis, MO), 2.5 ng/ml basic fibroblast growth factor (bFGF) (Gibco Life Technologies), and 10 ng/ml epidermal growth factor (EGF) (Gibco). Cells were grown on plastic. The medium was changed twice weekly and the cultures examined by inverted-phase microscopy. Once at 70% confluence, they were dissociated enzymatically with trypsin-EDTA (Sigma) and seeded for immediate propagation, or frozen in medium containing 10% DMSO (Sigma) for later propagation or other use. To obtain myotubes, the myoblasts were seeded into 35 mm dishes or in chamber slides in DMEM proliferating medium. At 70% confluence, proliferating medium was changed to differentiating medium (DMEM, 1% penicillin-streptomycin, L-glutamine and insulin, without FBS, or growth factors) and the myoblasts could differentiate into myotubes after 10 days (Zanotti et al., 2007). After the isolation, we analyzed phenotypic characteristic of the cell model carrying STIM1 L96V mutant, alongside with the non-mutated counterpart which represents control muscle cell. We evaluated various parameters on the proliferating and the differentiating myoblasts (T1, 5 days) and on the differentiated myotubes (T2, 10 days).

For fluorescence imaging analysis, both control and Leu96Val STIM1 myoblasts were seeded in quadruplicate in 96-well culture plates (96-well CellCarrier™, PerkinElmer) at 6,000/100 µL density and incubated at 37°C and 5% CO<sub>2</sub> to allow cell growth and proliferation. After 48 h incubation and cell washing, the growth medium was replaced by differentiation medium (T0) and incubation continued for further five (T1) or ten (T2) days, taking care to change the medium every 2 days.

## Cytosolic Calcium Measurements

Myoblasts or myotubes grown on coverslip were loaded for 30 min at room temperature with the cell permeant fluorescent Ca<sup>2+</sup> indicator 5 µM Fura-2-AM (Molecular Probes-Invitrogen, Italy) mixed to 0.05% (v/v) Pluronic F-127 (Molecular Probes) in normal physiological solution. Ratiometric images of Fura-2 fluorescence were monitored using an inverted Eclipse TE300 microscope (Nikon, Japan) with a 40X Plan-Fluor objective (Nikon, Japan). Fluorescence measurements were made using a QuantiCell 900 integrated imaging system (Visitech International Ltd., Sunderland, UK) as previously described (Conte et al., 2017). During the experiments, pairs of background subtracted images of Fura-2 fluorescence (510 nm) emitted after excitation at 340 and 380 nm were acquired and ratiometric images (340/380 nm) were calculated for each cell using QC2000 software. Subsequently fluorescence ratio values were converted to the resting cytosolic calcium concentration, [Ca<sup>2+</sup>]<sub>i</sub> (nM), after a calibration procedure using the following equation:  $[Ca^{2+}]_i = (R - R_{min}) / (R_{max} - R) * K_D * \beta$  where R is the ratio of the fluorescence emitted after excitation at 340 nm to the fluorescence after excitation at 380 nm; K<sub>D</sub> is the affinity constant of fura-2 for calcium, which was taken as 145 nM (Molecular Probes); and β is a parameter according to Grynkiewicz et al. (1985) that was determined experimentally *in situ* in ionomycin-permeabilized muscle fibers as previously described (Conte et al., 2017).

To measure SOCE, 2 µM Thapsigargin was used to passively deplete the Ca<sup>2+</sup> stores in the calcium free-solution and then extracellular Ca<sup>2+</sup> was applied to myoblasts or myotubes (SOCE protocol). The normal physiological solution was composed of 148 mM NaCl, 4.5 mM KCl, 2.5 mM CaCl<sub>2</sub>, 1 mM MgCl<sub>2</sub>, 0.44 mM NaH<sub>2</sub>PO<sub>4</sub>, 12 mM NaHCO<sub>3</sub>, and 5.5 mM glucose. The pH of all solutions was adjusted to 7.3–7.4 by bubbling them with 95% O<sub>2</sub>/5% CO<sub>2</sub>. The calcium free-solution has the same composition of normal physiological solution except that CaCl<sub>2</sub> was omitted and 10 mM ethylene glycol bis(β-aminoethyl ether)-N,N,N',N'-tetracetic acid (EGTA) was added. All chemicals cited above as well as ionomycin, caffeine and thapsigargin were purchased from Sigma (St. Louis, MO, USA).

## Fluorescent Probes, Image Acquisition, and Analysis

Cells were stained with a fluorophore dye cocktail containing Hoechst 33,342 (ThermoFisher) for nuclear staining and MitoTracker® Deep Red (ThermoFisher), 1 µM and 50 nM final concentration, respectively. MitoTracker® Deep Red enables the detection of cell shape and is also used to evaluate cytoplasmic morphological parameters along with mitochondrial mass and network features (texture). After 30 min incubation with the dye cocktail (37°C, 5% CO<sub>2</sub>), live cell image acquisitions were performed from 16 distinct areas/well using a Perkin Elmer Operetta High Content Imaging system (40x WD objective). Cytoplasmic and nuclear morphological parameters of differentiating control and STIM1 L96V myoblasts at T0, T1, and T2 time points were analyzed at single-cell level using Harmony 3.1 software. Briefly, images were first segmented into

nuclei and cytoplasm using “Find Nuclei” and “Find Cytoplasm” Building blocks on Hoechst and MitoTracker® Deep Red channels, respectively. After image segmentation, a set of basic intensity and morphological properties (e.g., area, roundness, etc.), and mitochondrial texture patterns of selected objects was calculated using “Calculate Intensity Properties,” “Calculate Morphology Properties” and “SER texture analysis” building blocks, respectively. Distinct mononuclear and multinuclear morphological phenotypes of skeletal muscle cells were manually identified and then used in the PhenoLOGIC™ machine learning module of the Harmony software. The PhenoLOGIC module requires users to supervise training selecting about 100 representative cells/class, thus allowing the software to distinguish different phenotypes. The software performs a linear discriminant analysis to create a linear combination of the most relevant parameters that are then applied to untrained sample wells to classify cells. This approach is very helpful, considering the morphological variety of differentiating skeletal muscle cells. As far as the mitochondrial texture properties are concerned, the analysis was performed using the SER features method. Briefly, the image texture features usually described as smooth, rough, granular, homogeneous/inhomogeneous, linear *etc.* were quantified calculating the numerical properties which quantitatively describe the texture. The SER (Spot, Edge, Ridge) features method includes a set of eight properties (spot, hole, edge, ridge, valley, saddle, bright, and dark) sensitive to distinct intensity patterns according to the property geometry designation. All results are reported as mean  $\pm$  SD from three independent experiments, each performed in quadruplicate. GraphPad Prism (GraphPad Software, Inc.) was used for calculating statistics and creation of graphs.

## Real Time PCR

Total RNA was extracted from myoblasts and myotubes using RNeasy Micro Kit (Qiagen C.N. 74004, Valencia) according to the manufacturer's protocols and RNA quantity was assessed using a spectrophotometer (ND-1000 NanoDrop, Thermo Scientific, United States). Reverse transcription and real-time PCR analysis were performed as previously described (Conte et al., 2017). The mRNA expression of genes was normalized to the best housekeeping gene: Beta-actin (*Actb*) selected from beta-2-microglobulin (*B2m*) and *ACTB* by Normfinder software. Genes were analyzed by the use of TaqMan Hydrolysis primer and probe gene expression assays that are produced by Life-Technologies with the following assay IDs: *ORAI1* assay ID: Hs03046013\_m1; *STIM1* assay ID: Hs00963373\_m1; *RYR1* assay ID: Hs00166991\_m1; *ATP2A1* (encoding SERCA1 protein) assay ID: Hs01092295\_m1; *CACNA1S* (encoding Cav1.1 protein) assay ID: Hs00163885\_m1; *ATP1A2* (encoding SERCA2 protein) assay ID: Hs00265131\_m1; *TRPC1* assay ID: Hs00608195\_m1; *TRPC4* assay ID: Hs01077392\_m1; *OGDH* assay ID: Hs01081865\_m1; *IDH3A* assay ID: Hs01051668\_m1; *PAX7* assay ID: Hs00242962\_m1; *MYF5* assay ID: Hs00271574\_m1, *MYOD1* assay ID: Hs00159528\_m1; *MEF2D* assay ID: Hs00954735\_m1; *MYOG* assay ID: Hs01072232\_m1; *TNNT3* (encoding Troponin protein) assay ID: Hs00952980\_m1; *DMD* (encoding Dystrophin protein) assay ID: Hs00758098\_m1; *B2M*

assay ID: Hs00984230\_m1 and *Actb* assay ID: Hs99999903\_m1. For genes that were poorly expressed, such as *Trpc1*, *Trpc4*, *Myf5*, and *Dmd*, preamplification by TaqMan PreAmp Master Mix (Life Technologies C.N. 4391128) was made before real-time experiments with a set-up of pre-amplification detailed in Conte et al. (2017). The real-time PCR protocols were performed in line with the guidelines for qPCR (Bustin et al., 2009).

## STATISTICS

Statistical analysis was performed using Student's *t*-test, with *p* < 0.05 or less considered as significant for calcium measurement and gene expression analysis. GraphPad Prism (GraphPad Software, Inc.) was used for calculating statistics (*t*-test, *chi*-square test, analysis of variance and Tukey HSD *post-hoc* test) and creation of graphs for high content fluorescence analysis.

## RESULTS

### Calcium Homeostasis

In engineered murine myoblasts, all TAM-associated STIM1 EF-hand mutations so far identified, including the L96V one, have been shown to induce protein clustering and excessive Ca<sup>2+</sup> entry independently from SR intraluminal Ca<sup>2+</sup> level (Böhm and Laporte, 2018). Particularly, C2C12 myoblasts transfected with STIM1 L96V-YFP displayed statistically significant STIM1 clustering regardless of SR Ca<sup>2+</sup> depletion (Böhm et al., 2014). Here, Ca<sup>2+</sup> homeostasis alterations associated with STIM1 L96V mutation have been investigated on skeletal muscle cells deriving from TAM patient's biopsy. The clinical, histological and functional phenotype of this patient has been already defined (Böhm et al., 2014). Free intracellular Ca<sup>2+</sup> was measured by using the ratiometric fluorescent dye Fura-2. Both STIM1 L96V myoblasts and myotubes, the latter obtained after 10 days in differentiation medium, showed higher basal cytoplasmic Ca<sup>2+</sup> level with respect with control cells (Figures 1A,D).

To examine the effect of STIM1 L96V mutation on SOCE, Ca<sup>2+</sup> was first depleted from the SR of myoblasts or myotubes with thapsigargin, in the absence of extracellular Ca<sup>2+</sup>, to avoid extracellular Ca<sup>2+</sup> entry during depletion, and then extracellular Ca<sup>2+</sup> was applied to myoblasts or myotubes to measure SOCE (Figures 1B,E, respectively). Both myoblasts and myotubes carrying STIM1 L96V mutation displayed a significant augmented SOCE compared to the respective control cells (Figures 1B,C,E,F).

Furthermore, to assess the Ca<sup>2+</sup> amount in the SR, we treated STIM1 L96V myotubes with 40 mM caffeine to induce extensive store depletion. Importantly, more Ca<sup>2+</sup> was released from the SR in STIM1 L96V myotubes than in control myotubes [Caffeine-induced  $\Delta[\text{Ca}^{2+}]_i = 320 \pm 27$  nM and  $214 \pm 35$  nM in mutant and control, respectively], thus demonstrating also an increase in the Ca<sup>2+</sup> SR content of STIM1 L96V muscle cells.

Thus, our functional assay conducted for the first time on patient-derived myoblasts and myotubes revealed that STIM1 L96V mutation is consistent with SOCE constitutive activation, i.e., with a gain of function effect.

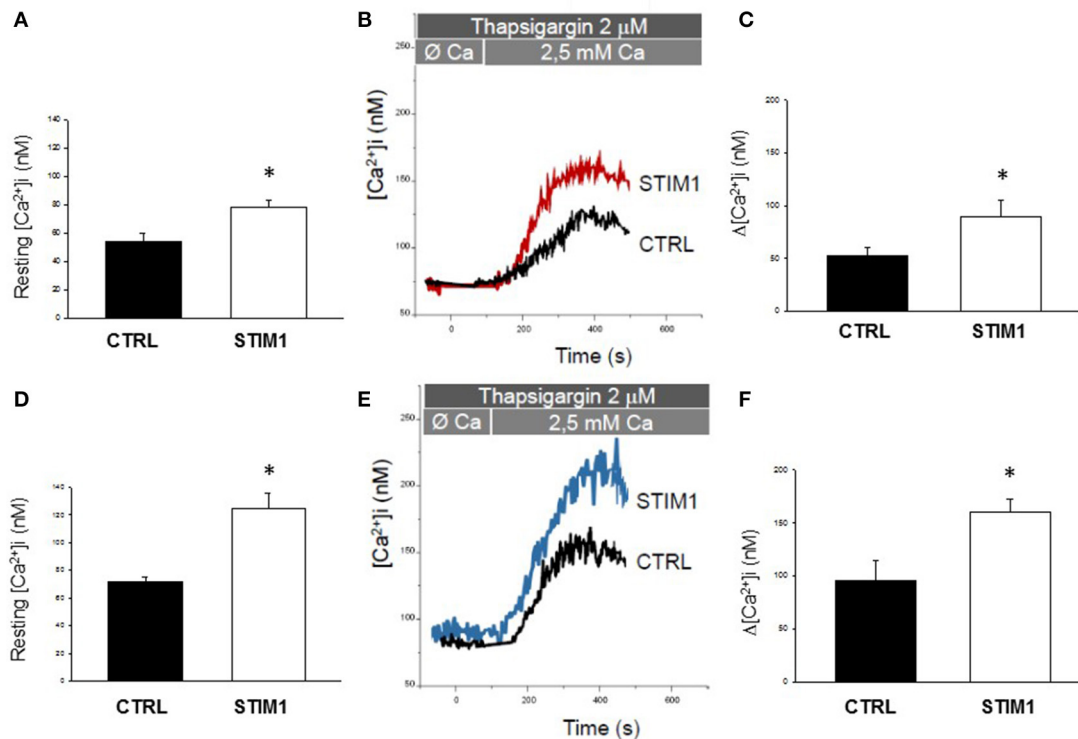


**FIGURE 1 |** Calcium homeostasis characterization of myoblast and myotubes carrying STIM1 L96V mutation. **(A–D)** Resting intracellular calcium, resting  $[Ca^{2+}]_i$  measured in control and STIM1 L96V myoblasts and control and STIM1 L96V myotubes. Each bar represents the mean  $\pm$  SEM of resting  $[Ca^{2+}]_i$  measured in 35–40 cells; **(B–E)** Representative traces of increased  $Ca^{2+}$  entry in store depleted thapsigargin treated cells after addition of extracellular calcium (see SOCE protocol described in Material and Methods) in control and STIM1 L96V myoblasts and in control and STIM1 L96V multinucleated myotubes **(C–F)** Amplitude values of  $[Ca^{2+}]_i$  increase observed with SOCE protocol in control and STIM1 L96V myoblasts and in control and STIM1 L96V multinucleated myotubes. Each bar represents the mean  $\pm$  SEM of  $[Ca^{2+}]_i$  increase measured in 25–30 cells. Statistical significance was determined by unpaired Student's *t*-test, with a value of  $P < 0.05$  considered significant, \*Significantly different.

## High Content Imaging of Differentiating Skeletal Muscle Cells

Different lines of evidence indicate that SOCE is a key factor controlling myoblasts fate (Louis et al., 2008; Darbellay et al., 2009, 2010; Michelucci et al., 2018) as well that mitochondria participate in the differentiating process of various cell types, including muscle cells (Noguchi and Kasahara, 2018). On this basis, cellular morphology properties and mitochondrial network features of control and STIM1 L96V differentiating cells have been investigated *in vitro* by automated fluorescence microscopy. The quantitative analysis of morphological changes associated with differentiation was performed on living myoblasts, at distinct time points after substitution of differentiation medium for growth medium (T0, T1, and T2, corresponding to 0, 5, and 10 days, respectively).

### Differentiation-Associated Morphological Features

As shown in **Figure 2A** (panels A–C), the myogenic differentiation process of control myoblasts is characterized by the presence of mononuclear cells at T0, followed by the increase of cell size as well as the emergence of multinuclear cells after 5 days (T1) and, to a greater extent, after 10 days (T2)

in differentiation medium. In parallel with the appearance of multinucleated elements, the number of control mononuclear cells progressively decreases (**Figure 2B**). In the case of STIM1 L96V cells, only rare multinucleated elements are present at T1, containing two-three nuclei [**Figure 2A** (panel E), arrowhead], whereas elements with more than 10 nuclei are already formed by control cells at this time [**Figure 2A** (panel B), arrow]. In parallel, mononuclear STIM1 L96V cells show a longer persistence, only at T2 their number being significantly reduced (**Figure 2B**).

### Cell Morphometry and Mitochondrial Texture Properties of Mononuclear Control and STIM1 L96V Cells (T0)

Both control and STIM1 L96V myoblasts at T0 are mononuclear cells, characterized by variable size and rounded or spindle-shaped morphology (**Figure 2**, asterisks and arrows, respectively, in panels A and D). The relative amount of rounded and spindle-shaped myoblasts in the two cell populations was calculated by using the PhenoLOGIC module, finding that the percentage of spindle-shaped cells in STIM1 L96V myoblasts was significantly higher than that of normal cells (47 and 38%, respectively;  $p = 0.005$ , chi-square test; data not shown). The comparative

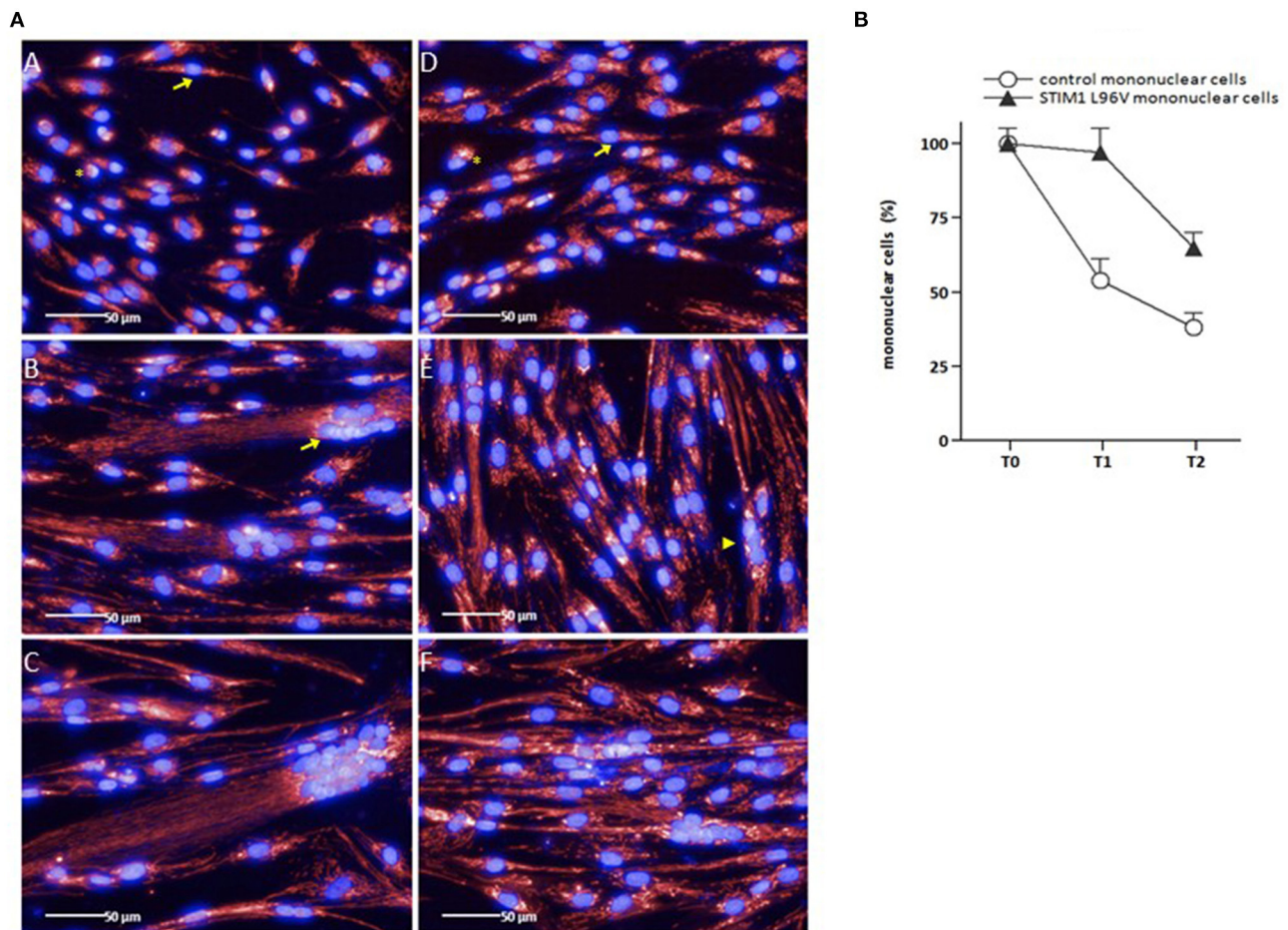


**FIGURE 2 |** Representative images of control and STIM1 L96V skeletal muscle cells at different time points in differentiation medium (A), and differentiation-associated decrease of control and STIM1 L96V mononuclear cells (B). (A) Control and STIM1 L96V mononuclear mononuclear cells were seeded in 96-well cell culture plates (6,000/100  $\mu$ L). Upon reaching sub-confluence ( $\sim$ 60%), growth medium was replaced by differentiation medium to induce myoblast differentiation and myotube formation. For fluorescence staining of mitochondria (red) and nuclei (blue), MitoTracker Deep Red and Hoechst 33,342 were added into the media (final concentration 50 nM and 1  $\mu$ M, respectively). After 30 min of incubation at 37°C, 5% CO<sub>2</sub>, live-cell images were recorded by automated fluorescence microscopy at day 0 (T0), 5 (T1), and 10 (T2) for control (panels A, B, C) and STIM1 L96V cells (panels D, E, F), respectively (Perkin Elmer Operetta High-Content Imaging System, 40x LWD objective). Asterisks and arrows in panels A and D indicate rounded and spindle-shaped control and STIM1 L96V myoblasts at T0, respectively. The arrow and arrowhead in panels B and E indicate a multinucleated control and STIM1 L96V cell at T1, respectively. (B) The percentage of mononuclear control and STIM1 L96V cells at distinct time points in differentiation medium is shown as mean  $\pm$  SD.

analysis of cell morphometry parameters reveals the features of control and STIM1 L96V myoblasts at T0 (Table 1). STIM1 L96V myoblasts are about 20% bigger than normal myoblasts, as indicated by cell area values, and have a more pronounced spindle-shaped morphology (roundness index: 0.68 and 0.61, respectively). The mitochondrial mass mean concentration (mitotracker intensity mean) of control and STIM1 L96V myoblasts is similar, whereas the total mitochondrial mass (mitotracker intensity sum) of STIM1 L96V myoblasts is higher, according to their increased cell size.

The effects of STIM1 L96V mutation on the mitochondrial architecture have been evaluated calculating the frequency of texture feature or combination of features using the “SER features” building block of the Harmony software

(Supplementary Material). All SER texture indexes of STIM1 L96V myoblasts were significantly different from those of control myoblasts, except for spot and hole feature (Figure 3A). The major differences concern in the order saddle, valley, edge and ridge, indicating that STIM1 L96V myoblasts at T0 are characterized by a more elongated and networked mitochondrial architecture with respect to control myoblasts.

#### Differentiation-Associated Modifications of Mononuclear Control and STIM1 L96V Cells

The differentiation-associated modifications of mononuclear cell morphometry of control and STIM1 L96V cells after 5 (T1) and 10 (T2) days in differentiation medium are reported in Tables 2, 3, respectively. The cell size of control cells

**TABLE 1** | Morphological features of control and STIM1 L96V myoblasts at T0.

Cell morphometry	Control myoblasts	STIM1 L96V myoblasts	P-value (unpaired t-test)
Cell area ( $\mu\text{m}^2$ )	409 $\pm$ 227	506 $\pm$ 274	<0.0001
Cell roundness*	0.68 $\pm$ 0.14	0.61 $\pm$ 0.15	<0.0001
Mito intensity Mean (AU)	256 $\pm$ 122	261 $\pm$ 98	0.09
Mito intensity Sum (AU)	1,017,364 $\pm$ 750,531	1,341,283 $\pm$ 894,914	<0.0001
Nuclear area ( $\mu\text{m}^2$ )	120 $\pm$ 41	141 $\pm$ 46	<0.0001
Nuclear roundness*	0.944 $\pm$ 0.038	0.946 $\pm$ 0.038	0.007
Nuclear Intensity Mean (AU)	1,118 $\pm$ 261	1,117 $\pm$ 236	0.87
Nuclear Intensity Sum (AU)	2,071,623 $\pm$ 596,194	2,440,722 $\pm$ 641,465	<0.0001

\*Cell and nuclear roundness are proportional to the square root of the area divided by the circumference: it is normalized to give 1 for a perfect circle and decreases for elongated objects. AU, Arbitrary Units. All data are expressed as mean  $\pm$  SD of measurements performed at single-cell level ( $n > 5,000$  cells/group).

progressively increases as well as the spindle-shaped morphology, the major increment occurring in the T0–T1 interval. Moreover, both mitotracker mean intensity and sum intensity values progressively increase, indicating a corresponding enhancement of mitochondrial mass and concentration (Table 2). As far as morphological modifications accompanying STIM1 L96V mononuclear cell differentiation are concerned, the results resemble those of control cells regarding size, spindle-shaped morphology and mitochondrial mass increase (Table 3). In contrast to control cells, however, the mitotracker mean intensity remains substantially unmodified from T0 to T2, suggesting that mitochondrial activity of mononuclear STIM1 L96V cells does not increase along with differentiation.

Differentiation-associated modifications of mitochondrial mass of control mononuclear cells were also accompanied by mitochondrial texture changes (Figure 3C). In the T0–T1 interval, the major variations of SER features concern the spot and hole filters, whose indexes reduce by around 18%, and the edge filter, which increases by 13%. This pattern suggests a relative increase of fragmentation over elongation in the mitochondrial architecture. Instead in the T1–T2 interval, SER

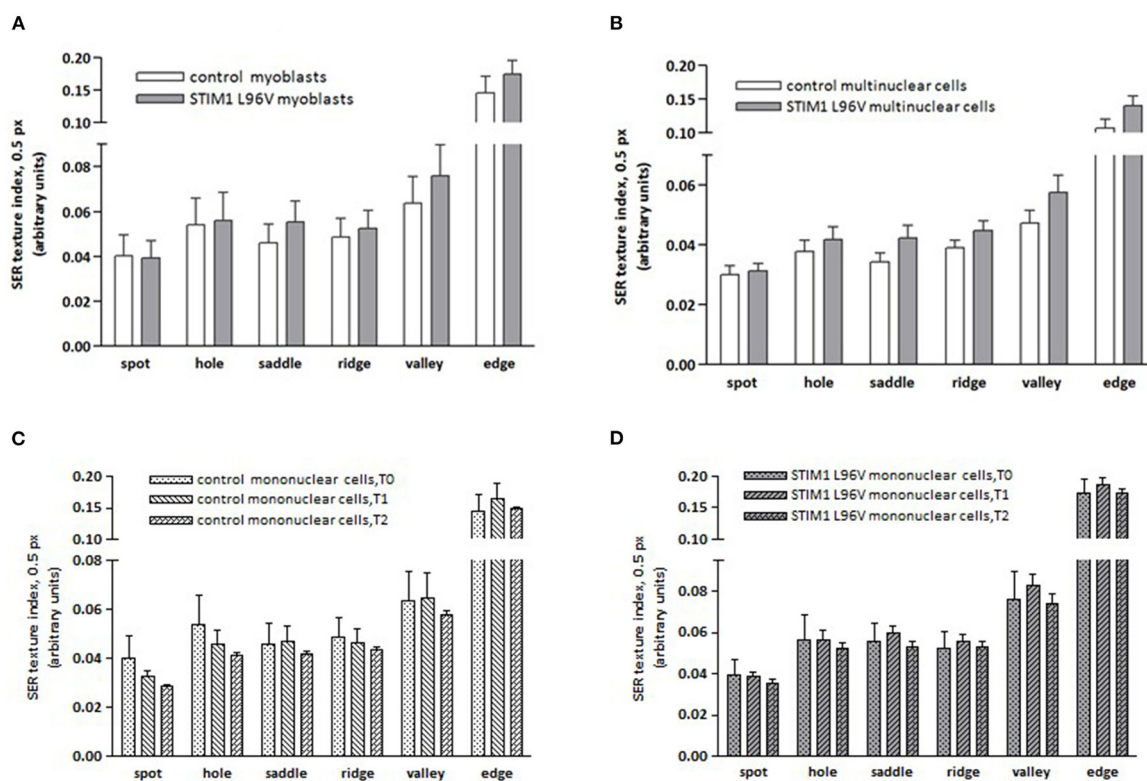


**FIGURE 3** | Mitochondrial SER texture indexes of control and STIM1 L96V skeletal muscle cells. **(A)** SER texture indexes of SER spot, hole, saddle, ridge, valley, and edge of normal and STIM1 L96V mononuclear cells at T0 are shown as mean  $\pm$  SD (cell number  $> 5,000$ /group). All SER features of STIM1 L96V myoblasts are significantly different from those of control myoblasts ( $p < 0.0001$ , unpaired *t*-test), except for spot and hole. **(B)** SER texture indexes of SER spot, hole, saddle, ridge, valley, and edge of normal and STIM1 L96V multinuclear cells are shown as mean  $\pm$  SD (cell number  $> 300$ ). All variations of SER texture indexes are significantly different ( $p < 0.005$  for spot;  $P < 0.0001$  for the remaining filters, unpaired *t*-test). **(C,D)** Differentiation-associated variations of mitochondrial SER texture indexes of control **(C)** and STIM1 L96V **(D)** mononuclear cells; the SER texture indexes at distinct time points in differentiation medium are shown as mean  $\pm$  SD (cell number  $> 5,000$  for T0 groups, and  $> 3,000$  for T1 and T2 groups). Time point-associated variations of SER texture indexes are significantly different for all SER features:  $P < 0.0001$ , ANOVA and Tukey HSD *post-hoc* test, in both control **(C)** and STIM1 L96V **(D)** mononuclear cells, except for hole in the T0–T1 comparison of STIM1 L96V cells.

**TABLE 2 |** Differentiation-associated modifications of control mononuclear cells.

Cell morphometry	T0	T1	T2	P-value (ANOVA, and Tukey HSD <i>post-hoc</i> test)
Cell area ( $\mu\text{m}^2$ )	409 $\pm$ 223	776 $\pm$ 56	944 $\pm$ 80	<0.0001 (T2>T1>T0)
Cell roundness*	0.68 $\pm$ 0.14	0.48 $\pm$ 0.039	0.44 $\pm$ 0.0168	<0.0001 (T0>T1>T2)
Mito intensity Mean (AU)	256 $\pm$ 122	359 $\pm$ 54	421 $\pm$ 20	<0.0001 (T2>T1>T0)
Mito intensity Sum (AU)	1,017,364 $\pm$ 750,531	3,214,531 $\pm$ 783,315	5,103,299 $\pm$ 530,463	<0.0001 (T2>T1>T0)
Nuclear area ( $\mu\text{m}^2$ )	120 $\pm$ 41	151 $\pm$ 4	148 $\pm$ 6	<0.0001 (T1, T2>T0)
Nuclear roundness*	0.944 $\pm$ 0.038	0.946 $\pm$ 0.04	0.945 $\pm$ 0.05	0.2
Nuclear Intensity Mean (AU)	1,118 $\pm$ 261	2,013 $\pm$ 50	1,997 $\pm$ 56	<0.0001 (T1, T2>T0)
Nuclear Intensity Sum (AU)	2,071,623 $\pm$ 596,194	4,803,092 $\pm$ 85,521	4,764,357 $\pm$ 88,105	<0.0001 (T1, T2>T0)

\*Cell and nuclear roundness are proportional to the square root of the area divided by the circumference: it is normalized to give 1 for a perfect circle and decreases for elongated objects. AU, Arbitrary Units. All data are expressed as mean  $\pm$  SD of measurements performed at single-cell level ( $n > 5,000$  cells for T0, and  $> 3,000$  cells/group for T1 and T2 groups).

**TABLE 3 |** Differentiation-associated modifications of STIM1 L96V mononuclear cells.

Cell morphometry	T0	T1	T2	P-value (ANOVA, and Tukey HSD <i>post-hoc</i> test)
Cell area ( $\mu\text{m}^2$ )	506 $\pm$ 274	749 $\pm$ 44	943 $\pm$ 61	<0.0001 (T2>T1>T0)
Cell roundness*	0.61 $\pm$ 0.15	0.4548 $\pm$ 0.0197	0.3942 $\pm$ 0.0181	<0.0001 (T0>T1>T2)
Mito intensity Mean (AU)	263 $\pm$ 98	265 $\pm$ 64	268 $\pm$ 58	0.09
Mito intensity Sum (AU)	1,341,283 $\pm$ 894,914	2,147,071 $\pm$ 365,087	3,292,538 $\pm$ 519,703	<0.0001 (T2>T1>T0)
Nuclear area ( $\mu\text{m}^2$ )	141 $\pm$ 46	168 $\pm$ 23	172 $\pm$ 36	<0.0001 (T1, T2>T0)
Nuclear roundness*	0.946 $\pm$ 0.038	0.950 $\pm$ 0.002	0.9339 $\pm$ 0.0058	0.2
Nuclear Intensity Mean (AU)	1,117 $\pm$ 236	1,818 $\pm$ 126	1,734 $\pm$ 135	<0.0001 (T1, T2>T0)
Nuclear Intensity Sum (AU)	2,440,722 $\pm$ 641,465	4,707,289 $\pm$ 73,993	4,718,524 $\pm$ 137,875	<0.0001 (T1, T2>T0)

\*Cell and nuclear roundness are proportional to the square root of the area divided by the circumference: it is normalized to give 1 for a perfect circle and decreases for elongated objects. AU, Arbitrary Units. All data are expressed as mean  $\pm$  SD of measurements performed at single-cell level (cell number  $> 5,000$  for T0 and T1 groups, and  $> 3,000$  for T2 group).

feature variations suggestive of mitochondrial fragmentation, i.e., decrease of spot, hole, and saddle, are quantitatively similar to the elongation-associated features (ridge and edge), thus indicating a balance in the mixed morphology of mitochondrial network. Mitochondrial texture modifications accompanying STIM1 L96V mononuclear cell differentiation resemble those of control cells in both T0–T1 and T1–T2 intervals. However, the variations of SER indexes indicative of network fragmentation are less pronounced than those of control cells in the T0–T1 interval, and a parallel increase of the saddle and valley features indicates a mitochondrial elongation (**Figure 3D**).

### Cell Morphometry and Mitochondrial Texture Properties of Control and STIM1 L96V Multinuclear Cells (T2)

A comparison of morphological features and mitochondrial architecture of multinuclear control and STIM1 L96V cells is reported in **Table 4** and **Figure 3B**, respectively. Multinuclear STIM1 L96V cells are smaller than corresponding normal cells. Curiously, STIM1 L96V cells are also more spindle-shaped, this feature being present during the entire differentiation process (**Tables 2, 3**). The nuclear parameters of STIM1 L96V cells are all lower than those of control cells, according to the

**TABLE 4 |** Morphological features of control and STIM1 L96V multinuclear cells (T2).

Cell morphometry	Control multinuclear cells	STIM1 L96V multinuclear cells	P-value (unpaired t-test)
Cell area [ $\mu\text{m}^2$ ]	3,906 $\pm$ 425	3,094 $\pm$ 892	<0.0001
Cell roundness*	0.3302 $\pm$ 0.0559	0.2643 $\pm$ 0.0461	<0.0001
Mito intensity Mean (AU)	408 $\pm$ 59	345 $\pm$ 51	<0.0001
Mito intensity Sum (AU)	19,191,957 $\pm$ 2,295,938	13,170,555 $\pm$ 5,595,763	<0.0001
Nuclear area [ $\mu\text{m}^2$ ]	791 $\pm$ 139	669 $\pm$ 107	<0.0001
Nuclear roundness*	0.7031 $\pm$ 0.042	0.6895 $\pm$ 0.0365	0.02
Nuclear Intensity Mean (AU)	2,652 $\pm$ 279	2,074 $\pm$ 235	<0.0001
Nuclear Intensity Sum (AU)	36,364,900 $\pm$ 10,586,040	23,063,770 $\pm$ 5,622,289	<0.0001

\*Cell and nuclear roundness are proportional to the square root of the area divided by the circumference: it is normalized to give 1 for a perfect circle and decreases for elongated objects. AU, Arbitrary Units. All data are expressed as mean  $\pm$  SD of measurements performed at single-cell level ( $n > 300$  for both control and STIM1 L96V multinuclear cells).

reduced number of nuclei in multinuclear STIM1 L96V cells. The mitotracker mean intensity of STIM1 multinuclear elements is slightly lower than that of control cells, suggesting a reduction of mitochondrial membrane potential. Interestingly, mitotracker mean intensity of STIM1 L96V multinuclear elements was higher than that of the corresponding mononuclear cells at T2, suggesting a fusion-associated increase of mitochondrial function. Mitochondrial texture features of multinuclear control and STIM1 L96V myotubes are reported in **Figure 3B**. The major variations concern saddle, valley, and hole features, indicating an elongated architecture, even though the increase of ridge, and edge indexes also denotes an increase of the fragmented phenotype.

## Gene Expression Analysis

### Genes Involved in Calcium Homeostasis and TA Formation

Tubular aggregates are displayed in patient derived muscle cells used in our study (Böhm et al., 2014). Different proteins involved in the uptake and  $\text{Ca}^{2+}$  storage such as STIM1, sarcoplasmic reticulum  $\text{Ca}^{2+}$ -ATPase (SERCA1a) or ryanodine receptor 1 molecule (RyR1) were previously shown to be components of the aggregates (Chevessier et al., 2005; Böhm et al., 2013). In addition, STIM1 could directly interact with other proteins, such as the canonical-type transient receptor potential cationic channels (TRPCs) or the dihydropyridine receptor (DHPR) (Kiselyov and Patterson, 2009; Lee et al., 2013). By qPCR, we found a significant down-regulation of mRNA level of *RyR1* and *Atp2a1* (encoding for SERCA1a) in myoblasts and myotube carrying STIM1 L96V mutation compared to control myoblasts

and myotubes, respectively (**Figure 4**). Any significant change was detected in the expression level of *Stim1*, *Cacna1s* (encoding for DHPR), *Atp1a2* (encoding for Na/K ATPase) and *Trpc4*. Importantly, a trend of reduction of *Trpc1* already observed in myoblasts carrying STIM1 L96V mutation, became significant in differentiated myotubes, while *Orail1* expression, resulted unchanged in myoblasts, was significantly reduced in myotubes carrying STIM1 L96V (**Figure 4**).

### Genes Involved in Mitochondrial Function

To assess if STIM1 L96V mutation could affect mitochondrial function, we analyzed mRNA expression level of two mitochondrial  $\text{Ca}^{2+}$ -sensitive dehydrogenases fundamental to generate NADH needed by the respiratory chain to generate ATP, such as an isoform of isocitrate dehydrogenases (*IDH3A*), which catalyzes the oxidative decarboxylation of the isocitrate in  $\alpha$ -ketoglutarate, and 2-oxoglutarate dehydrogenase (*OGDH*), a component of the  $\alpha$ -ketoglutarate dehydrogenase complex that converts  $\alpha$ -ketoglutarate to succinate (Denton and McCormack, 1980). A significant reduction of the expression of *IDH3A* and *OGDH* was detected in myoblasts carrying STIM1 L96V mutation with respect to control myoblasts, which is however observed only for *OGDH* in mutated differentiated myotubes (**Figure 4**).

### Genes Involved During the Differentiation of Myoblasts to Myotubes

High content imaging analysis revealed a defective myogenesis associated to STIM1 L96V mutant muscle cells with respect to control cells. On this basis, we gained insight into the mechanism underlying the myogenic pathway alteration by analyzing the mRNA levels in STIM1 L96V myoblasts and myotubes of the following genes: *Pax7* (paired box 7), which is a member of the upstream regulators of myogenesis and a marker of satellite cells; *Myf5* (Myogenic factor 5) and *MyoD1* (Myogenic differentiation 1), which are members of the myogenic regulatory factor (MRF) family; *Mef2D* (Myocyte enhancer factor 2D), which is a member of the myocyte enhancer factor 2 family (MEF2) and *Myog* (Myogenin), both markers of differentiation; finally, *Tnnt3* (Troponin), and *DMD* (Dystrophin), were chosen as markers of late differentiation.

Interestingly, in STIM1 L96V myoblasts we found a significant reduction in *DMD*, *Tnnt3* and an increase in *Myf5* and *Mef2D* mRNA levels with respect to control myoblasts. A significant reduction in *Pax7*, *DMD*, and *Tnnt3* was observed in mutated myotubes with respect to control ones (**Figure 5**). No significant alteration was observed for *MyoD1* and *Myog* expression levels both in STIM1 L96V myoblasts and myotubes with respect to control cells.

All these findings indicate an altered myogenic pathway associated to STIM1 L96V mutation.

## DISCUSSION

TAM is a rare hereditary myopathy actually without a cure caused by mutations of genes involved in  $\text{Ca}^{2+}$  homeostasis. In more detail, gain-of-function mutations of STIM1 or ORAI1

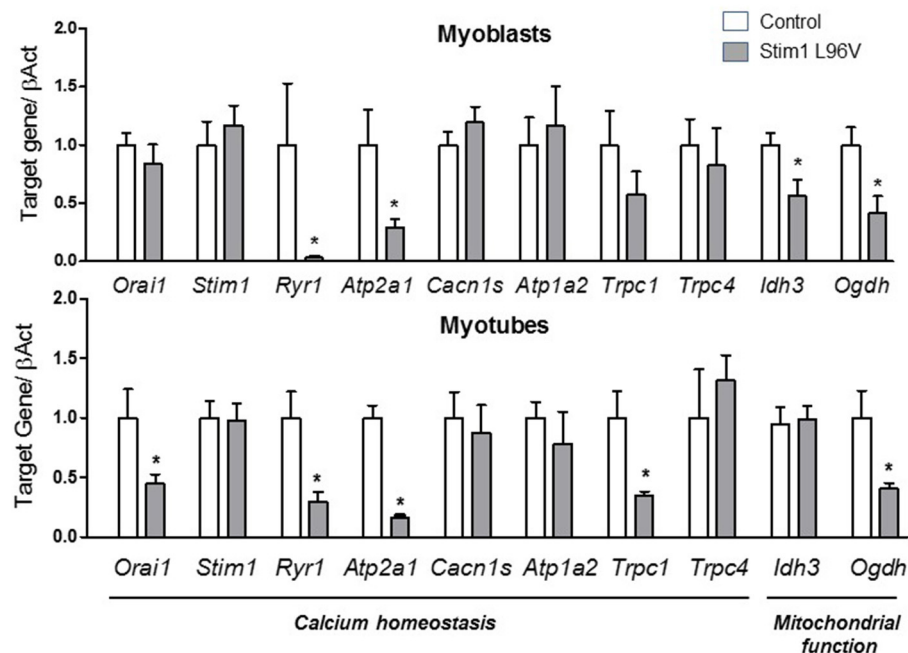


**FIGURE 4 |** Expression levels of selected genes involved in calcium homeostasis and mitochondrial function. The histograms show the relative content of transcript levels for *Orai1*, *Stim1*, *Ryr1*, *Atp2a1*, *Cacn1s*, *Atp1a2*, *Trpc1*, *Trpc4* genes involved in calcium homeostasis and *Ogdh*, and *Idh3* involved in mitochondrial function normalized to  $\beta$ -actin gene in STIM1 L96V myoblasts (upper Panel) and myotubes (bottom Panel) with respect of control cells. Data are expressed as fold-difference compared with control cells; samples were analyzed in triplicate, and results are expressed as the means  $\pm$  sem. Statistical significance was determined by unpaired Student's *t*-test, with a value of  $P < 0.05$  considered significant, \*Significantly different.

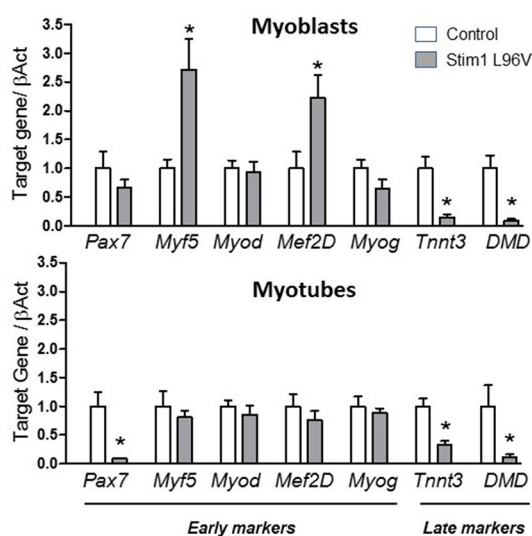


**FIGURE 5 |** Expression levels of selected genes involved in muscle differentiation. The histograms show the relative content of transcript levels for early markers of differentiation *Pax7*, *Myf5*, *Myod*, *Mef2D* and *Myog* genes, and later markers of differentiation *Tnnt3*, *DMD* genes normalized to  $\beta$ -actin gene in STIM1 L96V myoblasts (upper Panel) and myotubes (bottom Panel) with respect of control cells. Data are expressed as fold-difference compared with control cells; samples were analyzed in triplicate, and results are expressed as the means  $\pm$  sem. Statistical significance was determined by unpaired Student's *t*-test, with a value of  $P < 0.05$  considered significant, \*Significantly different.

genes inappropriately activate the SOCE process and induce an excessive extracellular  $\text{Ca}^{2+}$  entry despite repleted  $\text{Ca}^{2+}$  stores (Lacruz and Feske, 2015; Lee and Noguchi, 2016; Böhm and Laporte, 2018; Morin et al., 2020).  $\text{Ca}^{2+}$  homeostasis alterations affect a variety of cell functions, being  $\text{Ca}^{2+}$ -dependent signaling involved in multiple cellular processes (Carafoli and Krebs, 2016). As far as skeletal muscle cells are concerned, the  $\text{Ca}^{2+}$ -mediated coupling of excitation and contraction has long been well-established, but the recognition of  $\text{Ca}^{2+}$  relevance in muscle formation, growth and regeneration is also growing (Tu et al., 2016). Most of the STIM1 mutations responsible for TAM are located in the luminal  $\text{Ca}^{2+}$ -sensing EF-hand domain, and affect amino acids thought to be involved in  $\text{Ca}^{2+}$  coordination or maintaining the protein in a folded and inactive conformation (Böhm and Laporte, 2018). The patients carrying EF-hand mutations are mainly characterized by a muscle phenotype, a proximal muscle weakness being generally reported. However, a precise genotype/phenotype correlation is still undefined, the onset and severity of muscle involvement being not uniform for the different STIM1 EF-hand mutations (Morin et al., 2020). Symptoms vary greatly from patient to patient, with a wide phenotypical spectrum ranging from childhood-onset muscle weakness to adult-onset myalgia. Functional effects of STIM1 mutations at cellular level have been investigated mainly in heterologous expression systems and, only in the case of STIM1 A84G (Böhm et al., 2013) and G81A (Walter et al., 2015) mutations, also in patient-derived myoblasts.

In this study, we have investigated the  $\text{Ca}^{2+}$  homeostasis alterations of skeletal muscle cells from a TAM patient carrying the STIM1 L96V mutation. This mutation, along with the more recently reported L92V (Morin et al., 2020), is located in the hydrophobic cleft which contributes to keeping the STIM1 inactive conformation, according to molecular modeling simulations (Schober et al., 2019). We confirm in human myoblasts the STIM1 L96V-dependent  $\text{Ca}^{2+}$  overload already reported in engineered murine myoblasts and detect the  $\text{Ca}^{2+}$  alteration persistence also in differentiated cells. The resting  $\text{Ca}^{2+}$  level is set by the balance between influx and efflux mechanisms at rest (Li et al., 2010; Ríos, 2010) and whether STIM1 L96V is the main source for the resting  $\text{Ca}^{2+}$  dysregulation remain to be defined. Indeed, this is an unsolved aspect also for other described STIM1 mutants (Morin et al., 2020). In this regards, the use of SOCE inhibitors at different times of myogenesis process would be useful to explore the observed differences in resting  $\text{Ca}^{2+}$  level between patient-derived muscle cells and control cells. Notably, in view of the non-specific effects mediated by SOCE inhibitors actually available (Le Guilcher et al., 2020; Meizoso-Huesca and Launikonis, 2021), focused studies will be required based on the use of several tools to unequivocally solve this issue.

The measured excess of intraluminal and cytosolic  $\text{Ca}^{2+}$  is accompanied by expression profile modifications of genes involved in  $\text{Ca}^{2+}$  homeostasis. Our findings of expression profile regarding genes encoding proteins involved in  $\text{Ca}^{2+}$  homeostasis indicate an adaptive or compensatory response of the cells to the increased SOCE, which was already observable in myoblast and became clear in differentiated myotubes. Indeed, the significant reduction of *Orai1*, *RyR1*, and *Atp2a1* expression could be considered an attempt of muscle cells to counteract the  $\text{Ca}^{2+}$  homeostasis dysfunction. The parallel reduction of *Trpc1* could corroborate the involvement of these cationic channels into the STIM1-induced aggregate composition, as reported in other studies (Kiselyov and Patterson, 2009; Lee et al., 2013). Furthermore, *RyR1* expression reduction could be also correlate with the expression of the other RyR isoform expressed in skeletal muscle, i.e., *RyR3*. Indeed, *RyR3* isoform has a significant effect on resting  $\text{Ca}^{2+}$  levels and a precise balance between *RyR1* and *RyR3* expression physiologically tightly regulate the diversity of cellular responses that muscle cells undergo during their early development (Protasi et al., 2000; Perez et al., 2005). Particularly, in myotubes *RyR3* has virtually no role in initiating or maintaining EC coupling. Thus, it may be postulated that the reduction of *RyR1* gene expression we observed in *Stim1* mutant myotubes is likely related with a consequent *RyR1* and *RyR3* expression imbalance. This could be supported by the increased level of resting  $\text{Ca}^{2+}$  as well as by the significantly increased responsiveness to caffeine in STIM1 mutant muscle cells with respect to control cells. Indeed, it has been reported that altered expression of *RyR3* resulted in myotubes with significantly higher resting  $\text{Ca}^{2+}$  level as well as with a different caffeine sensitivity than myotubes expressing *RyR1* (Perez et al., 2005).

The STIM1/ORAI1-mediated SOCE is emerging as a critical process in regulating long-term muscle functions and a growing

evidence supports its relevance in muscle differentiation, development, and growth (Louis et al., 2008; Darbellay et al., 2009, 2010; Michelucci et al., 2018). To evaluate the cellular response to  $\text{Ca}^{2+}$  dyshomeostasis, in this study, we compared the morphological features of STIM1 L96V myoblasts and control myoblasts, and investigated the effects of STIM1 L96V mutation on *in vitro* myogenic differentiation process through high content imaging and gene expression analysis. Cells morphology and mitochondrial network are critical for several biological processes that control nuclear programs and are strictly related to  $\text{Ca}^{2+}$  handling in skeletal muscle (Favaro et al., 2019). Thus, we particularly focused on these cellular features. First of all, high content imaging was employed for evaluating similarities and differences between control and STIM1 L96V myoblasts at T0, i.e., when differentiation medium was substituted for growth medium. The variability of cellular shape and dimension of both control and STIM1 L96V myoblasts at T0 indicates that cells are in various growth stages and that some of them probably already started the differentiation process. This is most likely related to the use of non-synchronized cell cultures, an ex-ante choice undertaken with the aim of investigating differentiating muscle cells with minimal manipulation. Interestingly, STIM1 L96V myoblasts are larger and more spindle-shaped than control cells. More generally, the morphological features of STIM1 L96V myoblasts at T0 reflect the cellular adaptive response to the STIM1 mutation. In this respect, mitochondria might also be involved in cellular response to  $\text{Ca}^{2+}$  dyshomeostasis (Bagur and Hajnóczky, 2017). Mitochondria are dynamic organelles characterized by high mobility as well as shape changes, therefore they exhibit a mixed morphology, with small particles and tubular and highly networked structures (Karbowksi and Youle, 2003). Organizational changes of mitochondrial morphology are controlled by multiple processes, including biogenesis and fusion and fission events, which adapt mitochondrial shape to the cell physiological needs. Mitochondrial fusion and fission could be related to STIM1-mediated intracellular  $\text{Ca}^{2+}$  movements and SOCE and alterations of STIM1 expression or activity is associated with mitochondrial abnormalities in skeletal muscle cells (Goonasekera et al., 2014; Choi et al., 2019). SER texture analysis of mitochondrial network indicate that STIM1 L96V myoblasts at T0 are characterized by a more elongated and networked mitochondrial architecture with respect to control myoblasts. The  $\text{Ca}^{2+}$  overload associated with STIM1 L96V mutation could prematurely activate and/or upregulate the  $\text{Ca}^{2+}$ -dependent pathways, thus inducing an earlier onset of the differentiation process. This possibility is supported by the early appearance of spindle-shaped STIM1 L96V cells as well as by their more marked spindle-shaped morphology. If that was the case, it should be hypothesized that the mitochondrial system develops alongside the SR and myofibrils, as suggested by the elongated mitochondrial architecture observed in STIM1 L96V myoblasts in the early phase of differentiation.

High content imaging analysis of the differentiation process of control myoblasts shows a progressive increase of cell size and spindle-cell morphology. The parallel increase of mitochondrial mass and concentration also suggests an enhancement of

mitochondrial activity. Mitotraker deep red accumulation is indeed dependent upon mitochondrial membrane potential (Poot et al., 1996), and an increase of mitotracker signal intensity associated with myogenic differentiation has already been reported (Miyake et al., 2011). Differentiation-associated modifications of mitochondrial mass of control myoblasts are also accompanied by mitochondrial network modifications, the SER texture analysis likely indicating an initial prevalence of mitochondrial fragmentation followed by a balance condition of fragmented/elongated architecture. Indeed, the mitochondrial network SER modifications of differentiating control myoblasts are in agreement with results reported by Sin et al. (2016), who showed a mitochondrial dynamic remodeling in differentiating C2C12 myoblasts, characterized by a network fragmentation in the early phases of the process. Interestingly, the mitochondrial architecture modifications here reported could represent the morphological counterpart of the mitochondrial function modifications associated to human muscle cell differentiation (Hoffmann et al., 2018). In view of the well-established dysfunction of SR structure in TAM (Chevessier et al., 2005; Böhm et al., 2013, 2017; Morin et al., 2020), we cannot not rule out that mitochondrial alterations we observed herein are a secondary phenomenon to the altered SR functionality.

The STIM1 L96V mutation affects the myoblast differentiation process, the most striking differences with respect to control myoblasts being the longer persistence of mononuclear cells along with the formation of multinuclear elements with reduced size, mitochondrial mass and concentration, and nuclei number. Overall, these findings indicate that STIM1 L96V mutation and the associated  $\text{Ca}^{2+}$  overload induce a complex cell response affecting the myoblast differentiation program. In particular, the alterations of mitochondrial mass and texture along with the reduced expression of IDH3A and OGDH, two key genes of mitochondrial metabolism, strongly suggest a mitochondrial dysfunction associated with STIM1 L96V mutation. Interestingly, a recent reported mouse model bearing a gain-of-function mutation in STIM1 displays histological and muscle alteration associated with mitochondria dysfunction evidenced by the presence of enlarged mitochondria with abnormal morphology (Cordero-Sanchez et al., 2019).

A major phenotypic effect of STIM1 L96V mutation upon myoblast differentiation is represented by the reduced formation of multinuclear elements, this suggesting a STIM1 L96V-dependent delay in the fusion process. A critical event in muscle formation during both embryonic development and regeneration upon injury, is the fusion of myoblasts into multinucleated myotubes. Molecular and cellular mechanisms of myoblast fusion are less known than those of preceding events, even though significant advances have been recently achieved. Cell fusion is a complex event that requires the coordination of various processes culminating in the activation of dedicated proteins, named fusogens, responsible for mediating membrane fusion (Hernández and Podbilewicz, 2017; Sampath et al., 2018). It is generally acknowledged that the fusion of myoblasts into multinucleated myotubes is regulated by calcium-dependent signaling. In particular, the increase of intracellular  $\text{Ca}^{2+}$  determines the calcineurin-mediated activation of NFAT

transcription factor and myoblast fusion (Hindi et al., 2013). However, coordination and crosstalk of many signaling pathways are involved in myoblast fusion, and a complete picture of underlying cellular events is still lacking. In this context, it cannot be excluded that also a reduction of intracellular  $\text{Ca}^{2+}$  could be at some point required for cell fusion, as in the case of choriocarcinoma BeWo cells (Vatish et al., 2012), and that this event could be compromised by the STIM1 L96V-dependent  $\text{Ca}^{2+}$  overload.

By assessing the gene expression of some key myogenic factors leading to cell differentiation and fusion into multinucleated myotubes, we confirm the finding of our morphological imaging analysis highlighting an alteration of the myogenic pathway associated to TAM mutant. Particularly the gene expression increase of early differentiation markers such as *Myf5* and *Mef2D* together with the reduction of late differentiation markers such as *DMD* and *Tnnt3*, encoding for dystrophin and troponin, in mutant myoblasts and myotubes strongly supported an altered myogenesis associated to TAM mutant, mainly regarding the late differentiation phase. In comparison with respect to control cells, STIM1 Leu96Val myoblasts differentiation into myotubes is early started but is not concluded. Future focused studies aimed to detect the protein expression levels of the genes of interest will certainly contribute to gain further insight into the role of these differentiation biomarkers.

## Cellular Models for Personalized Therapeutics

To date, there is no specific treatment recommended for TAM patients. At least in principle, TAM could potentially benefit from treatment with SOCE/CRAC channel inhibitors, a group of putative immunomodulatory agents proposed for some chronic immune-related disorders (Riva et al., 2018; Stauderman, 2018). As far as preclinical investigations are concerned, there are two reported murine models bearing STIM1 gain-of function mutations and exhibiting a muscular phenotype (Gamage et al., 2018; Silva-Rojas et al., 2019), and only one is characterized by the luminal EF-hand mutation I115F (Cordero-Sanchez et al., 2019). In this respect, in our study, besides highlighting new etiopathological mechanisms underlying TAM disease, we validated a preclinical cellular model for TAM. We believe that preclinical investigations could benefit also from a preliminary phenotypic *in vitro* screening based upon the findings here reported, i.e., upon the ability of candidate SOCE/CRAC inhibitors to counteract the differentiation alterations associated with  $\text{Ca}^{2+}$  overload. As it is usually desired for neuromuscular disorders (Silva-Rojas et al., 2020; van Putten et al., 2020), a such experimental approach could finally allow a reliable translation in the clinical management of TAM patients.

## DATA AVAILABILITY STATEMENT

The raw data supporting the conclusions of this article will be made available by the authors, without undue reservation.

## ETHICS STATEMENT

The studies involving human participants were reviewed and approved by human muscle samples were provided by the Telethon biobank at Besta Neurological Institute in Milan. Research was conducted according to protocols approved by the Institutional Review Board of the Besta Neurological Institute and University of Bari, and in compliance with the Helsinki Declaration and local legislation. The patients/participants provided their written informed consent to participate in this study.

## AUTHOR CONTRIBUTIONS

EC and AL conceived and coordinated the study. LM, MM, and SG provided the muscle biopsy. PI and SG performed cell culture. EC and AL performed calcium cytofluorimetry experiments. AP and MC performed high content imaging experiments. EC and GC performed quantitative PCR experiments. PI, OC, and AD contributed ideas and critically interpreted results. EC, AP, MC,

and AL wrote the paper. All authors approved the final version of the manuscript.

## FUNDING

This work was in part supported by the research grants from Brain to the South (Fondazione con il Sud) with Project number 2018-PDR-00351 to OC.

## ACKNOWLEDGMENTS

We thank Prof. Lorenzo Puri for kindly providing the additional human control muscle cell line (HMB<sub>2</sub>).

## SUPPLEMENTARY MATERIAL

The Supplementary Material for this article can be found online at: <https://www.frontiersin.org/articles/10.3389/fcell.2021.635063/full#supplementary-material>

## REFERENCES

- Armand, A. S., Bourajaj, M., Martínez-Martínez, S., El Azzouzi, H., da Costa Martins, P. A., Hatzis, P., et al. (2008). Cooperative synergy between NEAT and MyoD regulates myogenin expression and myogenesis. *J. Biol. Chem.* 283, 29004–29010. doi: 10.1074/jbc.M801297200
- Bagur, R., and Hajnóczky, G. (2017). Intracellular Ca<sup>2+</sup> sensing: its role in calcium homeostasis and signaling. *Mol. Cell.* 66, 780–788. doi: 10.1016/j.molcel.2017.05.028
- Barone, V., Del Re, V., Gamberucci, A., Polverino, V., Galli, L., Rossi, D., et al. (2017). Identification and characterization of three novel mutations in the CASQ1 gene in four patients with tubular aggregate myopathy. *Hum. Mutat.* 38, 1761–1773. doi: 10.1002/humu.23338
- Böhm, J., Bulla, M., Urquhart, J. E., Malfatti, E., Williams, S. G., O'Sullivan, J., et al. (2017). ORAI1 Mutations with Distinct Channel Gating Defects in Tubular Aggregate Myopathy. *Hum. Mutat.* 38, 426–438. doi: 10.1002/humu.23172
- Böhm, J., Chevessier, F., De Paula, A. M., Koch, C., Attarian, S., Feger, C., et al. (2013). Constitutive activation of the calcium sensor STIM1 causes tubular-aggregate myopathy. *Am. J. Hum. Genet.* 92, 271–278. doi: 10.1016/j.ajhg.2012.12.007
- Böhm, J., Chevessier, F., Koch, C., Peche, A., Mora, M., Morandi, L., et al. (2014). Clinical, histological and genetic characterisation of patients with tubular aggregate myopathy caused by mutations in STIM1. *J. Med. Genet.* 51, 824–833. doi: 10.1136/jmedgenet-2014-102623
- Böhm, J., and Laporte, J. (2018). Gain-of-function mutations in STIM1 and ORAI1 causing tubular aggregate myopathy and Stormorken syndrome. *Cell Calcium* 76, 1–9. doi: 10.1016/j.ceca.2018.07.008
- Böhm, J., Lornage, X., Chevessier, F., Birck, C., Zanotti, S., Cudia, P., et al. (2018). CASQ1 mutations impair calsequestrin polymerization and cause tubular aggregate myopathy. *Acta Neuropathol.* 135, 149–151. doi: 10.1007/s00401-017-1775-x
- Bustin, S. A., Benes, V., Garson, J. A., Hellemans, J., Huggett, J., Kubista, M., et al. (2009). The MIQE guidelines: minimum information for publication of quantitative real-time PCR experiments. *Clin. Chem.* 55, 611–622. doi: 10.1373/clinchem.2008.112797
- Carafoli, E., and Krebs, J. (2016). Why calcium? How calcium became the best communicator. *J. Biol. Chem.* 291, 20849–20857. doi: 10.1074/jbc.R116.735894
- Chevessier, F., Bauché-Godard, S., Leroy, J. P., Koenig, J., Paturneau-Jouas, M., Eymard, B., et al. (2005). The origin of tubular aggregates in human myopathies. *J. Pathol.* 207, 313–323. doi: 10.1002/path.1832
- Cho, C. H., Woo, J. S., Perez, C. F., and Lee, E. H. (2017). A focus on extracellular Ca<sup>2+</sup> entry into skeletal muscle. *Exp. Mol. Med.* 49:e378. doi: 10.1038/emmm.2017.208
- Choi, J. H., Huang, M., Hyun, C., Oh, M. R., Lee, K. J., Cho, C. H., et al. (2019). A muscular hypotonia-associated STIM1 mutant at R429 induces abnormalities in intracellular Ca<sup>2+</sup> movement and extracellular Ca<sup>2+</sup> entry in skeletal muscle. *Sci. Rep.* 9:19140. doi: 10.1038/s41598-019-55745-z
- Conte, E., Camerino, G. M., Mele, A., De Bellis, M., Pierno, S., Rana, F., et al. (2017). Growth hormone secretagogues prevent dysregulation of skeletal muscle calcium homeostasis in a rat model of cisplatin-induced cachexia. *J. Cachexia Sarcopenia Muscle* 8, 386–404. doi: 10.1002/jcsm.12185
- Cordero-Sanchez, C., Riva, B., Reano, S., Clemente, N., Zaggia, I., Ruffinatti, F. A., et al. (2019). A luminal EF-hand mutation in STIM1 in mice causes the clinical hallmarks of tubular aggregate myopathy. *Dis. Model. Mech.* 13:dmm041111. doi: 10.1242/dmm.041111
- Darbellay, B., Arnaudeau, S., Ceroni, D., Bader, C. R., König, S., and Bernheim, L. (2010). Human muscle economy myoblast differentiation and excitation-contraction coupling use the same molecular partners, STIM1 and STIM2. *J. Biol. Chem.* 285, 22437–22447. doi: 10.1074/jbc.M110.118984
- Darbellay, B., Arnaudeau, S., König, S., Jousset, H., Bader, C., Demaurex, N., et al. (2009). STIM1- and Orail-dependent store-operated calcium entry regulates human myoblast differentiation. *J. Biol. Chem.* 284, 5370–5380. doi: 10.1074/jbc.M806726200
- Denton, R. M., and McCormack, J. G. (1980). The role of calcium in the regulation of mitochondrial metabolism. *Biochem. Soc. Trans.* 8, 266–268. doi: 10.1042/bst0080266
- Endo, Y., Noguchi, S., Hara, Y., Hayashi, Y. K., Motomura, K., Miyatake, S., et al. (2015). Dominant mutations in ORAI1 cause tubular aggregate myopathy with hypocalcemia via constitutive activation of store-operated Ca<sup>2+</sup> channels. *Hum. Mol. Genet.* 24, 637–648. doi: 10.1093/hmg/ddu477
- Favaro, G., Romanello, V., Varanita, T., Andrea Desbats, M., Morbidoni, V., Tezze, C., et al. (2019). DRP1-mediated mitochondrial shape controls calcium homeostasis and muscle mass. *Nat. Commun.* 10:2576. doi: 10.1038/s41467-019-10226-9
- Game, T. H., Gunnes, G., Lee, R. H., Louch, W. E., Holmgren, A., Bruton, J. D., et al. (2018). STIM1 R304W causes muscle degeneration and impaired platelet activation in mice. *Cell Calcium* 76, 87–100. doi: 10.1016/j.ceca.2018.10.001
- Goonasekera, S. A., Davis, J., Kwong, J. Q., Accornero, F., Wei-LaPierre, L., Sargent, M. A., et al. (2014). Enhanced Ca<sup>2+</sup> influx from STIM1-Orail induces muscle pathology in mouse models of muscular dystrophy. *Hum. Mol. Genet.* 23, 3706–3715. doi: 10.1093/hmg/ddu079

- Gryniewicz, G., Poenie, M., and Tsien, R. Y. (1985). A new generation of  $\text{Ca}^{2+}$  indicators with greatly improved fluorescence properties. *J. Biol. Chem.* 260, 3440–3450. doi: 10.1016/S0021-9258(19)83641-4
- Gudlur, A., Zeraik, A. E., Hirve, N., Rajanikanth, V., Bobkov, A. A., Ma, G., et al. (2018). Calcium sensing by the STIM1 ER-luminal domain. *Nat. Commun.* 9:4536. doi: 10.1038/s41467-018-06816-8
- Harris, E., Burki, U., Marini-Bettolo, C., Neri, M., Scotton, C., Hudson, J., et al. (2017). Complex phenotypes associated with STIM1 mutations in both coiled coil and EF-hand domains. *Neuromuscul. Disord.* 27, 861–872. doi: 10.1016/j.nmd.2017.05.002
- Hedberg, C., Niceta, M., Fattori, F., Lindvall, B., Ciolfi, A., D'Amico, A., et al. (2014). Childhood onset tubular aggregate myopathy associated with *de novo* STIM1 mutations. *J. Neurol.* 261, 870–876. doi: 10.1007/s00415-014-7287-x
- Hernández, J. M., and Podbilewicz, B. (2017). The hallmarks of cell-cell fusion. *Development* 144, 4481–4495. doi: 10.1242/dev.155523
- Hindi, S. M., Tajrishi, M. M., and Kumar, A. (2013). Signaling mechanisms in mammalian myoblast fusion. *Sci. Signal.* 6:re2. doi: 10.1126/scisignal.2003832
- Hoffmann, C., Höckele, S., Kappler, L., Hrabe de Angelis, M., Häring, H. U., and Weigert, C. (2018). The effect of differentiation and TGF $\beta$  on mitochondrial respiration and mitochondrial enzyme abundance in cultured primary human skeletal muscle cells. *Sci. Rep.* 8:737. doi: 10.1038/s41598-017-18658-3
- Karbowski, M., and Youle, R. (2003). Dynamics of mitochondrial morphology in healthy cells and during apoptosis. *Cell. Death Differ.* 10, 870–880. doi: 10.1038/sj.cdd.4401260
- Kegley, K. M., Gephart, J., Warren, G. L., and Pavlath, G. K. (2001). Altered Primary Myogenesis in NFATC3<sup>-/-</sup> mice leads to decreased muscle size in the adult. *Dev. Biol.* 232, 115–126. doi: 10.1006/dbio.2001.0179
- Kiselyov, K., and Patterson, R. L. (2009). The integrative function of TRPC channels. *Front. Biosci.* 14, 45–58. doi: 10.2741/3230
- Kiviluoto, S., Decuyper, J. P., De Smedt, H., Missiaen, L., Parys, J. B., and Bultynck, G. (2011). STIM1 as a key regulator for  $\text{Ca}^{2+}$  homeostasis in skeletal-muscle development and function. *Skelet. Muscle* 1:16. doi: 10.1186/2044-5040-1-16
- Lacruz, R. S., and Feske, S. (2015). Diseases caused by mutations in Orai1 and STIM1. *Ann N Y Acad Sci.* 1356, 45–79. doi: 10.1111/nyas.12938
- Le Guilcher, C., Luyten, T., Parys, J. B., Puchault, M., and Dellis, O. (2020). Synthesis and characterization of store-operated calcium entry inhibitors active in the submicromolar range. *Int. J. Mol. Sci.* 21:9777. doi: 10.3390/ijms21249777
- Lee, J. M., and Noguchi, S. (2016). Calcium dyshomeostasis in tubular aggregate myopathy. *Int. J. Mol. Sci.* 17:1952. doi: 10.3390/ijms17111952
- Lee, K. J., Woo, J. S., Hwang, J. H., Hyun, C., Cho, C. H., Kim, D. H., et al. (2013). STIM1 negatively regulates  $\text{Ca}^{2+}$  release from the sarcoplasmic reticulum in skeletal myotubes. *Biochem. J.* 453, 187–200. doi: 10.1042/BJ20130178
- Li, H., Ding, X., Lopez, J. R., Takeshima, H., Ma, J., Allen, P. D., et al. (2010). Impaired Orai1-mediated resting  $\text{Ca}^{2+}$  entry reduces the cytosolic  $[\text{Ca}^{2+}]$  and sarcoplasmic reticulum  $\text{Ca}^{2+}$  loading in quiescent junctophilin 1 knock-out myotubes. *J. Biol. Chem.* 285, 39171–39179. doi: 10.1074/jbc.M110.149690
- Li, T., Finch, E. A., Graham, V., Zhang, Z. S., Ding, J. D., Burch, J., et al. (2012). STIM1-Ca(2+) signaling is required for the hypertrophic growth of skeletal muscle in mice. *Mol. Cell. Biol.* 32, 3009–3017. doi: 10.1128/MCB.06599-11
- Lopez, J. J., Jardin, I., Albarrán, L., Sanchez-Collado, J., Cantonero, C., Salido, G. M., et al. (2020). Molecular basis and regulation of store-operated calcium entry. *Adv. Exp. Med. Biol.* 1131, 445–469. doi: 10.1007/978-3-030-12457-1\_17
- Louis, M., Zanou, N., Van Schoor, M., and Gailly, P. (2008). TRPC1 regulates skeletal myoblast migration and differentiation. *J. Cell. Sci.* 121(Pt 23), 3951–3959. doi: 10.1242/jcs.037218
- Meizoso-Huesca, A., and Launikonis, B. S. (2021). The Orai1 inhibitor BTP2 has multiple effects on  $\text{Ca}^{2+}$  handling in skeletal muscle. *J. Gen. Physiol.* 153:e202012747. doi: 10.1085/jgp.202012747
- Michelucci, A., García-Castañeda, M., Boncompagni, S., and Dirksen, R. T. (2018). Role of STIM1/Orai1-mediated store-operated  $\text{Ca}^{2+}$  entry in skeletal muscle physiology and disease. *Cell Calcium.* 76, 101–115. doi: 10.1016/j.ceca.2018.10.004
- Miyake, T., McDermott, J. C., and Gramolini, A. O. (2011). A method for the direct identification of differentiating muscle cells by a fluorescent mitochondrial dye. *PLoS ONE* 6:e28628. doi: 10.1371/journal.pone.0028628
- Morin, G., Biancalana, V., Echaniz-Laguna, A., Noury, J. B., Lornage, X., Moggio, M., et al. (2020). Tubular aggregate myopathy and stormorken syndrome: mutation spectrum and genotype/phenotype correlation. *Hum. Mutat.* 41, 17–37. doi: 10.1002/humu.23899
- Nesin, V., Wiley, G., Kousi, M., Ong, E. C., Lehmann, T., Nicholl, D. J., et al. (2014). Activating mutations in STIM1 and Orai1 cause overlapping syndromes of tubular myopathy and congenital myosis. *Proc. Natl. Acad. Sci. U.S.A.* 111, 4197–4202. doi: 10.1073/pnas.1312520111
- Noguchi, M., and Kasahara, A. (2018). Mitochondrial dynamics coordinate cell differentiation. *Biochem. Biophys. Res. Commun.* 500, 59–64. doi: 10.1016/j.bbrc.2017.06.094
- Park, C. Y., Hoover, P. J., Mullins, F. M., Bachhawat, P., Covington, E. D., Raunser, S., et al. (2009). STIM1 clusters and activates CRAC channels via direct binding of a cytosolic domain to Orai1. *Cell* 136, 876–890. doi: 10.1016/j.cell.2009.02.014
- Perez, C. F., López, J. R., and Allen, P. D. (2005). Expression levels of RyR1 and RyR3 control resting free  $\text{Ca}^{2+}$  in skeletal muscle. *Am. J. Physiol. Cell. Physiol.* 288, C640–C649. doi: 10.1152/ajpcell.00407.2004
- Phuong, T. T., Yun, Y. H., Kim, S. J., and Kang, T. M. (2013). Positive feedback control between STIM1 and NFATc3 is required for C2C12 myoblast differentiation. *Biochem. Biophys. Res. Commun.* 430, 722–728. doi: 10.1016/j.bbrc.2012.11.082
- Poot, M., Zhang, Y. Z., Krämer, J. A., Wells, K. S., Jones, L. J., Hanzel, D. K., et al. (1996). Analysis of mitochondrial morphology and function with novel fixable fluorescent stains. *J. Histochem. Cytochem.* 44, 1363–1372. doi: 10.1177/44.12.8985128
- Prakriya, M. (2009). The molecular physiology of CRAC channels. *Immunol. Rev.* 231, 88–98. doi: 10.1111/j.1600-065X.2009.00820.x
- Protasi, F., Takekura, H., Wang, Y., Chen, S. R., Meissner, G., Allen, P. D., et al. (2000). RYR1 and RYR3 have different roles in the assembly of calcium release units of skeletal muscle. *Biophys. J.* 79, 2494–2508. doi: 10.1016/S0006-3495(00)76491-5
- Ríos, E. (2010). The cell boundary theorem: a simple law of the control of cytosolic calcium concentration. *J. Physiol. Sci.* 60, 81–84. doi: 10.1007/s12576-009-0069-z
- Riva, B., Griglio, A., Serafini, M., Cordero-Sanchez, C., Aprile, S., Di Paola, R., et al. (2018). Pyrtriazoles, a novel class of store-operated calcium entry modulators: discovery, biological profiling, and *in vivo* proof-of-concept efficacy in acute pancreatitis. *J. Med. Chem.* 61, 9756–9783. doi: 10.1021/acs.jmedchem.8b01512
- Sampath, S. C., Sampath, S. C., and Millay, D. P. (2018). Myoblast fusion confusion: the resolution begins. *Skelet. Muscle* 8:3. doi: 10.1186/s13395-017-0149-3
- Schober, R., Bonhenry, D., Lunz, V., Zhu, J., Krizova, A., Frischauf, I., et al. (2019). Sequential activation of STIM1 links  $\text{Ca}^{2+}$  with luminal domain unfolding. *Sci. Signal.* 12:eaax3194. doi: 10.1126/scisignal.aax3194
- Silva-Rojas, R., Laporte, J., and Böhm, J. (2020). STIM1/Orai1 loss-of-function and gain-of-function mutations inversely impact on SOCE and calcium homeostasis and cause multi-systemic mirror diseases. *Front. Physiol.* 11:604941. doi: 10.3389/fphys.2020.604941
- Silva-Rojas, R., Treves, S., Jacobs, H., Kessler, P., Messaddeq, N., Laporte, J., et al. (2019). STIM1 over-activation generates a multi-systemic phenotype affecting the skeletal muscle, spleen, eye, skin, bones and immune system in mice. *Hum. Mol. Genet.* 28, 1579–1593. doi: 10.1093/hmg/ddy446
- Sin, J., Andres, A. M., Taylor, D. J., Weston, T., Hiraumi, Y., Stotland, A., et al. (2016). Mitophagy is required for mitochondrial biogenesis and myogenic differentiation of C2C12 myoblasts. *Autophagy* 12, 369–380. doi: 10.1080/15548627.2015.1115172
- Stathopoulos, P. B., Zheng, L., Li, G. Y., Plevin, M. J., and Ikura, M. (2008). Structural and mechanistic insights into STIM1-mediated initiation of store-operated calcium entry. *Cell* 135, 110–122. doi: 10.1016/j.cell.2008.08.006
- Stauderman, K. A. (2018). CRAC channels as targets for drug discovery and development. *Cell Calcium* 74, 147–159. doi: 10.1016/j.ceca.2018.07.005
- Stiber, J., Hawkins, A., Zhang, Z. S., Wang, S., Burch, J., Graham, V., et al. (2008). STIM1 signalling controls store-operated calcium entry required for development and contractile function in skeletal muscle. *Nat. Cell. Biol.* 10, 688–697. doi: 10.1038/ncb1731
- Stiber, J. A., and Rosenberg, P. B. (2011). The role of store-operated calcium influx in skeletal muscle signaling. *Cell Calcium.* 49, 341–349. doi: 10.1016/j.ceca.2010.11.012

- Tu, M. K., Levin, J. B., Hamilton, A. M., and Borodinsky, L. N. (2016). Calcium signaling in skeletal muscle development, maintenance and regeneration. *Cell Calcium* 59, 91–97. doi: 10.1016/j.ceca.2016.02.005
- van Putten, M., Hmeljak, J., Aartsma-Rus, A., and Dowling, J. J. (2020). Moving neuromuscular disorders research forward: from novel models to clinical studies. *Dis. Model. Mech.* 13:dmm044370. doi: 10.1242/dmm.044370
- Vatish, M., Tesfa, L., Grammatopoulos, D., Yamada, E., Bastie, C. C., and Pessin, J. E. (2012). Inhibition of Akt activity and calcium channel function coordinately drive cell-cell fusion in the BeWO choriocarcinoma placental cell line. *PLoS ONE* 7:e29353. doi: 10.1371/journal.pone.0029353
- Walter, M. C., Rossius, M., Zitzelsberger, M., Vorgerd, M., Muller-Felber, W., Ertl-Wagner, B., et al. (2015). 50 years to diagnosis: Autosomal dominant tubular aggregate myopathy caused by a novel STIM1 mutation. *Neuromuscul. Disord.* 25, 577–584. doi: 10.1016/j.nmd.2015.04.005
- Wei-Lapierre, L., Carrell, E. M., Boncompagni, S., Protasi, F., and Dirksen, R. T. (2013). Orai1-dependent calcium entry promotes skeletal muscle growth and limits fatigue. *Nat. Commun.* 4:2805. doi: 10.1038/ncomms3805
- Yang, X., Jin, H., Cai, X., Li, S., and Shen, Y. (2012). Structural and mechanistic insights into the activation of stromal interaction molecule 1 (STIM1). *Proc. Natl. Acad. Sci. U.S.A.* 109, 5657–5662. doi: 10.1073/pnas.1118947109
- Zanotti, S., Saredi, S., Ruggieri, A., Fabbri, M., Blasevich, F., Romaggi, S., et al. (2007). Altered extracellular matrix transcript expression and protein modulation in primary Duchenne muscular dystrophy myotubes. *Matrix Biol.* 26, 615–624. doi: 10.1016/j.matbio.2007.06.004
- Zhu, J., Feng, Q., and Stathopoulos, P. B. (2017). The STIM-Orai pathway: STIM-Orai structures: isolated and in complex. *Adv. Exp. Med. Biol.* 993, 15–38. doi: 10.1007/978-3-319-57732-6\_2

**Conflict of Interest:** The authors declare that the research was conducted in the absence of any commercial or financial relationships that could be construed as a potential conflict of interest.

Copyright © 2021 Conte, Pannunzio, Imbrici, Camerino, Maggi, Mora, Gibertini, Cappellari, De Luca, Coluccia and Liantonio. This is an open-access article distributed under the terms of the Creative Commons Attribution License (CC BY). The use, distribution or reproduction in other forums is permitted, provided the original author(s) and the copyright owner(s) are credited and that the original publication in this journal is cited, in accordance with accepted academic practice. No use, distribution or reproduction is permitted which does not comply with these terms.



# SARAF and Orai1 Contribute to Endothelial Cell Activation and Angiogenesis

Isabel Galeano-Otero<sup>1,2,3</sup>, Raquel Del Toro<sup>1,2,3</sup>, Abdel-Majid Khatib<sup>4</sup>,  
Juan Antonio Rosado<sup>5</sup>, Antonio Ordóñez-Fernández<sup>2,3,6</sup> and Tarik Smani<sup>1,2,3\*</sup>

<sup>1</sup> Department of Medical Physiology and Biophysics, University of Seville, Seville, Spain, <sup>2</sup> Group of Cardiovascular Pathophysiology, Institute of Biomedicine of Seville, University Hospital of Virgen del Rocío/University of Seville/CSIC, Seville, Spain, <sup>3</sup> CIBERCV, Madrid, Spain, <sup>4</sup> LAMC, INSERM U1029, Pessac, France, <sup>5</sup> Department of Physiology, University of Extremadura, Cáceres, Spain, <sup>6</sup> Department of Surgery, University of Seville, Seville, Spain

## OPEN ACCESS

### Edited by:

Isabel Merida,  
Consejo Superior de Investigaciones  
Científicas (CSIC), Spain

### Reviewed by:

Xuexin Zhang,  
Pennsylvania State University College  
of Medicine, United States  
Yoshiaki Suzuki,  
Nagoya City University, Japan

### \*Correspondence:

Tarik Smani  
tasmani@us.es

### Specialty section:

This article was submitted to  
Signaling,  
a section of the journal  
Frontiers in Cell and Developmental  
Biology

**Received:** 10 December 2020

**Accepted:** 01 February 2021

**Published:** 04 March 2021

### Citation:

Galeano-Otero I, Del Toro R,  
Khatib A-M, Rosado JA,  
Ordóñez-Fernández A and Smani T  
(2021) SARAF and Orai1 Contribute  
to Endothelial Cell Activation  
and Angiogenesis.  
Front. Cell Dev. Biol. 9:639952.  
doi: 10.3389/fcell.2021.639952

Angiogenesis is a multistep process that controls endothelial cells (ECs) functioning to form new blood vessels from preexisting vascular beds. This process is tightly regulated by pro-angiogenic factors, such as vascular endothelial growth factor (VEGF), which promote signaling pathways involving the increase in the intracellular  $\text{Ca}^{2+}$  concentration ( $[\text{Ca}^{2+}]_i$ ). Recent evidence suggests that store-operated calcium entry (SOCE) might play a role in angiogenesis. However, little is known regarding the role of SARAF, SOCE-associated regulatory factor, and Orai1, the pore-forming subunit of the store-operated calcium channel (SOCC), in angiogenesis. Here, we show that SOCE inhibition with GSK-7975A blocks aorta sprouting, as well as human umbilical vein endothelial cell (HUVEC) tube formation and migration. The intraperitoneal injection of GSK-7975A also delays the development of retinal vasculature assessed at postnatal day 6 in mice, since it reduces vessel length and the number of junctions, while it increases lacunarity. Moreover, we find that SARAF and Orai1 are involved in VEGF-mediated  $[\text{Ca}^{2+}]_i$  increase, and their knockdown using siRNA impairs HUVEC tube formation, proliferation, and migration. Finally, immunostaining and *in situ* proximity ligation assays indicate that SARAF likely interacts with Orai1 in HUVECs. Therefore, these findings show for the first time a functional interaction between SARAF and Orai1 in ECs and highlight their essential role in different steps of the angiogenesis process.

**Keywords:** Orai1, SARAF, SOCE, HUVEC, angiogenesis

## INTRODUCTION

Angiogenesis is defined as the formation of new blood vessels from existing vasculature for the purpose of expanding vascular networks to the tissues (Stapor et al., 2014). This process includes microvascular growth and endothelial sprouting, which itself involves endothelial cell (EC) proliferation, migration, and tube formation (Mentzer and Konerding, 2014). Angiogenesis

**Abbreviations:** ARC, arachidonate-regulated channels;  $[\text{Ca}^{2+}]_i$ , intracellular  $\text{Ca}^{2+}$  concentration; CRAC,  $\text{Ca}^{2+}$  release-activated  $\text{Ca}^{2+}$ ; EC, endothelial cells; EGF, epidermal growth factor; EGM-2<sup>TM</sup>, Endothelial Growth Medium BulletKit-2; FGF, fibroblast growth factor; GSK, GSK-7975A; HUVEC, human umbilical vein EC; SARAF, SOCE-associated regulatory factor; SOAR, STIM1 Orai1 activation region; SOCE, store-operated calcium entry; SOCC, store-operated calcium channels; STIM1, stromal interacting molecule 1; VEGF, vascular endothelial growth factor.

displays fine-tuned regulation that is mainly stimulated by oxygen deficiency, which may happen in both physiological (e.g., reproduction (Logsdon et al., 2014) or tissue repair (Ingason et al., 2018)) and pathological situations (e.g., diabetic retinopathy (Li et al., 2011) or cancer (Folkman, 1971)). This process requires the action of several growth factors, including vascular endothelial growth factor (VEGF), considered as the most pro-angiogenic factor, and fibroblast growth factor (FGF) and epidermal growth factor (EGF), which are secreted by parenchymal cells and triggered by the hypoxic environment (Adair and Montani, 2010).

Vascular endothelial growth factor promotes angiogenesis by its binding to VEGF receptors, VEGFR1 and VEGFR2 (Dragoni et al., 2011). Previous studies demonstrated that VEGF addition to ECs mediates the classical intracellular  $\text{Ca}^{2+}$  release followed by extracellular  $\text{Ca}^{2+}$  entry (Faehling et al., 2002; Jho et al., 2005). VEGF-induced increase in the intracellular  $\text{Ca}^{2+}$  concentration ( $[\text{Ca}^{2+}]_i$ ) was related to the activation of the store-operated calcium entry (SOCE) pathway (Li et al., 2011), which is required to the angiogenic activity in EC (Chen et al., 2016). Within the key elements of SOCE, Orai1, the pore-forming subunit of the store-operated calcium channel (SOCC), and stromal interacting molecule 1 (STIM1), are the most studied proteins (Avila-Medina et al., 2020). Both assemble to allow the activation of  $\text{Ca}^{2+}$  release-activated  $\text{Ca}^{2+}$  (CRAC) channels, responsible for SOCE currents. Previous studies demonstrated that Orai1 and STIM1 are involved in the proliferation and CRAC currents of EC (Abdullaev et al., 2008). Likewise, it has been proved that siRNA-mediated inhibition of Orai1 and STIM1 affected angiogenesis *in vitro* using human umbilical vein EC (HUVEC) and endothelial progenitor cells (Lodola et al., 2012).

Recently, SARAF (SOCE-associated regulatory factor) has been proposed as a new regulator of STIM1 activation. SARAF blocks the spontaneous activation of STIM1 under resting conditions (Palty et al., 2012). Likewise, SARAF attenuates arachidonate-regulated channel (ARC) activity, constituted by subunits of Orai1 and Orai3 (Albarran et al., 2016b). Other studies showed that Orai1 is essential for the interaction between STIM1 and SARAF (Palty et al., 2012; Jardín et al., 2018). Interestingly, it has been demonstrated that SARAF and Orai1 work together to boost SOCE in highly proliferated cancers cells, MEG01 and NG115-401L, independently of STIM1 (Albarran et al., 2016a). Nevertheless, to the best of our knowledge the role of SARAF in angiogenesis has not been addressed. Therefore, in this study we investigate the role of SARAF and Orai1 using different angiogenic approaches.

## MATERIALS AND METHODS

All animal assays were done in accordance with the recommendations of the Royal Decree 53/2013 in agreement with the Directive 2010/63/EU of the European Parliament and approved by the local Ethics Committee on human Research of the “Virgen del Rocio” University Hospital of Seville.

## Cell Culture and Transfection

Human umbilical vein endothelial cells (HUVEC; Lonza, Basilea, Switzerland) were cultured in 25-cm<sup>2</sup> flasks with enriched Endothelial Growth Medium BulletKit-2 (EGM-2) and were incubated at 37°C at 5% CO<sub>2</sub>. Primary cultures were thawed following the recommended seeding density from cryopreservation. After 24 h, the growth medium was replaced to refresh the medium. HUVECs were cultured and used at passages 3–10. HUVECs were transfected at 70% confluence with 3  $\mu\text{l}$  of 10  $\mu\text{M}$  siRNAs of scramble, Orai1, or SARAF using Lipofectamine<sup>®</sup> RNAiMAX Transfection Reagent following the manufacturer's instructions. Scrambled siRNA has the same nucleotide composition as the input sequence that is used as negative control.

## Tube Formation Assay in $\mu$ -Slide Angiogenesis

We studied tube formation as described previously (DeCicco-Skinner et al., 2014). We used  $\mu$ -Slide Angiogenesis ibiTreat 15 wells from ibidi<sup>®</sup> following the instructions of the “Application Note 19: Tube Formation” available in the web of ibidi<sup>®</sup>. Briefly, 10  $\mu\text{l}$  of Matrigel was added to each well. Immediately,  $\mu$ -Slide was placed into the incubator to allow gel polymerization for 30 min. Next,  $1.10^4$  HUVECs suspended in 50  $\mu\text{l}$  of EGM-2 were added to each well of the  $\mu$ -Slide and were incubated at 37°C in 5% CO<sub>2</sub>; 18 h after, pictures were taken using a phase-contrast inverted microscope Olympus IX-71 ( $\times 4$ , objective). Next, the supernatant was discarded and 50  $\mu\text{l}$  serum-free medium was added with 6.25  $\mu\text{g}/\text{ml}$  of Calcein-AM.  $\mu$ -Slide was then incubated for 30 min at RT in the dark. To analyze siRNA-mediated inhibition assay, cells were transfected 24 h before experiments. To analyze SOCC inhibition by GSK-7975A, the drug or vehicle (DMSO) was added after cells seeding in  $\mu$ -slide wells. Mesh formation was determined using Angiogenesis Analyzer for ImageJ (Gilles, 2020).

## Mouse Retinal Angiogenesis

For retinal angiogenesis assay, neonatal mice (SV129) were injected intraperitoneally with increasing concentrations of GSK-7975A (2.6, 4.0, 7.9, 15.9, and 31.8 mg/kg) dissolved in DMSO at postnatal day P3, P4, and P5. Pups were sacrificed at P6. After that, retinas were isolated as previously (Del Toro et al., 2010). With little modification, briefly, eyes were extracted from the orbit and were fixed in 4% paraformaldehyde (PFA) at RT for 30 min. Next, retina was isolated and incubated with the permeabilization and blocking solution 2 h at 4°C. After that, retinas were incubated at 4°C overnight with 1:50 biotinylated isolectin B4 (IB4). Next day, retina was incubated with 1:200 Cy3 streptavidin for 2 h at RT. Before mounting with Dako, retina was postfixed with PFA for 20 min. Fluorescence images were collected with fluorescence microscope Olympus BX-61 ( $\times 4$  objective). AngioTool software (Zudaire et al., 2011) was used to evaluate different parameters of vessel formation, such as total number of vessels and number of junctions, and lacunarity. Lacunarity is an index that measures and describes the

distribution of the sizes of gaps or lacunae within retinal vessels (Gould et al., 2011).

## Endothelial Cell Migration

HUVEC migration *in vitro* was evaluated by wound-healing assay (Rodriguez et al., 2005). Briefly, HUVECs were seeded in a 6-well plate and were cultured upon reaching 90–95% confluence. Then, using a sterile 2–200- $\mu$ l pipette tip, a scratch was done. Next, after washing with PBS 1 $\times$ , 1 ml of EGM-2 was added to each well. For siRNA experiments, HUVECs were transfected 48 h before scratching at 70% confluence. To analyze SOCC inhibition by GSK-7975A, the drug or vehicle (DMSO) was added after scratching. Pictures were taken by an inverted phase-contrast microscope Olympus IX71 ( $\times 10$  objective) immediately, 12 and 24 h after scratching. The cell-free area in the wound was measured using Fiji ImageJ (NIH; Bethesda, MD, United States).

## Cell Proliferation

HUVECs were seeded on coverslips, and cell transfection was done 48 hours before the assay. The cells were fixed with formalin, permeabilized with PBS 1  $\times$  0.5% Triton X-100, and blocked with PBS 1 $\times$  and 1% bovine serum albumin 0.5% TWEEN<sup>®</sup> 20. HUVECs were then incubated with a mouse anti-Ki67 antibody for 2 h at room temperature (RT). After that, coverslips were incubated 45 min in the dark at RT with Goat anti-Mouse Alexa Fluor<sup>®</sup> 594 (H + L) (1:200). HUVECs were incubated with DAPI diluted in PBS 1 $\times$  during 5 min to visualize the nucleus. The coverslips were mounted using Dako. Cells were then photographed using an Olympus BX-61 fluorescence microscope ( $\times 10$  objective). To analyze the proliferation, we considered Ki67<sup>+</sup> or proliferating cells whose merge between the two channels matched (channel red: Ki67, channel blue: DAPI), using CellCounter of ImageJ (NIH; Bethesda, MD, United States).

## Spatial Co-localization Study by Immunofluorescence and Proximity Ligation Assay

In order to examine the co-localization of Orai1 and SARAF proteins, we performed immunofluorescence and *in situ* Proximity Ligation Assay (PLA). Briefly, HUVECs were seeded on coverslips, fixed with formalin, permeabilized with PBS 1  $\times$  0.5% Triton X-100, and blocked with PBS 1  $\times$  1% bovine serum albumin + 0.5% TWEEN<sup>®</sup> 20. Cells were then incubated with mouse anti-Orai1 (1:200) and rabbit anti-SARAF (1:200) antibodies for 2 h at RT. After that, the coverslips were incubated 45 min in the dark at RT with Goat anti-mouse Alexa Fluor<sup>®</sup> 594 (H + L) (1:400) and Goat anti-rabbit Alexa Fluor<sup>®</sup> 488 (1:400). Staining with DAPI was used to visualize the nucleus of HUVEC. The coverslips were mounted using Dako. Cells were photographed by a Nikon A1R + laser scanning confocal microscope ( $\times 40$  objective). The Pearson correlation coefficient (PCC) was calculated using Jacob plugin of ImageJ software (Bolte and Cordelières, 2006).

For PLA assay, we used the Duolink *in situ* PLA detection kit (Sigma-Aldrich, St Louis, MO, United States). HUVECs were seeded on ibidi  $\mu$ -Slide VI<sup>0.4</sup> ibitreat and fixed with formalin

during 25 min following the manufacturer's instruction. After blocking for 30 min, cells were incubated with mouse anti-Orai1 and rabbit anti-SARAF antibodies for 2 h at RT. After that, cells were incubated with Duolink PLA anti-rabbit PLUS and anti-mouse MINUS included in the kit during 1 h at 37°C. Next, for the ligation step, we added hybridized oligonucleotides with the ligase to cells and further incubated them for 30 min at 37°C. Cells were then incubated with the polymerase diluted in the amplification buffer for 100 min at 37°C. The three last steps were done in a preheated humidity chamber. HUVECs were then washed following the instructions and incubated with DAPI for nucleus visualization. Cells were photographed using the Olympus IX-71 fluorescence microscope ( $\times 20$  objective).

## Aorta Ring Assay

Aorta ring assay was done following a modified protocol described by Baker et al. (Baker et al., 2012). Thoracic aortas were obtained from 250 to 300 g male Wistar rats. After dissection, aorta was sliced in 0.5-mm divisions. Then, rings were incubated in EGM-2 at 37°C overnight. Next day, 50  $\mu$ l of Matrigel was added to wells of a 24-well plate which was incubated for 15 min at 37°C. Each aortic ring was collocated over the Matrigel drop, and 50  $\mu$ l of Matrigel was added again to seal the ring. After 15 min of incubation at 37°C, we added 500  $\mu$ l of EGM-2 with increasing concentrations (10, 30, 50, 70, and 100  $\mu$ M) of GSK-7975A, or DMSO as vehicle. Photos were taken immediately and each 48 h until day 6, using a phase-contrast microscope Olympus IX-71 ( $\times 10$ , objective). Cell sprouting was evaluated using Fiji ImageJ.

## Intracellular Calcium Study

Ca<sup>2+</sup> measurement was carried out in HUVECs loaded with 2 to 5  $\mu$ M Fura-2 AM using an image system. The recording system consists of an inverted microscope Leica (Wetzlar, Germany) equipped with a 20 $\times$ /0.75 NA objective, a monochromator (Polychrome V, Till Photonics, Munich, Germany), and a light-sensitive CCD camera, controlled by HP software (Hamamatsu Photonics, Japan). Changes in intracellular Ca<sup>2+</sup> are represented as the ratio of Fura-2 AM fluorescence induced at an emission wavelength of 510 nm due to excitation at 340 and 380 nm (ratio =  $F_{340}/F_{380}$ ). Experiments were done in free Ca<sup>2+</sup> solution (in mM: 140 NaCl, 2.7 KCl, 4 MgCl<sub>2</sub>, 0.5 EGTA, 10 HEPES, pH = 7.4), and Ca<sup>2+</sup> influx was determined from changes in Fura-2 fluorescence after re-addition of Ca<sup>2+</sup> (2.5 mM). HUVECs were incubated 5 min with 30 ng/ml of VEGF and/without 30 ng/ml of anti-VEGF before Ca<sup>2+</sup> addition; 10  $\mu$ M of GSK-7975A was added before the end of the experiment. The Ca<sup>2+</sup> influx ( $\Delta$ ratio) was calculated as the difference between the peak ratio after extracellular Ca<sup>2+</sup> re-addition and its level right before.

## RNA Isolation and Quantification

We used miRNeasy kit to extract RNAs from cells. Briefly, HUVECs were collected using 1 ml of QIAzol Lysis Reagent included in the kit and Cell Scrapers (Greiner Bio-One North America, Monroe, NC, United States). After mixing with 200  $\mu$ l of chloroform, we followed the manufacturers' instruction to get the eluted RNA. RNA was quantified using NanoDrop<sup>TM</sup>, and

1 µg of RNA was retro-transcribed into cDNA using iScript™ Advanced cDNA Synthesis Kit. To determine genes' expression, we used 2.5 µl of cDNA of each primer (Orai1, SARAF, 18S; **Table 1**), and 5 µl of iTaq Universal SYBR Green Supermix in a total volume of 10 µl of reaction. qRT-PCR was performed using an Applied Biosystems Viia7 7900HT thermocycler (Thermo Fisher Scientific, Waltham, MA, United States).

## Statistical Analysis

Analyses were performed with GraphPad (GraphPad Software, Inc.). The results are presented as the mean and standard error of the mean (SEM). All variables were normally distributed. We used ordinary one-way ANOVA, and we performed multiple comparisons using T test without correction (Fisher's LSD test). To calculate the IC50 value in the dose-response inhibition analysis [log(inhibitor) vs. normalized responses], we used Hill equation,  $Y = 100/[1 + 10^{\{(\log IC_{50} - \log X) * n\}}]$ , where  $n$  is the Hill slope.

## Reagents

To culture HUVECs, we used Endothelial Growth Medium BulletKit-2 (EGM-2™ BulletKit; Lonza, Basilea, Switzerland) enriched with EGM™-2 SingleQuots™ (2% FBS, hydrocortisone, hFGF-B, VEGF, R3-IGF-1, hEGF, ascorbic acid, gentamicin/ampicillin, and heparin). In order to transfect HUVECs, we used Lipofectamine® RNAiMAX Transfection Reagent (Thermo Fisher Scientific, Waltham, MA, United States) and the siRNAs of scramble, Orai1, or SARAF (Ambion, Thermo Fisher Scientific, Waltham, MA, United States). SOCC inhibition was studied using GSK-7975A (Aobious, Gloucester, MA, United States) (Derler et al., 2013). The drug was dissolved in dimethyl sulfoxide (DMSO; Sigma-Aldrich, St Louis, MO, United States), considered as vehicle in a different set of experiments. VEGF (Sigma-Aldrich, St Louis, MO, United States), anti-VEGF (Cat. No. MAB293-SP; R&D, Minneapolis, MN, United States), and Fura-2 AM (Cat. No. F1225; Thermo Fisher Scientific, Waltham, MA, United States) were used for intracellular calcium study. Cell immunofluorescence permeabilization and blocking solution included PBS 1× with 0.5% Triton X-100 (Sigma-Aldrich, St Louis, MO, United States) and PBS 1× + 1% bovine serum albumin (BSA; Sigma-Aldrich, St Louis, MO, United States) and 0.5% TWEEN® 20 (Sigma-Aldrich, St Louis, MO, United States), respectively. Mouse retina permeabilization and blocking solution included TNB blocking buffer [0.1 M Tris-HCl, pH 7.5;

0.15 M NaCl; 0.5% (w/v) blocking reagent from Perkin-Elmer] and 0.3% Triton X-100. We worked with these antibodies: mouse anti-Ki67 (1:50; Cat. No. 550609; BD Biosciences Pharmingen, San Diego, CA, United States), mouse anti-Orai1 (1:200; Cat. No. ab175040; Abcam, Cambridge, United Kingdom), rabbit anti-SARAF (1:200; Cat. No. PA5-24237; Thermo Fisher Scientific, Waltham, MA, United States), biotinylated isolectin B4 (IB4; 1:50; The Jackson Laboratory, Farmington, CO, United States), Goat anti-Mouse Alexa Fluor® 594 (H + L) (Life technologies, Carlsbad, CA, United States), Goat anti-rabbit Alexa Fluor® 488 (Life Technologies, Carlsbad, CA, United States), Cy3 streptavidin (The Jackson Laboratory, Farmington, CO, United States), and 4',6-diamidino-2-phenylindole (DAPI; Sigma-Aldrich, St Louis, MO, United States). The coverslips were mounted using Dako Fluorescence Mounting medium (Dako; Agilent Technologies, Santa Clara, CA, United States). We used Corning™ Matrigel™ Matrix (Corning, NY, United States) to perform tube formation and rat aorta ring assays. To visualize live cells, we used Calcein-AM (Sigma-Aldrich, St Louis, MO, United States). To extract RNA from cells, we used miRNeasy kit (Qiagen, Hilden, Germany). RNA was retro-transcribed into cDNA using iScript™ Advanced cDNA Synthesis Kit (Bio-Rad, Hercules, CA, United States) and quantified using iTaq Universal SYBR Green Supermix (Bio-Rad, Hercules, CA, United States). Primers of Orai1, SARAF, and 18S were purchased from Sigma (Sigma-Aldrich, St Louis, MO, United States).

## RESULTS

### SOCC Inhibition With GSK-7975A Prevents Sprouting Angiogenesis, HUVEC Tube Formation, and Migration

To examine the role of SOCC in angiogenesis, we used the *ex vivo* model of rat aorta ring assay to check whether the formation of microvessels can be affected by SOCC inhibition with GSK-7975A (GSK), a widely used SOCC inhibitor (Derler et al., 2013). As shown in **Figure 1A**, in control aorta rings embedded in Matrigel and immersed in endothelial cell culture medium (EGM-2) enriched with growth factors, the outgrowth of well-formed sprouts took place after 4 days in culture. Slightly fewer sprouts were observed in aortic ring incubated with 1% of DMSO (vehicle), although they were not significantly different than in control. By contrast, the addition of increasing concentrations of GSK prevented aortic sprouting. Data analysis in **Figures 1B,C** shows that the number of new branches diminished drastically in GSK-treated aortic rings in a dose-dependent manner with an IC50 of 34.22 µM, as compared to the vehicle group.

Next, we assessed the effect of GSK *in vitro*, using HUVEC-induced tube formation assay. As depicted in **Figures 2A,B**, the addition of GSK to HUVEC seeded on Matrigel resulted in a reduced capacity of HUVEC to align and form mesh-like structures. HUVEC preincubation with DMSO (vehicle) did not affect significantly the formation of meshes as compared to control. Furthermore, using a well-established wound healing assay, we observed in **Figure 2C**, after scratching HUVEC,

**TABLE 1** | Forward and reverse primers used to quantify the mRNA expression of Orai1, SARAF, and 18S.

Primer	Sequence (5'–3')
Orai1	Forward: 5'-CCATAAGACGGACCGACAGT-3' Reverse: 5'-GGGAAGGTGAGGACTTAGGC-3'
SARAF	Forward: 5'-CAGTGGGAATGTAAGACGGACTT-3' Reverse: 5'-ACTCATAGCCTTCACAGCTCACC-3'
18S	Forward: 5'-AACGAGACTCTGGCATGCT-3' Reverse: 5'-GCCACTTGTCCTCTAAGA-3'

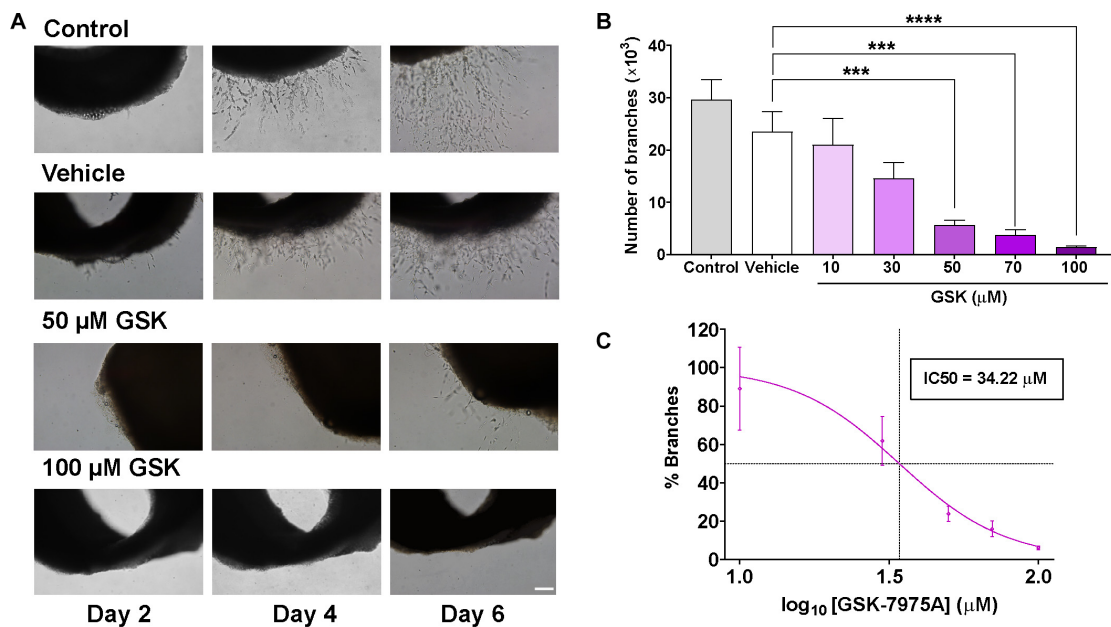


**FIGURE 1 |** SOCC inhibition by GSK-7975A reduces aorta sprouting. Aorta was cultured in the endothelial cell culture medium (EGM-2) enriched with growth factors. **(A)** Phase-contrast imaging ( $\times 10$  objective; scale bar = 200  $\mu\text{m}$ ) shows sprouting of aorta rings on day 2, 4, and 6 in untreated aorta (control), in aortic ring treated with DMSO (Vehicle), and in aortic rings incubated with GSK at 0, 50, and 100  $\mu\text{M}$ . **(B)** Bar graph shows the number of branches in control rat aorta rings (gray) and in aorta treated with vehicle (DMSO; white) and with 10, 30, 50, 70, and 100  $\mu\text{M}$  of GSK (purple) ( $n = 6$ ). **(C)** Curve shows the dose-dependent inhibition of % branches mediated by GSK-7975A in the rat aorta ring assay.  $\text{IC}_{50} = 34.22 \mu\text{M}$ . The fit was done using Hill equation as described in Methods (Hill slope:  $-2.443$ , 95% CI  $\text{IC}_{50}$  22.86 to 44.85,  $R^2 = 0.5762$ ). Values are presented as means  $\pm$  S.E.M. (\*\*\*), and (\*\*\*\*) indicate significance with  $p < 0.01$ , and  $p < 0.0001$ , respectively.

both in control and vehicle groups, a significant reduction in the wound size during the first 12 h. In contrast, treatment of HUVEC with 70  $\mu\text{M}$  GSK significantly attenuated cell migration, reaching the maximal significant effect 24 h after cell treatment (Figure 2D).

Altogether, these data indicate that pharmacological inhibition of SOCC with GSK impaired angiogenesis as assessed by tube formation, cell migration, and aorta ring assays.

## Intraperitoneal Injection of GSK-7975A Affects Retinal Angiogenesis

To further confirm the role of SOCC in angiogenesis, we evaluated the effect of intraperitoneal injection of GSK in retinal vascularization, using a mouse model of retinal angiogenesis (Del Toro et al., 2010). Increasing concentrations of GSK (from 2.6 to 31.8 mg/kg) were injected in neonatal mice at P3, P4, and P5, and retinal vessel formation was analyzed at P6. Figure 3A shows that vessel development was attenuated in the presence of increasing concentration of GSK. This delay in vessel formation was evident in the retina of mouse pups injected with 31.8 mg/kg GSK. AngioTool analysis determined that the total vessel length was significantly smaller when GSK was used at 31.8 mg/kg (Figure 3B) (Zudaire et al., 2011). Figure 3C shows that the maximum average of lacunarity, an index describing the distribution of the sizes of gaps between vessels, was also observed with 31.8 mg/kg GSK. In addition, the number of junctions decreased significantly with GSK concentrations higher

than 4.0 mg/kg (Figure 3D). Figure 3E shows that in this case the effect of GSK was dose dependent with an  $\text{IC}_{50}$  value of 18.4 mg/kg. Supplementary Figure 1 in supporting information confirmed that all these parameters were significantly affected with 31.8 mg/kg GSK, as compare with the retina treated with the same amount of DMSO used as vehicle. These findings further confirm that the vascularization of retina can be affected by the SOCC inhibitor.

## Role of SARAF and Orai1 in VEGF-Induced $\text{Ca}^{2+}$ Entry

To determine the role of the SOCE molecular component in angiogenesis, we used siRNA to examine the role of Orai1 and SARAF involvement in VEGF-mediated intracellular  $\text{Ca}^{2+}$  mobilization. As shown in Figures 4A,B, the transfection of HUVEC with siRNA of Orai1 and SARAF reduced drastically the expression of both Orai1 and SARAF mRNA; meanwhile, HUVEC transfection with scramble of RNA did not inhibit significantly the expression of Orai1 or SARAF, as compared to non-transfected control cells. Next, Figures 4C,D show that the re-addition of extracellular  $\text{Ca}^{2+}$  in HUVECs incubated with VEGF evoked a significant increase in  $[\text{Ca}^{2+}]_i$ . The induced  $[\text{Ca}^{2+}]_i$  increase was significantly inhibited in HUVECs incubated both with VEGF and anti-VEGF. Furthermore, Figure 4E shows that VEGF stimulated a significant  $\text{Ca}^{2+}$  influx in cells transfected with scramble siRNA, which was slightly higher than in control non-transfected HUVEC. By

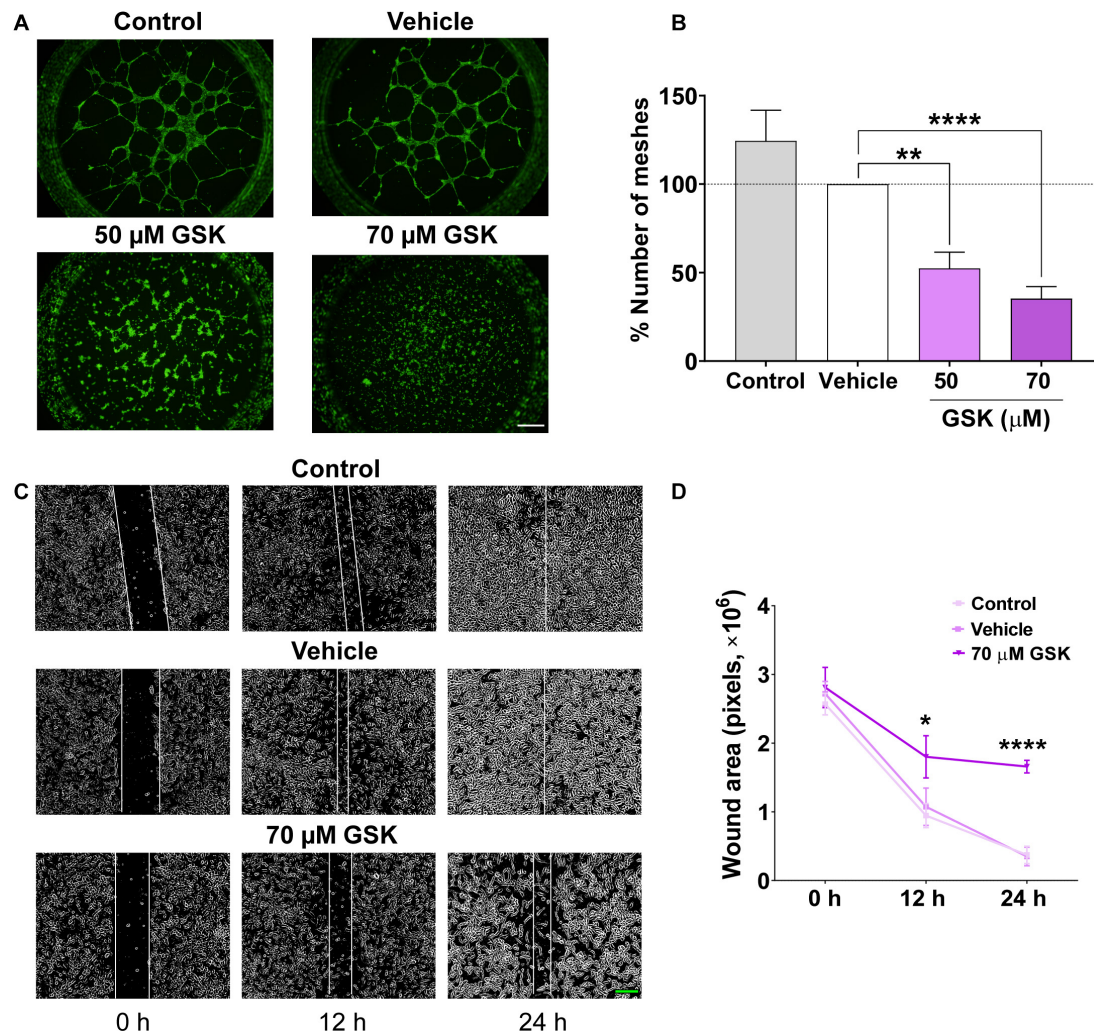


**FIGURE 2 |** GSK-7975A decreases HUVEC tube formation and migration. **(A)** Fluorescence images ( $\times 4$  objective; scale bar = 500  $\mu\text{m}$ ) are from HUVECs (control, vehicle, 50 and 70  $\mu\text{M}$  of GSK) incubated with Calcein-AM and seeded on Matrigel. **(B)** Bar graph shows normalized means of the percentage of meshes to the number in HUVECs treated with vehicle (gray). Bars are for untreated HUVECs, for HUVECs treated with vehicle (white), and with 50 or 70  $\mu\text{M}$  of GSK ( $n = 6$ ). **(C)** Phase-contrast imaging ( $\times 10$  objective; green scale bar = 200  $\mu\text{m}$ ) of the HUVEC wound healing assay. HUVEC was cultured in the endothelial cell culture medium (EGM-2) enriched with growth factors. Images are from control cells and for those treated with vehicle and 70  $\mu\text{M}$  of GSK, taken at 0, 12, and 24 h. **(D)** Graph shows summary data of the evolution of the wound area ( $n = 6$  per group). Values are presented as the means  $\pm$  S.E.M. (\*), (\*\*), and (\*\*\*\*) indicate significance with  $p < 0.05$ ,  $p < 0.01$ , and  $p < 0.0001$ , respectively.

contrast, VEGF-induced  $\text{Ca}^{2+}$  influx was significantly inhibited in HUVEC transfected with siRNA of Orai1 and SARAF. The addition of GSK at the end of each experiment successfully inhibited the  $\text{Ca}^{2+}$  influx, or what remained of this  $\text{Ca}^{2+}$  entry in transfected cells, confirming its SOCE nature. As depicted in **Figure 4F**, the downregulation of Orai1 and SARAF decreased VEGF-elicited  $\text{Ca}^{2+}$  response almost by 50%, as compared to cells transfected with scramble.

## Orai1 and SARAF Participate in HUVEC Tube Formation, Proliferation, and Migration

The tube formation, migration, and proliferation of EC are considered critical early steps in the initiation of angiogenesis.

Thereby, we examined the role of Orai1 and SARAF in these processes. As illustrated in **Figure 5A**, we observed that the transfection of HUVEC with siRNA against Orai1 and SARAF, seeded on Matrigel, prevented HUVEC capacity to mediate tube formation. **Figure 5B** indicates that Orai1 and SARAF silencing reduced mesh-like structures by approximately 60 and 40%, respectively, as compared to scramble. We also observed significantly less mesh formation in HUVECs transfected with scramble siRNA, as compared to control. Furthermore, **Figures 5C,D** illustrate that the incubation of HUVEC with EGM-2 enriched with growth factors promoted nucleus staining with Ki67 in control and cells transfected with scramble, indicating HUVEC proliferation. Conversely, Orai1 and SARAF downregulation by siRNA attenuated the amount of Ki67-positive HUVEC by 30 and 40%,

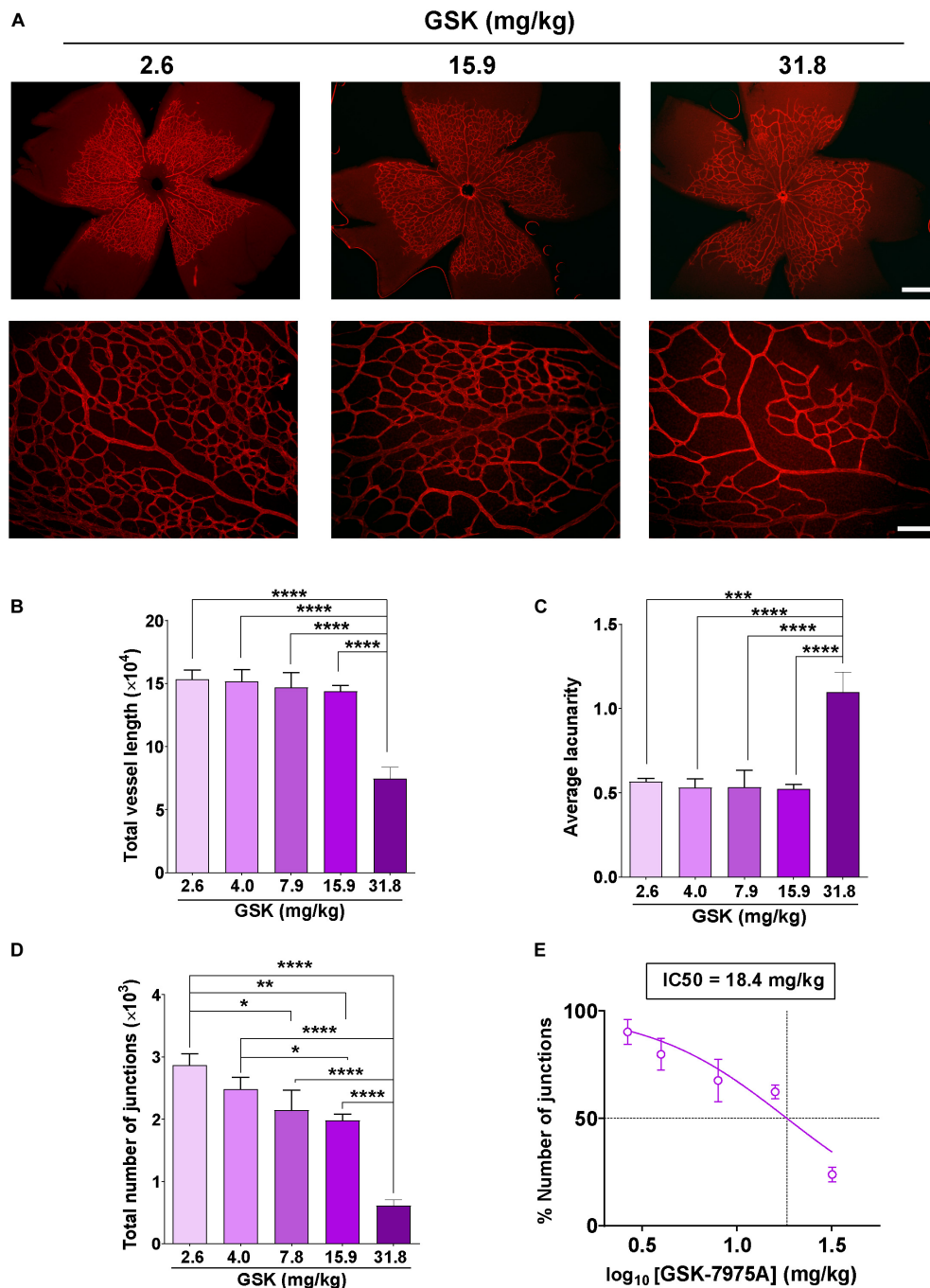
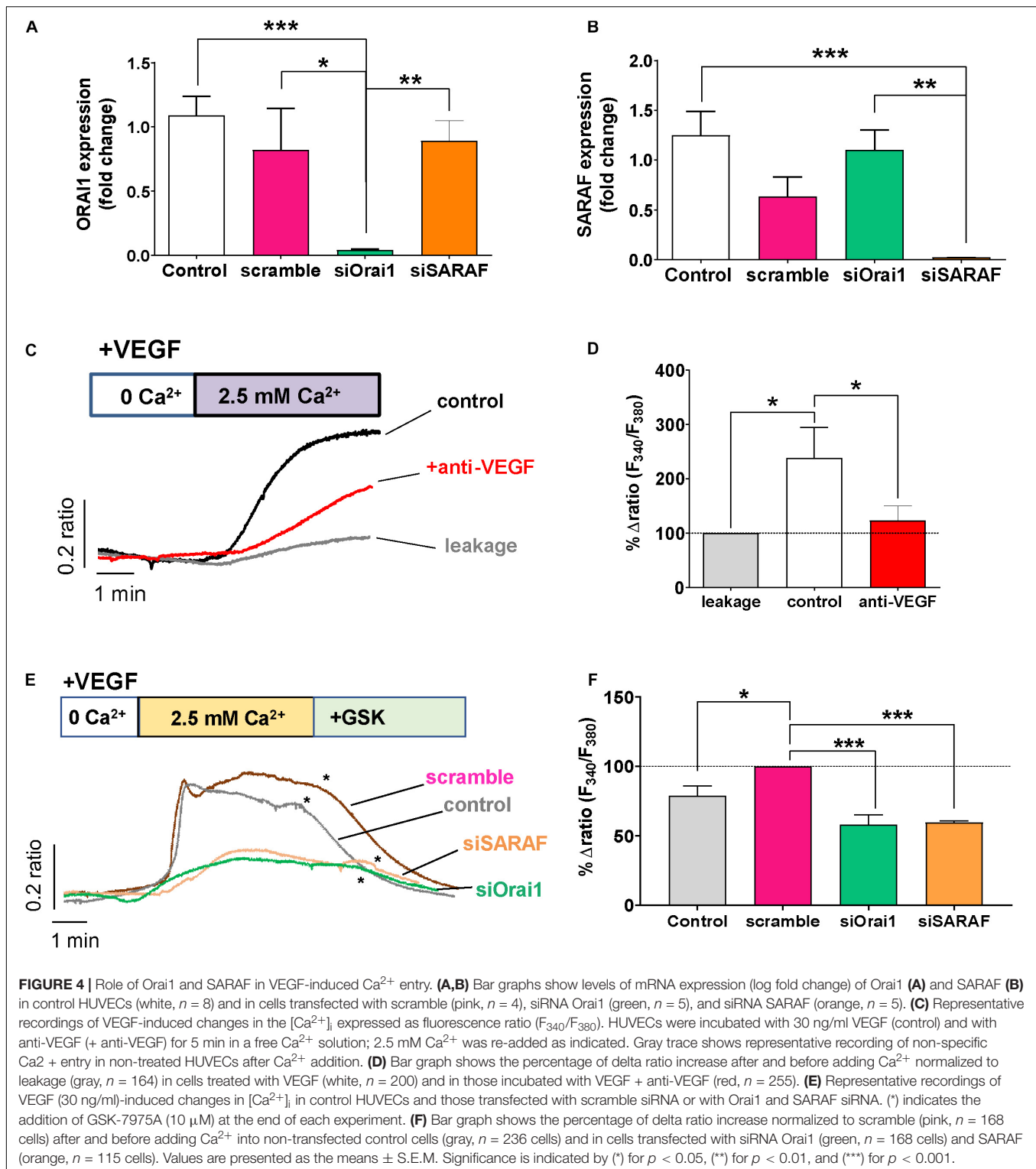


**FIGURE 3 |** GSK-7975A alters the vascularization of the retina. **(A)** Representative images of retinal blood vessels stained with Isolectin B4. Retina was isolated from P6 mouse injected with 2.6, 15.9, and 31.8 mg/kg of GSK. Fluorescence images were taken with objectives  $\times 4$  (top; scale bar = 500  $\mu\text{m}$ ) and  $\times 20$  (bottom; scale bar = 100  $\mu\text{m}$ ). **(B–D)** Bar graphs show summary data of total vessel length **(B)**, the average of lacunarity **(C)**, and the total number of junctions **(D)** of mouse retina vessels injected with 2.6, 4.0, 7.9, 15.9, and 31.8 mg/kg of GSK ( $n = 4$  to 8). **(E)** Curve shows the dose-dependent inhibition of % number of junctions affected by GSK-7975A IC<sub>50</sub> = 18.4 mg/kg. The fit was done using the Hill equation (Hill slope: -1.185, 95% CI IC<sub>50</sub> 14.50 to 24.66,  $R^2 = 0.6480$ ). Values are presented as the means  $\pm$  S.E.M. (\*), (\*\*), (\*\*\*), and (\*\*\*\*) indicate significance with  $p < 0.05$ ,  $p < 0.01$ ,  $p < 0.001$ , and  $p < 0.0001$ , respectively.

respectively. We next evaluated cell migration using the wound-healing assay. **Figures 5E,F** indicate that while control HUVECs and those transfected with siRNA scramble closed the wound within 24 h, HUVECs transfected with siRNA of

Orai1 and SARAF inefficiently sealed the wound over the same time frame. Therefore, these data demonstrated that Orai1 and SARAF are required for HUVEC tube formation, proliferation, and migration.



## Orai1 and SARAF Colocalize in HUVECs

Since our previous results strongly suggest a co-activation of Orai1 and SARAF in angiogenesis, we further examined the endogenous localizations of these proteins in HUVEC. Immunofluorescence images and analysis shows in **Figure 6A**

that SARAF and Orai1 are uniformly distributed in HUVEC. Merge image and Pearson's correlation coefficient (PCC), which estimate the correlation ratio, suggested a possible colocalization of SARAF and Orai1 in HUVECs since PCC was near 0.5 ( $r = 0.46$ ). Then, we used proximity ligation assay (PLA)

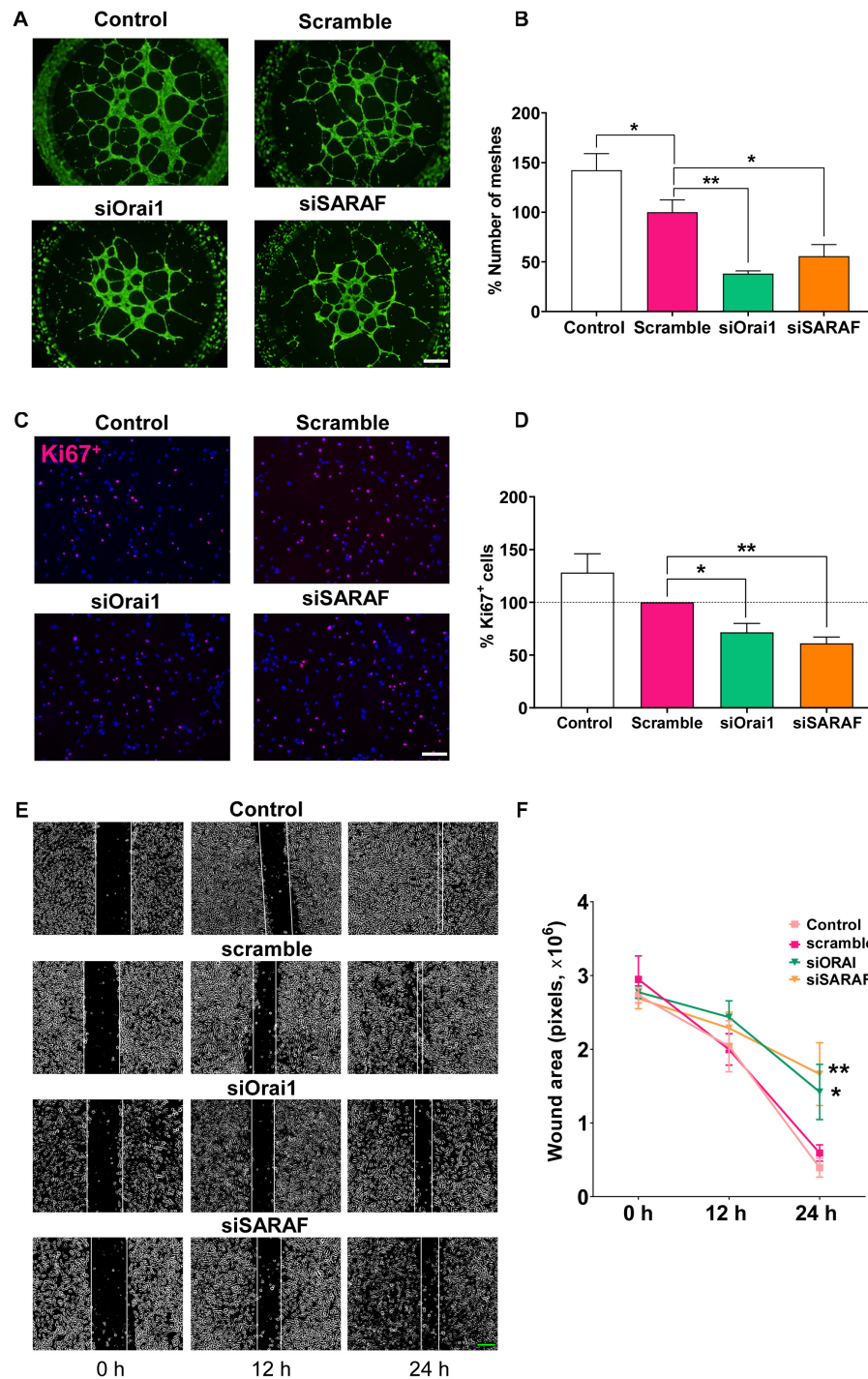


**FIGURE 5 |** siRNA-mediated inhibition of Orai1 and SARAF attenuates HUVEC tube formation, proliferation, and migration. **(A)** Fluorescence images ( $\times 4$  objective; scale bar = 500  $\mu\text{m}$ ) and **(B)** summary data (% of meshes number normalized to scramble) obtained from HUVECs embedded on Matrigel and stained with Calcein-AM of control (white) and transfected with scramble (pink), siRNA Orai1 (green), and siRNA SARAF (orange) ( $n = 5$  to 6). **(C)** Merged representative images ( $\times 20$  objective; scale bar = 100  $\mu\text{m}$ ) of HUVECs stained with Ki67<sup>+</sup> (red) and DAPI (blue) in control and in cells transfected with scramble, or siRNA Orai1 and SARAF ( $n = 5$ ). **(D)** Bar graph shows the percentage of Ki67<sup>+</sup> control (white bar) and transfected HUVECs with siOrai1 and siSARAF, normalized to scramble. **(E)** Phase-contrast imaging ( $\times 10$  objective; scale bar = 200  $\mu\text{m}$ ) of the HUVEC wound healing assay modified with ImageJ. Images were taken at 0, 12, and 24 h after the scratch from control HUVECs and from cells transfected with scramble siRNA, and siRNA against Orai1 and SARAF. **(F)** Graph shows summary data of the evolution of the wound area in experiments as in **(E)** ( $n = 4$ ). Values are presented as the means  $\pm$  S.E.M. Significance is indicated by (\*) and (\*\*) for  $p < 0.05$  and  $p < 0.01$ , respectively.

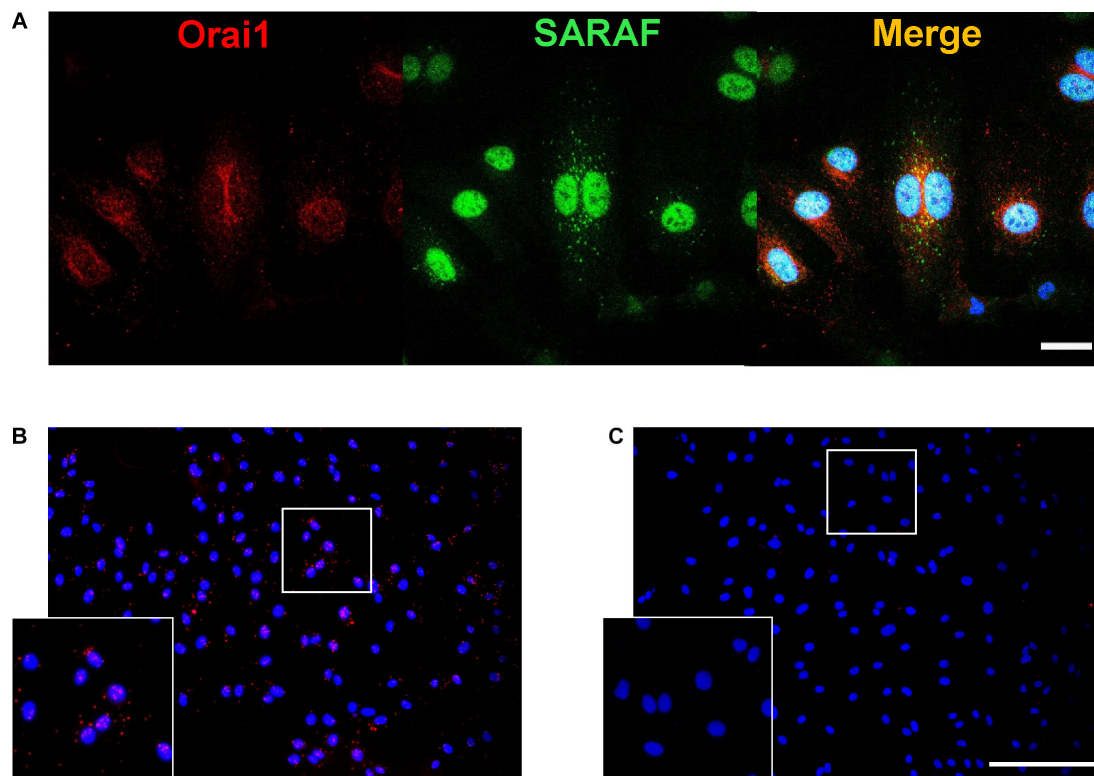


**FIGURE 6 |** SARAF and Orai1 colocalization in HUVECs. **(A)** Representative images with immunofluorescence ( $\times 40$  objective with  $\times 2$  zoom; scale bar =  $25\ \mu\text{m}$ ) using specific antibodies show localization of SARAF (green) and Orai1 (red) in HUVECs stained with anti-rabbit SARAF and anti-mouse Orai1. Blue channel corresponds to DAPI. Merge image shows possible colocalization of SARAF with Orai1 as indicated by yellow color. **(B,C)** Representative images of fluorescence ( $20\times$ ; scale bar =  $100\ \mu\text{m}$ ) in HUVECs using primary antibodies against Orai1 and SARAF **(B: both; C: only Orai1)** conjugated with the appropriate proximity ligation assay (PLA) probes. The bottom box is a zoom of **(B and C)** original images ( $20\times$ ). Red puncta indicate that proteins are in close proximity ( $<40\ \text{nm}$ ). HUVECs were cultured in the endothelial cell culture medium (EGM-2) enriched with growth factors, and nuclei are shown in blue as stained by DAPI.

technique and we determined 644 of red puncta in 165 cells in HUVECs when incubated with primary antibodies against SARAF and Orai1 (**Figure 6B**), indicating that both proteins are in close proximity ( $<40\ \text{nm}$ ). **Figure 6C** shows that no PLA signal was detected in HUVEC conjugated with anti-Orai1 antibody, but without anti-SARAF antibody.

## DISCUSSION

Angiogenesis is a dynamic multiphase process that includes the formation of new vessels from preexisting vascular beds, involving EC proliferation and migration, vascular patterning, and a final remodeling phase that ends in a stabilization of the new network for blood circulation (Ucuzian et al., 2010). The process of angiogenesis is tightly regulated by pro-angiogenic factors such as VEGF which binds to its receptors on ECs and mediates  $[\text{Ca}^{2+}]_i$  increase (Munaron et al., 2008). The close relationship between EC physiology and  $\text{Ca}^{2+}$  signaling has been extensively studied (Filippini et al., 2019). Nevertheless, only few studies reported the role of SOCE in angiogenesis. In the current study, we described that SOCE activation plays a key role in several angiogenesis hallmarks,

such as EC proliferation and migration, vessel sprouting, and tube formation. In fact, we demonstrated that GSK-7975A, a selective blocker of the CRAC channel (Derler et al., 2013), efficiently prevented aorta sprouting as well as HUVEC tube formation and migration. We also showed for the first time that intraperitoneal injection of GSK-7975A delayed the development of the retinal vasculature assessed at postnatal day 6 in mice. GSK-7975A reduced vessel length and their number of junctions, while it increased lacunarity, suggesting that SOCE might be required for normal vessel development. GSK-7975A inhibited especially and dose-dependently the number of branch junctions an essential step for vessel maturation and interconnected network formation, which may be independent of the number of new formed vessels and gaps that exist within them. The observed pharmacological inhibition of SOCE is consistent with previous studies which demonstrated that other more or less specific inhibitors of SOCE, Synta66 (Li et al., 2011), SFK-96365 (Chen et al., 2011; Savage et al., 2019), or 2-APB (Chen et al., 2011; Pafumi et al., 2015; Ye et al., 2018), similarly attenuated vessel formation in different *in vitro* and *in vivo* models of angiogenesis. Of note, none of these blockers have been injected to evaluate their effect on physiological developmental angiogenesis.

Within the key proteins of SOCE in the last years, Orai1 emerged as a possible new target to control angiogenesis, especially in tumor vascularization (as reviewed in Vashisht et al., 2015). Our data agree with previous studies that used VEGF or thapsigargin, the inhibitor of sarco/endoplasmic reticulum  $\text{Ca}^{2+}$ -ATPase, to demonstrate the activation of SOCE and CRAC current in ECs. Abdullaev et al. (2008) showed that Orai1 knockdown also inhibited the proliferation of HUVEC. Likely, Li et al. (2011) used siRNAs, a dominant negative, or neutralizing antibodies to demonstrate that Orai1 is also necessary for HUVEC tube formation, as well as for VEGF-induced  $\text{Ca}^{2+}$  influx. In contrast, a previous study by Antigny et al. (2012) suggested that silencing of Orai1 did not affect tube formation when they used the EA.hy926 EC cell line; meanwhile, they suggest that STIM1, TRPC3, TRPC4, and TRPC5 are involved in this process (Antigny et al., 2012). However, in another study, Antigny et al. (2011) proposed that thapsigargin activated STIM1- and Orai1-dependent  $[\text{Ca}^{2+}]_i$  increase in the same EC cell line. Our results support the involvement of Orai1 in HUVEC migration, proliferation, and Matrigel-based tube formation assays. At the same time, we demonstrated that VEGF-induced  $[\text{Ca}^{2+}]_i$  increase was significantly attenuated following Orai1 and SARAF downregulation, confirming that VEGF triggers SOCE in HUVEC. HUVEC treatment by VEGF may activate other  $\text{Ca}^{2+}$ -conducting channels since silencing of Orai1 and SARAF did not block completely the induced  $[\text{Ca}^{2+}]_i$  increase, as reviewed elsewhere (Smani et al., 2018).

To the best of our knowledge, this study is the first to evaluate the participation of SARAF in angiogenesis. The role of SARAF, product of the *tmem66* gene, in SOCE was described for the first time in 2012 (Palty et al., 2012). Now, there is a growing body of evidences indicating its role in the regulation of  $\text{Ca}^{2+}$  homeostasis in excitable and non-excitable cells (Albarran et al., 2016b). SARAF was identified as a blocker of spontaneous STIM1 activation under resting conditions in HEK cells (Palty et al., 2012). Later on, SARAF was demonstrated to regulate Orai1 activation through its binding to the STIM1 Orai1 activation region (SOAR) (Jha et al., 2013). Furthermore, Albarran et al. (2016b) found that SARAF is also expressed in the plasma membrane where it constitutively interacts with Orai1 and modulates  $\text{Ca}^{2+}$  entry through ARC (arachidonic acid regulated  $\text{Ca}^{2+}$ ) channels in neuroblastoma cell lines SH-SY5Y and NG115-401L. In the current study, using *in situ* PLA and immunofluorescence assays we demonstrated that Orai1 and SARAF are distributed in close subcellular vicinity suggesting their interaction. Indeed, Pearson's correlation coefficient and the PLA puncta's signal that occurs when proteins are < 40 nm apart (Bagchi et al., 2015) confirmed a strong colocalization of Orai1 and SARAF. This finding agrees with a previous data which demonstrated that SARAF colocalizes with STIM1 and Orai1, where it regulates the interaction between STIM1 and Orai1 during the initial steps of the activation of SOCE and transiently dissociates from STIM1 to associate with the C-terminus of Orai1 to promote  $\text{Ca}^{2+}$  entry (Albarran et al., 2016a).

Altogether, our data indicate that SARAF and Orai1 likely collaborate to maintain the  $\text{Ca}^{2+}$  influx required for different

steps of angiogenesis. We provided the first evidence of SARAF expression in HUVEC, which interacts with Orai1 to sustain SOCE, HUVEC proliferation, migration, and tube formation. These findings suggest that SARAF and Orai1 may be good candidates to target angiogenesis in both physiological and pathological processes, such as cancer.

## DATA AVAILABILITY STATEMENT

The original contributions presented in the study are included in the article/**Supplementary Material**, further inquiries can be directed to the corresponding author/s.

## ETHICS STATEMENT

The animal study was reviewed and approved by the Ethics Committee on Human Research of the "Virgen del Rocío" University Hospital of Seville.

## AUTHOR CONTRIBUTIONS

IG-O, RD, JR, and TS contributed to the study conceptualization. IG-O, RD, and A-MK contributed to the study methodology. IG-O and TS contributed to the writing—original draft preparation. JR, AO-F, A-MK, and RD contributed to the writing—review and editing. RD and TS contributed to the supervision. TS contributed to the project administration. JR, AO-F, and TS contributed to the funding acquisition. All authors have read and agreed to the published version of the manuscript.

## FUNDING

This research was funded by Agencia Estatal de Investigación [PID2019-104084GB-C22/AEI/10.13039/501100011033].

## ACKNOWLEDGMENTS

Graphical abstract was created with Biorender.com (<http://biorender.io>). We wish to thank Misses Isabel Mayoral González, Marta Martín Bórnez, and María Isabel Álvarez Vergara for their technical assistance.

## SUPPLEMENTARY MATERIAL

The Supplementary Material for this article can be found online at: <https://www.frontiersin.org/articles/10.3389/fcell.2021.639952/full#supplementary-material>

## REFERENCES

- Abdullaev, I. F., Bisailon, J. M., Potier, M., Gonzalez, J. C., Motiani, R. K., and Trebak, M. (2008). Stim1 and orai1 mediate crac currents and store-operated calcium entry important for endothelial cell proliferation. *Circ. Res.* 103, 1289–1299. doi: 10.1161/01.RES.0000338496.95579.56
- Adair, T. H., and Montani, J. P. (2010). *Overview of Angiogenesis*. San Rafael, CA: Morgan & Claypool Life Sciences.
- Albarran, L., Lopez, J. J., Amor, N. B., Martin-Cano, F. E., Berna-Erro, A., Smani, T., et al. (2016a). Dynamic interaction of SARAF with STIM1 and orai1 to modulate store-operated calcium entry. *Sci. Rep.* 6, 1–11. doi: 10.1038/srep24452
- Albarran, L., Lopez, J. J., Woodard, G. E., Salido, G. M., and Rosado, J. A. (2016b). Store-operated Ca<sup>2+</sup> entry-associated regulatory factor (SARAF) plays an important role in the regulation of arachidonate-regulated Ca<sup>2+</sup> (ARC) channels. *J. Biol. Chem.* 291, 6982–6988. doi: 10.1074/jbc.M115.704940
- Antigny, F., Girardin, N., and Frieden, M. (2012). Transient receptor potential canonical channels are required for in vitro endothelial tube formation. *J. Biol. Chem.* 287, 5917–5927. doi: 10.1074/jbc.M111.295733
- Antigny, F., Jousset, H., König, S., and Frieden, M. (2011). Thapsigargin activates Ca<sup>2+</sup> entry both by store-dependent, STIM1/Orai1-mediated, and store-independent, TRPC3/PLC/PKC-mediated pathways in human endothelial cells. *Cell Calcium* 49, 115–127. doi: 10.1016/j.ceca.2010.12.001
- Avila-Medina, J., Mayoral-González, I., Galeano-Otero, I., Redondo, P. C., Rosado, J. A., and Smani, T. (2020). Pathophysiological significance of store-operated calcium entry in cardiovascular and skeletal muscle disorders and angiogenesis. *Adv. Exp. Med. Biol.* 1131, 489–504. doi: 10.1007/978-3-030-12457-1\_19
- Bagchi, S., Fredriksson, R., and Wallén-Mackenzie, Å (2015). In situ proximity ligation assay (PLA). *Methods Mol. Biol.* 1318, 149–159. doi: 10.1007/978-1-4939-2742-5\_15
- Baker, M., Robinson, S. D., Lechertier, T., Barber, P. R., Tavora, B., D'Amico, G., et al. (2012). Use of the mouse aortic ring assay to study angiogenesis. *Nat. Protoc.* 7, 89–104. doi: 10.1038/nprot.2011.435
- Bolte, S., and Cordelières, F. P. (2006). A guided tour into subcellular colocalization analysis in light microscopy. *J. Microsc.* 224, 213–232. doi: 10.1111/j.1365-2818.2006.01706.x
- Chen, Y. F., Chiu, W. T., Chen, Y. T., Lin, P. Y., Huang, H. J., Chou, C. Y., et al. (2011). Calcium store sensor stromal-interaction molecule 1-dependent signaling plays an important role in cervical cancer growth, migration, and angiogenesis. *Proc. Natl. Acad. Sci. U.S.A.* 108, 15225–15230. doi: 10.1073/pnas.1103315108
- Chen, Y. F., Hsu, K. F., and Shen, M. R. (2016). The store-operated Ca<sup>2+</sup> entry-mediated signaling is important for cancer spread. *Biochim. Biophys. Acta Mol. Cell Res.* 1863, 1427–1435. doi: 10.1016/j.bbamer.2015.11.030
- DeCicco-Skinner, K. L., Henry, G. H., Cataisson, C., Tabib, T., Gwilliam, J. C., Watson, N. J., et al. (2014). Endothelial cell tube formation assay for the in vitro study of angiogenesis. *J. Vis. Exp.* e51312. doi: 10.3791/51312
- Del Toro, R., Prahst, C., Mathivet, T., Siegfried, G., Kaminker, J. S., Larrivee, B., et al. (2010). Identification and functional analysis of endothelial tip cell-enriched genes. *Blood* 116, 4025–4033. doi: 10.1182/blood-2010-02-270819
- Derler, I., Schindl, R., Fritsch, R., Heftberger, P., Riedl, M. C., Begg, M., et al. (2013). The action of selective CRAC channel blockers is affected by the Orai pore geometry. *Cell Calcium* 53, 139–151. doi: 10.1016/j.ceca.2012.11.005
- Dragoni, S., Laforenza, U., Bonetti, E., Lodola, F., Bottino, C., Berra-Romani, R., et al. (2011). Vascular endothelial growth factor stimulates endothelial colony forming cells proliferation and tubulogenesis by inducing oscillations in intracellular Ca<sup>2+</sup> concentration. *Stem Cells* 29, 1898–1907. doi: 10.1002/stem.734
- Faehling, M., Kroll, J., Föhr, K. J., Fellbrich, G., Mayr, U., Trischler, G., et al. (2002). Essential role of calcium in vascular endothelial growth factor A-induced signaling: mechanism of the antiangiogenic effect of carboxyamidotriazole. *FASEB J.* 16, 1805–1807. doi: 10.1096/fj.01-0938fje
- Filippini, A., D'Amore, A., and D'Alessio, A. (2019). Calcium mobilization in endothelial cell functions. *Int. J. Mol. Sci.* 20:4525. doi: 10.3390/ijms20184525
- Folkman, J. (1971). Tumor angiogenesis: therapeutic implications. *N. Engl. J. Med.* 285, 1182–1186. doi: 10.1056/NEJM19711118252108
- Gilles, C. (2020). *Angiogenesis Analyzer for ImageJ - Gilles Carpentier Research Web Site: Computer Image Analysis*. Available online at: <http://image.bio.methods.free.fr/ImageJ/?Angiogenesis-Analyzer-for-ImageJ&artpage=6-6&lang=en>
- Gould, D. J., Vadakkan, T. J., Poché, R. A., and Dickinson, M. E. (2011). Multifractal and lacunarity analysis of microvascular morphology and remodeling. *Microcirculation* 18, 136–151. doi: 10.1111/j.1549-8719.2010.00075.x
- Ingason, A. B., Goldstone, A. B., Paulsen, M. J., Thakore, A. D., Truong, V. N., Edwards, B. B., et al. (2018). Angiogenesis precedes cardiomyocyte migration in regenerating mammalian hearts. *J. Thorac. Cardiovasc. Surg.* 155, 1118–1127.e1. doi: 10.1016/j.jtcvs.2017.08.127
- Jardín, I., Albarran, L., Salido, G. M., López, J. J., Sage, S. O., and Rosado, J. A. (2018). Fine-tuning of store-operated calcium entry by fast and slow Ca<sup>2+</sup>-dependent inactivation: involvement of SARAF. *Biochim. Biophys. Acta Mol. Cell Res.* 1865, 463–469. doi: 10.1016/j.bbamer.2017.12.001
- Jha, A., Ahuja, M., Maléth, J., Moreno Claudia, C., Yuan Joseph, J., Kim, M. S., et al. (2013). The STIM1 CTID domain determines access of SARAF to SOAR to regulate Orai1 channel function. *J. Cell Biol.* 202, 71–78. doi: 10.1083/jcb.201301148
- Jho, D., Mehta, D., Ahmmed, G., Gao, X. P., Tirupathi, C., Broman, M., et al. (2005). Angiopoietin-1 opposes VEGF-induced increase in endothelial permeability by inhibiting TRPC1-dependent Ca<sup>2+</sup> influx. *Circ. Res.* 96, 1282–1290. doi: 10.1161/01.RES.0000171894.03801.03
- Li, J., Cubbon, R. M., Wilson, L. A., Amer, M. S., McKeown, L., Hou, B., et al. (2011). Orai1 and CRAC channel dependence of VEGF-activated Ca<sup>2+</sup> entry and endothelial tube formation. *Circ. Res.* 108, 1190–1198. doi: 10.1161/CIRCRESAHA.111.243352
- Lodola, F., Laforenza, U., Bonetti, E., Lim, D., Dragoni, S., Bottino, C., et al. (2012). Store-operated Ca<sup>2+</sup> entry is remodelled and controls in vitro angiogenesis in endothelial progenitor cells isolated from tumoral patients. *PLoS One* 7:e2541. doi: 10.1371/journal.pone.0042541
- Logsdon, E. A., Finley, S. D., Popel, A. S., and MacGabhann, F. (2014). A systems biology view of blood vessel growth and remodelling. *J. Cell. Mol. Med.* 18, 1491–1508. doi: 10.1111/jcmm.12164
- Mentzer, S. J., and Konerding, M. A. (2014). Intussusceptive angiogenesis: expansion and remodeling of microvascular networks. *Angiogenesis* 17, 499–509. doi: 10.1007/s10456-014-9428-3
- Munaron, L., Tomatis, C., Fiorio Pla, A., and Author, C. (2008). The secret marriage between calcium and tumor angiogenesis. *Techno. Cancer Res. Treat.* 7, 335–339.
- Pafumi, I., Favia, A., Gambarà, G., Papacci, F., Ziparo, E., Palombi, F., et al. (2015). Regulation of angiogenic functions by angiopoietins through calcium-dependent signaling pathways. *Biomed. Res. Int.* 2015:965271. doi: 10.1155/2015/965271
- Palty, R., Raveh, A., Kaminsky, I., Meller, R., and Reuveny, E. (2012). SARAF inactivates the store operated calcium entry machinery to prevent excess calcium refilling. *Cell* 149, 425–438. doi: 10.1016/j.cell.2012.01.055
- Rodriguez, L. G., Wu, X., and Guan, J. L. (2005). Wound-healing assay. *Methods Mol. Biol.* 294, 23–29. doi: 10.1385/1-59259-860-9:023
- Savage, A. M., Kurusamy, S., Chen, Y., Jiang, Z., Chhabria, K., MacDonald, R. B., et al. (2019). tmem33 is essential for VEGF-mediated endothelial calcium oscillations and angiogenesis. *Nat. Commun.* 10, 1–15. doi: 10.1038/s41467-019-08590-7
- Smani, T., Gómez, L. J., Regodon, S., Woodard, G. E., Siegfried, G., Khatib, A. M., et al. (2018). Trp channels in angiogenesis and other endothelial functions. *Front. Physiol.* 9:1731. doi: 10.3389/fphys.2018.01731
- Stapor, P., Wang, X., Goveia, J., Moens, S., and Carmeliet, P. (2014). Angiogenesis revisited – role and therapeutic potential of targeting endothelial metabolism. *J. Cell Sci.* 127, 4331–4341. doi: 10.1242/jcs.153908
- Ucuzian, A. A., Gassman, A. A., East, A. T., and Greisler, H. P. (2010). Molecular mediators of angiogenesis. *J. Burn Care Res.* 31, 158–175. doi: 10.1097/BCR.0b013e3181c7ed82
- Vashisht, A., Trebak, M., and Motiani, R. K. (2015). STIM and orai proteins as novel targets for cancer therapy. a review in the theme: cell and molecular

- processes in cancer metastasis. *Am. J. Physiol. Cell Physiol.* 309, C457–C469. doi: 10.1152/ajpcell.00064.2015
- Ye, J., Huang, J., He, Q., Zhao, W., Zhou, X., Zhang, Z., et al. (2018). Blockage of store-operated  $\text{Ca}^{2+}$  entry antagonizes Epstein-Barr virus-promoted angiogenesis by inhibiting  $\text{Ca}^{2+}$  signaling-regulated VEGF production in nasopharyngeal carcinoma. *Cancer Manag. Res.* 10, 1115–1124. doi: 10.2147/CMARS159441
- Zudaire, E., Gambardella, L., Kurcz, C., and Vermeren, S. (2011). A computational tool for quantitative analysis of vascular networks. *PLoS One* 6:e27385. doi: 10.1371/journal.pone.0027385
- Conflict of Interest:** The authors declare that the research was conducted in the absence of any commercial or financial relationships that could be construed as a potential conflict of interest.
- Copyright © 2021 Galeano-Otero, Del Toro, Khatib, Rosado, Ordóñez-Fernández and Smani. This is an open-access article distributed under the terms of the Creative Commons Attribution License (CC BY). The use, distribution or reproduction in other forums is permitted, provided the original author(s) and the copyright owner(s) are credited and that the original publication in this journal is cited, in accordance with accepted academic practice. No use, distribution or reproduction is permitted which does not comply with these terms.



# Corrigendum: SARAF and Orai1 Contribute to Endothelial Cell Activation and Angiogenesis

Isabel Galeano-Otero<sup>1,2,3</sup>, Raquel del-Toro<sup>1,2,3</sup>, Abdel-Majid Khatib<sup>4</sup>, Juan Antonio Rosado<sup>5</sup>, Antonio Ordóñez-Fernández<sup>2,3,6</sup> and Tarik Smani<sup>1,2,3\*</sup>

## OPEN ACCESS

**Approved by:**  
Frontiers Editorial Office,  
Frontiers Media SA, Switzerland

**\*Correspondence:**  
Tarik Smani  
tasmani@us.es

**Specialty section:**  
This article was submitted to  
Signaling,  
a section of the journal  
Frontiers in Cell and Developmental  
Biology

**Received:** 19 March 2021  
**Accepted:** 22 March 2021  
**Published:** 20 April 2021

**Citation:**  
Galeano-Otero I, del-Toro R,  
Khatib A-M, Rosado JA,  
Ordóñez-Fernández A and Smani T  
(2021) Corrigendum: SARAF and  
Orai1 Contribute to Endothelial Cell  
Activation and Angiogenesis.  
Front. Cell Dev. Biol. 9:683097.  
doi: 10.3389/fcell.2021.683097

<sup>1</sup> Department of Medical Physiology and Biophysics, University of Seville, Seville, Spain, <sup>2</sup> Group of Cardiovascular Pathophysiology, Institute of Biomedicine of Seville, University Hospital of Virgen del Rocío/University of Seville/CSIC, Seville, Spain, <sup>3</sup> CIBERCV, Madrid, Spain, <sup>4</sup> LAMC, INSERM U1029, Pessac, France, <sup>5</sup> Department of Physiology, University of Extremadura, Caceres, Spain, <sup>6</sup> Department of Surgery, University of Seville, Seville, Spain

**Keywords:** Orai1, SARAF, SOCE, HUVEC, angiogenesis

## A Corrigendum on

**SARAF and Orai1 Contribute to Endothelial Cell Activation and Angiogenesis**  
by Galeano-Otero, I., Del Toro, R., Khatib, A.-M., Rosado, J. A., Ordóñez-Fernández, A., and Smani, T. (2021). *Front. Cell Dev. Biol.* 9:639952. doi: 10.3389/fcell.2021.639952

There is an error in the Funding statement. The correct funding statement is: “This research was funded by Agencia Estatal de Investigación [PID2019-104084GB-C22/AEI/10.13039/501100011033]”.

The authors apologize for this error and state that this does not change the scientific conclusions of the article in any way. The original article has been updated.

Copyright © 2021 Galeano-Otero, del-Toro, Khatib, Rosado, Ordóñez-Fernández and Smani. This is an open-access article distributed under the terms of the Creative Commons Attribution License (CC BY). The use, distribution or reproduction in other forums is permitted, provided the original author(s) and the copyright owner(s) are credited and that the original publication in this journal is cited, in accordance with accepted academic practice. No use, distribution or reproduction is permitted which does not comply with these terms.



# Molecular Components of Store-Operated Calcium Channels in the Regulation of Neural Stem Cell Physiology, Neurogenesis, and the Pathology of Huntington's Disease

Ewelina Latoszek and Magdalena Czeredys\*

Laboratory of Neurodegeneration, International Institute of Molecular and Cell Biology in Warsaw, Warsaw, Poland

## OPEN ACCESS

### Edited by:

Joanna Gruszczynska-Biegala,  
Mossakowski Medical Research  
Centre, Polish Academy of Sciences,  
Poland

### Reviewed by:

Claire Mary Kelly,  
Cardiff Metropolitan University,  
United Kingdom  
Andrea Faedo,  
Axxam, Italy

### \*Correspondence:

Magdalena Czeredys  
mczeredys@iimcb.gov.pl

### Specialty section:

This article was submitted to  
Signaling,  
a section of the journal  
Frontiers in Cell and Developmental  
Biology

**Received:** 22 January 2021

**Accepted:** 10 March 2021

**Published:** 01 April 2021

### Citation:

Latoszek E and Czeredys M  
(2021) Molecular Components  
of Store-Operated Calcium Channels  
in the Regulation of Neural Stem Cell  
Physiology, Neurogenesis,  
and the Pathology of Huntington's  
Disease.  
Front. Cell Dev. Biol. 9:657337.  
doi: 10.3389/fcell.2021.657337

One of the major  $\text{Ca}^{2+}$  signaling pathways is store-operated  $\text{Ca}^{2+}$  entry (SOCE), which is responsible for  $\text{Ca}^{2+}$  flow into cells in response to the depletion of endoplasmic reticulum  $\text{Ca}^{2+}$  stores. SOCE and its molecular components, including stromal interaction molecule proteins, Orai  $\text{Ca}^{2+}$  channels, and transient receptor potential canonical channels, are involved in the physiology of neural stem cells and play a role in their proliferation, differentiation, and neurogenesis. This suggests that  $\text{Ca}^{2+}$  signaling is an important player in brain development. Huntington's disease (HD) is an incurable neurodegenerative disorder that is caused by polyglutamine expansion in the huntingtin (HTT) protein, characterized by the loss of  $\gamma$ -aminobutyric acid (GABA)-ergic medium spiny neurons (MSNs) in the striatum. However, recent research has shown that HD is also a neurodevelopmental disorder and  $\text{Ca}^{2+}$  signaling is dysregulated in HD. The relationship between HD pathology and elevations of SOCE was demonstrated in different cellular and mouse models of HD and in induced pluripotent stem cell-based GABAergic MSNs from juvenile- and adult-onset HD patient fibroblasts. The present review discusses the role of SOCE in the physiology of neural stem cells and its dysregulation in HD pathology. It has been shown that elevated expression of STIM2 underlying the excessive  $\text{Ca}^{2+}$  entry through store-operated calcium channels in induced pluripotent stem cell-based MSNs from juvenile-onset HD. In the light of the latest findings regarding the role of  $\text{Ca}^{2+}$  signaling in HD pathology we also summarize recent progress in the *in vitro* differentiation of MSNs that derive from different cell sources. We discuss advances in the application of established protocols to obtain MSNs from fetal neural stem cells/progenitor cells, embryonic stem cells, induced pluripotent stem cells, and induced neural stem cells and the application of transdifferentiation. We also present recent progress in establishing HD brain organoids and their potential use for examining HD pathology and its treatment. Moreover, the significance of stem cell therapy to restore normal neural cell function, including  $\text{Ca}^{2+}$  signaling in the central nervous system in HD patients will be considered. The transplantation of MSNs or their precursors remains a promising treatment strategy for HD.

**Keywords:** store-operated  $\text{Ca}^{2+}$  entry, store-operated  $\text{Ca}^{2+}$  channels,  $\text{Ca}^{2+}$  homeostasis, neural stem cells, induced pluripotent stem cells, brain organoids, Huntington's disease

## INTRODUCTION

Store-operated  $\text{Ca}^{2+}$  entry (SOCE) is the process by which calcium ( $\text{Ca}^{2+}$ ) flows from the extracellular space into the cytoplasm in response to the depletion of endoplasmic reticulum (ER)  $\text{Ca}^{2+}$  stores. Upon a decrease in  $\text{Ca}^{2+}$  in the ER,  $\text{Ca}^{2+}$  sensors, named stromal interaction molecules (STIMs; e.g., STIM1 and STIM2) (Liou et al., 2005; Roos et al., 2005; Zhang et al., 2005) interact with highly selective Orai1-3  $\text{Ca}^{2+}$  channels at the plasma membrane (Feske et al., 2006; Peinelt et al., 2006; Prakriya et al., 2006), which causes  $\text{Ca}^{2+}$  influx. The current mediated by Orai channels is called  $\text{Ca}^{2+}$  release-activated  $\text{Ca}^{2+}$  current (ICRAC) and is highly selective for  $\text{Ca}^{2+}$  (Hoth and Penner, 1993; Lewis and Cahalan, 1995; Moccia et al., 2015). Besides, there also exists store-operated  $\text{Ca}^{2+}$  current ( $\text{I}_{\text{SOC}}$ ), which is characterized by non-selective outward currents that are operated by STIM and transient receptor potential canonical 1 (TRPC1) channel (Golovina et al., 2001; Trepakova et al., 2001; Strübing et al., 2003; Ma et al., 2015; Majewski and Kuznicki, 2015; Lopez et al., 2016; Lopez et al., 2020). SOCE has been detected in both non-excitable cells (Feske et al., 2005; Parekh and Putney, 2005; Prakriya and Lewis, 2015; Putney et al., 2017) and neurons (Emptage et al., 2001; Baba et al., 2003; Klejman et al., 2009; Gemes et al., 2011; Gruszczynska-Biegala et al., 2011; Wu et al., 2011, 2016; Hartmann et al., 2014; Samtleben et al., 2015; Czeredys et al., 2017). Recent research has shown that  $\text{Ca}^{2+}$  signaling, including the SOCE process has been involved in the physiology of neural stem cells (NSCs) and neurogenesis (Tonelli et al., 2012; Toth et al., 2016; Glaser et al., 2019).

Stem cells are unspecialized cells that are characterized by their ability to self-renew to increase their pool. They also have the potential to differentiate (specialize) into specific types of cells (e.g., neuronal cells) (Hima Bindu and Srilatha, 2011; Tonelli et al., 2012; Zakrzewski et al., 2019). NSCs represent a population of multipotent cells, which can self-renew and proliferate without limitation, and finally, differentiate into neurons, astrocytes, and oligodendrocytes (Oikari et al., 2016; Golas, 2018). In contrast, neural progenitor cells (NPCs) are also multipotent and can differentiate into more than one cell type, but have a limited ability to proliferate and are unable to self-renew (Oikari et al., 2016; Golas, 2018). However, Golas, note that researchers use the term NSCs and NPCs interchangeably (Golas, 2018). NSCs/NPCs are present in fetal neural tissue, but also neonatal and adult brain (Yin et al., 2013; Martínez-Cerdeño and Noctor, 2018; Obernier and Alvarez-Buylla, 2019). The major stem cell niches in the adult brain are NSCs in the subgranular zone (SGZ) of the hippocampal dentate gyrus and subventricular zone (SVZ), which is situated on the outside wall of each lateral ventricle of the vertebrate brain (Ma et al., 2009). In these regions, NSCs can proliferate, self-renew, and give birth to both neurons and glial cells. In adulthood, neurogenesis continues to occur throughout life (Galvan and Jin, 2007).

Stem cells can differentiate into different specialized, mature cell types. There are five types of stem cell development potential, which can be arranged hierarchically. The first type is totipotency, in which cells differentiate into embryonic and extra-embryonic cell (EC) types. Among these are the fertilized egg cell, the

zygote. Zygotes have the highest differentiation potential because they can create a whole, complete organism (Hima Bindu and Srilatha, 2011; Zakrzewski et al., 2019). The second type are pluripotent cells. These cells can differentiate into any somatic cell, forming cells of all germ layers. However, they cannot transform into trophoblast cells (Hima Bindu and Srilatha, 2011; Zakrzewski et al., 2019). This type of cell includes embryonic stem cells (ESCs) and induced pluripotent stem cells (iPSCs). Dental pulp stem cells (DPSCs) and stem cells from human exfoliated deciduous teeth (SHEDs) can differentiate into several lineages, such as neurons, hepatocytes, endothelial cells, and odontoblasts (Rosa et al., 2016). The third type is multipotent cells, which are present during embryo development in the gastrula stage, consisting of mesoderm, endoderm, and ectoderm cells. They can differentiate into cells that belong to specific tissue. One example is adult NSCs, which can develop mature neurons and glial cells and have an ectodermal origin (Ma et al., 2009; Tonelli et al., 2012). Additionally, multipotent cells are hematopoietic stem cells, which have a mesodermal origin and can develop into several types of blood cells (Zakrzewski et al., 2019). Lung cells derive from lung endodermal progenitor cells (Parekh et al., 2020). The next type is oligopotent stem cells, which can differentiate into a few cell types. One example is myeloid stem cells, which can divide into white blood cell lineages (Hima Bindu and Srilatha, 2011; Zakrzewski et al., 2019). In turn, unipotent cells have lower potency and can develop only one specific cell type (e.g., muscle stem cells that give rise to mature muscle cells) (Hima Bindu and Srilatha, 2011). The fate of stem cells is determined by factors in the cell environment and tissue-specific niches, such as growth factors and neurotrophins (e.g., transforming growth factor  $\beta$  [TGF- $\beta$ ], fibroblast growth factor [FGF], and nerve growth factor [NGF]), cytokines (activin A), and other signaling molecules (Xiao and Le, 2016; Tan et al., 2019). One of them is  $\text{Ca}^{2+}$ , which plays a critical role in various stages of stem cell differentiation as a component of signaling pathways (Tan et al., 2019).

Huntington's disease (HD) is a heritable neurodegenerative disorder that is characterized by unintentional movements, cognitive decline, and behavioral impairment. A mutant form of huntingtin (mHTT) protein contains an expansion of polyglutamine residues (polyQ) in its amino-terminal part that causes its aggregation (Ross, 2002) and the loss of  $\gamma$ -aminobutyric acid (GABA)-ergic medium spiny neurons (MSNs) in the striatum (Vonsattel and DiFiglia, 1998; Zoghbi and Orr, 2000). When mHTT has between 39 and 60 glutamine repeats, late-onset HD begins, usually at 30–50 years of age. Early HD onset characterizes the juvenile form of HD, in which disease progression occurs before the age of 21, and the polyQ chain contains over 60 glutamine repeats (Quigley, 2017). Huntington's disease is also considered a neurodevelopmental disorder (Wood, 2018; Lebouc et al., 2020).

Recent research has shown the transcriptional dysregulation of several genes, including genes that are involved in the calcium signalosome in the striatum in YAC128 mice (i.e., a mouse model of HD) (Czeredys et al., 2013). SOCE was shown to be significantly elevated in several models of HD, including cellular models (Vigont et al., 2014, 2015) and MSNs from the

YAC128 mice model (Wu et al., 2011, 2016; Czeredys et al., 2017). Furthermore, patch-clamp recordings revealed that  $I_{SOCE}$  increased in cellular HD models (Wu et al., 2011; Vigont et al., 2015). STIM2 plays a key role in the dysregulation of SOCE in YAC128 mice. An increase in STIM2 expression was observed in both aged MSN cultures and in the striatum in YAC128 mice (Wu et al., 2016). Abnormal synaptic neuronal SOCE (nSOCE) likely underlies synaptic loss in MSNs (Wu et al., 2016; Wu J. et al., 2018). The knockdown of molecular components of SOCE, including the  $Ca^{2+}$  sensor STIM2 and  $Ca^{2+}$  channels TRPC1, TRPC6, Orai1, and Orai2, resulted in the stabilization of dendritic spines and restored elevations of nSOCE in YAC128 MSNs (Wu et al., 2016; Wu J. et al., 2018). Although a few compounds have been shown to stabilize elevations of SOCE, such as tetrahydrocarbazoles (Czeredys et al., 2017, 2018) and the quinizone derivative EVP4593 (an NF- $\kappa$ B antagonist which restores synaptic nSOCE and rescues abnormal spines in YAC128 MSNs *in vitro* and *in vivo*) (Wu et al., 2011, 2016), future research is needed to determine whether they can serve as drug candidates for HD therapy (Czeredys, 2020). No effective treatments are currently available for HD. One option for HD patients could be stem cell therapy, but this approach is still under investigation and many issues must be improved to increase the reliability of transplants (Bachoud-Lévi et al., 2020). It is difficult to obtain a genuine MSN fate, therefore further advances are required to achieve suitable donor cells for replacement therapy for HD.

The present review focuses on  $Ca^{2+}$  signaling via store-operated  $Ca^{2+}$  channels under physiological conditions in NSC development and the pathology of HD. The role of STIM, Orai, and TRPC proteins in NSC proliferation and differentiation and neurogenesis is discussed. The dysregulation of SOCE that has been detected in iPSC-based GABAergic MSNs from juvenile- and adult-onset HD patient fibroblasts and its contribution to HD pathology is also presented. We discuss advances in the application of established protocols to obtain MSNs from iPSCs and other stem cell sources. We also discuss recent progress in brain organoid technology and its potential use for examining HD pathology and treatment. Finally, we summarize the latest findings on the transplantation of precursors of MSNs into HD patient brains. Stem cell therapy is a promising treatment strategy for HD.

## **$Ca^{2+}$ SIGNALING VIA STORE-OPERATED $Ca^{2+}$ CHANNELS IN NSCs UNDER PHYSIOLOGICAL CONDITIONS**

$Ca^{2+}$  signaling is a crucial player in early neural development, which is distinguished by the fast proliferation of ECs, which then differentiate to produce many specialized cell types, including neurons. One of the major pathways of  $Ca^{2+}$  entry in non-excitable cells, such as NPCs, is SOCE (Shin et al., 2010). In human embryonic stem cells (hESCs), SOCE but not voltage-gated  $Ca^{2+}$  channel (VGCC)-mediated  $Ca^{2+}$  entry is detected (Huang et al., 2017). SOCE has been recently measured using Fura-2-acetoxymethyl ester (Fura2-AM) in human neural progenitor cells (hNPCs) and spontaneously differentiated

neurons that derive from pluripotent hESCs (Gopurappilly et al., 2019). In embryonic and adult mouse NSCs/NPCs from the ganglionic eminence (GE) and anterior SVZ, respectively, SOCE was mediated by  $Ca^{2+}$  release-activated  $Ca^{2+}$  (CRAC) channel proteins STIM1 and Orai1. The knockdown of STIM1 or Orai1 significantly decreased SOCE in NPCs *in vitro*. Moreover, SOCE was lost in NPCs from transgenic mice that lacked Orai1 or STIM1 and in knock-in mice that expressed a loss-of-function Orai1 mutant (R93W). In NPCs, the SOCE process was initiated by epidermal growth factor (EGF) and acetylcholine the latter of which involved the contribution of muscarinic receptors. CRAC channels regulated calcineurin/nuclear factor of activated T cell (NFAT)-mediated gene expression. The inhibition or ablation of STIM1 and Orai1 expression significantly attenuated the proliferation of embryonic and adult NPCs that were cultured as neurospheres and also *in vivo* in the SVZ in adult mice. This observation indicated that CRAC channels are crucial determinants of mammalian neurogenesis (Somasundaram et al., 2014).  $Ca^{2+}$  entry through SOCE, regulated by Orai channels in hNPCs and neurons that differentiated from hNPCs, was shown to be negatively regulated by septin 7 (SEPT7), a protein that is a member of the family of filament-forming guanosine triphosphatases, called septins (Deb et al., 2020).

To understand the role of SOCE in human NSC physiology, Gopurappilly et al. (2018) knocked down STIM1 in hNPCs. These cells were characterized by an efficient SOCE process that was significantly reduced by STIM1 knockdown. The global transcriptomic approach of STIM1-knockdown hNPCs indicated the downregulation of genes that are related to cell proliferation and DNA replication processes, whereas genes that are related to neural differentiation, including postsynaptic signaling, were upregulated. Additionally, STIM1-knockdown NPCs substantially attenuated the average size of neurospheres and their numbers. In parallel, they exhibited spontaneous differentiation into a neuronal lineage. These findings indicate that gene expression that is modulated by STIM1-mediated SOCE is responsible for the regulation of self-renewal and the differentiation of hNPCs. The authors considered that the loss of SOCE *in vivo* could result in the attenuation of an appropriate number of hNPCs that are needed for normal brain development (Gopurappilly et al., 2018). Additionally, Pregno et al. (2011) showed that the neuregulin-1/Erb-B2 receptor tyrosine kinase 4 (ErbB4)-induced migration of ST14A striatal progenitors cells was modulated by *N*-methyl-D-aspartate receptor (NMDAR) activation in a  $Ca^{2+}$ -dependent manner that was made possible by SOCE.

In mouse ESCs, both SOCE components STIM1 and Orai1 were expressed and functionally active (Hao et al., 2014). Their knockdown reduced SOCE in ECs. STIM1 and Orai1 expression levels were enhanced during neural differentiation. STIM1 was suggested to play an important role in the early stage of neural lineage entry. In contrast to Hao et al. (2014), Gopurappilly et al. (2018) observed that STIM1 and STIM2, but not Orai1, were shown to be involved in the early neural differentiation of ESCs. Moreover, STIM1 knockdown resulted in substantial cell loss and blocked the proliferation of neural progenitors that were derived from mouse ESCs. Hao et al. (2014) concluded

that inhibition of the neural differentiation of mouse ESCs by STIM1 and STIM2 knockdown is independent of Orai1-mediated SOCE. Additionally, STIM1 is involved in the terminal differentiation of mouse neural progenitors into neurons and astrocytes (Hao et al., 2014). Furthermore, upregulation of the Stim1b isoform was detected in differentiating cells compared with cells that underwent proliferation in zebrafish neurospheres (Tse et al., 2018).

In mouse SVZ cells, the expression of TRPC1 and Orai1 channels and their activator STIM1 was reported, and these cells were characterized by functional SOCE (Domenichini et al., 2018). The application of SOCE inhibitors *in vitro* (SKF-96365 or YM-58483) decreased the stem cell population by attenuating their proliferation and dysregulating SVZ stem cell self-renewal by driving their asymmetric division instead of symmetric proliferative division. Domenichini et al. (2018) detected TRPC1, Orai1, and STIM1 expression in mouse brain sections *in vivo* in sex-determining region Y-box2 (SOX2)-positive SVZ NSCs. The inhibition of SOCE reduced the population of stem cells in the adult mouse brain and impaired the ability of SVZ cells to create neurospheres *in vitro*. These results indicated that SOCE plays a key role in the regulation of NSC activation and self-renewal (Domenichini et al., 2018).

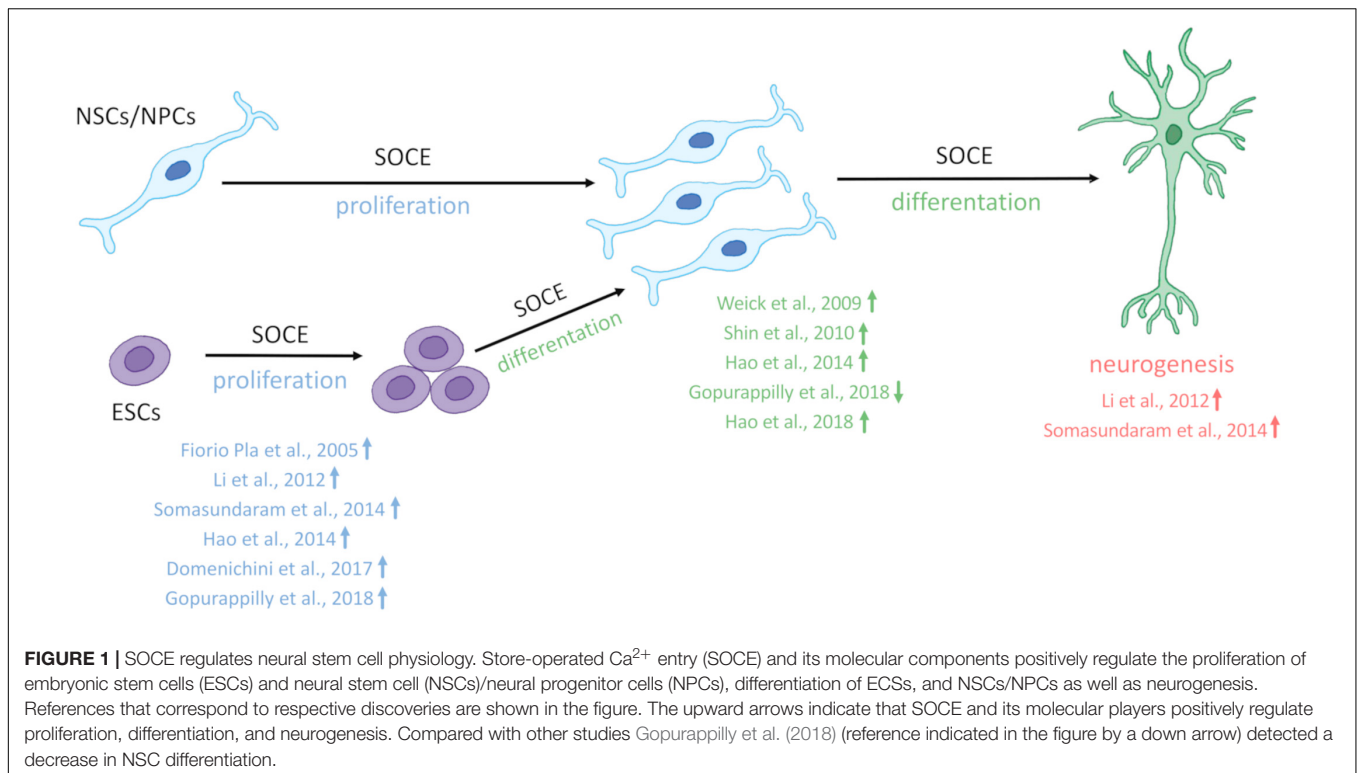
Several studies established a role for TRPC channels in NSC regulation.  $\text{Ca}^{2+}$  entry through TRPC1 channels appears to play a critical role in basic fibroblast growth factor (bFGF)-induced NSCs proliferation (Fiorio Pla et al., 2005). TRPC1 and TRPC4 modulate neurite extension in hESCs (Weick et al., 2009), whereas they regulate their proliferation in oligodendrocyte precursor cells (Paez et al., 2011). Additionally, Li et al. (2012) reported the role of TRPC1 and SOCE in adult hippocampal neurogenesis. The TRPC1-mediated elevation of  $\text{Ca}^{2+}$  entry was shown to be essential for the proliferation of adult hippocampal NPCs. Upon TRPC1 knockdown, the induction of cell cycle arrest in the G0/G1 phase was observed and caused the up- or downregulation of 10 cell cycle genes, indicating that these genes may regulate the effects of TRPC1 on adult NPCs proliferation. Antagonists of SOCE and canonical TRPC inhibited the increase in SOCE and adult NPC proliferation. Moreover, the knockdown of Orai1 and STIM1 inhibited SOCE and proliferation in adult NPCs (Li et al., 2012). The role of TRPCs as SOCE channels was also examined with regard to modulating induction of the neuronal differentiation of NPCs with a neural cell surface antigen of A2B5 (A2B5+ NPCs) that were obtained from the postnatal day 12 rat brain. In neural cells that differentiated from A2B5+ NPCs, SOCE substantially increased compared with proliferating cells, and the application of SOCE inhibitors normalized these processes. Pharmacological inhibitors of SOCE and an siRNA against TRPC5 normalized the amplitude of SOCE and inhibited neural differentiation from A2B5+ NPCs (Shin et al., 2010). TRPC3 was recently shown to play an important role in the survival, pluripotency, and neural differentiation of mouse embryonic stem cells (mESCs) (Hao et al., 2018). The CRISPR/Cas9-facilitated knockout of TRPC3 caused apoptosis and compromised mitochondrial membrane potential in undifferentiated mESCs and neurons during

the course of differentiation. Furthermore, TRPC3 knockout impaired the pluripotency of mESCs and strongly attenuated the neural differentiation of mESCs by inhibiting the expression of genes that encode neural progenitors, neurons, astrocytes, and oligodendrocytes (Hao et al., 2018).

SOCE is crucial for the physiology of NSCs and regulates  $\text{Ca}^{2+}$  signaling in newly developing neurons in the brain (Figure 1). The main molecular components of SOCE that directly regulate  $\text{Ca}^{2+}$  signaling in NSC development and their main physiological functions are listed in Table 1.

## MOLECULAR COMPONENTS OF SOCE AND $\text{Ca}^{2+}$ SIGNALING PATHWAYS MIGHT CONTRIBUTE TO NEURODEVELOPMENTAL CHANGES IN HD

Increasing evidence from iPSCs and a three-dimensional (3D) organoid model of HD indicates that HD is also a neurodevelopmental disease (Conforti et al., 2018; Świtońska et al., 2018; Wiatr et al., 2018). Neural cells that were differentiated from juvenile HD patient-derived iPSC lines exhibited deficits in neurodevelopment and adult neurogenesis. RNA sequencing (RNAseq) analyses of these cells showed that one-third of the genes that were altered are involved in the regulation of neuronal development and maturation (HD iPSC Consortium., 2017). Additionally, in neurons that were differentiated from iPSCs from juvenile HD patients, RNAseq revealed the upregulation of several genes that encode proteins that are involved in  $\text{Ca}^{2+}$  signaling, including inositol-1,4,5-triphosphate receptor 1 (IP3R1), TRPC6, and CRAC channels, and the downregulation of genes that encode proteins that are involved in cyclic adenosine monophosphate (cAMP) response element-binding protein (CREB), glutamate, and GABA signaling, axonal guidance, and synaptic function (HD iPSC Consortium., 2017). Transcriptomic analysis of juvenile-onset HD found that iPSC-derived NSCs had significantly different expression levels of genes that are involved in signaling, the cell cycle, axonal guidance, and neuronal development compared with controls, whereas NSCs that contained medium-length polyQ tracts were characterized by changes in  $\text{Ca}^{2+}$  signaling (HD iPSC Consortium., 2012). The dysregulation of several  $\text{Ca}^{2+}$  signalosomes that are involved in  $\text{Ca}^{2+}$  binding and  $\text{Ca}^{2+}$  signaling were identified in iPSC-based GABAergic MSNs from late-onset HD patient fibroblasts (Nekrasov et al., 2016). These findings corroborate the importance of  $\text{Ca}^{2+}$  dysregulation in neurodevelopmental changes that are observed in HD pathology. The treatment of neural stem or progenitor cells with isoxazole-9, which increases  $\text{Ca}^{2+}$  influx via NMDARs and VGCCs, was neuroprotective in juvenile- and adult-onset iPSC-derived neurons and restored cortico-striatal synapses in R6/2 mice, a model of HD (HD iPSC Consortium., 2017). In rat cortical neuronal cultures, STIM proteins negatively regulate NMDA (Gruszczynska-Biegala et al., 2020) and STIM1 inhibits L-type VGCCs (Park et al., 2010; Wang et al., 2010;



Dittmer et al., 2017). Therefore, the elevation of SOCE might affect these receptors in HD.

Additionally, neuronal differentiation is delayed in iPSC-derived MSNs from juvenile HD patients (Mathkar et al., 2019). Differentiated HD NPCs had a higher number of the stem cell marker Nestin on days 14, 28, and 42, however, no increased proliferation was observed. Both the knockdown of mHTT and inhibition of the Notch pathway stabilized Nestin expression in these cells (Mathkar et al., 2019). Recent data also clearly showed that HD has a neurodevelopmental component and thus is not simply a neurodegenerative disease (Barnat et al., 2020). In the developing cortex from fetal tissues that carried mHTT with 39, 40, and 42 polyQ repeats, which can lead to manifestations of adult-onset HD, Barnat et al. identified several cellular abnormalities. These changes included the abnormal localization of mHTT and junctional complex proteins, disruptions of neuroprogenitor cell polarity and differentiation, improper ciliogenesis, and defects in mitosis and cell cycle progression. Additionally, mHTT was shown to attenuate cell proliferation and shift neurogenesis toward the neuronal lineage (Barnat et al., 2020).

## DYSREGULATION OF SOCE IN iPSC-DERIVED MODELS FROM HD PATIENTS

In recent studies, iPSC-based GABAergic MSNs from HD patient fibroblasts that exhibit progressive HD pathology *in vitro* were generated by several groups (An et al., 2012; Jeon et al., 2012; Nekrasov et al., 2016). Nekrasov et al. (2016)

reported that iPSC-based GABAergic MSN neurons from HD patient fibroblasts (40–47 CAG repeats) representing adult-onset HD manifested progressive HD phenotype, including mHTT aggregation, an increase in the number of phagosomes, and an increase in neuronal death overtime. They also observed that these neurons were characterized by dysregulated SOCE what was measured using the patch-clamp technique (Nekrasov et al., 2016). In HD iPSC-based GABAergic MSNs, SOC currents were shown to be mediated by  $I_{\text{CRAC}}$  and  $I_{\text{SOC}}$ , which were upregulated simultaneously compared with wildtype iPSC-based GABAergic MSNs (Vigont et al., 2018). The molecular mechanism by which SOCE is elevated in MSNs from adult-onset HD fibroblasts is unrevealed. Transcriptome analysis has been previously demonstrated that the expression of genes encoding Orai and TRP channels and STIM proteins did not differ significantly between iPSCs-derived MSN cultures compared to control and their protein levels were not further studied (Nekrasov et al., 2016). Furthermore, the SOCE inhibitor EVP4593 stabilized  $I_{\text{SOC}}$  and  $I_{\text{CRAC}}$  in HD iPSC-based GABAergic MSNs (Vigont et al., 2018). The mechanism of action of EVP4593 is still unknown, but Vigont et al. (2018) suggested that this compound may target SOCE regulatory proteins (e.g., STIM proteins) that are involved in both  $I_{\text{CRAC}}$  and  $I_{\text{SOC}}$  because EVP4593 equally affected both  $I_{\text{CRAC}}$  and  $I_{\text{SOC}}$ . Besides EVP4593 attenuated the number of phagosomes and exerted neuroprotective effects during neuronal aging (Nekrasov et al., 2016).

A recent publication by Vigont et al. (2021) indicates that  $\text{Ca}^{2+}$  signaling is highly elevated in iPSC-based GABAergic MSNs cultures from juvenile-onset HD patient containing 76 repetitions of CAG in mHTT. Authors specifically demonstrated

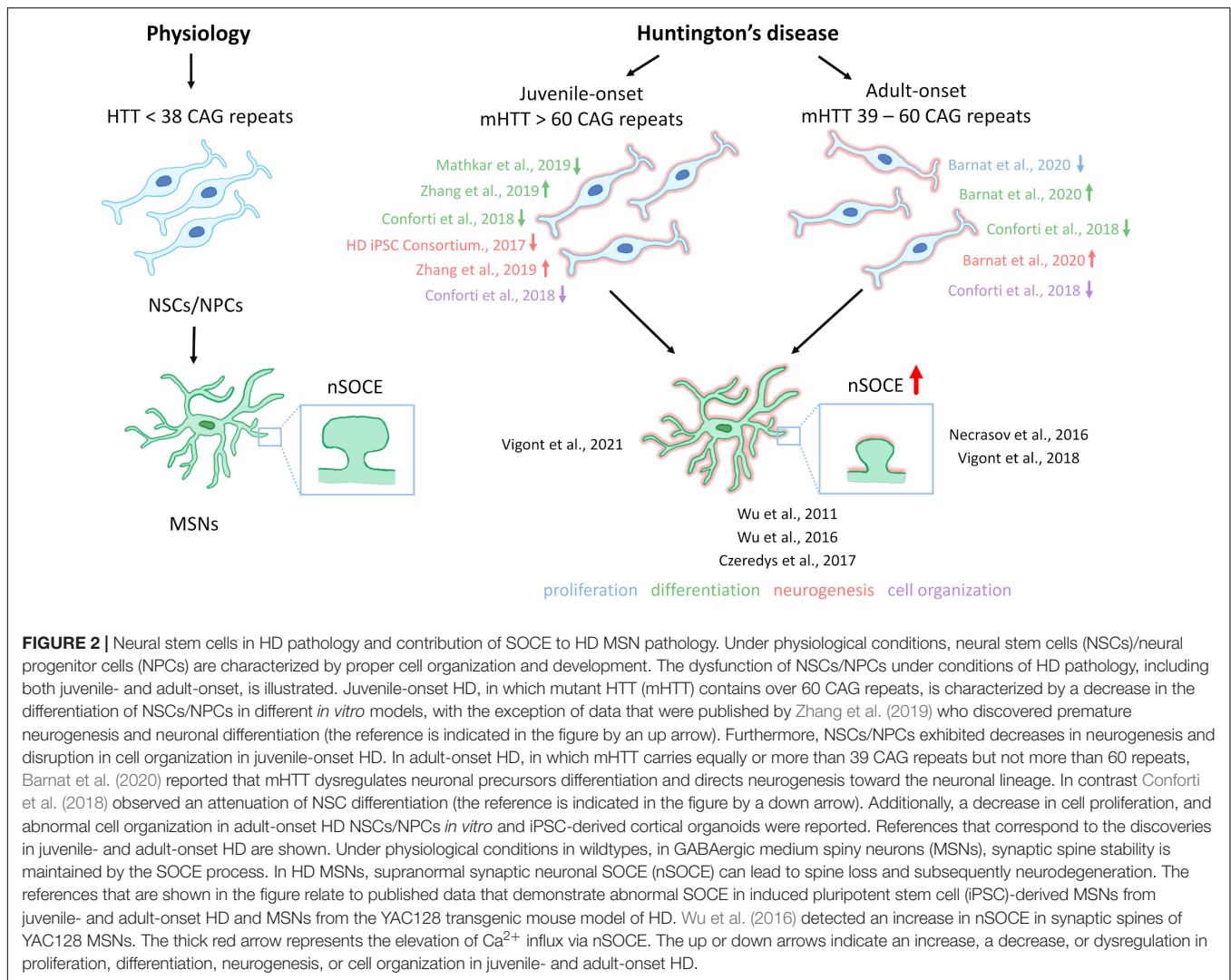
**TABLE 1** | Molecular components of SOCE in neural stem cell physiology.

Molecular component of SOCE	Function in neural stem cell physiology	References
<b>STIM1, Orai1</b>	<ul style="list-style-type: none"> <li>- Their inhibition or removal attenuated the proliferation of embryonic NPCs cultured as neurospheres <i>in vitro</i>.</li> <li>- Their inhibition or removal attenuated the proliferation of adult NPCs that were cultured as neurospheres <i>in vitro</i> and <i>in vivo</i> in the SVZ of adult mice.</li> </ul>	Somasundaram et al., 2014
<b>STIM1</b>	<ul style="list-style-type: none"> <li>- Its knockdown in hNPCs caused the downregulation of genes that are involved in cell proliferation and DNA replication and the upregulation of genes that are involved in neural differentiation.</li> <li>- Its knockdown in NPCs attenuated neurospheres size and number.</li> <li>- STIM1 knockdown increased spontaneous differentiation into the neuronal lineage.</li> </ul>	Gopurappilly et al., 2018
<b>STIM1, Orai1</b>	<ul style="list-style-type: none"> <li>- STIM1 and Orai1 expression levels increased during neural differentiation.</li> <li>- STIM1 plays a role in the early stage of neural lineage entry.</li> <li>- STIM1 and STIM2 but not Orai1 are involved in the early neural differentiation of ES cells.</li> <li>- STIM1 knockdown caused severe cell loss and inhibited the proliferation of neural progenitors that were derived from mouse ESCs.</li> <li>- STIM1 or STIM2 knockdown in EC cells is independent of Orai1-mediated SOCE.</li> <li>- STIM1 is involved in the terminal differentiation of mouse ESCs into neurons and astrocytes.</li> </ul>	Hao et al., 2014
<b>STIM1</b>	<ul style="list-style-type: none"> <li>- Upregulation of the Stim1b isoform was shown in differentiating cells compared with those that underwent proliferation in zebrafish neurospheres.</li> </ul>	Tse et al., 2018
<b>TRPC1, Orai1, STIM1</b>	<ul style="list-style-type: none"> <li>- Mouse SVZ cells express TRPC1, Orai1, and STIM1.</li> <li>- TRPC1, Orai1, and STIM1 are expressed in mouse brain sections <i>in vivo</i> in SOX2-positive SVZ NSCs.</li> <li>- Application of SOCE inhibitors <i>in vitro</i> (SKF-96365 or YM-58483) decreased the stem cell population by attenuating their proliferation and dysregulating SVZ stem cell self-renewal.</li> <li>- Inhibition of SOCE reduced the population of stem cells in the adult mouse brain and impaired the ability of SVZ cells to create neurospheres <i>in vitro</i>.</li> </ul>	Domenichini et al., 2018
<b>TRPC1</b>	<ul style="list-style-type: none"> <li>- <math>Ca^{2+}</math> entry through these channels regulates bFGF-induced NSC proliferation.</li> </ul>	Fiorio Pla et al., 2005
<b>TRPC1, TRPC4</b>	<ul style="list-style-type: none"> <li>- They modulate neurite extension in hESCs.</li> </ul>	Weick et al., 2009
<b>TRPC1, Orai1, STIM1</b>	<ul style="list-style-type: none"> <li>- TRPC1-mediated elevation of <math>Ca^{2+}</math> entry plays a role in adult hippocampal neurogenesis.</li> <li>- TRPC1-mediated elevation of <math>Ca^{2+}</math> entry is essential for the proliferation of adult hippocampal NPCs.</li> <li>- TRPC1 knockdown induces cell cycle arrest in the G0/G1 phase and dysregulates genes that are involved in cell cycle regulation.</li> <li>- Antagonist inhibition of TRPC1-mediated elevation of <math>Ca^{2+}</math> entry inhibited adult NPC proliferation.</li> <li>- Knockdown of Orai1 or STIM1 inhibited SOCE and proliferation in adult NPCs.</li> </ul>	Li et al., 2012
<b>TRPC5</b>	<ul style="list-style-type: none"> <li>- Pharmacological inhibition of SOCE and siRNA against TRPC5 blocked neural differentiation from A2B5+ NPCs.</li> </ul>	Shin et al., 2010
<b>TRPC3</b>	<ul style="list-style-type: none"> <li>- Plays a role in the survival, pluripotency, and neural differentiation of mESCs.</li> <li>- TRPC3 knockout caused apoptosis and disrupted mitochondrial membrane potential in both undifferentiated mESCs and neurons that were undergoing differentiation.</li> <li>- TRPC3 knockout impaired the pluripotency of mESCs and attenuated the neural differentiation of mESCs.</li> </ul>	Hao et al., 2018

higher levels of store-operated and voltage-gated calcium uptakes in these cells using the patch-clamp technique. Upregulation of  $Ca^{2+}$  sensor, STIM2 was detected in juvenile-onset HD MSNs, and shRNA-mediated suppression of STIM2 attenuated SOCE, but not affected VGCC. Moreover, G418, which is a known selective antagonist of STIM2 (Parvez et al., 2008) decreased SOCE in these cells. Vigont et al. (2021) concluded that elevated expression of STIM2 underlies the excessive  $Ca^{2+}$  entry through nSOCs in juvenile-onset HD pathology. Additionally, the neuroprotective effect of SOCE inhibitor, EVP4593 was shown in the stabilization of high protein levels of both total HTT and STIM2 via regulation of their expression (Vigont et al., 2021). Interestingly, the severity of  $Ca^{2+}$  influx via SOCE was independent of CAG repeat length between juvenile- and adult-onset HD iPSCs-derived MSNs (Vigont et al., 2021). Additionally, a similar increase of voltage-gated calcium uptakes was observed

in both juvenile- and adult-onset HD iPSCs-derived MSNs (Vigont et al., 2021).

Till now, the elevation of SOCE was observed in different HD models including MSNs from transgenic YAC128 mice and iPSCs-based GABAergic MSNs from juvenile- and adult-onset HD patient fibroblasts. The involvement of STIM2 in the regulation of the impaired SOCE was confirmed in both a mouse model of HD and juvenile-onset HD iPSCs-derived MSNs. Therefore, one postulation is that the dysregulation of nSOCE underlying HD pathology and neuronal store-operated calcium channels (nSOCs) such as STIM2 could be a novel therapeutic target for HD. Interestingly, STIM2 suppression resulted in attenuation of SOCE in wildtype iPSCs-derived MSNs indicating that STIM2 is responsible for mediating SOC channels in these neurons (Vigont et al., 2021). As shown in **Figure 2**, elevations of SOCE might underlie the pathology



of juvenile- and adult-onset HD. In mature HD MSNs from YAC128 mice, the dysregulation of synaptic spines resulted from abnormal nSOCE mediated by STIM2. The dysregulation of  $Ca^{2+}$  signaling pathways was demonstrated in iPSC-derived NPCs and MSNs from HD patients, suggesting its possible role in neurodevelopmental changes in HD.

Further studies using models based on cells from HD patients may bring new findings in understanding HD pathology, therefore it is important to develop techniques to obtain MSNs and cerebral organoids modeling HD. On the other hand, the transplantation of MSN progenitors or iPSC-derived MSNs without a mutation of HTT and with proper  $Ca^{2+}$  signaling could result in an advantage in HD patients.

## MODELING HD USING DIFFERENT PROTOCOLS TO OBTAIN MSNs

Reprogramming of somatic cells into iPSCs and then differentiating them into MSNs allows the generation of cells that

can be a valuable source for research of mechanisms leading to HD pathology. iPSC-based neurons are also crucial because it is impossible to obtain MSNs from living patients. Furthermore, post-mortem samples can be disrupted and unreliable in terms of disease progression and severity. Therefore, an unlimited source of iPSC-based MSNs can be invaluable. Recently, GABAergic MSNs that are based on HD iPSCs were suggested to be used as a platform for personal HD screening (Bezprozvanny and Kiselev, 2017; Vigont et al., 2018).

Human iPSCs can be obtained from somatic cells [(e.g., human fibroblasts, blood cells, keratinocytes from hair, and renal tubular epithelial cells from urine (Raab et al., 2014)], which are transduced by a lentiviral vector with a combination of four reprogramming transcription factors, including octamer-binding transcription factor 3/4 (Oct3/4), SOX2, Kruppel-like factor 4 (Klf4), and c-Myc (Takahashi et al., 2007). Park et al. (2008) were the first who reprogramming fibroblasts from HD patients into iPSCs. The generated iPSC line contained 72 CAG polyglutamine repeats in one allele and 19 in the other (Park et al., 2008). Recently reprogramming of iPSCs

with the application of non-integrative methods has become more popular (Schlaeger et al., 2015). In February 2020, The European Bank for induced Pluripotent Stem Cells (EBiSC) and CHDI Foundation, in cooperation with Censo Biotechnologies, generated widely available iPSC lines from HD patients<sup>1</sup>.

However, other cell types are also used to obtain MSNs, including embryonic stem cells that are pluripotent stem cells isolated from the inner cell mass (embryoblasts) of donated blastocysts. When they differentiate into neuronal progenitors, in addition to neurons, they can further transform into astrocytes and oligodendrocytes (Im et al., 2009). The advantage of iPSCs over ESCs during HD stem cell therapy is also evident. In the case of ESCs, allogenic immunological rejection and tumor formation were reported (Im et al., 2009; Liu et al., 2016). NSCs/NPCs are also used as sources of stem cells to generate human HD MSNs (Lin et al., 2015; Golas, 2018).

Various protocols to obtain MSNs from iPSCs have been developed (Zhang et al., 2010; Delli Carri et al., 2013; Arber et al., 2015; Lin et al., 2015; Liu et al., 2016; Nekrasov et al., 2016; Adil et al., 2018; Golas, 2018; Csobonyeiova et al., 2020; Grigor'eva et al., 2020; Xu et al., 2020; Vigont et al., 2021). These protocols may be based on other already established protocols that are modified.

Adult-onset HD iPSCs-based GABAergic MSNs cultures, which were characterized by abnormal  $\text{Ca}^{2+}$  influx via SOCs, were cultured using the protocol that consists of four steps (Nekrasov et al., 2016). From the start of differentiation to receiving terminally differentiated neurons, more than 60 days elapse. To obtain HD iPSC-based GABAergic MSNs in the induction step, the authors used Noggin, TGF- $\beta$  RI kinase inhibitor VI (SB-431542), and dorsomorphin to inhibit the bone morphogenetic protein (BMP)/TGF- $\beta$  pathway and differentiate hPSCs into neuroepithelial cells (Nekrasov et al., 2016). The combined use of Noggin/SB-431542 and dihydrochloride (LDN-193189), referred to as dual SMAD inhibition, was applied in earlier protocols (Delli Carri et al., 2013; Nicoleau et al., 2013). Maintaining the use of Noggin and adding purmorphamine resulted in cell differentiation into lateral ganglionic eminence (LGE) progenitors (Nekrasov et al., 2016). However, most protocols are based on the use of only one of these factors (Delli Carri et al., 2013; Nicoleau et al., 2013; Adil et al., 2018; Grigor'eva et al., 2020). Striatal projection neurons derive especially from the LGE (Reddington et al., 2014). In the next step of the protocol of Nekrasov et al. (2016) neural rosettes were mechanically reconstructed to separate NPCs from other cell types. The self-arranged formation of rosettes by neuroectodermal or neuroepithelial progenitor cells is a morphological signal that neuronal induction has started (Golas, 2018; Comella-Bolla et al., 2020). This is a transition stage to differentiation into a neuronal or glial lineage entry in response to relevant developmental signals (Elkabetz et al., 2008). To differentiate NPCs into mature HD iPSC-based GABAergic MSNs, brain-derived neurotrophic factor (BDNF) and forskolin were used (Nekrasov et al., 2016; Comella-Bolla et al., 2020). Forskolin is a cAMP signal conduction activator and not widely used

for MSN terminal differentiation. However, it is a morphogen that is used for the direct differentiation of fibroblasts into cholinergic and glutaminergic neurons and motoneurons (Xu et al., 2020). Dibutyryl-cAMP (db-cAMP) is a cAMP analog that is used more frequently (Zhang et al., 2010; Nicoleau et al., 2013; Victor et al., 2014; Lin et al., 2015; Adil et al., 2018; Grigor'eva et al., 2020). Finally, Nekrasov et al. (2016) obtained HD iPSCs-based GABAergic MSNs cultures that expressed synaptic GABA transporter 1 (GAT1), had dendritic spines, formed synapses, and manifested an HD phenotype, which was more prominent with the culture age.

Grigor'eva et al. (2020) developed a new three-step protocol for human iPSCs differentiation into striatal MSNs. The protocol assumes dual SMAD inhibition to obtain neuroectodermal cells. For this purpose, the authors used SB-431542 and LDN-193189. These small molecules inhibit BMP/TGF- $\beta$  signaling and induce ventral telencephalic specification, enhanced by the addition of purmorphamine. This combination significantly enhanced neural induction (Grigor'eva et al., 2020). Ventral telencephalic identity induction was also performed using sonic hedgehog (SHH) (Zhang et al., 2010; Delli Carri et al., 2013; Nicoleau et al., 2013; Lin et al., 2015), for which purmorphamine is an agonist (Ma et al., 2012). Ma et al. (2012) showed that 0.65  $\mu\text{M}$  purmorphamine can be the equivalent of 200 ng/ml SHH for generating LGE-like progenitors. As a factor that improves the survival of neurons, bFGF, also known as FGF2 was used (Zhang et al., 2010; Nekrasov et al., 2016; Grigor'eva et al., 2020). In the next stage, subsequent precursors of GABAergic projection MSNs (pMSNs) were cultivated, which was an important attribute of their protocol (Grigor'eva et al., 2020). Finally, the terminal differentiation of cells into MSNs was performed by adding activin A, which promotes the differentiation of cells toward the LGE. Arber et al. (2015) were the first, who proposed the use of activin A as an inducer of LGE phenotype in neuronal precursors from hESCs and hiPSCs in an SHH-independent manner during the derivation of MSNs. This methodology was later used by Fjodorova et al. (2019) who differentiated hPSCs, hESCs, and hiPSCs into HD MSNs. Additionally, both BDNF and ascorbic acid (AA) were supplemented in the media. The high-frequency use of BDNF at the stage of regionalization and maturation indicates that this is an important and necessary factor that allows the generation of MSNs. The obtained cells expressed striatal marker dopamine- and cAMP-regulated neuronal phosphoprotein (DARPP-32), forkhead box protein P2 (FOXP2), and calbindin 1 (CALB1). The authors skipped the stage of the manual collection of rosette-like structures compared with the protocol of Nekrasov et al. (2016), but they observed the formation of these structures (Grigor'eva et al., 2020). They also did not extend co-cultivation on feeder cells compared with Zhang et al. (2010), who cultured iPSCs on irradiation-inactivated mouse embryonic fibroblasts (MEFs). However, Grigor'eva et al. (2020) used Matrigel or poly-D-lysine/laminin-coated plates. They also demonstrated the possibility of pMSNs cryopreservation from day 20 to 180 of differentiation. After reseeded, cell survival was over 95%, and pMSNs were able to differentiate into terminal neurons. Terminally differentiated MSNs were characterized after

<sup>1</sup> cells.ebisc.org

58-day pMSNs were obtained, which took 12 days to mature (Grigor'eva et al., 2020).

To obtain juvenile-onset HD iPSCs-derived MSNs, which characterize by abnormal SOCE (Vigont et al., 2021), applied protocol based on double inhibition of the SMAD cascade using SB-431542 and LDN-193189. Next, purmorphamine treatment directed cells into LGE, and further neuronal maturation has been achieved with the application of neurotrophic factors BDNF and GDNF as well as forskolin (Nekrasov et al., 2016; Comella-Bolla et al., 2020). Neuronal maturation took approximately 20 days and differentiated neurons expressed neuronal and striatal markers. However, no visible differences in neuronal morphology and viability between control and mutant cells were detected. Additionally, the protocol described by Vigont et al. (2021) allows cryopreservation of NPCs.

One of the most rapid protocols that involve the transdifferentiation of fibroblasts into MSNs has been recently established (Victor et al., 2014). These authors transduced fibroblasts with lentiviruses to obtain the co-expression of microRNA (miR)-9/9\* and miR-124 (miR-9/9\*-124), which play a key role in differentiating NPCs into mature neurons. The induced neurons (iNs) were then transduced with lentivirus to express transcription factors that are involved in development of the striatum, such as chicken ovalbumin upstream promoter (COUP)-transcription factor (TF)-interacting protein 2 (CTIP2), distal-less homeobox 1 (DLX1), DLX2, and myelin transcription factor 1 like (MYT1L). Neuronal culture medium was supplemented with valproic acid (VPA), db-cAMP, BDNF, and retinoic acid (RA). Thirty-five days after transduction, the obtained cells were positive for markers of MSNs, including microtubule-associated protein 2 (MAP2), GABA, and DARPP-32 (Victor et al., 2014). Other reports present that MSNs can also be produced based on the transdifferentiation of somatic cells (Richner et al., 2015; Gascón et al., 2017; Victor et al., 2018).

Wu M. et al. (2018) developed a protocol, called XLSBA, that involves the differentiation of ESCs by replacing protein components with small molecules and adding the  $\gamma$ -secretase inhibitor DAPT to enhance neural differentiation. This protocol allowed the generation of MSNs that can be used as a cell-based therapy for HD patients. To obtain MSNs that expressed appropriate markers and exhibited electrophysiological properties, 21–24 days is needed. The shorter time to obtain MSNs increases the ability to control the conditions and reduce variability between successive neuron generations. Additionally, the restriction of protein elements eliminates difficulties in quality control and reduces costs. In this protocol, the authors replaced Noggin with LDN-193189 and SB-431542, thereby achieving the effect of dual SMAD inhibition. To inhibit WNT signaling, they used the tankyrase inhibitor (XAV-939). By combining four small molecules (XAV939, LDN-193189, SB-431542, and SAG, the SHH signaling agonist), they obtained precursors of LGE that express the striatal markers CTIP2 and DARPP-32. The only protein factors that were used were BDNF and glial cell line-derived neurotrophic factor (GDNF) for terminal differentiation (Wu M. et al., 2018). Similar to Grigor'eva et al. (2020), they used AA for maturation. Finally, Wu et al. achieved 90% of DARPP-32-positive GABAergic

MSNs that are suitable for cell transplantation (Wu M. et al., 2018). Additionally, hESCs were used by several groups as *in vitro* models of HD to understand the mechanisms of neurodegeneration in HD patients (Niclis et al., 2009; Bradley et al., 2011; Dumevska et al., 2016; Xie et al., 2016).

Currently, no protocols are available that can generate MSNs from iNSCs that are obtained directly *in vitro*. The only successful attempts differentiate iPSC-derived NPCs (Lin et al., 2015), HD-iPSC-derived NSCs (Zhang et al., 2010), and striatal human neural stem cell (hNSC) lines (El-Akabawy et al., 2011) into MSNs. However, Al-Gharaibeh et al. (2017) obtained iNSCs from iPSCs (iPSCs-NSCs), which expressed the NSC markers Nestin and SOX2. After intra-striatal transplantation into YAC128 mice, iPSCs-NSCs differentiated into region-specific MSNs. These cells co-expressed a neuronal nuclei (NeuN), which is a marker of mature neurons, and the region-specific marker DARPP-32. Additionally, iNSC-treated mice exhibited the amelioration of motor deficits and an increase in BDNF levels in the striatum (Al-Gharaibeh et al., 2017). Evidence indicates that induced neural stem cells (iNSCs), NSCs, and NPCs do not form teratomas after transplantation in animal models (Gao et al., 2016; Deng et al., 2018). Furthermore, NSCs/NPCs can be induced from somatic cells (Han et al., 2012; Ring et al., 2012; Capetian et al., 2016; Choi and Hong, 2017; Kim et al., 2017). **Table 2** summarizes small molecules, inhibitors, transcription factors, and growth factors that are widely used for the differentiation of iPSCs (Zhang et al., 2010; Delli Carri et al., 2013; Arber et al., 2015; Nekrasov et al., 2016; Adil et al., 2018; Comella-Bolla et al., 2020; Grigor'eva et al., 2020; Vigont et al., 2021), ESCs (Nicoleau et al., 2013; Arber et al., 2015; Wu M. et al., 2018), and NPCs (Lin et al., 2015), NSCs (El-Akabawy et al., 2011) and fibroblast transdifferentiation into MSNs (Victor et al., 2014). The table also shows the steps of MSNs development where they are used *in vitro*.

Finally, **Figure 3** shows a schematic representation of the protocols that are established to obtain MSNs *in vitro* from different cell sources.

## MODELING HD USING BRAIN ORGANOIDs

By developing 3D culture methods based on the ability of iPSCs to self-organize and gene editing, the first organoids could be created, which can mimic brain tissue architecture. The complexity and characterization of their structures allow them to be used as an efficient and suitable model for drug and toxicity testing as a substitute for animal models (Csobonyeiova et al., 2020). It is now possible to create different types of organoids, including midbrain, cerebral, and hippocampal organoids, that can be used to understand disease development and progression (Lancaster and Knoblich, 2014; Yadav et al., 2020). Advances in obtaining 3D organoids that may serve as a model for studying HD has been made in recent years. **Figure 4** shows schematic methods of culturing iPSC-derived 3D organoids and assembloids for modeling HD.

Huntington's disease is characterized by motor dysfunction and incoordination. Kawada et al. (2017) created motor nerve organoids that derived from human iPSCs. Authors first

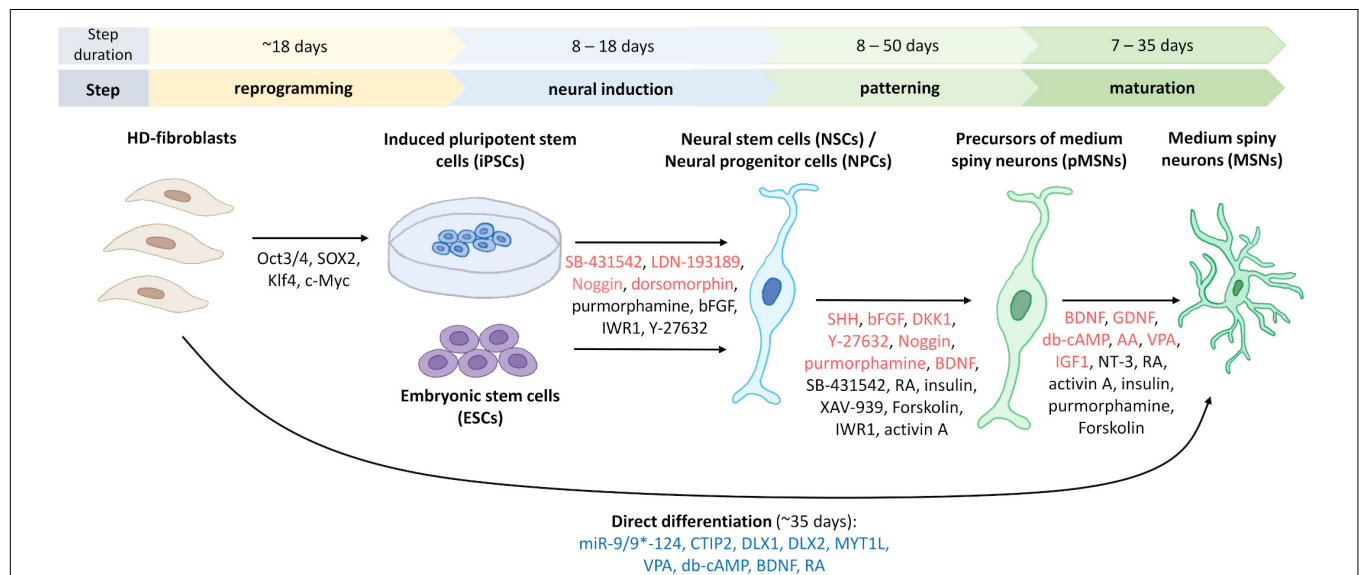
**TABLE 2 |** Small molecules, inhibitor, transcription factors, and growth factors used for iPSC, ECS, and NPC differentiation and transdifferentiation.

Substance/Factor	Function	Differentiation step	References
TGF- $\beta$ RI kinase inhibitor VI (SB-431542)	<ul style="list-style-type: none"> <li>- BMP/TGF-<math>\beta</math> signaling inhibition</li> <li>- Enhanced neuronal differentiation</li> <li>- Induction of ventral telencephalic specification</li> <li>- PSC differentiation into neuroepithelial cells</li> </ul>	Neural induction	Delli Carri et al., 2013; Nicoleau et al., 2013; Arber et al., 2015; Adil et al., 2018; Comella-Bolla et al., 2020; Grigor'eva et al., 2020; Vigont et al., 2021
		Patterning	Delli Carri et al., 2013
Noggin	<ul style="list-style-type: none"> <li>- BMP/TGF-<math>\beta</math> signaling inhibition</li> <li>- PSC differentiation into neuroepithelial cells</li> </ul>	Neural induction and patterning	Delli Carri et al., 2013; Nicoleau et al., 2013; Nekrasov et al., 2016
Purmorphamine	<ul style="list-style-type: none"> <li>- BMP signaling inhibition</li> <li>- Enhanced neuronal differentiation</li> </ul>	Neural induction	El-Akabawy et al., 2011; Adil et al., 2018
		Patterning	El-Akabawy et al., 2011; Nekrasov et al., 2016; Adil et al., 2018; Grigor'eva et al., 2020; Vigont et al., 2021
		Maturation	El-Akabawy et al., 2011
Brain-derived neurotrophic factor	<ul style="list-style-type: none"> <li>- Neuronal survival factor</li> <li>- Increase the proportion of DARPP-32-positive neurons</li> </ul>	Patterning	Zhang et al., 2010; Delli Carri et al., 2013; Lin et al., 2015; Adil et al., 2018; Grigor'eva et al., 2020
		Maturation	El-Akabawy et al., 2011; Delli Carri et al., 2013; Nicoleau et al., 2013; Victor et al., 2014; Arber et al., 2015; Lin et al., 2015; Nekrasov et al., 2016; Wu M. et al., 2018; Comella-Bolla et al., 2020; Grigor'eva et al., 2020; Vigont et al., 2021
Dihydrochloride (LDN-193189)	<ul style="list-style-type: none"> <li>- BMP/TGF-<math>\beta</math> signaling inhibition</li> <li>- Induction of ventral telencephalic specification</li> </ul>	Neural induction	Arber et al., 2015; Wu M. et al., 2018; Comella-Bolla et al., 2020; Grigor'eva et al., 2020; Vigont et al., 2021
Sonic hedgehog	<ul style="list-style-type: none"> <li>- Induction of forebrain neurogenesis</li> <li>- Promote differentiation into DARPP-32-positive neurons</li> </ul>	Patterning	Zhang et al., 2010; El-Akabawy et al., 2011; Delli Carri et al., 2013; Nicoleau et al., 2013; Lin et al., 2015
Basic fibroblast growth factor	<ul style="list-style-type: none"> <li>- Neuronal survival factor</li> </ul>	Neural induction	Al-Gharaibeh et al., 2017
		Patterning	Zhang et al., 2010; Nekrasov et al., 2016; Grigor'eva et al., 2020; Vigont et al., 2021
Glial cell line-derived neurotrophic factor	<ul style="list-style-type: none"> <li>- Neuronal survival factor</li> </ul>	Maturation	Arber et al., 2015; Lin et al., 2015; Adil et al., 2018; Wu M. et al., 2018; Vigont et al., 2021
Dorsomorphin	<ul style="list-style-type: none"> <li>- BMP signaling inhibition</li> <li>- Enhanced neuronal differentiation</li> <li>- Induction of ventral telencephalic specification</li> <li>- PSC differentiation into neuroepithelial cells</li> </ul>	Neural induction	Arber et al., 2015; Nekrasov et al., 2016; Grigor'eva et al., 2020
Forskolin	<ul style="list-style-type: none"> <li>- cAMP pathway activator</li> </ul>	Patterning and maturation	Nekrasov et al., 2016
		Maturation	Comella-Bolla et al., 2020; Vigont et al., 2021
Activin A	<ul style="list-style-type: none"> <li>- TGF-<math>\beta</math>/BMP signaling pathway activation</li> <li>- Induction of forebrain neurogenesis</li> <li>- Differentiation in the lateral ganglionic eminence</li> <li>- Promote differentiation into DARPP-32-positive neurons</li> </ul>	Patterning and maturation	Arber et al., 2015; Grigor'eva et al., 2020
Dibutyl- $\gamma$ -cAMP	<ul style="list-style-type: none"> <li>- Cell-permeable analog of cAMP</li> <li>- Enhance the output of depolarized neurons</li> <li>- Stimulate GABAergic MSNs neurogenesis</li> </ul>	Maturation	Zhang et al., 2010; El-Akabawy et al., 2011; Nicoleau et al., 2013; Victor et al., 2014; Lin et al., 2015; Adil et al., 2018; Grigor'eva et al., 2020
Ascorbic acid	<ul style="list-style-type: none"> <li>- Formation and maintenance of the neural microenvironment</li> <li>- Neuroprotective</li> </ul>	Maturation	Wu M. et al., 2018; Comella-Bolla et al., 2020; Grigor'eva et al., 2020

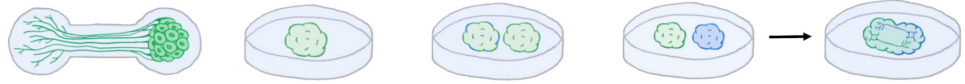
(Continued)

**TABLE 2 |** Continued

Substance/Factor	Function	Differentiation step	References
ROCK inhibitor (Y-27632)	- Stem cell survival factor	Neural induction	Compagnucci et al., 2016; Comella-Bolla et al., 2020
		Patterning	Zhang et al., 2010; Delli Carri et al., 2013; Lin et al., 2015; Compagnucci et al., 2016; Grigor'eva et al., 2020
Valproic acid; Valpromide	- Stimulation of GABAergic MSN neurogenesis	Maturation	Zhang et al., 2010; El-Akabawy et al., 2011; Nicoleau et al., 2013; Victor et al., 2014
Neurotrophin-3	- Neurotrophic factor	Maturation	Victor et al., 2014
Retinoid acid	- Induce GABAergic differentiation	Patterning and maturation	El-Akabawy et al., 2011; Victor et al., 2014
WNT inhibitor dickkopf 1	- WNT signaling inhibition	Patterning	Zhang et al., 2010; El-Akabawy et al., 2011; Delli Carri et al., 2013; Nicoleau et al., 2013; Adil et al., 2018
Insulin	- Proliferation improvement	Patterning Maturation	Delli Carri et al., 2013; Shahbazi et al., 2019 Delli Carri et al., 2013; Lin et al., 2015; Shahbazi et al., 2019
Insulin-like growth factor 1	- Synapse formation	Maturation	Lin et al., 2015; Nieto-Estévez et al., 2016; Adil et al., 2018
Tankyrase inhibitor (IWR1)	- WNT signaling inhibition	Neural induction and patterning	Comella-Bolla et al., 2020
Tankyrase inhibitor (XAV-939)	- WNT signaling inhibition	Patterning	Wu M. et al., 2018



**FIGURE 3 |** Generation of human striatal MSNs from fibroblasts and stem cells. To reprogram fibroblasts into induced pluripotent stem cells (iPSCs), four transcription factors are used to transduce cells from HD patients (Victor et al., 2018). Indicated in red are the most commonly used factors for neural induction of iPSCs or embryonic stem cells (ESCs) to obtain neural stem cells (NSCs)/neural progenitor cells (NPCs), and for differentiation of progenitors and mature GABA-ergic medium spiny neurons, pMSNs and MSNs, respectively. Marked in black are factors used for neural induction or differentiation only in one or two protocols, which are discussed in the manuscripts. For direct differentiation, microRNA-9/9\*-124, and other factors that are indicated in blue were used (Victor et al., 2014). The duration of each of the differentiation steps differs according to the various protocols. Figure summarizes fourteen protocols describing the generation of human striatal MSNs from iPSCs (Zhang et al., 2010; Delli Carri et al., 2013; Arber et al., 2015; Nekrasov et al., 2016; Adil et al., 2018; Comella-Bolla et al., 2020; Grigor'eva et al., 2020; Vigont et al., 2021), fibroblasts (Victor et al., 2014), ESCs (Nicoleau et al., 2013; Arber et al., 2015; Wu M. et al., 2018), NSCs (El-Akabawy et al., 2011), and NPCs (Lin et al., 2015). Using bFGF and neural media for culturing, it is possible to differentiate iPSCs to induced neural stem cells (iNSCs) and then transplant them into the striatal region of the mouse brain where they differentiate into MSNs (not shown) (Al-Gharaibeh et al., 2017).

References	Kawada et al., 2017	Conforti et al., 2018 (based on Lancaster and Knoblich, 2014)	Zhang et al., 2019 (based on Lancaster et al., 2013)	Miura et al., 2020	
Type of structure	Motor nerve organoid in microdevice chamber	Cortical organoid	(Chimeric) Cerebral organoids	Human striatal and cortical organoids	Cortico-striatal assembloid
					
Initial cell type	hiPSC lines	HD-iPSCs-21Q, 28Q, 60Q, 109Q	Chimeric cerebral organoid: IsoHD-30Q hEPSCs co-cultured with IsoHD-81Q-GFP <sup>+</sup> hEPSCs Cerebral organoids: IsoHD-30Q hEPSCs, 45Q, 65Q, 81Q and hiPSCs-18Q, 71Q, 191Q	hiPSCs	human cortical spheroid (hCS) + 3D human striatal spheroid (hStrS)
Formation time span	20 – 30 days	45 days	28 days	80 days	72h
Additional molecules	RA, SAG	RA	RA, GSK inhibitor (CHIR-99021)	RXRG agonist (SR-11237) for hStrS	

**FIGURE 4 |** Generation of human iPSC-derived three-dimensional brain structures modeling HD. All illustrated HD organoids, including two region-specific brain organoids that consist of the three-dimensional (3D) human striatal spheroid (hStrS) and human cortical spheroid (hCS) that were used to create the assembloid by Miura et al. (2020), originated from induced pluripotent stem cells (iPSCs). Cortical organoids (Conforti et al., 2018; Zhang et al., 2019) and the chimeric organoids (Zhang et al., 2019) represent 3D cell models of Huntington's disease. Motor nerve organoids extended axons as a result of their culture in the special chamber with microchannels (Kawada et al., 2017). The organoid formation time differs depending on the protocol. Neural differentiation inducers were used in the organoids formation process: retinoic acid (RA) (Kawada et al., 2017; Conforti et al., 2018; Zhang et al., 2019), retinoid X receptor  $\gamma$  (RXRG) agonist, SR-11237 (Miura et al., 2020), glycogen synthase kinase (GSK) inhibitor, CHIR-99021 (Zhang et al., 2019), and sonic hedgehog signaling agonist (SAG) (Kawada et al., 2017).

differentiated human-induced pluripotent stem cells (hiPSCs) into spinal motor neurons. They then placed these neurons in the vessel with low adhesion. Under these conditions, the cells began to form spheroids. The spheroids were then moved into a culture microdevice, which was a special chamber for the spheroid that turns into a microchannel that ends in the chamber to axon terminals. Finally, after 20–30 days of culture in the microdevice, the spheroid-forming neurons spontaneously extended the axons. In this way, nerve organoids were formed that consisted of a unidirectional fascicle and neural spheroid (Kawada et al., 2017). The resulting motor nerve organoids may be a good model of HD to study disturbances in  $\text{Ca}^{2+}$  homeostasis and provide insights into the projection of neural networks and synaptic plasticity.

Another attempt to model HD was made by Conforti et al. (2018) who investigated HD-iPSC-derived striatal and cortical neurons and HD-iPSC-based 3D cerebral organoids that corresponded to adult- and juvenile-onset HD. Selected HD-iPSC lines that were used to generate neurons or organoids carried 60, 109, and 180 CAG repeats, whereas the control lines carried 21, 28, and 33 CAG repeats in HTT. To obtain MSNs, both SB-431542 and LDN-193189 were used for neural induction, similar to MSNs that were obtained previously (Shi et al., 2012; Comella-Bolla et al., 2020; Grigor'eva et al., 2020), whereas striatal differentiation was performed according to the Delli Carri et al. (2013) protocol. Cortical projection neurons were differentiated using the three-stage protocol (Shi et al., 2012). To obtain 3D cortical organoids, a methodology describing cerebral organoids generation was applied (Lancaster and Knoblich, 2014). According to the hanging drop method, on day 3, Conforti et al. (2018) obtained

HD-iPSC-derived spheroids. After being placed on the horizontal shaker, spheroids formed embryonic bodies (EBs). The EBs were then neuroectodermally differentiated using neural induction medium. The resulting cell aggregates were placed in drops of Matrigel with the medium for neural differentiation. In the next stage, neuroepithelial bud expansion and promotion occurred for further development into the cortical part of the brain (Conforti et al., 2018). Conforti et al. (2018) established that mHTT affects human neurodevelopment through the negative regulation of striatal and cortical specification in both juvenile- and adult-onset HD iPSC-derived cerebral organoids where a decrease in neuronal differentiation and cell disorganization were detected. They found that mHTT that carried longer CAG expansions led to the total failure of neuroectodermal acquisition, whereas cells that contained shorter CAG repeats were characterized by several abnormalities in neural rosette formation and improper cortical organoid cytoarchitecture. Moreover, HD lines exhibited a slower exit from pluripotency in a CAG-dependent manner and defects in cortical and striatal progenitors, neuronal specification, and terminal neuronal maturation. Analyses of gene expression in HD organoids confirmed that they overlapped with the immature ventricular zone/SVZ, whereas control organoids corresponded to mature human fetal cortical areas. Huntington's disease organoids also exhibited a reduction of the expression of genes that are related to the regulation of neuronal migration and differentiation. Additionally, the downregulation of mHTT and inhibition of its effector metalloprotease ADAM10 rescued defects in neuronal induction and striatal differentiation in HD lines. These data confirmed the role of mHTT in abnormal neurodevelopment in HD (Conforti et al., 2018).

Additionally, Zhang et al. (2019) investigated the correlation between prolonged CAG repetitions (polyQ tail) of huntingtin and control, juvenile- and adult-onset HD and the influence on early neurodevelopment in HD hESC-derived cerebral organoids. The authors used isogenic HD ESCs with 30, 45, 65, and 81 CAG repeats (IsoHD hESCs 30Q, 45Q, 65Q, and 81Q, respectively) and HD hiPSCs with 18Q, 71Q, and 191Q to create organoids. They also generated chimeric cerebral organoids from co-cultures of IsoHD hESCs 81Q labeled with a green fluorescent protein and IsoHD hESCs 30Q. The protocol that was used by Zhang et al. (2019) was based on Lancaster et al. (2013) protocol for the induction of cerebral organoid formation. hESCs were first used to create EBs, after which deposition in Matrigel formed a neuroectoderm with a neuroepithelium (Zhang et al., 2019). To obtain shaping toward the forebrain, a glycogen synthase kinase (GSK) inhibitor, CHIR-99021 was added to the medium. On day 28 of culture, the obtained organoids resembled the human brain, corresponding to 2–3 months of human brain development *in vivo*. Expression of the cortical and forebrain markers CTIP2 and forkhead box G1 (FOXP1), respectively, was detected in these organoids. Additionally, the presence of radial (neuroepithelial) structures that expressed paired box protein 6 (PAX6) was detected (Zhang et al., 2019). In contrast to Conforti et al. (2018), Zhang et al. (2019) found premature neurogenesis and neuronal differentiation in IsoHD-81Q cerebral organoids corresponding to juvenile-onset HD. Zhang et al. (2019) showed that ventricular zone-like neuroepithelial progenitor layer expansion was blunted by an increase in the number of CAG repeats in mHTT because of premature neurogenesis in these organoids. Furthermore, impairments in cell cycle regulatory processes and an increase in activity of an upstream regulator of the cell cycle (i.e., the ataxia telangiectasia mutated [ATM]-p53 pathway) were identified, which might be responsible for premature neuronal differentiation. Upon the application of ATM antagonists, the partial rescue of blunted neuroepithelial progenitor expansion was detected in HD organoids (Zhang et al., 2019). The authors proposed that the length of HTT polyQ tails controls the ratio between NPC proliferation and differentiation in the early stages of nervous system development (Zhang et al., 2019).

Finally, Miura et al. (2020) were the first to develop a protocol to generate human 3D brain organoids that resemble the LGE, corresponding to the striatum during development. To obtain these organoids, hiPSCs were used. Neuronal differentiation was induced using SMAD and WNT modulators and the application of activin A, which promotes differentiated cells in the striatal direction. To obtain LGE patterning, transcriptomic research was performed. Miura et al. found that the gene that encodes retinoid X receptor  $\gamma$  (RXRG) was highly expressed in the early developing striatum. By adding the RXRG agonist SR-11237, they increased the proportion of CTIP2-positive cells, which are a marker of early striatal cells. Moreover, they found that neurons that were obtained from human striatal spheroids (hStrSs) had electrophysiological characteristics of striatal MSNs (Miura et al., 2020). The authors assembled hStrSs with human cortical spheroids (hCSs) shaped like the cerebral cortex to form cortico-striatal assembloids. They found that the resulting structure sent axonal projection neurons into

hStrSs and functionally connected with MSNs. Lastly, cortico-striatal assembloids were used to examine defects in cortico-striatal circuits in patients with 22q13.3 deletion syndrome (22q13.3DS) (Miura et al., 2020). They may also serve as a model to investigate cortico-striatal circuits or transneuronal cortico-striatal spreading of mHTT in HD (Pecho-Vrieseling et al., 2014; Miura et al., 2020).

The further development of 3D organoids that model HD is needed. These models will likely provide novel insights into the regulation of synaptic plasticity and maturation of striatal and motor neurons (Chang et al., 2020). Different signal pathways, including  $\text{Ca}^{2+}$  signaling, can also be studied using these models. Although 3D organoid technology still has many obstacles to overcome, it will certainly contribute to our understanding of complex processes of neurodevelopment, disease progression, and pathogenesis. Patient-derived organoids may also be useful for generating personalized models of disease and thus personalized HD treatment strategies.

## APPLICATION OF STEM CELL IN HD THERAPY

Although a few compounds have been shown to stabilize elevations of SOCE in HD models, future studies are necessary to evaluate their potential for HD therapy (Czeredys, 2020). No treatments for HD are currently available, but this disease may be a good candidate for cell replacement therapy because it is characterized by the relatively focal loss of MSNs that is caused by a mutation of HTT (Rosser and Bachoud-Lévi, 2012). It was suggested that mHTT disrupts  $\text{Ca}^{2+}$  signaling in MSNs and those changes could be a cause of HD progression (Raymond, 2017; Pchitskaya et al., 2018; Czeredys, 2020). Therefore transplantation of MSN progenitors without a mutation of HTT appears to be beneficial for HD patients. To achieve regeneration in HD, donor cells should have the ability to be precisely differentiated into MSNs, and these cells should be functionally active (Precious and Rosser, 2012). The application of donor cells that are derived from the whole ganglionic eminence (WGE) in the ventral telencephalon in the fetal brain is a very promising approach (Döbrössy and Dunnett, 2003; Mazzocchi-Jones et al., 2009; Pauly et al., 2012). This brain region is the origin of cells that are committed to striatal MSN phenotypes (Deacon et al., 1994; Olsson et al., 1998; Straccia et al., 2016). Several groups reported that the transplantation of developing MSNs into the degenerating striatum in different animal models of HD led to functional recovery and ameliorated motor and cognitive deficits (Björklund et al., 1994; Kendall et al., 1998; Palfi et al., 1998; Brasted et al., 1999; McLeod et al., 2013; Schackel et al., 2013; Paganini et al., 2014). Similar recovery in rats grafted with human whole ganglionic eminence (hWGE) compared to rat WGE was shown, with the additional benefit of the hWGE stabilizing performance on the adjusting steps test (Lelos et al., 2016).

Evidence from initial clinical trials showed that human fetal-derived grafts that were transplanted into the striatum of three out of five HD patients survived and significantly improved motor and cognitive function over an approximately 6-year period (Bachoud-Lévi et al., 2000, 2006). Additionally, enhanced

fluorodeoxyglucose positron emission tomography showed that implanted cells were able to integrate into striatal neural circuits and created functional connections with cortical regions (Gaura et al., 2004). Other pilot studies performed by different groups reported some beneficial effects for HD patients who received fetal neurografts into the striatum (Hauser et al., 2002; Rosser et al., 2002; Gallina et al., 2008; Reuter et al., 2008; Barker et al., 2013). In longer-term follow-up data from these initial trials, where a total of 51 patients have been transplanted using human fetal cells, signs of long-term efficacy have been reported in 4 out of 30 patients for which clinical data and follow-up are available (Bachoud-Lévi, 2017). Interestingly, it was shown in post mortem analysis of HD patients that grafts might survive at least 10 years after transplantation (Bachoud-Lévi, 2009; Cicchetti et al., 2009). Preliminary stem cell transplants provided the basis for the largest fetal cell transplant trial Multicentric Intracerebral Grafting in Huntington's Disease (MIG-HD), which involved 45 HD patients. It was initiated to investigate the efficacy of transplantation as well as its applicability in a multicenter approach. However, the lack of clinical benefit was found in these trial, what might be related to graft rejection. Total motor score at month 32 did not differ between grafted and control groups. In 40% of the transplanted patients, antihuman leucocytes antigen antibodies were found (Krystkowiak et al., 2007; Bachoud-Lévi and on behalf the Multicentric Intracerebral Grafting in Huntington's Disease Group., 2020). In the German branch of MID-HD, where additional 22 patients were transplanted no clinical benefit was detected (Capetian et al., 2009; Krebs et al., 2011; Lopez et al., 2014). MID-HD studies failed to identify the methodology to reliably reproduce pilot results, although procedural improvements have significantly increased the safety of surgery (Bachoud-Lévi et al., 2020).

Limitations of human fetal tissue and other aspects that make their use difficult (Precious et al., 2017; Bachoud-Lévi et al., 2020) have prompted the need to search for alternative donor cell sources that can be cultured, expanded, and reprogrammed into MSNs before their therapeutic use (Csobonyeiova et al., 2020). ECs and adult iPSCs appear to be a good cell source for replacement therapy since they can be directed to MSN-like cell fates. However, it is difficult to obtain a genuine MSN fate, and further advances are needed to achieve suitable cells for replacement therapy for HD (Li and Rosser, 2017; Golas, 2018; Bachoud-Lévi et al., 2020). Interestingly, hWGE iPSC-derived MSNs that shared fundamental characteristics with hWGE-derived MSNs expect their methylation profiles, differentiated both *in vitro* and following transplantation into an HD model, therefore they might be useful as an alternative cell source for cell replacement therapy (Choompoo et al., 2020). Using iPSCs directly in cell therapy is still challenged because human clinical trials that used iPSCs found unexpected mutations that were caused by the reprogramming technique. Therefore, further research is needed to overcome this critical issue and make cell therapy more feasible (Yoshihara et al., 2017). Recently, hiPSC-derived NPCs that were transplanted into the neonatal mouse striatum differentiated into MSNs and successfully integrated into the host's brain circuitry without teratoma formation (Comella-Bolla et al., 2020). Moreover, *in vitro* differentiated human striatal progenitors, which were transplanted into the

striatum from a rat model of HD matured and integrated into host circuits (Besusso et al., 2020). Additionally, other cell types, such as mesenchymal stem cells, are being administrated intravenously to HD patients (Salado-Manzano et al., 2020).

## CONCLUDING REMARKS

$\text{Ca}^{2+}$  signaling via store-operated  $\text{Ca}^{2+}$  channels may control both physiological and pathological processes in neuronal cells. Here, we discussed the key role of SOCE in the regulation of NSC proliferation, differentiation, and neurogenesis. Several SOCE components play a crucial role in these processes, including STIM proteins and Orai and TRPC channels. Elevations of  $\text{Ca}^{2+}$  influx via SOC channels, mediated by an increase in STIM2 expression, was observed in HD transgenic mice and caused the dysregulation of dendritic spines in HD MSNs. Interestingly, the elevation of SOCE was also detected in iPSC-based MSNs that were obtained from both juvenile- and adult-onset HD patient fibroblasts. In juvenile-onset HD iPSC-based MSNs elevated expression of STIM2 underlies the excessive  $\text{Ca}^{2+}$  entry through SOC channels in HD pathology. Both neurodevelopmental alterations and  $\text{Ca}^{2+}$  signaling dysregulation were detected in iPSC-derived MSNs from juvenile HD patients. Furthermore, mHTT was shown to alter human neurodevelopment in adult-onset HD. mHTT was also recently suggested to compromise neurodevelopmental pathways, which can disturb synaptic homeostasis and boost the susceptibility of neurons to the pathological consequences of expanded polyglutamine repeats during HD progression (HD iPSC Consortium., 2017). The involvement of abnormal nSOCE in MSNs from juvenile- and adult-onset HD patients could be concerned with pathological changes that are observed in these patients. The various defects in neurodevelopment that were observed in juvenile- and adult-onset HD *in vitro* models may depend on the length of CAG repeats in mHTT. Whereas the severity of SOCE alterations did not depend on the length of CAG repetitions in different HD onsets. Only in MSNs derived from juvenile-onset HD fibroblasts upregulation of  $\text{Ca}^{2+}$  sensor STIM2 was shown to contribute to SOCE dysregulation. Considering impairments in  $\text{Ca}^{2+}$  homeostasis and the dysregulation of other signaling pathways by mHTT, neuronal progenitor cells or differentiated neurons without a mutation of HTT could be grafted to replace degenerated MSNs in HD patients. These therapies could serve as a promising treatment strategy to delay the progression of HD, but further research is needed (Glaser et al., 2019). Therefore, recent progress in the *in vitro* differentiation of MSNs that are derived from different cell sources is essential for HD patients. Additionally, establishing both iPSC-derived HD MSN cultures and HD brain organoids *in vitro* will help us understand the complexity of HD pathology and possible treatment strategies.

## AUTHOR CONTRIBUTIONS

MC conceived, designed, and wrote the manuscript. EL wrote the manuscript and drew the figures. Both authors contributed to the article and approved the submitted version.

## FUNDING

This study was supported by the National Science Centre in Poland (grant no. 2019/33/B/NZ3/02889 to MC).

## REFERENCES

- Adil, M. M., Gaj, T., Rao, A. T., Kulkarni, R. U., Fuentes, C. M., Ramadoss, G. N., et al. (2018). hPSC-Derived Striatal Cells Generated Using a Scalable 3D Hydrogel Promote Recovery in a Huntington Disease Mouse Model. *Stem Cell Reports* 10, 1481–1491. doi: 10.1016/j.stemcr.2018.03.007
- Al-Gharibeh, A., Culver, R., Stewart, A. N., Srinageshwar, B., Spelde, K., Frollo, L., et al. (2017). Induced Pluripotent Stem Cell-Derived Neural Stem Cell Transplantations Reduced Behavioral Deficits and Ameliorated Neuropathological Changes in YAC128 Mouse Model of Huntington's Disease. *Front Neurosci* 11:628. doi: 10.3389/fnins.2017.00628
- An, M. C., Zhang, N., Scott, G., Montoro, D., Wittkop, T., Mooney, S., et al. (2012). Genetic correction of Huntington's disease phenotypes in induced pluripotent stem cells. *Cell Stem Cell* 11, 253–263. doi: 10.1016/j.stem.2012.04.026
- Arber, C., Precious, S. V., Cambray, S., Risner-Janiczek, J. R., Kelly, C., Noakes, Z., et al. (2015). Activin A directs striatal projection neuron differentiation of human pluripotent stem cells. *Development* 142, 1375–1386. doi: 10.1242/dev.117093
- Baba, A., Yasui, T., Fujisawa, S., Yamada, R. X., Yamada, M. K., Nishiyama, N., et al. (2003). Activity-evoked capacitative Ca<sup>2+</sup> entry: implications in synaptic plasticity. *J Neurosci* 23, 7737–7741. doi: 10.1523/jneurosci.23-21-07737.2003
- Bachoud-Lévi, A. C. (2009). Neural grafts in Huntington's disease: viability after 10 years. *Lancet Neurol* 8, 979–981. doi: 10.1016/S1474-4422(09)70278-9
- Bachoud-Lévi, A. C. (2017). From open to large-scale randomized cell transplantation trials in Huntington's disease: Lessons from the multicentric intracerebral grafting in Huntington's disease trial (MIG-HD) and previous pilot studies. *Prog Brain Res* 230, 227–261. doi: 10.1016/bs.pbr.2016.12.011
- Bachoud-Lévi, A. C., and on behalf the Multicentric Intracerebral Grafting in Huntington's Disease Group (2020). Human Fetal Cell Therapy in Huntington's Disease: A Randomized, Multicenter, Phase II Trial. *Mov Disord* 35, 1323–1335. doi: 10.1002/mds.28201
- Bachoud-Lévi, A. C., Gaura, V., Brugières, P., Lefaucheur, J. P., Boissé, M. F., Maison, P., et al. (2006). Effect of fetal neural transplants in patients with Huntington's disease 6 years after surgery: a long-term follow-up study. *Lancet Neurol* 5, 303–309. doi: 10.1016/S1474-4422(06)70381-7
- Bachoud-Lévi, A. C., Massart, R., and Rosser, A. (2020). Cell therapy in Huntington's disease: Taking stock of past studies to move the field forward. *Stem Cells* 39, 144–155. doi: 10.1002/stem.3300
- Bachoud-Lévi, A. C., Rémy, P., Nguyen, J. P., Brugières, P., Lefaucheur, J. P., Bourdet, C., et al. (2000). Motor and cognitive improvements in patients with Huntington's disease after neural transplantation. *Lancet* 356, 1975–1979. doi: 10.1016/S0140-6736(00)03310-9
- Barker, R. A., Mason, S. L., Harrower, T. P., Swain, R. A., Ho, A. K., Sahakian, B. J., et al. (2013). The long-term safety and efficacy of bilateral transplantation of human fetal striatal tissue in patients with mild to moderate Huntington's disease. *J Neurol Neurosurg Psychiatry* 84, 657–665. doi: 10.1136/jnnp-2012-302441
- Barnat, M., Capizzi, M., Aparicio, E., Boluda, S., Wennagel, D., Kacher, R., et al. (2020). Huntington's disease alters human neurodevelopment. *Science* 369, 787–793. doi: 10.1126/science.aax3338
- Besusso, D., Schellino, R., Boido, M., Belloli, S., Parolisi, R., Conforti, P., et al. (2020). Stem Cell-Derived Human Striatal Progenitors Innervate Striatal Targets and Alleviate Sensorimotor Deficit in a Rat Model of Huntington Disease. *Stem Cell Reports* 14, 876–891. doi: 10.1016/j.stemcr.2020.03.018
- Bezprozvanny, I., and Kiselev, S. L. (2017). Neurons from skin mimic brain holes. *Oncotarget* 8, 8997–8998. doi: 10.18632/oncotarget.13709
- Björklund, A., Campbell, K., Sirinathsinghji, D. J., Fricker, R. A., and Dunnett, S. B. (1994). "Functional capacity of striatal transplants of rat Huntington model," in *Functional neural transplantation*, eds S. B. Dunnett and A. Björklund (New York: Ravel Press), 157–195.
- Bradley, C. K., Scott, H. A., Chami, O., Peura, T. T., Dumevska, B., Schmidt, U., et al. (2011). Derivation of Huntington's disease-affected human embryonic stem cell lines. *Stem Cells Dev* 20, 495–502. doi: 10.1089/scd.2010.0120
- Brasted, P. J., Watts, C., Torres, E. M., Robbins, T. W., and Dunnett, S. B. (1999). Behavioural recovery following striatal transplantation: effects of postoperative training and P-zone volume. *Exp Brain Res* 128, 535–538. doi: 10.1007/s002210050877
- Capetian, P., Azmitia, L., Pauly, M. G., Krajka, V., Stengel, F., Bernhardt, E. M., et al. (2016). Plasmid-Based Generation of Induced Neural Stem Cells from Adult Human Fibroblasts. *Front Cell Neurosci* 10:245. doi: 10.3389/fncel.2016.00245
- Capetian, P., Knoth, R., Maciaczyk, J., Pantazis, G., Ditter, M., Bokla, L., et al. (2009). Histological findings on fetal striatal grafts in a Huntington's disease patient early after transplantation. *Neuroscience* 160, 661–675. doi: 10.1016/j.neuroscience.2009.02.035
- Chang, Y., Kim, J., Park, H., and Choi, H. (2020). Modelling neurodegenerative diseases with 3D brain organoids. *Biol Rev Camb Philos Soc* 95, 1497–1509. doi: 10.1111/brv.12626
- Choi, K. A., and Hong, S. (2017). Induced neural stem cells as a means of treatment in Huntington's disease. *Expert Opin Biol Ther* 17, 1333–1343. doi: 10.1080/14712598.2017.1365133
- Choompoo, N., Bartley, O. J. M., Precious, S. V., Vinh, N. N., Schnell, C., Garcia, A., et al. (2020). Induced pluripotent stem cells derived from the developing striatum as a potential donor source for cell replacement therapy for Huntington disease. *Cytotherapy* 23, 111–118. doi: 10.1016/j.jcyt.2020.06.001
- Cicchetti, F., Saporta, S., Hauser, R. A., Parent, M., Saint-Pierre, M., Sanberg, P. R., et al. (2009). Neural transplants in patients with Huntington's disease undergo disease-like neuronal degeneration. *Proc Natl Acad Sci U S A* 106, 12483–12488. doi: 10.1073/pnas.0904239106
- Comella-Bolla, A., Orlandi, J. G., Miguez, A., Straccia, M., García-Bravo, M., Bombau, G., et al. (2020). Human Pluripotent Stem Cell-Derived Neurons Are Functionally Mature In Vitro and Integrate into the Mouse Striatum Following Transplantation. *Mol Neurobiol* 57, 2766–2798. doi: 10.1007/s12035-020-01907-4
- Compagnucci, C., Barresi, S., Petrini, S., Billuart, P., Piccini, G., Chierazzi, P., et al. (2016). Rho kinase inhibition is essential during *in vitro* neurogenesis and promotes phenotypic rescue of human induced pluripotent stem cell-derived neurons with Oligophrenin-1 loss of function. *Stem Cells Transl. Med.* 5, 860–869. doi: 10.5966/sctm.2015-0303
- Conforti, P., Besusso, D., Bocchi, V. D., Faedo, A., Cesana, E., Rossetti, G., et al. (2018). Faulty neuronal determination and cell polarization are reverted by modulating HD early phenotypes. *Proc Natl Acad Sci U S A* 115, E762–E771. doi: 10.1073/pnas.1715865115
- Csobonyeiova, M., Polak, S., and Danisovic, L. (2020). Recent Overview of the Use of iPSCs Huntington's Disease Modeling and Therapy. *Int J Mol Sci* 21, 2339. doi: 10.3390/ijms21062239
- Czeredys, M. (2020). Dysregulation of Neuronal Calcium Signaling via Store-Operated Channels in Huntington's Disease. *Front Cell Dev Biol* 8:611735. doi: 10.3389/fcell.2020.611735
- Czeredys, M., Gruszczynska-Biegala, J., Schacht, T., Methner, A., and Kuznicki, J. (2013). Expression of genes encoding the calcium signalosome in cellular and transgenic models of Huntington's disease. *Front Mol Neurosci* 6:42. doi: 10.3389/fnmol.2013.00042
- Czeredys, M., Maciag, F., Methner, A., and Kuznicki, J. (2017). Tetrahydrocarbazoles decrease elevated SOCE in medium spiny neurons from transgenic YAC128 mice, a model of Huntington's disease. *Biochem Biophys Res Commun* 483, 1194–1205. doi: 10.1016/j.bbrc.2016.08.106
- Czeredys, M., Vigont, V. A., Boeva, V. A., Mikoshiba, K., Kaznacheyeva, E. V., and Kuznicki, J. (2018). Huntingtin-Associated Protein 1A Regulates Store-Operated Calcium Entry in Medium Spiny Neurons From Transgenic YAC128 Mice, a Model of Huntington's Disease. *Front Cell Neurosci* 12:381. doi: 10.3389/fncel.2018.00381

## ACKNOWLEDGMENTS

The authors thank Dr. Tomasz Wegierski for critically reading the manuscript.

- Deacon, T. W., Pakzaban, P., and Isacson, O. (1994). The lateral ganglionic eminence is the origin of cells committed to striatal phenotypes: neural transplantation and developmental evidence. *Brain Res* 668, 211–219. doi: 10.1016/0006-8993(94)90526-6
- Deb, B. K., Chakraborty, P., Gopurappilly, R., and Hasan, G. (2020). SEPT7 regulates Ca<sup>2+</sup> entry through Orai channels in human neural progenitor cells and neurons. *Cell Calcium* 90, 102252. doi: 10.1016/j.ceca.2020.102252
- Delli Carri, A., Onorati, M., Castiglioni, V., Faedo, A., Camnasio, S., Toselli, M., et al. (2013). Human pluripotent stem cell differentiation into authentic striatal projection neurons. *Stem Cell Rev Rep* 9, 461–474. doi: 10.1007/s12015-013-9441-8
- Deng, J., Zhang, Y., Xie, Y., Zhang, L., and Tang, P. (2018). Cell Transplantation for Spinal Cord Injury: Tumorigenicity of Induced Pluripotent Stem Cell-Derived Neural Stem/Progenitor Cells. *Stem Cells Int* 2018, 5653787. doi: 10.1155/2018/5653787
- Dittmer, P. J., Wild, A. R., Dell'Acqua, M. L., and Sather, W. A. (2017). STIM1 Ca<sup>2+</sup> sensor control of L-type Ca<sup>2+</sup> channel-dependent dendritic spine structural plasticity and nuclear signaling. *Cell Rep* 19, 321–334. doi: 10.1016/j.celrep.2017.03.056
- Döbrössy, M. D., and Dunnett, S. B. (2003). Motor training effects on recovery of function after striatal lesions and striatal grafts. *Exp Neurol* 184, 274–284. doi: 10.1016/s0014-4886(03)00028-1
- Domenichini, F., Terrié, E., Arnault, P., Harnois, T., Magaud, C., Bois, P., et al. (2018). Store-Operated Calcium Entries Control Neural Stem Cell Self-Renewal in the Adult Brain Subventricular Zone. *Stem Cells* 36, 761–774. doi: 10.1002/stem.2786
- Dumevska, B., Peura, T., McKernan, R., Goel, D., and Schmidt, U. (2016). Derivation of Huntington disease affected Genea020 human embryonic stem cell line. *Stem Cell Res* 16, 430–433. doi: 10.1016/j.scr.2016.02.009
- El-Akabawy, G., Medina, L. M., Jeffries, A., Price, J., and Modo, M. (2011). Purmorphamine increases DARPP-32 differentiation in human striatal neural stem cells through the Hedgehog pathway. *Stem Cells Dev* 20, 1873–1887. doi: 10.1089/scd.2010.0282
- Elkabatz, Y., Panagiotakos, G., Al Shamy, G., Socci, N. D., Tabar, V., and Studer, L. (2008). Human ES cell-derived neural rosettes reveal a functionally distinct early neural stem cell stage. *Genes Dev* 22, 152–165. doi: 10.1101/gad.1616208
- Emptage, N. J., Reid, C. A., and Fine, A. (2001). Calcium stores in hippocampal synaptic boutons mediate short-term plasticity, store-operated Ca<sup>2+</sup> entry, and spontaneous transmitter release. *Neuron* 29, 197–208. doi: 10.1016/s0896-6273(01)00190-8
- Feske, S., Gwack, Y., Prakriya, M., Srikanth, S., Puppel, S. H., Tanasa, B., et al. (2006). A mutation in Orai1 causes immune deficiency by abrogating CRAC channel function. *Nature* 441, 179–185. doi: 10.1038/nature04702
- Feske, S., Prakriya, M., Rao, A., and Lewis, R. S. (2005). A severe defect in CRAC Ca<sup>2+</sup> channel activation and altered K<sup>+</sup> channel gating in T cells from immunodeficient patients. *J Exp Med* 202, 651–662. doi: 10.1084/jem.20050687
- Fiorio Pla, A., Maric, D., Brazer, S. C., Giacobini, P., Liu, X., Chang, Y. H., et al. (2005). Canonical transient receptor potential 1 plays a role in basic fibroblast growth factor (bFGF)/FGF receptor-1-induced Ca<sup>2+</sup> entry and embryonic rat neural stem cell proliferation. *J Neurosci* 25, 2687–2701. doi: 10.1523/JNEUROSCI.0951-04.2005
- Fjodorova, M., Louessard, M., Li, Z., De La Fuente, D. C., Dyke, E., Brooks, S. P., et al. (2019). CTIP2-Regulated Reduction in PKA-Dependent DARPP32 Phosphorylation in Human Medium Spiny Neurons: Implications for Huntington Disease. *Stem Cell Reports* 13, 448–457. doi: 10.1016/j.stemcr.2019.07.015
- Gallina, P., Paganini, M., Lombardini, L., Saccardi, R., Marini, M., De Cristofaro, M. T., et al. (2008). Development of human striatal anlagen after transplantation in a patient with Huntington's disease. *Exp Neurol* 213, 241–244. doi: 10.1016/j.expneurol.2008.06.003
- Galvan, V., and Jin, K. (2007). Neurogenesis in the aging brain. *Clin Interv Aging* 2, 605–610. doi: 10.2147/cia.s1614
- Gao, M., Yao, H., Dong, Q., Zhang, H., Yang, Z., Yang, Y., et al. (2016). Tumorigenicity and Immunogenicity of Induced Neural Stem Cell Grafts Versus Induced Pluripotent Stem Cell Grafts in Syngeneic Mouse Brain. *Sci Rep* 6, 29955. doi: 10.1038/srep29955
- Gascón, S., Masserdotti, G., Russo, G. L., and Götz, M. (2017). Direct Neuronal Reprogramming: Achievements, Hurdles, and New Roads to Success. *Cell Stem Cell* 21, 18–34. doi: 10.1016/j.stem.2017.06.011
- Gaura, V., Bachoud-Lévi, A. C., Ribeiro, M. J., Nguyen, J. P., Frouin, V., Baudic, S., et al. (2004). Striatal neural grafting improves cortical metabolism in Huntington's disease patients. *Brain* 127, 65–72. doi: 10.1093/brain/awh003
- Gemes, G., Bangaru, M. L., Wu, H. E., Tang, Q., Weihrauch, D., Koopmeiners, A. S., et al. (2011). Store-operated Ca<sup>2+</sup> entry in sensory neurons: functional role and the effect of painful nerve injury. *J Neurosci* 31, 3536–3549. doi: 10.1523/JNEUROSCI.5053-10.2011
- Glaser, T., Arnaud Sampaio, V. F., Lameu, C., and Ulrich, H. (2019). Calcium signalling: A common target in neurological disorders and neurogenesis. *Semin Cell Dev Biol* 95, 25–33. doi: 10.1016/j.semcdb.2018.12.002
- Golas, M. M. (2018). Human cellular models of medium spiny neuron development and Huntington disease. *Life Sci* 209, 179–196. doi: 10.1016/j.lfs.2018.07.030
- Golovina, V. A., Platoshyn, O., Bailey, C. L., Wang, J., Limsuwan, A., Sweeney, M., et al. (2001). Upregulated TRP and enhanced capacitative Ca(2+) entry in human pulmonary artery myocytes during proliferation. *Am J Physiol Heart Circ Physiol* 280, H746–H755. doi: 10.1152/ajpheart.2001.280.2.H746
- Gopurappilly, R., Deb, B. K., Chakraborty, P., and Hasan, G. (2018). Stable STIM1 Knockdown in Self-Renewing Human Neural Precursors Promotes Premature Neural Differentiation. *Front Mol Neurosci* 11:178. doi: 10.3389/fnmol.2018.00178
- Gopurappilly, R., Deb, B. K., Chakraborty, P., and Hasan, G. (2019). Measurement of Store-Operated Calcium Entry in Human Neural Cells: From Precursors to Differentiated Neurons. *Methods Mol Biol* 2029, 257–271. doi: 10.1007/978-1-4939-9631-5\_20
- Grigor'eva, E. V., Malankhanova, T. B., Surumbayeva, A., Pavlova, S. V., Minina, J. M., Kizilova, E. A., et al. (2020). Generation of GABAergic striatal neurons by a novel iPSC differentiation protocol enabling scalability and cryopreservation of progenitor cells. *Cytotechnology* 72, 649–663. doi: 10.1007/s10616-020-00406-7
- Gruszczynska-Biegala, J., Pomorski, P., Wisniewska, M. B., and Kuznicki, J. (2011). Differential roles for STIM1 and STIM2 in store-operated calcium entry in rat neurons. *PLoS One* 6:e19285. doi: 10.1371/journal.pone.0019285
- Gruszczynska-Biegala, J., Strucinska, J., Maciag, F., Majewski, L., Sladowska, M., and Kuznicki, J. (2020). STIM Protein-NMDA2 Receptor Interaction Decreases NMDA-Dependent Calcium Levels in Cortical Neurons. *Cells* 9, 160. doi: 10.3390/cells9010160
- Han, D. W., Tapia, N., Hermann, A., Hemmer, K., Höing, S., Araúzo-Bravo, M. J., et al. (2012). Direct reprogramming of fibroblasts into neural stem cells by defined factors. *Cell Stem Cell* 10, 465–472. doi: 10.1016/j.stem.2012.02.021
- Hao, B., Lu, Y., Wang, Q., Guo, W., Cheung, K. H., and Yue, J. (2014). Role of STIM1 in survival and neural differentiation of mouse embryonic stem cells independent of Orai1-mediated Ca<sup>2+</sup> entry. *Stem Cell Res* 12, 452–466. doi: 10.1016/j.scr.2013.12.005
- Hao, H. B., Webb, S. E., Yue, J., Moreau, M., Leclerc, C., and Miller, A. L. (2018). TRPC3 is required for the survival, pluripotency and neural differentiation of mouse embryonic stem cells (mESCs). *Sci China Life Sci* 61, 253–265. doi: 10.1007/s11427-017-9222-9
- Hartmann, J., Karl, R. M., Alexander, R. P., Adelsberger, H., Brill, M. S., Rühlmann, C., et al. (2014). STIM1 controls neuronal Ca<sup>2+</sup> signaling, mGluR1-dependent synaptic transmission, and cerebellar motor behavior. *Neuron* 82, 635–644. doi: 10.1016/j.neuron.2014.03.027
- Hauser, R. A., Furtado, S., Cimino, C. R., Delgado, H., Eichler, S., Schwartz, S., et al. (2002). Bilateral human fetal striatal transplantation in Huntington's disease. *Neurology* 58, 687–695. doi: 10.1212/wnl.58.5.687
- HD iPSC Consortium. (2012). Induced pluripotent stem cells from patients with Huntington's disease show CAG-repeat-expansion-associated phenotypes. *Cell Stem Cell* 11, 264–278. doi: 10.1016/j.stem.2012.04.027
- HD iPSC Consortium. (2017). Developmental alterations in Huntington's disease neural cells and pharmacological rescue in cells and mice. *Nat Neurosci* 20, 648–660. doi: 10.1038/nn.4532
- Hima Bindu, A., and Srilatha, A. (2011). Potency of Various Types of Stem Cells and their Transplantation. *Journal of Stem Cell Research & Therapy* 1, doi: 10.4172/2157-7633.100011\*\*Q,

- Hoth, M., and Penner, R. (1993). Calcium release-activated calcium current in rat mast cells. *J Physiol* 465, 359–386. doi: 10.1113/jphysiol.1993.sp019681
- Huang, J. J., Wang, Y. J., Zhang, M., Zhang, P., Liang, H., Bai, H. J., et al. (2017). Functional expression of the Ca<sup>2+</sup> signaling machinery in human embryonic stem cells. *Acta Pharmacol Sin* 38, 1663–1672. doi: 10.1038/aps.2017.29
- Im, W., Lee, S. T., Chu, K., Kim, M., and Roh, J. K. (2009). Stem Cells Transplantation and Huntington's Disease. *Int J Stem Cells* 2, 102–108. doi: 10.15283/ijsc.2009.2.2.102
- Jeon, I., Lee, N., Li, J. Y., Park, I. H., Park, K. S., Moon, J., et al. (2012). Neuronal properties, in vivo effects, and pathology of a Huntington's disease patient-derived induced pluripotent stem cells. *Stem Cells* 30, 2054–2062. doi: 10.1002/stem.1135
- Kawada, J., Kaneda, S., Kirihara, T., Maroof, A., Levi, T., Eggan, K., et al. (2017). Generation of a Motor Nerve Organoid with Human Stem Cell-Derived Neurons. *Stem Cell Reports* 9, 1441–1449. doi: 10.1016/j.stemcr.2017.09.021
- Kendall, A. L., Rayment, F. D., Torres, E. M., Baker, H. F., Ridley, R. M., and Dunnett, S. B. (1998). Functional integration of striatal allografts in a primate model of Huntington's disease. *Nat Med* 4, 727–729. doi: 10.1038/nm0698-727
- Kim, J. J., Shin, J. H., Yu, K. R., Lee, B. C., Kang, I., Lee, J. Y., et al. (2017). Direct Conversion of Human Umbilical Cord Blood into Induced Neural Stem Cells with SOX2 and HMGA2. *Int J Stem Cells* 10, 227–234. doi: 10.15283/ijsc17025
- Klejman, M. E., Gruszczynska-Biegala, J., Skibinska-Kijek, A., Wisniewska, M. B., Misztal, K., Blazejczyk, M., et al. (2009). Expression of STIM1 in brain and puncta-like co-localization of STIM1 and ORAI1 upon depletion of Ca(2+) store in neurons. *Neurochem Int* 54, 49–55. doi: 10.1016/j.neuint.2008.10.005
- Krebs, S. S., Trippel, M., Prokop, T., Omer, T. N., Landwehrmeyer, B., Weber, W. A., et al. (2011). Immune response after striatal engraftment of fetal neuronal cells in patients with Huntington's disease: Consequences for cerebral transplantations programs. *Clinical & Experimental Neuroimmunology* 2, 25–32. doi: 10.1111/j.1759-1961.2011.00018.x
- Krystkowiak, P., Gaura, V., Labalette, M., Rialland, A., Remy, P., Peschanski, M., et al. (2007). Alloimmunisation to donor antigens and immune rejection following foetal neural grafts to the brain in patients with Huntington's disease. *PLoS One* 2:e166. doi: 10.1371/journal.pone.0000166
- Lancaster, M. A., and Knoblich, J. A. (2014). Generation of cerebral organoids from human pluripotent stem cells. *Nat Protoc* 9, 2329–2340. doi: 10.1038/nprot.2014.158
- Lancaster, M. A., Renner, M., Martin, C. A., Wenzel, D., Bicknell, L. S., Hurles, M. E., et al. (2013). Cerebral organoids model human brain development and microcephaly. *Nature* 501, 373–379. doi: 10.1038/nature12517
- Lebouc, M., Richard, Q., Garret, M., and Baufreton, J. (2020). Striatal circuit development and its alterations in Huntington's disease. *Neurobiol Dis* 145, 105076. doi: 10.1016/j.nbd.2020.105076
- Lelos, M. J., Robertson, V. H., Vinh, N. N., Harrison, C., Eriksen, P., Torres, E. M., et al. (2016). Direct Comparison of Rat- and Human-Derived Ganglionic Eminence Tissue Grafts on Motor Function. *Cell Transplant* 25, 665–675. doi: 10.3727/096368915X690297
- Lewis, R. S., and Cahalan, M. D. (1995). Potassium and calcium channels in lymphocytes. *Annu Rev Immunol* 13, 623–653. doi: 10.1146/annurev.iy.13.040195.003203
- Li, M., and Rosser, A. E. (2017). Pluripotent stem cell-derived neurons for transplantation in Huntington's disease. *Prog Brain Res* 230, 263–281. doi: 10.1016/bs.pbr.2017.02.009
- Li, M., Chen, C., Zhou, Z., Xu, S., and Yu, Z. (2012). A TRPC1-mediated increase in store-operated Ca<sup>2+</sup> entry is required for the proliferation of adult hippocampal neural progenitor cells. *Cell Calcium* 51, 486–496. doi: 10.1016/j.ceca.2012.04.014
- Lin, L., Yuan, J., Sander, B., and Golas, M. M. (2015). In Vitro Differentiation of Human Neural Progenitor Cells Into Striatal GABAergic Neurons. *Stem Cells Transl Med* 4, 775–788. doi: 10.5966/sctm.2014-0083
- Liou, J., Kim, M. L., Heo, W. D., Jones, J. T., Myers, J. W., Ferrell, J. E., et al. (2005). STIM is a Ca<sup>2+</sup> sensor essential for Ca<sup>2+</sup>-store-depletion-triggered Ca<sup>2+</sup> influx. *Curr Biol* 15, 1235–1241. doi: 10.1016/j.cub.2005.05.055
- Liu, L., Huang, J. S., Han, C., Zhang, G. X., Xu, X. Y., Shen, Y., et al. (2016). Induced Pluripotent Stem Cells in Huntington's Disease: Disease Modeling and the Potential for Cell-Based Therapy. *Mol Neurobiol* 53, 6698–6708. doi: 10.1007/s12035-015-9601-8
- Lopez, J. J., Albarran, L., Gómez, L. J., Smani, T., Salido, G. M., and Rosado, J. A. (2016). Molecular modulators of store-operated calcium entry. *Biochim Biophys Acta* 1863, 2037–2043. doi: 10.1016/j.bbamcr.2016.04.024
- Lopez, J. J., Jardin, I., Sanchez-Collado, J., Salido, G. M., Smani, T., and Rosado, J. A. (2020). TRPC Channels in the SOCE Scenario. *Cells* 9, 126. doi: 10.3390/cells9010126
- Lopez, W. O., Nikkhah, G., Schültke, E., Furlanetti, L., and Trippel, M. (2014). Stereotactic planning software for human neurotransplantation: suitability in 22 surgical cases of Huntington's disease. *Restor Neurol Neurosci* 32, 259–268. doi: 10.3233/RNN-130340
- Ma, D. K., Bonaguidi, M. A., Ming, G. L., and Song, H. (2009). Adult neural stem cells in the mammalian central nervous system. *Cell Res* 19, 672–682. doi: 10.1038/cr.2009.56
- Ma, G., Wei, M., He, L., Liu, C., Wu, B., Zhang, S. L., et al. (2015). Inside-out Ca(2+) signalling prompted by STIM1 conformational switch. *Nat Commun* 6, 7826. doi: 10.1038/ncomms8826
- Ma, L., Hu, B., Liu, Y., Vermilyea, S. C., Liu, H., Gao, L., et al. (2012). Human embryonic stem cell-derived GABA neurons correct locomotion deficits in quinolinic acid-lesioned mice. *Cell Stem Cell* 10, 455–464. doi: 10.1016/j.stem.2012.01.021
- Majewski, L., and Kuznicki, J. (2015). SOCE in neurons: Signaling or just refilling? *Biochim Biophys Acta* 1853, 1940–1952. doi: 10.1016/j.bbamcr.2015.01.019
- Martínez-Cerdeño, V., and Noctor, S. C. (2018). Neural Progenitor Cell Terminology. *Front Neuroanat* 12:104. doi: 10.3389/fnana.2018.00104
- Mathkar, P. P., Suresh, D., Dunn, J., Tom, C. M., and Mattis, V. B. (2019). Characterization of Neurodevelopmental Abnormalities in iPSC-Derived Striatal Cultures from Patients with Huntington's Disease. *J Huntingtons Dis* 8, 257–269. doi: 10.3233/JHD-180333
- Mazzocchi-Jones, D., Döbrösy, M., and Dunnett, S. B. (2009). Embryonic striatal grafts restore bi-directional synaptic plasticity in a rodent model of Huntington's disease. *Eur J Neurosci* 30, 2134–2142. doi: 10.1111/j.1460-9568.2009.07006.x
- McLeod, M. C., Kobayashi, N. R., Sen, A., Baghbaderani, B. A., Sadi, D., Ulalia, R., et al. (2013). Transplantation of GABAergic cells derived from bioreactor-expanded human neural precursor cells restores motor and cognitive behavioral deficits in a rodent model of Huntington's disease. *Cell Transplant* 22, 2237–2256. doi: 10.3727/096368912X658809
- Miura, Y., Li, M. Y., Birey, F., Ikeda, K., Revah, O., Thete, M. V., et al. (2020). Generation of human striatal organoids and cortico-striatal assembloids from human pluripotent stem cells. *Nat Biotechnol* 38, 1421–1430. doi: 10.1038/s41587-020-00763-w
- Moccia, F., Zuccolo, E., Soda, T., Tanzi, F., Guerra, G., Mapelli, L., et al. (2015). Stim and Orai proteins in neuronal Ca(2+) signaling and excitability. *Front Cell Neurosci* 9:153. doi: 10.3389/fncel.2015.00153
- Nekrasov, E. D., Vigont, V. A., Klyushnikov, S. A., Lebedeva, O. S., Vassina, E. M., Bogomazova, A. N., et al. (2016). Manifestation of Huntington's disease pathology in human induced pluripotent stem cell-derived neurons. *Mol Neurodegener* 11, 27. doi: 10.1186/s13024-016-0092-5
- Niclis, J., Trounson, A. O., Dottori, M., Ellisdon, A., Bottomley, S. P., Verlinsky, Y., et al. (2009). Human embryonic stem cell models of Huntington disease. *Reprod Biomed Online* 19, 106–113. doi: 10.1016/s1472-6483(10)60053-3
- Nicoleau, C., Varela, C., Bonnefond, C., Maury, Y., Bugi, A., Aubry, L., et al. (2013). Embryonic stem cells neural differentiation qualifies the role of Wnt/ $\beta$ -Catenin signals in human telencephalic specification and regionalization. *Stem Cells* 31, 1763–1774. doi: 10.1002/stem.1462
- Nieto-Estévez, V., Defterali, C., and Vicario-Abejón, C. (2016). IGF-I: a key growth factor that regulates neurogenesis and synaptogenesis from embryonic to adult stages of the brain. *Front. Neurosci.* 10:52. doi: 10.3389/fnins.2016.00052
- Obernier, K., and Alvarez-Buylla, A. (2019). Neural stem cells: origin, heterogeneity and regulation in the adult mammalian brain. *Development* 146, dev156059. doi: 10.1242/dev.156059
- Oikari, L. E., Okolicsanyi, R. K., Qin, A., Yu, C., Griffiths, L. R., and Haupt, L. M. (2016). Cell surface heparan sulfate proteoglycans as novel markers of human neural stem cell fate determination. *Stem Cell Res* 16, 92–104. doi: 10.1016/j.scr.2015.12.011
- Olsson, M., Björklund, A., and Campbell, K. (1998). Early specification of striatal projection neurons and interneuronal subtypes in the lateral and medial

- ganglionic eminence. *Neuroscience* 84, 867–876. doi: 10.1016/s0306-4522(97)00532-0
- Paez, P. M., Fulton, D., Spreuer, V., Handley, V., and Campagnoni, A. T. (2011). Modulation of canonical transient receptor potential channel 1 in the proliferation of oligodendrocyte precursor cells by the golli products of the myelin basic protein gene. *J Neurosci* 31, 3625–3637. doi: 10.1523/JNEUROSCI.4424-10.2011
- Paganini, M., Biggeri, A., Romoli, A. M., Mechi, C., Ghelli, E., Berti, V., et al. (2014). Fetal striatal grafting slows motor and cognitive decline of Huntington's disease. *J Neurol Neurosurg Psychiatry* 85, 974–981. doi: 10.1136/jnnp-2013-306533
- Palfi, S., Condé, F., Riche, D., Brouillet, E., Dautry, C., Mittoux, V., et al. (1998). Fetal striatal allografts reverse cognitive deficits in a primate model of Huntington disease. *Nat Med* 4, 963–966. doi: 10.1038/nm0898-963
- Parekh, A. B., and Putney, J. W. (2005). Store-operated calcium channels. *Physiol Rev* 85, 757–810. doi: 10.1152/physrev.00057.2003
- Parekh, K. R., Nawroth, J., Pai, A., Busch, S. M., Senger, C. N., and Ryan, A. L. (2020). Stem cells and lung regeneration. *Am J Physiol Cell Physiol* 319, C675–C693. doi: 10.1152/ajpcell.00036.2020
- Park, C. Y., Shcheglovitov, A., and Dolmetsch, R. (2010). The CRAC channel activator STIM1 binds and inhibits L-type voltage-gated calcium channels. *Science* 330, 101–105. doi: 10.1126/science.1191027
- Park, I. H., Arora, N., Huo, H., Maherali, N., Ahfeldt, T., Shimamura, A., et al. (2008). Disease-specific induced pluripotent stem cells. *Cell* 134, 877–886. doi: 10.1016/j.cell.2008.07.041
- Parvez, S., Beck, A., Peinelt, C., Soboloff, J., Lis, A., Monteilh-Zoller, M., et al. (2008). STIM2 protein mediates distinct store-dependent and store-independent modes of CRAC channel activation. *FASEB J* 22, 752–761. doi: 10.1096/fj.07-9449.com
- Pauly, M. C., Piroth, T., Döbrössy, M., and Nikkhah, G. (2012). Restoration of the striatal circuitry: from developmental aspects toward clinical applications. *Front Cell Neurosci* 6:16. doi: 10.3389/fncel.2012.00016
- Pchitskaya, E., Popugaeva, E., and Bezprozvanny, I. (2018). Calcium signaling and molecular mechanisms underlying neurodegenerative diseases. *Cell Calcium* 70, 87–94. doi: 10.1016/j.ceca.2017.06.008
- Pecho-Vrieseling, E., Rieker, C., Fuchs, S., Bleckmann, D., Esposito, M. S., Botta, P., et al. (2014). Transneuronal propagation of mutant huntingtin contributes to non-cell autonomous pathology in neurons. *Nat Neurosci* 17, 1064–1072. doi: 10.1038/nn.3761
- Peinelt, C., Vig, M., Koomoa, D. L., Beck, A., Nadler, M. J., Koblan-Huberson, M., et al. (2006). Amplification of CRAC current by STIM1 and CRACM1 (Orai1). *Nat Cell Biol* 8, 771–773. doi: 10.1038/ncb1435
- Prakriya, M., and Lewis, R. S. (2015). Store-Operated Calcium Channels. *Physiol Rev* 95, 1383–1436. doi: 10.1152/physrev.00020.2014
- Prakriya, M., Feske, S., Gwack, Y., Srikanth, S., Rao, A., and Hogan, P. G. (2006). Orai1 is an essential pore subunit of the CRAC channel. *Nature* 443, 230–233. doi: 10.1038/nature05122
- Precious, S. V., and Rosser, A. E. (2012). Producing striatal phenotypes for transplantation in Huntington's disease. *Exp Biol Med (Maywood)* 237, 343–351. doi: 10.1258/ebm.2011.011359
- Precious, S. V., Zietlow, R., Dunnett, S. B., Kelly, C. M., and Rosser, A. E. (2017). Is there a place for human fetal-derived stem cells for cell replacement therapy in Huntington's disease? *Neurochem Int* 106, 114–121. doi: 10.1016/j.neuint.2017.01.016
- Pregno, G., Zamburlin, P., Gambarotta, G., Farcito, S., Licheri, V., Fregnan, F., et al. (2011). Neuregulin1/ErbB4-induced migration in ST14A striatal progenitors: calcium-dependent mechanisms and modulation by NMDA receptor activation. *BMC Neurosci* 12:103. doi: 10.1186/1471-2202-12-103
- Putney, J. W., Steinckwich-Besançon, N., Numaga-Tomita, T., Davis, F. M., Desai, P. N., D'Agostin, D. M., et al. (2017). The functions of store-operated calcium channels. *Biochim Biophys Acta Mol Cell Res* 1864, 900–906. doi: 10.1016/j.bbamcr.2016.11.028
- Quigley, J. (2017). Juvenile Huntington's Disease: Diagnostic and Treatment Considerations for the Psychiatrist. *Curr Psychiatry Rep* 19, 9. doi: 10.1007/s11920-017-0759-9
- Raab, S., Klingenstein, M., Liebau, S., and Linta, L. (2014). A Comparative View on Human Somatic Cell Sources for iPSC Generation. *Stem Cells Int* 2014, 768391. doi: 10.1155/2014/768391
- Raymond, L. A. (2017). Striatal synaptic dysfunction and altered calcium regulation in Huntington disease. *Biochem Biophys Res Commun* 483, 1051–1062. doi: 10.1016/j.bbrc.2016.07.058
- Reddington, A. E., Rosser, A. E., and Dunnett, S. B. (2014). Differentiation of pluripotent stem cells into striatal projection neurons: a pure MSN fate may not be sufficient. *Front Cell Neurosci* 8:398. doi: 10.3389/fncel.2014.00398
- Reuter, I., Tai, Y. F., Pavese, N., Chaudhuri, K. R., Mason, S., Polkey, C. E., et al. (2008). Long-term clinical and positron emission tomography outcome of fetal striatal transplantation in Huntington's disease. *J Neurol Neurosurg Psychiatry* 79, 948–951. doi: 10.1136/jnnp.2007.142380
- Richner, M., Victor, M. B., Liu, Y., Abernathy, D., and Yoo, A. S. (2015). MicroRNA-based conversion of human fibroblasts into striatal medium spiny neurons. *Nat Protoc* 10, 1543–1555. doi: 10.1038/nprot.2015.102
- Ring, K. L., Tong, L. M., Balestra, M. E., Javier, R., Andrews-Zwilling, Y., Li, G., et al. (2012). Direct reprogramming of mouse and human fibroblasts into multipotent neural stem cells with a single factor. *Cell Stem Cell* 11, 100–109. doi: 10.1016/j.stem.2012.05.018
- Roos, J., DiGregorio, P. J., Yeromin, A. V., Ohlsen, K., Lioudyno, M., Zhang, S., et al. (2005). STIM1, an essential and conserved component of store-operated Ca<sup>2+</sup> channel function. *J Cell Biol* 169, 435–445. doi: 10.1083/jcb.200502019
- Rosa, V., Dubey, N., Islam, I., Min, K. S., and Nör, J. E. (2016). Pluripotency of Stem Cells from Human Exfoliated Deciduous Teeth for Tissue Engineering. *Stem Cells Int* 2016, 5957806. doi: 10.1155/2016/5957806
- Ross, C. A. (2002). Polyglutamine pathogenesis: emergence of unifying mechanisms for Huntington's disease and related disorders. *Neuron* 35, 819–822. doi: 10.1016/s0896-6273(02)00872-3
- Rosser, A. E., and Bachoud-Lévi, A. C. (2012). Clinical trials of neural transplantation in Huntington's disease. *Prog Brain Res* 200, 345–371. doi: 10.1016/B978-0-444-59575-1.00016-8
- Rosser, A. E., Barker, R. A., Harrower, T., Watts, C., Farrington, M., Ho, A. K., et al. (2002). Unilateral transplantation of human primary fetal tissue in four patients with Huntington's disease: NEST-UK safety report ISRCTN no 36485475. *J Neurol Neurosurg Psychiatry* 73, 678–685. doi: 10.1136/jnnp.73.6.678
- Salado-Manzano, C., Perpiña, U., Straccia, M., Molina-Ruiz, F. J., Cozzi, E., Rosser, A. E., et al. (2020). Is the Immunological Response a Bottleneck for Cell Therapy in Neurodegenerative Diseases? *Front Cell Neurosci* 14:250. doi: 10.3389/fncel.2020.00250
- Samtleben, S., Wachter, B., and Blum, R. (2015). Store-operated calcium entry compensates fast ER calcium loss in resting hippocampal neurons. *Cell Calcium* 58, 147–159. doi: 10.1016/j.ceca.2015.04.002
- Schackel, S., Pauly, M. C., Piroth, T., Nikkhah, G., and Döbrössy, M. D. (2013). Donor age dependent graft development and recovery in a rat model of Huntington's disease: histological and behavioral analysis. *Behav Brain Res* 256, 56–63. doi: 10.1016/j.bbr.2013.07.053
- Schlaeger, T. M., Dameron, L., Brickler, T. R., Entwistle, S., Chan, K., Cianci, A., et al. (2015). A comparison of non-integrating reprogramming methods. *Nat Biotechnol* 33, 58–63. doi: 10.1038/nbt.3070
- Shahbazi, M., Cundiff, P., Zhou, W., Lee, P., Patel, A., D'Souza, S. L., et al. (2019). The role of insulin as a key regulator of seeding, proliferation, and mRNA transcription of human pluripotent stem cells. *Stem Cell Res. Ther.* 10:228. doi: 10.1186/s13287-019-1319-5
- Shi, Y., Kirwan, P., and Livesey, F. J. (2012). Directed differentiation of human pluripotent stem cells to cerebral cortex neurons and neural networks. *Nat Protoc* 7, 1836–1846. doi: 10.1038/nprot.2012.116
- Shin, H. Y., Hong, Y. H., Jang, S. S., Chae, H. G., Paek, S. L., Moon, H. E., et al. (2010). A role of canonical transient receptor potential 5 channel in neuronal differentiation from A2B5 neural progenitor cells. *PLoS One* 5:e10359. doi: 10.1371/journal.pone.0010359
- Somasundaram, A., Shum, A. K., McBride, H. J., Kessler, J. A., Feske, S., Miller, R. J., et al. (2014). Store-operated CRAC channels regulate gene expression and proliferation in neural progenitor cells. *J Neurosci* 34, 9107–9123. doi: 10.1523/JNEUROSCI.0263-14.2014
- Straccia, M., Carrere, J., Rosser, A. E., and Canals, J. M. (2016). Human t-DARPP is induced during striatal development. *Neuroscience* 333, 320–330. doi: 10.1016/j.neuroscience.2016.07.022

- Strübing, C., Krapivinsky, G., Krapivinsky, L., and Clapham, D. E. (2003). Formation of novel TRPC channels by complex subunit interactions in embryonic brain. *J Biol Chem* 278, 39014–39019. doi: 10.1074/jbc.M306705200
- Świtońska, K., Szlachcic, W. J., Handschuh, L., Wojciechowski, P., Marczak, E., Stelmazczuk, M., et al. (2018). Identification of Altered Developmental Pathways in Human Juvenile HD iPSC With 71Q and 109Q Using Transcriptome Profiling. *Front Cell Neurosci* 12:528. doi: 10.3389/fncel.2018.00528
- Takahashi, K., Tanabe, K., Ohnuki, M., Narita, M., Ichisaka, T., Tomoda, K., et al. (2007). Induction of pluripotent stem cells from adult human fibroblasts by defined factors. *Cell* 131, 861–872. doi: 10.1016/j.cell.2007.11.019
- Tan, Y. Z., Fei, D. D., He, X. N., Dai, J. M., Xu, R. C., Xu, X. Y., et al. (2019). L-type voltage-gated calcium channels in stem cells and tissue engineering. *Cell Prolif* 52, e12623. doi: 10.1111/cpr.12623
- Tonelli, F. M., Santos, A. K., Gomes, D. A., da Silva, S. L., Gomes, K. N., Ladeira, L. O., et al. (2012). Stem cells and calcium signaling. *Adv Exp Med Biol* 740, 891–916. doi: 10.1007/978-94-007-2888-2\_40
- Toth, A. B., Shum, A. K., and Prakriya, M. (2016). Regulation of neurogenesis by calcium signaling. *Cell Calcium* 59, 124–134. doi: 10.1016/j.ceca.2016.02.011
- Trepakova, E. S., Gericke, M., Hirakawa, Y., Weisbrod, R. M., Cohen, R. A., and Bolotina, V. M. (2001). Properties of a native cation channel activated by Ca<sup>2+</sup> store depletion in vascular smooth muscle cells. *J Biol Chem* 276, 7782–7790. doi: 10.1074/jbc.M010104200
- Tse, M. K., Hung, T. S., Chan, C. M., Wong, T., Dorothea, M., Leclerc, C., et al. (2018). Identification of Ca<sup>2+</sup> signaling in neural stem/progenitor cells during differentiation into neurons and glia in intact and dissociated zebrafish neurospheres. *Sci China Life Sci* 61, 1352–1368. doi: 10.1007/s11427-018-09315-6
- Victor, M. B., Richner, M., Hermansteyne, T. O., Ransdell, J. L., Sobieski, C., Deng, P. Y., et al. (2014). Generation of human striatal neurons by microRNA-dependent direct conversion of fibroblasts. *Neuron* 84, 311–323. doi: 10.1016/j.neuron.2014.10.016
- Victor, M. B., Richner, M., Olsen, H. E., Lee, S. W., Monteys, A. M., Ma, C., et al. (2018). Striatal neurons directly converted from Huntington's disease patient fibroblasts recapitulate age-associated disease phenotypes. *Nat Neurosci* 21, 341–352. doi: 10.1038/s41593-018-0075-7
- Vigont, V. A., Grekhnev, D. A., Lebedeva, O. S., Gusev, K. O., Volovikov, E. A., Skopin, A. Y., et al. (2021). STIM2 Mediates Excessive Store-Operated Calcium Entry in Patient-Specific iPSC-Derived Neurons Modeling a Juvenile Form of Huntington's Disease. *Front Cell Dev Biol* 9:625231. doi: 10.3389/fcell.2021.625231
- Vigont, V. A., Zimina, O. A., Glushankova, L. N., Kolobkova, J. A., Ryazantseva, M. A., Mozhayeva, G. N., et al. (2014). STIM1 Protein Activates Store-Operated Calcium Channels in Cellular Model of Huntington's Disease. *Acta Naturae* 6, 40–47. doi: 10.32607/20758251-2014-6-4-40-47
- Vigont, V., Kolobkova, Y., Skopin, A., Zimina, O., Zenin, V., Glushankova, L., et al. (2015). Both Orai1 and TRPC1 are Involved in Excessive Store-Operated Calcium Entry in Striatal Neurons Expressing Mutant Huntingtin Exon 1. *Front Physiol* 6:337. doi: 10.3389/fphys.2015.00337
- Vigont, V., Nekrasov, E., Shalygin, A., Gusev, K., Klushnikov, S., Illarioshkin, S., et al. (2018). Patient-Specific iPSC-Based Models of Huntington's Disease as a Tool to Study Store-Operated Calcium Entry Drug Targeting. *Front Pharmacol* 9:696. doi: 10.3389/fphar.2018.00696
- Vonsattel, J. P., and DiFiglia, M. (1998). Huntington disease. *J Neuropathol Exp Neurol* 57, 369–384. doi: 10.1097/00005072-199805000-00001
- Wang, Y., Deng, X., Mancarella, S., Hendron, E., Eguchi, S., Soboloff, J., et al. (2010). The calcium store sensor, STIM1, reciprocally controls Orai and CaV1.2 channels. *Science* 330, 105–109. doi: 10.1126/science.1191086
- Weick, J. P., Austin Johnson, M., and Zhang, S. C. (2009). Developmental regulation of human embryonic stem cell-derived neurons by calcium entry via transient receptor potential channels. *Stem Cells* 27, 2906–2916. doi: 10.1002/stem.212
- Wiatr, K., Szlachcic, W. J., Trzeciak, M., Figlerowicz, M., and Figiel, M. (2018). Huntington Disease as a Neurodevelopmental Disorder and Early Signs of the Disease in Stem Cells. *Mol Neurobiol* 55, 3351–3371. doi: 10.1007/s12035-017-0477-7
- Wood, H. (2018). Huntington disease - a neurodevelopmental disorder? *Nat Rev Neurol* 14, 632–633. doi: 10.1038/s41582-018-0075-y
- Wu, J., Ryskamp, D. A., Liang, X., Egorova, P., Zakharova, O., Hung, G., et al. (2016). Enhanced Store-Operated Calcium Entry Leads to Striatal Synaptic Loss in a Huntington's Disease Mouse Model. *J Neurosci* 36, 125–141. doi: 10.1523/JNEUROSCI.1038-15.2016
- Wu, J., Ryskamp, D., Birnbaumer, L., and Bezprozvanny, I. (2018). Inhibition of TRPC1-Dependent Store-Operated Calcium Entry Improves Synaptic Stability and Motor Performance in a Mouse Model of Huntington's Disease. *J Huntingtons Dis* 7, 35–50. doi: 10.3233/JHD-170266
- Wu, J., Shih, H. P., Vigont, V., Hrdlicka, L., Diggins, L., Singh, C., et al. (2011). Neuronal store-operated calcium entry pathway as a novel therapeutic target for Huntington's disease treatment. *Chem Biol* 18, 777–793. doi: 10.1016/j.chembiol.2011.04.012
- Wu, M., Zhang, D., Bi, C., Mi, T., Zhu, W., Xia, L., et al. (2018). A Chemical Recipe for Generation of Clinical-Grade Striatal Neurons from hESCs. *Stem Cell Reports* 11, 635–650. doi: 10.1016/j.stemcr.2018.08.005
- Xiao, N., and Le, Q. T. (2016). Neurotrophic Factors and Their Potential Applications in Tissue Regeneration. *Arch Immunol Ther Exp (Warsz)* 64, 89–99. doi: 10.1007/s00005-015-0376-4
- Xie, P., Sun, Y., Zhou, X., Chen, J., Du, J., Lu, G., et al. (2016). Generation of human embryonic stem cell line chHES-458 from abnormal embryos with HTT gene mutation. *Stem Cell Res* 17, 627–629. doi: 10.1016/j.scr.2016.11.002
- Xu, Z., Su, S., Zhou, S., Yang, W., Deng, X., Sun, Y., et al. (2020). How to reprogram human fibroblasts to neurons. *Cell Biosci* 10, 116. doi: 10.1186/s13578-020-00476-2
- Yadav, A., Seth, B., and Chaturvedi, R. K. (2020). Brain Organoids: Tiny Mirrors of Human Neurodevelopment and Neurological Disorders. *Neuroscientist* doi: 10.1177/1073858420943192
- Yin, X., Li, L., Zhang, X., Yang, Y., Chai, Y., Han, X., et al. (2013). Development of neural stem cells at different sites of fetus brain of different gestational age. *Int J Clin Exp Pathol* 6, 2757–2764.
- Yoshihara, M., Hayashizaki, Y., and Murakawa, Y. (2017). Genomic Instability of iPSCs: Challenges Towards Their Clinical Applications. *Stem Cell Rev Rep* 13, 7–16. doi: 10.1007/s12015-016-9680-6
- Zakrzewski, W., Dobrzyński, M., Szymonowicz, M., and Rybak, Z. (2019). Stem cells: past, present, and future. *Stem Cell Res Ther* 10, 68. doi: 10.1186/s13287-019-1165-5
- Zhang, J., Ooi, J., Utami, K. H., Langley, S. R., Aning, O. A., Park, D. S., et al. (2019). Expanded huntingtin CAG repeats disrupt the balance between neural progenitor expansion and differentiation in human cerebral organoids. *bioRxiv* doi: 10.1101/850586
- Zhang, N., An, M. C., Montoro, D., and Ellerby, L. M. (2010). Characterization of Human Huntington's Disease Cell Model from Induced Pluripotent Stem Cells. *PLoS Curr* 2:RRN1193. doi: 10.1371/currents.RRN1193
- Zhang, S. L., Yu, Y., Roos, J., Kozak, J. A., Deerinck, T. J., Ellisman, M. H., et al. (2005). STIM1 is a Ca<sup>2+</sup> sensor that activates CRAC channels and migrates from the Ca<sup>2+</sup> store to the plasma membrane. *Nature* 437, 902–905. doi: 10.1038/nature04147
- Zoghbi, H. Y., and Orr, H. T. (2000). Glutamine repeats and neurodegeneration. *Annu Rev Neurosci* 23, 217–247. doi: 10.1146/annurev.neuro.23.1.217

**Conflict of Interest:** The authors declare that the research was conducted in the absence of any commercial or financial relationships that could be construed as a potential conflict of interest.

Copyright © 2021 Latoszek and Czeredys. This is an open-access article distributed under the terms of the Creative Commons Attribution License (CC BY). The use, distribution or reproduction in other forums is permitted, provided the original author(s) and the copyright owner(s) are credited and that the original publication in this journal is cited, in accordance with accepted academic practice. No use, distribution or reproduction is permitted which does not comply with these terms.

## GLOSSARY

22q13.3DS, 22q13.3 deletion syndrome; 3D, three-dimensional; A2B5+ NPCs, NPCs with neural cell surface antigen of A2B5; AA, ascorbic acid; ATM, ataxia telangiectasia mutated; BDNF, brain-derived neurotrophic factor; bFGF, basic fibroblast growth factor; BMP, bone morphogenetic protein;  $\text{Ca}^{2+}$ , calcium; CALB1, calbindin 1; cAMP, cyclic adenosine monophosphate; CHIR-99021, GSK inhibitor; CRAC,  $\text{Ca}^{2+}$  release-activated  $\text{Ca}^{2+}$ ; CREB, cAMP-response element-binding protein; CTIP2, chicken ovalbumin upstream promoter (COUP)-transcription factor (TF)-interacting protein 2; DARPP, dopamine- and cAMP-regulated neuronal phosphoprotein; db-cAMP, dibutyl-cAMP; DKK1, dickkopf 1; DLX, distal-less homeobox; DPSCs, dental pulp stem cells; EBiSC, European Bank for induced Pluripotent Stem Cells; EBs, embryonic bodies; ECs, embryonic cells; EGF, epidermal growth factor; ER, endoplasmic reticulum; ErbB-4, Erb-B2 receptor tyrosine kinase 4; ESCs, embryonic stem cells; FGF, fibroblast growth factor; FOXG1, forkhead box protein G1; FOXP2, forkhead box protein P2; Fura-2AM, Fura-2-acetoxymethyl ester; GABA,  $\gamma$ -aminobutyric acid; GAT1, GABA transporter 1; GDNF, glial cell line-derived neurotrophic factor; GE, ganglionic eminence; GSK, glycogen synthase kinase; hCSs, human cortical spheroids; HD, Huntington's disease; hESCs, human embryonic stem cells; hiPSCs, human-induced pluripotent stem cells; hNPCs, human neural progenitor cells; hNSC, human neural stem cell; hStrSs, human striatal spheroids; HTT, huntingtin; hWGE, human whole ganglionic eminence;  $\text{I}_{\text{CRAC}}$ ,  $\text{Ca}^{2+}$  release-activated  $\text{Ca}^{2+}$  current; IGF1, insulin-like growth factor 1; iNs, induced neurons; iNSCs, induced neural stem cells; IP3R1, inositol-1,4,5-triphosphate receptor 1; iPSCs, induced pluripotent stem cells; iPSCs-NSCs, iNSCs from iPSCs;  $\text{I}_{\text{SOC}}$ , store-operated  $\text{Ca}^{2+}$  current; isogenic HD ESCs, IsoHD hESCs; IWR1, tankyrase inhibitor; Klf4, Kruppel-like factor 4; KO, knockout; LDN-193189, dichydrochloride; LGE, lateral ganglionic eminence; MAP2, microtubule-associated protein 2; MEFs, mouse embryonic fibroblasts; mESCs, mouse ESCs; mHTT, mutant HTT; MIG-HD, multicentric intracerebral grafting in Huntington's Disease; miR, microRNA; MSNs,  $\gamma$ -aminobutyric acid (GABA)-ergic medium spiny neurons; MYT1L, myelin transcription factor 1 like; NeuN, neuronal nuclei; NFAT, nuclear factor of activated T cells; NGF, nerve growth factor; NMDAR, *N*-methyl-D-aspartate receptor; NPCs, neural progenitor cells; NSCs, neural stem cells; nSOCE, neuronal store-operated  $\text{Ca}^{2+}$  entry; nSOCs, neuronal store-operated calcium channels; NT-3, neurotrophin-3; OCT3/4, octamer-binding transcription factor-3/4; PAX6, paired box protein 6; pMSNs, precursors of (GABA)-ergic MSNs; polyQ, polyglutamine residues; RA, retinoic acid; RNAseq, RNA sequencing; ROCK, Rho-associated protein kinase; RXRG, retinoid X receptor gamma; SAG, SHH signaling agonist; SB-431542, TGF- $\beta$  RI kinase inhibitor VI; SCs, stem cells; SEPT7, septin 7; SGZ, subgranular zone; SHEDs, stem cells from human exfoliated deciduous teeth; SHH, sonic hedgehog; SKF-96365, SOCE inhibitor; SOCE, store-operated  $\text{Ca}^{2+}$  entry; SOX2, sex determining region Y-box2; SR-11237, RXRG agonist; STIMs, stromal interaction molecule proteins; SVZ, subventricular zone; TGF- $\beta$ , transforming growth factor beta; TRPC, transient receptor potential canonical; VGCC, voltage-gated  $\text{Ca}^{2+}$  channel; VPA, valproic acid; WGE, whole ganglionic eminence; XAV-939, tankyrase inhibitor; Y-27632, ROCK inhibitor; YM-58483, SOCE inhibitor.



# ORAI1 Ca<sup>2+</sup> Channel as a Therapeutic Target in Pathological Vascular Remodelling

Heba Shawer<sup>1</sup>, Katherine Norman<sup>1,2</sup>, Chew W. Cheng<sup>1</sup>, Richard Foster<sup>1,2</sup>, David J. Beech<sup>1</sup> and Marc A. Bailey<sup>1\*</sup>

<sup>1</sup> School of Medicine, The Leeds Institute of Cardiovascular and Metabolic Medicine, University of Leeds, Leeds, United Kingdom, <sup>2</sup> School of Chemistry, University of Leeds, Leeds, United Kingdom

## OPEN ACCESS

### Edited by:

Agnese Secondo,  
University of Naples Federico II, Italy

### Reviewed by:

Irene Frischaut,  
Johannes Kepler University of Linz,  
Austria

Silvia Martin-Puig,  
Spanish National Centre  
for Cardiovascular Research, Spain

### \*Correspondence:

Marc A. Bailey  
m.a.bailey@leeds.ac.uk

### Specialty section:

This article was submitted to  
Signaling,  
a section of the journal  
Frontiers in Cell and Developmental  
Biology

**Received:** 15 January 2021

**Accepted:** 08 March 2021

**Published:** 06 April 2021

### Citation:

Shawer H, Norman K, Cheng CW, Foster R, Beech DJ and Bailey MA (2021) ORAI1 Ca<sup>2+</sup> Channel as a Therapeutic Target in Pathological Vascular Remodelling. *Front. Cell Dev. Biol.* 9:653812. doi: 10.3389/fcell.2021.653812

In the adult, vascular smooth muscle cells (VSMC) are normally physiologically quiescent, arranged circumferentially in one or more layers within blood vessel walls. Remodelling of native VSMC to a proliferative state for vascular development, adaptation or repair is driven by platelet-derived growth factor (PDGF). A key effector downstream of PDGF receptors is store-operated calcium entry (SOCE) mediated through the plasma membrane calcium ion channel, ORAI1, which is activated by the endoplasmic reticulum (ER) calcium store sensor, stromal interaction molecule-1 (STIM1). This SOCE was shown to play fundamental roles in the pathological remodelling of VSMC. Exciting transgenic lineage-tracing studies have revealed that the contribution of the phenotypically-modulated VSMC in atherosclerotic plaque formation is more significant than previously appreciated, and growing evidence supports the relevance of ORAI1 signalling in this pathologic remodelling. ORAI1 has also emerged as an attractive potential therapeutic target as it is accessible to extracellular compound inhibition. This is further supported by the progression of several ORAI1 inhibitors into clinical trials. Here we discuss the current knowledge of ORAI1-mediated signalling in pathologic vascular remodelling, particularly in the settings of atherosclerotic cardiovascular diseases (CVDs) and neointimal hyperplasia, and the recent developments in our understanding of the mechanisms by which ORAI1 coordinates VSMC phenotypic remodelling, through the activation of key transcription factor, nuclear factor of activated T-cell (NFAT). In addition, we discuss advances in therapeutic strategies aimed at the ORAI1 target.

**Keywords:** ORAI1, STIM1, calcium, vascular remodelling, store operated calcium entry, vascular smooth muscle, pharmacology

## INTRODUCTION

Cardiovascular disease (CVD) defines the conditions affecting the heart and blood vessels. CVD is currently the leading cause of global mortality, accounting for an estimated 17 million deaths annually (WHO, 2017). This figure is anticipated to rise as the prevalence in low and middle-income countries increases. CVD is associated with classical risk factors, including obesity (Poirier et al., 2006), smoking (Keto et al., 2016), family history (Dorairaj and Panniyammakal, 2012; Jeemon et al., 2017), and diabetes (Rydén et al., 2013; Shah et al., 2015). Atherosclerotic CVD (e.g.,

ischaemic heart disease, peripheral arterial disease, cerebrovascular disease, renovascular disease), pulmonary hypertension and aneurysm formation have all been associated with pathological remodelling behaviour of the native vascular smooth muscle cells (VSMC) within the arterial wall. Similarly, failure of surgical revascularisation to treat atherosclerotic CVD lesions (bypass grafting with autologous vein or prosthetic graft) or percutaneous coronary intervention/peripheral artery endovascular intervention (angioplasty+/-stenting) is associated with neointimal hyperplasia (NIH) which is also a manifestation of pathological vascular remodelling. The ability to selectively inhibit such pathological remodelling of VSMC is therefore considered to be a potentially fruitful therapeutic strategy across this range of cardiovascular pathologies. In order to achieve this, an identifiable, specific, druggable target is required. In this review we present an update on the evidence supporting the ORAI1  $\text{Ca}^{2+}$  channel as a potential therapeutic target and the current status of inhibitor development. The focus is on atherosclerotic CVD and NIH as little evidence exists regarding aneurysm disease in this context and we recently reviewed the evidence supporting ORAI1 as a target in pulmonary hypertension (Rode et al., 2018).

## VSMC Phenotypic Switching

The VSMC is a specialised cell type which is optimised for vascular contractility and the modulation of vascular tone via its contractile apparatus, which depends on smooth muscle contractile proteins such as alpha smooth muscle actin ( $\alpha$ -SMA), smooth muscle myosin heavy chain (SM-MHC) and smooth muscle 22 alpha (SM22 $\alpha$ ). These “contractile” VSMCs usually reside in the tunica media of the vessel wall and are classically associated with diseases arising from altered vascular tone, such as hypertension. VSMC intracellular free calcium levels and L-type  $\text{Ca}^{2+}$  channel activity are hallmarks of excessive vascular contractility and are targeted by calcium channel blocking anti-hypertensive drugs in the clinic.

When new blood vessels form during embryogenesis, the local VSMC sub-populations envelop the angiogenic endothelial cells to build the vascular tree. Unlike other specialised cell types, such as the cardiomyocyte, VSMCs are not terminally differentiated. In cases of vascular injury, the contractile VSMCs retain the ability to de-differentiate to an immature, plastic, secretory, and “synthetic” state. These phenotypically modulated VSMCs have reduced expression of contractile proteins, while displaying high indices of proliferation, migration, synthesis and secretion of cytokines and tropoelastins. This phenotypic switch generates a range of de-differentiated VSMC phenotypes, including macrophage-like, osteoblast-like and myofibroblast-like VSMC phenotypes, as reviewed in Sorokin et al. (2020). This heterogeneity in VSMC populations within the healthy vessel wall was evident in the heterogeneity of the single VSMCs transcriptional profiles defined by single cell RNA-sequencing (Dobnikar et al., 2018).

The critical driver of this process is platelet derived growth factor BB (PDGF-BB) signalling through the PDGF receptor beta, PDGFR $\beta$  (Owens et al., 2004; Thomas et al., 2009). *In vitro* and *in vivo* studies have shown that PDGF-BB negatively regulates

expression of VSMC contractile markers and promotes the phenotypic switch toward a plastic and secretory phenotype. Production of PDGF-BB by activated platelets, macrophages, endothelial cells and even phenotypically modulated VSMCs themselves has been described in atherosclerosis and post-surgical NIH mouse models. This results in downregulation of VSMC contractile markers, and subsequent stimulation of VSMC proliferation and migration, reviewed in Owens et al. (2004). There is evidence to support the concept that as the de-differentiated VSMC lay down new elastin and repopulate the vessel, the elastin itself drives the VSMC back toward their contractile phenotype. This is evidenced by the synthetic behaviour of VSMC obtained from elastin-deficient mice and the reduced NIH observed after elastin delivery to the vessel in porcine model of CVD (Karnik et al., 2003). It has been argued by Owens and others that this is likely to be an evolutionarily conserved mechanism for repairing vascular trauma that conferred a survival advantage to early man. Major trauma is not the main driver of vascular injury in developed societies; rather the risk factors driving the development of CVD cause much less severe but sustained injury to our vasculature. Therefore, VSMC phenotypic modulation becomes sustained and the vascular remodelling response itself becomes part of the pathological process.

## Pathological Vascular Remodelling in Atherosclerosis and NIH

Atherosclerosis is associated with pathological intimal thickening, neovascularisation, and lipoprotein depositions (Virmani et al., 2000). Phenotypically-modulated VSMCs in atherosclerosis have low expression of VSMC contractile markers, and a heightened ability to proliferate and migrate. Synthetic VSMCs have also been associated with increased secretory activities and increased production of extra-cellular matrix (ECM) components, which contribute to the intimal thickening and atherosclerosis progression (Okada et al., 1993; Andreeva et al., 1997). It was long assumed that the role of VSMC was rather limited in atherosclerotic plaque formation. These assumptions were based on conventional VSMC identification approaches; low levels of antibody staining for “classical” VSMC markers, such as  $\alpha$ -SMA and SM-MHC were observed in the atherosclerotic plaque. However, as discussed above, the classical VSMC markers are downregulated in phenotypically-modulated VSMC therefore potentially rendering them undetectable via this approach. Recent transgenic lineage-tracing studies have enabled fate tracking of VSMC even following remodelling and loss of contractile protein expression. These elegant studies demonstrated that more than 80% of cells within lesions are phenotypically-modulated VSMC that lack VSMC identification markers (Shankman et al., 2015). Compelling evidence supports the adverse effect of VSMC remodelling to macrophage-like foam cells in lesion pathogenesis. This was demonstrated in a study from the Owens laboratory that utilised an SMC lineage-tracing murine model to study the impact of SMC-specific deletion of the pluripotency factor, Krüppel-like factor 4 (Klf4), which is crucial for the PDGF-induced VSMC phenotypic switch, on

atherosclerotic plaque development (Deaton et al., 2009). They showed that loss of Klf4 in VSMC was associated with reduced plaque formation, and improved plaque stability (Shankman et al., 2015), highlighting the key role of VSMC remodelling in the pathogenesis of atherosclerosis and the potential beneficial outcome of inhibiting the extrinsic phenotypic switch to target atherosclerosis. Critically, the same group have demonstrated that VSMC remodelling mediated by the transcription factor Octamer-Binding Protein 4 (Oct4) is crucial for plaque stability, and that Oct4 conditional deletion in VSMC had adverse effects on lesion pathogenesis as shown by the reduced VSMC content in the protective fibrous cap, implying that VSMC phenotypic switching could be beneficial in maintaining plaque stability, and preventing rupture (Otsuka et al., 2015). Additionally, VSMC apoptosis was also shown to be a key feature of plaque vulnerability (Clarke and Bennett, 2006).

The VSMC phenotypic switch is also a key player in the development of NIH. Post-coronary intervention patients remain at risk of developing NIH, with even greater risk in patients with comorbidities, including diabetes and obesity (Silber et al., 2013). Drug-eluting stents that target VSMC proliferation have been shown to improve the clinical outcome following bypass surgery, percutaneous coronary angioplasty, and peripheral revascularisation (Moses et al., 2003), yet a recent systematic review and meta-analysis suggested increased mortality risk 5 years following femoropopliteal application of drug-coated balloons and stents (Katsanos et al., 2018). Despite the beneficial effects of the drug-coated stents and balloons in preventing NIH following angioplasty, the reported possible deleterious long-term side effects of these devices raised concerns about their safety and emphasised the clinical need for new effective therapeutic strategies.

Taken together, strong evidence supports the crucial role of VSMC in the pathophysiology of atherosclerosis, and NIH. VSMC could be directed toward either beneficial or unfavourable remodelling during lesion development. Nevertheless, suitable (and druggable) molecular therapeutic targets to control VSMC phenotypic remodelling remain elusive.

## Store-Operated Calcium Entry (SOCE)

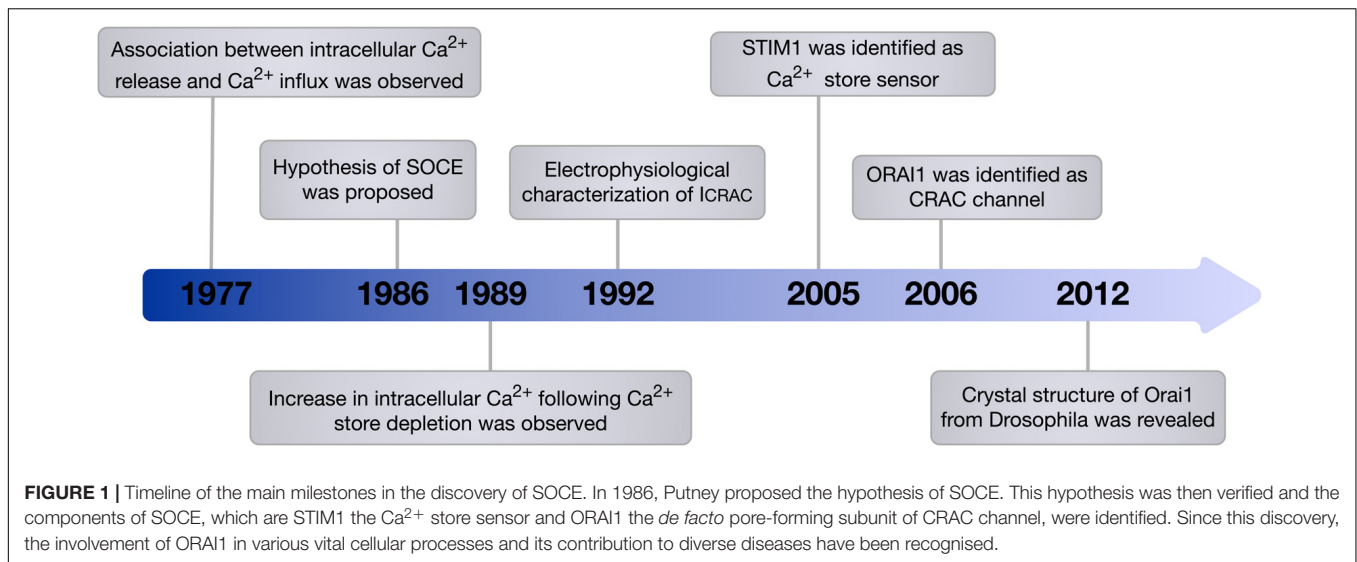
Calcium ( $\text{Ca}^{2+}$ ) is a universal second messenger and signalling ion that is crucial for a wide range of cellular processes with a temporal range from milliseconds (e.g., contraction) to hours/days (e.g., gene transcription). The concentration of global as well as compartmentalised  $\text{Ca}^{2+}$  within the cell regulates  $\text{Ca}^{2+}$ -dependent regulatory pathways that define VSMC function and phenotype, cytoskeletal remodelling and cell proliferation (Beech, 2007). Cytosolic  $\text{Ca}^{2+}$  influx occurs through plasmalemmal  $\text{Ca}^{2+}$  channels, including voltage-gated and receptor-operated  $\text{Ca}^{2+}$  channels, that allow modulated extracellular  $\text{Ca}^{2+}$  influx into the cell. Additionally,  $\text{Ca}^{2+}$  fluxes out of and into the major intracellular  $\text{Ca}^{2+}$  store, the endoplasmic reticulum (ER), are controlled by ryanodine receptors (RyR) and inositol trisphosphate receptors ( $\text{IP}_3\text{R}$ ) on the ER membrane. PDGF-BB, which drives VSMC phenotypic switch, triggers a global rise in intracellular  $\text{Ca}^{2+}$  through the binding of PDGF-BB to its receptor, PDGFR $\beta$ , initiating

phosphorylation of the PDGF receptor tyrosine kinase residues, leading to activation of number of signalling pathways implicated in proliferative vascular diseases, including phospholipase C (PLC) and phosphatidylinositol 3-kinase (PI3K). The activated PLC enzymes generate  $\text{IP}_3$ , which in turn promotes the activation of  $\text{IP}_3\text{R}$  and the release of  $\text{Ca}^{2+}$  waves from the ER to the cytosol.

The phenomenon of extracellular  $\text{Ca}^{2+}$  influx following intracellular  $\text{Ca}^{2+}$  release was first observed by Putney in 1977 (Putney, 1977) and formalised into the theory of capacitative  $\text{Ca}^{2+}$  entry in 1986 (Putney, 1986). The proposed hypothesis was then verified by the observed increase in  $\text{Ca}^{2+}$  influx in parotid acinar cells following stimulation of store depletion using the sarco/endoplasmic reticulum  $\text{Ca}^{2+}$ -ATPase (SERCA) pump inhibitor, thapsigargin (Takemura et al., 1989). Afterward, via whole-cell patch-clamp analysis in mast cells,  $\text{Ca}^{2+}$  current following store depletion was recorded and characterised as  $\text{Ca}^{2+}$ -selective inwardly rectifying current, which was termed calcium-release-activated-calcium current ( $\text{I}_{\text{CRAC}}$ ) (Hoth and Penner, 1992). Today the process of extracellular  $\text{Ca}^{2+}$  influx upon depletion of the intracellular stores is most commonly described as store-operated  $\text{Ca}^{2+}$  entry or SOCE and throughout this review we will use this term.

Despite the physiological phenomenon of SOCE being well established, the molecular machinery encoding SOCE remained elusive for many years. In 2005, STIM1 was identified as the ER membrane  $\text{Ca}^{2+}$  store sensor and a key component of SOCE (Liou et al., 2005; Roos et al., 2005). It has since been demonstrated that a small pool of STIM1 also exists in the plasma membrane (Li et al., 2015). Identification of patients who presented with severe combined immune deficiency (SCID) due to impairment of SOCE in T cells was a key discovery that provided a chance to pinpoint genes encoding calcium-release-activated-calcium current (CRAC) channels (Feske et al., 2005). ORAI1, which is also known as calcium release-activated calcium modulator 1 (CRACM1) and transmembrane protein 142A (TMEM142A) was identified in 2006 by Feske et al. (2006) through a genome-wide screen of linkage in SCID patients that identified a missense mutation in ORAI1, which resulted in impaired  $\text{I}_{\text{CRAC}}$  in T cells, as well as a genome-wide RNA interference screen in *Drosophila melanogaster* which provided support that ORAI1 is the key component of CRAC channels (Figure 1). In addition, genome-wide RNA-interference screens have identified ORAI1 as a key component of SOCE in *D. melanogaster* S2 cells, and confirmed the requirement of ORAI1 for generation of  $\text{I}_{\text{CRAC}}$  (Zhang et al., 2006). Ectopic co-expression of ORAI1 and STIM1 was able to augment SOCE in human embryonic kidney cells (HEK293) and Jurkat T cells, implying their independent role in generating  $\text{I}_{\text{CRAC}}$  (Peinelt et al., 2006). Furthermore, Prakriya et al. (2006) revealed that ORAI1 is the *de facto* pore-forming subunit of CRAC channels, demonstrating that ORAI1 is located at the cell surface, and that mutations within ORAI1 alter the properties of the CRAC current.

It was long thought that SOCE was mediated by members of the transient receptor potential (TRP) channel superfamily, mainly canonical TRP (TRPC) channels, most commonly, TRPC1. Attenuation of SOCE upon TRPC1 knockdown in



human submandibular gland (HSG) cells (Liu et al., 2003), and in salivary gland acinar cells isolated from TRPC1 knockout mice (Liu et al., 2007), as well as the augmentation of  $\text{Ca}^{2+}$  influx following thapsigargin-mediated store-depletion in cells expressing TRPC1 (Zhu et al., 1996; Liu et al., 2003) provided support for this view. Induced expression of mutant TRPC1 that either encodes truncated protein or harbours mutations at the negatively charged residues in the pore-forming region resulted in remarkable reduction of SOCE, implying that TRPC1 could be a molecular component of CRAC channels (Liu et al., 2003).

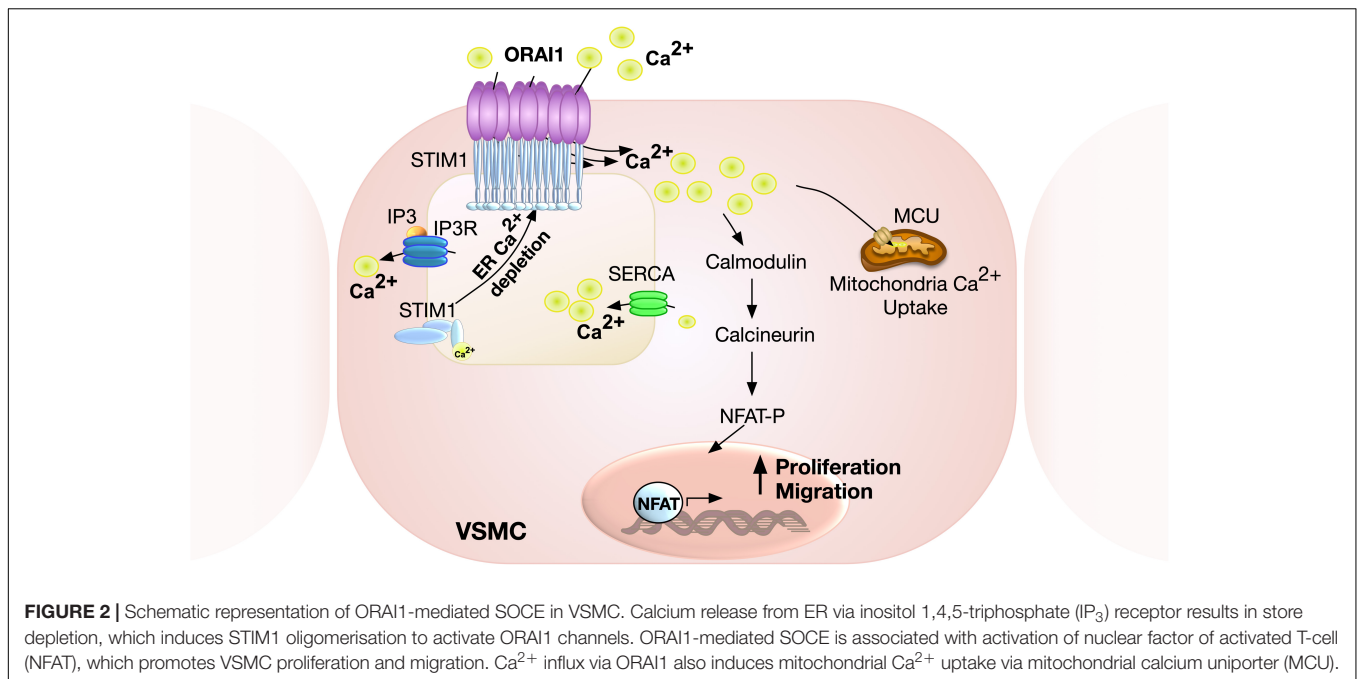
The discovery of ORAI1 as the *de facto* CRAC channel created debate regarding TRPC1 as a direct component of CRAC channels or indirect modulator of SOCE. ORAI1 was shown to associate with TRPC1, with enhanced interaction upon store depletion, suggesting the involvement of ORAI1/TRPC1 channel in SOCE (Jardin et al., 2008). Induced interaction between ORAI1 and TRPC1 was observed in murine pulmonary arterial smooth muscle cells with elevated SOCE in response to acute hypoxia (Ng et al., 2012). Ávila-Medina et al. (2016) showed via an *in situ* proximity ligation assay that the three channels, ORAI1, TRPC1 and voltage-gated  $\text{Ca}^{2+}$  channel (Cav1.2) are localised in close proximity in VSMC, suggesting possible functional interactions to modulate  $\text{Ca}^{2+}$  signalling. Electrostatic interaction between TRPC1 and STIM1 was reported to be essential for TRPC1 channel gating (Zeng et al., 2008). Moreover, inhibition of the interaction between ORAI1 and STIM1, using an antibody directed against the C-terminal region of ORAI1, impaired STIM1 and TRPC1 association and altered TRPC1 function from a store-operated channel into a store-independent (receptor-operated) channel in human platelet cells (Jardin et al., 2008).

Arguing against the role of TRPC1 as a CRAC channel, the activity of TRPC1 was reported to be independent of the ER  $\text{Ca}^{2+}$  sensor STIM1, as shown by the lack of effect of STIM1 silencing or overexpression on the channel's activity in HEK293 cells (Wayne et al., 2009). Nonetheless, an alternative model of communication with intracellular stores was suggested by an enhanced TRPC1 interaction with the  $\text{IP}_3$  receptor upon store

depletion in human platelets, implying that the role of TRPC1 could include coupling to the  $\text{IP}_3$  receptor in the ER (Rosado et al., 2002). This model was again challenged by the observation that TRPC1 is localised on the intracellular membranes in platelets rather than the plasma membrane (Hassock et al., 2002). It was also reported that TRPC1-induced expression failed to enhance SOCE (Sinkins et al., 1998; Strübing et al., 2001), and VSMC isolated from TRPC1 knockout mice showed no change in SOCE relative to wild type (Dietrich et al., 2007). Despite the evidence supporting the involvement of TRPC1 in SOCE, there is still considerable controversy surrounding the contradictory results of the involvement of TRPC1 in SOCE.

## STIM1

Live cell imaging and electrophysiology studies have shown that following pharmacological store depletion, STIM1 undergoes oligomerisation, aggregation and translocation to the ER-plasma membrane junctions to activate ORAI1 channels (Wu et al., 2006; Liou et al., 2007; Luik et al., 2008; McKeown et al., 2012). This distribution, however, was not observed in PDGF-mediated ORAI1 activation in VSMC, revealing an alternative non-clustering mechanism of ORAI1 activation that is likely to be more relevant to the physiological setting (McKeown et al., 2012). STIM1 is an ER membrane protein consisting of multiple structural domains, with the N-terminus located in ER lumen encompassing canonical EF-hand, hidden EF-hand, and sterile alpha motif (SAM) domains. The  $\text{Ca}^{2+}$  sensing ability of STIM1 is mediated by the low  $\text{Ca}^{2+}$  binding affinity of the canonical EF-hand intra-ER domain.  $\text{Ca}^{2+}$  depletion and release from the EF-hand domain result in exposure of its hydrophobic residues, EF-SAM monomer transformation into an oligomer, elongation of the C-terminal cytosolic domain, and exposure of its CRAC activation domain (CAD) (Huang et al., 2006; Stathopoulos et al., 2006; Covington et al., 2010; Yang et al., 2012b). The ORAI1 channel is subsequently activated by direct interaction with CAD, generating ICRAC (Spassova et al., 2006; Park et al., 2009; **Figure 2**). STIM1 regulation of  $\text{Ca}^{2+}$  signalling is



not limited to modulating ORAI1 activity. Other Ca<sup>2+</sup> channels revealed to be regulated by STIM1 include TRPC1 (Zeng et al., 2008), and the voltage-gated Ca<sup>2+</sup> channel, Cav1.2 (Wang et al., 2010). Interestingly, while STIM1 activates ORAI1 channels, its interaction with Cav1.2 attenuates the channel's activity (Wang et al., 2010), supporting a bimodal function of STIM1 in regulating Ca<sup>2+</sup> signalling by activating SOCE on one hand and inhibiting voltage-gated Ca<sup>2+</sup> channels on the other.

### ORAI1 Channel

The human *ORAI1* gene is 16.128 Kb in length, located at chromosome 12q24.31 (GRCh38/hg38), and is translated into two protein isoforms: ORAI1 $\alpha$  (around 33 KDa) and ORAI1 $\beta$  (around 23 KDa) due to different translation initiation sites (Fukushima et al., 2012). Both ORAI1 $\alpha$  and ORAI1 $\beta$  assemble to generate functional CRAC channels, and have similar sub-cellular localisation. Nonetheless, ORAI1 $\beta$  has higher mobility in the plasma membrane as it lacks arginine-rich residues that promote ORAI1 $\alpha$  interaction with the phosphatidylinositol-4,5-bisphosphate (PIP<sub>2</sub>) of plasma membrane (Calloway et al., 2011). The ORAI1 protein structure comprises four transmembrane (TM) domains, extracellular TM1-TM2 loop, intracellular TM2-TM3 loop, extracellular TM3-TM4 loop, and cytoplasmic N- and C-termini (Figure 3). ORAI1 was shown to undergo post-translational modifications, including glycosylation of the asparagine 233 residue located at the extracellular loop-2 (Gwack et al., 2007), and phosphorylation of serine residues at positions 27 and 30 (Kawasaki et al., 2010). ORAI1 assembles to form either homomeric or heteromeric channels. Three members of the ORAI family have been identified, with ORAI2 and ORAI3 encoded by separate genes, *ORAI2* and *ORAI3*, respectively. ORAI channels can assemble as hetero-pentameric channels comprising three ORAI1 and two ORAI3 subunits to

generate arachidonate-regulated Ca<sup>2+</sup> (ARC) channel, which is activated independent of store depletion. ARC channels show receptor-mediated activation by intracellular arachidonic acid. Interestingly, only ORAI1 $\alpha$  and not ORAI1 $\beta$  participates in the formation of ARC channels (Desai et al., 2015).

ORAI1 monomers are arranged to generate a central ion conduction pore, involving the TM1 domain from each monomer, to generate a circle of TM1 domains. These amino acid residues, surrounding the ion conductance pore, determine the biophysical features of the channel. The glutamic acid residues at position 106 form an outer ring thought to act as a selectivity filter (McNally et al., 2009). Crystal structure determination of the *D. melanogaster* Orail revealed assembly as an unusual and unexpected hexameric complex (Hou et al., 2012). However, the data on functional stoichiometry of human ORAI1 (hORAI1) is contradictory. High resolution scanning transmission electron microscopy (STEM) imaging of hORAI1 proteins indicated that they were mainly found as monomers and dimers, with a small fraction found as hexamers (Peckys et al., 2016). Early electrophysiological analysis of hexameric and tetrameric concatemer of hORAI1 suggested that the biophysical properties of the tetrameric concatemer match that of the native CRAC currents, whereas the hexameric concatemer lacked key fingerprint features of CRAC currents (Thompson and Shuttleworth, 2013). More recent electrophysiology studies, however, reported that hexameric hORAI1 concatemer exhibited the key biophysical features of CRAC channels, including Ca<sup>2+</sup> selectivity, generating unitary current and rapid Ca<sup>2+</sup> dependent channel inactivation (Yen et al., 2016). Similarly, recent analysis of Ca<sup>2+</sup> currents mediated by dimeric, trimeric, tetrameric, pentameric, and hexameric concatemers of hORAI1 showed inwardly rectifying store-operated Ca<sup>2+</sup> current in all oligomeric concatemers similar to that of native CRAC

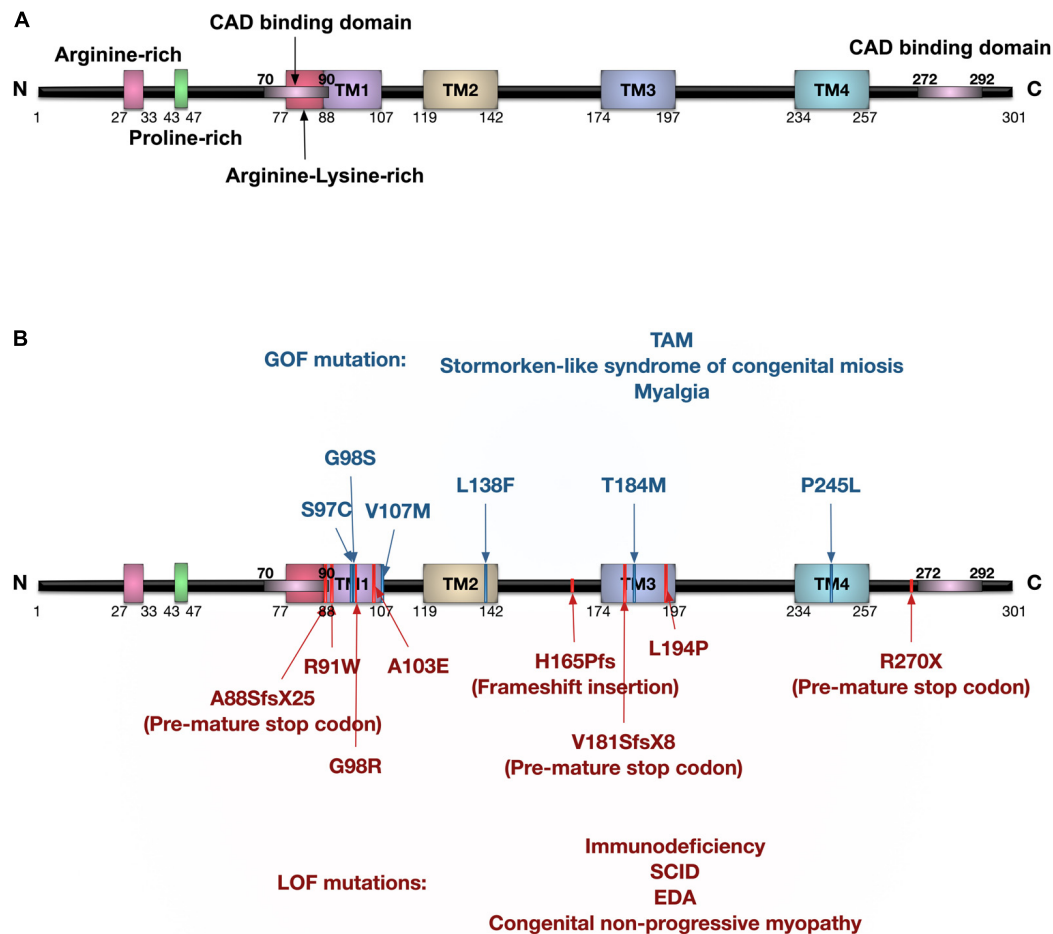


**FIGURE 3 |** Protein domain structure of human ORAI1 and the reported ORAI1 mutations. **(A)** Human ORAI1 protein comprises four transmembrane (TM) domains, two extracellular loops between TM1-TM2, and between TM3-TM4, one intracellular loop between TM2-TM3, arginine rich domain, proline-rich domain, arginine-lysine rich domain, amino terminus (N), and carboxy terminus (C) containing CRAC activation domain (CAD) binding domains (purple lines). **(B)** The blue lines represent gain-of-function (GOF) single nucleotide polymorphisms (SNPs) reported in tubular aggregate myopathy (TAM) patients with elevated CRAC channel activity. The red lines represent ORAI1 loss-of-function (LOF) mutations reported in patients with immunodeficiency, severe combined immune deficiency (SCID), and ectodermal dysplasia anhidrosis (EDA).

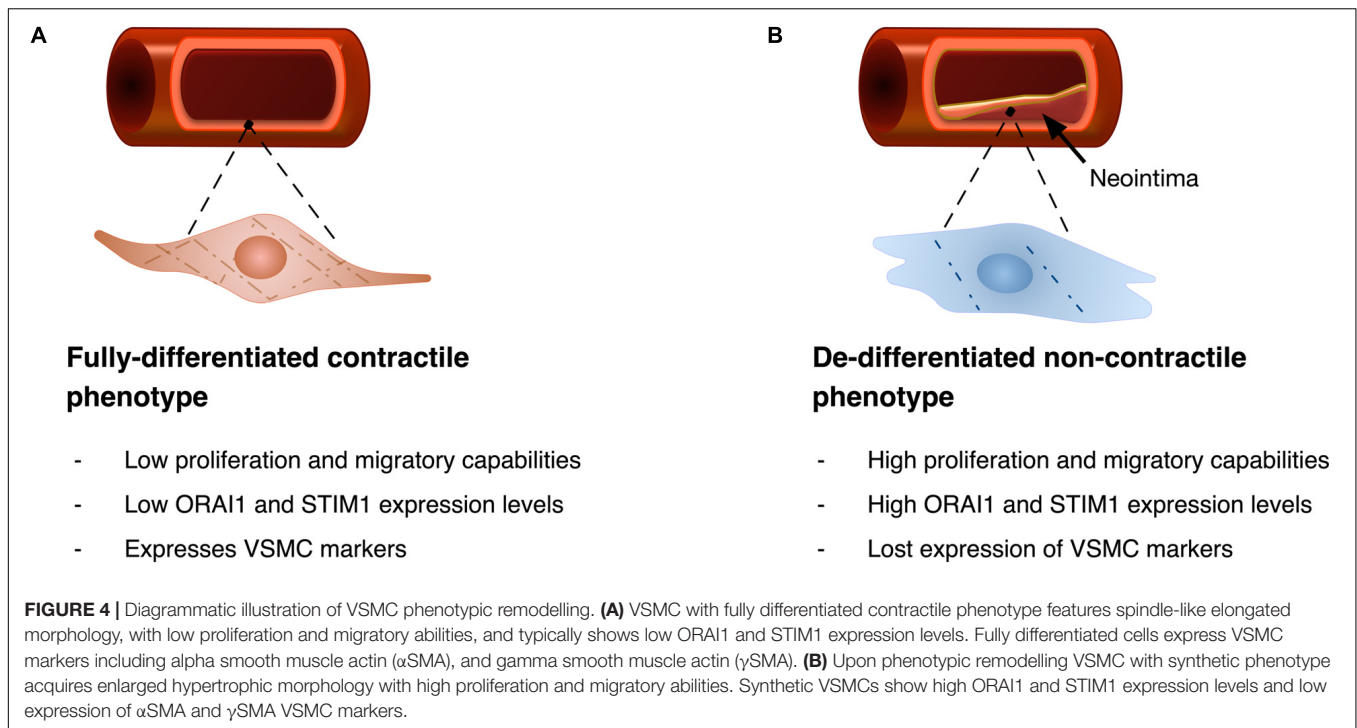
channels (Cai et al., 2016). This study also found that the hORAI1 tetrameric concatemer only contributed with the N-terminal dimer of the construct to generate the channel; unlike the hORAI1 hexamer, in which all subunits contributed to formation of the channel, suggesting that hORAI1 exists in a hexameric configuration (Cai et al., 2016). This is in accord with the atomic force microscopy imaging study that suggested that hORAI1 assembles as a hexamer (Balasuriya et al., 2014). Although several lines of evidence support the idea that hORAI1 channels exist as hexamers, debate remains.

Recent studies have shed the light on the contribution of the different ORAI homologs in the pattern of  $\text{Ca}^{2+}$  signals and revealed their involvement in  $\text{Ca}^{2+}$  oscillatory responses (Yoast et al., 2020; Zhang et al., 2020). These oscillations in cytosolic  $\text{Ca}^{2+}$  concentration, with varying spatiotemporal features, are fundamental cellular signals that are efficiently decoded to activate specific gene transcription and certain cellular responses. The pattern of  $\text{Ca}^{2+}$  response in cells that lacked

either one, two, or the three ORAI homologs was studied and it was shown that ORAI2 and ORAI3 play an essential role in maintaining agonist-induced  $\text{Ca}^{2+}$  oscillatory responses, while ORAI1 mainly mediates plateaus. These findings suggest that ORAI2 and ORAI3 heteromerisation with ORAI1 plays a role in mediating the channel response to low agonist concentrations, and modulating CRAC channel-mediated gene transcription processes (Yoast et al., 2020).

## ORAI1 in Pathological Vascular Smooth Muscle Cell Remodelling

Contractile VSMC exhibit almost no proliferation and low expression of ORAI1 and STIM1 proteins. Increased expression of these proteins was shown to be associated with VSMC de-differentiation and remodelling (i.e., the synthetic phenotype, Figure 4). In proliferating cultures of human saphenous vein VSMC (hVSMC), ORAI1 is abundantly expressed and is crucial



for SOCE. Where siRNA-induced *ORAI1* silencing suppressed SOCE, and this reduction of SOCE was rescued by transfecting cells with *ORAI1* cDNA, verifying the role of ORAI1 in SOCE in hVSMC (Li et al., 2011b). Inhibition of SOCE either by siRNA-mediated *ORAI1* silencing or pharmacologically using the potent and selective CRAC channel blocker Synta66 (S66) reduced hVSMC migration, with slight reduction of cell proliferation and no effect on cell viability (Li et al., 2011b). Similarly, in human aortic VSMC cultures, impairment of  $I_{CRAC}$  via siRNA-mediated *ORAI1* silencing significantly hampered cell proliferation (Baryshnikov et al., 2009). Although the secretory behaviour of VSMC plays a crucial role in pathologic ECM remodelling, little is known about the role of ORAI1 in ECM production and secretion in VSMCs.

Whilst ORAI1 is upregulated in synthetic and proliferative VSMC, the L-type voltage gated  $Ca_v1.2$  channel was downregulated, which is a trend thought to contribute to the loss of the VSMC contractile function in synthetic phenotype (Gollasch et al., 1998; Ihara et al., 2002).  $Ca_v1.2$  channel blockers in VSMC promote STIM1-induced ORAI1 activation through promoting STIM1 re-localisation to the ER-PM junctions, in  $Ca_v1.2$  and store-depletion independent fashion, leading to induced VSMC remodelling (Johnson et al., 2020). These findings not only support the implication of ORAI1/STIM1 signalling in VSMC remodelling but also imply the risk of potential aggravation of vascular remodelling by the  $Ca_v1.2$  channel blockers, which are routinely used anti-hypertensive medications.

PDGF pro-migratory signalling, an essential component in VSMC phenotypic switching (Yamasaki et al., 2001), was shown to activate ORAI1 channels in hVSMC without inducing ORAI1

redistribution in the plasma membrane (McKeown et al., 2012). In agreement with these findings, Ogawa et al. (2012) showed that PDGF induces pulmonary arterial VSMC proliferation through activation of SOCE. Silencing of either *Orai1* or *Stim1* in cultured rat aortic VSMC disrupted PDGF-induced  $Ca^{2+}$  entry and reduced cell migration, verifying that PDGF mediates its effect in VSMC through the ORAI1/STIM1 signalling pathway (Bisaillon et al., 2010). On the other hand, pharmacological potentiation of ORAI1 channel activity using the ORAI1 enhancer (IA65) was shown to promote the PDGF-induced VSMC migration (Azimi et al., 2020). The pro-migratory and proliferative effect of ORAI1 is thought to be mediated through activation of the transcription factor, nuclear factor for activated T cells (NFAT), which potentially promotes the expression of pro-proliferative factors (e.g., IL6, cyclin A, and cyclin D1), as observed from the reduced NFAT nuclear translocation following silencing of *Orai1* or *Stim1* in VSMC (Aubart et al., 2009; Zhang et al., 2011b). *Orai1* silencing in primary VSMC isolated from rabbit aorta resulted in reduced DNA synthesis and cell proliferation (Yang et al., 2012a). In cultured rat synthetic VSMC, knockout of either *Orai1* or *Stim1* reduced cellular proliferative and migratory ability (Potier et al., 2009). Similar results were reported with siRNA-induced silencing of *Stim1* in cultured rat VSMC, resulting in reduced cell proliferation and migration. This effect of *Stim1* silencing on VSMC proliferation and migration was reversed by re-expression of *Stim1* (Guo et al., 2009), demonstrating its vital role in regulating VSMC proliferation. These data highlight the role of ORAI1/STIM1 and SOCE in regulating VSMC switch to a proliferative and migratory phenotype, a process that plays a key role in the aetiology of various vascular pathologies.

In addition to the activation of ORAI1 by PDGF signalling, Urotensin-II-induced VSMC proliferation was mediated through activating SOCE and promoting ORAI1/STIM1 and ORAI1/TRPC interactions (Rodríguez-Moyano et al., 2013). Similar findings were observed by *in vitro* treatment of human coronary VSMC with angiotensin-II, which stimulated VSMC remodelling to proliferative phenotype, and resulted into ORAI1 upregulation leading to augmented SOCE (Liu et al., 2020). Additionally, the angiotensin-II-stimulated human coronary VSMC (Liu et al., 2020) and rat aortic VSMC (Guo et al., 2011) proliferation was hampered by either *ORAI1* or *STIM1* silencing. Sphingosine-1-phosphate (S1P) is another signalling molecule that was shown to induce STIM1 rearrangement, resulting in subsequent activation of ORAI1-mediated SOCE in VSMC. This S1P-triggered activation of SOCE was shown to be higher in synthetic VSMC relative to those with the contractile phenotype, supporting the crucial role ORAI1-mediated SOCE in promoting phenotypic remodelling (Hopson et al., 2011).

The phenotypic modulation of VSMC could lead to their differentiation to an osteoblast-like cells, which is characterised by the expression of osteogenic markers and secretion of calcified matrix, a process known as vascular calcification. This osteogenic differentiation of VSMC is a key player in vascular calcification that can lead to vascular stiffness and atherosclerotic plaque rupture (Durham et al., 2018). ORAI1 has been reported to play a role in this osteogenic reprogramming of human aortic VSMC and vascular calcification. For example, *in vitro* induction of the osteogenic signalling in human aortic VSMC by  $\beta$ -glycerophosphate exposure, as a phosphate donor, or by high extracellular glucose treatment resulted in an upregulation of ORAI1 and STIM1 levels, and this effect on vascular osteogenic signalling was suppressed by ORAI1 silencing or pharmacological inhibition (Ma et al., 2019, 2020; Zhu et al., 2020).

## Evidence Implicating ORAI1 in Pathological Vascular Remodelling in Atherosclerosis and NIH

Mutations in the *ORAI1* gene have been reported in a range of diseases (Figure 3 and Tables 1, 2), including: tubular aggregate myopathy (TAM), SCID, congenital miosis, ectodermal dysplasia anhidrosis (EDA), and Stormorken-like syndrome (Böhm et al., 2017; Garibaldi et al., 2017). The clinical manifestation of ORAI1 deficiency is mainly immunodeficiency, global muscular hypotonia, and defects in dental enamel calcification (Table 1; Feske et al., 2006; McCarl et al., 2009; Badran et al., 2016; Lian et al., 2018). Of interest to the present study however, neo-vascularisation of the cornea was observed in a patient with compound heterozygous missense mutations 308C>A (A103E) and 581T > C (L194P) in the *ORAI1* gene (McCarl et al., 2009). There is also a growing body of evidence linking upregulation of ORAI1 in a wide range of important human diseases from cancer to heart failure. The implication of ORAI1 in human cardiovascular abnormalities was highlighted by the reported association of ORAI1 mutations with Kawasaki disease (KD) susceptibility, which is the leading cause of cardiovascular complications during childhood. These studies have identified

rare missense variants in KD patients (Onouchi et al., 2016; Thiha et al., 2019). The reported variants in KD patients, interestingly, include a variant that cause p.Gly98Asp mutation within the TM1 domain that generates the ion conduction pore, which is a mutation known to lead to a constitutive ORAI1 channel activation (Zhang et al., 2011a). These findings signify the potential involvement of ORAI1-mediated signalling in cardiovascular pathologies.

## ORAI1 in the Pathological VSMC Remodelling in NIH and Re-Stenosis

The key role of ORAI1/STIM1 signalling in promoting migration and proliferation of cultured VSMC was supported by *in vivo* studies, where STIM1 (Aubart et al., 2009; Guo et al., 2009) and ORAI1 (Bisaillon et al., 2010) levels were elevated in injured rat carotid arteries following balloon angioplasty, relative to uninjured arteries. Similar elevation of ORAI1 and STIM1 was observed in the intimal hyperplastic lesion in mouse carotid arteries following carotid ligation (Zhang et al., 2011b), and an increased expression of ORAI1 and STIM1 in neointimal VSMC was associated with elevated expression of proliferation markers (Zhang et al., 2011b). Formation of NIH following balloon angioplasty and the expression level of proliferation markers were significantly reduced by either *Stim1* knockdown (Aubart et al., 2009; Guo et al., 2009) or *Orai1* knockdown (Zhang et al., 2011b) induced by viral delivery of siRNA or short-hairpin RNA (shRNA) in rats, respectively, supporting the *in vivo* role of ORAI1 and STIM1 in the pathogenesis of NIH.

It was also shown that angiotensin-II, which is a driver of VSMC remodelling, promotes ORAI1 and STIM1 expression in rat carotid arteries after balloon angioplasty, and that silencing of either *Orai1* or *Stim1* reduced the angiotensin-II-promoted NIH formation in injured rat carotids (Guo et al., 2011). In support, Mancarella et al. (2013) studied the role of STIM1 in SMC function via targeted deletion of *Stim1* specifically in murine smooth muscle tissues using Cre-Lox technology. This murine model was carrying the cre-recombinase transgene under the control of the SM22 $\alpha$  smooth muscle-specific promoter that enabled the deletion of *Stim1* in the different smooth muscle tissues. This lack of Stim1 in smooth muscle tissues resulted in abnormal development and impaired contractile response in intestinal and vascular smooth muscles. Development of NIH following carotid artery ligation was shown to be significantly reduced in mice with *Stim1* SMC-specific conditional deletion relative to controls (Mancarella et al., 2013). This study emphasises the role of STIM1 in the formation of NIH. Nonetheless, the reported involvement of STIM1 in NIH does not necessarily indicate similar contribution of ORAI1, due to the multiple pathways and channels involving STIM1 activation.

ORAI1 has been shown to directly interact with various proteins implicated in NIH formation, including members of TRPC family. TRPC1, TRPC3, TRPC4, and TRPC6 were shown to have a role in modulating VSMC proliferation and formation of NIH (Kumar et al., 2006; Jia et al., 2017). Nonetheless, little is known about the potential involvement

**TABLE 1** | Human ORAI1 (NM\_032790.3) mutations and the associated disorders.

ORAI1 function	Mutation	Position of mutation	Effect on $I_{CRAC}$	Disease phenotype	References
Gain-of-function	Heterozygous missense mutation 290C>G (S97C)	TM1	Constitutive activation of $I_{CRAC}$	TAM, congenital miosis	Garibaldi et al., 2017
	Heterozygous missense mutations 292G>A (G98S)	TM1	STIM1-independent constitutive activation of $I_{CRAC}$	TAM, myalgia, occasional mild hypocalcemia, frequent episodes of bleeding from mouth, nose, and bowel	Böhm et al., 2017
	Heterozygous missense mutations 319G>A (V107M)	TM1	STIM1-independent Constitutive activation of $I_{CRAC}$	TAM, myalgia	Böhm et al., 2017
	Heterozygous missense mutations 551C>T (T184M)	TM3	Constitutive activation of $I_{CRAC}$	Mild general weakness, myalgia, hypereosinophilia, pectus excavatum, arched palate, asymptomatic hyperCKemia	Böhm et al., 2017
	Heterozygous missense mutation 292G>A (G98S)	TM1	Constitutive activation of $I_{CRAC}$	TAM, slowly progressive diffuse muscle weakness, hypocalcemia	Endo et al., 2014
	Heterozygous missense mutation 412C>T (L138F)	TM2	Constitutive activation of $I_{CRAC}$	TAM, slowly progressive diffuse muscle weakness	Endo et al., 2014
	Heterozygous missense mutation 734C>T (P245L)	TM4	Prolonged $I_{CRAC}$ activation and reduced inactivation relative to WT	TAM, stormorken-like syndrome of congenital miosis	Nesin et al., 2014
Loss-of-Function	Homozygous missense mutation 271C>T (R91W)	TM1	Defects in SOCE and $I_{CRAC}$	Hereditary SCID, EDA, congenital non-progressive myopathy	Feske et al., 2006
	Homozygous non-sense mutation resulting from frameshift insertion (258_259insA)	Premature termination (A88SfsX25) at the end of TM1	Defects in SOCE and $I_{CRAC}$	SCID due to proliferation defects in T-cells, global muscular hypotonia, defects in dental enamel calcification	McCarl et al., 2009
	Compound heterozygous for two missense mutations 308C>A (A103E) and 581T>C (L194P)	TM1 and TM3 pore-domains	Defects in SOCE and $I_{CRAC}$	SCID, global muscular hypotonia, defects in dental enamel calcification, chronic pulmonary disease due to respiratory muscle insufficiency, eczema, neo-vascularisation of cornea, EDA	McCarl et al., 2009
	Homozygous for missense mutation 581T>C (L194P)	TM3	Defects in SOCE and $I_{CRAC}$	Immunodeficiency, anemia, thrombocytopenia, congenital muscular hypotonia, anhidrosis	Lian et al., 2018
	Homozygous missense mutation 808C>T (R270X) resulting in pre-mature stop codon	C-terminally truncation	Defects in SOCE and $I_{CRAC}$	Immunodeficiency due to proliferation defects in T-cells	Badran et al., 2016
	Homozygous missense mutation, resulting from frameshift insertion 493_494insC (H165Pfs)	C-terminally truncation	Reduced but not abolished $I_{CRAC}$	Immunodeficiency, with normal T-cell numbers and proliferation	Chou et al., 2015
	Homozygous missense mutation 292G>C (G98R)	TM1	Defects in SOCE and $I_{CRAC}$	Immunodeficiency, autoimmune haemolytic anemia, thrombocytopenia, anhidrosis, congenital muscular hypotonia	Lian et al., 2018
	Homozygous for single nucleotide deletion resulting in frameshift mutation (del541C)	Premature termination (V181SfsX8) within TM3	Defects in SOCE and $I_{CRAC}$	Immunodeficiency, reduced T-cell proliferation, muscular hypotonia, EDA	Lian et al., 2018

$I_{CRAC}$ , calcium-release-activated-calcium current; SOCE, store-operated calcium entry; TM, transmembrane; TAM, tubular aggregate myopathy; SCID, severe combined immune deficiency; EDA, ectodermal dysplasia anhidrosis.

**TABLE 2 |** ORAI1 mutations and resulting phenotype in animal models.

Mutation	Position of mutation	Model organism	Disease phenotype	References
Global <i>Orai1</i> knockout in C57BL/6 background	Exon-1 deletion	Mice	Perinatal lethality	Gwack et al., 2008
Global amorphic mutation	ORAI1 <sup>R93W/R93W</sup> in TM1 pore-domain	Mice	Perinatal lethality	Bergmeier et al., 2009; Maus et al., 2017
Global <i>Orai1</i> knockout in mixed ICR background	Exon-1 deletion	Mice	Small size, eyelid irritation, and sporadic hair loss; and impaired B-cell proliferation and decreased cytokine production	Gwack et al., 2008
			Small size, reduced and irregular enamel deposition, deficient multinucleated osteoclasts, decreased bone mineral resorption and bone volume, impaired osteoblast differentiation	Robinson et al., 2012
Global <i>Orai1</i> <sup>-/-</sup> via gene trap technology	Deletion of exon-2 and -3	Mice	Small size, defects in integrin activation, degranulation, decreased cytokine production, and defects in the <i>in vivo</i> allergic response, no defects in T cell proliferation and differentiation	Vig et al., 2008
Chimeric mice expressing amorphic mutant ORAI1 protein only in blood cells	ORAI1 <sup>R93W/R93W</sup> in TM1 pore-domain	Mice	Defects in platelet integrin activation, degranulation, and surface phosphatidylserine exposure	Bergmeier et al., 2009
Global <i>Orai1</i> knockout in mixed ICR background	Deletion of exon-2 and -3	Mice	Osteopenia, decreased bone mineral density and bone volume, despite normal osteoblast differentiation	Hwang et al., 2012
Global <i>Orai1</i> deficiency by injection of <i>Orai1</i> morpholinos	Targeting splice donor site of exon1 or translational start site	Zebrafish	Muscle weakness, severe heart failure, bradycardia, despite normal cardiomyocyte differentiation	Volkers et al., 2012
Brain- specific <i>Orai1</i> deletion	Deletion of exon-2 and -3	Mice	Diminished proliferation of adult neural progenitor cell	Somasundaram et al., 2014
T cell- specific <i>Orai1</i> deletion	<i>Orai1</i> deletion	Mouse model of EAE	Inhibition of pro-inflammatory cytokines production, and reduced EAE severity	Kaufmann et al., 2016
Global <i>Orai1</i> knockout <i>Orai1</i> <sup>-/-</sup> in mixed ICR background	<i>Orai1</i> deletion	Mice	Sterile males, severe defects in spermatogenesis, and in elongating spermatid development	Davis et al., 2016
Ectodermal tissues -specific <i>Orai1</i> deletion	Deletion of exon-2 and -3	Mice	Impairment of sweat secretion, despite of normal development of sweat glands.	Concepcion et al., 2016
T cell- specific <i>Orai1/Orai2</i> double deficient mice	<i>Orai2</i> null, <i>Orai1</i> T cell-specific knockout	Mice	Impaired T-cell dependent immune response	Vaeth et al., 2017
Pancreatic acinar cell- specific, tamoxifen-inducible <i>Orai1</i> deletion	Deletion of exon-2 and -3	Mice	Lack of antimicrobial secretions from pancreatic acinar cells, resulting in intestinal bacterial outgrowth with dysbiosis and increased mortality	Ahuja et al., 2017

TM, transmembrane; EAE, experimental autoimmune encephalomyelitis.

of ORAI1/TRPC complexes in promoting VSMC proliferation. HOMER1 is a scaffolding protein that has been shown to be able to interact with ORAI1 and a number of TRPC channels. ORAI1 interaction with HOMER1 was shown to be enhanced in VSMC

following balloon-injury of carotid arteries, relative to uninjured arteries (Jia et al., 2017). Interestingly, *Homer1* silencing in rat aortic proliferative VSMC resulted in reduction of SOCE, VSMC proliferation, and migration, implying the involvement of

ORAI1/HOMER1 interaction in modulating VSMC phenotypic remodelling (Jia et al., 2017).

### ORAI1 in the Pathological VSMC Remodelling in Atherosclerosis

ORAI1 expression was reported to be elevated in atherosclerotic lesions of Apolipoprotein-E null ( $ApoE^{-/-}$ ) mice on a high-cholesterol diet. *In vivo* silencing of *Orai1* using viral delivery of siRNA against *Orai1* or pharmacological inhibition of ORAI1, using an inhibitor with poor specificity, reduced atherosclerotic plaque formation in  $ApoE^{-/-}$  mice fed high-cholesterol diet (Liang et al., 2016). ORAI1-mediated SOCE was shown to be essential for the formation of foam cells, which are macrophages loaded with low-density lipoproteins, a critical step in atherogenesis. *Orai1*-knockdown macrophages exhibited remarkable reduction in their ability to bind and uptake lipoproteins, which subsequently reduced foam cell formation, and atherosclerotic plaque formation (Liang et al., 2016).

Inflammation and cytokine secretion are also major components of the development of atherosclerosis and NIH. Inflammation in atherosclerotic lesions is mediated by pro-inflammatory T helper 1 (Th1) cells that secrete inflammatory cytokines, including interferon- $\gamma$  (IFN- $\gamma$ ) (Frostegard et al., 1999), which in turn induces macrophage activation and promotes intimal thickening through the promotion of growth factor-induced mitogenesis in VSMC (Ferns et al., 1991; Yokota et al., 1992; Tellides et al., 2000). Knockdown of leukotriene-C4 synthase, which produces the pro-inflammatory mediator leukotriene-C4, and activates ORAI1/ORAI3 channels in VSMC, suppressed neointimal formation in balloon-injured rat carotid artery (Zhang et al., 2015). Furthermore, the emerging role of ORAI1 in lipid metabolism suggests potential involvement of ORAI1 in lipid deposition in atherosclerotic plaque. Maus et al. (2017) revealed that the absence of SOCE due to ORAI1 or STIM1/STIM2 disruption resulted in increased deposition of lipid droplets in murine liver, skeletal muscle, and heart muscle. Additionally, TAM patients with ORAI1 loss-of-function p.Gly98Arg mutation showed deposition of lipid droplets in skeletal muscles, and increased lipid content in patient fibroblasts relative to healthy donors, due to impaired lipolysis (Maus et al., 2017). SOCE was shown to modulate the expression of key enzymes involved in the mitochondrial fatty acid oxidation, and regulate the expression of neutral lipases and a number of transcription regulators that modulate lipolysis (Maus et al., 2017). This is in accord with the previously reported reduction of SOCE associated with lipid accumulation in rat liver cells (Wilson et al., 2015). The involvement of ORAI1 in lipid metabolism foreshadows its potential role in pathogenic mechanisms underlying atherosclerosis, including lipid deposition and formation of the fatty streak.

The ORAI1/ORAI3 ARC store-independent channel was reported to be activated in VSMC after thrombin-mediated induced phenotypic remodelling (González-Cobos et al., 2013). Platelet activation contributes to the initiation and progression of atherosclerosis (Methia et al., 2001; Pratico et al., 2001; Massberg et al., 2002) and platelet adhesion to vascular endothelium was observed before the development of atherosclerotic lesions in

$ApoE^{-/-}$  mice (Massberg et al., 2002). Defective SOCE in both *Orai1* $^{-/-}$  or *Stim1* $^{-/-}$  mice resulted in impaired platelet activation and thrombus formation (Varga-Szabo et al., 2008; Braun et al., 2009). Similarly, introduction of a SNP in the EF-hand of murine STIM1 impaired its activation in response to ER  $Ca^{2+}$  deletion and resulted in macrothrombocytopenia and impaired platelet activation (Grosse et al., 2007). Furthermore, gain-of-function mutations in STIM1 were observed in patients with York Platelet syndrome (Markello et al., 2015) and thrombocytopenia (Nesin et al., 2014). Impaired platelet function was also observed in patients with ORAI1 mutations (Table 1; Nagy et al., 2018). The involvement of ORAI1-mediated SOCE in normal platelet function implies the potential involvement of ORAI1 abnormalities in platelet activation and adhesion in atherosclerosis.

### Pharmacological Modulation of SOCE

The link between SOCE and vascular remodelling rendered CRAC channels as promising therapeutic targets. Newly identified inhibitors of SOCE have increased understanding of the physiological roles of SOCE and emerged as attractive candidates with the potential to enable pharmacological modulation of CRAC channels. Nonetheless, many of these agents have indefinite mechanism of action and those with the specificity to distinguish between different  $Ca^{2+}$  channels remains elusive (Table 3).

**Lanthanides ( $Gd^{3+}$  and  $La^{3+}$ )** are widely studied potent inhibitors of CRAC channels, which block SOCE at the nanomolar concentration range. At a concentration of 5  $\mu M$ ,  $Gd^{3+}$  was reported to block SOCE in rat synthetic VSMC and in the A7R5 VSMC line (Potier et al., 2009). Sensitivity to inhibition by lanthanides is a key feature of CRAC currents that differentiate CRAC channels from other  $Ca^{2+}$  channels.  $Gd^{3+}$  is equipotent toward the three ORAI homologs, ORAI1, ORAI2, and ORAI3 (Zhang et al., 2020). Despite the high potency of lanthanides, their efficiency as CRAC channel inhibitors is limited by their high plasma protein binding affinity, low solubility in presence of other multivalent ions, and their limited specificity as CRAC channel inhibitors at higher concentration (Figure 5). At concentrations more than 1  $\mu M$ , lanthanides inhibit activity of voltage-gated calcium ion channels (Reichling and MacDermott, 1991), and TRPC channels (Halaszovich et al., 2000; Trebak et al., 2002). It is thought that lanthanides exhibit their activity as CRAC channel blockers through binding to acidic residues on the extracellular loop of ORAI1, rather than competing for the  $Ca^{2+}$  binding sites within the ion conduction pore of the channel. In support of this theory, the ability of  $Gd^{3+}$  to inhibit CRAC channel activity was significantly reduced in cells expressing mutant *ORAI1* gene carrying charge-neutralising mutations of aspartate (D) residues within the TM1-TM2 extracellular loop of ORAI1 (Yeromin et al., 2006). Similarly, McNally et al. (2009) showed that mutations of acidic residues in the human *ORAI1* gene at either of Q108, D110, D112, or D114 of the TM1-TM2 loop reduced the potency of  $La^{3+}$  inhibition. However, mutation at position 106, which serves as the ion selectivity filter and

**TABLE 3 |** Features of ORAI1 channel pharmacological inhibitors.

Compound	Reported potential mode of action	Other targets	Effective concentrations
Lanthanides ( $Gd^{3+}$ and $La^{3+}$ )	Direct binding to the extracellular loop of ORAI1 channel	Cav1.2 and TRP channels	Effective at low nanomolar concentration 5 $\mu$ M $Gd^{3+}$ blocked SOCE in rat synthetic VSMC and in A7R5 VSMC line
2-APB	Maintain STIM1 at its resting state Direct inhibition to ORAI1	ORAI2, ORAI3, IP <sub>3</sub> receptor, SERCA pumps, and members of the TRP channel superfamily	IC <sub>50</sub> of 10 $\mu$ M in Jurkat T cells, 4.8 $\mu$ M in IP <sub>3</sub> R-knockout DT-40, 2.9 $\mu$ M in CHO cells, and 6.5 $\mu$ M in HeLa cells
Carboxyamidotriazole (CAI)	Indirect inhibition, mitochondrial membrane depolarisation	Inhibits non-voltage gated calcium influx	IC <sub>50</sub> of around 0.5 $\mu$ M in HEK293 cells
The 7-azaindole series, compound (14 d)	Unclear	Unknown	IC <sub>50</sub> of 150 $\pm$ 22 nM in Jurkat T cells
The indazole-3-carboxamide series, compound (12 d)	Unclear	Unknown	IC <sub>50</sub> of 0.67 $\mu$ M in RBL-2H3 cells
pyrtriazole series, compound (39)	Unclear	Selective for SOCE over CaVs, TRPV1 and TRPM8	IC <sub>50</sub> of 4.4 $\mu$ M in HEK293 cells
DPB162-AE	Reduction of STIM1 clustering upon store depletion Inhibit STIM1/ORAI1 functional coupling	Induce Ca <sup>2+</sup> leak from the ER	IC <sub>50</sub> of 27 nM in DT-40 cells, 190 nM in CHO cells, and 620 nM in HeLa cells
SKF-96365	Unclear	TRPC, Cav1.2, voltage-gated Na <sup>+</sup> channels, ATP sensitive K <sup>+</sup> channels, and ER Ca <sup>2+</sup> pumps	IC <sub>50</sub> of 12 $\mu$ M in Jurkat T cells
Synta66	Potentially binds to the extracellular loop 1 and 3 regions of ORAI1	No off-targets have yet been identified	IC <sub>50</sub> of 3 $\mu$ M in RBL cells, 1 $\mu$ M in Jurkat T cell and 26 nM in VSMC
CM4620	Unclear	No off-targets have yet been identified	IC <sub>50</sub> of $\sim$ 0.1 $\mu$ M in Orai1/STIM1 overexpressing HEK293
YM-58483	Unclear	Inhibits TRPC3, and TRPC5 activity Enhances the activity of TRPM4 channels	IC <sub>50</sub> of 10–100 nM in Jurkat T cells
GSK7975A	Altering channel pore geometry	ORAI3, L-type Ca <sup>2+</sup> , and TRPV6 channels	IC <sub>50</sub> of 4 $\mu$ M in HEK293 cells
AnCoA4	Interaction with the C-terminus of ORAI1 Inhibition STIM1/ORAI1 interaction	Unknown	20 $\mu$ M AnCoA4 resulted in 80% SOCE inhibition in HEK293 cells
RO2959	Unclear	5-hydroxytryptamine receptor 2B (5-HT <sub>2B</sub> ) and the peripheral benzodiazepine (BZD) receptors	IC <sub>50</sub> of 400 nM in RBL cells, 25 nM in CHO cells, and 260 nM in CD4 <sup>+</sup> T cells
JP111	Unclear	No off-targets have yet been identified	IC <sub>50</sub> of 299 nM in HEK293 cells

IC<sub>50</sub>, Half-maximal inhibitory concentration; DT-40, Chicken lymphoblast cell line; CHO, Chinese hamster ovary cells, RBL, Rat chemically induced basophils; TRP, transient receptor potential.

is located within TM1 domain that generates the central ion conduction pore, did not affect the ability of  $La^{3+}$  to inhibit the channel activity. These observations suggest that lanthanides bind to residues at the extracellular TM1-TM2 loop, rather than binding deeper in the ion conduction pore of ORAI1 channels (McNally et al., 2009).

**Imidazole antimycotic drugs** including SKF-96365 (Figure 5), econazole and miconazole were shown to inhibit I<sub>CRAC</sub> in a wide range of cell types. SKF-96365 was first identified in Ca<sup>2+</sup> signalling studies as an inhibitor of receptor-mediated Ca<sup>2+</sup> influx, with inhibitory effect in the micromolar range

in platelets, neutrophils and endothelial cells (Merritt et al., 1990; Franzius et al., 1994). It was also shown to inhibit SOCE in Jurkat T cells (Chung et al., 1994). In a mouse model of atherosclerosis, *in vivo* administration of SKF-96365 remarkably reduced atherosclerotic plaque development (Liang et al., 2016). Nonetheless, the observed effect is not necessarily attributed to SOCE inhibition. A wide spectrum of ion channels were reported to be targeted by SKF-96365, including receptor- and store-operated TRPC channels, voltage gated Ca<sup>2+</sup> channels (Merritt et al., 1990; Singh et al., 2010), voltage gated sodium channels (Chen et al., 2015), and ATP sensitive potassium channels (K<sub>ATP</sub>)

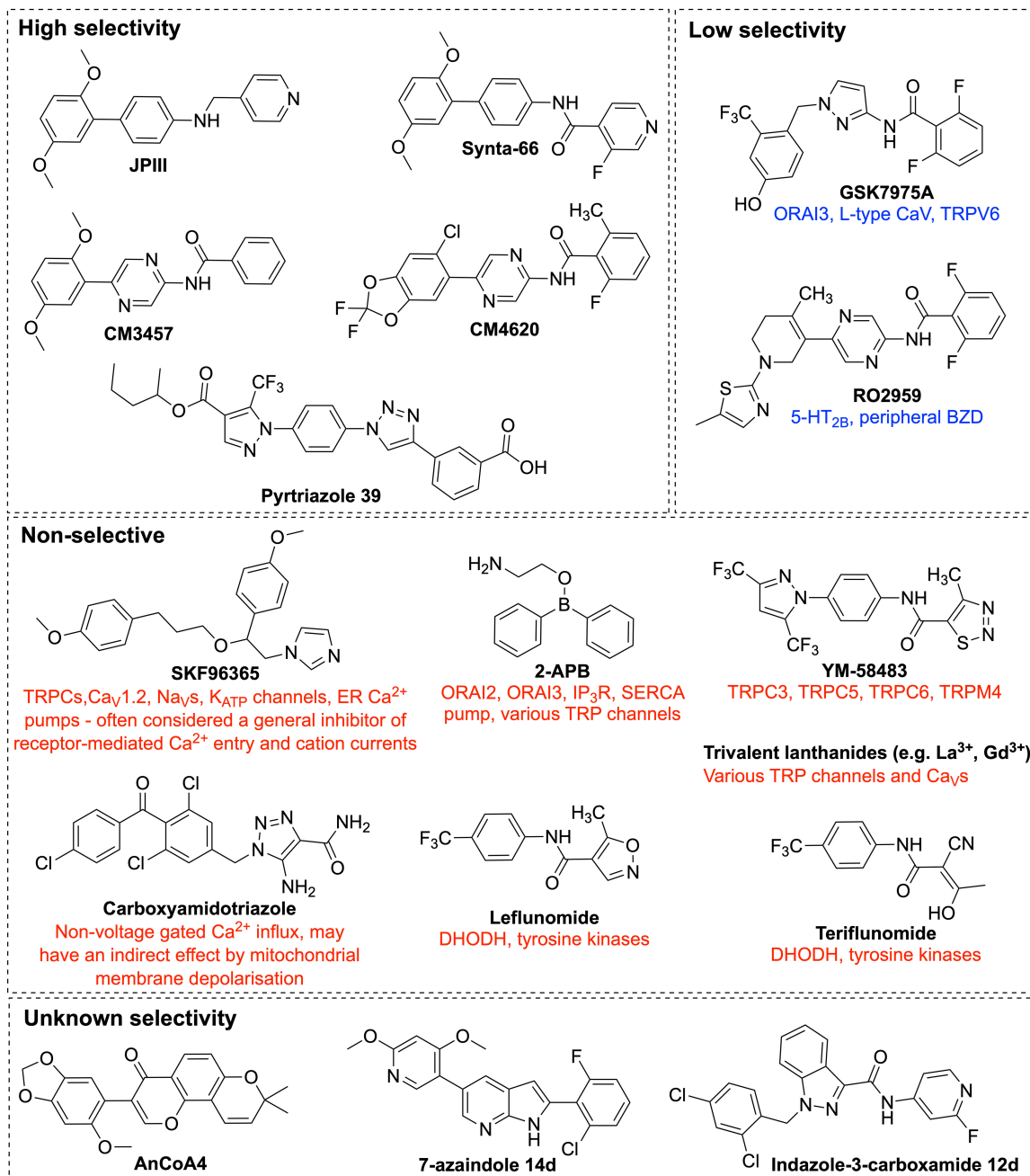


**FIGURE 5 |** Chemical structures of ORAI1 channel pharmacological inhibitors. Illustration of the chemical structures of ORAI1 channel inhibitors and a list of their previously reported off-targets. The ORAI1 inhibitors were grouped by their reported specificity against ORAI1. 2-APB, 2-Aminoethylidiphenyl Borate; TRP, transient receptor potential; 5-HT<sub>2B</sub>, 5-hydroxytryptamine receptor 2B; BZD, benzodiazepine receptors; DHODH, dihydro-orotate dehydrogenase.

(Tanahashi et al., 2016). Furthermore, earlier studies reported that SKF-96365 not only acts as an ion influx inhibitor, micromolar concentrations of SKF-96365 also inhibited ER Ca<sup>2+</sup> pumps in human endothelial cells (Iouzalet et al., 1996), and activated reverse operation of Na<sup>+</sup>/Ca<sup>2+</sup> exchanger (NCX) resulting in Ca<sup>2+</sup> uptake and sustained intracellular Ca<sup>2+</sup> elevation in cancer cells (Song et al., 2014). SKF-96365 has served as a powerful tool to characterise mechanisms of Ca<sup>2+</sup>

entry, however, the multiple targets of SKF-96365 could hinder its use as I<sub>CRAC</sub> inhibitor and limit its translation toward potential therapies. Analogues of SKF-96365 were reported to have higher potency in inhibiting SOCE in B lymphocyte cells; however, further studies are still needed to assess their specificity (Dago et al., 2018).

**Carboxyamidotriazole (CAI)** (Figure 5) was identified as a Ca<sup>2+</sup> influx inhibitor, showing antiproliferative and

antimetastatic effects in multiple cancer cell lines and *in vivo* xenograft models (Kohn and Liotta, 1990; Hupe et al., 1991; Kohn et al., 1992; Wasilenko et al., 1996; Wu et al., 1997). Its anticancer activity has been linked to inhibition of SOCE, but investigations have been complicated by it being a general inhibitor of non-voltage gated calcium influx (Enfissi et al., 2004). Whilst most research on CAI has focused on its anticancer effects, it has also shown promise in other fields. Through a reduction in pro-inflammatory cytokines, CAI has shown benefits in a rat model of rheumatoid arthritis (Zhu et al., 2015) and a mouse model of inflammatory bowel disease (Guo et al., 2012), although the exact molecular mechanism was not known. There is also much evidence for CAI as an anti-angiogenic agent in cancer (Luzzi et al., 1998; Bauer et al., 2000; Faehling et al., 2002) and retinal neovascularisation (Afzal et al., 2010), although it does not appear to have been investigated for pathological vascular remodelling.

**2-Aminoethylidiphenyl Borate (2-APB)** is one of the most thoroughly studied SOCE inhibitors (**Figure 5**). It was initially thought to have inhibitory effect on  $\text{Ca}^{2+}$  signalling through being a membrane permeable  $\text{IP}_3$  receptor-antagonist (Maruyama et al., 1997; Missiaen et al., 2001), and was also reported to be associated with store-operated  $\text{Ca}^{2+}$  channel inhibition; nonetheless, this inhibition was interpreted as a potential consequence of  $\text{IP}_3$  receptor inhibition (Ma et al., 2000). Then, Gregory et al. (2001) showed via whole-cell patch-clamp analysis of rat hepatoma cells that 2-APB inhibited inward  $\text{Ca}^{2+}$  current induced by  $\text{IP}_3$ , implying that 2-APB could be acting as a blocker of SOCE. This finding was further supported by the ability of 2-APB to block SOCE in  $\text{IP}_3$  receptor-knockout cells, and the observed more potent inhibition when applied extracellularly relative to intracellularly (Bakowski et al., 2001; Ma et al., 2001; Prakriya and Lewis, 2001). It was reported that this inhibitory effect is mediated via enhancing STIM1 intramolecular interactions, which subsequently maintain STIM1 at its resting state, as well as a potential direct inhibition of ORAI1 as shown by the observed 2-APB inhibition of SOCE in a STIM-independent constitutively active ORAI1 mutant (Wei et al., 2016). Interestingly, 2-APB was shown to exhibit a bimodal effect on SOCE, in which low concentrations (1–5  $\mu\text{M}$ ) promote SOCE, while higher ones (more than 10  $\mu\text{M}$ ) have a strong inhibitory effect (Prakriya and Lewis, 2001). Besides the inhibition of ORAI1, 2-APB at 50  $\mu\text{M}$  concentration showed weak inhibitory effect of ORAI2, and significantly potentiated the activity of ORAI3 channels in a store-independent manner (Lis et al., 2007; Peinelt et al., 2008). 2-APB was also shown to inhibit SERCA pumps (Bilmen et al., 2002; Peppiatt et al., 2003) and to modulate the activity of members of the TRP channel superfamily, including members of TRPM subfamily, TRPM6, TRPM7 (Li et al., 2006) and TRPM8 (Hu et al., 2004), TRPV subfamily, TRPV1, TRPV2, and TRPV3 (Hu et al., 2004) and members of TRPC subfamily, TRPC3 (Trebak et al., 2002) and TRPC6 (Hu et al., 2004). Its multiple targets and limited specificity promoted the need to develop analogues of 2-APB with improved selectivity and potency. Zhou et al. (2007), assessed the potency of 166 2-APB analogues and two analogues (DPB025 and DPB083) were identified to have

higher specificity to SOCE inhibition relative to that of 2-APB. Additionally, analogues including DPB161-AE, DPB163, and DPB162-AE that are around 100-fold more potent than 2-APB itself were identified (Zhou et al., 2007; Goto et al., 2010). It was, however, shown that the effect of DPB162-AE on  $\text{Ca}^{2+}$  signalling is not limited to inhibition of CRAC channels, but also induced  $\text{Ca}^{2+}$  leak from the ER resulting in  $\text{Ca}^{2+}$  store depletion without inhibiting SERCA pumps (Bittremieux et al., 2017). The mechanisms underlying the diverse effects of 2-APB and its analogues on SOCE remain poorly understood and more studies are still need to clarify their mechanism of action. Due to its wide range of protein targets, various clinically relevant biological effects have been observed and recently reviewed, including immunomodulatory, anti-cancer, neuroprotective, and in the GI system (Rosalez et al., 2020). Of relevance to CVD, 2-APB has been studied and shown benefits in models of atherosclerosis (Ewart et al., 2017; Simo-Cheyou et al., 2017), hypertension (Bencze et al., 2015), and vascular calcification (Lee et al., 2020), although these effects have mostly been attributed to its effects on TRP channels or the  $\text{IP}_3$  receptor.

**YM-58483**, also known as bis(trifluoromethyl)pyrazole-2 (BTP2 or Pyr2) (**Figure 5**), is a pyrazole derivative that was identified as an  $\text{I}_{\text{CRAC}}$  blocker with an  $\text{IC}_{50}$  of 10–100 nM in Jurkat T cells (Ishikawa et al., 2003; Zitt et al., 2004). YM-58483-mediated  $\text{I}_{\text{CRAC}}$  inhibition resulted in reduced T cell activation, and proliferation, as well as reduced cytokine production. It exhibits higher specificity in inhibiting CRAC channels over voltage gated  $\text{Ca}^{2+}$  channels, without off-target effects observed on ER  $\text{Ca}^{2+}$  pumps or potassium channels. Despite its remarkable potency, its inhibitory effect on  $\text{I}_{\text{CRAC}}$  is limited by the long incubation time that is needed to achieve this high potency, with around 75% inhibition of  $\text{I}_{\text{CRAC}}$  achieved within 2 h of incubation with Jurkat T cells (Zitt et al., 2004). The inhibitory effect of YM-58483 was only observed when applied extracellularly implying that it probably interacts with the extracellular side of CRAC channels (Zitt et al., 2004). In contrast, others suggested that YM-58483 inhibits  $\text{I}_{\text{CRAC}}$  through binding to an actin reorganisation protein, Drebrin, and thus disrupting actin cytoskeleton (Mercer et al., 2010). Besides inhibiting CRAC channels, YM-58483 was shown to promote the activity of TRPM4 channels at low nanomolar concentrations (Takezawa et al., 2006) and inhibit the activity of number of TRPC channels, including TRPC3, and TRPC5 (He et al., 2005). It has mostly been studied for its effects in inflammatory disease, including asthma and rheumatoid arthritis (Yoshino et al., 2007; Miyoshi et al., 2018; Sogkas et al., 2018), as well as pain and neurology (Qi et al., 2016; Orem et al., 2020). Of relevance to vascular pathology, YM-58483 and SKF-96365 have been used to characterise SOCE in models of diabetic vasculopathy, in which SOCE is reduced compared to non-diabetic VSMCs (Schach et al., 2020).

**GSK7975A, GSK5503A, and GSK5498A** are pyrazole derivatives developed by GlaxoSmithKline for inflammatory and immune disorders. GSK5498A was reported to inhibit  $\text{I}_{\text{CRAC}}$  at  $\text{IC}_{50}$  of around 1  $\mu\text{M}$  in HEK293 co-expressing STIM1 and ORAI1 (Ashmole et al., 2012). GSK7975A was shown to be effective in models of acute pancreatitis

(Gerasimenko et al., 2013; Voronina et al., 2015). GSK7975A and GSK5503A were shown to have similar inhibitory effects on  $I_{CRAC}$ . Similar to the earlier pyrazole derivative YM-58483, GSK7975A, and GSK5503A showed slow onset of  $I_{CRAC}$  inhibition. GSK7975A inhibits both ORAI1 and ORAI3 at similar  $IC_{50}$  of around 4  $\mu$ M in HEK293 cells expressing STIM1, as well as ORAI1 or ORAI3 (Derler et al., 2013). It was also reported that GSK7975A largely inhibits both ORAI1 and ORAI2, with less inhibitory effect against ORAI3 (Zhang et al., 2020). Its inhibitory effect was suggested to be mediated through direct interaction with ORAI1 channel, without affecting STIM1 oligomerisation or ORAI1-STIM1 interactions (Derler et al., 2013). This inhibitory effect was significantly reduced in cells expressing pore mutant ORAI1, relative to those expressing wildtype ORAI1, suggesting mechanism of inhibition via altering the pore geometry of ORAI1 channels (Derler et al., 2013). GSK7975A showed partial inhibition of the activity of L-type  $Ca^{2+}$  channels, and blocked TRPV6 channel activity. Failure to differentiate between ORAI1 and ORAI3 channels, as well as inhibition of L-type  $Ca^{2+}$ , and TRPV6 channels, limit its specificity as an ORAI1 channel blocker.

**Synta66 (S66) (Figure 5)** is an  $I_{CRAC}$  inhibitor showing an inhibitory effect in the micromolar concentration range. A lack of off-target effects on the inwardly rectifying  $K^{+}$  current or  $Ca^{2+}$  pumps suggested selectivity against  $I_{CRAC}$  (Ng et al., 2008). Its remarkable selectivity was then revealed by radioligand binding assays and functional assays which showed that S66 did not affect the activity of wide spectrum of receptors, and ion channels, including voltage-gated  $Ca^{2+}$  channels, and  $Na^{+}$  channels (Di Sabatino et al., 2009). In support, Li et al. (2011b) showed that S66 did not affect STIM1 aggregation, or the activity of TRPC5 channels, TRPC1/5 channels, or even the store operated non-selective cationic current. S66 showed remarkable inhibition of ORAI1 activity, whereas it showed only minimal activation of ORAI2 and inhibition of ORAI3 in HEK293 cells that lacked the three native ORAI homologs and expressed a specific individual ORAI homolog along with STIM1 (Zhang et al., 2020). Computational docking simulations have shown that S66 potentially binds to the extracellular loop 1 and 3 regions of ORAI1, which are regions at close proximity to the selectivity filter. The inhibitory effect of S66 was also shown to be weakened in cells expressing ORAI1 mutations affecting the channel selectivity. This was demonstrated by the impaired S66-mediated SOCE inhibition by the ORAI1 mutation (E106D) within the region that encodes for the glutamate residues that form the channel selectivity filter. Similar impairment of the S66 inhibitory effect was observed with other ORAI1 mutations that result into non-selective currents, like the mutant ORAI1 that carries mutations within its extracellular loop1 or loop 3 regions (Waldherr et al., 2020). S66 is a potent inhibitor of SOCE in VSMCs isolated from human saphenous veins with an  $IC_{50}$  of around 26 nM and resulted in significant reduction of VSMC migration (Li et al., 2011b). It has also been found to inhibit endothelial cell migration and tube formation *in vitro* and angiogenesis *in vivo* (Li et al., 2011a). Interestingly, S66 showed remarkably higher potency in inhibiting  $I_{CRAC}$  in VSMC than its reported potency in the RBL cells (Ng et al., 2008), Jurkat T cell

(Di Sabatino et al., 2009), and in leucocytes (Li et al., 2011b). The high potency of S66 in VSMC relative to other cell types raises the promise to selectively modulate CRAC channels in VSMC, and to enable targeting vascular remodelling. Nonetheless, the lack of information regarding the mechanisms underlying S66-induced  $I_{CRAC}$  inhibition and its poor aqueous solubility render it far from being translated into therapies.

**RO2959** was developed by Roche as a CRAC channel blocker that is effective in the nanomolar concentration range. It showed higher selectivity for ORAI1 inhibition over ORAI2 and ORAI3. It was screened against a range of ion channels, but showed no off-target effects on voltage-gated  $Ca^{2+}$  channels,  $Na^{+}$ ,  $K^{+}$  channels, members of TRPC or TRPM channels, indicating specificity in inhibiting ORAI1 channels. It was also screened against cell receptors and transporters and two receptors were considered to be inhibited by RO2959, which are the 5-hydroxytryptamine receptor 2B (5-HT2B) and the peripheral benzodiazepine (BZD) receptors, showing 87 and 89% inhibition, respectively, at 3  $\mu$ M concentration of RO2959 (Chen et al., 2013). RO2959-mediated  $I_{CRAC}$  inhibition in human  $CD4^{+}$  T cells resulted in reduction of cell proliferation and cytokine production, signifying the role of  $I_{CRAC}$  in T cell function (Chen et al., 2013). Nevertheless, the mechanism of action of RO2959 remains elusive.

**AnCoA4** was discovered by a commercial small molecule microarray of 12,000 compounds (Sadaghiani et al., 2014). Rather than screening against whole cells, this technique uses minimal functional domains, which are purified isolated domains of ORAI1 and STIM1 known to be vital for SOCE. This is to allow only small molecules that directly bind to ORAI1 or STIM1 to be identified as hits, avoiding those that indirectly affect SOCE. AnCoA4, at 20  $\mu$ M concentration, showed 80% inhibition of SOCE in HEK293 cells co-expressing STIM1 and ORAI1. A binding site for AnCoA4 on the C-terminus of ORAI1 was proposed, using a fluorescence aggregation assay, surface plasmon resonance and the FRED docking algorithm. AnCoA4 was also found to inhibit the ORAI1/STIM1 interaction, on the C-terminus, and to compete with STIM1 for ORAI1 binding, supporting the binding region prediction (Sadaghiani et al., 2014).

**The 7-azaindole series** of SOCE inhibitors was developed based on the structures of YM-58483 and Synta-66, a series of 7-azaindole SOCE inhibitors were developed for inflammatory respiratory diseases. Lead compound (14 d) inhibited SOCE with an  $IC_{50}$  of  $150 \pm 22$  nM in Jurkat T cells, and its administration in a rat model of allergic respiratory inflammation was associated with a dose-dependent inhibition of eosinophils, showing promise as a therapeutic strategy (Esteve et al., 2015).

**The indazole-3-carboxamide series** was also developed as anti-inflammatory compounds, and shows moderate SOCE inhibition, with lead compound (12 d) showing dose-dependent inhibition of mast cell activation and pro-inflammatory cytokine release in the range of 0.28–1.60  $\mu$ M  $IC_{50}$  in RBL-2H3 cells (Bai et al., 2017). In this series, the “reverse” amide bond isomers were found to have significantly reduced activity, with most only inhibiting at  $>100$   $\mu$ M. This effect has not been reported in any other ORAI1 inhibitors, and most of those containing amide

bonds are in reverse to 12 d (YM-58483, Synta-66, RO2959, GSK series, CalciMedica series). Compound (12 d) has also been developed into an indole derivative, MCS-01, which inhibits  $\text{Ca}^{2+}$  influx at 1.6  $\mu\text{M}$  and is being developed as a topical mast cell stabilising treatment to improve diabetic wound healing (Tellechea et al., 2020).

**Leflunomide and teriflunomide** were identified as weakly potent ORAI1 inhibitors alongside several other FDA-approved drugs (Rahman and Rahman, 2017). Leflunomide is used clinically as a dihydro-orotate dehydrogenase inhibitor to treat rheumatoid and psoriatic arthritis; teriflunomide was later approved for the treatment of multiple sclerosis (Fragoso and Brooks, 2015). These were identified in a virtual ligand-based screen for 3D shape and electrostatics using the structures of Synta66, AnCoA4, YM-58483 and its analogue Pyr6 as bait. Leflunomide and its active metabolite teriflunomide were identified as being able to inhibit SOCE at clinically relevant concentrations, with  $\text{IC}_{50}$  of around 10  $\mu\text{M}$  for leflunomide and 21  $\mu\text{M}$  for teriflunomide.

**CM4620** is a small-molecule ORAI1 inhibitor developed by CalciMedica, which has shown potent inhibition of ORAI1 activity with  $\text{IC}_{50}$  of 119 nM and a less potent effect against ORAI2 channels with an  $\text{IC}_{50}$  of 895 nM (CalciMedica, 2016). CM4620 was showed to be effective in reducing the severity of acute pancreatitis in pre-clinical models (Waldron et al., 2019), and reached clinical trials for acute pancreatitis and is currently being tested in Phase II clinical trials for use in patients with severe COVID-19 pneumonia (Miller et al., 2020). These ongoing clinical trials emphasise the efficacy, safety, and tolerability of ORAI1 inhibitors in patients and highlights the promising potential of using ORAI1 inhibition as new therapies. An older compound, CM3457, has shown inhibition of various interleukins and other immune functions in different cell lines (Ramos et al., 2012). It was also shown to be selective over a small panel of potassium, sodium and calcium channels, mostly those involved in cardiac function, and is effective in rat models of arthritis and asthma (Ramos et al., 2012).

**The pyrtriazole series** has been developed as an anti-inflammatory SOCE inhibitors based on the structures of the Pyr family of compounds. Lead Pyrtriazole compound (39) showed an  $\text{IC}_{50}$  of 4.4  $\mu\text{M}$  for SOCE inhibition in HEK293 cells and was reported to be selective for SOCE over voltage gated  $\text{Ca}^{2+}$  channels, TRPV1 and TRPM8, although an analogue was found to activate TRPV1. Pyrtriazole 39 was taken into a mouse model of acute pancreatitis and found to reduce oedema, inflammation and apoptosis, all hallmarks of pancreatitis. This series also contains two compounds which were unexpectedly found to be SOCE activators, activating the channel at 198–236% entry and 142–197% entry at 10  $\mu\text{M}$  in three different cell lines (Riva et al., 2018).

**Rhizen Pharmaceuticals** have developed inhibitors of SOCE for the treatment of cancers, two of which have reached clinical trials. RP3128 is orally active and effective in a guinea pig model of asthma (Vakkalanka et al., 2013; Sutovska et al., 2016), and was taken into a Phase I dose escalation safety study (Barde et al., 2020). Another compound, RP4010, has been investigated for esophageal squamous cell cancer and is potent and effective in

several cancer cell lines and in xenograft mouse models (Cui et al., 2018). It required around 2 h to demonstrate maximal inhibition of SOCE, and so may have an indirect effect on the channel rather than directly blocking ORAI1 (Cui et al., 2018). It was entered into Phase I safety studies for the treatment of relapsed non-Hodgkin's lymphoma, but the trial has been terminated, because of pharmacokinetic (PK) and safety reasons (US National Library of Medicine, 2017).

**JPIII (4-(2,5-dimethoxyphenyl)-N-[(pyridin-4-yl)methyl]aniline)** is a novel analogue of S66 that we have recently identified as a potent ORAI1 inhibitor with sufficiently improved pharmacokinetics compared to S66 (Bartoli et al., 2020). JPIII showed potent inhibitory effects of SOCE at the nanomolar range, with  $\text{IC}_{50}$  of 399 nM in HEK293 cells. Besides its potency, JPIII also showed remarkable selectivity against ORAI1, and did not affect the activity of ORAI3, TRPC5, TRPC6, TRPC4, TRPC5, TRPM2, or hERG channels. It also showed high efficacy, without any obvious side-effects when administered *in vivo* in murine models (Bartoli et al., 2020). The high potency at the target, the selectivity, the improved pharmacokinetics compared to S66, which is limited by its poor aqueous solubility, as well as the *in vivo* safety and efficacy in pre-clinical models highlight the great potential of JPIII to be used as an *in vivo* tool to study the effects of ORAI1 inhibition on VSMC biology. It is, however, limited by lack of information about the mechanism by which it inhibits ORAI1 activity.

These ORAI1 channel inhibitors are valuable tools to study the role of SOCE in health and disease, and paves the way for the development of therapeutic ORAI1 inhibitors that target pathologic remodelling. The reported implications of ORAI1-mediated signalling in VSMC phenotypic switching and in vascular pathologies highlight the therapeutic promise of ORAI1-targeted approaches. This is further supported by the role of ORAI1 in immune cell function, inflammation, and lipid homeostasis, which are key components in the development of atherosclerosis and NIH. A number of pharmacological inhibitors have now reached clinical trials for severe plaque psoriasis, acute pancreatitis, asthma and coronavirus disease 2019 (COVID-19)-associated severe pneumonia (Stauderman, 2018; Miller et al., 2020), which highlights the therapeutic potential of the ORAI1 channel inhibitors and the tolerability of the ORAI1 inhibitors in patients. Activators of ORAI1 activity, as shown in the recently developed enhancer of ORAI1 activity, IA65 (Azimi et al., 2020), could also be useful tools to help further define the role of ORAI1 in pathophysiology.

Understanding the nature of ORAI1 involvement in health and diseases holds promise to allow fine-tuning of VSMC phenotypic remodelling to its normal physiological levels. The nature of ORAI1 involvement in vascular development, angiogenesis, vascular physiology and vascular diseases is still unclear. This could be attributed to lack of information regarding ORAI1 dysregulation in adults, because of the early mortality associated with ORAI1 mutations, as well as the perinatal lethality of ORAI1 deletion in animal models. Further studies are still needed to elucidate the role of ORAI1 in vascular development, physiology and diseases, as well as the *in vivo* consequences that

could be associated with ORAI1 inhibition or over-activation in VSMC. The rapidly increasing knowledge of the implications of ORAI1 signalling in vascular remodelling holds promise to generate novel therapeutic tools for atherosclerosis and to prevent NIH following endovascular intervention.

## AUTHOR CONTRIBUTIONS

HS, KN, and MB wrote the manuscript. CC and RF reviewed and edited the manuscript. DB provided intellectual input.

## REFERENCES

- Afzal, A., Caballero, S., Palii, S. S., Jurczyk, S., Pardue, M., Geroski, D., et al. (2010). Targeting retinal and choroid neovascularization using the small molecule inhibitor carboxyamidotriazole. *Brain Res. Bull.* 81, 320–326. doi: 10.1016/j.brainresbull.2009.08.001
- Ahuja, M., Schwartz, D. M., Tandon, M., Son, A., Zeng, M., Swaim, W., et al. (2017). Orai1-mediated antimicrobial secretion from pancreatic acini shapes the gut microbiome and regulates gut innate immunity. *Cell Metab.* 25, 635–646. doi: 10.1016/j.cmet.2017.02.007
- Andreeva, E. R., Pugach, I. M., and Orekhov, A. N. (1997). Collagen-synthesizing cells in initial and advanced atherosclerotic lesions of human aorta. *Atherosclerosis* 130, 133–142. doi: 10.1016/s0021-9150(96)06056-x
- Ashmole, I., Duffy, S. M., Leyland, M. L., Morrison, V. S., Begg, M., and Bradding, P. (2012). CRACM/Orai ion channel expression and function in human lung mast cells. *J. Allergy Clin. Immunol.* 129, 1628–1635.e2. doi: 10.1016/j.jaci.2012.01.070
- Aubart, F. C., Sassi, Y., Coulombe, A., Mougenot, N., Vignaud, C., Leprince, P., et al. (2009). RNA interference targeting STIM1 suppresses vascular smooth muscle cell proliferation and neointima formation in the rat. *Mol. Ther.* 17, 455–462. doi: 10.1038/mt.2008.291
- Ávila-Medina, J., Calderón-Sánchez, E., González-Rodríguez, P., Monje-Quiroga, F., Rosado, J. A., Castellano, A., et al. (2016). Orai1 and TRPC1 proteins co-localize with Ca(V)1.2 channels to form a signal complex in vascular smooth muscle cells. *J. Biol. Chem.* 291, 21148–21159. doi: 10.1074/jbc.M116.742171
- Azimi, I., Stevenson, R. J., Zhang, X., Meizoso-Huesca, A., Xin, P., Johnson, M., et al. (2020). A new selective pharmacological enhancer of the Orai1 Ca<sup>2+</sup> channel reveals roles for Orai1 in smooth and skeletal muscle functions. *ACS Pharmacol. Transl. Sci.* 3, 135–147. doi: 10.1021/acscptsci.9b00081
- Badran, Y. R., Massaad, M. J., Bainter, W., Cangemi, B., Naseem, S. U. R., Javad, H., et al. (2016). Combined immunodeficiency due to a homozygous mutation in ORAI1 that deletes the C-terminus that interacts with STIM 1. *Clin. Immunol.* 166–167, 100–102. doi: 10.1016/j.clim.2016.03.012
- Bai, S., Nagai, M., Koerner, S. K., Veves, A., and Sun, L. (2017). Structure-activity relationship study and discovery of indazole 3-carboxamides as calcium-release activated calcium channel blockers. *Bioorg. Med. Chem. Lett.* 27, 393–397. doi: 10.1016/j.bmcl.2016.12.062
- Bakowski, D., Glitsch, M. D., and Parekh, A. B. (2001). An examination of the secretion-like coupling model for the activation of the Ca<sup>2+</sup> release-activated Ca<sup>2+</sup> current ICRAC in RBL-1 cells. *J. Physiol.* 532, 55–71. doi: 10.1111/j.1469-7793.2001.0055g.x
- Balasuriya, D., Srivats, S., Murrell-Lagnado, R. D., and Edwardson, J. M. (2014). Atomic force microscopy (AFM) imaging suggests that stromal interaction molecule 1 (STIM1) binds to Orai1 with sixfold symmetry. *FEBS Lett.* 588, 2874–2880. doi: 10.1016/j.febslet.2014.06.054
- Barde, P. J., Viswanadha, S., Veeraghavan, S., Vakkalanka, S. V., and Nair, A. (2020). A first-in-human study to evaluate the safety, tolerability and pharmacokinetics of RP3128, an oral calcium release-activated calcium (CRAC) channel modulator in healthy volunteers. *J. Clin. Pharm. Ther.* 00, 1–11. doi: 10.1111/jcpt.13322
- Bartoli, F., Bailey, M. A., Rode, B., Mateo, P., Antigny, F., Bedouet, K., et al. (2020). Orai1 channel inhibition preserves left ventricular systolic function and normal Ca<sup>2+</sup> handling after pressure overload. *Circulation* 141, 199–216. doi: 10.1161/CIRCULATIONAHA.118.038891
- Baryshnikov, S. G., Pulina, M. V., Zulian, A., Linde, C. I., and Golovina, V. A. (2009). Orai1, a critical component of store-operated Ca<sup>2+</sup> entry, is functionally associated with Na<sup>+</sup>/Ca<sup>2+</sup> exchanger and plasma membrane Ca<sup>2+</sup> pump in proliferating human arterial myocytes. *Am. J. Physiol.* 297, C1103–C1112. doi: 10.1152/ajpcell.00283.2009
- Bauer, K. S., Cude, K. J., Dixon, S. C., Kruger, E. A., and Figg, W. D. (2000). Carboxyamido-triazole inhibits angiogenesis by blocking the calcium-mediated nitric-oxide synthase-vascular endothelial growth factor pathway. *J. Pharmacol. Exp. Ther.* 292, 31–37.
- Beech, D. J. (2007). Ion channel switching and activation in smooth-muscle cells of occlusive vascular diseases. *Biochem. Soc. Trans.* 35(Pt 5), 890–894. doi: 10.1042/BST0350890
- Bencze, M., Behuliak, M., Vavrinova, A., and Zicha, J. (2015). Broad-range TRP channel inhibitors (2-APB, flufenamic acid, SKF-96365) affect differently contraction of resistance and conduit femoral arteries of rat. *Eur. J. Pharmacol.* 765, 533–540. doi: 10.1016/j.ejphar.2015.09.014
- Bergmeier, W., Oh-Hora, M., McCarl, C. A., Roden, R. C., Bray, P. F., and Feske, S. (2009). R93W mutation in Orai1 causes impaired calcium influx in platelets. *Blood* 113, 675–678. doi: 10.1182/blood-2008-08-174516
- Bilmen, J. G., Wootton, L. L., Godfrey, R. E., Smart, O. S., and Michelangeli, F. (2002). Inhibition of SERCA Ca<sup>2+</sup> pumps by 2-aminoethoxydiphenyl borate (2-APB). *Eur. J. Biochem.* 269, 3678–3687. doi: 10.1046/j.1432-1033.2002.03060.x
- Bisaillon, J. M., Motiani, R. K., Gonzalez-Cobos, J. C., Potier, M., Halligan, K. E., Alzawahra, W. F., et al. (2010). Essential role for STIM1/Orai1-mediated calcium influx in PDGF-induced smooth muscle migration. *Am. J. Physiol.* 298, C993–C1005. doi: 10.1152/ajpcell.00325.2009
- Bittremieux, M., Gerasimenko, J. V., Schuermans, M., Luyten, T., Stapleton, E., Alzayady, K. J., et al. (2017). DPB162-AE, an inhibitor of store-operated Ca<sup>2+</sup> entry, can deplete the endoplasmic reticulum Ca<sup>2+</sup> store. *Cell Calcium* 62, 60–70. doi: 10.1016/j.ceca.2017.01.015
- Böhm, J., Bulla, M., Urquhart, J. E., Malfatti, E., Williams, S. G., O'Sullivan, J., et al. (2017). ORAI1 mutations with distinct channel gating defects in tubular aggregate myopathy. *Hum. Mutat.* 38, 426–438. doi: 10.1002/humu.23172
- Braun, A., Varga-Szabo, D., Kleinschnitz, C., Pleines, I., Bender, M., Austinat, M., et al. (2009). Orai1 (CRACM1) is the platelet SOC channel and essential for pathological thrombus formation. *Blood* 113, 2056–2063. doi: 10.1182/blood-2008-07-171611
- Cai, X., Zhou, Y., Nwokonko, R. M., Loktionova, N. A., Wang, X., Xin, P., et al. (2016). The Orai1 store-operated calcium channel functions as a hexamer. *J. Biol. Chem.* 291, 25764–25775. doi: 10.1074/jbc.M116.758813
- CalciMedica, I. (2016). *Pancreatitis Treatment*. WO/2016/138472A1.
- Calloway, N., Owens, T., Corwith, K., Rodgers, W., Holowka, D., and Baird, B. (2011). Stimulated association of STIM1 and Orai1 is regulated by the balance of PtdIns(4,5)P(2) between distinct membrane pools. *J. Cell Sci.* 124, 2602–2610. doi: 10.1242/jcs.084178
- Chen, G., Panicker, S., Lau, K.-Y., Apparsundaram, S., Patel, V. A., Chen, S.-L., et al. (2013). Characterization of a novel CRAC inhibitor that potently blocks human T cell activation and effector functions. *Mol. Immunol.* 54, 355–367. doi: 10.1016/j.molimm.2012.12.011

All authors contributed to the article and approved the submitted version.

## FUNDING

This work was supported by the British Heart Foundation grant (FS/18/12/33270) to MB and DB, a British Heart Foundation student scholarship (FS/17/66/33480) to HS, and a Medical Research Council studentship to KN (MR/N013840/1) and Leeds Cardiovascular Endowment support to CC.

- Chen, K. H., Liu, H., Yang, L., Jin, M. W., and Li, G. R. (2015). SKF-96365 strongly inhibits voltage-gated sodium current in rat ventricular myocytes. *Pflugers Arch.* 467, 1227–1236. doi: 10.1007/s00424-014-1565-4
- Chou, J., Badran, Y. R., Yee, C. S. K., Bainter, W., Ohsumi, T. K., Al-Hammadi, S., et al. (2015). A novel mutation in ORAI1 presenting with combined immunodeficiency and residual T-cell function. *J. Allergy Clin. Immunol.* 136, 479–482.e1. doi: 10.1016/j.jaci.2015.03.050
- Chung, S. C., McDonald, T. V., and Gardner, P. (1994). Inhibition by SKF 96365 of  $\text{Ca}^{2+}$  current, IL-2 production and activation in T lymphocytes. *Br. J. Pharmacol.* 113, 861–868.
- Clarke, M., and Bennett, M. (2006). The Emerging role of vascular smooth muscle cell apoptosis in atherosclerosis and plaque stability. *Am. J. Nephrol.* 26, 531–535.
- Concepcion, A. R., Vaeth, M., Wagner, L. E., Eckstein, M., Hecht, L., Yang, J., et al. (2016). Store-operated  $\text{Ca}^{2+}$  entry regulates  $\text{Ca}^{2+}$ -activated chloride channels and eccrine sweat gland function. *J. Clin. Invest.* 126, 4303–4318. doi: 10.1172/jci89056
- Covington, E. D., Wu, M. M., and Lewis, R. S. (2010). Essential role for the CRAC activation domain in store-dependent oligomerization of STIM1. *Mol. Biol. Cell* 21, 1897–1907. doi: 10.1091/mbc.E10-02-0145
- Cui, C., Chang, Y., Zhang, X., Choi, S., Tran, H., Penmetsa, K. V., et al. (2018). Targeting Orai1-mediated store-operated calcium entry by RP4010 for anti-tumor activity in esophagus squamous cell carcinoma. *Cancer Lett.* 432, 169–179. doi: 10.1016/j.canlet.2018.06.006
- Dago, C. D., Maux, P. L., Roisnel, T., Brigaudeau, C., Bekro, Y.-A., Mignen, O., et al. (2018). Preliminary structure-activity relationship (SAR) of a novel series of pyrazole SKF-96365 analogues as potential store-operated calcium entry (SOCE) inhibitors. *Int. J. Mol. Sci.* 19:856. doi: 10.3390/ijms19030856
- Davis, F. M., Goulding, E. H., D'Agostin, D. M., Janardhan, K. S., Cummings, C. A., Bird, G. S., et al. (2016). Male infertility in mice lacking the store-operated  $\text{Ca}^{2+}$  channel Orai1. *Cell Calcium* 59, 189–197. doi: 10.1016/j.ceca.2016.02.007
- Deaton, R. A., Gan, Q., and Owens, G. K. (2009). Sp1-dependent activation of KLF4 is required for PDGF-BB-induced phenotypic modulation of smooth muscle. *Am. J. Physiol.* 296, H1027–H1037. doi: 10.1152/ajpheart.01230.2008
- Derler, I., Schindl, R., Fritsch, R., Heftberger, P., Riedl, M. C., Begg, M., et al. (2013). The action of selective CRAC channel blockers is affected by the Orai pore geometry. *Cell Calcium* 53, 139–151. doi: 10.1016/j.ceca.2012.11.005
- Desai, P. N., Zhang, X., Wu, S., Janoshazi, A., Bolimuntha, S., Putney, J. W., et al. (2015). Multiple types of calcium channels arising from alternative translation initiation of the Orai1 message. *Sci. Signal.* 8:ra74. doi: 10.1126/scisignal.aaa8323
- Di Sabatino, A., Rovedatti, L., Kaur, R., Spencer, J. P., Brown, J. T., Morisset, V. D., et al. (2009). Targeting Gut T Cell  $\text{Ca}^{2+}$  release-activated  $\text{Ca}^{2+}$  Channels Inhibits T Cell Cytokine Production and T-Box Transcription Factor T-Bet in inflammatory bowel disease. *The Journal of Immunology* 183, 3454–3462. doi: 10.4049/jimmunol.0802887
- Dietrich, A., Kalwa, H., Storch, U., Mederos, Y., Schnitzler, M., Salanova, B., et al. (2007). Pressure-induced and store-operated cation influx in vascular smooth muscle cells is independent of TRPC1. *Pflugers Arch.* 455, 465–477. doi: 10.1007/s00424-007-0314-3
- Dobnikar, L., Taylor, A. L., Chappell, J., Oldach, P., Harman, J. L., Oerton, E., et al. (2018). Disease-relevant transcriptional signatures identified in individual smooth muscle cells from healthy mouse vessels. *Nat. Commun.* 9:4567. doi: 10.1038/s41467-018-06891-x
- Dorairaj, P., and Panniyammakal, J. (2012). Should your family history of coronary heart disease scare you? *Mt Sinai J. Med.* 79, 721–732. doi: 10.1002/msj.21348
- Durham, A. L., Speer, M. Y., Scatena, M., Giachelli, C. M., and Shanahan, C. M. (2018). Role of smooth muscle cells in vascular calcification: implications in atherosclerosis and arterial stiffness. *Cardiovasc. Res.* 114, 590–600. doi: 10.1093/cvr/cvy010
- Endo, Y., Noguchi, S., Hara, Y., Hayashi, Y. K., Motomura, K., Murakami, N., et al. (2014). G.O.1: Dominant mutations in ORAI1 cause tubular aggregate myopathy with hypocalcemia via constitutive activation of store-operated  $\text{Ca}^{2+}$  channels. *Neuromuscular Dis.* 24:792. doi: 10.1016/j.nmd.2014.06.009
- Enfissi, A., Prigent, S., Colosetti, P., and Capiod, T. (2004). The blocking of capacitative calcium entry by 2-aminoethyl diphenylborate (2-APB) and carboxyamidotriazole (CAI) inhibits proliferation in Hep G2 and Huh-7 human hepatoma cells. *Cell Calcium* 36, 459–467. doi: 10.1016/j.ceca.2004.04.004
- Esteve, C., González, J., Gual, S., Vidal, L., Alzina, S., Sentellas, S., et al. (2015). Discovery of 7-azaindole derivatives as potent Orai inhibitors showing efficacy in a preclinical model of asthma. *Bioorg. Med. Chem. Lett.* 25, 1217–1222. doi: 10.1016/j.bmcl.2015.01.063
- Ewart, M. A., Ugusman, A., Vishwanath, A., Almabrouk, T. A. M., Alganga, H., Katwan, O. J., et al. (2017). Changes in IP3 receptor expression and function in aortic smooth muscle of atherosclerotic mice. *J. Vasc. Res.* 54, 68–78. doi: 10.1159/000461581
- Faehling, M., Kroll, J., Fohr, K. J., Fellbrich, G., Mayr, U., Trischler, G., et al. (2002). Essential role of calcium in vascular endothelial growth factor a-induced signaling: mechanism of the antiangiogenic effect of carboxyamidotriazole. *FASEB J.* 16, 1805–1807. doi: 10.1096/fj.01-0938fje
- Ferns, G. A., Reidy, M. A., and Ross, R. (1991). Balloon catheter de-endothelialization of the nude rat carotid. Response to injury in the absence of functional T lymphocytes. *Am. J. Pathol.* 138, 1045–1057.
- Feske, S., Gwack, Y., Prakriya, M., Srikanth, S., Puppel, S.-H., Tanasa, B., et al. (2006). A mutation in Orai1 causes immune deficiency by abrogating CRAC channel function. *Nature* 441:179. doi: 10.1038/nature04702
- Feske, S., Prakriya, M., Rao, A., and Lewis, R. S. (2005). A severe defect in CRAC  $\text{Ca}^{2+}$  channel activation and altered  $\text{K}^{+}$  channel gating in T cells from immunodeficient patients. *J. Exp. Med.* 202, 651–662. doi: 10.1084/jem.20050687
- Fragoso, Y. D., and Brooks, J. B. B. (2015). Leflunomide and teriflunomide: altering the metabolism of pyrimidines for the treatment of autoimmune diseases. *Expert Rev. Clin. Pharmacol.* 8, 315–320. doi: 10.1586/17512433.2015.1019343
- Franzius, D., Hoth, M., and Penner, R. (1994). Non-specific effects of calcium entry antagonists in mast cells. *Pflugers Arch.* 428, 433–438.
- Frostegard, J., Ulfgrén, A. K., Nyberg, P., Hedin, U., Swedenborg, J., Andersson, U., et al. (1999). Cytokine expression in advanced human atherosclerotic plaques: dominance of pro-inflammatory (Th1) and macrophage-stimulating cytokines. *Atherosclerosis* 145, 33–43. doi: 10.1016/S0021-9150(99)00011-8
- Fukushima, M., Tomita, T., Janoshazi, A., and Putney, J. W. (2012). Alternative translation initiation gives rise to two isoforms of Orai1 with distinct plasma membrane mobilities. *J. Cell Sci.* 125, 4354–4361. doi: 10.1242/jcs.104919
- Garibaldi, M., Fattori, F., Riva, B., Labasse, C., Brochier, G., Ottaviani, P., et al. (2017). A novel gain-of-function mutation in ORAI1 causes late-onset tubular aggregate myopathy and congenital miosis. *Clin. Genet.* 91, 780–786. doi: 10.1111/cge.12888
- Gerasimenko, J. V., Gryshchenko, O., Ferdek, P. E., Stapleton, E., Hébert, T. O. G., Bychkova, S., et al. (2013).  $\text{Ca}^{2+}$  release-activated  $\text{Ca}^{2+}$  channel blockade as a potential tool in antipneumonia therapy. *Proc. Natl. Acad. Sci.* 110, 13186–13191. doi: 10.1073/pnas.1300910110
- Gollasch, M., Haase, H., Ried, C., Lindschau, C., Morano, I., Luft, F. C., et al. (1998). L-type calcium channel expression depends on the differentiated state of vascular smooth muscle cells. *FASEB J.* 12, 593–601. doi: 10.1096/fasebj.12.7.593
- González-Cobos, J. C., Zhang, X., Zhang, W., Ruhle, B., Motiani, R. K., Schindl, R., et al. (2013). Store-independent Orai1/3 channels activated by intracrine leukotrieneC(4): role in neointimal hyperplasia. *Circ. Res.* 112, 1013–1025. doi: 10.1161/CIRCRESAHA.111.300220
- Goto, J.-I., Suzuki, A. Z., Ozaki, S., Matsumoto, N., Nakamura, T., Ebisui, E., et al. (2010). Two novel 2-aminoethyl diphenylborinate (2-APB) analogues differentially activate and inhibit store-operated  $\text{Ca}^{2+}$  entry via STIM proteins. *Cell Calcium* 47, 1–10. doi: 10.1016/j.ceca.2009.10.004
- Gregory, R. B., Rychkov, G., and Barritt, G. J. (2001). Evidence that 2-aminoethyl diphenylborate is a novel inhibitor of store-operated  $\text{Ca}^{2+}$  channels in liver cells, and acts through a mechanism which does not involve inositol trisphosphate receptors. *Biochem. J.* 354, 285–290. doi: 10.1042/bj3540285
- Grosse, J., Braun, A., Varga-Szabo, D., Beyersdorf, N., Schneider, B., Zeitlmann, L., et al. (2007). An EF hand mutation in Stim1 causes premature platelet activation and bleeding in mice. *J. Clin. Invest.* 117, 3540–3550. doi: 10.1172/JCI32312
- Guo, L., Ye, C., Hao, X., Zheng, R., Ju, R., Wu, D., et al. (2012). Carboxyamidotriazole ameliorates experimental colitis by inhibition of cytokine production, nuclear factor-kappaB activation, and colonic fibrosis. *J. Pharmacol. Exp. Ther.* 342, 356–365. doi: 10.1124/jpet.112.192849

- Guo, R. W., Wang, H., Gao, P., Li, M. Q., Zeng, C. Y., Yu, Y., et al. (2009). An essential role for stromal interaction molecule 1 in neointima formation following arterial injury. *Cardiovascular Research* 81, 660–668. doi: 10.1093/cvr/cvn338
- Guo, R.-W., Yang, L.-X., Li, M.-Q., Pan, X.-H., Liu, B., and Deng, Y.-L. (2011). Stim1- and Orail-mediated store-operated calcium entry is critical for angiotensin II-induced vascular smooth muscle cell proliferation. *Cardiovasc. Res.* 93, 360–370. doi: 10.1093/cvr/cvr307
- Gwack, Y., Srikanth, S., Feske, S., Cruz-Guilloty, F., Oh-hora, M., Neems, D. S., et al. (2007). Biochemical and functional characterization of Orail proteins. *J. Biol. Chem.* 282, 16232–16243. doi: 10.1074/jbc.M609630200
- Gwack, Y., Srikanth, S., Oh-Hora, M., Hogan, P. G., Lamperti, E. D., Yamashita, M., et al. (2008). Hair loss and defective T- and B-cell function in mice lacking ORAI1. *Mol. Cell Biol.* 28, 5209–5222. doi: 10.1128/MCB.00360-08
- Halaszovich, C. R., Zitt, C., Jüngling, E., and Lückhoff, A. (2000). Inhibition of TRP3 Channels by Lanthanides: block from the cytosolic side of the plasma membrane. *J. Biol. Chem.* 275, 37423–37428. doi: 10.1074/jbc.M007010200
- Hassock, S. R., Zhu, M. X., Trost, C., Flockerzi, V., and Authi, K. S. (2002). Expression and role of TRPC proteins in human platelets: evidence that TRPC6 forms the store-independent calcium entry channel. *Blood* 100, 2801–2811. doi: 10.1182/blood-2002-03-0723
- He, L.-P., Hewavitharana, T., Soboloff, J., Spassova, M. A., and Gill, D. L. (2005). A functional link between store-operated and TRPC channels revealed by the 3,5-bis(trifluoromethyl)pyrazole derivative, BTP2. *J. Biol. Chem.* 280, 10997–11006. doi: 10.1074/jbc.M411797200
- Hopson, K. P., Truelove, J., Chun, J., Wang, Y. M., and Waeber, C. (2011). S1P activates store-operated calcium entry via receptor- and non-receptor-mediated pathways in vascular smooth muscle cells. *Am. J. Physiol.* 300, C919–C926. doi: 10.1152/ajpcell.00350.2010
- Hoth, M., and Penner, R. (1992). Depletion of intracellular calcium stores activates a calcium current in mast cells. *Nature* 355:353. doi: 10.1038/355353a0
- Hou, X., Pedi, L., Diver, M. M., and Long, S. B. (2012). Crystal structure of the calcium release-activated calcium channel Orail. *Science* 338, 1308–1313. doi: 10.1126/science.1228757
- Hu, H.-Z., Gu, Q., Wang, C., Colton, C. K., Tang, J., Kinoshita-Kawada, M., et al. (2004). 2-Aminoethoxydiphenyl Borate Is a Common Activator of TRPV1, TRPV2, and TRPV3. *J. Biol. Chem.* 279, 35741–35748. doi: 10.1074/jbc.M404164200
- Huang, G. N., Zeng, W., Kim, J. Y., Yuan, J. P., Han, L., Muallem, S., et al. (2006). STIM1 carboxyl-terminus activates native SOC. *Icrac and TRPC1 channels. Nature Cell Biology* 8:1003. doi: 10.1038/ncb1454
- Hupe, D. J., Boltz, R., Cohen, C. J., Felix, J., Ham, E., Miller, D., et al. (1991). The inhibition of receptor-mediated and voltage-dependent calcium entry by the antiproliferative L-651,582. *J. Biol. Chem.* 266, 10136–10142.
- Hwang, S. Y., Foley, J., Numaga-Tomita, T., Petranka, J. G., Bird, G. S., and Putney, J. W. (2012). Deletion of Orail alters expression of multiple genes during osteoclast and osteoblast maturation. *Cell Calcium* 52, 488–500. doi: 10.1016/j.ceca.2012.10.001
- Ihara, E., Hirano, K., Hirano, M., Nishimura, J., Nawata, H., and Kanaide, H. (2002). Mechanism of down-regulation of L-type  $\text{Ca}^{2+}$  channel in the proliferating smooth muscle cells of rat aorta. *J. Cell Biochem.* 87, 242–251. doi: 10.1002/jcb.10295
- Iouzalen, L., Lantoin, F., Pernollet, M. G., Millanvoe-Van Brussel, E., Devynck, M. A., and David-Dufilho, M. (1996). SK&F 96365 inhibits intracellular  $\text{Ca}^{2+}$  pumps and raises cytosolic  $\text{Ca}^{2+}$  concentration without production of nitric oxide and von Willebrand factor. *Cell Calcium* 20, 501–508.
- Ishikawa, J., Ohga, K., Yoshino, T., Takezawa, R., Ichikawa, A., Kubota, H., et al. (2003). A pyrazole derivative, YM-58483, potently inhibits store-operated sustained  $\text{Ca}^{2+}$  influx and IL-2 production in T lymphocytes. *J. Immunol.* 170, 4441–4449. doi: 10.4049/jimmunol.170.9.4441
- Jardin, I., Lopez, J. J., Salido, G. M., and Rosado, J. A. (2008). Orail mediates the interaction between STIM1 and hTRPC1 and regulates the mode of activation of hTRPC1-forming  $\text{Ca}^{2+}$  channels. *J. Biol. Chem.* 283, 25296–25304. doi: 10.1074/jbc.M802904200
- Jeemon, P., Hari Krishnan, S., Sanjay, G., Sivasubramanian, S., Lekha, T. R., Padmanabhan, S., et al. (2017). A PROgramme of lifestyle intervention in families for cardiovascular risk reduction (PROLIFIC Study): design and rationale of a family based randomized controlled trial in individuals with family history of premature coronary heart disease. *BMC Public Health* 17:10. doi: 10.1186/s12889-016-3928-6
- Jia, S. P., Rodriguez, M., Williams, A. G., and Yuan, J. P. (2017). Homer binds to Orail and TRPC channels in the neointima and regulates vascular smooth muscle cell migration and proliferation. *Sci. Rep.* 7:5075. doi: 10.1038/s41598-017-04747-w
- Johnson, M. T., Gudlur, A., Zhang, X., Xin, P., Emrich, S. M., Yoast, R. E., et al. (2020). L-type  $\text{Ca}^{2+}$  channel blockers promote vascular remodeling through activation of STIM proteins. *Proc. Natl. Acad. Sci. U.S.A.* 117, 17369–17380. doi: 10.1073/pnas.2007598117
- Karnik, S. K., Brooke, B. S., Bayes-Genis, A., Sorensen, L., Wythe, J. D., Schwartz, R. S., et al. (2003). A critical role for elastin signaling in vascular morphogenesis and disease. *Development* 130, 411–423. doi: 10.1242/dev.00223
- Katsanos, K., Spiliopoulos, S., Kitrou, P., Krokidis, M., and Karnabatidis, D. (2018). Risk of death following application of paclitaxel-coated balloons and stents in the femoropopliteal artery of the leg: a systematic review and meta-analysis of randomized controlled trials. *J. Am. Heart Assoc.* 7:e011245. doi: 10.1161/JAHA.118.011245
- Kaufmann, U., Shaw, P. J., Kozhaya, L., Subramanian, R., Gaida, K., Unutmaz, D., et al. (2016). Selective ORAI1 inhibition ameliorates autoimmune central nervous system inflammation by suppressing effector but not regulatory T cell function. *J. Immunol.* 196, 573–585. doi: 10.4049/jimmunol.1501406
- Kawasaki, T., Ueyama, T., Lange, I., Feske, S., and Saito, N. (2010). Protein kinase C-induced phosphorylation of Orail regulates the intracellular  $\text{Ca}^{2+}$  level via the store-operated  $\text{Ca}^{2+}$  channel. *J. Biol. Chem.* 285, 25720–25730. doi: 10.1074/jbc.M109.022996
- Keto, J., Ventola, H., Jokelainen, J., Linden, K., Keinonen-Kiukaanniemi, S., Timonen, M., et al. (2016). Cardiovascular disease risk factors in relation to smoking behaviour and history: a population-based cohort study. *Open Heart* 3:e000358. doi: 10.1136/openhrt-2015-000358
- Kohn, E. C., and Liotta, L. A. (1990). L651582: a novel antiproliferative and antimetastasis agent. *J. Natl. Cancer Inst.* 82, 54–60. doi: 10.1093/jnci/82.1.54
- Kohn, E. C., Sandeen, M. A., and Liotta, L. A. (1992). In vivo efficacy of a novel inhibitor of selected signal transduction pathways including calcium, arachidonate, and inositol phosphates. *Cancer Res.* 52, 3208–3212.
- Kumar, B., Dreja, K., Shah, S. S., Cheong, A., Xu, S. Z., Sukumar, P., et al. (2006). Upregulated TRPC1 channel in vascular injury in vivo and its role in human neointimal hyperplasia. *Circ. Res.* 98, 557–563. doi: 10.1161/01.Res.0000204724.29685.Db
- Lee, C.-T., Ng, H.-Y., Kuo, W.-H., Tain, Y.-L., Leung, F.-F., and Lee, Y.-T. (2020). The role of TRPM7 in vascular calcification: Comparison between phosphate and uremic toxin. *Life Sci.* 260, 118280. doi: 10.1016/j.lfs.2020.118280
- Li, J., Bruns, A. F., Hou, B., Rode, B., Webster, P. J., Bailey, M. A., et al. (2015). Orail3 surface accumulation and calcium entry evoked by vascular endothelial growth factor. *Arterioscler. Thromb. Vasc. Biol.* 35, 1987–1994. doi: 10.1161/ATVBAHA.115.305969
- Li, J., Cubbon, R. M., Wilson, L. A., Amer, M. S., McKeown, L., Hou, B., et al. (2011a). Orail and CRAC channel dependence of VEGF-Activated  $\text{Ca}^{2+}$  entry and endothelial tube formation. *Circ. Res.* 108, 1190–1198. doi: 10.1161/CIRCRESAHA.111.243352
- Li, J., McKeown, L., Ojelabi, O., Stacey, M., Foster, R., O'Regan, D., et al. (2011b). Nanomolar potency and selectivity of a  $\text{Ca}^{2+}$  release-activated  $\text{Ca}^{2+}$  channel inhibitor against store-operated  $\text{Ca}^{2+}$  entry and migration of vascular smooth muscle cells. *Br. J. Pharm.* 164, 382–393. doi: 10.1111/j.1476-5381.2011.01368.x
- Li, M., Jiang, J., and Yue, L. (2006). Functional characterization of homo- and heteromeric channel kinases TRPM6 and TRPM7. *J. Gen. Physiol.* 127, 525–537. doi: 10.1085/jgp.200609502
- Lian, J., Cuk, M., Kahlfuss, S., Kozhaya, L., Vaeth, M., Rieux-Laucat, F., et al. (2018). ORAI1 mutations abolishing store-operated  $\text{Ca}^{2+}$  entry cause anhidrotic ectodermal dysplasia with immunodeficiency. *J. Allergy Clin. Immunol.* 142, 1297.e–1310.e. doi: 10.1016/j.jaci.2017.10.031
- Liang, S. J., Zeng, D. Y., Mai, X. Y., Shang, J. Y., Wu, Q. Q., Yuan, J. N., et al. (2016). Inhibition of Orail store-operated calcium channel prevents foam cell formation and atherosclerosis. *Arterioscler. Thromb. Vasc. Biol.* 36, 618–628. doi: 10.1161/Atvbaha.116.307344
- Liou, J., Fivaz, M., Inoue, T., and Meyer, T. (2007). Live-cell imaging reveals sequential oligomerization and local plasma membrane targeting of stromal

- interaction molecule 1 after  $\text{Ca}^{2+}$  store depletion. *Proc. Natl. Acad. Sci. U.S.A.* 104, 9301–9306. doi: 10.1073/pnas.0702866104
- Liou, J., Kim, M. L., Heo, W. D., Jones, J. T., Myers, J. W., Ferrell, J. E., et al. (2005). STIM is a  $\text{Ca}^{2+}$  sensor essential for  $\text{Ca}^{2+}$ -store-depletion-triggered  $\text{Ca}^{2+}$  influx. *Curr. Biol.* 15, 1235–1241. doi: 10.1016/j.cub.2005.05.055
- Lis, A., Peinelt, C., Beck, A., Parvez, S., Monteilh-Zoller, M., Fleig, A., et al. (2007). CRACM1, CRACM2, and CRACM3 are store-operated  $\text{Ca}^{2+}$  channels with distinct functional properties. *Curr. Biol.* 17, 794–800. doi: 10.1016/j.cub.2007.03.065
- Liu, B., Zhang, B., Roos, C. M., Zeng, W., Zhang, H., and Guo, R. (2020). Upregulation of Orai1 and increased calcium entry contribute to angiotensin II-induced human coronary smooth muscle cell proliferation: Running Title: Angiotensin II-induced human coronary smooth muscle cells proliferation. *Peptides* 133, 170386. doi: 10.1016/j.peptides.2020.170386
- Liu, X., Cheng, K. T., Bandyopadhyay, B. C., Pani, B., Dietrich, A., Paria, B. C., et al. (2007). Attenuation of store-operated  $\text{Ca}^{2+}$  current impairs salivary gland fluid secretion in TRPC1(−/−) mice. *Proc. Natl. Acad. Sci. U.S.A.* 104, 17542–17547. doi: 10.1073/pnas.0701254104
- Liu, X., Singh, B. B., and Ambudkar, I. S. (2003). TRPC1 is required for functional store-operated  $\text{Ca}^{2+}$  channels: role of acidic amino acid residues in the S5-S6 region. *J. Biol. Chem.* 278, 11337–11343. doi: 10.1074/jbc.M213271200
- Luik, R. M., Wang, B., Prakriya, M., Wu, M. M., and Lewis, R. S. (2008). Oligomerization of STIM1 couples ER calcium depletion to CRAC channel activation. *Nature* 454:538. doi: 10.1038/nature07065
- Luzzi, K. J., Varghese, H. J., MacDonald, I. C., Schmidt, E. E., Kohn, E. C., Morris, V. L., et al. (1998). Inhibition of angiogenesis in liver metastases by carboxyamidotriazole (CAI). *Angiogenesis* 2, 373–379. doi: 10.1023/a:1009259521092
- Ma, H.-T., Patterson, R. L., van Rossum, D. B., Birnbaumer, L., Mikoshiba, K., et al. (2000). Requirement of the inositol trisphosphate receptor for activation of store-operated  $\text{Ca}^{2+}$  channels. *Science* 287, 1647–1651. doi: 10.1126/science.287.5458.1647
- Ma, H.-T., Venkatachalam, K., Li, H.-S., Montell, C., Kurosaki, T., Patterson, R. L., et al. (2001). Assessment of the role of the inositol 1,4,5-trisphosphate receptor in the activation of transient receptor potential channels and store-operated  $\text{Ca}^{2+}$  entry channels. *J. Biol. Chem.* 276, 18888–18896. doi: 10.1074/jbc.M100944200
- Ma, K., Liu, P., Al-Maghout, T., Sukkar, B., Cao, H., Voelkl, J., et al. (2019). Phosphate-induced Orai1 expression and store-operated  $\text{Ca}^{2+}$  entry in aortic smooth muscle cells. *J. Mol. Med. (Berl)* 97, 1465–1475. doi: 10.1007/s00109-019-01824-7
- Ma, K., Sukkar, B., Zhu, X., Zhou, K., Cao, H., Voelkl, J., et al. (2020). Stimulation of Orai1 expression, store-operated  $\text{Ca}^{2+}$  entry, and osteogenic signaling by high glucose exposure of human aortic smooth muscle cells. *Pflugers Arch.* 472, 1093–1102. doi: 10.1007/s00424-020-02405-1
- Mancarella, S., Potireddy, S., Wang, Y. J., Gao, H., Gandhirajan, R. K., Autieri, M., et al. (2013). Targeted STIM deletion impairs calcium homeostasis, NFAT activation, and growth of smooth muscle. *FASEB J.* 27, 3408–3408. doi: 10.1096/fj.11-183350.ERR
- Markello, T., Chen, D., Kwan, J. Y., Horkayne-Szakaly, I., Morrison, A., Simakova, O., et al. (2015). York platelet syndrome is a CRAC channelopathy due to gain-of-function mutations in STIM1. *Mol. Gen. Metab.* 114, 474–482. doi: 10.1016/j.ymgme.2014.12.307
- Maruyama, T., Kanaji, T., Nakade, S., Kanno, T., and Mikoshiba, K. (1997). 2APB, 2-aminoethoxydiphenyl borate, a membrane-penetrable modulator of  $\text{Ins}(1,4,5)\text{P}_3$ -induced  $\text{Ca}^{2+}$  release. *J. Biochem.* 122, 498–505.
- Massberg, S., Brand, K., Gruner, S., Page, S., Muller, E., Muller, I., et al. (2002). A critical role of platelet adhesion in the initiation of atherosclerotic lesion formation. *Journal of Experimental Medicine* 196, 887–896. doi: 10.1084/jem.20012044
- Maus, M., Cuk, M., Patel, B., Lian, J., Ouimet, M., Kaufmann, U., et al. (2017). Store-operated  $\text{Ca}^{2+}$  entry controls induction of lipolysis and the transcriptional reprogramming to lipid metabolism. *Cell Metab.* 25, 698–712. doi: 10.1016/j.cmet.2016.12.021
- McCarl, C.-A., Picard, C., Khalil, S., Kawasaki, T., Röther, J., Papolos, A., et al. (2009). Orai1 deficiency and lack of store-operated  $\text{Ca}^{2+}$  entry cause immunodeficiency, myopathy and ectodermal dysplasia. *J. Allergy Clin. Immunol.* 124, 1311–1318.e7. doi: 10.1016/j.jaci.2009.10.007
- McKeown, L., Moss, N. K., Turner, P., Li, J., Heath, N., Burke, D., et al. (2012). PDGF maintains stored calcium through a non-clustering Orai1 mechanism but evokes clustering if the ER is stressed by store-depletion. *Circu.Res.* 111, 66–76. doi: 10.1161/CIRCRESAHA.111.263616
- McNally, B. A., Yamashita, M., Engh, A., and Prakriya, M. (2009). Structural determinants of ion permeation in CRAC channels. *Proc. Natl. Acad. Sci. U.S.A.* 106, 22516–22521. doi: 10.1073/pnas.0909574106
- Mercer, J. C., Qi, Q., Mottram, L. F., Law, M., Bruce, D., Iyer, A., et al. (2010). Chemico-genetic identification of Drebrin as a regulator of calcium responses. *Intl. J. Biochem.* 42, 337–345. doi: 10.1016/j.biocel.2009.11.019
- Merritt, J. E., Armstrong, W. P., Benham, C. D., Hallam, T. J., Jacob, R., Jaxa-Chamiec, A., et al. (1990). SK&F 96365, a novel inhibitor of receptor-mediated calcium entry. *Biochem. J.* 271, 515–522.
- Methia, N., Andre, P., Denis, C. V., Economopoulos, M., and Wagner, D. D. (2001). Localized reduction of atherosclerosis in von Willebrand factor-deficient mice. *Blood* 98, 1424–1428. doi: 10.1182/blood.V98.5.1424
- Miller, J., Bruen, C., Schnaus, M., Zhang, J., Ali, S., Lind, A., et al. (2020). Auxora versus standard of care for the treatment of severe or critical COVID-19 pneumonia: results from a randomized controlled trial. *Crit. Care* 24:502. doi: 10.1186/s13054-020-03220-x
- Missiaen, L., Callewaert, G., De Smedt, H., and Parys, J. B. (2001). 2-Aminoethoxydiphenyl borate affects the inositol 1,4,5-trisphosphate receptor, the intracellular  $\text{Ca}^{2+}$  pump and the non-specific  $\text{Ca}^{2+}$  leak from the non-mitochondrial  $\text{Ca}^{2+}$  stores in permeabilized A7r5 cells. *Cell Calcium* 29, 111–116. doi: 10.1054/ceca.2000.0163
- Miyoshi, M., Liu, S., Morizane, A., Takemasa, E., Suzuki, Y., Kiyoi, T., et al. (2018). Efficacy of constant long-term delivery of YM-58483 for the treatment of rheumatoid arthritis. *Eur. J. Pharmacol.* 824, 89–98. doi: 10.1016/j.ejphar.2018.02.006
- Moses, J. W., Leon, M. B., Popma, J. J., Fitzgerald, P. J., Holmes, D. R., O'Shaughnessy, C., et al. (2003). Sirolimus-eluting stents versus standard stents in patients with stenosis in a native coronary artery. *N. Engl. J. Med.* 349, 1315–1323. doi: 10.1056/NEJMoa035071
- Nagy, M., Mastenbroek, T. G., Mattheij, N. J. A., de Witt, S., Clemetson, K. J., Kirschner, J., et al. (2018). Variable impairment of platelet functions in patients with severe, genetically linked immune deficiencies. *Haematologica* 103, 540–549. doi: 10.3324/haematol.2017.176974
- Nesin, V., Wiley, G., Kousi, M., Ong, E.-C., Lehmann, T., Nicholl, D. J., et al. (2014). Activating mutations in STIM1 and Orai1 cause overlapping syndromes of tubular myopathy and congenital miosis. *Proc. Natl. Acad. Sci. U.S.A.* 111, 4197–4202. doi: 10.1073/pnas.1312520111
- Ng, L. C., O'Neill, K. G., French, D., Airey, J. A., Singer, C. A., Tian, H. L., et al. (2012). TRPC1 and Orai1 interact with STIM1 and mediate capacitative  $\text{Ca}^{2+}$  entry caused by acute hypoxia in mouse pulmonary arterial smooth muscle cells. *Am. J. Physiol.* 303, C1156–C1172. doi: 10.1152/ajpcell.00065.2012
- Ng, S. W., di Capite, J., Singaravelu, K., and Parekh, A. B. (2008). Sustained activation of the tyrosine kinase Syk by antigen in mast cells requires local  $\text{Ca}^{2+}$  influx through  $\text{Ca}^{2+}$  release-activated  $\text{Ca}^{2+}$  channels. *J. Biol. Chem.* 283, 31348–31355. doi: 10.1074/jbc.M804942200
- Ogawa, A., Firth, A. L., Smith, K. A., Maliakal, M. V., and Yuan, J. X. J. (2012). PDGF enhances store-operated  $\text{Ca}^{2+}$  entry by upregulating STIM1/Orai1 via activation of Akt/mTOR in human pulmonary arterial smooth muscle cells. *Am. J. Physiol.* 302, C405–C411. doi: 10.1152/ajpcell.00337.2011
- Okada, Y., Katsuda, S., Watanabe, H., and Nakanishi, I. (1993). Collagen synthesis of human arterial smooth muscle cells: effects of platelet-derived growth factor, transforming growth factor-beta 1 and interleukin-1. *Acta Pathol Jpn* 43, 160–167. doi: 10.1111/j.1440-1827.1993.tb01127.x
- Onouchi, Y., Fukazawa, R., Yamamura, K., Suzuki, H., Kakimoto, N., Suenaga, T., et al. (2016). Variations in Orai1 gene associated with kawasaki disease. *PLoS One* 11:e0145486. doi: 10.1371/journal.pone.0145486
- Orem, B. C., Partain, S. B., and Stirling, D. P. (2020). Inhibiting store-operated calcium entry attenuates white matter secondary degeneration following SCI. *Neurobiol Dis* 136:104718. doi: 10.1016/j.nbd.2019.104718
- Otsuka, F., Kramer, M. C. A., Woudstra, P., Yahagi, K., Ladich, E., Finn, A. V., et al. (2015). Natural progression of atherosclerosis from pathologic intimal thickening to late fibroatheroma in human coronary arteries: A pathology study. *Atherosclerosis* 241, 772–782. doi: 10.1016/j.atherosclerosis.2015.05.011

- Owens, G. K., Kumar, M. S., and Wamhoff, B. R. (2004). Molecular regulation of vascular smooth muscle cell differentiation in development and disease. *Physiol. Rev.* 84, 767–801. doi: 10.1152/physrev.00041.2003
- Park, C. Y., Hoover, P. J., Mullins, F. M., Bachhawat, P., Covington, E. D., Raunser, S., et al. (2009). STIM1 clusters and activates CRAC channels via direct binding of a cytosolic domain to Orai1. *Cell* 136, 876–890. doi: 10.1016/j.cell.2009.02.014
- Peckys, D. B., Alansary, D., Niemeyer, B. A., and de Jonge, N. (2016). Visualizing quantum dot labeled Orai1 proteins in intact cells via correlative light and electron microscopy. *Microsc. Microanal.* 22, 902–912. doi: 10.1017/S1431927616011491
- Peinelt, C., Lis, A., Beck, A., Fleig, A., and Penner, R. (2008). 2-Aminoethoxydiphenyl borate directly facilitates and indirectly inhibits STIM1-dependent gating of CRAC channels. *J. Physiol.* 586(Pt 13), 3061–3073. doi: 10.1113/jphysiol.2008.151365
- Peinelt, C., Vig, M., Koomoa, D. L., Beck, A., Nadler, M. J. S., Koblan-Huberson, M., et al. (2006). Amplification of CRAC current by STIM1 and CRACM1 (Orai1). *Nat. Cell Biol.* 8:771. doi: 10.1038/ncb1435
- Peppiatt, C. M., Collins, T. J., Mackenzie, L., Conway, S. J., Holmes, A. B., Bootman, M. D., et al. (2003). 2-Aminoethoxydiphenyl borate (2-APB) antagonises inositol 1,4,5-trisphosphate-induced calcium release, inhibits calcium pumps and has a use-dependent and slowly reversible action on store-operated calcium entry channels. *Cell Calcium* 34, 97–108. doi: 10.1016/S0143-4160(03)00026-5
- Poirier, P., Giles, T. D., Bray, G. A., Hong, Y., Stern, J. S., Pi-Sunyer, F. X., et al. (2006). Obesity and cardiovascular disease. Pathophysiology, Evaluation, and Effect of Weight Loss. *Arterioscler Thromb Vasc Biol.* 26, 968–976. doi: 10.1161/01.ATV.0000216787.85457.f3
- Potier, M., Gonzalez, J. C., Motiani, R. K., Abdullaev, I. F., Bisailon, J. M., Singer, H. A., et al. (2009). Evidence for STIM1- and Orai1-dependent store-operated calcium influx through I-CRAC in vascular smooth muscle cells: role in proliferation and migration. *FASEB J.* 23, 2425–2437. doi: 10.1096/fj.09-131128
- Prakriya, M., Feske, S., Gwack, Y., Srikanth, S., Rao, A., and Hogan, P. G. (2006). Orai1 is an essential pore subunit of the CRAC channel. *Nature* 443:230. doi: 10.1038/nature05122
- Prakriya, M., and Lewis, R. S. (2001). Potentiation and inhibition of  $\text{Ca}^{2+}$  release-activated  $\text{Ca}^{2+}$  channels by 2-aminoethylidiphenyl borate (2-APB) occurs independently of IP(3) receptors. *J. Physiol.* 536(Pt 1), 3–19. doi: 10.1111/j.1469-7793.2001.t01-1-00003.x
- Pratico, D., Tillmann, C., Zhang, Z. B., Li, H. W., and FitzGerald, G. A. (2001). Acceleration of atherogenesis by COX-1-dependent prostanoid formation in low density lipoprotein receptor knockout mice. *Proc. Natl. Acad. Sci. U.S.A.* 98, 3358–3363. doi: 10.1073/pnas.061607398
- Putney, J. W. Jr. (1977). Muscarinic, alpha-adrenergic and peptide receptors regulate the same calcium influx sites in the parotid gland. *J. Physiol.* 268, 139–149.
- Putney, J. W. (1986). A model for receptor-regulated calcium entry. *Cell Calcium* 7, 1–12. doi: 10.1016/0143-4160(86)90026-6
- Qi, Z., Wang, Y., Zhou, H., Liang, N., Yang, L., Liu, L., et al. (2016). The Central Analgesic Mechanism of YM-58483 in Attenuating Neuropathic Pain in Rats. *Cell Mol. Neurobiol.* 36, 1035–1043. doi: 10.1007/s10571-015-0292-5
- Rahman, S., and Rahman, T. (2017). Unveiling some FDA-approved drugs as inhibitors of the store-operated  $\text{Ca}^{2+}$  entry pathway. *Sci. Rep.* 7:12881. doi: 10.1038/s41598-017-13343-x
- Ramos, S., Grigoryev, S., Rogers, E., Roos, J., Whitten, J., Stauderman, K., et al. (2012). CM3457, a potent and selective oral CRAC channel inhibitor, suppresses T and mast cell function and is efficacious in rat models of arthritis and asthma (72.3). *J. Immunol.* 188(1 Supplement), 72.3.
- Reichling, D. B., and MacDermott, A. B. (1991). Lanthanum actions on excitatory amino acid-gated currents and voltage-gated calcium currents in rat dorsal horn neurons. *J. Physiol.* 441, 199–218.
- Riva, B., Griglio, A., Serafini, M., Cordero-Sanchez, C., Aprile, S., Di Paola, R., et al. (2018). Pyrrizoles, a novel class of store-operated calcium entry modulators: discovery, biological profiling, and in vivo proof-of-concept efficacy in acute pancreatitis. *J. Med. Chem.* 61, 9756–9783. doi: 10.1021/acs.jmedchem.8b01512
- Robinson, L. J., Mancarella, S., Songsawad, D., Tourkova, I. L., Barnett, J. B., Gill, D. L., et al. (2012). Gene disruption of the calcium channel Orai1 results in inhibition of osteoclast and osteoblast differentiation and impairs skeletal development. *Lab. Invest.* 92, 1071–1083. doi: 10.1038/labinvest.2012.72
- Rode, B., Bailey, M. A., Marthan, R., Beech, D. J., and Guibert, C. (2018). Orai1 channels as potential therapeutic targets in pulmonary hypertension. *Physiology* 33, 261–268. doi: 10.1152/physiol.00016.2018
- Rodríguez-Moyano, M., Díaz, I., Dionisio, N., Zhang, X., Ávila-Medina, J., Calderón-Sánchez, E., et al. (2013). Urotensin-II promotes vascular smooth muscle cell proliferation through store-operated calcium entry and EGFR transactivation. *Cardiovasc. Res.* 100, 297–306. doi: 10.1093/cvr/cvt196
- Roos, J., DiGregorio, P. J., Yeromin, A. V., Ohlsen, K., Lioudyno, M., Zhang, S. Y., et al. (2005). STIM1, an essential and conserved component of store-operated  $\text{Ca}^{2+}$  channel function. *J. Cell Biol.* 169, 435–445. doi: 10.1093/jcb.200502019
- Rosado, J. A., Brownlow, S. L., and Sage, S. O. (2002). Endogenously expressed Trp1 is involved in store-mediated  $\text{Ca}^{2+}$  entry by conformational coupling in human platelets. *J. Biol. Chem.* 277, 42157–42163. doi: 10.1074/jbc.M207320200
- Rosalde, M. N., Estevez-Fregoso, E., Alatorre, A., Abad-García, A., and Soriano-Urúa, M. A. (2020). 2-Aminoethylidiphenyl Borinate: A Multitarget Compound with Potential as a Drug Precursor. *Curr. Mol. Pharm.* 13, 57–75. doi: 10.2174/1874467212666191025145429
- Rydén, L., Grant, P. J., Anker, S. D., Berne, C., Cosentino, F., Danchin, N., et al. (2013). ESC Guidelines on diabetes, pre-diabetes, and cardiovascular diseases developed in collaboration with the EASD The Task Force on diabetes, pre-diabetes, and cardiovascular diseases of the European Society of Cardiology (ESC) and developed in collaboration with the European Association for the Study of Diabetes (EASD). *Eur. Heart J.* 34, 3035–3087. doi: 10.1093/eurheartj/eh108
- Sadaghiani, A. M., Lee, S. M., Odegaard, J. I., Leveson-Gower, D. B., McPherson, O. M., Novick, P., et al. (2014). Identification of Orai1 channel inhibitors by using minimal functional domains to screen small molecule microarrays. *Chem. Biol.* 21, 1278–1292. doi: 10.1016/j.chembiol.2014.08.016
- Schach, C., Wester, M., Leibl, F., Redel, A., Gruber, M., Maier, L. S., et al. (2020). Reduced store-operated  $\text{Ca}^{2+}$  entry impairs mesenteric artery function in response to high external glucose in type 2 diabetic ZDF rats. *Clin. Exp. Pharmacol. Physiol.* 47, 1145–1157. doi: 10.1111/1440-1681.13300
- Shah, A. D., Langenberg, C., Rapsomaniki, E., Denaxas, S., Pujades-Rodriguez, M., Gale, C. P., et al. (2015). Type 2 diabetes and incidence of cardiovascular diseases: a cohort study in 1.9 million people. *Lancet Diabetes Endocrinol.* 3, 105–113. doi: 10.1016/S2213-8587(14)70219-0
- Shankman, L. S., Gomez, D., Cherepanova, O. A., Salmon, M., Alencar, G. F., Haskins, R. M., et al. (2015). KLF4-dependent phenotypic modulation of smooth muscle cells has a key role in atherosclerotic plaque pathogenesis. *Nat. Med.* 21:628. doi: 10.1038/nm.3866
- Silber, S., Serruys, P. W., Leon, M. B., Meredith, I. T., Windecker, S., Neumann, F.-J., et al. (2013). Clinical outcome of patients with and without diabetes mellitus after percutaneous coronary intervention with the resolute zotarolimus-eluting stent: 2-year results from the prospectively pooled analysis of the international global RESOLUTE Program. *JACC: Cardiovasc. Interv.* 6, 357–368. doi: 10.1016/j.jcin.2012.11.006
- Simo-Cheyou, E. R., Tan, J. J., Grygorczyk, R., and Srivastava, A. K. (2017). STIM-1 and Orai-1 channel mediate angiotensin-II-induced expression of Egr-1 in vascular smooth muscle cells. *J. Cell Physiol.* 232, 3496–3509. doi: 10.1002/jcp.25810
- Singh, A., Hildebrand, M. E., Garcia, E., and Snutch, T. P. (2010). The transient receptor potential channel antagonist SKF96365 is a potent blocker of low-voltage-activated T-type calcium channels. *Br. J. Pharmacol.* 160, 1464–1475. doi: 10.1111/j.1476-5381.2010.00786.x
- Sinkins, W. G., Estacion, M., and Schilling, W. P. (1998). Functional expression of TrpC1: a human homologue of the Drosophila Trp channel. *Biochem. J.* 331(Pt 1), 331–339.
- Sogkas, G., Rau, E., Atschekzei, F., Syed, S. N., and Schmidt, R. E. (2018). The Pyrazole Derivative BTP2 Attenuates IgG Immune Complex-induced Inflammation. *Inflammation* 41, 42–49. doi: 10.1007/s10753-017-0661-y
- Somasundaram, A., Shum, A. K., McBride, H. J., Kessler, J. A., Feske, S., Miller, R. J., et al. (2014). Store-operated CRAC channels regulate gene expression and proliferation in neural progenitor cells. *J. Neurosci.* 34, 9107–9123. doi: 10.1523/JNEUROSCI.0263-14.2014
- Song, M., Chen, D., and Yu, S. P. (2014). The TRPC channel blocker SKF 96365 inhibits glioblastoma cell growth by enhancing reverse mode of the  $\text{NaCa}^{+}/\text{Ca}^{2+}$  exchanger and increasing intracellular  $\text{Ca}^{2+}$ . *Br. J. Pharmacol.* 171, 3432–3447. doi: 10.1111/bph.12691

- Sorokin, V., Vickneson, K., Kofidis, T., Woo, C. C., Lin, X. Y., Foo, R., et al. (2020). Role of vascular smooth muscle cell plasticity and interactions in vessel wall inflammation. *Front. Immunol.* 11:599415. doi: 10.3389/fimmu.2020.599415
- Spassova, M. A., Soboloff, J., He, L.-P., Xu, W., Dziadek, M. A., and Gill, D. L. (2006). STIM1 has a plasma membrane role in the activation of store-operated  $\text{Ca}^{2+}$  channels. *Proc. Natl Acad. Sci. U.S.A.* 103, 4040–4045. doi: 10.1073/pnas.0510050103
- Stathopoulos, P. B., Li, G. Y., Plevin, M. J., Ames, J. B., and Ikura, M. (2006). Stored  $\text{Ca}^{2+}$  depletion-induced oligomerization of stromal interaction molecule 1 (STIM1) via the EF-SAM region: An initiation mechanism for capacitive  $\text{Ca}^{2+}$  entry. *J. Biol. Chem.* 281, 35855–35862. doi: 10.1074/jbc.M608247200
- Stauderman, K. A. (2018). CRAC channels as targets for drug discovery and development. *Cell Calcium* 74, 147–159. doi: 10.1016/j.ceca.2018.07.005
- Strübing, C., Krapivinsky, G., Krapivinsky, L., and Clapham, D. E. (2001). TRPC1 and TRPC5 form a novel cation channel in mammalian brain. *Neuron* 29, 645–655. doi: 10.1016/S0896-6273(01)00240-9
- Sutovska, M., Kocmalova, M., Franova, S., Vakkalanka, S., and Viswanadha, S. (2016). Pharmacodynamic evaluation of RP3128, a novel and potent CRAC channel inhibitor in guinea pig models of allergic asthma. *Eur. J. Pharmacol.* 772, 62–70. doi: 10.1016/j.ejphar.2015.12.047
- Takemura, H., Hughes, A. R., Thastrup, O., and Putney, J. W. (1989). Activation of calcium entry by the tumor promoter thapsigargin in parotid acinar cells. Evidence that an intracellular calcium pool and not an inositol phosphate regulates calcium fluxes at the plasma membrane. *J. Biol. Chem.* 264, 12266–12271.
- Takezawa, R., Cheng, H., Beck, A., Ishikawa, J., Launay, P., Kubota, H., et al. (2006). A pyrazole derivative potently inhibits lymphocyte  $\text{Ca}^{2+}$  influx and cytokine production by facilitating transient receptor potential melastatin 4 channel activity. *Mol. Pharmacol.* 69, 1413–1420. doi: 10.1124/mol.105.021154
- Tanahashi, Y., Wang, B., Murakami, Y., Unno, T., Matsuyama, H., Nagano, H., et al. (2016). Inhibitory effects of SKF96365 on the activities of  $\text{K}^{+}$  channels in mouse small intestinal smooth muscle cells. *J. Vet Med. Sci.* 78, 203–211. doi: 10.1292/jvms.15-0346
- Tellechea, A., Bai, S., Dangwal, S., Theocharidis, G., Nagai, M., Koerner, S., et al. (2020). Topical application of a mast cell stabilizer improves impaired diabetic wound healing. *J. Invest. Dermatol.* 140, 901–911.e11. doi: 10.1016/j.jid.2019.08.449
- Tellides, G., Tereb, D. A., Kirkiles-Smith, N. C., Kim, R. W., Wilson, J. H., Schechner, J. S., et al. (2000). Interferon-gamma elicits arteriosclerosis in the absence of leukocytes. *Nature* 403, 207–211. doi: 10.1038/35003221
- Thiha, K., Mashimo, Y., Suzuki, H., Hamada, H., Hata, A., Hara, T., et al. (2019). Investigation of novel variations of ORAI1 gene and their association with Kawasaki disease. *J. Hum. Genet.* 64, 511–519. doi: 10.1038/s10038-019-0588-2
- Thomas, J. A., Deaton, R. A., Hastings, N. E., Shang, Y., Moehle, C. W., Eriksson, U., et al. (2009). PDGF-DD, a novel mediator of smooth muscle cell phenotypic modulation, is upregulated in endothelial cells exposed to atherosclerosis-prone flow patterns. *Am. J. Physiol.* 296, H442–H452. doi: 10.1152/ajpheart.00165.2008
- Thompson, J. L., and Shuttleworth, T. J. (2013). How Many OraIs Does It Take to Make a CRAC Channel? *Sci. Rep.* 3, 1961. doi: 10.1038/srep01961
- Trebak, M., Bird, G. S., McKay, R. R., and Putney, J. W. Jr. (2002). Comparison of human TRPC3 channels in receptor-activated and store-operated modes: Differential sensitivity to channel blockers suggests fundamental differences in channel composition. *J. Biol. Chem.* 277, 21617–21623. doi: 10.1074/jbc.M202549200
- US National Library of Medicine (2017). *Safety and Efficacy Study of RP4010, in Patients With Relapsed or Refractory Lymphomas*. Available online at: <https://clinicaltrials.gov/ct2/show/NCT03119467?term=RP4010&draw=2&rank=1> (Accessed 10 January 2021).
- Vaeth, M., Yang, J., Yamashita, M., Zee, I., Eckstein, M., Knosp, C., et al. (2017). ORAI2 modulates store-operated calcium entry and T cell-mediated immunity. *Nat. Commun.* 8, 14714. doi: 10.1038/Ncomms14714
- Vakkalanka, S., Merikapudi, G., Babu, G., Routhu, K., Veeraraghavan, S., and Viswanadha, S. (2013). Pre-clinical characterization of RP3128, a novel and potent CRAC channel inhibitor for the treatment of respiratory disorders. *Eur. Respir. J.* 42(Suppl 57):1583.
- Varga-Szabo, D., Braun, A., Kleinschnitz, C., Bender, M., Pleines, I., Pham, M., et al. (2008). The calcium sensor STIM1 is an essential mediator of arterial thrombosis and ischemic brain infarction. *J. Exp. Med.* 205, 1583–1591. doi: 10.1084/jem.20080302
- Vig, M., DeHaven, W. I., Bird, G. S., Billingsley, J. M., Wang, H., Rao, P. E., et al. (2008). Defective mast cell effector functions in mice lacking the CRACM1 pore subunit of store-operated calcium release-activated calcium channels. *Nat. Immunol.* 9, 89–96. doi: 10.1038/ni1550
- Virman, R., Kolodgie, F. D., Burke, A. P., Farb, A., and Schwartz, S. M. (2000). Lessons from sudden coronary death - A comprehensive morphological classification scheme for atherosclerotic lesions. *Arterioscler. Thromb. Vasc. Biol.* 20, 1262–1275.
- Volkers, M., Dolatabadi, N., Gude, N., Most, P., Sussman, M. A., and Hassel, D. (2012). Orai1 deficiency leads to heart failure and skeletal myopathy in zebrafish. *J. Cell Sci.* 125, 287–294. doi: 10.1242/jcs.090464
- Voronina, S., Collier, D., Chvanov, M., Middlehurst, B., Beckett, A. J., Prior, I. A., et al. (2015). The role of  $\text{Ca}^{2+}$  influx in endocytic vacuole formation in pancreatic acinar cells. *Biochem. J.* 465, 405–412. doi: 10.1042/BJ20140398
- Waldherr, L., Tiffner, A., Mishra, D., Sallinger, M., Schober, R., Frischauf, I., et al. (2020). Blockage of Store-Operated  $\text{Ca}^{2+}$  Influx by Synta66 is Mediated by Direct Inhibition of the  $\text{Ca}^{2+}$  Selective Orai1 Pore. *Cancers* 12, 2876. doi: 10.3390/cancers12102876
- Waldron, R. T., Chen, Y., Pham, H., Go, A., Su, H.-Y., Hu, C., et al. (2019). The Orai  $\text{Ca}^{2+}$  channel inhibitor CM4620 targets both parenchymal and immune cells to reduce inflammation in experimental acute pancreatitis. *J. Physiol.* 597, 3085–3105. doi: 10.1113/jp277856
- Wang, Y., Deng, X., Mancarella, S., Hendron, E., Eguchi, S., Soboloff, J., et al. (2010). The calcium store sensor, STIM1, reciprocally controls Orai and  $\text{CaV}1.2$  channels. *Science* 330, 105–109. doi: 10.1126/science.1191086
- Wasilenko, W. J., Palad, A. J., Somers, K. D., Blackmore, P. F., Kohn, E. C., Rhim, J. S., et al. (1996). Effects of the calcium influx inhibitor carboxyamido-triazole on the proliferation and invasiveness of human prostate tumor cell lines. *Int J Cancer* 68, 259–264. doi: 10.1002/(SICI)1097-0215(19961009)68:2<259::AID-IJC20>3.0.CO;2-4
- Wayne, D., Bertina, J., John, P., Jeremy, S., Takuro, T., Gary, B., et al. (2009). TRPC channels function independently of STIM1 and Orai1. *J. Physiol.* 587, 2275–2298. doi: 10.1113/jphysiol.2009.170431
- Wei, M., Zhou, Y., Sun, A., Ma, G., He, L., Zhou, L., et al. (2016). Molecular mechanisms underlying inhibition of STIM1-Orai1-mediated  $\text{Ca}^{2+}$  entry induced by 2-aminoethoxydiphenyl borate. *Pflugers Arch.* 468, 2061–2074. doi: 10.1007/s00424-016-1880-z
- WHO (2017). *Cardiovascular Diseases*. Available online at: [http://www.who.int/cardiovascular\\_diseases/world-heart-day-2017/en/](http://www.who.int/cardiovascular_diseases/world-heart-day-2017/en/) (accessed October 2017).
- Wilson, C. H., Ali, E. S., Scrimgeour, N., Martin, A. M., Hua, J., Tallis, G. A., et al. (2015). Steatosis inhibits liver cell store-operated  $\text{Ca}^{2+}$  entry and reduces ER  $\text{Ca}^{2+}$  through a protein kinase C-dependent mechanism. *Biochem. J.* 466, 379–390. doi: 10.1042/bj20140881
- Wu, M. M., Buchanan, J., Luik, R. M., and Lewis, R. S. (2006).  $\text{Ca}^{2+}$  store depletion causes STIM1 to accumulate in ER regions closely associated with the plasma membrane. *J. Cell Biol.* 174, 803–813. doi: 10.1083/jcb.200604014
- Wu, Y., Palad, A. J., Wasilenko, W. J., Blackmore, P. F., Pincus, W. A., Schechter, G. L., et al. (1997). Inhibition of head and neck squamous cell carcinoma growth and invasion by the calcium influx inhibitor carboxyamido-triazole. *Clin. Cancer Res.* 3, 1915–1921.
- Yamasaki, Y., Miyoshi, K., Oda, N., Watanabe, M., Miyake, H., Chan, J., et al. (2001). Weekly dosing with the platelet-derived growth factor receptor tyrosine kinase inhibitor SU9518 significantly inhibits arterial stenosis. *Circu. Res.* 88, 630–636.
- Yang, B., Gwozdz, T., Dutko-Gwozdz, J., and Bolotina, V. M. (2012a). Orai1 and  $\text{Ca}^{2+}$ -independent phospholipase A2 are required for store-operated  $\text{I}_{\text{cat-SOC}}$  current,  $\text{Ca}^{2+}$  entry, and proliferation of primary vascular smooth muscle cells. *Am. J. Physiol. Cell Physiol.* 302, C748–C756. doi: 10.1152/ajpcell.00312.2011
- Yang, X., Jin, H., Cai, X., Li, S., and Shen, Y. (2012b). Structural and mechanistic insights into the activation of Stromal interaction molecule 1 (STIM1). *Proc. Natl. Acad. Sci. U.S.A.* 109, 5657–5662. doi: 10.1073/pnas.1118947109
- Yen, M., Lokteva, L. A., and Lewis, R. S. (2016). Functional analysis of orai1 concatemers supports a hexameric stoichiometry for the CRAC channel. *Biophys. J.* 111, 1897–1907. doi: 10.1016/j.bpj.2016.09.020

- Yeromin, A. V., Zhang, S. L., Jiang, W., Yu, Y., Safrina, O., and Cahalan, M. D. (2006). Molecular identification of the CRAC channel by altered ion selectivity in a mutant of Orai. *Nature* 443, 226. doi: 10.1038/nature05108
- Yoast, R. E., Emrich, S. M., Zhang, X., Xin, P., Johnson, M. T., Fike, A. J., et al. (2020). The native ORAI channel trio underlies the diversity of  $\text{Ca}^{2+}$  signaling events. *Nat. Commun.* 11:2444. doi: 10.1038/s41467-020-16232-6
- Yokota, T., Shimokado, K., Kosaka, C., Sasaguri, T., Masuda, J., and Ogata, J. (1992). Mitogenic activity of interferon gamma on growth-arrested human vascular smooth muscle cells. *Arterioscler. Thromb.* 12, 1393–1401.
- Yoshino, T., Ishikawa, J., Ohga, K., Morokata, T., Takezawa, R., Morio, H., et al. (2007). YM-58483, a selective CRAC channel inhibitor, prevents antigen-induced airway eosinophilia and late phase asthmatic responses via Th2 cytokine inhibition in animal models. *Eur. J. Pharmacol.* 560, 225–233. doi: 10.1016/j.ejphar.2007.01.012
- Zeng, W., Yuan, J. P., Kim, M. S., Choi, Y. J., Huang, G. N., Worley, P. F., et al. (2008). STIM1 Gates TRPC Channels, but Not Orai1, by Electrostatic Interaction. *Mol. Cell* 32, 439–448. doi: 10.1016/j.molcel.2008.09.020
- Zhang, S. L., Yeromin, A. V., Hu, J., Amcheslavsky, A., Zheng, H., and Cahalan, M. D. (2011a). Mutations in Orai1 transmembrane segment 1 cause STIM1-independent activation of Orai1 channels at glycine 98 and channel closure at arginine 91. *Proc. Natl. Acad. Sci. U.S.A.* 108, 17838–17843. doi: 10.1073/pnas.1114821108
- Zhang, S. L., Yeromin, A. V., Zhang, X. H.-F., Yu, Y., Safrina, O., Penna, A., et al. (2006). Genome-wide RNAi screen of  $\text{Ca}^{2+}$  influx identifies genes that regulate  $\text{Ca}^{2+}$  release-activated  $\text{Ca}^{2+}$  channel activity. *Proc. Natl. Acad. Sci. U.S.A.* 103, 9357–9362. doi: 10.1073/pnas.0603161103
- Zhang, W., Halligan, K. E., Zhang, X. X., Baisillon, J. M., Gonzalez-Cobos, J. C., Motiani, R. K., et al. (2011b). Orai1-mediated I-CRAC is essential for neointima formation after vascular injury. *Circu. Res.* 109, 534–U189. doi: 10.1161/circresaha.111.246777
- Zhang, W., Zhang, X., González-Cobos, J. C., Stolwijk, J. A., Matrougui, K., and Trebak, M. (2015). Leukotriene-C4 synthase, a critical enzyme in the activation of store-independent Orai1/Orai3 channels, is required for neointimal hyperplasia. *J. Biol. Chem.* 290, 5015–5027. doi: 10.1074/jbc.M114.625822
- Zhang, X., Xin, P., Yoast, R. E., Emrich, S. M., Johnson, M. T., Pathak, T., et al. (2020). Distinct pharmacological profiles of ORAI1, ORAI2, and ORAI3 channels. *Cell Calcium* 91:102281. doi: 10.1016/j.ceca.2020.102281
- Zhou, H., Iwasaki, H., Nakamura, T., Nakamura, K., Maruyama, T., Hamano, S.-I., et al. (2007). 2-Aminoethyl diphenylborinate analogues: Selective inhibition for store-operated  $\text{Ca}^{2+}$  entry. *Biochem. Biophys. Res. Commun.* 352, 277–282. doi: 10.1016/j.bbrc.2006.10.174
- Zhu, L., Li, J., Guo, L., Yu, X., Wu, D., Luo, L., et al. (2015). Activation of NALP1 inflammasomes in rats with adjuvant arthritis; a novel therapeutic target of carboxyamidotriazole in a model of rheumatoid arthritis. *Br J Pharmacol* 172, 3446–3459. doi: 10.1111/bph.13138
- Zhu, X., Jiang, M., Peyton, M., Boulay, G., Hurst, R., Stefani, E., et al. (1996). Trp a novel mammalian gene family essential for agonist-activated capacitative  $\text{Ca}^{2+}$  entry. *Cell* 85, 661–671. doi: 10.1016/S0092-8674(00)81233-7
- Zhu, X., Ma, K., Zhou, K., Voelkl, J., Alesutan, I., Leibrock, C., et al. (2020). Reversal of phosphate-induced ORAI1 expression, store-operated  $\text{Ca}^{2+}$  entry and osteogenic signaling by  $\text{MgCl}_2$  in human aortic smooth muscle cells. *Biochem. Biophys. Res. Commun.* 523, 18–24. doi: 10.1016/j.bbrc.2019.11.005
- Zitt, C., Strauss, B., Schwarz, E. C., Spaeth, N., Rast, G., Hatzelmann, A., et al. (2004). Potent inhibition of  $\text{Ca}^{2+}$  release-activated  $\text{Ca}^{2+}$  channels and T-lymphocyte activation by the pyrazole derivative BTP2. *J. Biol. Chem.* 279, 12427–12437. doi: 10.1074/jbc.M309297200

**Conflict of Interest:** The authors declare that the research was conducted in the absence of any commercial or financial relationships that could be construed as a potential conflict of interest.

Copyright © 2021 Shawer, Norman, Cheng, Foster, Beech and Bailey. This is an open-access article distributed under the terms of the Creative Commons Attribution License (CC BY). The use, distribution or reproduction in other forums is permitted, provided the original author(s) and the copyright owner(s) are credited and that the original publication in this journal is cited, in accordance with accepted academic practice. No use, distribution or reproduction is permitted which does not comply with these terms.

# Advantages of publishing in Frontiers



## OPEN ACCESS

Articles are free to read  
for greatest visibility  
and readership



## FAST PUBLICATION

Around 90 days  
from submission  
to decision



## HIGH QUALITY PEER-REVIEW

Rigorous, collaborative,  
and constructive  
peer-review



## TRANSPARENT PEER-REVIEW

Editors and reviewers  
acknowledged by name  
on published articles

## Frontiers

Avenue du Tribunal-Fédéral 34  
1005 Lausanne | Switzerland

**Visit us:** [www.frontiersin.org](http://www.frontiersin.org)

**Contact us:** [frontiersin.org/about/contact](http://frontiersin.org/about/contact)



## REPRODUCIBILITY OF RESEARCH

Support open data  
and methods to enhance  
research reproducibility



## DIGITAL PUBLISHING

Articles designed  
for optimal readership  
across devices



## FOLLOW US

@frontiersin



## IMPACT METRICS

Advanced article metrics  
track visibility across  
digital media



## EXTENSIVE PROMOTION

Marketing  
and promotion  
of impactful research



## LOOP RESEARCH NETWORK

Our network  
increases your  
article's readership